NASA Conference Publication 2300

Tribology
in the 80's

Volume I—Sessions 1 to 4

Proceedings of an
International conference held at
NASA Lewis Research Center
Cleveland, Ohio
April 18-21, 1983

N/\S/

National Aeronautics
and Space Administration

**Scientific and Technical
Information Branch**

19960229 142

1984

DISCLAIMER NOTICE
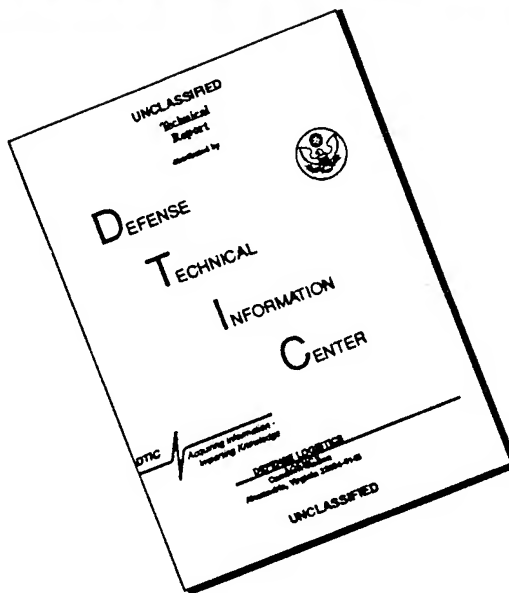
THIS DOCUMENT IS BEST QUALITY AVAILABLE. THE COPY FURNISHED TO DTIC CONTAINED A SIGNIFICANT NUMBER OF PAGES WHICH DO NOT REPRODUCE LEGIBLY.

DEDICATION

The proceedings of this conference is dedicated to Edmond E. Bisson as was the conference itself. Ed retired from NASA Lewis Research Center in 1973 and currently resides in Fairview Park, Ohio, where he writes and prepares lectures, consults, and serves as Editor-in-Chief for the American Society of Lubrication Engineers.

The tribology organization at NASA Lewis exists because of the pioneering spirit of Ed Bisson. The activity had its beginning at Langley Laboratory, Langley Field, Virginia, prior to World War II. Shortly thereafter the activity moved to the Lewis Research Center in Cleveland, Ohio. Ed recognized the need for a group dedicated to gaining a better fundamental understanding of adhesion, friction, wear, and lubrication processes. He sought the sustaining support of NACA and later NASA for the research. And he created an environment which attracted capable engineers and scientists.

Ed Bisson is a truly exceptional individual. Throughout his many years of managing the research work in tribology, bearings, gears, and seals, he demonstrated the utmost in administrative skills. More importantly, he also maintained a close contact with the technical aspects of the research work by reading and editing all technical papers emanating from the group. Many of the pioneering papers in solid film lubrication, high temperature behavior of materials, synthetic lubricants, and bearing concepts bear his name as one of the authors. His book, coauthered with William J. Anderson and entitled Advanced Bearing Technology, is widely used and referenced by tribologists throughout the world.

Researchers in this and other fields tend to gravitate to either fundamental studies or the more practical engineering applications. Ed Bisson always recognized the importance of both approaches. He knew that it was necessary to conduct fundamental research for tribology to grow as a science. He was also practical enough to recognize the need to solve existing engineering problems. He ensured that both areas were adequately addressed and helped to bring about interaction and mutual appreciation for both approaches among staff members.

A number of internationally recognized tribologists, either presently or formerly with NASA, were initiated into the field under the supervision of Ed Bisson. Literally hundreds of technical papers were published by various authors as a result of programs initiated or supported by him. A host of awards were bestowed on various members of the group through the years of his management. These recipients will readily admit that the creative environment which made these awards possible was a direct result of Ed Bisson's efforts.

Thus, in recognition of his many contributions to the field of tribology and his determined efforts in the advancement of the field, both as a scientific endeavor and an engineering discipline, we dedicated to Edmond E. Bisson the International Conference on Tribology in the 80's and its proceedings.

PREFACE

Since many of you may not be familiar with the NASA Lewis Research Center, I want to briefly introduce you to our Center and the work we do.

Lewis Research Center is one of eight major NASA field centers in the United States. In addition to these eight centers are several small satellite organizations and our Headquarters in Washington.

NASA Lewis is located on 350 acres adjacent to the Cleveland Hopkins International Airport. We have an additional 6000 acres at Sandusky, Ohio (about 60 miles west), where some larger facilities, including an experimental wind turbine, are located. Onsite we employ about 2600 civil service employees and another 700 support service contractors. Typically, our budget is about $600 million a year. About a third of that supports our inhouse research efforts, some of which you will be learning about in the next few days. The other two-thirds supports our contracts and grants with various industries and universities. You will also be hearing some results of these contractual endeavors during this conference.

Basically, there are four major program thrusts at Lewis, the largest being that of aeronautical propulsion R&T. Lewis, now over 40 years old, was formed in 1941 primarily for research on aircraft engines – originally recip-rocating engines and then jet engines. That research still constitutes about half our effort here at Lewis. Aeronautical propulsion covers everything from fundamental research in materials and tribology, which you will be hearing about, through components and internal aerodynamics, and eventually to total engine systems that are tested in our various wind tunnels and engine testing facilities.

A second major thrust is space propulsion. We have people working on various types of advanced rocket engines – for example, the Centaur engine, which is a second-stage engine. The Centaur engine has been operational for 20 years. It is now being reconfigured to operate from the bay of the Shuttle as an upper-stage vehicle to deliver satellites to high Earth orbits and Earth escape trajectories. Some of our other research propulsion devices include electric thrusters and advanced chemical propulsion systems.

A third major area is space power R&T. This is an area the Center emphasized during the 1960's with such devices as solar cells, batteries, fuel cells, and various dynamic systems. Since the early 1970's and until recently only a relatively small effort had continued at Lewis in this research area. However, through our strategic planning of the last year, it was decided to make this work a major new thrust for the Center. Through such efforts, we are trying to return Lewis to its former role as NASA's lead center in space power R&D for the future.

The fourth area is communications R&T. Starting in the mid 1970's, Lewis essentially became NASA's lead center in communications technology. The Ad-vanced Communication Technology Satellite Program is a major effort in this area. When this advanced satellite is launched in the late 1980's, it will open up the wave bands of a 20-30 GHz system.

Over the last decade we have been applying these major technologies to terrestrial-energy applications such as windmills and automotive propulsion, both gas-turbine and Stirling-cycle systems. Much of our technology is being funded and applied by the U.S. Department of Energy (DOE). Lewis Research

Center has managed and directed DOE programs through both inhouse and contracted efforts.

Another special area is launch vehicle operations for upper-stage propulsion systems. Centaur vehicle operations have been managed from Lewis for the last 20 some years. The Centaur has been a second-stage engine on both the Atlas and Titan rockets, and thus has carried many of the communications satellites to their high Earth orbits. Our Centaur program has been very successful. In fact, we have had 99 successful launches and, within the next month we will complete, hopefully, the 100th successful launch of that system.

This is just a brief overview of the work we are doing at Lewis Research Center. I hope you will find this conference rewarding, not just the formal papers that are to be presented, but also the discussions – both the more formal ones following the papers and the informal ones. And I urge you to participate actively in this conference, because participation of all attendees is the real value of any conference.

Neal T. Saunders
Director
Materials and Structures Directorate

FOREWORD

This proceedings of the International Conference in Tribology in the 80's is the result of a program by the Structures and Mechanical Technologies Division of the NASA Lewis Research Center to bring together the most outstanding and internationally known people in the field of tribology. Thirty-six invited presentations were made relative to the understanding and technical advancement of various disciplines and subdisciplines of the field. These included papers on the status of understanding on each of the eight session topics as well as an examination of the current state-of-knowledge and the directions to be taken for the remainder of the decade for each subject. Presentations by two preeminent tribologists from England, the "cradle of Tribology," set the theme for the conference. Professor David Tabor of the University of Cambridge began the conference with an overview paper on the "Status and Direction of Tribology as a Science in the 80's." Then, at the dinner meeting, Professor Duncan Dowson of the University of Leeds spoke of the future with his presentation on "Tribology for the 90's and Beyond." It is noteworthy to mention that both of these gentlemen are recipients of the prestigious Tribology Gold Medal, tribology's highest award, from the Institution of Mechanical Engineers in London. The conference was honored to have four of the ten living winners of this award in attendance, the other two being Professor Harmen Blok of The Netherlands and Robert L. Johnson of the United States.

In addition to furthering the understanding and the exchange of knowledge among some of the world's tribologists, there were several other purposes for the conference: (1) to gain attention in other scientific communities and in industry for some of the important elements being studied in tribology, (2) to help transform this information into broad, practical uses, and (3) to try to eliminate the general vagueness that exists, even among some tribologists, with the meaning of the word tribology.

Let us spend a minute with the definition and significance of the word tribology. Websters New Collegiate Dictionary has the definition "a science that deals with the design, friction, wear, and lubrication of interacting surfaces in relative motion (as in bearings or gears)." As was so succinctly stated by Professor Terence F. J. Quinn[1], "tribology is a subject which has suffered from lack of precision over the terms used to identify its various constituents." But the word itself has different connotations, according to the various authorities connected with the subject. The Jost Committee, in its report[2] to the British Government in 1966, was responsible for introducing the word tribology into current usage. The Committee defined tribology as "the study of the interactions between surfaces in relative motion and the practice related thereto." More recently, D. Scott[3], past editor of the tribology journal Wear, simply used "the science and technology of lubrication, friction and wear" as his definition. The Jost Committee's definition is perhaps deliberately vague so as to encompass the many complex interactions and practices involved and the obvious interdisciplinary nature of the science.

This conference covered a wide range of subjects extending from fundamental research with tribological materials of all kinds and their surface effects up to the final applications in mechanical components. An attempt was made to exemplify this in the design of the conference logo, which is shown on the cover. First and central to all efforts in tribology is basic research

work, which is illustrated in the middle of the logo with a drawing of the Stribeck curve[4] for delineating the various lubrication regimes. This curve is superimposed on a sketch showing two rubbing surfaces (roughness exaggerated) under load and separated by a lubricant. Around these illustrations are shown a bearing, seal, and gear to indicate the ultimate use and technology application.

The conference had a definite international flavor with 72 of the 311 registrants representing 14 countries other than the United States: 20 from Japan, 14 from England, 10 from the Federal Republic of Germany, 9 from Canada, 6 from The Netherlands, 3 each from France and Sweden, and 1 each from Australia, Finland, India, Ireland, Israel, Italy, and Switzerland.

The most important and critical elements needed for the success of this or any technical conference are the interest and support of the participants. Of the technical presentations, 11 were by NASA Lewis personnel, and the remainder were by individuals from universities, industry, and other government agencies – 12 from the United States and 13 from other countries. In addition to the 36 technical papers, there were about 70 invited discussions of these papers solicited prior to the conference plus others that were offered during and after the meeting. Those who served as chairmen of the various technical sessions were: Marshall B. Peterson, Wear Sciences; J. M. Georges, Professor, University Claude Bernard–Lyon I, France; Kenneth C. Ludema, Professor, University of Michigan; Masahisa Matsunaga, Professor, Chiba Institute of Technology, Japan; Lavern D. Wedeven, NASA Lewis Research Center; Robert L. Fusaro, NASA Lewis Research Center; Olog Vingsbo, Professor, Uppsala University, Sweden; and Robert L. Johnson, Consultant and Professor, Rensselaer Polytechnic Institute. Debra J. Drdek served as Conference Coordinator in making all the physical arrangements and Susan F. Gott was the Conference Secretary.

Many other people at the Lewis Research Center contributed to the success of this conference. Among these are some personnel of the Engineering and Technical Services Directorate and the Technical Information Services Division. I thank these people as well as the participants. In particular, a special thank you to Donald H. Buckley, Chief of the Tribology Branch, and the members of his group who helped to make this conference possible.

References

1. Quinn, T. F. J.: NASA Interdisciplinary Collaboration in Tribology – A Review of Oxidational Wear. NASA CR-3686, 1983.
2. Lubrication (Tribology), Education and Research; a report on the Present Position and industry's needs. H.M.S.O., 1966.
3. Scott, D.: Introduction to Tribology. Fundamentals of Tribology, Editors N. P. Suh and N. Saka, eds., The M.I.T. Press, 1980, pp. 1-13.
4. Stribeck, R.: Characteristics of Plain and Roller Bearings (in German), Zeit, V. D., vol. 46, 1902, pp. 1341-48, 1432-38, 1463-70.

William R. Loomis
NASA Lewis Research Center

Conference Chairman

CONTENTS

Volume I

SESSION 3 – FUTURE DIRECTION OF RESEARCH IN
WEAR AND WEAR RESISTANT MATERIALS
Chairman: K. C. Ludema, University of Michigan

SESSION 4 – THE FUTURE FOR LIQUID LUBRICANTS AND ADDITIVES
Chairman: M. Matsunaga, Chiba Institute of Technology

Volume II*

SESSION 5 - STATUS AND NEW DIRECTIONS IN EHL
Chairman: L. D. Wedeven, NASA Lewis Research Center

*Pages 507 to 881 are published under separate cover.

STATUS AND DIRECTION OF TRIBOLOGY AS A SCIENCE IN THE 80's

Understanding and Prediction

David Tabor
Cavendish Laboratory
Cambridge, England

"It is better to predict without certainty than never to have predicted at all". Henri Poincaré, "Science and Hypothesis", 1905, Chapt. IX , p. 144, Walter Scott Publishing Co., London.

The most challenging research problems in Tribology for the next decade or beyond can be classified horizontally into two categories (I) understanding of basic mechanisms and (II) prediction of practical performance. Vertically they may be classified in terms of particular themes or fields of interest.

The full paper will discuss areas where it seems more fundamental work is required:

(i) Adhesion and friction of clean and contaminated surfaces: with metals the role of ductility, workhardening and surface shear; the mode of removal of surface contaminants: with polymers the connection between friction and chemical structure and morphology: with ceramics the nature of adhesive forces and modes of junction rupture.

(ii) Lubrication: hydrodynamic and elastodynamic lubrication are well understood though many applied problems will continue to attract attention. On the other hand a fundamental attack on the viscous properties of lubricants in molecular terms (avoiding Eyring and molecular dynamics) is long overdue: it may come from current ideas in polymer flow. Similarly there is scope for more realistic molecular models of boundary lubrication, and for a better understanding of the mechanical as well as the chemical properties of dry film lubricants.

(iii) New materials: here is a whole field for investigation for both the material scientist and the tribologist.

(iv) Surface characterisation at the engineering level (topography) and at the atomic level (various spectroscopies). Analytical topography has probably reached maturity but its application to practical problems in tribology is essential. Spectroscopic studies can shed new light on atomic mechanisms in adhesion, friction, lubrication and wear but care must be taken to match the resolving power of our instruments to our level of understanding or perhaps a little beyond.

(v) Wear: This is probably the field in which most research will emerge as Dowson has suggested. It is an area which highlights the contrast between basic research (which I strongly favour) and the needs of the engineer (which I well appreciate). At the basic level the research worker attempts to isolate and understand a single mechanism and creates conditions under which this mechanism dominates. Typical mechanisms include adhesion, abrasion, delamination, oxidation, fatigue, surface cell-formation, corrosion, erosion, and (in brittle solids) crack formation. By

contrast the engineer works with real systems where usually several mechanisms operate simultaneously and interact with one another. It is a humbling discovery that the main cause of failure in automotive engines is the presence of adventitious dirt.

This leads into the second column of the horizontal classification: prediction. Apart from situations where full lubrication is achieved, can the research physicist and chemist, the material scientist and the tribologist predict the performance of a particular tribological system in terms of the materials, surface finish, speeds, loads and ambient conditions? Are quantitative formulae, such as those proposed by Kragelski and his school, realistic, practical and reliable? Can they be merged with the construction of "wear-maps"? Do these provide the practising engineer with the design date he requires? Or must we rely on the experience of the engineer and his intelligent application of fundamental knowledge to the system he is operating? The limits of our ability to predict performance remain a major long term challenge: can it, in fact, ever be surmounted?

INTRODUCTION

It is a great honour to be asked to present this introductory paper at such an important and pretigious Conference. The title that the organisers have suggested describes the main thrust of this Conference. I have, however, chosen as my own subtitle "Understanding and Prediction" because I believe that the most challenging research problems facing Tribology in the next decade and beyond can be classified horizontally in those two words, that is

I   the understanding of basic mechanisms
    and
II the prediction of practical performance based on our understanding.

Vertically the classification may be presented in terms of particular themes or fields of interest. A Table indicating the interrelations between these categories, covering a small typical range of themes is given below (Table 1).

In what follows I shall deal primarily with those areas where it seems to me that more basic understanding is both necessary and timely: but I shall also refer to more practical implications and the problems involved. However, the Conference includes a number of introductory lectures on future directions of research in half-a-dozen specific areas which cover almost the whole of Tribology. Consequently my own contribution may appear redundant. I hope nevertheless to introduce a number of themes and concepts which may not emerge in the more specific sessions. In what follows I shall deal in turn with adhesion, friction, lubrication and wear.

(i) Adhesion and friction of clean and contaminated surfaces
(a) Adhesion of metals

We now have ample evidence (ref. 1) not least from N.A.S.A., that clean metals if pressed together can adhere very strongly indeed. The strength of adhesion is usually expressed as the force to pull the surfaces apart. Although I do not approve of multiplying specialist jargon I prefer to give this a specific name and call it the "pull-off" force to distinguish it from thermodynamic adhesion and from surface forces. The pull-off force undoubtedly depends on the strength of the bond formed between the surfaces. Thus with similar metals, as Buckley and his group have shown, the pull-off force falls off very rapidly as the amount of bonding of d-electrons increases. This has been interpreted in terms of reduced bond-strength. Other important atomic parameters include cohesive or lattice energies and, for dissimilar metals, lattice misfit.

2

However, the pull-off force also depends on the applied load, the surface geometry (gross and microscopic) and the ductility of the metal (ref. 2). It seems to me that ductility has been a neglected parameter in this field and in a later talk I shall describe simple experimental procedures which, I believe, can sort out ductility from the other variables. Ductility may also be an important parameter in the behaviour of hexagonal metals of different c/a ratios. It may also be relevant to the adhesion and frictional properties of ceramics.

(b) The effect of contaminant films

Practically all published work agrees that extremely small amounts of oxygen or other contaminants can greatly reduce the adhesion between metals (ref. 1,3). However, there are situations where modest amounts of oxide produce a relatively small decrease in adhesion (ref. 4,5). Further, in systems such as sapphire on nickel a monolayer of oxygen can increase the adhesion. This result is of great interest and deserves critical theoretical and experimental study. In the practical field it may be relevant to the problem of forming strong bonds between metals and ceramics.

There is another aspect of contaminant films which may form either by interaction with the environment or by diffusion through the solid itself. The surface film may change the mechanical properties of the first few atomic layers of metal adjacent to the surface film. Work in this area is somewhat piecemeal and deserves more systematic study. Finally the way in which surface films are ruptured or removed needs to be examined afresh. Our picture is either at the level of a rather gross process or at the level of Auger spectroscopy. Something inbetween is required.

(c) Ceramics - adhesion and rupture

We understand fairly well the nature of the metal-metal bond though there are still a number of very challenging problems for the theoretical solid state physicist (ref. 6,7). By contrast we understand far less about the forces and bonding if two pieces of ceramic are brought into contact.This is particularly true if the bonding within the ceramics is primarily covalent since it is extremely difficult to define the state of atoms at the free surface. Are there dangling bonds ready to link up with those of another contacting surface? Or do the surface valency bonds back-bond or rehydridise? If so do they need thermal activation before they can take part in bond formation with another surface?

These concepts also have a bearing on the friction and wear of ceramic materials and will be discussed in somewhat greater detail in a later paper.

(d) Surface energy, fracture mechanics and the adhesion of solids

In many studies of the adhesion of solids use is made of thermodynamic concepts involving surface and interfacial energies. The surface free energy of a solid is the thermodynamically reversible energy involved in creating a unit area of surface. Consider two bodies 1 and 2 with surface energies γ_1 and γ_2 respectively which are brought into atomic contact. If the interfacial energy (defined like surface energy) is γ_{12} then for each unit of interface that is formed the energy released is

$$\Delta\gamma = \gamma_1 + \gamma_2 - \gamma_{12} \qquad\qquad (1)$$

This quantity is known as the thermodynamic work of adhesion since in principle a similar amount of work is needed to separate the bodies. Relation (1) has been applied very successfully to liquids. It cannot be applied unequivocally to solids

even if they are ideally brittle for the following reason. Consider the adhesion between two identical solids; here $\gamma_1 = \gamma_2 = \gamma$ and the interface has no identity i.e. $\gamma_{12} = 0$. Then $\Delta\gamma = 2\gamma$. We may thus take a bar of solid 1, start a crack in one side and pull it until the crack begins to grow. By the principle of fracture mechanics crack-growth will commence when the release rate of stored elastic energy in the solid is just equal to the surface energy involved in extending the crack. This would be valid if the cracking process were reversible. But because of the atomic (particulate) nature of real solids it is found that there are instabilities in the opening and closing of the crack (ref. 8,9,10). According to these theories the work to extend the crack is always greater than 2γ the excess being dissipated as waves in the solid (phonons). Similarly the energy release on closing the crack is less than 2γ. Thus the thermodynamic surface energy of a solid composed of atoms (as distinct from some hypothetical smoothed-out continuum) cannot be determined with precision from fracture studies, even for an ideally brittle material. Presumably the same applies to adhesion.

Of course with metals the fracture energy (or the equivalent adhesion) is greatly magnified because of plastic deformation at the crack-tip, another example of the importance of ductility. With elastomers and polymers the fracture energy, and adhesion are similarly increased because of hysteresis losses and flow. There may also be electrostatic forces due to charge separation at the interface.

In recent years a great deal of exciting work has been carried out (ref. 11) on the effect of liquid media on the fracture process (Rehbinder effect). This must go on and its implications in the friction and wear of solids, especially brittle solids, must be explored further. However, it seems to me that even with ideally brittle solids there is a large gap between the atomics of fracture and the applied field of fracture mechanics. More cross-fertilisation in these fields could be beneficial.

(e) Adhesion of elastomers and polymers

We now have a far better basic understanding of the adhesion of elastomers and polymers than we had a decade or so ago. The adhesion is a function of the thermo-dynamic energy of adhesion and the viscoelastic properties (ref. 12,13,14), or deform-ation-loss properties of the polymer (ref. 15). Surface roughness may also be impor-tant (ref. 16). There are also certain systems where electric charge separation at the interface is important (ref. 17), but there are numerous systems where charge transfer plays only a small part.

In recent years chemical treatments of the surfaces have been used to change the adhesion of polymers and fundamental studies in this field have proved very fruitful and stimulating (ref. 18). It is natural to ask if such treatments can be applied to sliding surfaces and, if so, whether the treated surface is viable.

(f) Friction of elastomers and polymers

A study of the friction of soft elastomers in contact with smooth surfaces has revealed that gross sliding does not usually occur. A ruck or buckle is formed in the elastomer due to an instability generated by the surface traction. This ruck travels along the interface so that movement of the elastomer resembles the motion of a cater-pillar (ref. 19). This process, often described as Schallamach waves of detachment, involves adhesion and dehesion of the elastomer and energy losses due to hysteresis. This will be discussed in a later session.

The friction of polymers can be explained qualitatively in terms of adhesion,

deformation, rupture, cracking etc. Thermal effects and rate effects are more marked than with metals and are fairly well understood. To some extent we also understand the relation between molecular architecture and frictional behaviour but we need to know more in the hope that, in due course, we may be able to design polymers for specific tribological applications. I have in mind the brilliant work by chemists of the United States Navy in producing a strong, bondable transparent non-wettable polymer.

(ii) Lubrication

(a) Hydrodynamic and elastohydrodynamic lubrication (ref. 20)

These fields of lubrication are well understood in terms of the properties of the lubricant, the gross geometry of the solids, their microtopography, and their deformation properties. Hydrodynamic lubrication still provides a host of practical problems which in turn produce a steady stream of theoretical and computational papers. No doubt this will continue but it is unlikely that new fundamental ideas will arise.

This also applies to E.H.L. and with the development of independent techniques for determining lubricant rheology in terms of temperature, pressure and shear rate (ref. 21) the main creative period has probably passed. However the mechanism of film breakdown is still a challenging problem. The possibility that it is mainly due to temperature flashes may now be explored with sensitive infra-red devices. Of course there will still be considerable scope for tackling applied problems.

(b) Lubricant viscosity

A fundamental study of the viscous properties of lubricants in molecular terms is long overdue. The present approach to liquid viscosity is three-pronged. The first is that due to Eyring and originally was meant to apply only to simple liquids. The general idea is that the molecules, on account of their thermal motion, are able to jump from one site to another with a frequency v_0 determined by the temperature, ($v_0 = kT/h$) and by an exponential term $\exp - \varepsilon/kT$ where ε is the energy required to form a "hole" into which the molecule can jump. In equilibrium, molecules jump as many times in one direction as in another so that there is no overall movement in any one direction. If, however, a shear stress is applied the jump rate is increased in the direction in which the shear stress can do work and reduced in the opposite direction. This leads to a net flow and results in an equation for the viscosity of the liquid in terms of basic molecular properties (see Figure 1). The approach is referred to as a "stress-aided thermally activated" process. It has been applied with astonishing success to the behaviour of lubricant molecules with 30 carbons in the chain and several side groups and describes the effects of pressure, temperature and shear rate with surprising accuracy. We know however that the model cannot be right. First of all the whole straggly molecule cannot jump as one unit: it simply cannot move in that way. Secondly even if it could jump it is inconceivable that the jump frequency would be the same as for a monatomic molecule. Thirdly even for simple liquids there is no evidence that molecules jump from one site to another: they appear to shuffle and gradually change their place by very small movements. This has led to an alternative approach, a modification of Eyring, in which the emphasis is placed on the free volume available for molecular movement. This treatment is again limited to small molecules. Finally there is the approach known as molecular dynamics where the behaviour of a group of molecules contained in a box of specified volume is solved computationally. The molecules are assumed to be elastic solids with some suitable law of force between them. They are placed in the box with a given velocity in random directions and allowed to interact with one another according

5

to classical collision theory. Molecules that pass through one wall of the box are allowed to re-enter from the other side thus maintaining the number of molecules and the energy of the system. This approach provides a very reliable and realistic picture of the behaviour of an assembly of molecules. However because of computational complexity it is limited to the number of molecules, their size, and, even more important, to the degrees of molecular freedom that can be handled. It seems to me that there is a challenge for liquid-state scientists to break away from the existing models and venture into new paths. The following is one suggestion.

Recently as part of a study of diffusion in polymers Rennie and I studied the effect of hydrostatic pressure on the diffusion of hydrocarbons through a molten polymer (ref. 22). The pressure reduces the diffusion coefficient and from this the activation volume ϕ for diffusion may be deduced (see Figure 2). It turns out that ϕ is almost independent of the size of the diffusant and bears no relation to it. For example for a hydrocarbon with 260 carbons in the chain (molecular volume ca 7000 Å^3) the value of ϕ is less than 100 Å^3. What does this mean? It implies that the hydrocarbon, by a process known as reptation, snakes its way through the empty spaces in the polymer matrix (Figure 3). However it does not move as a continuous entity like a rope being drawn through a tube. On the contrary it moves by rotations or crank-like motions of a small part of the chain involving only 3 or 4 carbons at a time. These rotations are thermally activated processes, each rotation producing a local translation over a distance comparable with the lengths of a C-C bond. If this is a general feature of the movement of hydrocrabon chains past similar molecules such ideas could be fed into a theory of hydrocarbon viscosity perhaps borrowing techniques from molecular models of polymer flow (ref. 23).

(c) Boundary lubrication

During the last 10 years or so there has been some revival of interest in the frictional behaviour and breakdown of boundary films, though much of this appears to be similar to older work. A different approach which has produced some promising results (as well as some unanswered questions) concerns the direct measurement of the shear properties of boundary films under carefully controlled conditions. The most definitive experiments were carried out between crossed cylinders of mica on which Langmuir-Blodgett monolayers could be deposited (ref. 24). The mica surfaces were mounted on glass substrates (Figure 4) so that very high contact pressures could be reached (of order 10 kg mm^{-2}). Using multiple beam optical interferometry the area of contact could be determined reliably and the thickness of the Langmuir-Blodgett sandwich could be measured to an accuracy of $\pm$ 2 Å. From the area of contact and the force required to produce sliding the shear strength τ of the film could be calculated. There are five interesting results. First and most surprising is the viability of these films even when subjected to contact pressures comparable to the yield pressure of metals. In these experiments the sliding speeds were rather small so that frictional heating could not have been marked. On the other hand on account of the small thickness of the sandwich (ca 50 Å = 5 nm) the shear rates are enormous; nevertheless the film survives repeated traversals. Secondly the sandwich thickness remains virtually constant during sliding: it is within experimental error equal to the thickness under static load and this in turn is essentially the same as the thickness of an uncompressed film. Thus not only is the film highly incompressible – shear does not tilt the molecules out of the vertical orientation. Thirdly some experiments carried out over a small temperature range showed that τ decreases with increasing temperature. Fourthly the shear strength τ increases linearly with contact pressure (see Figure 5). Fifthly certain polymeric films examined in a similar way show similar behaviour but in addition show a retardation effect, that is the increase of τ with pressure takes a finite time to reach its maximum equilibrium

value (ref. 25).   These experiments provide a means of modelling the shear behaviour in terms of various rate-process parameters.   However they do not indicate how such films break down.   It is possible that temperature is a far more important parameter causing breakdown than shear, shear-rate, or pressure.   The subject merits a new look.

(d)   Dry film lubrication (including oxides)

Certain surface films can greatly reduce friction and wear.   With metal surfaces these include oxides, chlorides and sulphides which may be formed in situ.   More generally lamellar solids such as MoS_2 and graphite may be applied to the surface. There are three basic problems here.   First how are the films attached to the substrate;   second what are the strengths and shear-strength properties of the films; third, how do they break-down?

Sometimes these surface films crack and allow the underlying substrate to exude through the cracks (see below).   In other cases they form blisters and peel away from the substrate.   Is this due to the generation of compressive stresses in the film?   If so can it be explained in terms of Kendall's ideas of the effect of compressive stresses on the peeling apart of elastomeric joints?   In his view peeling occurs because the additional elastic strain energy facilitates crack propagation and separation at the interface (ref. 26).   Of course a detailed study of such a mechanism in relation to oxides and similar films requires a knowledge of their surface energies.

(e) Oxide films in electrical contacts

Oxide films play an extremely important part in the practical functioning of both static and sliding electrical contacts.   A tremendous amount of applied research has been carried out on the general behaviour, electrical characteristics, reliability, and effective lifetime of such contacts.   The amount of basic work is surprisingly meagre.   For example, it is only recently that Williamson has shown, in a simple basic study, how electrical joints operating under alternating currents, can stabilise their behaviour and achieve very long lives (ref. 27).   In general local oxidation leads to a deterioration of the contact, a rise in contact resistance and an increase in local temperature, so accelerating the oxidation process.   However local softening intervenes, producing an enlarged area of contact, a drop in contact resistance and a reduced temperature at which the contact can operate over very long periods.   With electrical contacts, the cracking of an oxide which allows metal to exude through the cracks seems to be a common feature (see Figure 6). We may ask if a similar situation applies in well lubricated <u>sliding</u> systems.   Does the tessellated structure of the oxide remain for protracted periods or is it removed in a gross manner even in the presence of lubricant films.   There appears to be little overlap between those engaged in research on electrical contacts and tribologists involved in surface oxidation.

Again the role of electrical currents in sliding contacts needs critical exploration.   The field is complicated, to my mind largely because experiments are carried out on poorly characterised surfaces.

Finally we may note that in power conduction in electrical traction a tremendous effort has been expended in the empirical selection of conductors which give satisfactory power transmission.   Far less fundamental work has been carried out on why certain combinations work well electrically and whether such satisfactory electrical performance must always be accompanied by heavy wear.

(iii) New materials

The explosion in new materials, covering metals, metalloids, cermets, ceramics and polymers presents the tribologist with a dazzling choice. This has been further expanded by the new techniques of ion deposition (and similar processes) by which surface films of the most diverse composition and structure may be formed. Many of these films are of materials which do not exist in the bulk state. The material scientist and the tribologist have the possibility of choosing surfaces with clearly specified strength and surface properties. One problem is how to characterise these properties. Another is how to limit one's appetite to a sensible range of materials. I do not think this Conference expects me to offer advice as to the best possible choices: I recognise that we are faced with an "embarras du choix".

(iv) Surface characterisation

(a) Topography at the engineering level

We now have extremely sensitive and elegant stylus equipment which can trace the surface topography along a given datum line with a high degree of precision. By carrying out such traces along closely parallel lines a full three dimensional map of the surface may be plotted. The data obtained may be processed digitally and analysed to provide information about the statistical height of asperities, the prevalence of peaks (an asperity higher than its immediate neighbours), average asperity slopes, effective curvature of asperity tips and other features. Indeed the processing of topographical information, as Whitehouse has pointed out, has led to the development of commercially available software which often provides an enormous number of surface parameters, most of which are redundant (ref. 28). During the last decade or so some very valuable theoretical treatments have emerged which make it possible to characterise the surface in a useful way (ref. 29). They often differ in detail but as far as concerns the main features, they are generally in accord with one another. One interesting conclusions is that the average slope of the surface asperities is probably the most significant <u>single</u> parameter determining the deformation properties of the surface. Another and far more important general conclusion is that there is no absolute description of surface topography: it depends on the scale at which the characterisation is being made. Consequently surface topography should be studied at the same scale as the surface process that is being studied. This is a general principle of very wide application in practically all fields of scientific research.

With our present knowledge of surface topography it is possible to understand the way in which the asperities deform when two surfaces are brought together, but it is still not possible to calculate quantitatively the true area of contact. This is because there is, as yet, no unequivocal way of deciding on the appropriate lateral sampling length. For example an unanswered question is - if there are small asperities between larger ones at what level can a particular range of asperity sizes be neglected. Of course there is a lower limit to the area of true contact whatever assumptions are made about the sampling length. This is the area that would be attained if all the asperities deformed plastically at the yield pressure of the softer metal. In spite of these problems progress is being made and in due course it may be possible to calculate quantitatively the true area of contact, the contact pressures, the overall approach of the two bodies under load etc. This may then be applied to sliding surfaces if we can make reasonable assumptions concerning interfacial shear strength. Another problem is the way in which the asperities fail during sliding (shear, fracture, tearing): this is part of the general problem involved in analysing the frictional processes. These models do not cope with the

effect of work-hardening for metals, or with the effect of temperature and time dependent deformation for polymers. Such effects are probably not important in static contact but may be important in sliding contact. The theoretical models already available could be modified to deal, at least approximately, with these effects. Of course at a practical level surface topography must be incorporated into our thinking over a wide range of tribological engineering applications.

(b) Surface characterisation at the atomic and electronic level

We now have a large array of techniques for studying the solid surface at the atomic and electronic level (ref. 1). These include electron diffraction, field ion microscopy and a whole suite of electronic and photonic spectroscopies. Their number is still growing and one of the most exciting recent developments is that of microprobe electron tunnelling (ref. 30). These techniques provide different pieces of information and in due course it should prove possible to coordinate all of them and provide a coherent self consistent description of the surface. The same may be achieved for surfaces covered with adsorbed films of gases, lubricants and frictionally transferred films. Thus surface studies of this type can provide us with an extremely basic understanding of some of the most important processes involved in adhesion, friction, lubrication and wear. In the long run, they could well provide us with information that would enable us to select materials and surface treatments most suited for a particular application. In spite of the fact that such surface studies are expensive and time consuming they should be continued. However, we must be sensible about this. If we do not match the resolving power of our instruments to our level of understanding (or a little beyond) we may accumulate data which, for the time being, are virtually useless.

(v) Wear

Duncan Dowson has pointed out in his fascinating book on the history of tribology (ref. 31) that whereas the past period has been mainly concerned with the mechanisms of friction and lubrication the future will probably concentrate on the study of wear. This is an area which highlights the contrast between basic research, which I strongly favour, and the needs of the engineer which I well appreciate. At the basic level the research worker attempts to isolate and understand a single mechanism. To do this he sets up apparatus and creates conditions under which this mechanism dominates. Thus we now have groups of dedicated scientists demonstrating the importance of adhesion, abrasion, delamination, oxidation, fatigue, surface cell-formation, corrosion, erosion, and (with brittle solids) crack formation. No one doubts the validity of these expositions or the integrity of their proponents. If indeed a practical system operates under conditions where wear is dominated by one of these mechanisms the results are of the greatest practical value. But the real systems with which the engineer works usually involve several wear mechanisms which operate simultaneously and interact with one another. Here prediction based on a detailed knowledge of individual mechanisms is very uncertain.

It is not my purpose in this review to discuss individual wear mechanisms in detail - there is a whole session devoted to this theme. I hope it will also include a critical assessment of non-destructive methods of wear detection. I may however make a few comments. First I think that all those who concentrate on a particular wear mechanism should make an effort to indicate the conditions under which such mechanisms <u>cease to be important</u>. For example, is there a critical tractive stress below which delamination does not occur; is there a critical amount of surface contamination above which adhesive wear falls off: is there a toughness parameter which indicates when wear due to cracking is avoided? And in many wear studies on metals

9

where experiments are carried out in air why do we pay so little attention to the way in which the oxide is worn away? Is it abraded, is it torn up, is it detached by adhesion, is it broken up and incorporated into the surface layers of the metal?

Again in the wear of thermoplastics in the presence of a liquid it is found that the wear rate is higher the larger the solubility parameter of the liquid. It is known that there is an accompanying reduction in fracture toughness; but apparently there is also a reduction in fatigue resistance. Which of these properties is responsible for the observed wear behaviour and under what conditions? To some extent this is as much a problem for the polymer scientist as for the tribologist.

Finally in the study of brittle solids a substantial body of work has been published on the way in which various patterns of cracks are formed as a result of normal stresses, tangential stresses, elastic and elasto-plastic deformation. Many workers continue to apply and modify existing classical theory but in order to obtain better agreement between theory and experiment are forced to introduce empirical corrections. A new analysis has recently emerged that may remove this empiricism. It is based on the idea that since most ceramics and glasses are not completely densified some compaction occurs during indentation. The loss in volume leads to stress distributions not given by existing classical theory and these appear to explain many of the deformation and crack features observed in practice. This modest paper (ref. 32) may well prove to be a seminal paper in the field.

This discussion leads into column II of the horizontal classification: prediction of practical performance based on fundamental understanding. There are indeed systems where such predictions are possible. For example in full hydrodynamic lubrication we can specify the mechanical properties of the solid surfaces, the level of surface topography and the viscosity characteristics of the oil; and then predict with some certainty the performance of the system in terms of speeds, loads and ambient conditions. With some knowledge of lubricant chemistry and with adequate knowledge of the fatigue or creep properties of the solids we can also predict when the oil should be changed or the bearing replaced. The reason is clear. On the whole such systems involve bulk properties of the solids and of the lubricant. Indeed under ideal conditions, surface properties do not come into the picture.

As soon as we are confronted with a system where surface properties are involved we are in trouble. As Wolfgang Pauli is reported to have said "God made solids, but surfaces were made by the Devil". Suppose we have acquired a vast fundamental knowlege of surface structure, physical and chemical properties, topography, deformation characteristics etc. can we predict the behaviour of a practical system in terms of our knowledge? I have recently been much exercised by the publications of Professor Kragelsky and his school and have been both impressed and puzzled by the analytical expressions they provide for predicting friction and wear (ref. 33,34). The friction calculations, although complicated, employ parameters every single one of which is clearly defined. Similarly in calculating fatigue wear, on a model not unlike that derived at IBM, they are able to predict wear rates over 10 orders of magnitude for materials as diverse as automobile tyres, brakes, clutch plates, gears and cam mechanisms (see Figure 7). Wear equations which are not too complicated are also developed for other types of wear. In addition they provide detailed guidance on the selection of materials for rubbing parts. In this area they conclude that "before full field tests, the materials should be bench tested in standard conditions and also in conditions simulating the operating ones" (ref. 24, vo. 1, p.196). This is familiar engineering practice. Nevertheless the whole thrust of their analytical work is to enable the engineer to chose materials and surface parameters and predict performance.

How are we to regard this approach? It is certainly interesting and challenging: is it in fact realistic? To my mind the friction equations, however brilliant, are too complicated. On the other hand the treatment of wear might well be expressed as K.L. Johnson suggests (ref. 35) in the form of "wear-maps" resembling the "deformation maps" pioneered by Professor Ashby. These maps, which might have to be multidimensional, would (a) predict the wear mechanisms most likely to apply in particular circumstances (b) provide a wear equation applicable to that particular regime. No doubt bench-tests would also be required. The main difficulty, once again, is that in practice wear might be the result of interacting mechanisms with no single process dominating. In that case we have to rely on the experience of the engineer and his intelligent application of fundamental knowledge to the system he is operating. It may indeed turn out that the quality of the man rather than the ingenuity of the equation or the systemisation of the wear processes will prove to be the most important factor. I have raised these issues partly because the Russian work is not being presented as a specific contribution to this Conference, but also because I believe the challenge to predict is as important and as demanding as the fundamental study of tribological processes.

TABLE I

Understanding and Prediction

(Typical sample)

Basic Understanding	Prediction
Adhesion mechanisms of metals	Material combinations, surface geometries, operating conditions favouring high or low adhesion.
Contaminant films	Effectiveness of surface films especially their viability
Ceramic adhesion	Factors favouring sintering and metal-ceramic bonding. Wear prediction in tribology.
Adhesion and friction of elastomers and polymers.	Design of polymers (chemistry and structure) for specific applications.
Viscous properties of lubricating oils	Chemical synthesis of more effective products.
Dry film lubrication	Selection of films for increased life.
Electrical contacts.	Practical performance, stability, and life of static and sliding contacts.

REFERENCES

1. Buckley, D.H.: "Surface Effects in Adhesion, Friction, Wear and Lubrication", 1981, Elsevier.

2. Gane, N., Pfaelzer, P.F. and Tabor, D.: "Adhesion between Clean Surfaces at Light Loads", Proc. Roy. Soc. London A340, 1974, pp. 495-517.

3. Bowden, F.P. and Tabor, D.: "Friction and Lubrication of Solids", Part I, 1950; Part II, 1964, Clarendon Press, Oxford.

4. Pethica, J.B. and Tabor, D.: "Contact of Characterised Metal Surfaces at Very Low Loads: Deformation and Adhesion", Surface Science, 89, 1979, pp. 182-188.

5. Pashley, M.D. and Tabor, D.: "Adhesion and Deformation Properties of Clean and Characterised Metal Micro-Contacts", Vacuum, 31, 1981, pp. 619-623.

6. Ferante, J. and Smith, J.W.: "A Theory of Adhesion at a Bi-metallic Interface: Overlap Effects", Surface Science, 38, 1973, pp. 77-92.

7. Inglesfield, J.E.: "Adhesion between Al Slabs and Mechanical Properties", J. Phys. F: Metal Phys. 6, 1976, pp. 687-710.

8. Thomson, R., Hsieh, C. and Rana, V.: "Lattice Trapping of Fracture Cracks", J. Appl. Phys. 42, 1971, pp. 3154-3160.

9. Hsieh, C. and Thomson, R.: "Lattice Theory of Fracture and Crack-Creep", J. Appl. Phys. 44, 1973, pp. 2051-2063.

10. Sinclair, J.E.: "The Influence of the Interatomic Force Law and of Kinks on the Propagation of Brittle Cracks", Phil. Mag. 31, 1975, pp. 647-671.

11. Latanision, R.M.: "Surface Effects in Crystal Plasticity", in Fundamentals of Tribology, Ed. Suh, N.P. and Saka, N., 1980, pp. 255-294, M.I.T.

12. Gent, A.N. and Petrich, R.P.: "Adhesion of Viscoeleastic Materials to Rigid Substrates", Proc. Roy. Soc. London, A310, 1969, pp. 433-448.

13. Greenwood, J.A. and Johnson, K.L.: "The Mechanisms of Adhesion of Viscoelastic Solids", Phil. Mag. A43, 1981, pp. 697-711.

14. Maugis, D. and Barquins, M: "Fracture Mechanics and the Adhesion of Viscoelastic Bodies", J. Phys. D: Appl. Phys. 11. 1978, pp. 1989-2023.

15. Andrews, E.H. and King, N.E.: "Surface Energetics in Adhesion in Polymer Surfaces", Ed. Clark, D.T. and Feast, W.J., 1978, Wiley, pp. 47-63.

16. Fuller, K.N.G. and Tabor, D.: "The Effects of Surface Roughness on the Adhesion of Elastic Solids", Proc. Roy. Soc. London, A345, 1975, pp. 327-342.

17. Deryagin, B.V., Krotova, N.A. and Smilga, V.P.: "Adhesion of Solids", Translated from the Russian by Johnston, R.K., 1978, Consultants Bureau, N.Y.

13

18. Andrews, E.H., Pingsheng, He. and Vlachos, C.: "Adhesion of Epoxy Resin to Glass", Proc. Roy. Soc. London, A381, 1982, pp. 345-360.

19. Schallamach, A.: "How does Rubber Slide?", Wear, 17, 1971, pp. 301-312.

20. Cameron, A.: "Basic Lubrication Theory", 1981, Ellis-Horwood, Chichester, UK.

21. Bair, S. and Winer, W.O.: "A Rheological Model of Elastohydrodynamic Contacts Based on Primary Laboratory Data", Trans. ASME J. Lubrication Technology 101, 3, 1979, pp. 258-265.

22. Rennie, A.R. and Tabor, D.: "Duffision in Molten Polymers: the Influence of Hyrdostatic Pressure". Proc. Roy. Soc. London, A383, 1982, pp. 1-14.

23. Tabor, D: "The Role of Surface and Intermolecular Forces in Thin Film Lubrication", in "Microscopic Aspects of Adhesion and Lubrication", Ed. Georges,J.M. 1982, pp. 651-682, Elsevier.

24. Briscoe, B.J. and Evans, D.C.B.: "The Shear Properties of Langmuir-Blodgett Layers". Proc. Roy. Soc. London A380, 1982, pp.389-407.

25. Briscoe, B.J. and Tabor, D.: "Shear Properties of Polymeric Films", J. Adhesion, 9, 1978, pp.145-155.

26. Kendall, K.: "The Effect of Shrinkage on Interfacial Cracking in a Bonded Laminate". J. Phys. D: Appl. Phys. 8, 1975, pp. 1722-1723.

27. Williamson, J.B.P.: "The Micro-world of the Contact Spot", Holm Conf. on Electrical Contacts, 1981, pp.1-10, Illinois, Inst. Tech.

28. Whitehouse, D.J.: "The Parameter Rash - Is there a Cure", Wear, 83, 1983, pp. 75-78.

29. Thomas, T.R. (Editor), "Rough Surfaces", 1982, Longman.

30. Binning, G., Rohrer, H., Gerber, Ch., and Weibel, E.: "Surface Studies by Scanning Tunneling Microscopy", Phys. Rev. Lett. 49, 1982. pp. 57-64.

31. Dowson, D.: "History of Tribology", 1979, Longman, London.

32. Yoffe, E.: "Elastic Stress Fields Caused by Indenting Brittle Materials", Phil. Mag. A 46, 1982, pp.617-628.

33. Kragelsky, I.V., Dobychin, M.N. and Kombalov, V.S.: "Friction and Wear: Calculation Methods", 1982, Pergamon.

34. Kragelsky, I.V. and Alisin, V.V. (Editors), "Friction, Wear, Lubrication: Tribology Handbook", Vols. 1,2 and 3, 1981, Mir Publishers (in English) Moscow.

35. Johnson, K.L., Private communication, 1983.
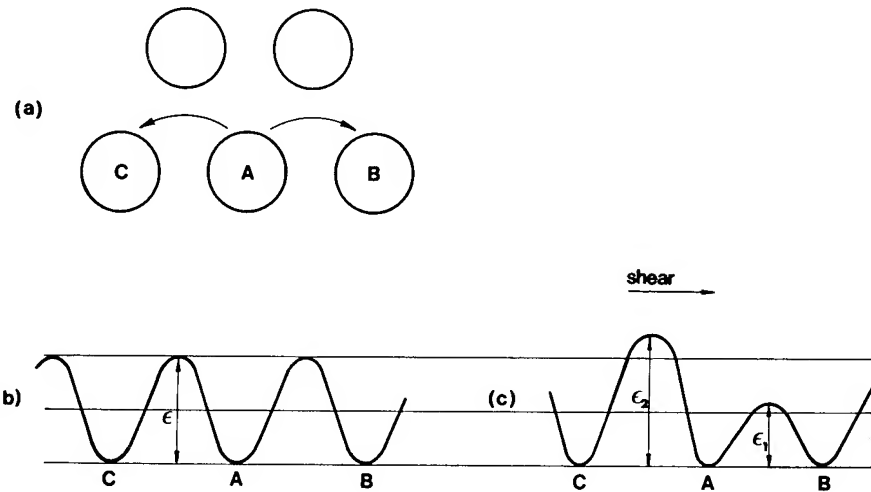
Figure 1. The Eyring Model of vis-
cosity for small molecules.

	Vol. of Molecule Å^3	Activation Volume Å^3
C18	450	45
C45	1200	50
C 260	7000	80

(A)

(B)

Diffusion in Molten
Linear PE at 150°C

log D
(m^2s^{-1})

(C)

Error bar

Pressure (MNm^{-2})
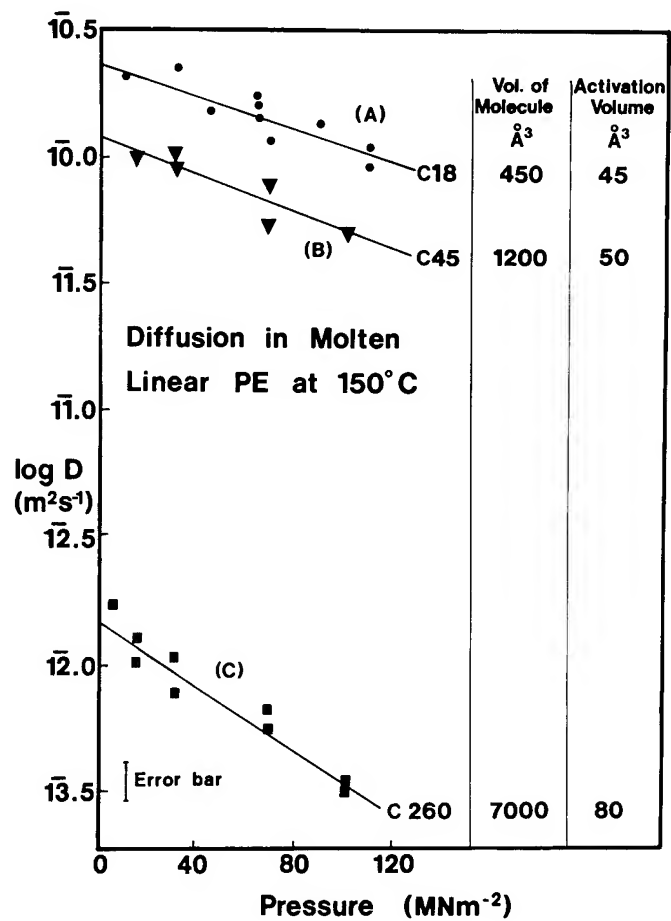
Figure 2. Effect of hydrostatic
pressure on diffusion in
molten P.E.
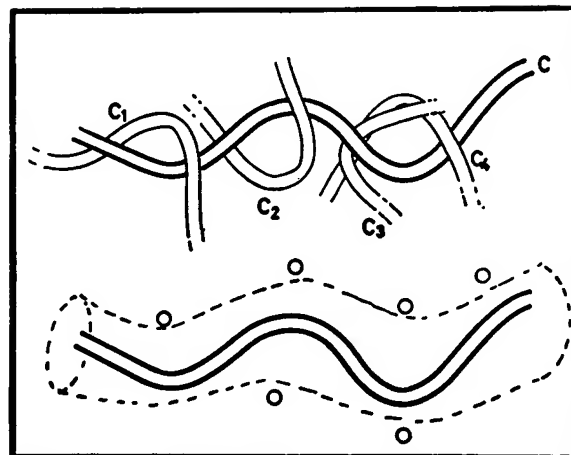
Figure 3. The reptation of one long
chain molecule through
available free space.
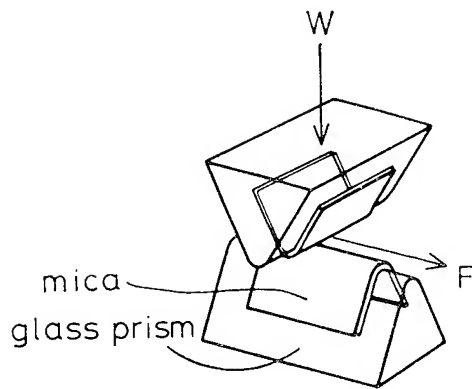
Figure 4.   Arrangement of mica
            surfaces attached to glass
            mounts.
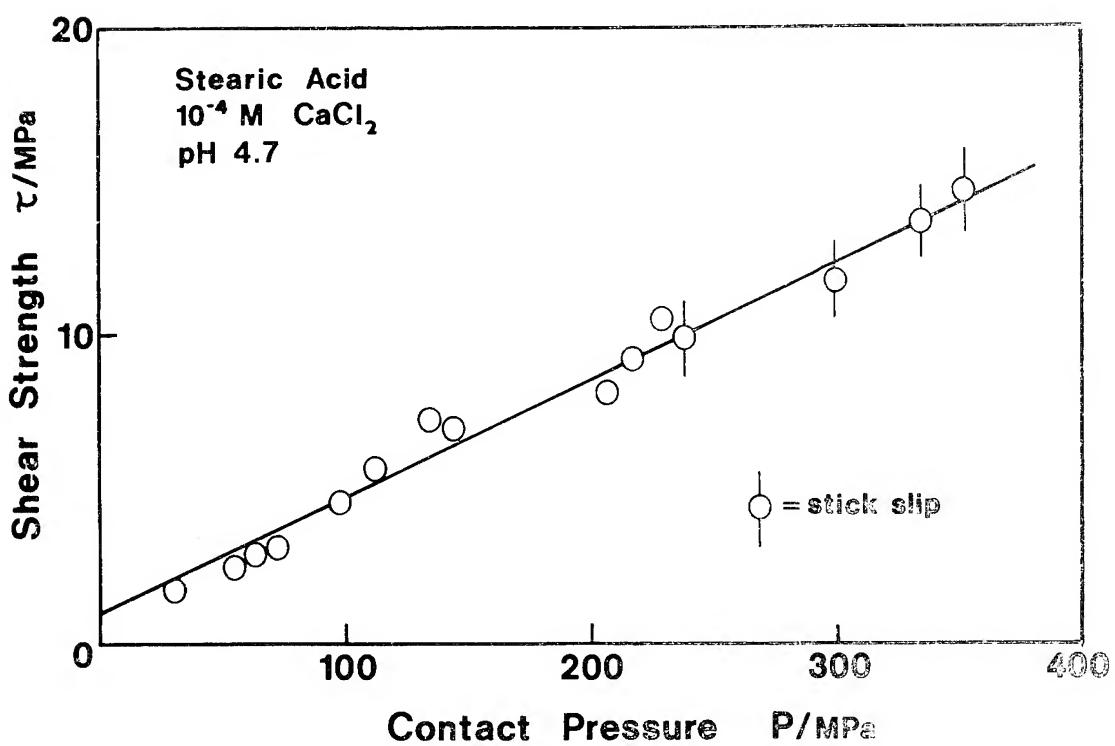
Figure 5.   Shear strength τ of
            Langmuir-Blodgett films.

Oxide

Exuded Metal

⌐¬ 100 µm
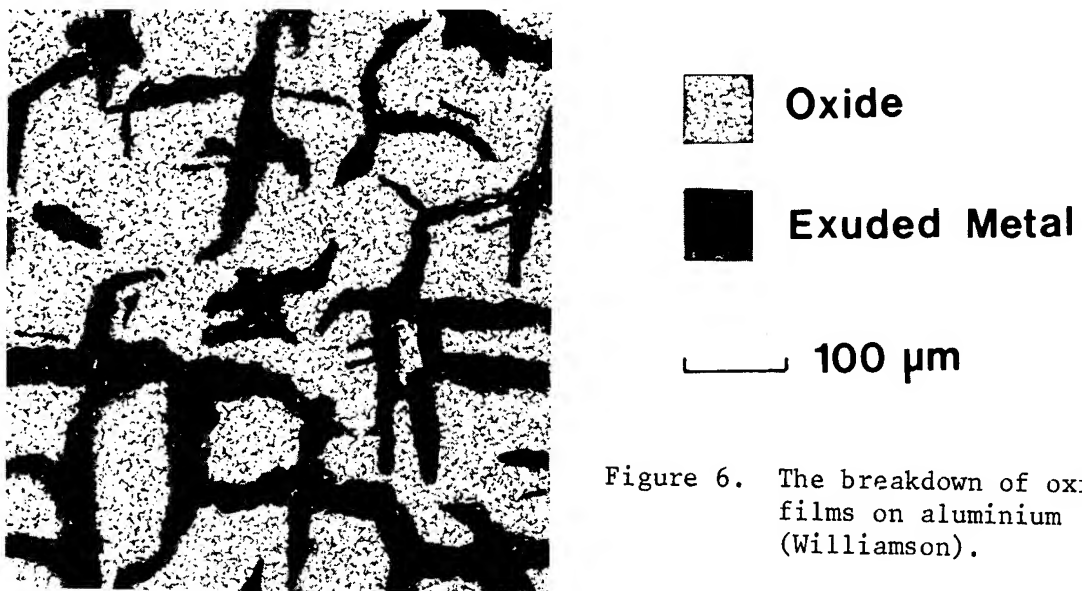
Figure 6. The breakdown of oxide films on aluminium (Williamson).

x bronze on steel

o tread rubber {rolling}

● tread rubber {sliding} on concrete

□ metals on abrasive

■ metals on abrasive paper
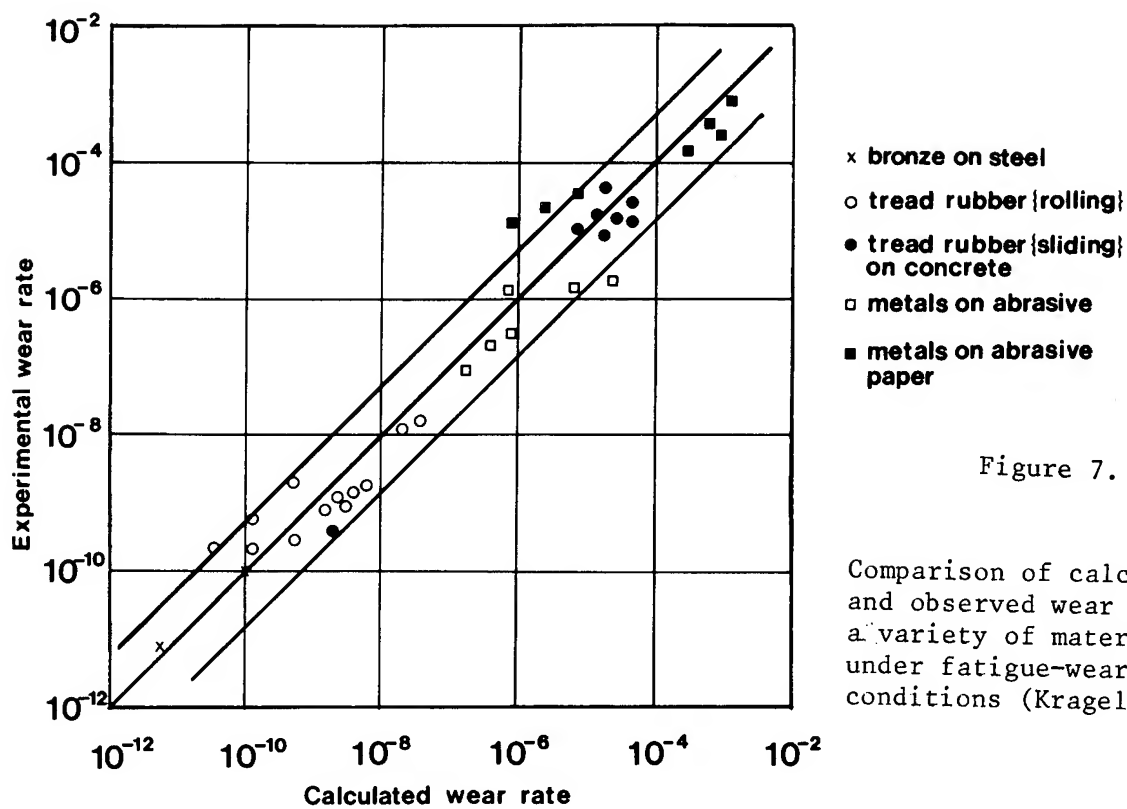
Figure 7.

Comparison of calculated and observed wear rates for a variety of materials under fatigue-wear conditions (Kragelsky).

17

IMPORTANCE AND DEFINITION OF MATERIALS IN TRIBOLOGY

Status of Understanding

Donald H. Buckley
National Aeronautics and Space Administration
Lewis Research Center
Cleveland, Ohio 44135

SUMMARY

In general, tribological systems consist of three basic components: the material surfaces in contact, the lubricant, and the environment. This paper addresses the materials in contact and the influence of both bulk and surface properties, indicating the importance of material characterization, on tribological behavior. Since metals and metallic alloys are the most widely used class of materials in practical devices, attention is focused principally on them.

With respect to surface behavior, the effect of contaminants both from within the material and from the environment on adhesive behavior is addressed. The various surface events that can alter adhesion, friction, and wear are discussed. These include surface reconstruction, segregation, chemisorption, and compound formation. Examples of these events are presented. It is demonstrated that minor nuances in the structure of the outermost layers of solids can have a pronounced effect on tribological properties.

The transition from surface to bulk properties is achieved with an indication of the relationship of surface to bulk energetics. Surface energetics are involved in adhesion, but separation of adhered junctions usually occurs in the bulk of one of the two contacting materials and accordingly involves bulk cohesive energies. Data are presented that show the interrelationship between those cohesive energies and wear behavior. Another manifestation of the relationship is the adhesive transfer of metallic alloy constituents to metallic oxides and its predictability from the free energy of metal oxide formation. Analogous behavior is presented for friction and adhesive transfer of metals to nonmetal surfaces with the degree of metal valence and saturation.

The presence of crystallinity in metallic alloys is shown to affect friction and wear as the alloys in the amorphous state have superior tribological properties. Further, alloys can serve as a reservoir for species that can undergo surface segregation and thus can markedly alter surface interactions. Temperature, time, and the stress of contacting solids are shown to be capable of altering alloy surface chemistry, crystal structure, and reaction rates.

The paper addresses the importance of characterizing the materials of solids in contact in order to achieve a fundamental understanding of adhesion, friction, and wear and accordingly of methods for their control.

INTRODUCTION

In examining any tribological system, three fundamental components must be considered. These components are the material surfaces to be lubricated, the lubricant, and the environment. Considerable research has been devoted to characterizing and understanding both liquid and solid lubricant structures, their rheological properties, and their performance. Even the additives that

are placed in lubricants to serve various functions (antiwear, antifoam, anti-oxidant, corrosion inhibition, etc.) have been the focus of considerable attention from the viewpoint of structure.

In recent years there has been an increase in cognizance of the importance of the environment, particularly with respect to its role in interacting with lubricants, both liquids and solids. The role of oxygen in the degradation of both liquids and solids has been fairly well established. Further, the influence of water dissolved in oils and its effect on the lubricating ability of the oil has been studied. The effect of water vapor on graphite and its ability to lubricate has been known for some time. More recently the effect of water on the performance of molybdenum disulfide has been determined. With graphite, the presence of water is now known to be necessary for lubrication; and with molybdenum disulfide, it is known to be detrimental.

The attention that has been focused by researchers through the years on the lubricant and the environment has not been enjoyed by the materials requiring lubrication. Neither the surface or bulk properties of the materials have been given a great deal of fundamental consideration with regard to those properties that are important to adhesion, friction, and wear. With respect to the surfaces of solids, most chemists, in considering the reaction of lubricants, still think of the surfaces of bearing and gear steels as being iron and postulate surface reactions of lubricants and additives as occurring exclusively with iron. It is now well established that the surface of steel frequently contains very little exposed iron. Further, small concentrations of alloying agents can segregate to the surface of a solid and completely dominate surface reactions.

With respect to the solids themselves, a host of different properties basic to materials may bear a relationship to the adhesion, friction, and wear properties of those solids. Understanding the relative interrelationships between the basic properties of solids and their tribological performance can do much to reduce empirical testing and to assist in further moving tribology into the realm of science and away from the practice of an art.

The objective of the present paper is to review the properties of surfaces and bulk materials that are of fundamental significance to the adhesion, friction, and wear of mechanical components. Attention will be focused on metals and alloys primarily because the host of components in practical mechanical devices are predominantly made up of these materials. The various events that take place on the surface will be considered and their relationship to tribology established via experimental data. The bulk properties of metals and alloys that bear a relationship to adhesion, friction, and wear will be considered and the interrelationship with adhesion, friction, and wear established.

RESULTS AND DISCUSSION

Surfaces

The study of surface behavior is not of recent origin. Back in 1916, Langmuir established the method for the adsorption of monolayers on solid surfaces (ref. 1). In 1932, Lennard-Jones established a quantum-mechanical representation of the variation of the potential energy of an adatom with distance from a solid surface (ref. 2). Further, in 1931, Taylor recognized that metal surfaces were covered with contaminants (ref. 3), and in 1935, Roberts established the crucial experiment for achieving a clean metal surface

20

(ref. 4). In 1939, Oatley determined that argon ions could be used to clean a metal surface, a technique that is commonly used today for the generation of clean metal and alloy surfaces (ref. 5).

A number of surface analytical tools have their origins in years long since gone by. For example, the Auger effect, which was discovered in 1925, led to modern Auger spectroscopy (ref. 6). Low-energy electron diffraction (LEED) had its beginnings in the late 1920's (ref. 7). Mueller developed the field emission microscope in 1936 (ref. 8) and the field ion microscope in 1951 (ref. 9).

Despite an understanding of the nature of surfaces and the availability of concepts for surface analytical tools in the 1920's and 1930's, a real understanding of the fundamental properties of surfaces had to await the achievement of ultra-high-vacuum systems. The reason for this is that both the preparation and maintenance of a clean surface, particularly a metal or an alloy, and the use of surface analytical tools require a vacuum of 10^{-8} to 10^{-9} Pa. Vacuums of these pressure levels became achievable in the 1950's and readily available to the researcher via commercial systems in the 1960's. Today, the vacuum systems, surface tools, and techniques for generating well characterized surfaces are all available and are routinely employed in the study of catalysis, corrosion, and physical metallurgy. Attention currently is being focused on increasing characterization of surfaces in tribology.

Iron is the basic component of steels, one of the most widely used alloys in mechanical systems. It is therefore an element worthy of study. Iron, like steel, has a surface that is covered with oxides and adsorbates. It is a relatively easy task to use the technique originally established by Oatley, namely, argon ion bombardment, to clean an iron surface (thereby removing adsorbed films and oxides). Further, if this is done in a vacuum of 10^{-8} to 10^{-9} Pa, the surface can be maintained free from adsorbtion and oxide formation for at least an hour. However, an examination of the surface of the iron with, for example, Auger emission spectroscopy or LEED will establish that the surface of the iron is in fact not clean. Contaminants from the bulk segregate to the surface and are readily seen thereon with surface analyses. For example, iron, even when triple-zone refined to only a few parts per million of contaminant, will exhibit either sulfur or carbon or both on the surface.

Figure 1 presents LEED patterns of an iron single-crystal surface of the (011) orientation. The pattern in the upper left of the figure is that of the iron surface containing a carbon contaminant film. The carbon source was the bulk iron. Mild heating of the iron after cleaning allowed the carbon to segregate to the surface, producing the ringlike structure shown in figure 1. The use of argon ion bombardment dislodged the carbon contaminant from the surface and left behind the carbon-free surface shown in the LEED pattern in the upper right of figure 1. The iron surface was, however, in a strained state as a result of the bombardment with the argon ions. Mild heating eliminated the strain, and a clean, strain-free iron surface is presented in the lower LEED pattern of figure 1.

If adhesion experiments are conducted with two iron surfaces containing the carbon contaminant surface film shown in figure 1, adhesion between the solids is very poor. Conversely, when the surfaces are clean, very strong adhesive bond forces approaching the cohesive energy of iron are measured. The bond energy is less than the cohesive energy because lattice disregistry at the interface generates misfit dislocations. The role of lattice disregistry at interfaces and the influence of misfit dislocations at interfaces on epitaxial film growth were observed by van der Merwe long before the present author studied lattice disregistry in adhesion (ref. 10).

21

Environmental contamination of clean metal surfaces must be continuously monitored during surface studies to maintain the condition of a clean surface. The field ion micrograph of figure 2 for an iridium surface indicates that under certain circumstances contamination can occur fairly rapidly even at vacuum pressures of 10^{-8} Pa. The original photograph shown in figure 2 contained red and green dots denoting atomic sites that had undergone a change due either to adsorption or removal of atoms from the surface. These changes in the surface took place at 78 K in the course of 1 hour. Such contamination can alter adhesion behavior at the atomic level (refs. 11 and 12).

Surface Events

A number of events can occur on a solid surface in the clean state that can alter its behavior. These events, which include reconstruction, segregation, chemisorption, and compound formation, are shown schematically in figure 3.

Reconstruction takes place when the outermost layers of atoms of the solid surface undergo a change in structure. A recent example of this obtained in our laboratory (ref. 13) was for the surface of silicon carbide. On heating silicon carbide above 800° C, silicon-to-carbon bond scission occurred and the silicon evaporated from the surface leaving the carbon behind. The carbon in the outermost layers collapsed into a pseudo-graphitic structure. The surface reconstruction resulted in a marked change in the friction coefficient for the silicon carbide, from approximately 0.8 before reconstruction to 0.2 thereafter.

The second surface event shown in figure 3 is segregation. The segregation of alloy species to grain boundaries in alloys and its effect on mechanical properties have been known by metallurgists for some time (ref. 14). The same segregation can occur on the surfaces of solids, and segregation has been observed to exert considerable influence on adhesion, friction, and wear. Segregation effects in tribology have been studied for copper- and iron-base alloys with in some instances, because of segregation, as little as 1 at.% of alloying element completely dominating adhesion behavior (refs. 15 and 16).

With some alloy systems the segregation process is irreversible and, once alloying elements segregate to the surface, they remain there. Examples are carbon to the surface of iron, sulfur to the surface of iron, aluminum to the surface of both iron and copper, and indium and tin to the surface of copper. Recent studies with amorphous alloys also indicate the segregation of boron to the surface of ferrous alloys (ref. 17). In each case, the segregation produces a notably significant effect on adhesion, friction, and wear.

The third surface event shown in figure 3 is chemisorption. The adhesive behavior of materials in solid-state contact is extremely sensitive to minor nuances in the structure of adsorbed species. For example, minor modifications in the hydrocarbon structure can produce marked differences in measured adhesive forces. This is demonstrated in the data of table I. Simply increasing the number of carbon atoms from one to two produces a significant change in adhesive behavior for a clean iron surface containing a chemisorbed layer of each of the hydrocarbons methane and ethane. Further, altering the degree of bond saturation has an effect, as indicated in table I with the data for ethane, ethylene, and acetylene. In addition, altering the surface active species in the two-carbon-atom structure can produce significant differences. A comparison in table I of the results for vinyl chloride and ethylene oxide demonstrates this effect. LEED patterns for these two species indicate that

ethylene oxide produces a closely packed molecular structure on the iron surface that completely masks the iron but that vinyl chloride does not completely cover the surface, even at saturation.

Not only the quality of the adsorbed species on a solid surface, but the concentration thereof as well, alters adhesive behavior. Hydrogen sulfide adsorbs dissociatively on a clean iron surface. Concentrations from fractions to a monolayer of sulfur on a clean iron surface were measured with respect to their influence on iron adhesive forces. The data of figure 4 reflect three different degrees of surface coverage, the c(2X4) coverage being minimal, the c(1X2) structure being intermediate, and the monolayer representing maximum surface coverage. The greater the surface coverage of sulfur on iron, the lower the adhesive force for the iron. These results have been observed with other elements as well, notwithstanding some evidence to the contrary (ref. 18).

The fourth surface event shown in figure 3 is compound formation. When clean metal surfaces are brought into solid-state contact, adhesive transfer from one surface to another always occurs. Figure 5 presents two field ion micrographs. The one on the left is for iridium in the atomically clean state, and that on the right is for the iridium after having been contacted by clean platinum. Platinum has been transferred to the iridium in the contact process. This transfer process can lead to the formation of surface compounds.

With metals in contact with both metals and nonmetals, compound formation has been observed to occur on a solid surface. Examples are gold on tungsten (ref. 11), gold on silicon (ref. 19), and phosphorus on iron (ref. 20). The formation of a compound produces strong interfacial bonds at the contacting surfaces and influences adhesive behavior.

Interrelationship of Surface to Bulk Properties

In the preceding discussion, mention was made of the fact that when two clean metal surfaces are brought into solid-state contact, adhesion always occurs. Transfer of the cohesively weaker metal to the cohesively stronger is always observed to occur. However, adhesion is a surface process and the outermost layer of the atoms in the surface of each solid is involved. What then is the interrelationship between cohesive binding in an elemental metal and its surface state?

Surface energy is generally believed to be related to the adhesive behavior of solids in solid-state contact (ref. 21). It is difficult to obtain either theoretical or experimentally determined reliable surface energy values. Notwithstanding this fact, an attempt was made to correlate bulk cohesive energies for some metals with their surface energies in the data of figure 6. Although scatter exists in the data, there appears to be a correlation between cohesive energy and surface energy for the elemental metals indicated. The reason for such an attempted correlation is that reliable cohesive energy values exist but reliable surface energy values do not. Thus it may be possible to predict adhesive transfer behavior from cohesive energy data.

Figures 7 and 8 demonstrate the concept of the cohesively weaker material transferring to the cohesively stronger. The implication incident to the transfer is that the adhesive binding energy at the interface is stronger than the cohesive binding energy in the cohesively weaker of the two materials. In figure 7, gold transferred to a single crystal of silicon on adhesive contact because gold is cohesively weaker than silicon. The transfer of the gold to the silicon is shown in both the photomicrograph and the energy dispersive X-ray map of figure 7.

23

Germanium, a sister element to silicon in the periodic table, has many common properties with silicon. One notable difference, however, is that it is cohesively weaker. It is also cohesively weaker than gold. Adhesion experiments with gold contacting germanium of the same surface orientation as the silicon (111) resulted in the adhesive transfer of germanium to gold. Photomicrographs of the germanium surface (fig. 8) show chevron-shaped fracture pits resulting from the plucking of the germanium on separation of the solids. Thus, without any real knowledge of the surface energies of the solids or the resulting interface energy on contact, the adhesive transfer behavior shown in figures 7 and 8 can be predicted from cohesive binding energies readily available in the literature (ref. 22).

Bulk Properties

If there is a relationship between the cohesive binding energies of elemental metals and their adhesive transfer, which in reality reflects adhesive wear behavior, a relationship should exist between cohesive binding energies and certain other forms of wear. For example, erosive wear involves the removal of material from a solid surface by the impingement of solid-state interactions. The energy of impact is transferred to and dissipated in the eroded solid. When the energy associated with impact is sufficiently high, it may be anticipated that the energy will be dissipated by the removal of metallic atoms from the solid surface. The data in figure 9 reflect a relationship between the erosive wear of some elemental metals and their cohesive binding energies. The data of figure 9(a) are those of the present author and those of 9(b) are taken from the work of Hutchings (ref. 23). Despite differences between the two studies in experimental conditions, a general relationship exists.

Attempts to correlate the abrasive wear resistance of metals and inorganic nonmetals have shown similar correlations. Vijh has taken wear data from various sources and demonstrated the correlation (ref. 24).

The data thus far discussed with respect to adhesive behavior have been for metals and alloys in the absence of ordinary surface oxides. Surfaces in the normal air environment, however, are covered with oxides as is well known. An examination of the basic behavior of materials in solid-state contact in the presence of such oxides indicates some fundamental relationships to bulk properties.

Sliding friction experiments were conducted with copper-base alloys in which each alloy contained 1 at.% of a different alloying species. These copper-base alloys were made to slide on an ordinary oxidized bearing steel surface. No attempt was made to intentionally remove the oxides from either surface. However, in the course of sliding, all of the copper-base alloys transferred to the steel surface.

Figure 10 presents Auger spectra for the bearing steel surface before and after sliding contact with a Co - 1-at.% Ni binary alloy. Before sliding, the bearing steel surface contained carbon from the steel itself and adsorbed carbon monoxide, oxygen from the carbon monoxide, and iron oxides and had iron peaks associated with the iron oxide. After sliding contact with the copper-base alloy, the bearing steel surface contained the original Auger peaks and in addition thereto copper peaks associated with the transfer of copper to the steel surface. This transfer was observed with all of the alloys.

A comparison of the relative peak intensities of copper to iron in the Auger spectra can provide some quantitative insight into the amount of copper

alloy transferred to the steel surface if all else is kept constant except the particular atomic species dissolved in the copper binary alloy. A correlation was found between the mass of alloy transferred to the bearing steel surface and the strength of the bond between the alloying element and oxygen. Data for this interrelationship are presented in figure 11.

An examination of figure 11 indicates a direct correlation between the amount of copper alloy transferred to the bearing steel surface and the free energy of formation of the metal oxide for the 1-at.% alloying element present in the copper.

Other bulk properties of solids can be related to their adhesion, friction, and wear behavior. One such property is the degree of d-valence bond character of the transition metals. Pauling, many years ago, quantified the percentage of d-valence bond character for the transition metals (ref. 25). This relationship has been shown to be related to the adhesive bonding of the transition metals to themselves and to other materials (refs. 26 and 27). In general, those metals with a high degree of valence bond unsaturation such as titanium and zirconium manifest a strong adhesive bond force at the interface. The strong bonding occurs for the metals in contact with themselves as well as with nonmetals.

Titanium, with a very high degree of bond unsaturation, shows a strong affinity for nonmetals such as diamond. Figure 12 presents a replication electron micrograph of the diamond (111) surface after a single sliding pass of a titanium rider across that surface, together with an energy dispersive X-ray profile of the surface. That titanium transferred to the diamond with a single sliding pass indicates that the adhesive bond force at the interface between the diamond and the titanium is stronger than the titanium cohesive bond.

Figure 13 presents a plot of the coefficient of friction as a function of percentage of d-valence bond character of the transition metals. The data indicate a correlation between friction coefficient and percentage of d-valence bond character. The more active the metal, the higher the coefficient of friction. Thus, there is a fundamental relationship between the adhesion and friction properties of the transition metals and the bulk property known as d-valence bond character.

The influence of alloying elements on the behavior of elemental metals has already been discussed to some extent. Other basic relationships between friction properties of metals and the effect of alloying elements have been established. For example, the abrasive wear resistance as well as the friction coefficient for simple ferrous-base binary alloys has been shown to be related to the solute-to-solvent atomic radius ratio in the binary alloy. This relationship is demonstrated in figure 14.

The data of figure 14 indicate that, when the solute-to-solvent atomic radius ratio is unity, the friction coefficient is at a minimum. Deviation in the radius ratio from unity in either direction results in an increase in friction coefficient. Deviation from unity in the lattice radius ratio produces strain in the crystal lattice of the solvent iron and thereby increases the shear strength. Accordingly, this accounts for an increase in friction coefficient. The relationship of figure 14 indicates another bulk property of metal alloys that can be related to tribological performance.

When moving from simple binary alloys to more complex systems involving many elemental constituents, more than a single basic property of an alloy may be relatable to the adhesion, friction, and wear behavior of the alloy. A current form of alloy that appears to be very promising for tribological applications is the amorphous metal or metallic glass. Certain alloy compositions, upon very rapid quenching from the liquid state, solidify into the

25

amorphous state with an absence of crystallinity. There are currently a host of alloy compositions that exhibit this property in the solid state. These alloys undergo transformations from the amorphous to the crystalline state at various temperatures depending on their composition.

Friction data over a range of temperatures for three ferrous-base metallic glasses as a function of temperature are presented in figure 15. At room temperature, the friction coefficients are low for the metallic glasses in the amorphous state. As the temperature is increased toward the transformation temperature from the amorphous to the crystalline state for these alloys, which is approximately 450° C, friction coefficients increase. Thus, for these alloys the amorphous state has superior friction properties to the crystalline state (ref. 28).

Wear studies on the amorphous glasses also indicate that wear is considerably less for the metallic glasses than it is for other alloys having comparable mechanical properties. For example, under an equivalent set of mechanical conditions, 304 stainless steel exhibits considerable wear, but the metallic glass exhibits no discernible wear (ref. 28).

The lack of crystallinity is not the only property of metallic glasses that influences tribological behavior. If the temperature is increased above 500° C (fig. 15), the friction coefficient markedly decreases for all three metallic glasses. All the metallic glasses in figure 15 contain boron. With heating above 500° C, the boron and the nitrogen segregate from the alloyed bulk to the solid surface and combine to form boron nitride. (The nitrogen is trapped in the alloy from the environment upon solidification). Evidence for this is found in the XPS (X-ray photoelectron spectroscopy) data of figure 16.

Examination of figure 16 reveals the presence of boron nitride in the spectra at high temperatures not seen in the lower temperature spectrum. The boron nitride can account for the marked reduction observed in friction coefficients above 500° C in figure 15. With other metallic glass compositions, different species segregate to the solid surface and influence friction behavior. For example, with some nickel-base metallic glasses containing phosphorus, the element phosphorus segregates to the surface and thereby brings about conditions of reduced friction.

The presence of alloy constituents can alter not only the tribological properties of a surface, but the oxides that form thereon as well. The chemistry and nature of the oxides on a conventional bearing steel can be completely dominated by alloying elements. An example of this is presented in the Auger data of figure 17 for 440C bearing steel. The Auger spectra of figure 17 were taken at two temperatures, 600° and 700° C. Marked differences in the surface oxides are reflected in these Auger spectra. At 600° C, the spectra contained oxygen and iron Auger peaks reflective of iron oxide being the oxide present on the alloy surface. At 700° C, however, the oxide on the surface was no longer iron oxide but chromium oxide. Thus, simply changing the temperature by 100 degrees C produced a complete change in the metallic oxide that covered the bearing surface. This indicates the importance of alloying elements in the control of surface films as well as surface properties.

Mechanical Effects

In the study of the tribological behavior of materials, cognizance of the mechanical parameters involved must be continuously maintained. The presence of relative motion between surfaces in contact and the imposition of loads on those surfaces impart energy to the surfaces that can be dissipated in a

26

variety of ways, many of which include changes in basic properties and structure. Increases in energy imparted by mechanical activity can cause in metals and alloys crystal transformations, order-disorder reactions, texturing, recrystallization, segregation, and strain.

The influence of mechanical effects can be demonstrated with the aid of simple erosion experiments on aluminum single-crystal surfaces having different surface orientations. The orientations of three aluminum single crystals and their weight losses in erosion experiments are presented in table II. The data of table II reveal very little difference in the erosive wear resistance of the three orientations of aluminum despite differences in atomic packing at the surface and a logical inference that differences in erosive wear behavior would accordingly be anticipated.

The absence of differences in erosive wear resistance for the three orientations of aluminum in table II can be explained by X-ray diffraction patterns of the three single-crystal surfaces. X-ray diffraction patterns for the (110) orientation are presented in figure 18 before and after erosion. Before erosion, Laue spots are readily apparent in the pattern. After erosion, however, ring structures are visible in the pattern, reflecting that surface recrystallization has taken place on the single-crystal surface. The patterns for all three orientations after erosion indicate that recrystallization has occurred. The recrystallization, therefore, presents essentially the same surface for the incoming eroding particles and, as a consequence thereof, the weight losses of table II are essentially the same for the three orientations.

Mechanical activity at the surface not only alters the properties of metals themselves, but also can influence interactive chemistry between environmental constituents and the solid surface. For example, straining metal under load can alter the chemical reactivity of the solid surface. This is demonstrated in the data of figure 19.

Figure 19 is a plot of the chlorine Auger peak intensity as a function of the exposure of iron to benzyl chloride, statically and during sliding contact. The data indicate a higher concentration of chlorine on the iron surface at each exposure level during sliding contact. Thus, the mechanical action of sliding promotes increased reactivity and a greater concentration of reactant on the solid surface.

CONCLUSIONS

A consideration of real solid surfaces involved in tribological systems indicates that attention must be paid to small concentrations of alloying elements in metals and alloys because the presence of these species can alter not only bulk behavior but surface behavior as well and, in certain instances, can completely dominate friction and wear properties.

A number of surface events such as reconstruction, segregation, chemisorption, and compound formation influence to a greater or lesser extent adhesion, friction, and wear. For example, minor nuances in the molecular composition of chemisorbed species can produce significant differences in adhesive behavior.

Such bulk properties as cohesive energy, d-valence bond character, lattice radius ratio for alloys, and the presence or absence of crystallinity have all been shown to be related to friction and wear performance. Some of these properties such as cohesive energy can be shown to relate to surface behavior via adhesion and friction results.

27

The imposition of mechanical effects such as load and relative motion between two solids in solid-state contact introduces mechanical energies to the interface that can alter behavior. For example, surface physical and metallurgical properties can change and influence wear behavior. Further, chemical interactions of environmental constituents with the surface can be altered by the mechanical activity.

REFERENCES

1. Langmuir, I.: The Constitution and Fundamental Properties of Solids and Liquids, Part I – Solids. J. Am. Chem. Soc., vol. 38, no. 11, Nov. 1916, pp. 2221-2295.
2. Lennard-Jones, J. E.: Processes of Adsorption and Diffusion on Solid Surfaces. Trans. Faraday Soc., vol. 28, 1932, pp. 333-359.
3. Taylor, H. S.: The Activation Energy of Adsorption Processes. J. Am. Chem. Soc., vol. 53, no. 2, Feb. 1931, pp. 578-597.
4. Roberts, J. K.: The Adsorption of Hydrogen on Tungsten. Proc. R. Soc., London, Ser. A, vol. 152, no. 876, Nov. 1935, pp. 445-477.
5. Oatley, C. W.: The Adsorption of Oxygen and Hydrogen on Platinum and the Removal of These Gases by Positive Ion Bombardment. Proc. Phys. Soc., London, vol. 51, pt. 2, Mar. 1939, pp. 318-328.
6. Auger, P.: The Compound Photoelectric Effect. J. Phys. Radium, vol. 6, 1925, pp. 205-208.
7. Davisson, C.; and Germer, L. H.: Diffraction of Electrons by a Crystal of Nickel. Phys. Rev., vol. 30, no. 6, Dec. 1927, pp. 705-740.
8. Muller, E. W.: Versuche zur Theorie dur Elektonenemission unter dur Einwirkung Hoher Feldstarken. Phys. Z., vol. 37, 1936, pp. 838-842.
9. Muller, E. W.: Das Feldionenmikroskop (The Field-ion Microscope). Z. Phys., vol. 131, 1951, pp. 136-142.
10. van der Merwe, J. H.: On the Stresses and Energies Associated with Inter-Crystalline Boundaries. Proc. Phys. Soc., London, vol. A63, pt. 6, June 1950, pp. 616-637.
11. Brainard, W. A.; and Buckley, D. H.: Preliminary Studies by Field Ion Microscopy of Adhesion of Platinum and Gold to Tungsten and Iridium. NASA TN D-6492, 1971.
12. Brainard, W. A.; and Buckley, D. H.: Adhesion of Polymers to Tungsten as Studied by Field Ion Microscopy. NASA TN D-6524, 1971.
13. Miyoshi, K.; and Buckley, D. H.: Changes in Surface Chemistry of Silicon Carbide (0001) Surface with Temperature and Their Effect on Friction. NASA TP-1756, 1980.
14. McLean, D. H.: Grain Boundaries in Metals. Clarendon Press, Oxford, 1957.
15. Buckley, D. H.: A LEED Study of the Adhesion of Gold to Copper and Copper Aluminum Alloys. NASA TN D-5351, 1969.
16. Ferrante, J.; and Buckley, D. H.: A Review of Surface Segregation, Adhesion, and Friction Studies Performed on Copper-Aluminum, Copper-Tin, and Iron Aluminum Alloy. ASLE Trans., vol. 15, no. 1, 1972, pp. 18-24.
17. Miyoshi, K.; and Buckley, D. H.: Friction and Surface Chemistry of Some Ferrous-Base Metallic Glasses. NASA TP-1991, 1982.
18. Hartweck, W.; and Grabke, H. J.: Effect of Adsorbed Atoms on the Adhesion of Iron Surfaces. Sur. Sci., vol. 89, 1979, pp. 174-181.
19. Mouttet, C.; Gaspard, J. P.; and Lambin, P.: Electronic Structure of the Si-Au Surface. Sur. Sci., vol. 111, 1981, pp. L755-L758.

20. Egert, B.; and Panzner, G.: Electron Spectroscopic Study of Phosphorous Segregated to α-Iron Surfaces. Sur. Sci., vol. 118, 1982, pp. 345-368.
21. Maugis, D.: Adherence of Solids. Microscopic Aspects of Adhesion and Lubrication, J. M. Georges, ed., Elsevier Scientific Publishing Co., Amsterdam, 1982, pp. 221-252.
22. Gschneidner, K. A., Jr.: Physical Properties and Interrelationships of Metallic and Semi-Metallic Elements. Solid State Physics, vol. 16, F. Seitz and D. Trumbull, eds., Academic Press, 1964, pp. 275-426.
23. Hutchings, I. M.: Prediction of the Resistance of Metals to Erosion by Solid Particles. Wear, vol. 35, 1975, pp. 371-374.
24. Vijh, A. K.: The Influence of Solid State Cohesion of Metals and Non-Metals on the Magnitude of Their Abrasive Wear Resistance. Wear, vol. 35, 1975, pp. 205-209.
25. Pauling, L. C.: The Nature of the Chemical Bond and the Structures of Molecules and Crystals, 3d ed., Cornell University Press, 1960.
26. Buckley, D. H.: The Metal to Metal Interface and Its Effect on Adhesion and Friction. J. Colloid Interface Sci., vol. 58, no. 1, Jan. 1977, pp. 36-53.
27. Miyoshi, K.; and Buckley, D. H.: Friction and Wear of Single-Crystal Manganese-Iron Ferrite. Wear, vol. 66, 1981, pp. 157-173.
28. Miyoshi, K.; and Buckley, D. H.: Surface Chemistry, Microstructure, and Friction Properties of Some Ferrous-Base Metallic Glasses at Temperatures to 750° C. NASA TP-2006, 1982.

TABLE I. - EFFECT OF VARIOUS HYDROCARBONS ON ADHESION OF CLEAN IRON

HYDROCARBON CHEMISORBED TO IRON	ADHESIVE FORCE*, DYNES
CLEAN Fe	>400
ETHANE C_2H_6	280
ETHYLENE $H_2C = CH_2$	170
ACETYLENE $HC \equiv CH$	80
VINYL CHLORIDE $H_2C = CHCl$	30
ETHYLENE OXIDE $H_2C \overset{O}{\diagup\!\diagdown} CH_2$	<10

*LOAD 20 DYNES, 10^{-10} TORR, 20^0 C, BOTH SURFACES (001) PLANES

CS-54407

TABLE II. - EROSION OF ALUMINUM SINGLE CRYSTALS

ORIENTATION	WEIGHT LOSS ON A 2-min EROSION TEST, g
(100)	0.0120
(110)	.0115
(111)	.0118

CS-82-1830
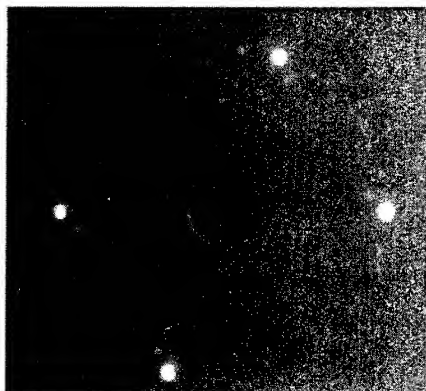
CARBON CONTAMINANTS

ARGON BOMBARDED
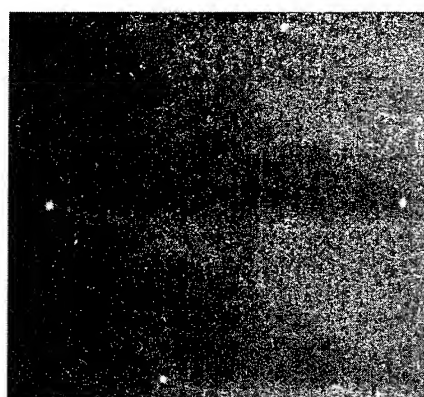
CLEAN SURFACE (110 V)   CS-78-1970

Figure 1. - LEED patterns of iron (011) surface.

30
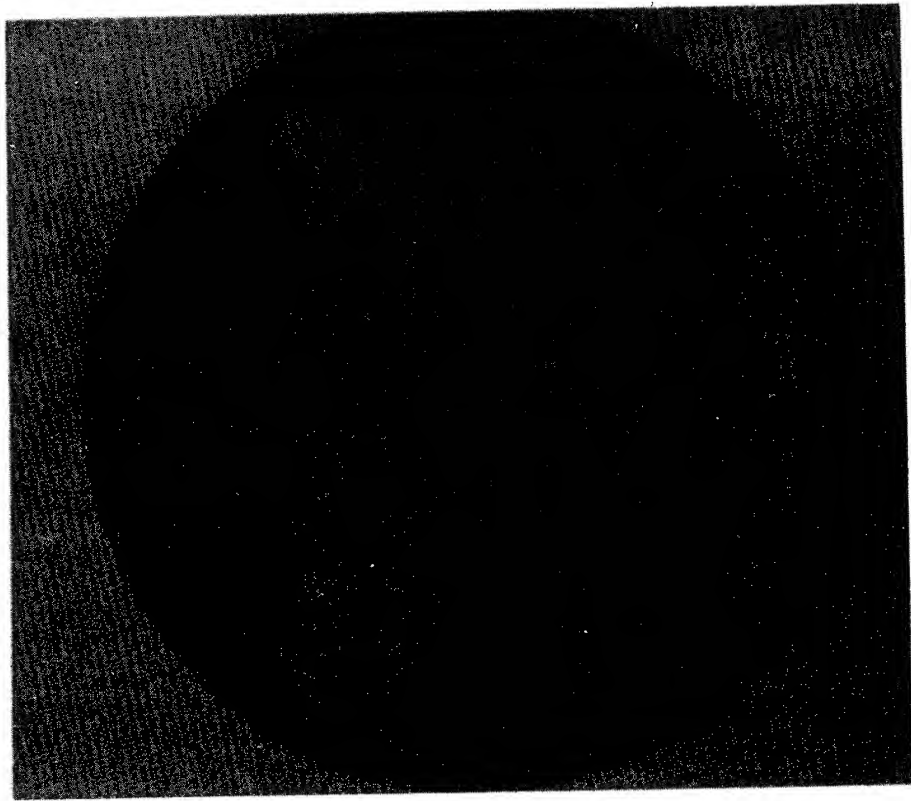
Figure 2. - Field ion micrograph of contaminated iridium surface, 1 hr after field evaporation at 78 K and 2×10^{-8} Pa.

RECONSTRUCTION SEGREGATION CHEMISORPTION COMPOUND FORMATION
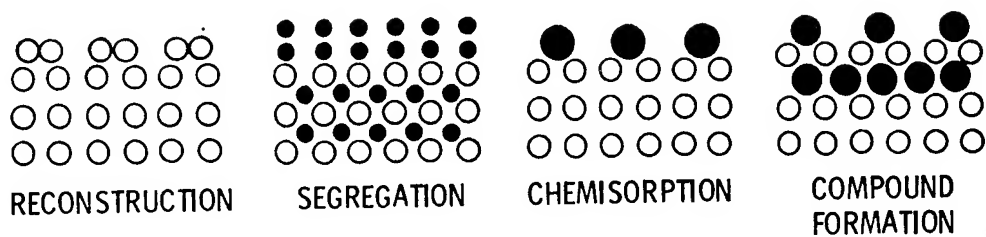
Figure 3. - Possible surface events.
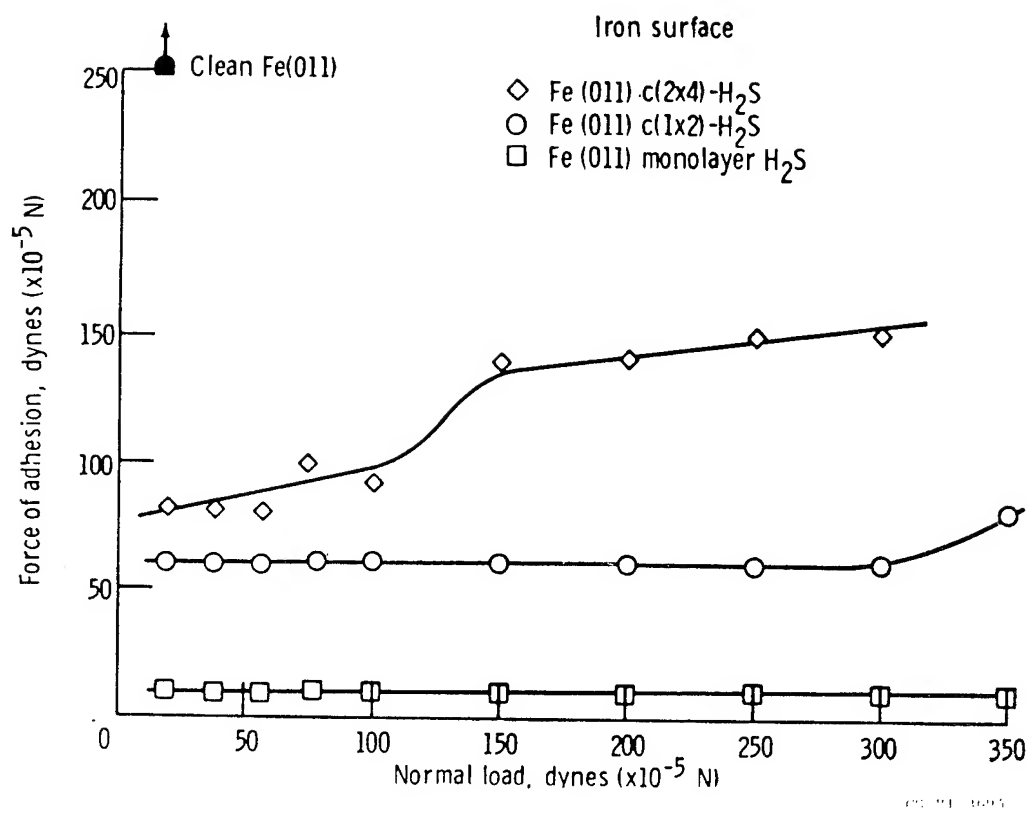
Figure 4. - Influence of hydrogen sulfide on adhesion of iron (011) surface.
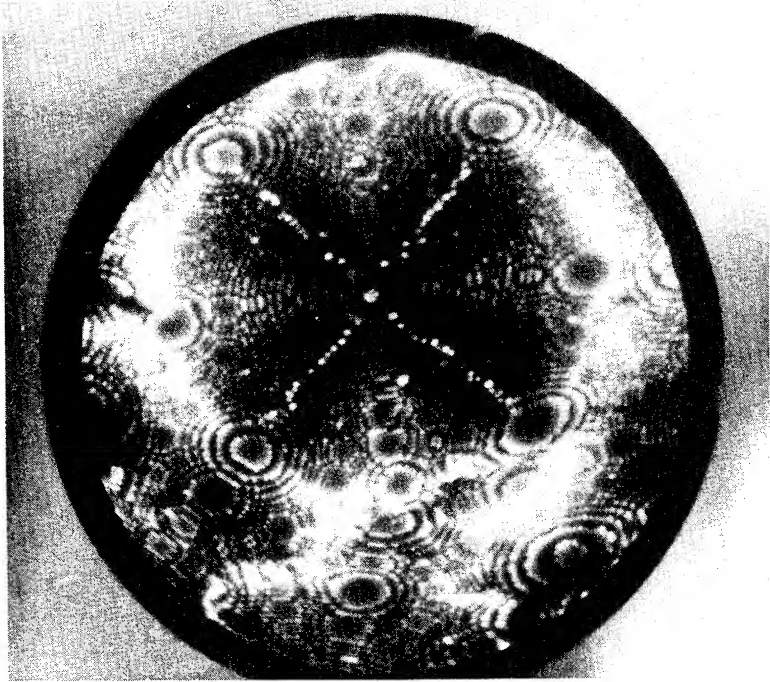
IRIDIUM PRIOR TO CONTACT
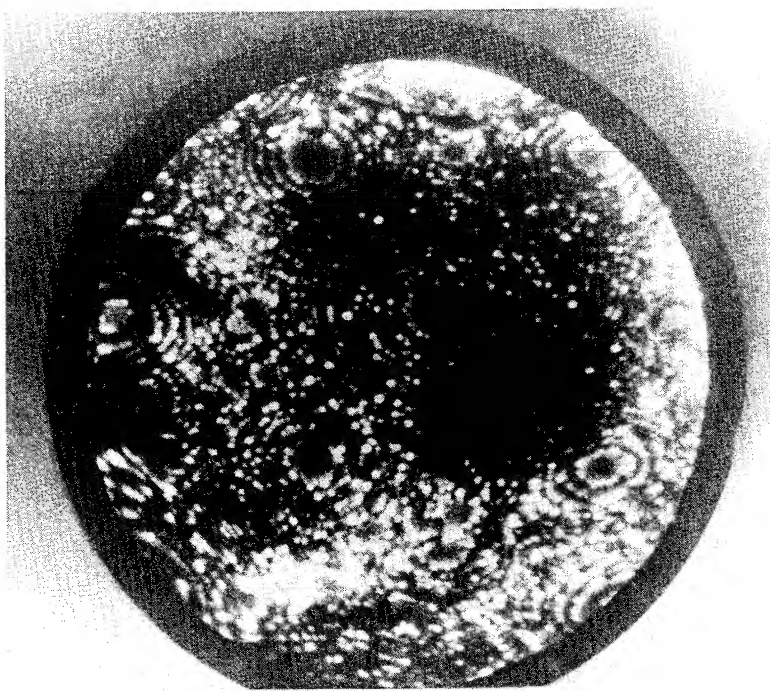
IRIDIUM AFTER PLATINUM CONTACT AT 19.0 kV   CS-██-███

IMAGE GAS, HELIUM; LIQUID-NITROGEN COOLING

Figure 5. - Field ion micrographs of iridium-platinum contact.

33
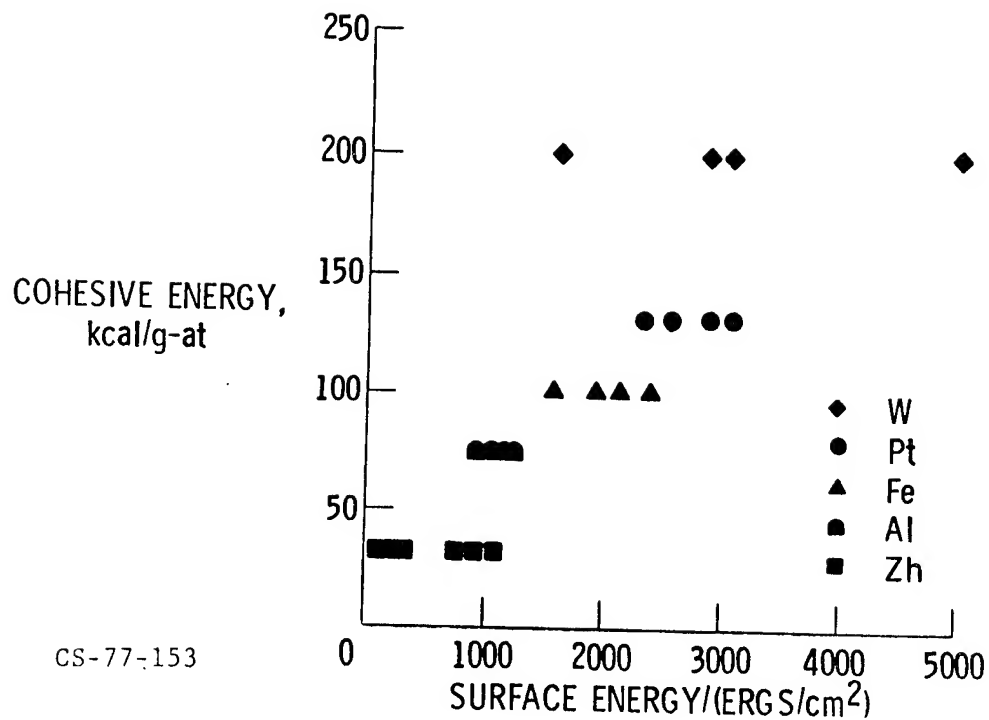
Figure 6. - Experimentally determined surface energies for some metals.

34

PHOTOMICROGRAPH

X-RAY MAP FOR GOLD   CS-79518

Figure 7. - Gold transferred to silicon (111) surface after adhesive contact. Load, 30 g; surface condition, sputter cleaned; temperature, 23° C; vacuum, 10^{-8} Pa.
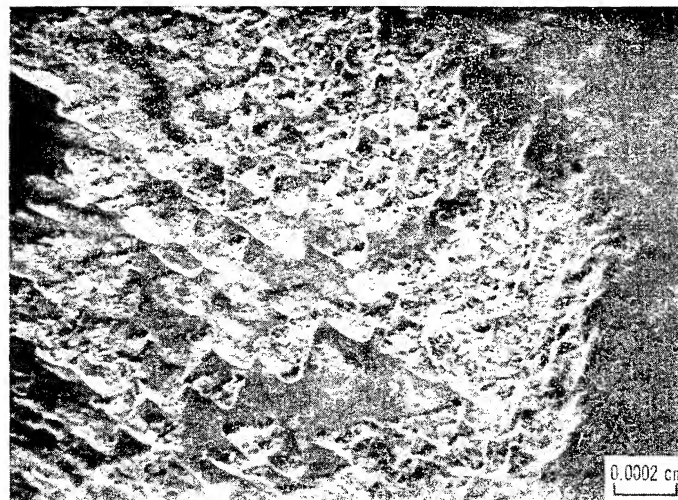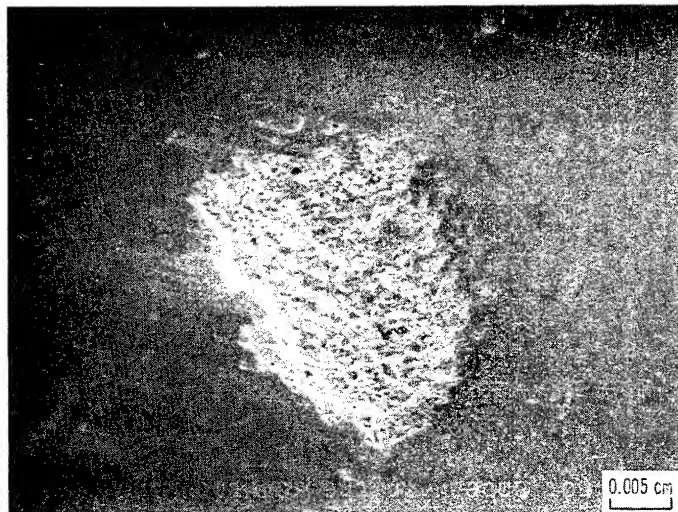
CS-78-708

Figure 8. - Adhesion of gold (111) surface to germanium (111) surface. Load, 30 g; temperature, 23° C; vacuum, 10^{-8} Pa. (Fracture occurred in germanium.)

36
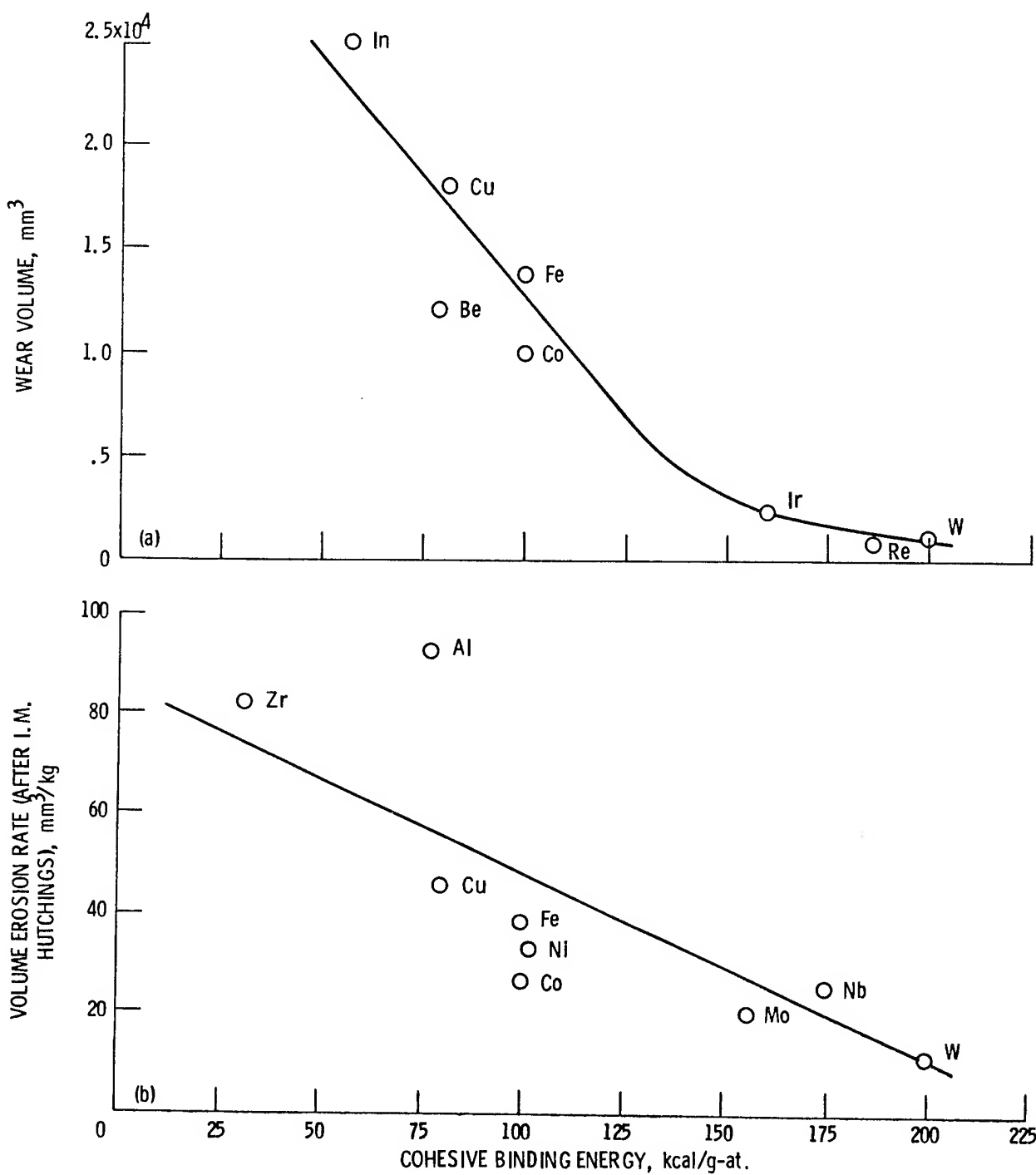
(a) Glass beads; impact time, 10 sec; impact pressure, 560 kPa; distance, 5 mm.

(b) Quartz sand; impact angle, 45°; impingement velocity, 82 m/sec.

Figure 9. - Erosive wear resistance as a function of cohesive binding energy of some elemental metals.

37
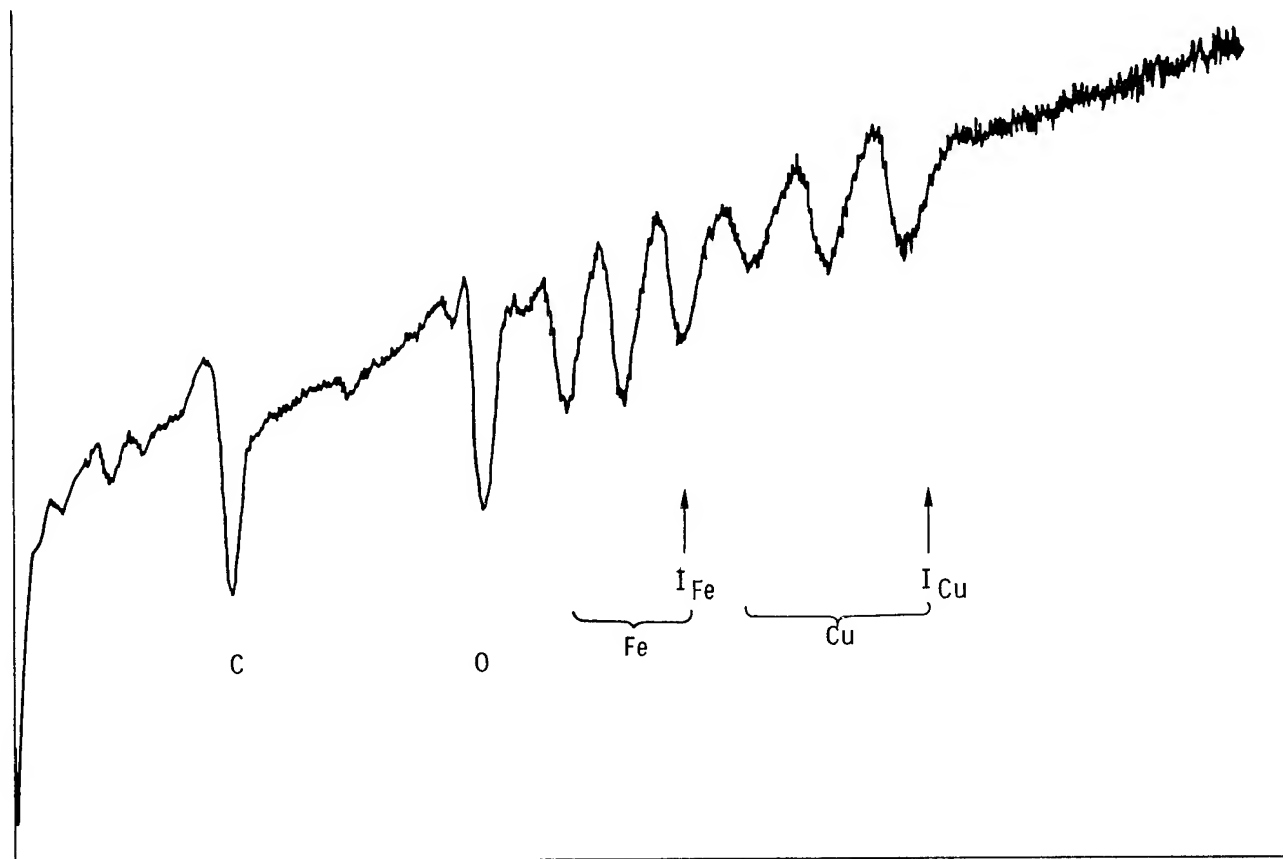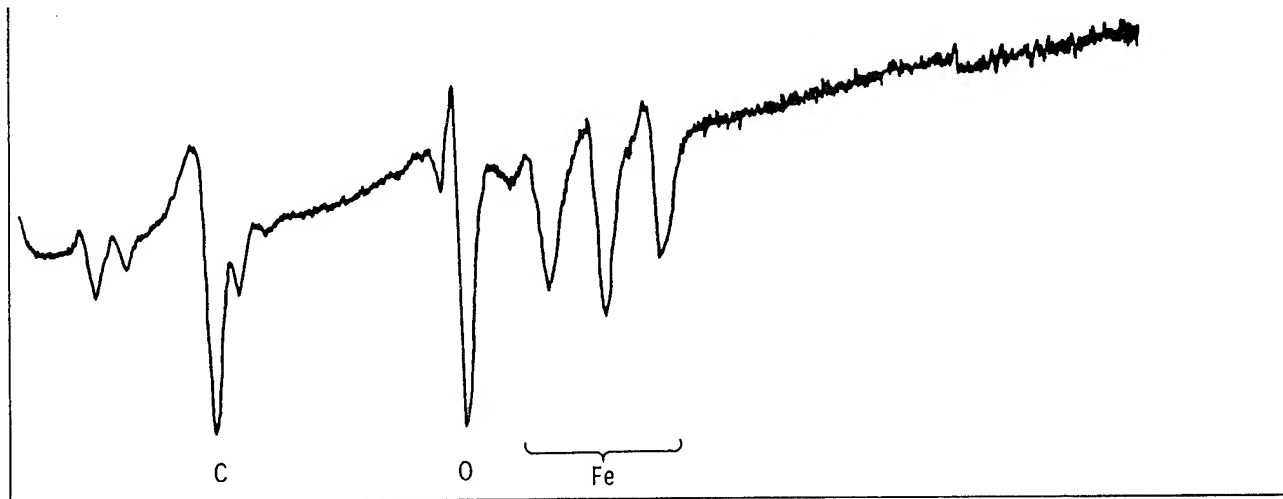
(a) Before friction experiment.

(b) After 250 passes of a Cu - 1 at. % Ni alloy over surface.

Figure 10. - Auger emission spectroscopy spectrum of AISI 52100 bearing steel surface. Sliding velocity, 60 mm/min; load, 100 g; specimen temperature, 25° C.
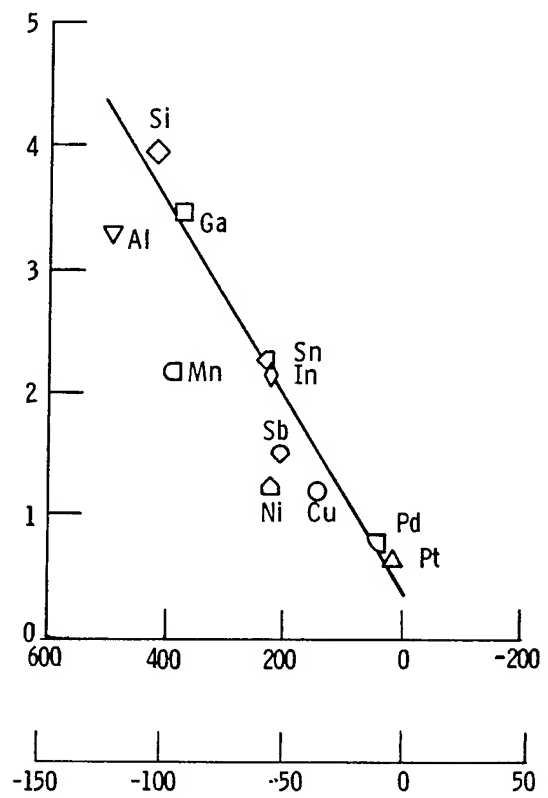
Figure 11. - Relative Auger peak intensities for binary copper alloys as a
function of free energy of formation of the oxides of the elements alloyed
with copper in a concentration of 1 at.%.

TITANIUM COPPER
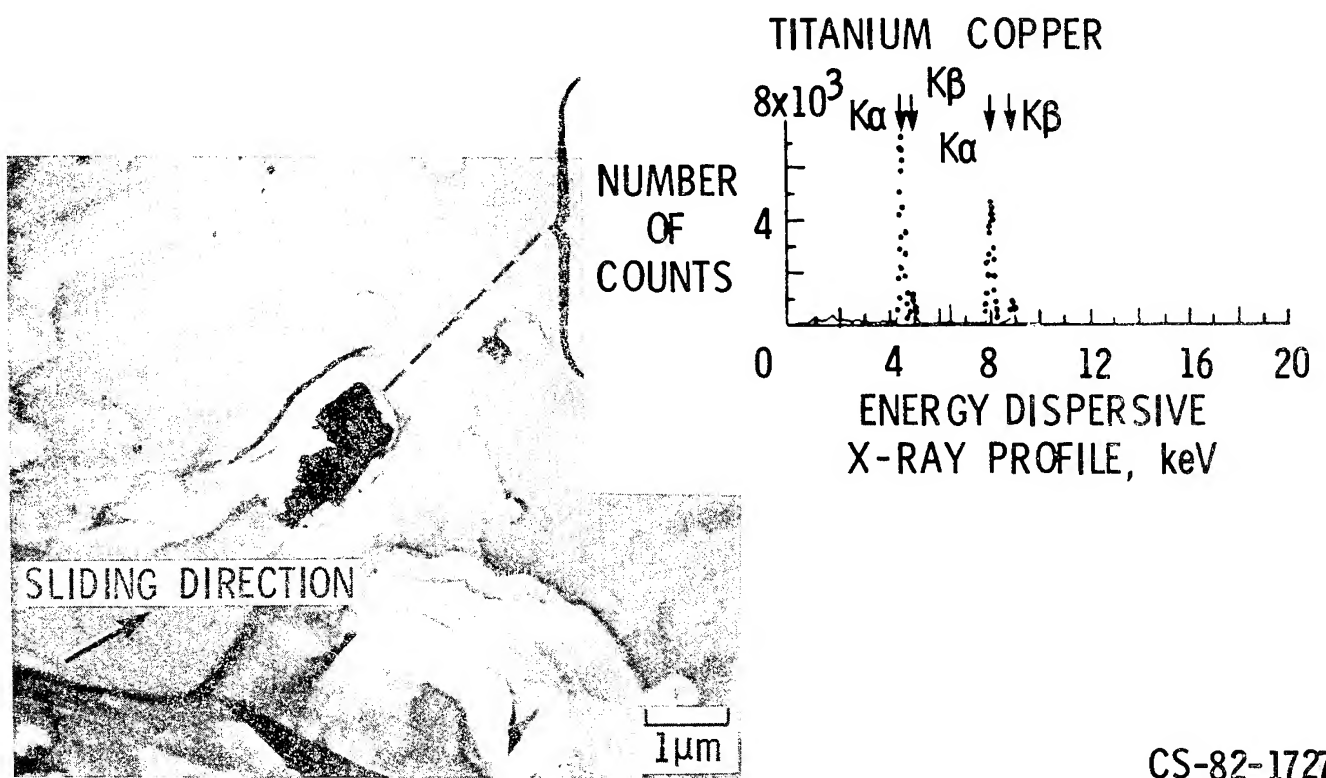
Figure 12. - Replication electron micrograph of wear track on diamond (111)
surface. Single pass of Ti rider; 110|; sliding velocity, 3 mm/min; load,
0.2 N; temperature, 23° C; vacuum, 10^{-8} Pa.
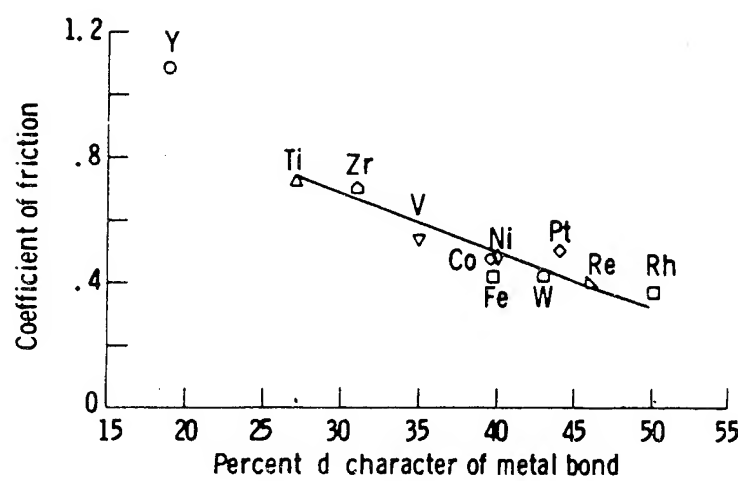
Figure 13. - Coefficient of friction for diamond (111) surface in sliding
contact with transition metals in vacuum, as a function of percentage of
d-valence bond character.
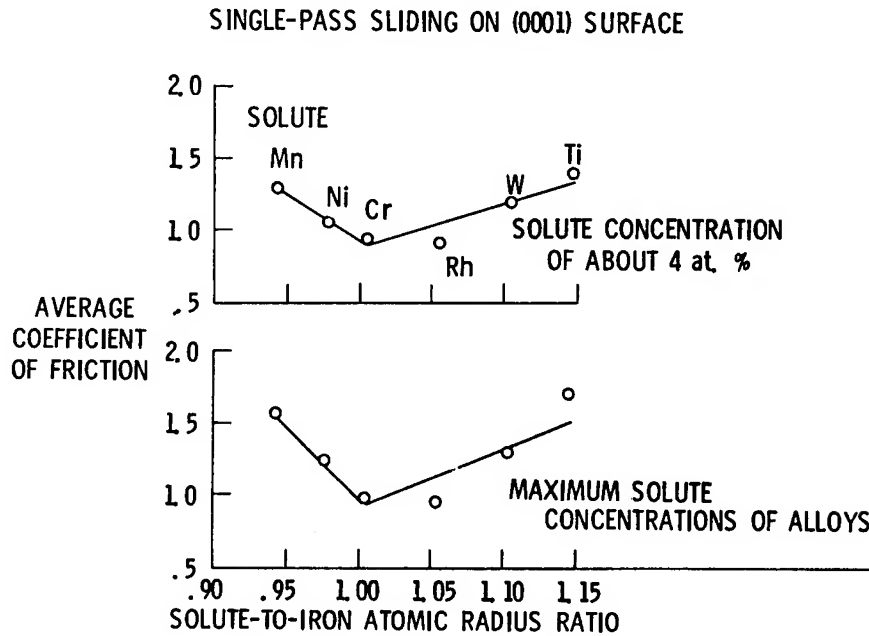
Figure 14. - Coefficient of friction for various iron-base binary alloys as a function of solute-to-iron atomic radius ration.
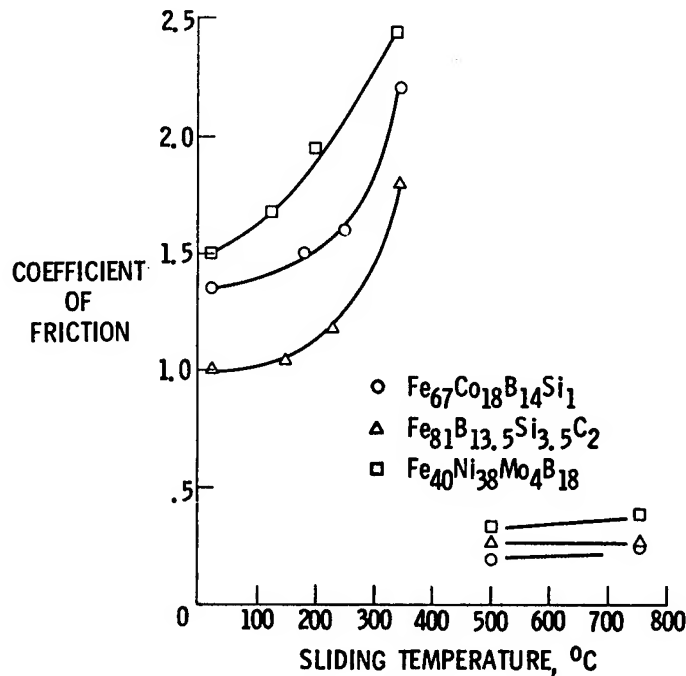
CS-82-1711

Figure 15. - Coefficient of friction for various metallic glasses as a function of sliding temperature.

41
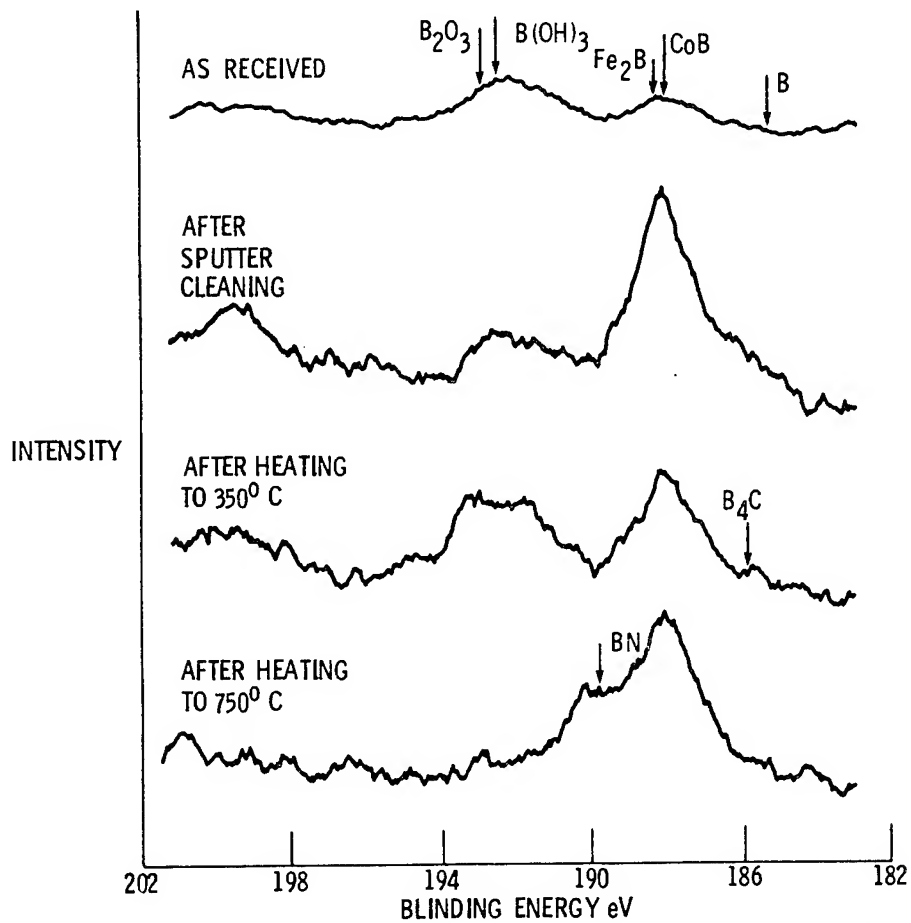
Figure 16. – B_{1s} XPS peaks on $Fe_{67}Co_{18}B_{14}Si_1$ surface.
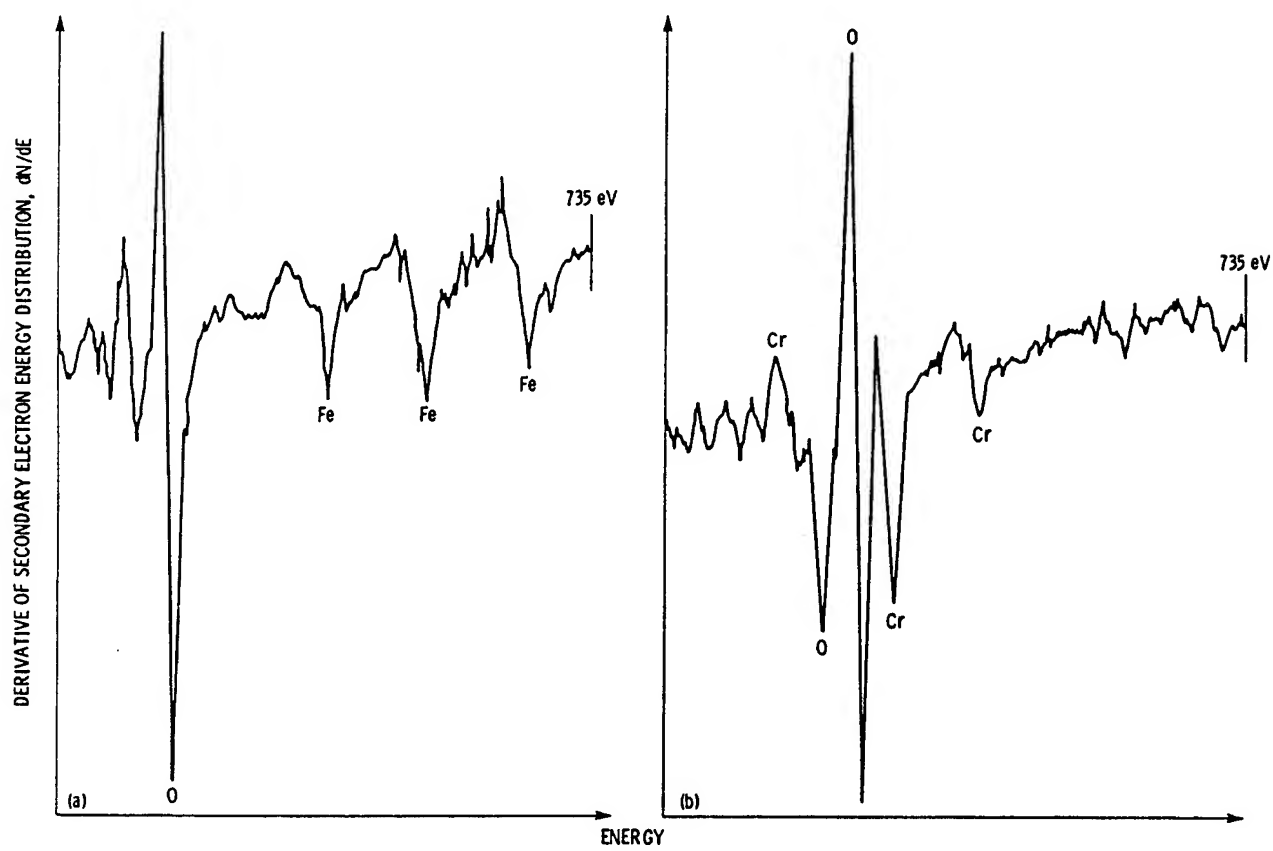
(a) For 60 min at 600° C.

(b) For 40 min at 700° C.

Figure 17. - AES spectra following heating in oxygen at 10^{-4} Pa.
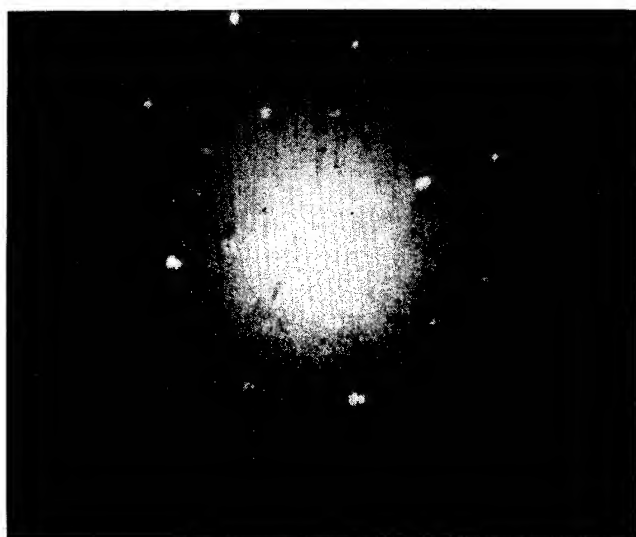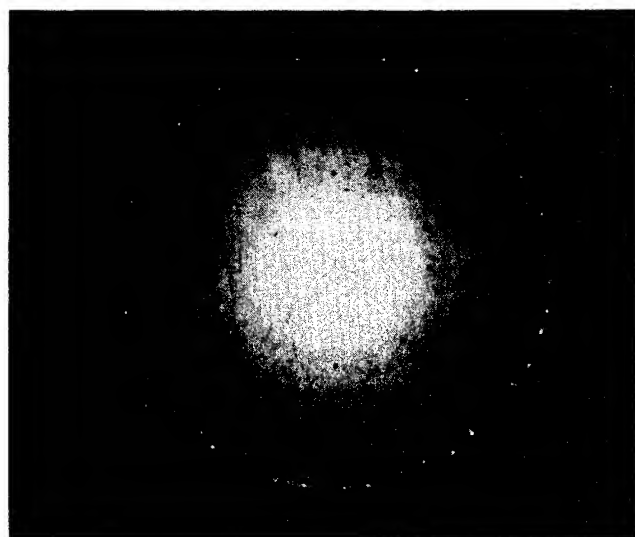
BEFORE EROSION   AFTER EROSION

Figure 18. - X-ray diffraction patterns obtained from aluminum (110) single crystal.

43
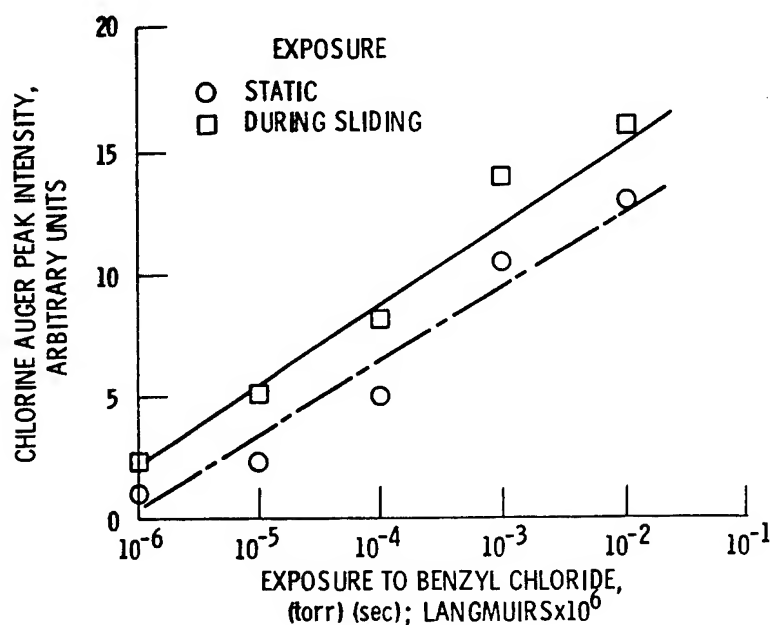
Figure 19. - Chlorine Auger peak intensity as a function of iron exposure to benzyl chloride, both static and during sliding. Sliding velocity, 30 cm/min; load, 100 g; temperature, 23° C.

NATURE OF THE SURFACE AND ITS EFFECT

ON SOLID-STATE INTERACTIONS

J. M. Georges
Laboratoire de Technologie des Surfaces - ERA 666
Ecole Centrale de Lyon
Ecully, France

An important aspect of the friction and wear of solids is the nature and the mechanical behavior of the surface films. A description of the mechanical, physical, and chemical behavior of surface films is achieved by an investigation of boundary lubrication. The purpose of this paper is to demonstrate two major points. First, the sliding of two solid surfaces under boundary lubricating conditions can create third bodies in the interface. Second, the nature and the evolution of the interface are dictated by the colloidal behavior of the products generated. To illustrate these two propositions, we present some recent work at our laboratory.

SLIDING GENERATES THIRD BODIES

Over the last 20 years, experimental techniques have been developed which allow delicate measurements to be made of the intimate contact between two solid bodies (ref. 1). In these studies two molecularly smooth surfaces of mica, or mica covered with a surfactant monolayer, can be brought together in a controlled manner with a normal load N. One of the main results is that it is possible to place statically in contact a monolayer against a monolayer so that the real contact area coincides with the apparent contact area of the two bodies, according to the Hardy models (ref. 2). The authors are able by these ways to measure attractive and repulsive forces (ref. 3).

If a tangential displacement d is gradually applied to the two contacting bodies, the contact is initially static and then it slides. Mindlin (ref. 4) demonstrates that the tangential force problem can be solved without modifying appreciably the normal pressure distribution of the Hertz theory. He found that the tangential stress rises to infinity at the edge of the contact region, which is physically impossible. Therefore, Mindlin made the assumption that slip will occur wherever the tangential stress is greater than the product of the normal pressure p and the coefficient of friction f. For a circular contact area of radius a, the tangential stress in absence of slip is axisymmetric so that slip may be expected to occur on an outer annulus (radius r, c < r < a). The radius of the inner region of nonslip decreases when the tangential force T is increased. It was found that $c = a(1 - T/fN)^{1/3}$. When T = fN, c = 0 and the gross slip occurs between the two bodies.

Far from the contacting surfaces where slip occurs on an annulus, the tangential relative displacement d of the two elastic bodies is a nonlinear function of the tangential force involving a purely elastic component and a nonelastic slip component. When two bodies have the same elastic properties, Mindlin found that

$$d = \frac{3fN(1 - v)}{8Ga} [1 - (1 - T/fN)^{2/3}]$$

where G is the elastic shear modulus of one body and ν the Poisson ratio.
The gross slip is for

$$d^* = \frac{3fN(1 - \nu)}{8Ga}$$

Numerical application is useful. If we assume the Hertzian contact of a
highly polished steel ball (radius of curvature, 60 μm) against a steel flat
with a load of 10 N, the Hertzian contact area diameter is 2a = 140 μm. If we
further assume that the static friction coefficient is f = 0.1, we find that
a tangential displacement of d* = 0.1 μm is enough to create gross slip. We
then observe for this case d*/a = 0.0014, which is a very small value.

As shown recently, these relations take into account the presence of a
thin film in the interface. When the film behaves as a solid, it is possible
to show that the slope T/d at the origin is a function of the thickness and
the shear modulus of the film (ref. 5). By measuring the tangential force at
the beginning of gross slip, some authors (refs. 6 and 23) have determined the
mean tangential stress of the surface film.

The major problem is to determine the relative displacement d without
surface deterioration. The study of the durability of the boundary films has
been fully developed in the literature. Recently, Martin and Mansot have
addressed this problem (refs. 7 and 8).

A sphere/plane combination is used with a very smooth AISI 52100 steel
substrate. The total equivalent rugosity measured with a talystep is found
equal to 10 nm. Before contact is made, a thin organic film is deposited on
both surfaces through adsorption of an amphiphilic complex ester in a dodecane
solution. An incomplete monolayer adsorbed on the surface is in equilibrium
with the presence of ester micelles in the solution (ref. 7 and fig. 2).
Evolution of the tangential force and the electrical contact resistance ECR
are recorded (fig. 3) for unidirectional sliding of a few Hertzian diameters
distance d at a slow velocity (50 μm/s). Three zones are distinguishable.
The ECR value in the zone I (static contact) is not easily reproduced. Its
relative high value (> 1 Ω) indicates the presence of a material within the
interface (the sole calculated constriction resistance is equal to 0.01 Ω).
The transitional state II corresponds to the behavior before gross slip. ECR
changes in this period have not been detected with our equipment, but ECR
increases have already been detected (ref. 9). Undoubtedly there are very
small ECR variations during the transitional state.

The dynamic state III can be estimated. Under our conditions, the whole
contact area is sliding after a displacement of about 0.1 μm. A sudden and
large increase of ECR (3 decades) is observed as soon as gross slip occurs.
This drop is so instantaneous that it is impossible to predict if it corre-
sponds to the transitional or dynamic state. After this drop, the ECR signal
relaxes to a nearly stable value in the same way the friction force T does,
and a good correlation is observed between the two evolutions.

The significance of ECR changes during the dynamic state has been ana-
lyzed (ref. 10). The electrical transport phenomena, in the sliding inter-
face, have been attributed to tunneling conduction, suggesting a possible
quantitative approach to the interface thickness change that actually takes
place when sliding occurs (ref. 10).

We can show that the first Hertzian diameter sliding distance corre-
sponds to the basic shearing mechanism of the two contacting adsorbed layers.

Careful examination of the surface after the friction experiments, using electron microscopy (TEM) with the direct replica technique, showed no evidence of damage to the steel surfaces. It seems reasonable to assume, therefore, that the frictional force depends on the shear strength of the lubricant bifilm present in the interface.

An examination after 2 or 3 Hertzian diameters reveals the presence of some agglomerations of matter in the interface. The extent of these agglomerations is so small in comparison with the Hertzian dimension that its effects on the friction force are not detectible. These agglomerations are the beginning of the third body coalescence (refs. 11 to 13). The visualization is very effective when the case of a contact with a solid monolayer film interface of stearic acid deposited on an oxide surface is investigated (ref. 11).

The main results, shown in figure 4, are as follows. The area of experimental static contact corresponded to that calculated using Hertz formulae; the pressure (15×10^7 Pa) was similar to that obtained by Bailey and Courtney-Pratt (ref. 6). For a displacement $d = 10$ μm (fig. 4a) the bilayer broke up and sliding occurred within a "mush" in the contact region. Some piled-up material appeared at the front of the slider (a in fig. 4a) forming a protruding lip around the contact region (b in fig. 4a). During frictional contact the piled-up material increased in volume (a and b in fig. 4b), although the distance covered was very small (four Hertzian diameters, about 200 μm). Material was removed at a' (fig. 4b) and a very small amount of material scratched the slider-plane interface (c in fig. 4b); and the thickness of the interface increased slightly. The small amount of very flat material coming from the inlet face which formed in the interface (a in fig. 4b) is designated as a lump. For greater sliding distances (40 Hertzian diameters, about 2000 μm) the phenomenon increased without changing its nature (fig. 4c). In particular, scratching developed at e and an accumulation of piled-up material was seen (fig. 4c). The number of lumps was generally small, and the piled-up material produced in the scratches lifted the slider. At the same time, the friction coefficient quickly increased and fluctuated ($f \simeq 0.3 \pm 0.1$).

A lump has a circular appearance (with a diameter of about 2.5 μm and a thickness of less than 50 nm) and is composed essentially of CoO particles linked by fatty acids and water. Numerous observations have shown that the lumps behaved plastically. The question then arises as to whether this piled-up material can scratch a solid surface. Electron microscope observations of carbon replicas (fig. 5) indicate the formation of such initial scratch (e in fig. 4b). The scratch produced by the lump takes the form of a thin deposit of crushed material. From the observations it was not possible to determine precisely the true profile of the scratch, which in this particular case had a groove form. Cracks were observed in the glass which were very similar to the fractures occurring when a rigid indentor slides over a brittle surface (ref. 14). The form of these cracks is determined by the indentor (lump) geometry and its associated stress fields.

If all the approximations necessary to apply this model to a fracture mechanics analysis of the observed cracks are considered, the load supported by the lumps is of the order of 0.01 to 0.05 N, which corresponds to a very high average pressure of 2×10^9 Pa.

Sliding is also responsible for the third body generated in the mixed lubrication regime. Mixed lubrication is considered to be an intermediary regime between boundary and elastohydrodynamic lubrication (EHL). When the

pure EHL regime is studied, no solid film or agglomeration of products is formed on the surfaces. But in the mixed regime, the chemical decomposition of the additive contributes to a continuous film formation in both sliding and rolling situations (ref. 15). Figure 6 shows microscopic aspects of surfaces after experiments with similar conditions (time, lubricant, rolling speed U, load, temperature) except for the sliding speed ΔU. With pure rolling, reaction films do not form. However, as soon as the slide/roll ratio reaches 2.5, different types of films appear.

COLLOIDAL EVOLUTION OF THE INTERFACE

General Principles

Prior to motion and friction, the environment reacts with the surfaces. For instance, the additives or lubricant base are adsorbed or they react with the metallic surfaces to create new condensed products. We have similar phenomena with oxygen and oxides films (ref. 27). The nature of friction interface layers depends on environmental conditions. Its thickness is generally small (molecular scale). Because of its patchy nature, the chemical and structural determination of its composition is difficult even with modern analytical tools (ESCA, AUGER, SIMS...). The components of the metallic surface are essentially hydrated oxides and adsorbed lubricant, depending on machining and cleaning procedures used. These products are the basic materials that produce the colloidal paste during friction. We assume that in the favorable areas of the friction interface these products mix to generate a paste. The shape of the interface under boundary lubrication can be considered as a convergent inlet. Surface products are first picked up and mixed in the convergent inlet, and then, during their transit in the interface, they form a colloidal medium. This paste, depending on its rheological behavior, is considered the entity primarily responsible for the formation of individual wear scratches. Under specific conditions, such as very high local pressures, contact supertemperatures, presence of dissolved oxygen, water, etc., this paste may be chemically transformed during friction, as is demonstrated by the electrical contact resistance study, to produce adherent films (table I and refs. 16 and 17).

When friction begins, wear is mainly abrasive. Material loss is correlated with the scratches parallel to the direction of sliding. The scratch origin seems to be related to the lumps adhering to a solid body. These lumps behave very similarly to the built-up edge in cutting processes.

In these analyses, scaling factors have to be kept in mind. Wear measurements assume that wear is uniform in the contact area and the wear corresponds to that of region I of table II. Wear loss is essentially due to the oxide and chemical layers which cover the surfaces. The scale in this case corresponds to III on table II. Between the two domains I and III we have accumulations of matter (lumps) and scratches (II). In this sense we have abrasive behavior. But, the main cause of material removal is perhaps adhesive.

48

The studies of the antiwear properties of the lubricant additives are very useful for knowledge of the interface behavior. We consider here the case of pure ethyl 2 hexyl zinc dithiophosphate in solution in n-dodecane. The friction materials are cast iron (flat) and AISI 52100 steel (sphere).

Many authors have studied the chemical decomposition of additives with temperature in the presence of solid surfaces. The mechanisms are not yet understood, but when the temperature is near 190° C, the additive degradation leads to several products (table III and refs. 18 to 20). When the temperature is below 40° C, the additive is adsorbed physically on the iron. For temperatures higher than 60° C, a chemical reaction occurred with iron. This reaction is complex and corresponds to a loss of zinc (ref. 21). The thickness of the reaction layer is very small (50 nm) (ref. 22).

Electrical contact resistance (ECR) measurements are very sensitive to interface material change during friction (ref. 23). Figure 7 shows the evolution of ECR values versus time with a plane on plane tribometer under boundary conditions (low speed). This evolution is characterized by the formation of an interface film which consists of a dielectric substance that is (very often) strongly adherent to worn metallic surfaces. The ECR value at the beginning of the test is low (< 0.1 Ω) (stage I), and the character of the worn surface is very similar to that observed in tests with pure n-dodecane. Then in stage II, the ECR is found to increase exponentially, and optical microscopic observations show that the increase is related to the appearance of a brown film and subsequently to the formation of a blue film. Stage III corresponds to the development of the blue film. Stage I corresponds to the abrasive wear of an interface (high wear rate), and stage II corresponds to the corrosive wear (low wear rate) (ref. 24).

Wear particles created during stage I (fig. 7) are aggregates (fig. 8), which are very similar to gel particles. We found spherical particles (diameter, 15 nm) of iron oxide. The composition of the gel is rich in phosphorus, sulfur, zinc, and carbon generated by the zinc DTP (ref. 20).

When stage III is reached, the surface is covered by a tribochemical reaction film (ref. 24). Observations of parts of this solid film were made by TEM (fig. 9). X-ray analyses have shown that these parts are homogeneous (iron and zinc phosphate or polyphosphate). The product is found to be amorphous and an insulator; it looks like a glassy material. Similar results were obtained recently with different antiwear additives (ref. 25).

We can assume that in the high pressure conditions of the contact interface the colloidal substances created by the sliding conditions are agglomerated and pressed together to create a glassy material.

Recently, Desportes and Martin (ref. 20) used the nuclear magnetic resonance 31 phosphorus technique to analyze degradation products formed during a wear test. The solution of ZDTP in pure dodecane (called a reference solution) was tested in friction and stage III (fig. 7) was reached. Table IV gives the nature of the different degradation products detected and the corresponding phosphorus concentrations. Spectrum of reference solution reveals the presence of many products probably due to the ZDTP synthesis. Then it seems that no new product is formed during friction; this point has been confirmed by infrared and chromatographic analyses (ref. 20).

These results are important for many reasons. First, during wear tests, degradation products do not appear in the solution and ZDTP disappears.

Second, products like SP(SR)(OR)$_2$, SP(SR)$_2$OR, and SP(SR)$_3$ are formed in great quantity during thermal degradation (Coy (ref. 26), Watkins (ref. 19), and table III). In this investigation in the friction test these products are not formed. We can assume that thermal effect is not the only process occurring in tribochemical reactions. Third, the presence of basic ZDTP is not clear. According to these results, this product is generated by the friction test. But it is also possible that basic ZDTP has been present in the reference solution, but not detected, because of the exchange with acid traces due to the presence of dithiophosphoric acid, which would be destroyed during friction.

Tribochemical films created during friction are not just a consequence of reactions between environment and surfaces. They imply the mechanical behavior effects at the interface when colloidal products are sheared.

Role of Contact Pressure

Kapsa (ref. 24) studied the effects of the apparent contact pressure on the formation of tribochemical films using the plane on plane tribometer with the same material and lubricant (dodecane + ZDTP) already described (fig. 7). The apparent contact area is 10 mm^2, and different loads (between 50 and 3000 N) are investigated. Figure 10 shows the different evolutions of the ECR as a function of the apparent contact pressure. Stages I, II, and III are detectable and are similar to those shown in figure 7. Stage III, corresponding to the presence of tribochemical film, is always present in the pressure range of 30 to 235 MPa. The ECR value, at this stage, does not depend on the pressure. Islands of blue films cover the metallic surfaces. The percent of apparent surface covered is independent of the pressure (25 to 30 percent). The size of the islands (diameter, 3 to 6 μm), the chemical nature of films, and the thickness of the interface are also independent of the pressure.

But the pressure effect regulates the induction period. If the pressure is too low, tribochemical film is not formed because the abrasive products in the interface are not sufficiently sheared. If the pressure is too high, seizure occurs before the protective tribochemical film is formed.

An interesting observation according to Kapsa (ref. 24) is presented in figure 11. Tribochemical films are formed at a given pressure (80 MPa). Then the pressure is increased in steps, gradually. The ECR evolution shows that for a first range of pressure (80 to 150 MPa) no effect is observable. Then, after every pressure increase, the ECR value decreases suddenly and then increases to reach the stationary value (pressure range, 150 to 235 MPa).

After a pressure of 235 MPa, the ECR limit decreases with pressure. We conclude that a tribochemical film protects the surface against seizure. If no film is created the seizure pressure is 234 MPa (fig. 11). After film formation, the pressure is higher (340 MPa). These experiments show that for a broad range of apparent contact pressure the nature of the phenomena is the same and the local behavior of the film is the predominantly important phenomenon.

CONCLUSIONS

The nature of a surface plays a very important part in tribology. The effects like adsorption, chemical reaction between environment and the solids, are the starting point of complex phenomena. Mechanical effects created by the two bodies in contact are responsible for the interfacial body formation. We emphasize that the colloidal nature of products is created by friction. The high pressures can compact these particles and create a glassy material.

REFERENCES

1. Tabor D.; and Winterton, R. H. S.: Proc. Roy. Soc. A3/2, (1969), 435-450.
2. Hardy, W. B.: Phil. Trans. Roy. Soc. A 230 1 (1931).
3. Israelachvili, J. N.; and Adams, G. E.: Nature, 262, (1976), 774-776.
4. Mindlin, R. D.: Trans. ASME, Int. App. Mech. 16, (1949), 259-268.
5. Tonck, A.; Sabot, J.; and Georges J. M.: Microdisplacements Between Two Elastic Bodies Separated by a Thin Film of Polystyrene, to be proposed to ASME-ASLE Lubrication Conference 1983.
6. Bailey, A. I.; and Courtney-Pratt, J. S.: Proc. Roy. Soc., London A 291, (1955), 500-515.
7. Mansot, J. L.; Candau, S. J.; and Martin, J. M.: Amphiphilic Complex Esters as Lubricant Additives – Part I – Molecular Structure of Paraffinic Solution, to be published in Colloids and Surfaces.
8. Mansot, J. L.; and Martin, J. M.: Amphiphilic Complex Esters as Lubricant Additives – Part II – Role of Ester Molecules in Modifying Friction, proposed to Colloid and Surfaces.
9. Courtney-Pratt, J. S.; and Eisner, E.: Proc. Roy. Soc., London, A 238, (1956), 529-549.
10. Mansot, J. L.: Aspects Microscopiques de l'Action des Réducteurs de Frottement en Lubrification Limite, Thèse de Docteur Ingénieur, 82-02, Ecole Centrale, Lyon, (1982).
11. Georges, J. M.; and Mathia, T.: J. Mech. Appl., 2, 2, (1978), 16-265.
12. Godet, M.; Play, D.; Berthe, D.: J. of Lub. Tech., 102, 2, (1980), 153-163.
13. Israelachvili, J.; and Tabor, D.: Wear, 24, (1973), 386-390.
14. Swain, M. W.; and Hagan, J. T.: J. Phys. D. 9, (1976), 2207.
15. Georges, J. M.; Tonck, A.; Meille, G.; and Belin, M.: ASLE Preprint 82 LC 4C 3, (1982).
16. Georges, J. M.: Colloidal Behavior of Films in Boundary Lubrication in Microscopic Aspects of Adhesion and Lubrication, Elsevier, (1982), 729-761.
17. Georges, J. M.; et al.: Wear, 53, (1979), 9-34.
18. Rounds, F.: ASLE Trans. 21, 2, (1978), 91-101.
19. Watkins, R. C.: Tribology Int., (1982), 13-15.
20. Desportes, J. L.: Etude de la Réaction Tribochimique du DTPZn, Thèse 3ème Cycle, Université Claude Bernard, Lyon, 1203, (1982).
21. Dacre, B.; and Bovington, C. H.: ASLE Preprint 81 LC 6A 5.
22. Tonck, A.; et al.: Tribology Int., (1979), 209-213.
23. Allen, A. E. M.; and Drauglis, E.: Wear 14, 5, (1969).
24. Kapsa, Ph.: "Etude Microscopique et Macroscopique de l'Usure en Régime de Lubrification Limite, Thèse de Doctorat d'Etat, Université Claude Bernard, Lyon, 8219, (1982).

25. Basset, D.; Hermant, M.; and Martin, J. M.: Oil Soluble Fluorinatez Compound as Antiwear Additives in Lubricant, proposed to ASME ASLE Lubrication Conference, 1983.
26. Coy, R. C.; and Jones, R. B.: ASLE Preprint 79 LC 6A 5.
27. Quinn, T. F. J.: The Role of Oxide Films in Microscopic Aspects of Adhesion and Lubrication, Elsevier, 1982, 579-594.

TABLE I

SCALE

1nm   10nm   100nm   1000nm   10000nm

APPARENT CONTACT AREA

FILM THICKNESS

MOLECULE OXIDE

SCRATCHES PARTICLE AGGLOMERATION

WEAR MEASUREMENTS

ABRASION EFFECTS

ADHESION EFFECTS

$$\begin{bmatrix} III \end{bmatrix} \qquad \begin{bmatrix} II \end{bmatrix} \qquad \begin{bmatrix} I \end{bmatrix}$$

TABLE II

THERMAL DECOMPOSITION OF ZDTP

Volatile	Oil soluble	Oil insoluble
H_2S	RS − SR	Zn polyphosphate
Olefin	RSR	
	RSH	
	$SP(SP)(OR_2)$	
	$SP(SR)_2(OR)$	
	$SP(SR)_3$	

TABLE III - According to Coy |26|, Watkins |19|

54

PRODUCTS	CHEMICAL SHIFT (in ppm)	REFERENCE SOLUTION %	SOLUTION AFTER WEAR PROCEDURE %
Basic DTPZn	103,2		6.7
DTPZn	98.2	87.1	80.5
	85.7	1.0	4.4
$((RO)_2 P(S) S)_2$	83.5	2.5	2.4
$(RO)_2 P(S) S(S) P(OR)_2$	79	2.1	2.1
$(RO)_2 P(S) OR$	69	0.5	0.5
$(RO)_2 P(S) H$	63	3.6	0.6
$(RO) P(S) O Zn$	46-48	3.1	2.9

TABLE IV - NMR 31P ANALYSIS OF LUBRICANT SOLUTIONS
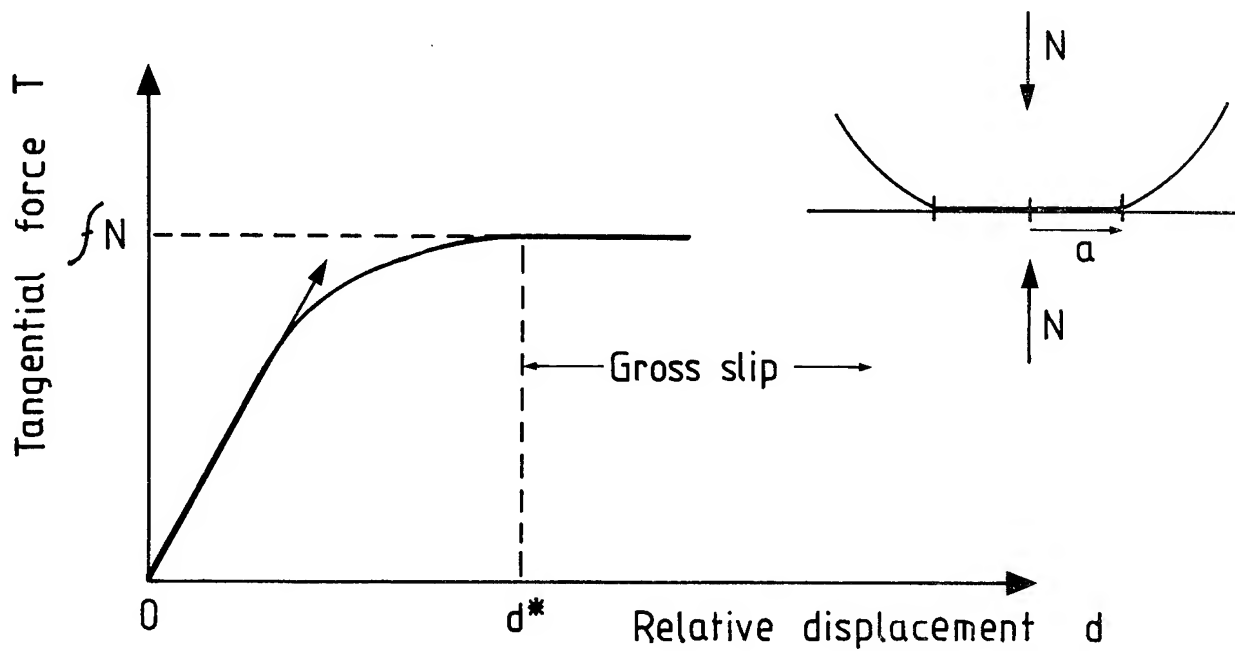
Figure 1 : Tangential force T versus relative displacement d
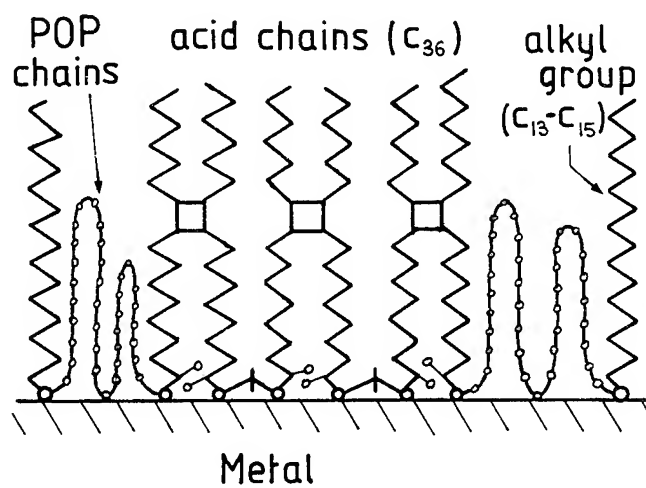
Figure 2 : Amphiphilic complex esters as lubricant additive adsorbed on the steel surface.
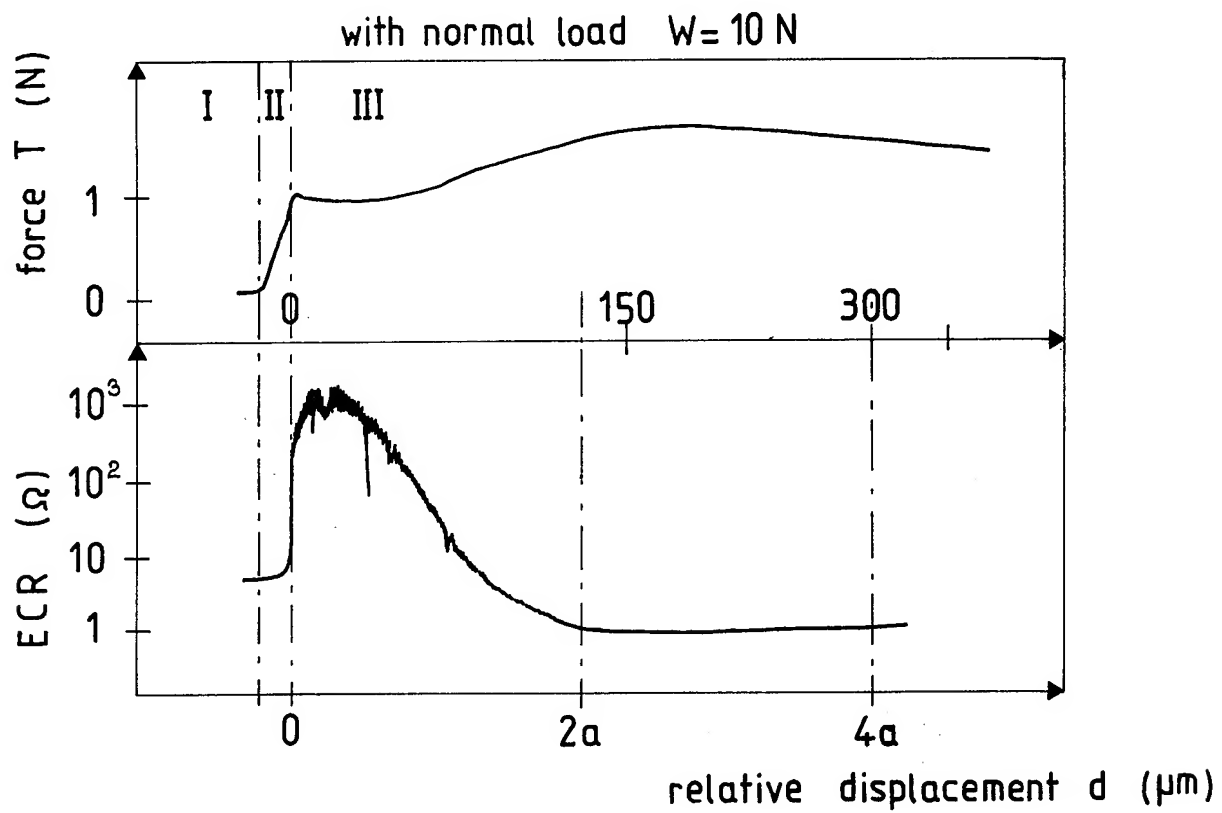
figure 3 : Pin on flat friction test
          Steel surfaces lubricated with a complex ester (figure 2)
          Temperature 20°C |8|
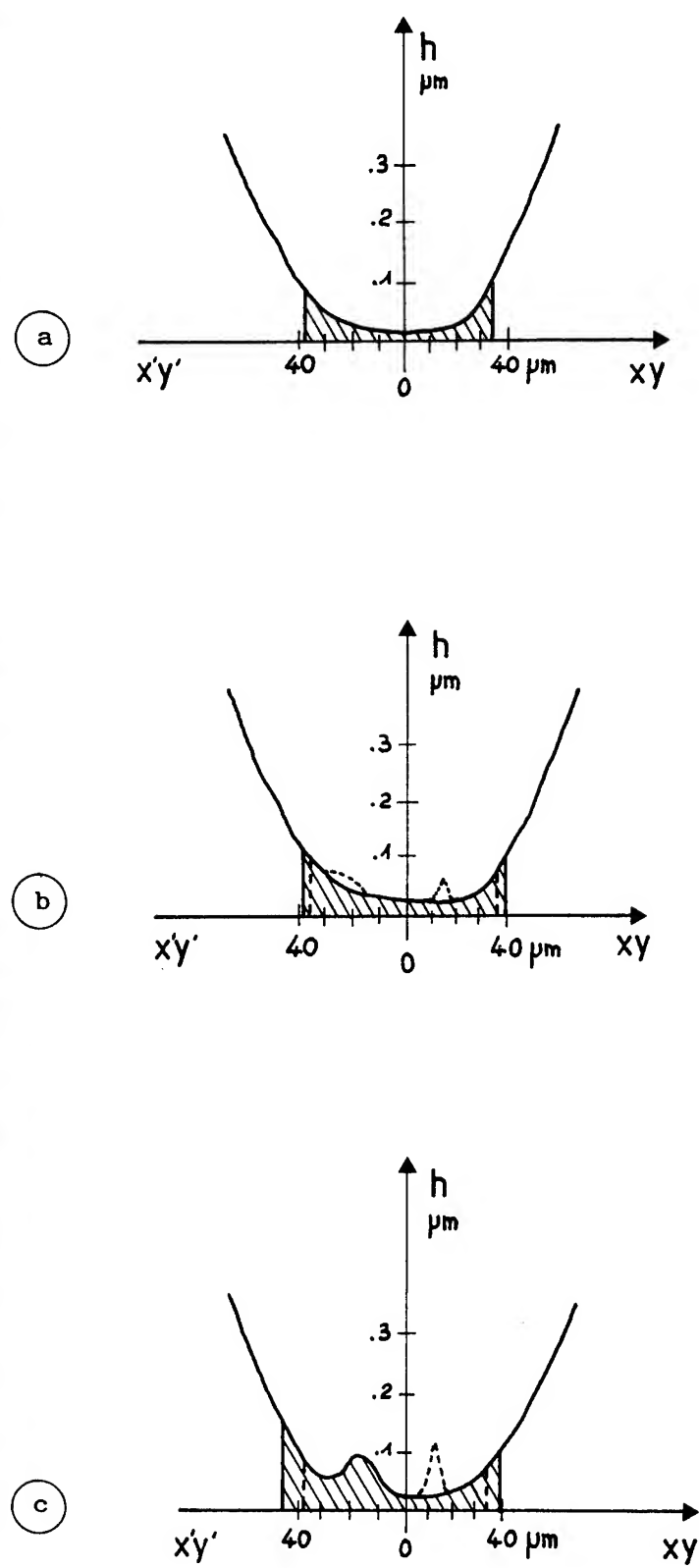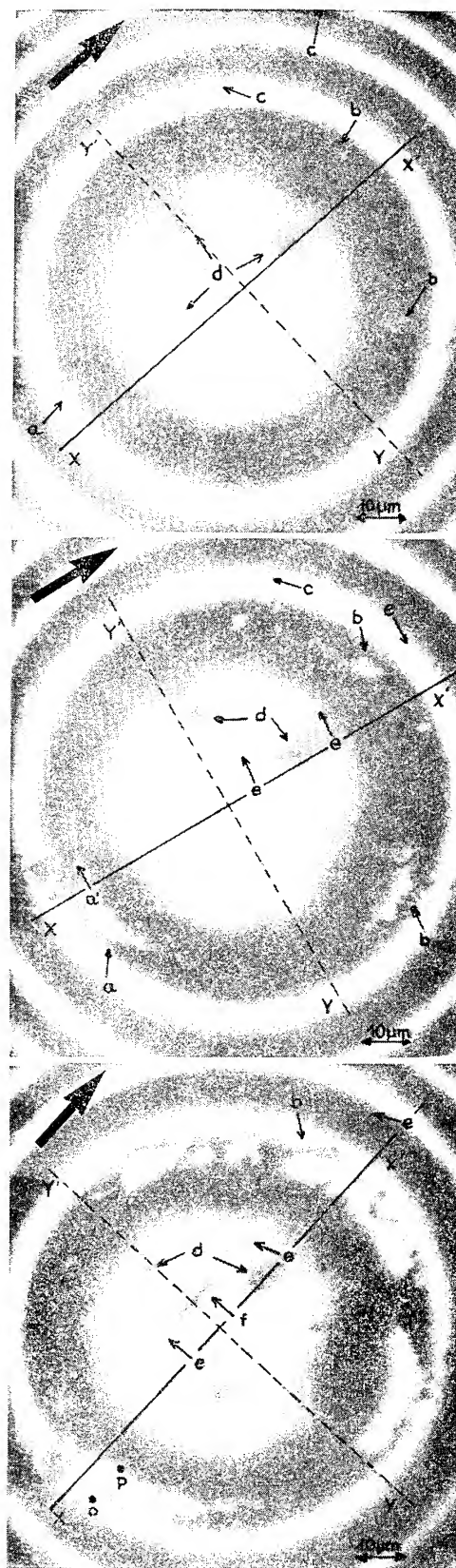
Figure 4 : Soda lime glass surfaces covered with CoO (30 nm) and a chemisorbed
stearic acid monolayer
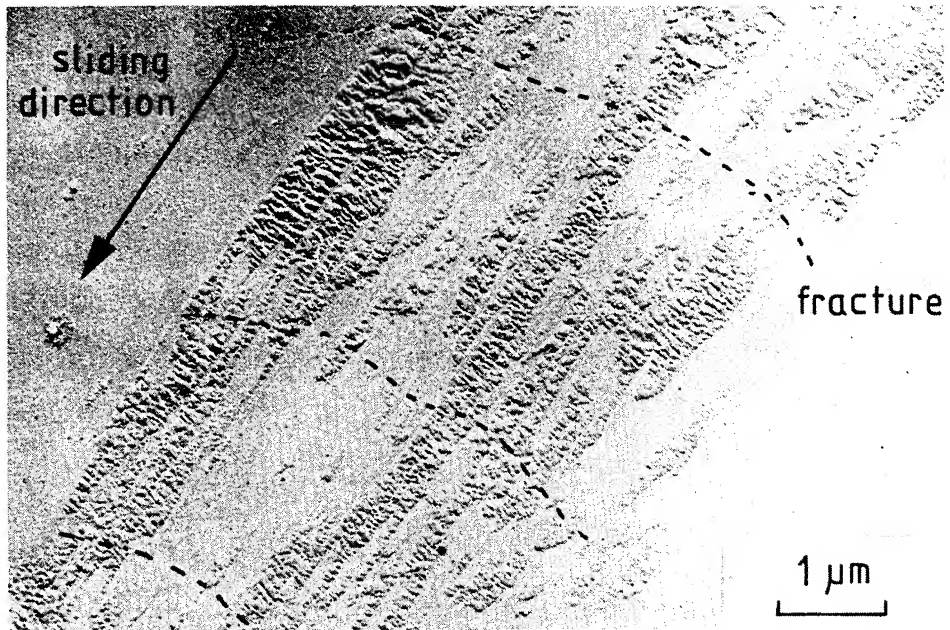
Figure 5 : Transmission electron micrograph of a direct carbon replica of a worn plane surface showing a fragment produced by a lump
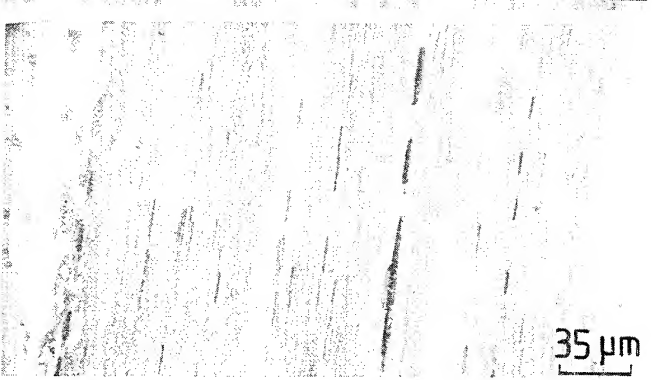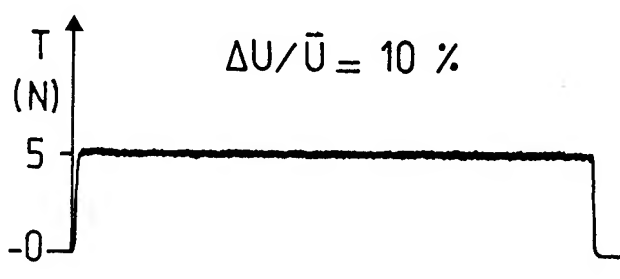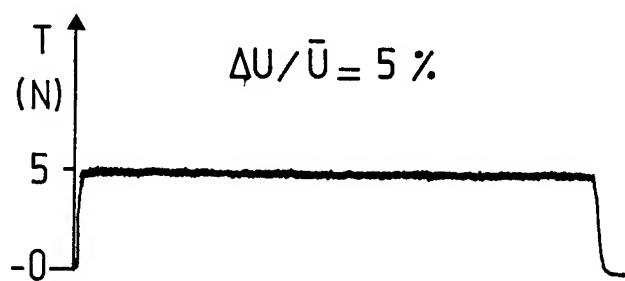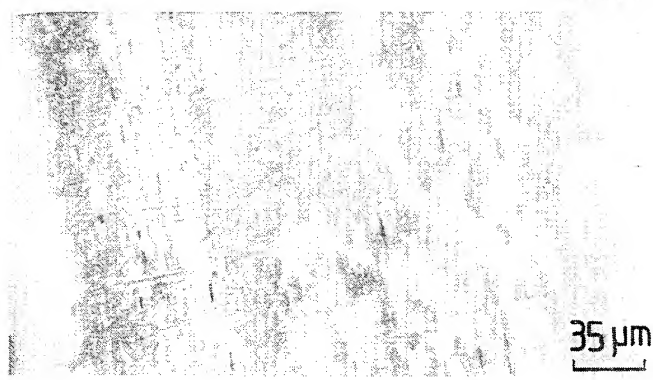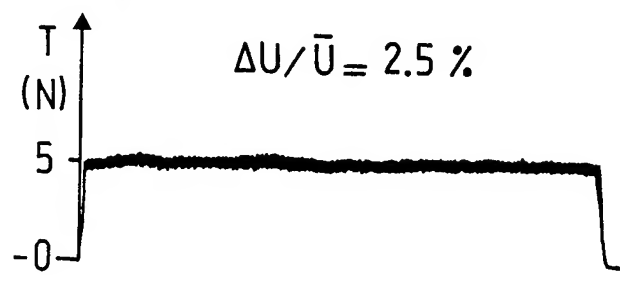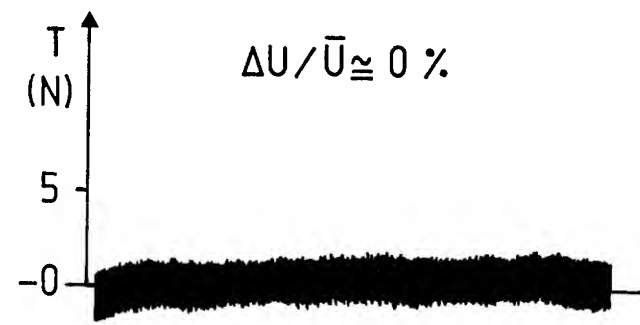
Figure 6 : Mixed lubrication – Sphere/cylinder test lubricated with
dodecane + 1 % TCP |15| – Mean rolling speed $\bar{U}$ = 1 m/s,
pressure p_m = 10^9 Pa.
Microphotograph of the surface of cylinders and corresponding records of
traction forces T, versus time, for a 90 s tests and varying ΔU.

60
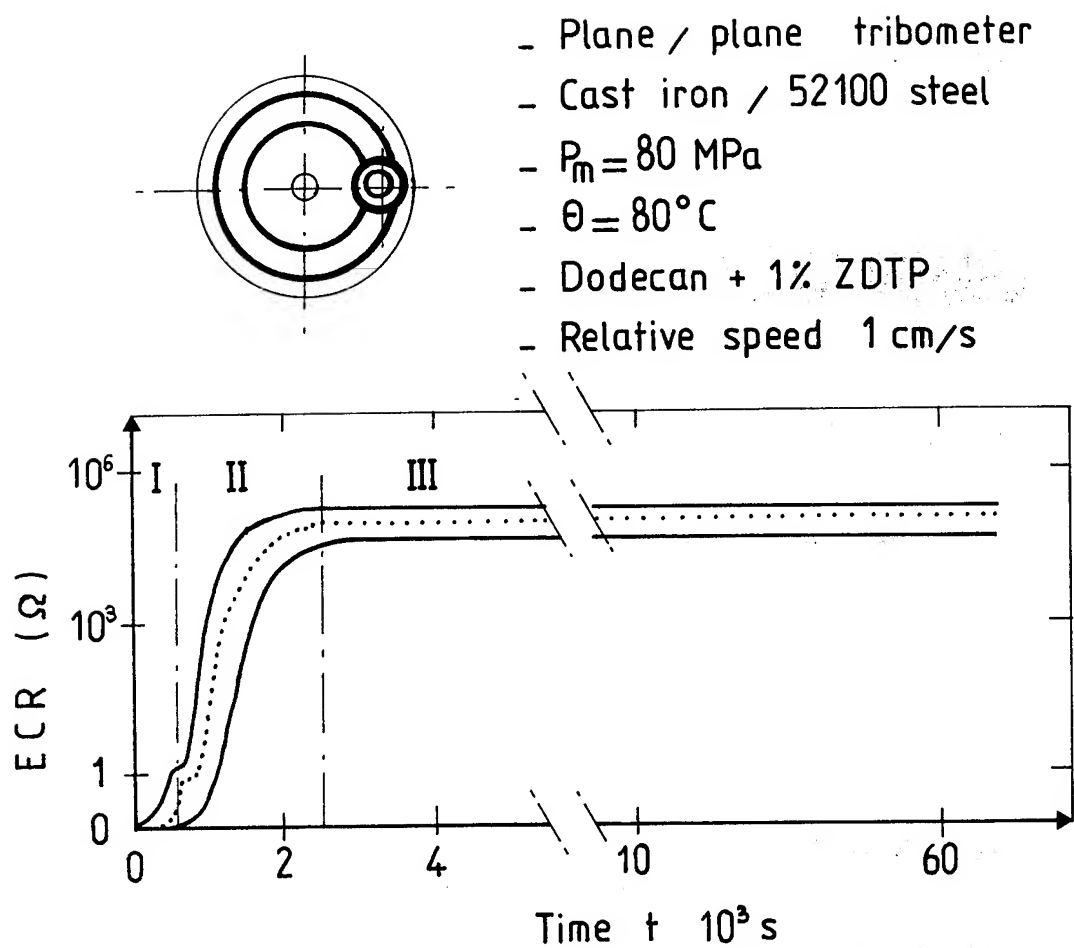
Figure 7 : Plane/plane test
Evolution of electrical contact resistance (ECR) versus time
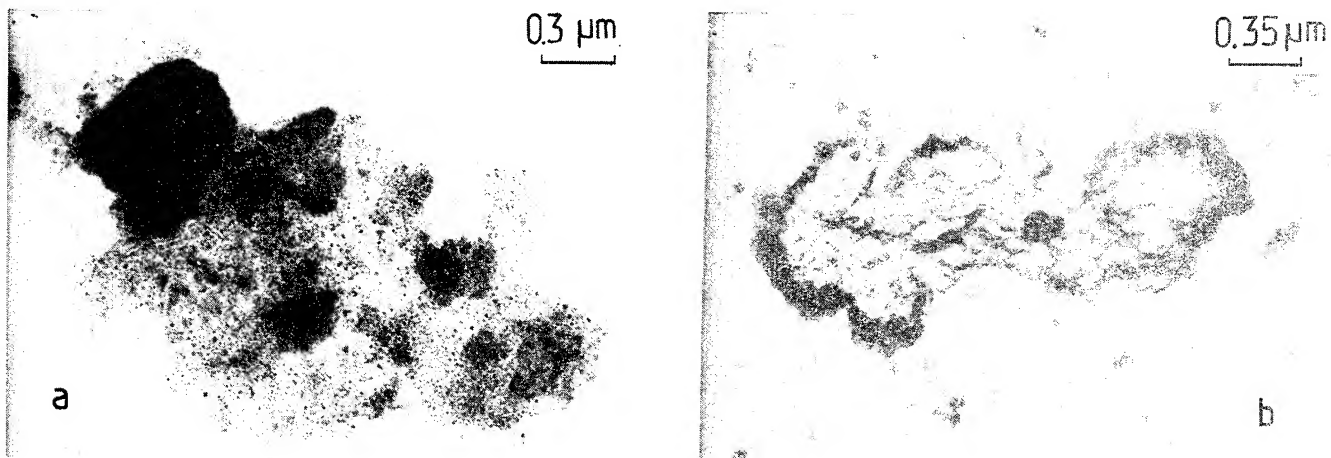
Figure 8 : Wear particles generated in stage I |20|

8a. Direct observation of the particle by TEM
8b. Microphotograph obtained on Pt/C replica of a wear particle
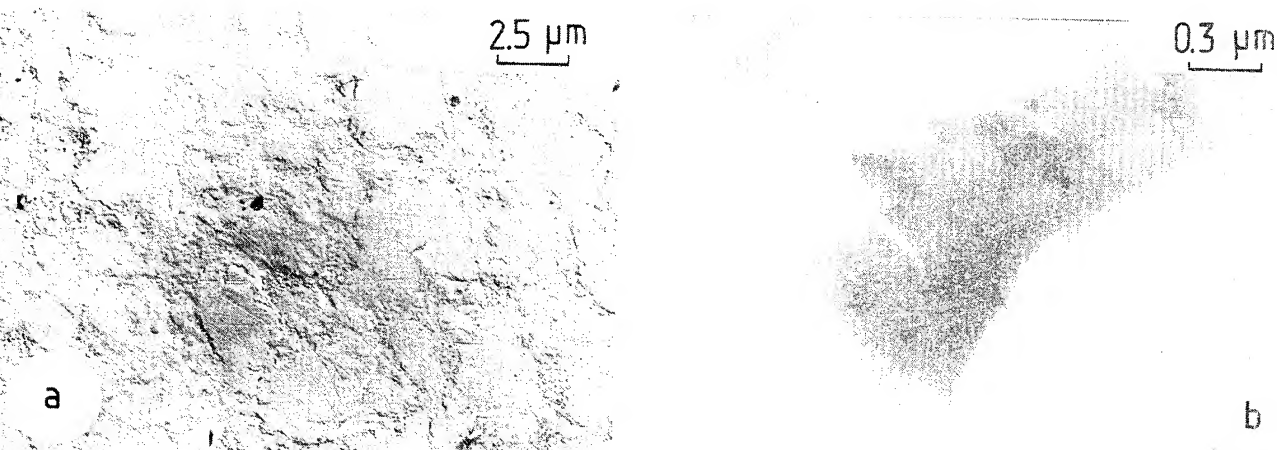
Figure 9 : Tribochemical films created with ZDTP

9a. Microphotograph obtained on Pt/C replica of friction surface
covered by tribochemical ZDTP film.
9b. Direct observation in TEM of a piece of tribochemical ZDTP film
deposited on a carbon layer
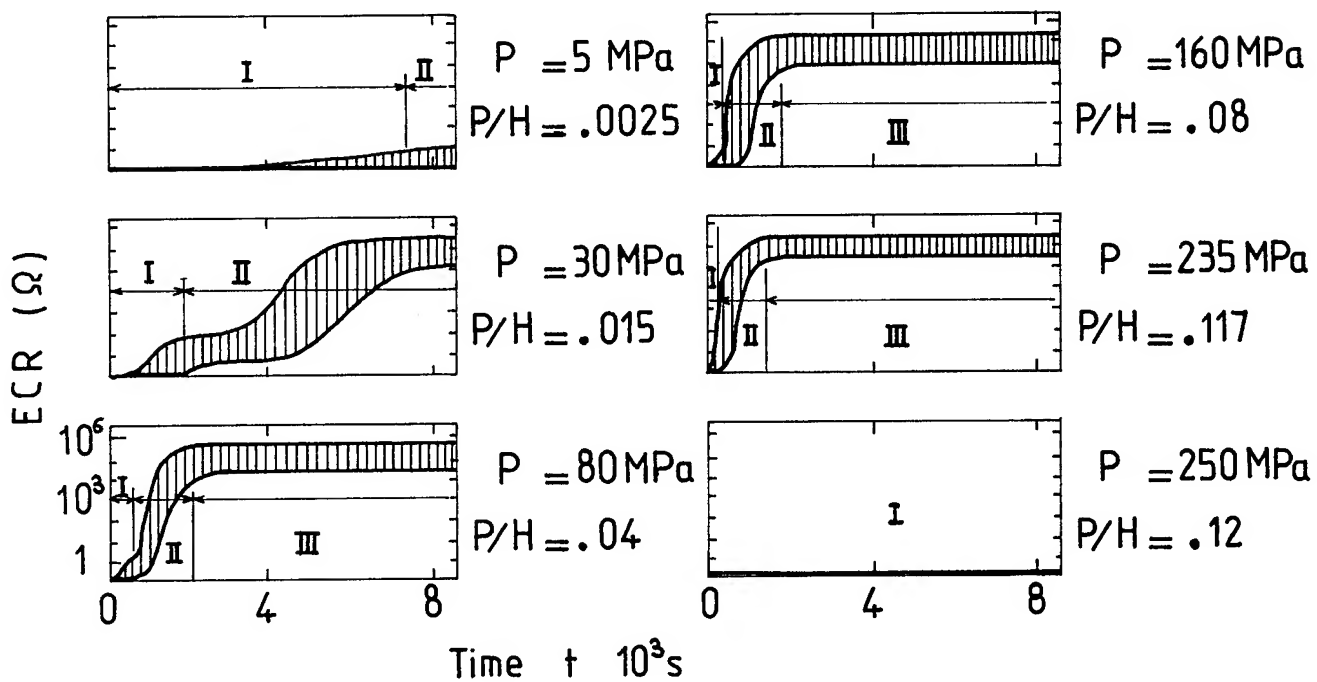
Figure 10 : Plane/plane tribometer. Same conditions as figure 7.
Evolution of ECR versus time for different apparent pressure P.
H is the hardness of cast iron, H = 2000 MPa
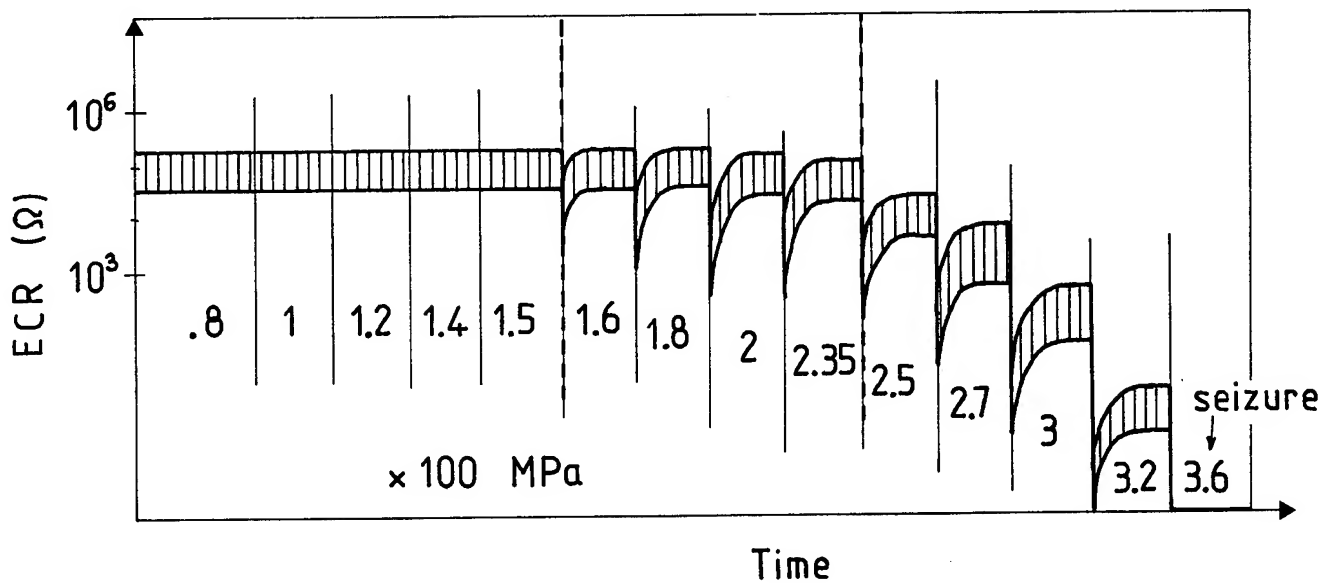
Figure 11 : Plane/plane tribometer. Same conditions as figure 7.
Evolution of ECR in function of applied pressure.

63

DISCUSSION

J. F. Hutton
Thornton Research Centre
Chester, England

Professor Georges refers to thermal degradation studies of ZDTPs carried out by my colleagues R.C. Coy and R.B. Jones. These degradation studies were part of an extensive programme carried out in our laboratories in the 1970's. The publications start with the pioneering use of XPS (ESCA) for the analysis of surface films by Bird and Galvin[1] and finish with a study of the two fundamental types of film laid down by ZDTPs.[2] Professor Georges points out that NMR analysis of oils shows that soluble products found in thermal degradations are different from those found during a tribological rubbing test. I wish to point out that in one of our series of papers Coy and Jones[3] demonstrated this very result and further, stated that the products found in a rubbing test were similar to those found in oxidation tests. The disulphide $((RO)_2PS.S)_2$, noted in Table IV, is a typical product of oxidation. Hence, the work published by my colleagues does not conflict with that of the Lyon School but is in general agreement. However, we have taken the matter further and pointed out the importance of oxidation in laboratory tests as well as in engines.

The paper[3] also throws some light on the observation by Professor Georges and his colleagues that basic ZDTP is present after a tribological test. It is true that basic ZDTP can be present in a fresh commercial additive. However, even if a "pure" laboratory-prepared additive is used, some basic ZDTP can be found in a tribological test. This product has also been observed in oxidation processes.

It seems to be in order to mention another result of Coy and Jones[3] namely, that the soluble products found during the testing of simple

formulations differ substantially from those found during the testing of fully-formulated motor oils. Hence, although the Lyon studies are fascinating and complicated, and useful in gaining new information, the results cannot be applied directly to real lubricants in real situations.

Finally, it should be remembered that the chemical changes observed in a lubricant are not necessarily those that are relevant to the function of surface films and hence to lubricant performance. Thus, it is still possible that film formation involves thermal degradation locally. It is noteworthy that the composition of the "deposited" surface films (as opposed to the "reacted" metal sulphide films) is quite similar to the solid product of thermal degradation.[2,4]

REFERENCES

1. R.J. Bird and G.D. Galvin, Wear, 37 (1976) 143.

2. F.T. Barcroft, R.J. Bird, J.F. Hutton and D. Park, Wear, 77 (1982) 355.

3. R.C. Coy and R.B. Jones, "Tribology - Key to the Efficient Vehicle", Mechanical Engineering Publication Ltd., London, 1982, p.17.

4. R.J. Bird, R.C. Coy and J.F. Hutton, Trans. ASLE, 23 (1980) 121.

DISCUSSION

K. C. Tripathi
Warner-Lambert Company
Milford, Connecticut

The author has summarized the conclusions of a number of studies at the Ecole Centrale, Lyon on interfacial tribochemical reactions of relatively simple and complex complex ZDTP with glass/AISI 52100 steel and cast-iron AISI/52100 steel combinations. Electrical Contact Resistance (ECR) measurements have been used to investigate interfacial tribochemical reactions and explain the nature and colors of surface films formed under varying pressures and sliding and rolling speeds. Basically, three zones have been observed, the first two are called "transitional" and the third "dynamic." The studies of ECR using ester and ZDTP show that while the direction of changes in the zones I and II are similar, the changes in zone III proceed in opposite directions. With the ester the ECR decreases, indicating a film breakdown, while with the ZDPT it increases, indicating a protective film. The loads and speeds in two studies are different and do not allow any quantitative comparisons of the interfacial films.

A similar study was conducted at Birmingham University in England by G. W. Rowe and his colleagues./1/ They used three point surface profilometry as a technique to investigate the mechanism of the "break-in" or "running-in" phenomenon of plain bearings. The initial changes observed by the author in the ECR (Zones I and II) before the steady state (Zone III) can also be explained by the changes in surface roughness profiles of the contacting surfaces since asperity contact of moving surfaces will indicate low electrical resistance. During the initial stages, the lubricant gets entrapped only by surface valleys and therefore, the observation of a patchy film. Surface wear then occurs through the

microwear at the tip of the asperities. The nature of lubricants and that of contaminants, speeds and stresses were shown to effect the asperity wear. When the asperities have been smoothed out, the lubricant film or the film of the reaction product becomes more uniform and the steady state is reached. The electrical resistance will be a function of the resistance of the film and is likely to be higher than the initial resistance. The initial patchy film and the steady states observed by Georges could thus be explained on the basis of above studies.

It is interesting that the author has been able to observe agglomerates of wear products ("mush" as called by the author) during the initial wear stages. It is quite conceivable that these agglomerates are the products of tribochemical reactions of the lubricant at asperties and the scratches observed are a result of the abrasive wear due to the particles produced in the smoothening out process of the asperties in the initial stage zone. However, more work needs to be done to understand the nature of the particles, their size distribution and chemical composition of the "mush" and their effect on the wear and fatigue process in rolling and sliding. A three body wear study is badly needed to understand all these aspects which are so very important for practical wear problems.

The author has observed that scratches are produced by this "mush" which he considers as colloidal particles. The discussor feels the need for identifying the metallic and non-metallic constituents of this "mush" in order to relate them to the wear process of the initial stage as well as that of the stationary stage. The discussor/2/ has also observed that the fine particles generated initially in the break-in process may start abrasive wear which under rolling and sliding condition can lead finally to adhesive and fatigue wear causing a catastrophic failure of the contacting surfaces of components (Fig. 1). A recent Canadian

study/3/ has also shown that wear debris generated in simple pin-on-disc experiment effects wear rates, appearances and subsurface structure of pins and dies.

Regarding the studies of the antiwear mechanism of ZDTP the discussor/4/ has also observed the formation of a blue film in geared roller tests. This blue film is a protective one. However, the chemical composition of this film is not known. The author has called this a "glassy" film. No characterization of this glassy film has been presented. It has been assumed that the film is a result of compaction of the colloidal solution formed in dynamic stage. Watkins et. al./5/ have recently confirmed the hydrolytic mechanism of the formation of the glassy film of ZDTP. By their experiments on the effect of water removal from the reaction, they conclude that the presence of water is essential for the production of the glassy film.

It is interesting that the author considers that mechanisms of formation of the blue film is related to contact pressure and not to thermal effect. Both these effects are related to each other. The higher the loads and speeds, the higher would be the contact pressure. The discussor wonders as to how the two could be separated in order to make a definitive statement?

The discussor has found that there exists a trigger mechanism which starts the formation of the blue film/4/. It was observed in geared roller tests that sliding rather than rolling speeds determines the trigger point. According to our observations sliding and, therefore, the contact temperature rather than the pressure determines the formation of the blue film.

References:

/1/ B. K. N Rao, H. Kaliszer and G. W. Rowe, Wear, 73 (1981) 157-162.

/2/ K. C. Tripathi, "A Tribological Failure Analysis of Roller cam followers in I.C. Engins", Unpublished work.

/3/ J. S. Sheasby and J. H. Vandergeest, Wear, 73 1981 283-296.

/4/ K. C. Tripathi and T. Clarke, "Joint IH-N.W. University -NSF Study of Gear Failures" (1982), to be published.

/5/ R. C. Watkins, et. al., Tribology International, Feb. 1982, pp. 9-11-Pt.I and pp. 13-15, Pt.II.
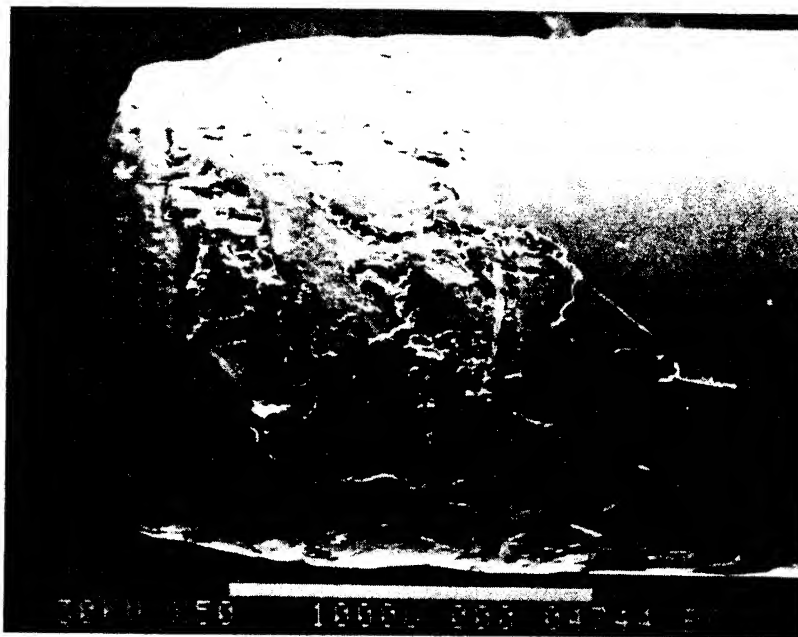
Fig. 1:   Low magnification scanning electron photomacrograph of spalled end of a bearing in roller cam follower of an IC engine.

RESPONSE

J. M. Georges
Laboratoire de Technologie des Surfaces - ERA 666
Ecole Centrale de Lyon
Ecully, France

I wish to thank Dr. K. C. Tripathi for his supporting comments and additional examples.

Further works must precise the mechanical and physical properties of these films.

IMPORTANCE OF PROPERTIES OF SOLIDS TO FRICTION

AND WEAR BEHAVIOUR

Horst Czichos
Bundesanstalt für Materialprüfung (BAM)
(Federal Institute for Materials Research and Testing)
Berlin-Dahlem
Federal Republic of Germany

It is now generally recognized that friction and wear are not "intrinsic material properties" but rather characteristics of the pertinent "tribological system", consisting generally of four material components: a pair of solids, an interfacial medium and an environmental atmosphere. Numerous properties of the interacting components have been identified to affect friction and wear.

In this paper, the main properties of solids which influence friction and wear are discussed and published rules which relate material properties to friction and wear are considered. In addition, recent experimental results on the tribological behaviour of metals and polymers illustrating the effect of some important "interaction characteristics" on friction and wear are presented. Finally, a framework for the systematic compilation and documentation of relevant tribological parameters in experimental friction and wear investigations is given.

1. INTRODUCTION

In tribology - as in all areas of contemporary technology - there is a broad spectrum of materials available today for the various technical applications. In tables 1 and 2 a survey of tribologically relevant materials is given. The tables which are extracted from Glaeser's article on "Wear Resistant Materials" in the Wear Control Handbook indicate that materials in tribology range from structural alloys, stainless steels, cast irons and copper alloys to carbides, ceramics, polymers and carbons, literally covering all technologically important types of materials. From tables 1 and 2 it can also be seen that different types of materials are suited for different types of tribological action. In this connection the following question arises: what material properties - or more generally what properties of solids - determine the friction and wear behaviour?

A general answer to this question is extremely difficult because, as is known, friction and wear are influenced by a great number of processes, conditions and parameters so that no simple "property-behaviour-relations" exist. In addition, because friction and wear result per definition from the "interaction of materials in relative motion" the tribological behaviour is determined by "interaction characteristics" rather than by intrinsic properties of single components.

71

Materials \ Tribological action	Sliding (a)	Sliding (b)	Rolling (a)	Rolling (b)	Impact	Rolling Abrasion	Sliding Abrasion
Structural Alloys							
Surface Treatments	X	X				X	X
Hard Surfacing	X				X	X	X
Soft Coatings	X	X					
Alloy Steels		X	X	X	X	X	X
Tool Steels	X	X	X	X	X	X	X
Stainless Steels							
Precipitation Hardened			X	X			
Martensitic		X	X	X			X
Cast Irons							
Graphitic	X	X	X			X	X
White Irons	X					X	X
High Temperature Alloys							
Refractory Metals	X	X			X		
Super Alloys		X	X				

(a): unlubricated, (b): lubricated

Table 1: Materials for tribological applications
(after Glaeser, WCH, 1980)

Materials \ Tribological action	Sliding (a)	Sliding (b)	Rolling (a)	Impact	Rolling Abrasion	Sliding Abrasion
Copper Base Alloys						
Bronze		X				
BE Copper		X		X		
Soft Bearing Alloys						
Babbitts		X				
Carbides	X		X			X
Ceramics	X					X
Polymers						
Thermosets	X					
Thermoplastics	X	X				
Elastomers		X			X	X
Carbons	X					
Lubricating Composites	X	X				

(a): unlubricated, (b): lubricated

Table 2: Materials for tribological applications
(after Glaeser, WCH, 1980)

Although it appears on one hand impossible to discuss tribologically relevant material properties in terms of "first principles" there are on the other hand some general material-related aspects which obviously characterize the friction and wear behaviour. For example, the tribological behaviour of metals is mainly determined by processes of deformation, work hardening and fracture of surface asperities whereas for polymeric materials, surface energies and friction-induced surface heating and for ceramics localized brittle fracture are important phenomena.

In this paper it is attempted to present a survey on the present state of our understanding of the importance of properties of solids to friction and wear behaviour. The survey concentrates on two main questions:

(i)   what are the fundamental friction and wear processes?

(ii) how are the fundamental friction and wear processes connected with properties of solids?

The discussion is restricted to basic phenomena with respect to the tribological behaviour of materials under sliding conditions.

2. BACKGROUND

The great variety of material-related aspects of tribology is obvious in considering the tribological literature. According to the BAM Documentation Service on Tribology, which publishes an annual systematic bibliography of titles covering the entire field of friction, lubrication and wear, about 5000 to 6000 papers are published worldwide annually in the field of tribology. In order to get an idea of the tribologically relevant material aspects a survey of the published literature dealing with material aspects in tribology has been made by H. Tischer of the BAM Documentation Service on Tribology considering the tribology literature of 1977/1978. The results of this literature survey are compiled in table 3. It can be seen that approximately 50 % of the papers considered deal with metals and semi-metals. About one quarter of the published literature is devoted to studies of organic materials and polymers. The other two groups concern tribological studies on composite materials and minerals or ceramics. In table 3 also the main groups of material properties studied in the published literature are compiled. These tribology relevant properties range from bulk material properties over surface properties to properties relevant to design. In the following it is discussed how the various properties of materials are connected with the fundamental mechanisms of friction and wear.

Type of material	Percentage of published papers
● Metals and semimetals	47 %
● Organic materials, polymers	24 %
● Composite materials	16 %
● Minerals, ceramics	13 %
Total (1230 papers)	100 %

Material properties	Percentage of published papers
● Bulk material properties (Composition, physical properties, microstructure, strength properties, hardness, etc.)	39 %
● Surface properties, (Surface energy, heat treatment, etc.)	31 %
● Surface topography, waviness	16 %
● Adsorbed surface layers	7 %
● Properties relevant to design	7 %
Total (540 papers)	100 %

Table 3: Overview on materials aspects in the tribological literature

I. | Introduction of mechanical energy into the contact zone |

→ formation of real area of contact

II. | Transformation of mechanical energy |

→ elastic deformation and elastic hysteresis
→ plastic deformation
→ ploughing
→ adhesion

III. | Dissipation of mechanical energy |

(a) | Thermal transformation |

→ generation of heat and entropy

(b) | Storage |

→ generation of point defects and dislocations
→ strain energy storage
→ phase transformations

(c) | Emission |

→ thermal radiation and conduction
→ phonons (acoustic waves, noise)
→ photons (triboluminescence)
→ electrons (exo-electrons)

Table 4: Energy-based overview on friction phenomena

3. FRICTION MECHANISMS AND THE IMPORTANCE OF PROPERTIES OF SOLIDS

3.0 General considerations

Despite the considerable amount of work that has been devoted to the study of friction since the early investigations of Leonardo da Vinci, Amontons, Coulomb and Euler (ref. 1) there is no "simple" model to predict or to calculate friction of a given pair of materials. Although it is now well recognized by tribologists that friction is a very complex phenomenon, non-tribologists are often not aware of the complexity of friction and often still misinterpret friction as a kind of materials property. However, to quote the physicist and Nobel-laureate Richard P. Feynman from his famous Feynman-Lectures: "The tables that list purported values of the friction coefficient of "steel on steel" or "copper on copper" and the like are all false because they ignore a couple of important factors". So, what is our present status of understanding friction and the importance of properties of solids to it?

From the results of various studies it is obvious that friction originates from complicated molecular-mechanical interactions between contacting bodies (ref. 2). In quoting a summarizing description of Nam P. Suh (ref. 3), the "genesis of friction" may be characterized as follows: "The coefficient of friction between sliding surfaces is due to the various combined effects of asperity deformation, ploughing by wear particles and hard surface asperities and adhesion between the flat surfaces. The relative contribution of these components depends on the condition of the sliding interface which is affected by the history of the sliding, the specific materials used, the surface topography and the environment".

Similarly, David Tabor pointed out that today we recognize that three basic phenomena are involved in the friction of unlubricated solids (ref. 4):

I.   The area of real contact between the sliding surfaces.

II. The type of strength of bond that is formed at the interface where contact occurs.

III. The way in which the material in and around the contacting regions is sheared and ruptured during sliding.

Because friction is essentially an energy dissipation process, an energy consideration of friction may also be useful (ref. 2). According to that the whole course of the "loss" process of mechanical energy due to friction may be formally divided into different phases as compiled in table 4. Firstly, mechanical energy is introduced into the contact zone by the formation of the real area of contact. Secondly, a transformation of mechanical energy takes place mainly by the effect of plastic deformation, ploughing and adhesion. Thirdly, the dissipation phenomena include the effects of thermal dissipation, storage or emission. In the following some of the main

basic aspects of friction with respect to the importance of proper-
ties of solids to it are considered.

3.1 Real area of contact

In recent years there has been an increasing interest in
surface topography and its role in tribocontact formation and per-
formance. (See ref. 5 for a recent comprehensive book which contains
numerous references.) These studies assume that the surfaces of
tribological contacts are covered with asperities of a certain
heights distribution which deform elastically or plastically under
the given load. The summation of individual contact spots gives the
real area of contact. The basic properties and parameters relevant
to the real area of a tribocontact are summarized in figure 1. There
are two classes of properties, namely deformation properties and
surface topography characteristics. Without going into details it
can be said that, for example, the behaviour of metals in contact
is determined by a deformation criterion, namely the so called
plasticity index. Depending on the value of the plasticity index
(Ψ) an elastic or plastic deformation mode results which can be
characterized in a simplified manner by the formulas given in
figure 1. If in addition to the normal load a tangential force is
introduced a junction growth of asperity contacts may occur leading
to a considerably larger area of contact.

The overall picture of a tribocontact summarized in a simpli-
fied manner in figure 1 is influenced by some other phenomena, e.g.:

- Microasperities may contain no dislocations and may be therefore
  much harder than the average of the bulk material, (ref. 6).

- Surface films (e.g. oxides) may change the deformation
  properties of the materials. It has been found, for example,
  that a surface layer of oxide 50 Å thick increases the
  effective hardness of nickel by a factor of about 5, (ref. 7).

- The influence of temperature may lead to creep and sintering
  and may considerably increase the area of contact, (ref. 8).

3.2 Adhesion component of friction

The adhesion component of friction is due to the formation
and rupture of interfacial adhesion bonds. These bonds are the
results of interfacial interatomic forces. There have been theore-
tical papers to explain this interaction, expecially for the contact
of clean metals, in terms of the electronic structures of the
contacting partners (see e.g. ref. 9 to 11). Theoretically the
attractive interaction forces between two contacting solids include,
at least in principle, all those types of interaction that contribute
to the cohesion of solids, such as metallic, covalent and ionic
i.e. primary chemical bonds (short-range forces) as well as
secondary van der Waals bonds (long-range forces). For example, two
pieces of clean gold placed in contact will form metallic bonds

Fig. 1: Characteristics of tribocontact

Tribocontact

F_N

Deformation properties

- elastic modulus E
- yield pressure p_y
- hardness H

solid (1)

solid (2)

Surface topography

- asperity distribution
- tip radius β
- deviation of asperity heights σ^*
- slope of asperities Θ

Deformation criterion

$$\psi = \frac{E'}{p_y} \cdot \left(\frac{\sigma^*}{\beta}\right)^{1/2} \qquad \begin{array}{l} \psi < 0.6 \ : \text{elastic} \\ \psi > 1 \quad : \text{plastic} \end{array}$$

Area of contact

- elastic: $A_{0r} = c \cdot \left(\frac{F_N}{E'}\right)^n \quad \frac{2}{3} < n < 1$

- plastic: $A_{0r} = c \cdot \frac{F_N}{p_y} \approx \frac{F_N}{H}$

- junction growth:

$$A_r = A_{0r} \left[1 + \alpha\left(\frac{F_F}{F_N}\right)^2\right]^{1/2} \quad \alpha \approx 9$$

Fig. 1: Characteristics of tribocontact

Adhesion component of friction

F_N

(1)

F_F

Θ

(2)

β

- simplest model:

$$f_a = \frac{F_F}{F_N} \approx \frac{\tau_{s_{12}}}{p_y}$$

$\tau_{s_{12}}$: interfacial shear strength
p_y : yield pressure

- surface energy theory: $f_a = \frac{\tau_{s_{12}}}{p_y} \left[1 - 2\frac{W_{12} \cdot \tan\Theta}{\beta \cdot p_y}\right]^{-1}$

where $W_{12} = \gamma_1 + \gamma_2 - \gamma_{12}$: surface energy

- fracture mechanic model: $f_a = c\frac{\sigma_{12} \cdot \delta_c}{n^2 \cdot (F_N \cdot H)^{1/2}}$

σ_{12} : interfacial tensile strength
δ_c : critical crack opening factor
n : work hardening factor
H : hardness

Fig. 2: Characteristics of adhesion models
of friction

over the regions of atomic contact and the interface will have the strength of bulk gold. With clean diamond the surface forces will resemble valency forces. With rock salt the surface forces will be partly ionic. All these forces are essentially short-range forces. Long-range van der Waals forces act in the adhesion between soft rubber-like materials and between polymeric solids. It is evident from these examples of metals, ceramics and polymers that interfacial adhesion is as natural as cohesion which determines the bulk strength of materials within a solid.

The adhesion component of friction has been described by Bowden and Tabor in a highly simplified model as the quotient of the interfacial shear strength and the yield pressure of the asperities, see figure 2 (ref. 4). Because for most materials this ratio is of the order of 0.2, the friction coefficient may have this value. Because of junction growth (see figure 1) the adhesion component of friction may however increase for clean metals to values of about 10 to 100. If, on the other hand, the contacting surfaces are separated by a film with an effective shear strength of about one half of that of the parent metals, a friction coefficient of 0.1 may result.

The simplified Bowden and Tabor model of the adhesion component of friction has been extended by some other theories taking into account further properties of solids (see figure 2):

- A surface energy theory which introduces the surface energy of the contacting partners as an important parameter, (ref. 12).

- A fracture mechanic model which considers the fracture of an adhesive junction and introduces as influencing parameters a critical crack opening factor and a work hardening factor, (ref. 13).

In considering the adhesion component of friction it must be emphasized that the relevant influencing properties like the interfacial shear strength or the surface energy are characteristics related to the given pair of materials rather than to the single components involved.

3.3 Ploughing component of friction

It is obvious that if one surface in a sliding tribocontact is considerably harder than the other the harder asperities may penetrate into the softer surface. In tangential motion a certain force results because of the ploughing resistance. This may considerably contribute to the friction resistance as pointed out already by L. Gümbel in 1925 in his book on "Friction and Lubrication in Mechanical Engineering" (ref. 14).

As compiled in a simplified manner in figure 3 basic possibilities of ploughing are

- ploughing by asperities

- ploughing by penetrated wear particles.

In the simplest model, i.e. the case of a sliding conical asperity the friction coefficient is related to the tangens of the slope of the ploughing asperity (ref. 12). Because normal surface asperities seldom have an effective slope exceeding 5° or 6°, it follows that the coefficient friction should have a value of $f \sim 0.05$. This value may be regarded, however, only as a lower friction coefficient limit for the ploughing component of friction, due to the neglections of the experimentally observed fact that a pile-up of material ahead of the grooving path occurs in most cases of ploughing during sliding (ref. 15).

Because during ploughing of brittle surface material, micro-cracking may occur, an extended model has been suggested by Zum Gahr (ref. 16). In this fracture mechanic model of ploughing, properties of materials like the fracture toughness, the elastic modulus and the hardness are main influencing parameters.

The other possibility of ploughing, namely ploughing by penetrated wear particles was investigated by Nam P. Suh and co-workers, (ref. 17). Their analysis showed that the contribution of ploughing to friction is very sensitive to the ratio of the radius of curvature of the particle to the depth of penetration. This analysis indicates that in addition to the materials properties the geometric properties of asperities or penetrated wear particles may considerably influence the friction behaviour of sliding surfaces.

3.4 Deformation component of friction

Because of the deformation during sliding contact, mechanical energy may be dissipated through plastic deformation effects. A.P. Green (ref. 18) analysed the deformation of the surface asperity contact using the slip-line field for a rigid-perfectly plastic material. In a similar way in applying a two-dimensional stress analysis of L. Prandtl, Drescher has worked out a slip-line deformation model of friction as summarized in figure 4, (ref. 19). In this model it is assumed that under an asperity contact (AB in figure 4) three regions of plastically deformed material may develop which are described in figure 4 by the regions ABE, BED, BDC. The maximum shear stress in these areas is equal to the flow shear stress of the pertinent material. An important parameter in this model ist the factor λ, the proportion of the plastically supported load which is related in a complicated manner to the ratio of the hardness to the elastic modulus. If the asperity contact is com-pletely plastic and the asperity slope is 45°, a friction coeffi-cient of $f = 1.0$ results. This value goes down to $f = 0.55$, if the asperity slope approaches zero. In discussing the deformation component of friction Drescher pointed out that this model is a
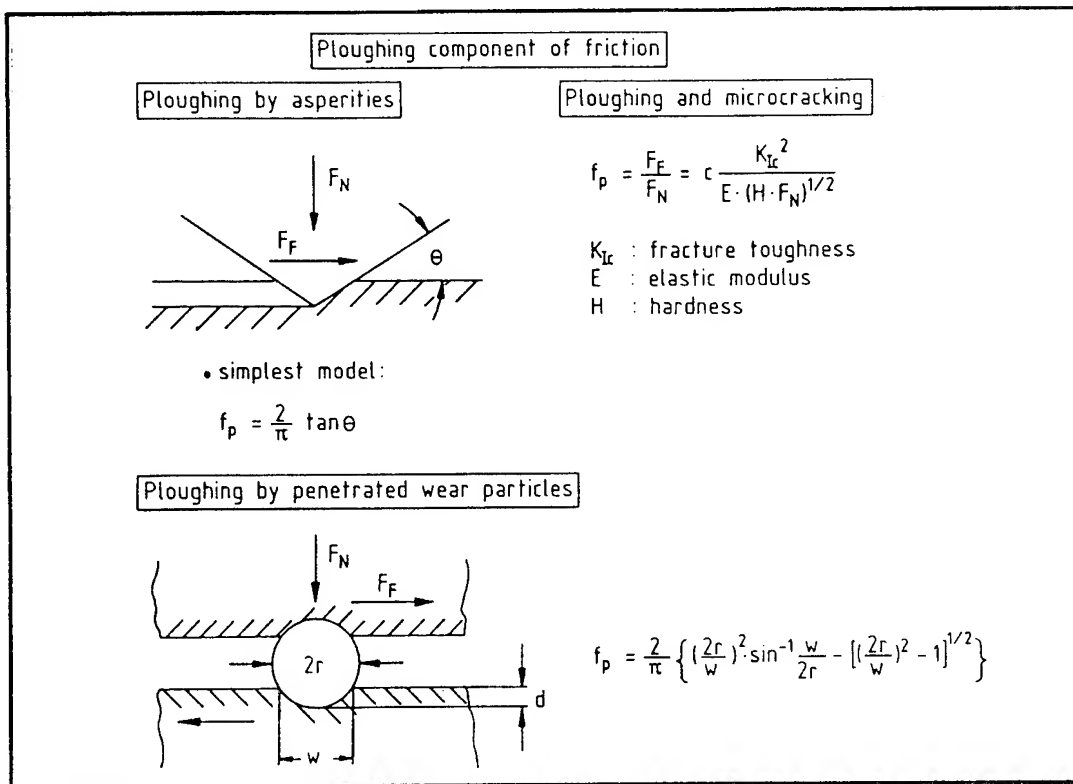
Fig. 3: Characteristics of ploughing models of friction

Fig. 4: Characteristics of deformation models of friction

80

Ploughing component of friction

Ploughing by asperities

F_N ↓ F_F → θ

- simplest model:

$$f_p = \frac{2}{\pi} \tan\theta$$

Ploughing and microcracking

$$f_p = \frac{F_F}{F_N} = c\,\frac{K_{Ic}^2}{E \cdot (H \cdot F_N)^{1/2}}$$

K_{Ic} : fracture toughness
E : elastic modulus
H : hardness

Ploughing by penetrated wear particles

F_N ↓ F_F → $2r$ d w

$$f_p = \frac{2}{\pi}\left\{ \left(\frac{2r}{w}\right)^2 \sin^{-1}\frac{w}{2r} - \left[\left(\frac{2r}{w}\right)^2 - 1\right]^{1/2} \right\}$$

Fig. 3: Characteristics of ploughing models of friction

Deformation component of friction

Slip line field theories

F_N ↓ F_F →   A B C E D ϑ

$$f_d = \frac{F_F}{F_N} = \lambda \cdot \tan\,\text{arc}\,\sin\left[\frac{\sqrt{2}}{4}\cdot\frac{(2+\vartheta)}{(1+\vartheta)}\right]$$

where $\lambda = \lambda(E',H)$ proportion of plastically supported load

E': elastic modulus
H : hardness

Energy-based plastic deformation model

$$f_d = \frac{A_r}{F_N}\,\tau_{max}\cdot F\!\left(\frac{\tau_s}{\tau_{max}}\right)$$

$$\text{where } F\!\left(\frac{\tau_s}{\tau_{max}}\right) = 1 - 2\,\frac{\ln\left(1+\frac{\tau_s}{\tau_{max}}\right) - \frac{\tau_s}{\tau_{max}}}{\ln\left[1-\left(\frac{\tau_s}{\tau_{max}}\right)^2\right]}$$

A_r : real area of contact
τ_{max} : ultimate shear strength of material
τ_s : average interfacial shear strength

Fig. 4: Characteristics of deformation models of friction

80

very simple one and that some other material properties should be considered like

- microstructure of the materials

- work hardening effects

- thermal softening

- influence of interfacial layers.

A recent model of the slip-line theory of the deformation component of friction was advanced by Challen and Oxley (ref. 20).

Another model of the deformation component of friction which relates friction mainly to plastic deformation was suggested recently by Heilmann and Rigney (ref. 21). The main assumption is that the frictional work performed is equal to the work of plastic deformation during steady state sliding. As summarized in figure 4 there are three main parameters characterizing this model:

- The real area of contact (see Section 3.1).

- The ultimate shear strength of the material which can be achieved during shear.

- The average shear strength actually achieved at the interface during sliding. This quantity may depend on many experimental parameters like operating conditions (load, sliding velocity, temperature) and other material characteristics such as crystal structure, microstructure, work-hardening rate and recovery rate.

4. WEAR MECHANISMS AND THE IMPORTANCE OF PROPERTIES OF SOLIDS

4.0 General considerations

Similarly as friction, the wear behaviour of materials is also a very complicated phenomenon in which various mechanisms and influencing factors are involved. A great step forward in our understanding of wear was the classification of wear mechanisms given by Burwell in the 50's, (ref. 22), according to which wear mechanisms may be divided into four broad general classes under the headings of abrasion, adhesion, surface fatigue and tribochemical processes.

In recent years an increasing number of studies have been devoted to wear (see, e.g., refs. 23 to 27) which indicate that wear, i.e., "the removal of material from interacting surfaces in relative motion" results through various interaction processes. In quoting a summarizing description of Nam P. Suh (ref. 28) it may be said that "wear of materials occurs by many different mechanisms depending on the materials, the environmental and operating conditions and the geometry of the wearing bodies. These wear mechanisms may be classified into two groups: those primarily dominated by the mechanical behaviour of solids and those primarily dominated by

the chemical behaviour of materials. What determines the dominant wear behaviour are mechanical properties, chemical stability of materials, temperature and operating conditions".

Tabor in his recent critical synoptic view of wear (ref. 29) for simplicity divided wear processes into three groups:"The first is that in which wear arises primarily from adhesion between the sliding surfaces, the second is that deriving primarily from non-adhesive processes and the third is that very broad class in which there is interaction between the adhesive and non-adhesive processes to produce a type of wear that seems to have characteristics of its own. The way in which these mechanisms interact with one another depends extremely sensitively on the specific operating conditions. In addition the frictional process itself can produce profound structural changes and modifications of the physical and chemical properties of the sliding surfaces. Consequently unless a single wear process dominates these surface changes and complex inter-actions must necessarily make wear predictions extremely difficult and elusive".

In order to discuss the importance of materials on the wear behaviour the whole chain of events which leads to the generation of loose wear particles must be considered. The chain of events that leads to the generation of wear particles and material removal from a given tribological system is initiated by two broad classes of tribological processes as summarized in table 5 (ref. 23):

I.   Stress interactions

These are due to the combined action of load forces and frictional forces and lead to wear processes described broadly as surface fatigue and abrasion.

II.   Material interactions

These are due to intermolecular forces either between the interacting solid bodies or between the interacting solid bodies and the environmental atmosphere (and/or the interfacial medium) and lead to wear processes, described broadly as tribochemical reactions and adhesion.

4.1 Surface fatigue and delamination wear mechanisms

As is known from the mechanical behaviour of bulk materials under repeated mechanical stressing, microstructural changes in the material may occur which result in gross mechanical failure. Similarly under repeated tribological loading, surface fatigue phenomena may occur leading finally to the generation of wear particles. These effects are mainly based on the action of stresses in or below the surfaces without needing a direct physical solid contact of the surfaces under consideration. This follows from the observation that surface fatigue effects are observed to occur in journal bearings where the interacting surfaces are fully separated by a thick lubricant film (ref. 30). As is known, the

Tribological interactions

Stress interactions (load, frictional forces) ← Frictional heating → Material interactions (interatomic forces)

Surface fatigue | Abrasion | Tribochemical reactions | Adhesion

Stress cycles
Microstructural changes
Crack formation
Delamination

Micro-cutting
Micro-ploughing
Micro-cracking

Tribochemical films due to material/environment interactions

Transferred material due to adhesive joint formation and rupture

Material removal processes

Fatigued wear particles | Abraded wear particles | Tribochemical wear particles | Adhesive wear particles

Table 5: Tribological interactions and wear mechanisms

Surface fatigue and delamination wear mechanisms

F_N

F_F

tension   compression

cracks

• Fatigue wear model:

$$W_v = c \frac{\eta \cdot \gamma}{\bar{\varepsilon}_1^2 \cdot H} \cdot F_N \cdot s$$

η : line distribution of asperities
γ : particle size constant
$\bar{\varepsilon}_1$: strain to failure in one loading cycle
H : hardness

• Delamination wear model:

(i)   transmittance of stresses at contact points
(ii) incremental plastic deformation per cycle
(iii) subsurface void and crack nucleation
(iv) crack formation and propagation
(v)   delamination of sheet-like wear particles

Fig. 5: Characteristics of surface fatigue and delamination wear models

effect of fatigue wear is especially associated with repeated stress cycling in rolling contact. However, also in sliding the asperities undergo cyclic stressing leading to stress concentration effects and the generation and propagation of cracks. On the basis of the dislocation theory there are several possible mechanisms for crack initiation and propagation (see ref. 31). A contribution to the theory of surface fatigue wear mechanisms was put forward by J. Halling (ref. 32). This model incorporates the concept of fatigue failure and also of simple plastic deformation failure which is considered as fatigue failure in one cycle of loading. The main properties of materials relevant to surface fatigue in this model are listed in figure 5.

In studying the plastic-elastic stress fields in the subsurface regions of sliding asperity contacts and the possible dislocation interaction a "delamination theory of wear" has been put forward by Nam P. Suh, (ref. 33), in which the generation of sheet-like wear particles is explained on the basis of the chain of events, compiled in figure 5. In refining this theory some implications of crystal plasticity effects have been discussed including a specific dis-location model for hexagonal close packed metals under wear con-ditions and a correlation with stacking fault energy for face-centred cubic and hexagonal close packed metals (ref. 34). It appears that by the use of dislocation models it is now possible to explain the occurrence of sheet-like wear particles observed as early as in 1929 by Füchsel and interpreted through a process of stress-induced material separation (German:"Abblättern"), (ref. 35).

4.2 Abrasive wear mechanisms

The effect of abrasion occurs in contact situations in which direct physical contact between two surfaces is given, where one of the surfaces is considerably harder than the other. The harder surface asperities press into the softer surface with plastic flow of the softer surface occurring around the asperities from the harder surface. When a tangential motion is imposed the harder surface remove the softer material by combined effects of "micro-ploughing", "micro-cutting", and "micro-cracking".

As illustrated in figure 6 in the simplest model of abrasive wear processes the wear volume is related to the asperity slope of the penetrating abrasive particle and the hardness of the abraded material, (see ref. 12). From the comprehensive experimental work of Khrushov the following phenomenological observations on the influence of material properties on abrasive wear are drawn (ref.36):

- Technically pure metals in an annealed state and annealed steels show a direct proportionality between the relative wear resistance and the pyramid hardness.

- For non-metallic hard materials and minerals a linear relationship between wear resistance and hardness is similarly found.

84

- For metallic materials cold work-hardened by plastic deformation, the relative wear-resistance does not depend on the hardness resulting from cold work hardening.

- A heat treatment of structural steels (normal hardening and tempering) improves the abrasive wear resistance.

The simple abrasion model which includes only the hardness as material property has been recently extended. Hornbogen proposed a model to explain increasing relative wear rates with decreasing toughness of metallic materials (ref. 37). This model is based on the comparison of the strain that occurs during asperity interactions with the critical strain at which crack growth is initiated. The basic properties of materials relevant to that model are listed in figure 6. Another model was proposed by Zum Gahr who considered the detailed processes of micro-cutting, micro-ploughing and micro-cracking in the abrasive wear of ductile metals, (ref. 38). This model includes other micro-structural properties of the materials worn beside the flow pressure or hardness. Influences of capacity of work-hardening, ductility, homogeneity of strain distribution, crystal anisotropy and mechanical instability have been identified to influence the abrasive wear mechanisms.

4.3 Tribochemical wear mechanisms

Whereas the mechanisms of surface fatigue and abrasion can be described mainly in terms of stress interactions and deformation properties, in tribochemical wear as third partner, the environment and the dynamic interactions between the material components and the environment determine the wear processes. These interactions may be expressed as cyclic stepwise processes:

(i)   At the first stage the materials surfaces react with the environment. In this process reaction products are formed on the surfaces.

(ii) The second step consists of the attrition of the reaction products as a result of crack formation and abrasion in the contact process interactions of the materials. When this occurs "fresh", i.e. reactive surface parts of the materials are formed and stage (i) continues.

As a consequence of thermal and mechanical activation the asperities undergo the following changes:

(a)   The reactivity is increased due to the increased asperity temperature. Therefore the formation of surface layers is accelerated.

(b)   The mechanical properties of the surface asperity layers are changed: in general they have a tendency to brittle fracture.

85

Abrasive wear mechanisms

F_N, F_F, θ, s

- simplest model:

$$W_v = \frac{2}{\pi} \cdot \frac{\tan\theta}{H} \cdot F_N \cdot s$$

- extended models

$$W_v = n^2 \frac{p_y \cdot E \cdot F_N^{3/2}}{K_{Ic}^2 \cdot H^{3/2}} \cdot s$$

$$W_v = \frac{f_{abr}}{K_1 \cdot K_2 \cdot \tau_c} \cdot \frac{\cos\rho \cdot \sin\theta}{(\cos\frac{\theta}{2})^{1/2} \cdot \cos(\theta-\rho)} \cdot F_N \cdot s$$

E : elastic modulus
H : hardness
K_{Ic}: fracture toughness
n : workhardening factor
p_y : yield strength

f_{abr} : model factor (1 for micro-cutting)
K_1 : relation of normal and shear stress
K_2 : texture factor (1 for fcc-metals)
τ_c : shear stress for dislocation movement
ρ : friction angle at abrasive/material interface

Fig. 6: Characteristics of abrasive wear models

Tribochemical wear mechanisms

F_N, v, asperity contact, reaction layer, ρ, d

$$W_v = \frac{k''}{\xi^2 \rho^2} \cdot \frac{d}{H} \cdot \frac{F_N}{v} \cdot s$$

k″: velocity factor of oxydation
d: asperity contact diameter
ρ: thickness of reaction layer
ξ: critical thickness of reaction layer
H: hardness
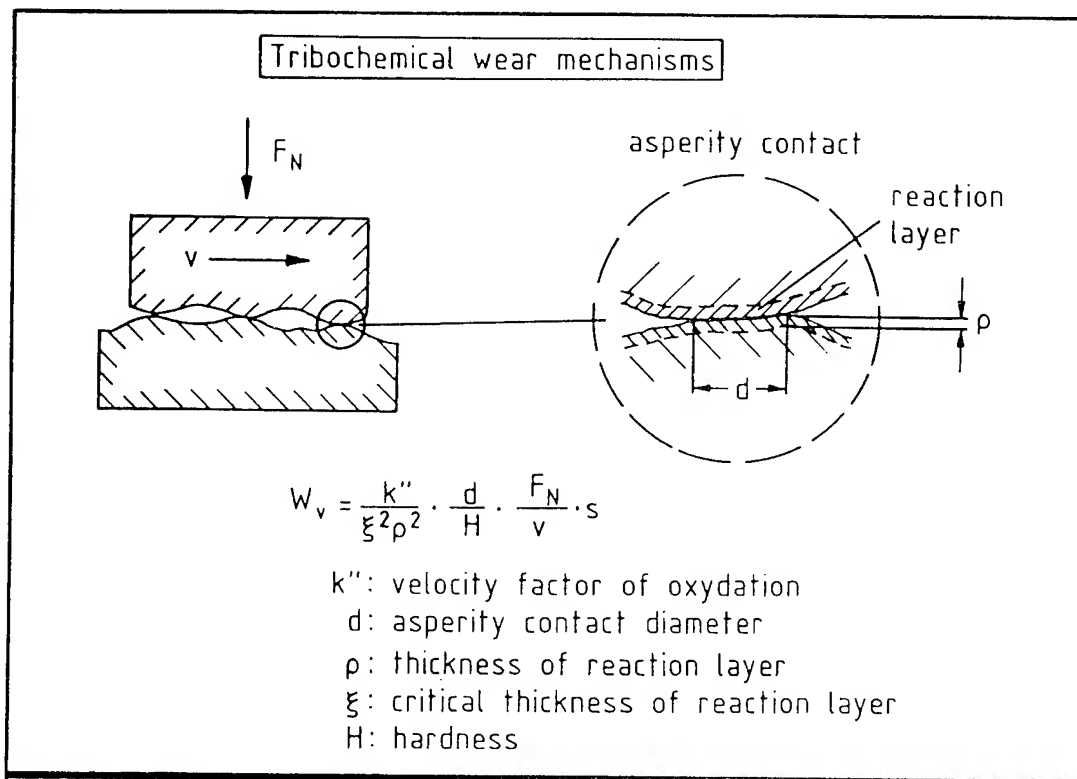
Fig. 7: Characteristics of tribochemical wear models

86

Starting with the assumption that tribochemically formed surface asperity layers are detached at a certain critical thickness, Quinn proposed a tribochemical wear hypothesis of the wear of steels, (ref. 39). In figure 7 the main characterizing parameters of tribo-chemical wear mechanisms according to Quinn are listed. Based on recent investigations on the oxidative wear of aluminium alloys, Eyre (ref. 40) concluded that tribochemical wear occurs by a process of oxidation, deformation and fracture to produce layers which are compacted into grooves in the metal surface. Oxidative surfaces become smoother with time as the troughs become filled with oxide, and oxidative wear then occurs by the fracture of plate-like debris.

4.4 Adhesive wear mechanisms

The adhesive wear processes are initiated by the interfacial adhesive junctions which form if solid materials are in contact on an atomic scale. As described in Section 3.2 depending on the nature of the solids in contact different adhesive junctions may result. The whole chain of events which lead to the generation of wear particles is summarized in figure 8. It is obvious that a number of properties of the contacting solids influence the adhesive wear mechanisms. Obviously the processes and parameters of adhesion (see Section 3.2) as well as those of fracture (see Sections 4.1 and 4.2) must be taken into account. Since both adhesion and fracture are influenced by surface contaminants and the effect of the environment it is quite difficult to relate adhesive wear processes with elementary bulk properties of materials. In vacuum where these influences are eliminated the following parameters have been observed to influence the adhesive wear processes of metal/metal pairs (ref. 41):

- Interfacial metallic adhesion bonding depends on the electronic structure of the contacting partners. It has been suggested that strong adhesion will occur if one metal can act as an electron donor, the other as an electron acceptor (ref. 9, 42, 43).

- Crystal structure exerts an influence on adhesive wear processes. Hexagonal metals in general exhibit lower adhesive wear charac-teristics than either body-centred cubic or face-centred cubic metals. This difference is assumed to be related to different plastic asperity contact deformation modes and the number of operable slip systems in the crystals, (ref. 44, 45).

- Crystal orientation influences the adhesive wear behaviour. In general high atomic density low surface energy grain orientations exhibit lower adhesion and less adhesive wear than other orien-tations (ref. 41).

- When dissimilar metals are in contact, the adhesive wear process will generally result in the transfer of particles of the cohesively weaker of the two materials to the cohesively stronger (ref. 41).

Fig 8: Characteristics of adhesive wear models

Table 6: Polymer pairs studied

The wear resulting through adhesive processes has been described phenomenologically by the well-known Archard equation, see figure 8, (ref. 46). This equation contains as only material property the hardness of the material. As is obvious from the above discussion, the Archard wear coefficient k depends on various properties of the materials in contact. However, it is not possible to describe the influence of materials properties on the wear coefficient k in a simple manner.

5. EXPERIMENTAL RESULTS ILLUSTRATING THE IMPORTANCE OF "INTERACTION CHARACTERISTICS" ON FRICTION AND WEAR BEHAVIOUR

The discussion on properties of solids with respect to friction and wear has shown that various factors influence the tribological behaviour of a given system. There are three groups of parameters which appear to be of special importance and which will be considered in some detail in connection with experimental friction and wear investigations on metals and polymers:

- Interfacial adhesion or surface energy

- Hardness of materials

- Surface topography characteristics.

A first example concerns the friction of thermoplastic polymers sliding against thermoplastic polymers. The materials studied are compiled in table 6. (Details of the experimental equipment used, the preparation of the specimens and the performance of the tests are given elsewhere, see ref. 47). The friction characteristics of the different polymer couples which were studied at very low sliding speeds are shown in figures 9 to 11. It can be seen that in any case a typical peak of the friction coefficient appears which is followed by different levels of friction for the various polymer/polymer combinations. Optical "in-situ" studies revealed (see ref. 47) that no detectable surface changes during sliding occurred, which indicated that the sliding took place in the original polymer/polymer interface. In order to relate the frictional behaviour of the polymer/ polymer pairs with material properties, the surface energies of the polymeric couples were calculated in using values of the surface energy, determined by Erhard (ref. 48). In table 7 the data of the experimentally determined frictional work and the calculated work of adhesion are compiled. In figure 12 the experimentally determined frictional work is plotted as a function of the calculated work of adhesion. It can be seen that in a logarithmic scale frictional work increases with the work of adhesion and that the experimental data seem to be in a reasonably good correlation with the theoretically calculated values. It appears that for the polymer combinations studied the adhesion component at the interface is the dominant factor governing the frictional behaviour of the polymer/polymer sliding pairs. Clearly the surface energy is an interaction characteristic rather than a simple material property.

89
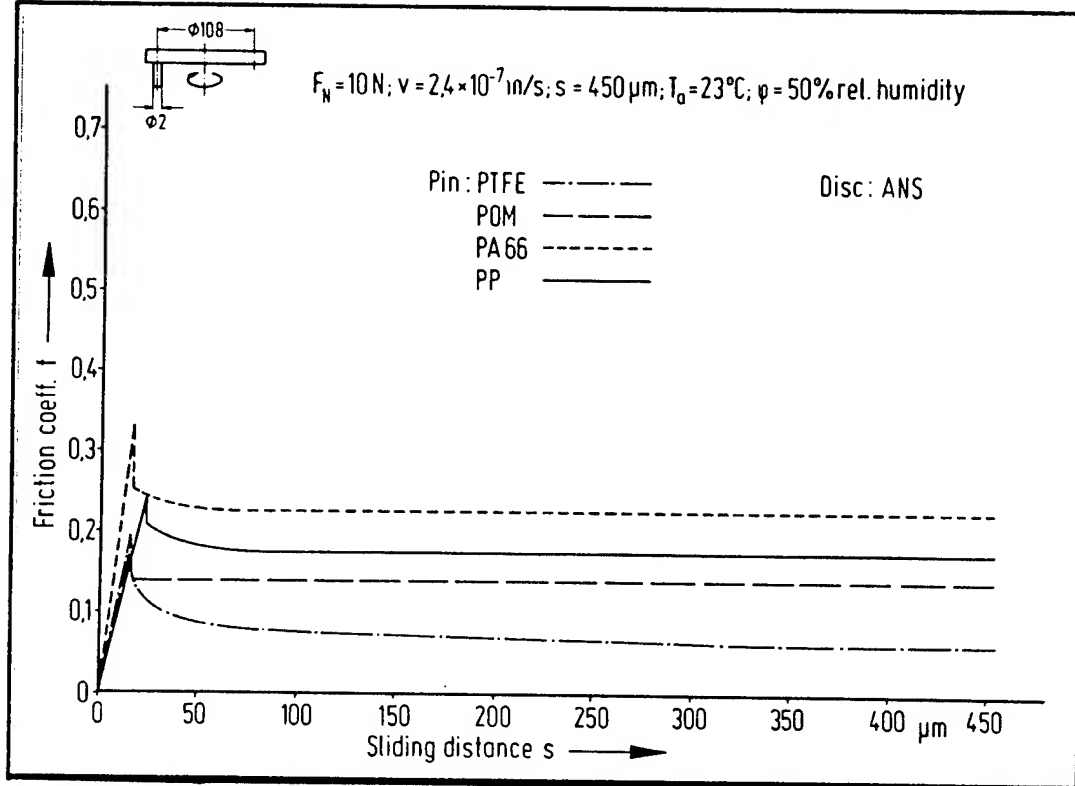
Fig. 9: Friction of polymer/polymer pairs
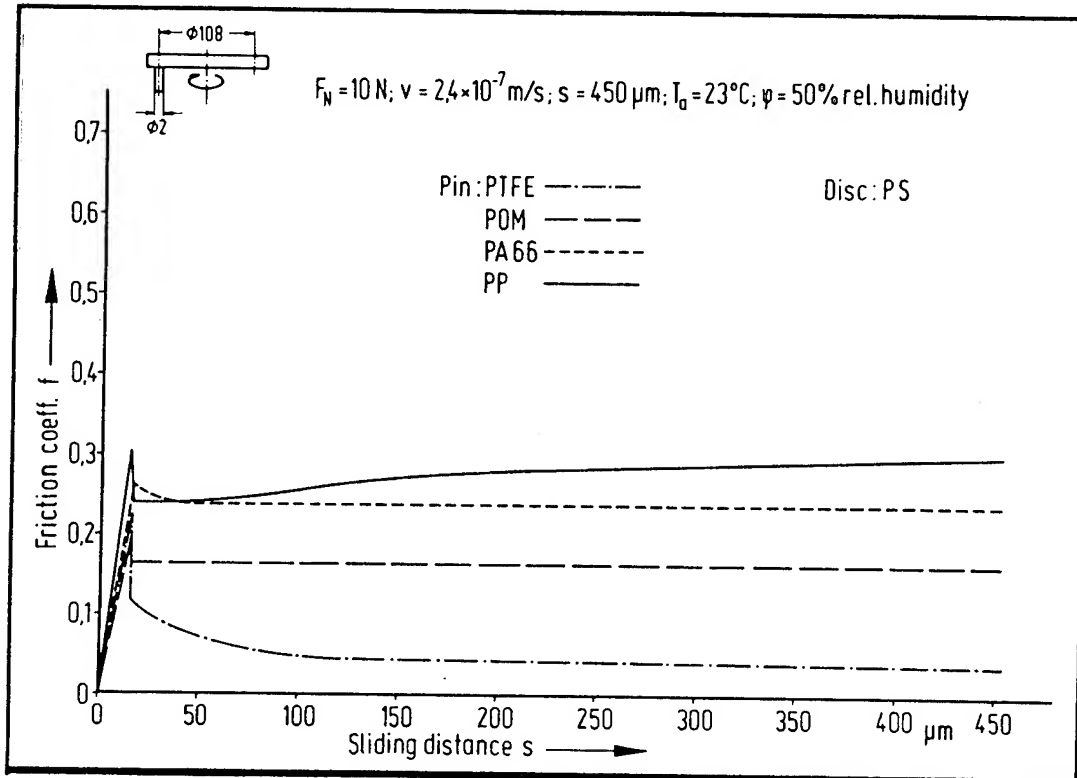
Fig. 10: Friction of polymer/polymer pairs
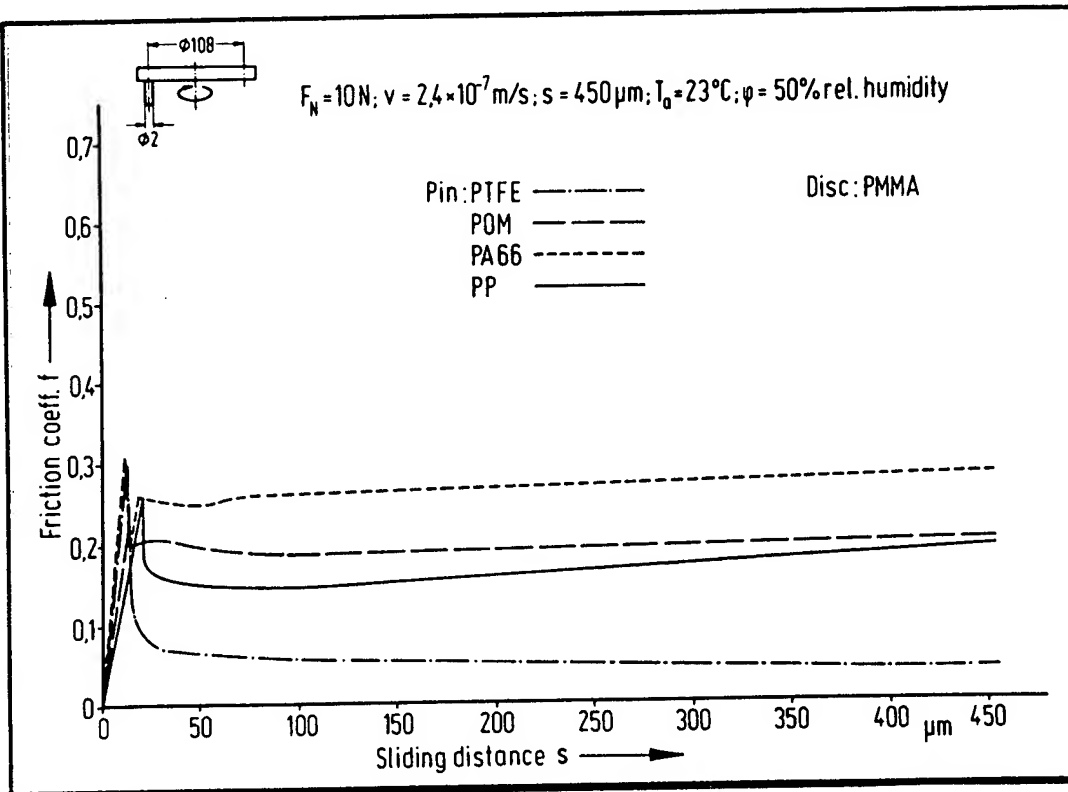
Fig. 11: Friction of polymer/polymer pairs

Pin	Disc	Frictional work E_F [Nmm]	Work of adhesion $\Delta\gamma = \gamma_1 + \gamma_2 - \gamma_{12}$ [10^{-6} Nmm/mm^2]
PTFE	ANS	0.328	54.7
	PS	0.343	55.4
	PMMA	0.324	53.6
PP	ANS	0.795	73.0
	PS	1.215	75.3
	PMMA	0.730	73.0
POM	ANS	0.619	84.5
	PS	0.760	81.0
	PMMA	0.850	87.3
PA66	ANS	0.987	88.0
	PS	0.864	83.1
	PMMA	1.128	92.1

Table 7: Work of friction and adhesion of polymers

91
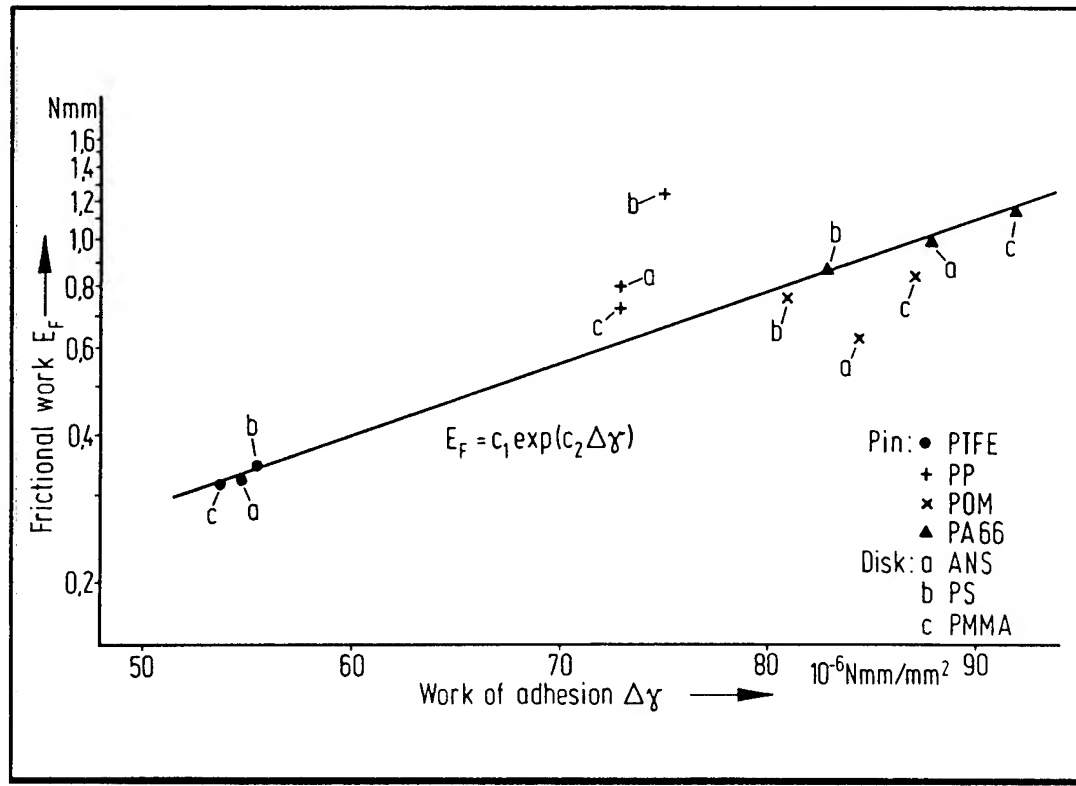
Fig. 12: Correlation between frictional work and work of adhesion

The equation shown in the figure:
$$E_F = c_1 \exp(c_2 \Delta \gamma)$$
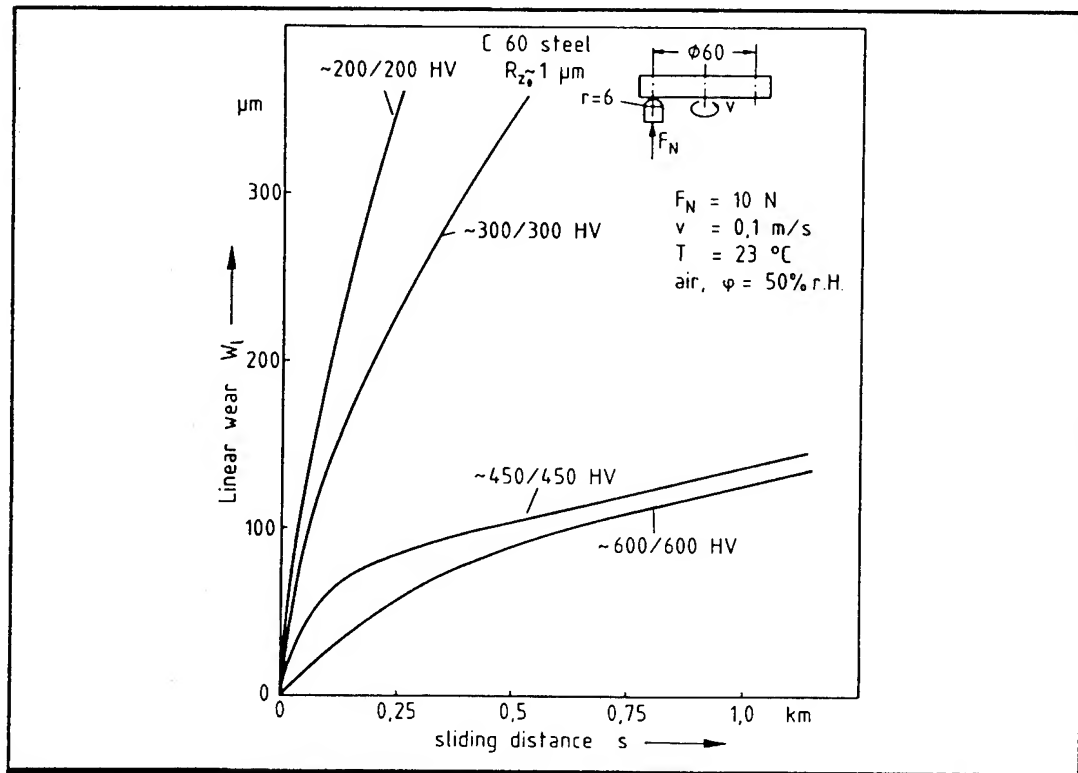
Fig. 13: Influence of hardness on sliding wear of steel

In another investigation the influence of hardness and surface topography on the sliding wear behaviour of plain carbon steel pairs was studied. The investigations were performed with a pin-on-disk configuration operating either in air (50 percent relative humidity) or under boundary lubrication (pure mineral oil). The specimens were prepared from one single batch and the different specimens were given different hardness and surface roughness values. (The experimental details and the material characteristics are described elsewhere, see ref. 49). In figure 13 wear as a function of sliding distance for specimen pairs of variable hardness is plotted. It can be seen that the wear curves decrease with increasing hardness as can be expected. The scanning electron micrographs of the pins shown in figures 14 to 17 indicate that different wear processes dominate: at low hardness adhesive processes prevail, which change to mainly tribochemical wear mechanisms for intermediate hardness, whereas for the highest hardness obviously abrasive processes dominate.

Some interesting effects are now observed if specimens of different hardness are combined. In figure 18 wear curves as function of sliding distance for two pairs of the same hardness ratio are plotted. (The initial mean peak-to-valley surface roughness R_z was the same for all specimens.) It can be seen that although the same material pair was used completely different wear curves result depending on the hardness values of the stationary and the moving partners: If the stationary pin is softer than the moving disk a comparably high initial amount of wear and a comparably low wear rate results (upper curve in figure 18) whereas if the stationary pin is harder than the moving disk a comparably lower initial amount of wear and a higher wear rate is observed (lower curve in figure 18).

In addition to the hardness ratio the surface roughness also plays an important role. This can be seen from figure 19 which shows wear curves for the same specimen pairs as in figure 18 but with different surface roughness values R_z. Also here a different influence of surface roughness must be noted: the influence of surface roughness is more pronounced for the specimen pair consisting of a soft stationary pin and a hard moving disk rather than for the specimen pair of a reversed hardness ratio.

In order to get an overview on the influences of both hardness and surface roughness, the steady state wear rate for all possible combinations of steel pairs of two hardnesses (~ 300 HV and ~ 600 HV) and two surface roughness values ($R_z \sim 1$ μm and $R_z \sim 4$ μm) were determined. In table 8 the relative wear rates are listed. It can be seen that the sliding combination of a rough soft stationary pin against a hard smooth moving disk has the lowest wear rate whereas sliding pairs consisting of either a rough soft stationary pin or a rough hard stationary pin against soft moving disk have the highest wear rate under the operating conditions chosen.

Fig. 14: Wear surface (C 60 steel, ~200 HV)
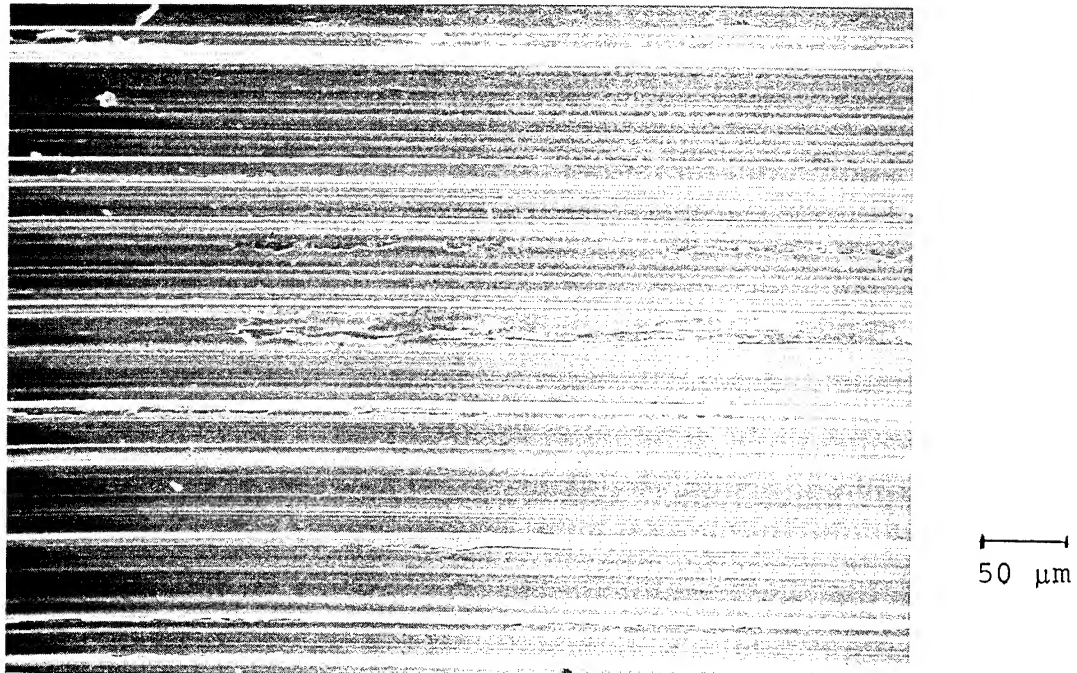
Fig. 15: Wear surface (C 60 steel, ~300 HV)
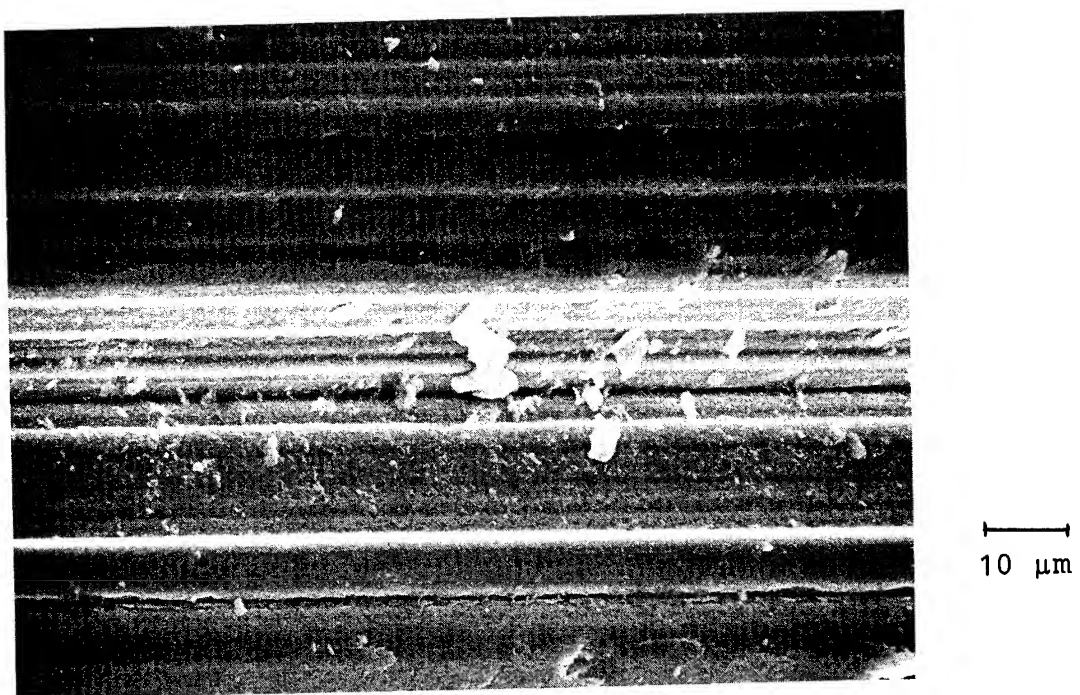
Fig. 16: Wear surface (C 60 steel, ∼450 HV)
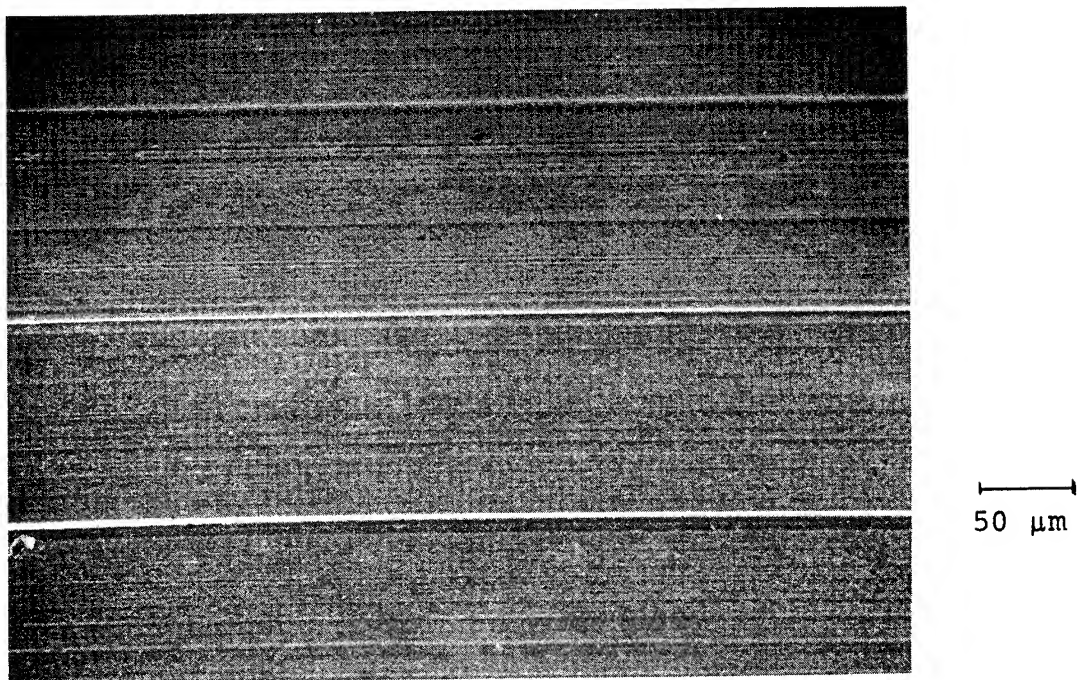
Fig. 17: Wear surface (C 60 steel, ∼600 HV)
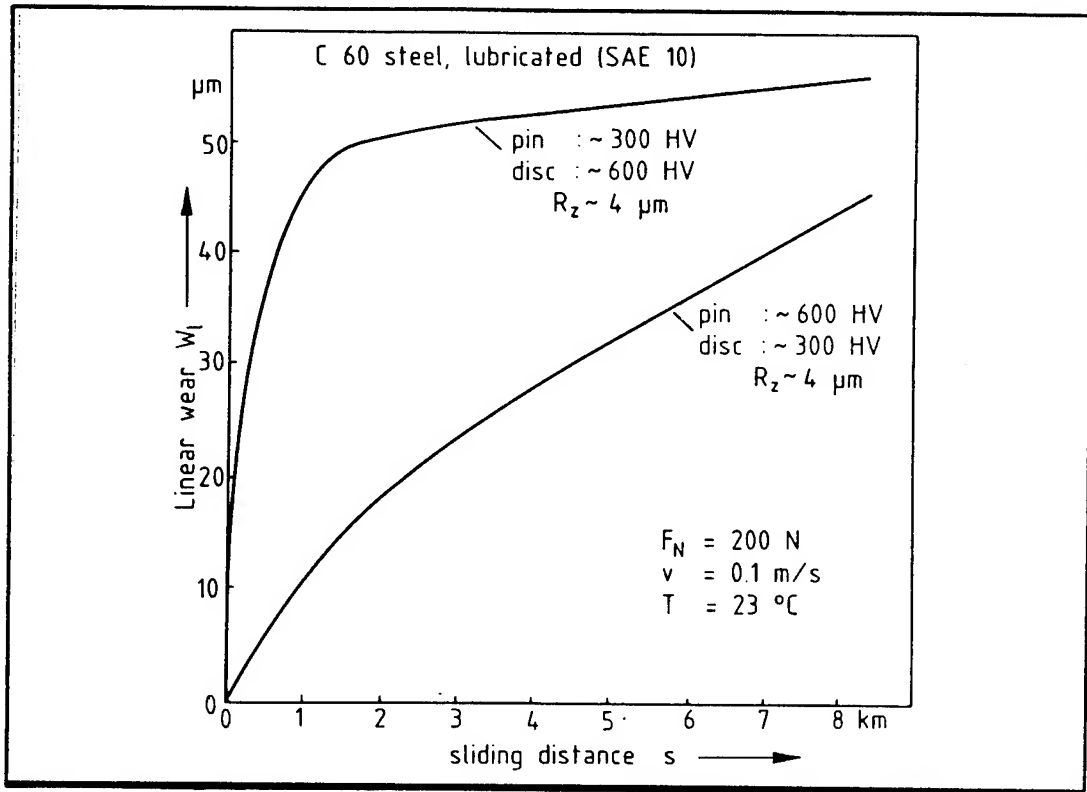
Fig. 18: Influence of hardness combinations
on sliding wear of steel
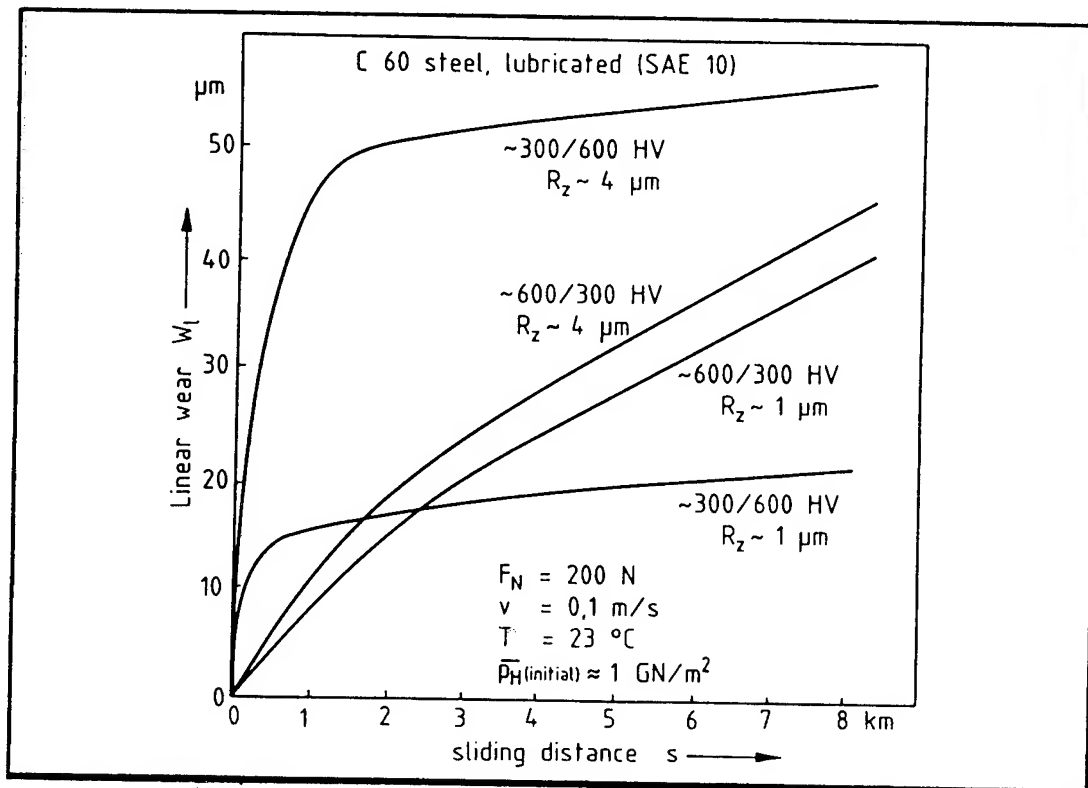
Fig. 19: Influence of hardness and surface
roughness on sliding wear of steel

96

disc (mov.)		~300 HV		~600 HV	
pin (stat.)	R_{zp} (µm)	1	4	1	4
~300 HV	1	20	22	2	3
	4	(25)	22	(1)	3
~600 HV	1	19	19	14	14
	4	(25)	20	12	11

Table 8: Relative wear rates of steel: dependence on hardness and roughness combinations

stationary pin [~300 HV]

30 µm / 100

moving disc [~300 HV]

stationary pin [~600 HV]

30 µm / 100

moving disc [~600 HV]

stationary pin [~300 HV]

30 µm / 100

moving disc [~600 HV]

stationary pin [~600 HV]

30 µm / 100

moving disc [~300 HV]

C 60 steel, $R_a \approx 1$ µm, lubricated (SAE 10)

$F_N = 200$ N, $v = 0,1$ m/s
$T = 23$ °C, $s = 8$ km
$\overline{p_H}$ (initial) ≈ 1 GN/m^2
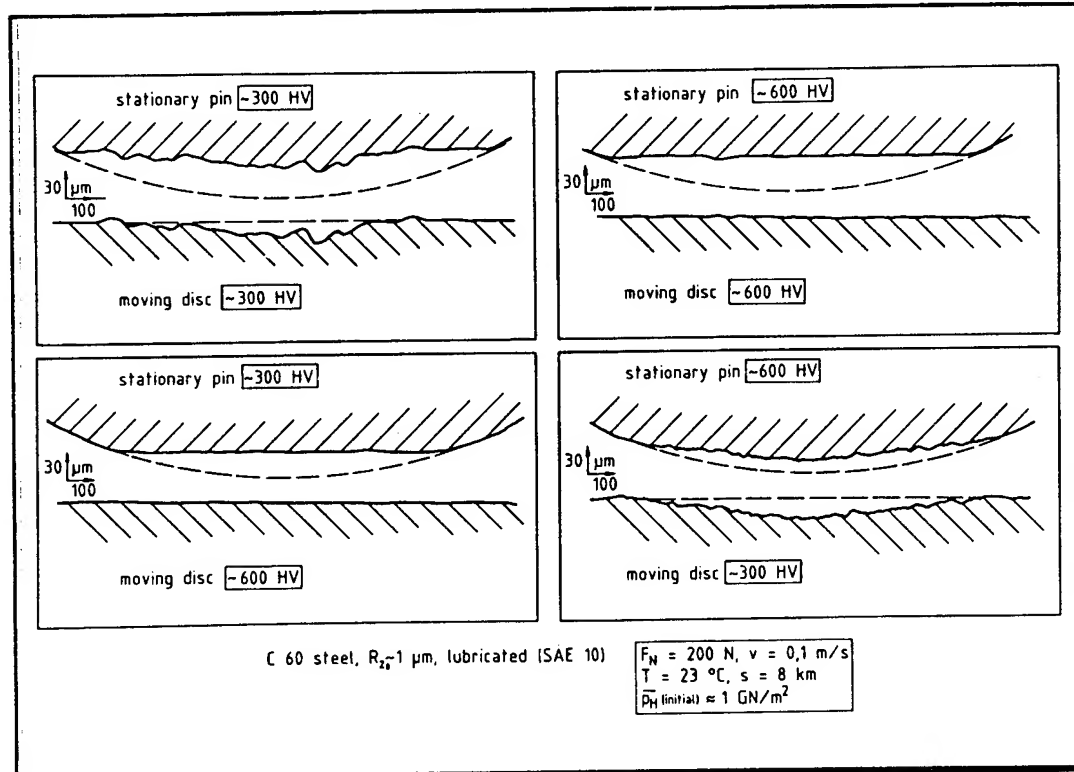
Fig. 20: Wear surfaces: influence of different hardness combinations

In addition to the wear rates also the surface topography of the worn surface is greatly influenced by the hardness ratio of the moving/stationary specimen pair. This can be seen from figure 20 which shows profilograms (perpendicular to the sliding direction) of the surfaces of the stationary pin and the moving disk. (In this case the initial surface roughness and all the operating conditions were the same for all specimen pairs.) Without going into details it is interesting to note that - contrary to common expectations - the surface of a hard stationary pin is more severely worn by a soft moving disk than by a hard moving disk (see diagrams on the right of figure 20). This again indicates that - depending on the hardness ratio of the stationary/moving sliding pair - different interfacial wear mechanisms dominate as discussed already above (see figures 14 to 17). In trying to understand this unexpected behaviour it must be noticed that the interfacial processes acting on pin and disk are not only influenced by the bulk material properties but also by the geometric contact conditions as discussed below (see figure 21.).

The experimental results discussed phenomenologically in this section clearly show that the friction and wear behaviour of a sliding tribosystem is greatly influenced by "interaction characteristics" - like surface energy, hardness and surface roughness ratios as well as the geometric contact condition of the stationary/moving sliding pairs - in addition to the single properties of solids discussed above.

6. SUMMARIZING DISCUSSION

The survey presented in this paper has shown that various properties of solids influence the tribological behaviour. The basic tribologically relevant properties may be classified into different groups:

- Surface and interface properties
- Physical properties
- Mechanical properties
- Microstructural parameters

The main parameters together with an indication of the basic tribological processes which are influenced by them are compiled in table 9. In addition to this it has been estimated that there are certain material-related criteria which must be fulfilled in order that certain tribological processes occur. Some of these criteria, which may be considered as rough guidelines only, are compiled in table 10 (see ref. 50).

In addition to the summary of tribologically important properties of solids as compiled in tables 9 and 10 attention must also be given to geometric properties of the components of sliding tribosystems as characterized for example by the so-called tribocontact

98

Basic tribologically relevant properties of solids

Surface and interface properties

• surface topography	→ deformation
• surface energy	→ adhesion, friction
• interfacial shear strength	→ friction, material transfer
• adsorbed layers, surface films	→ adhesion, friction, tribochemical effects

Physical properties

• bond type	→ adhesion, friction
• electronic structure	
• heat conductivity	→ thermal effects

Mechanical properties

• elastic modulus	→ deformation
• yield pressure	
• hardness	→ deformation, abrasion
• shear strength	→ deformation, friction
• fracture toughness	→ asperity fracture

Microstructural parameters

• crystal structure and orientation	→ deformation
• dislocation distribution	
• work-hardening and recovery	→ deformation, abrasion
• stacking fault energy	→ abrasion
• second phases	
• alloying elements	→ adhesion, abrasion

Table 9: Overview on tribologically relevant
properties of solids

Tribological processes	Criteria
• Elastic contact deformation	plasticity index < 1
• Plastic contact deformation	plasticity index > 1
• Stress distribution mode:	
— max. shear stress below surface	friction coeff. $< 0{,}25$
— max. shear stress at surface	friction coeff. $> 0{,}25$
• Adhesion and plastic flow	$\dfrac{\text{interfacial shear strength}}{\text{flow stress of material}} > 0{,}5$
• Fatigue failure (low cycle)	$\dfrac{\text{max. appl. (Hertzian) shear stress}}{\text{yield stress in shear}} > 0{,}2$
• Asperity fracture	$\dfrac{\text{applied strain}}{\text{critical strain of material}} > 1$
• Abrasive material removal	$\dfrac{\text{hardness of abrasive}}{\text{hardness of material}} > 1{,}3$

Table 10: Simplified material-related criteria
for tribological processes

99

parameter ε (ref. 51). In figure 21 the definition of this parameter together with its relevance for the components of sliding tribosystems is given. From the results of the experimental data shown in figures 18, 19, 20 it appears obvious that the tribocontact parameter must be taken into consideration if the influence of material properties like hardness and surface roughness on the friction and wear behaviour of a given tribosystem is discussed.

Finally it must be pointed out that - generally speaking - the properties of solids discussed in this paper and summarized in table 9 are only one part of the whole parameters of a "tribological system". Thorough systematic analyses of the basic parameters of tribological systems have shown (see ref. 51) that the friction and wear behaviour is determined by the parameter groups summarized in a highly simplified manner in figure 22, namely:

- the set of the operating variables
- the structure of the tribo-system, i.e.
  - the material components of the system
  - the tribologically relevant properties of the system's components
- the tribological interactions between the system's components
- the friction-induced energy losses and the wear-induced material losses resulting from the tribological interactions which are initiated by the action of the operating variables on the structure of the pertinent tribo-system.

Although a discussion of the details of the parameter groups of tribological systems summarized in figure 22 is beyond the scope of this paper, it is obvious that in order to understand the importance of certain properties of solids on the friction and wear behaviour in a given tribological situation a comprehensive systematic analysis of the basic influencing parameters is necessary. To support such systematic analyses a methodology together with a data sheet of relevant parameters has been worked out which is contained in a recent German Standard on Wear (see ref. 52). Table 11 shows a simple framework for the compilation of relevant properties of the components of tribological systems. The use of such data sheets may be helpful for both the planning of meaningful tribological tests (especially for the problem of laboratory simulation tests) and the documentation of the obtained results of tribological investigations.
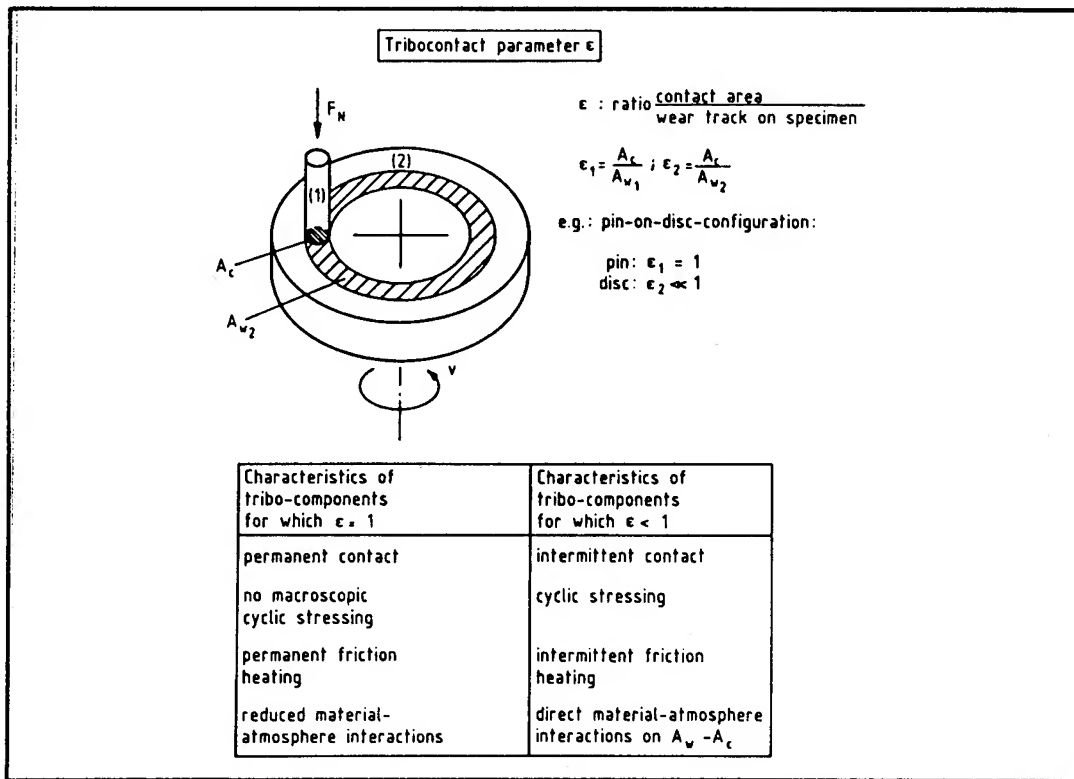
Fig. 21: The tribocontact parameter:
an important interaction characteristic
of tribological systems
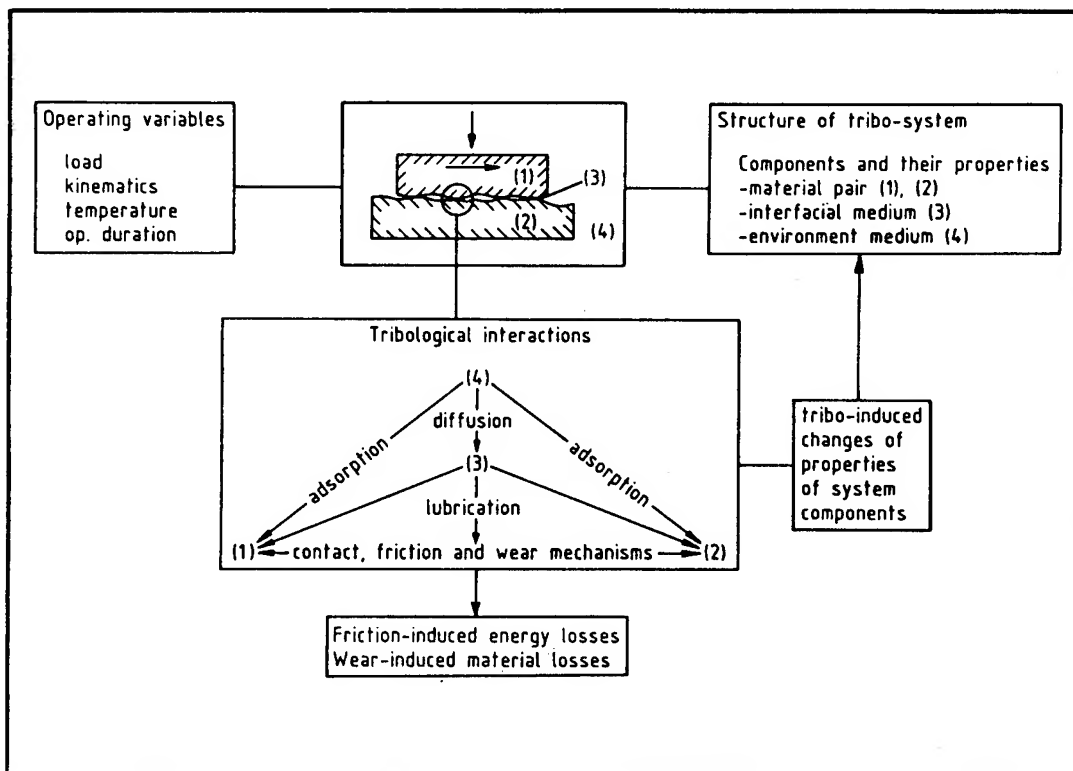
Fig. 22: Basic parameter groups of
tribological systems

101

I Technical function of the tribo-system

II Operating variables	
Type of motion :	Duration of operation t[ ]:

Load $F_N(t)$ [ ]	Velocity $v(t)$ [ ]	Temperature $T(t)$ [ ]

Other op. variables:	Location:

III Structure of the tribo-system

Properties of elements (initial/final)		Tribo-element (1)	Tribo-element (2)	Lubricant (3)	Atmosphere (4)
Designation of element and material					
Volume properties	Geometry/Dimensions/ Volume				
	Chemical composition				
	Phys.-mech. data: Hardness Viscosity $\eta(T,p)$ other				
Surface properties	Topography descriptors (c.l.a.,etc)			Other data:	
	Surface layer data (if different from volume)				

Contact area A[ ]		Tribological interactions: (1) (2) (3) (4)
Ratio: $\dfrac{\text{contact area}}{\text{total wear track}}$ ε [%]	ε(1) ε(2)	
App. lubrication mode:		

IV Tribological characteristics

Changes in properties of the elements	Friction data (vs time t or distance s)	Wear data (vs time t or distance s)

Other characteristics (e.g.: contact resistance, vibrations, noise, etc):	Appearance of worn surfaces:

Table 11: Data sheet

REFERENCES

1. Dowson, D.: History of Tribology, London: Longman, 1979.

2. Czichos, H.: Solid Friction - A Sub-Area of Tribology (in German), Umschau, (1971) 116.

3. Suh, N.P. and Sin, H.C.: The Genesis of Friction, Wear, 69 (1981) 91.

4. Tabor, D.: Friction - the Present State of Our Understanding, Trans ASME (JOLT), 103 (1981) 169.

5. Thomas, T.R. (Editor): Rough Surfaces, London: Longman, 1982.

6. Gane, N.: The Direct Measurement of the Strength of Metals on a Sub-Microscopic Scale, Proc. Roy. Soc. (London) Series A 317, (1970) 367.

7. Pethica, J.B. and Tabor, D.: Contact of Characterized Metal Surfaces at Very Low Loads: Deformation and Adhesion, Surf. Sci., 89 (1979) 182.

8. Maugis, D.: Creep, Hot Hardness and Sintering in the Adhesion of Metals at High Temperatures, Wear, 62 (1980) 349.

9. Czichos, H.: The Mechanism of the Metallic Adhesion Bond, J. Phys. D: Appl. Phys. 5 (1972) 1890.

10. Ferrante, J., and Smith, J.R.: A Theory of Adhesion at a Bimetallic Interface: Overlap Effects, Surf. Sci., 38 (1973) 77.

11. Ferrante, J. and Smith, J.R.: Metal Interfaces: Adhesive Energies and Electronic Barriers, Solid State Comm., 20 (1976) 393.

12. Rabinowicz, E.: Friction and Wear of Materials, New York: Wiley, 1965.

13. Marx, U. and Feller, H.G.: Correlation of Tribological and Mechanical Characteristics Studied on the Example of Gold, Gold-Tantal-Alloys and Nickel - Part III: Tribological Theories and Ranges of Validity (in German), Metall, 33 (1979) 380.

14. Gümbel, L.: Friction and Lubrication in Mechanical Engineering (in German), Berlin, 1925.

15. Landheer, D. and Zaat, J.H.: The Mechanism of Metal Transfer
    in Sliding Friction, Wear, 27 (1974) 129.

16. Zum Gahr, K.-H.: Abrasive Wear of Metallic Materials (in German),
    VDI-Fortschr. Ber., Reihe 5, Nr. 57, 1981, Düsseldorf,
    VDI-Verlag.

17. Sin, H.C., Saka, N. and Suh, N.P.: Abrasive Wear Mechanisms
    and the Grit Size Effect, Wear 55 (1979) 163.

18. Green, A.P.: The Plastic Yielding of Metal Junctions Due to
    Combined Shear and Pressure, J. Mech. Phys. Solids,
    2 (1955) 197.

19. Drescher, H.: The Mechanics of Friction Between Solid Bodies
    (in German), VDI-Z., 101 (1959) 697.

20. Challen, J.M. and Oxley, P.L.B.: An Explanation of the Different
    Regimes of Friction and Wear Using Asperity Deformation Models,
    Wear, 53 (1979) 229.

21. Heilmann, P. and Rigney, D.A.: An Energy-Based Model of Friction
    and Its Application to Coated Systems, Wear, 72 (1981) 195.

22. Burwell, J.T.: Survey of Possible Wear Mechanisms, Wear,
    1 (1959) 119.

23. Czichos, H. and Habig, K.H.: Basic Wear Mechanisms of Metallic
    Materials - Recent Results of Research (in German),
    VDI-Berichte, Nr. 194, 1973, p.23.

24. Briscoe, B.: Wear of Polymers - An Essay on Fundamental Aspects,
    Tribology international, 14 (1981) 231.

25. Rigney, D.A. (Editor): Fundamentals of Friction and Wear of
    Materials, Metals Park: ASM, 1980.

26. Habig, K.-H.: Wear and Hardness of Materials (in German),
    München: Hanser Verlag, 1980.

27. Czichos, H. et al.: Friction and Wear of Materials, Components
    and Constructions (in German), Grafenau: Expert-Verlag, 1982.

28. Suh, Nam P.: Surface Interactions, in: Tribological Technology,
    Vol. I (Editor: P. Senholzi), The Hague: Martinus Nijhoff
    Publishers, 1982, p.37-208.

29. Tabor, D.: Wear - A Critical Synoptic View, Proc. Internat. Conf.
    on Wear of Materials, New York: ASME, 1979, 1.

30. Lang, O.R.: Surface Fatigue of Plain Bearings,
    Wear, 43 (1977) 25.

31. Kuhlmann-Wilsdorf, D.: Dislocation Concepts in Friction and Wear, see ref. 25, p.119-186.

32. Halling, J.: A Contribution to the Theory of Mechanical Wear, Wear, 34 (1975) 239.

33. Suh, Nam P.: The Delamination Theory of Wear, Wear, 25 (1973) 111.

34. Hirth, J.P. and Rigney, D.A.: Crystal Plasticity and the Delamination Theory of Wear, Wear, 39 (1976) 133.

35. Füchsel, M.: On the Wear of Materials During Dry Friction (in German), Organ Fortschr. Eisenbahnwes.,84 (1929) 413.

36. Krushov, M.M.: Principles of Abrasive Wear, Wear, 28 (1974) 69.

37. Hornbogen, E.: The Role of Fracture Toughness in the Wear of Metals, Wear, 33 (1975) 251.

38. Zum Gahr, K.-H.: Abrasive Wear of Ductile Metals (in German), Z.f.Metallkunde, 73 (1982) 267.

39. Quinn, T.F.J.: The Effect of "Hot-Spot" Temperatures on the Unlubricated Wear of Steel, ASLE Trans., 10 (1967) 158.

40. Razavizadeh, K. and Eyre, T.S.: Oxidative Wear of Aluminium Alloys, Wear, 79 (1982) 325.

41. Buckley, D.H.: Surface Effects in Adhesion, Friction, Wear, and Lubrication, (Tribology Series Vol. 5), Amsterdam: Elsevier, 1981.

42. Buckley, D.H.: Adhesion of Metals to a Clean Iron Surface Studied with LEED and Auger Emission Spectroscopy, Wear, 20 (1972) 89.

43. Ohmae, N., Okuyama, T. and Tsukizoe, T.: Influence of Electronic Structure on the Friction in Vacuum of 3 d Transition Metals in Contact with Copper, Tribology international, 13 (1980) 177.

44. Buckley, D.H. and Johnson, R.L.: The Influence of Crystal Structure and Some Properties of Hexagonal Metals on Friction and Adhesion, Wear, 11 (1968) 405.

45. Habig, K.-H.: On the Dependence of Adhesion and Dry Friction of Metals on Structure and Orientation (in German), Material-prüfung, 10 (1968) 417.

46. Archard, J.F.: Wear Theory and Mechanisms, in: Wear Control Handbook (Editors: M.B. Peterson and W.O. Winer), New York: ASME, 1980, p.35-80.

47. Czichos, H. and Feinle, P.: Tribological Behaviour of Thermo-
    plastic Polymers - Contact Deformation, Friction and Wear,
    Surface Investigations (in German), Berlin: BAM-Research
    Report, No. 83, July 1982.

48. Erhard, G.: On the Sliding Friction of Polymer/Polymer Pairs
    (in German), Düsseldorf: Jahrbuch der VDI-Ges. Werkstoff-
    technik, 1981, p.7-15.

49. Czichos, H.: Systematics of Tribological Testing (in German), in:
    Tribologie - Reibung, Verschleiß, Schmierung (Editors: W. Bunk,
    J. Hansen, M. Geyer), Vol. 4, Berlin: Springer-Verlag,
    in print.

50. Childs, T.H.C.: The Sliding Wear Mechanisms of Metals, Mainly
    Steels, Tribology international, 13 (1980) 285.

51. Czichos, H.: Tribology - A Systems Approach to the Science and
    Technology of Friction, Lubrication and Wear, Amsterdam:
    Elsevier, 1978.

52. German Standard DIN 50 320: Wear - Terms, Systems Analysis of
    Wear Processes, Classification of the Field of Wear (available
    in English), Berlin: Beuth-Verlag, Dec. 1979.

DISCUSSION

Juniti Sato
Tokyo University of Mercantile Marine
Etchujima, Koto-ku
Tokyo, Japan

I would like to express my appreciation for the systematic compilation of numerous parameters in friction and wear conducted by Professor Czichos.

Being interested in the experimental results shown in Fig. 13 and Table 8, I would like to ask the author why the most beneficial pair is 300/600 Hv under lubricated condition in spite of 600/600 Hv under unlubricated condition.

I should also like to know the author's view on the critical condition to translate from mild wear to severe wear in relation to the properties of steel.

107

DISCUSSION

John A. Schey
Department of Mechanical Engineering
University of Waterloo
Waterloo, Ontario, N2L 3G1

The work of Dr. Czichos [1] has done much to alert tribologists to the importance of adopting a systems view of the complex material and process interactions typical of most friction and wear situations. Interactions become more complex yet when one of the contacting bodies suffers plastic deformation, as is the case in metalworking processes. The problem is fully considered in a recent monograph [2], and it should suffice here to highlight the special features introduced by plastic deformation, with special emphasis on the role of adhesion.

The complexity of the system is illustrated in Fig.1 [2]. Elastic contact, with contact limited to asperities, is characteristic of some sheet metalworking processes, but in the majority of instances the bulk of the workpiece undergoes plastic deformation, and the real area of contact may reach 100% of the apparent area of contact. A fundamental difference relative to other tribological systems is that, because of the plastic deformation of the workpiece, a substantial portion of the surface consists of virgin metal; this portion reaches 100% in metal cutting. Consequences can be severe.

1. In the absence of a suitable parting film, metal-to-metal contact sets in between tool and workpiece. Adhesion between the two assumes critical importance because it determines whether welding and metal transfer (usually in the form of tool pickup) will occur. Operation under high-adhesion conditions is possible in metal cutting, but damage to the workpiece surface often forces a

termination of plastic deformation processes. Tool pickup is, indeed, a danger whenever the lubricant film interposed between die and workpiece is locally disrupted. For this reason, a better understanding of factors governing adhesion is vital, yet our knowledge is still severely limited. The work of Buckley [3], Ferrante [4], and Czichos [1] has done much to develop models of adhesion on the basis of the electronic structure of metals. It is not clear how these models can be applied to the more complex alloys used in practice and, especially, to die materials. Unfortunately, models based on metallurgical properties such as crystal structure, hardness, stacking fault energy, solubility, etc. can give little more guidance. Yet the practical success of particular die-workpiece combinations cannot be denied, as evidenced by the example of the aluminum bronze dies used in the forming of stainless steels.

2. Desirable as reduced adhesion may be, a change of die material (or of surface coating) may unbalance the tribological system with undesirable consequences. An example of this is seen in Fig.2 [5] in which friction and surface damage (L = light, M = medium, H = heavy) in twist compression is shown for various workpiece materials rotating against steel (ST.), tungsten carbide (WC), or boronized steel (B) anvils. The boronized surface which, relative to an uncoated steel, reduces adhesion and surface damage in dry sliding, actually prevented the beneficial reactions evident with chlorinated paraffin in testing 4140 steel.

3. Adhesion may be changed also by the application of a soft metal coating to the workpiece surface. Such coatings have the advantage that they can follow the extension of the workpiece surface and thus prevent contact between substrate and die materials, even after substantial deformation has been imposed. Traditionally, metal films have been regarded as agents that lower

109

friction by their low shear strength. It now appears that this view is too narrow, and that the system comprising the coating and the superimposed lubricant must be considered. In this, the microtopography of the metal coating plays a powerful role. Thus, reflowed electrolytic tin or hot-dipped zinc coatings have the possible advantage of firm attachment to the substrate by reaction products. However, their smooth surface is a disadvantage, because it is unable to carry sufficient lubricant into the deformation zone and, most importantly, cannot prevent lubricant displacement in the deformation zone. In contrast, unreflowed electrolytic tin or electrolytically deposited zinc possess a favorable microtopography, with minute surface pockets that help to maintain a lubricant film and thus minimize tool pickup and workpiece damage. An example of this has been given by Apel and Nünninghoff [6]; an electrolytically deposited zinc coating survived 17 wiredrawing passes without damage and with hydrodynamic pockets still in evidence (Fig.3a), whereas a hot-dipped wire suffered severe scoring and loss of metal (Fig.3b).

4. The need for a systems view is evident also from the work on steel sheet used in pressworking, especially for automotive purposes. Die pickup is inadmissible because workpiece scoring would cause rejection of the part. Since the nominal composition of the sheet is fixed by formability, end use, and cost considerations, only surface topography is available as a freely controllable variable. It was recognized a long time ago that some minimum roughness is necessary to assure adequate entrapment volume for the lubricant. Adequate spacing of asperities was also recognized as a prerequisite for the control of the restraint applied by means of a blankholder. Figure 4 [1] summarizes the presently proposed criteria [7-12]. The manufacture and especially annealing conditions also have an effect, and, with advances in surface analytical tech-

niques, it can be shown that there are indeed variations in surface composition that may account for the differences observed in the scoring tendency (and friction ratio, Fig.4) of sheet of nominally the same composition but of different origins. Nevertheless, much remains to be done in both the geometrical and chemical characterization of surfaces.

5. The powerful tool-workpiece interactions also account for many of the difficulties of modelling friction in metalworking. While substantial advances have been made in the mathematical treatment of plastohydrodynamic lubrication [13], most practical situations involve mixed-film lubrication with often substantial proportions of boundary, E.P. and/or metal-to-metal contact. For ease of calculation, it is customary to describe interface friction with either a coefficient of friction (relating shear strength to interface pressure) or with a frictional shear factor (relating shear strength to the flow strength of the workpiece material). The latter treatment is of limited applicability from the physical point of view [14] but is, nevertheless, widely used because of the convenience it offers in the mathematical treatment of processes. The only truly valid descriptor of the interface is its shear strength under the conditions prevailing in the system, but it is doubtful whether this will ever be predictable from basic principles and properties, unless the interface is simply a continuous lubricant film of known rheological properties.

6. Wear under metalworking conditions can be severe and, especially in cutting processes, tool lives may be measured in only minutes. Adhesion, together with chemical stability and reactivity, again plays a vital role, and great advances in the development of tool materials would become possible if it could be predicted from basic principles.

REFERENCES

1. H. Czichos, Tribology--A Systems Approach to the Science and Technology of Friction, Lubrication, and Wear, Elsevier, Amsterdam, 1978.

2. J.A. Schey, Tribology in Metalworking: Friction, Lubrication, and Wear, American Society for Metals, Metals Park, OH, 1983 (to be published).

3. D.H. Buckley, Surface Effects in Adhesion, Friction, Wear and Lubrication, Elsevier, Amsterdam, 1981.

4. J. Ferrante, J.R. Smith and J.H. Rose, in: Microscopic Aspects of Adhesion and Lubrication (J.M. Georges, ed.), Elsevier, Amsterdam, 1982, pp.19-30.

5. J.A. Schey and J.A. Newnham, Lubric. Eng., 26, 1970, 129-137.

6. G. Apel and R. Nünninghoff, Stahl u. Eisen, 100, 1980, 1247-1253.

7. C.R. Weymueller, Metal Progr., 88(4), 1965, 213-233.

8. Am. Deep Dr. Res. Group, Sheet Metal Ind., 54, 1977, 147-153.

9. M. Littlewood and J.F. Wallace, ibid., 41, 1964, 925-930.

10. R.D. Butler and R.J. Pope, ibid., 44, 1967, 579-592, 597.

11. R.R. Hilsen and L.M. Berwick, in: Formability Topics--Metallic Materials, STP 647, ASTM, Philadelphia, pp.220-237.

12. A. Bragard et al, in: Sheet Metal Forming and Formability (Proc. 10th IDDRG Congress), Portcullis Press, Redhill, 1978, pp.253-278.

13. W.R.D. Wilson, J. Appl. Metalwork., 1(1), 1979, 7-19.

14. J.A. Schey, in Metal Forming Plasticity (H. Lippmann, ed.), Springer, Berlin, 1979, pp.336-348.
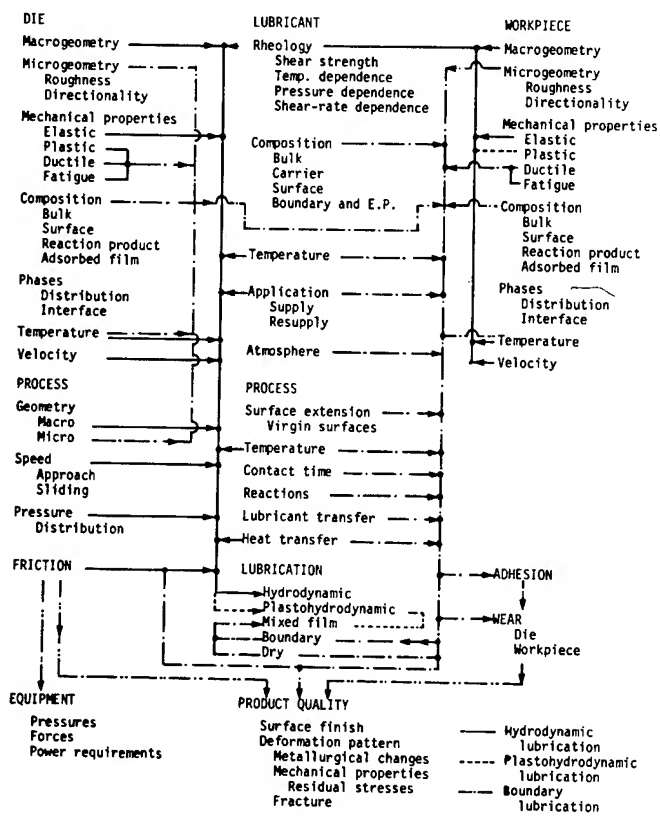
Fig.1. Tribological interactions in metalworking processes (2).
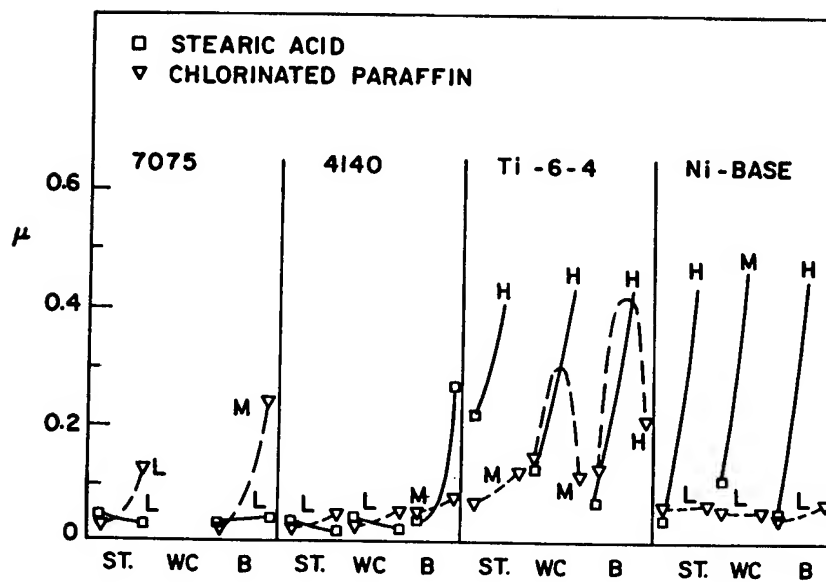

Fig.2. Friction and surface damage in twist-compression testing (after 5).

113

a

b
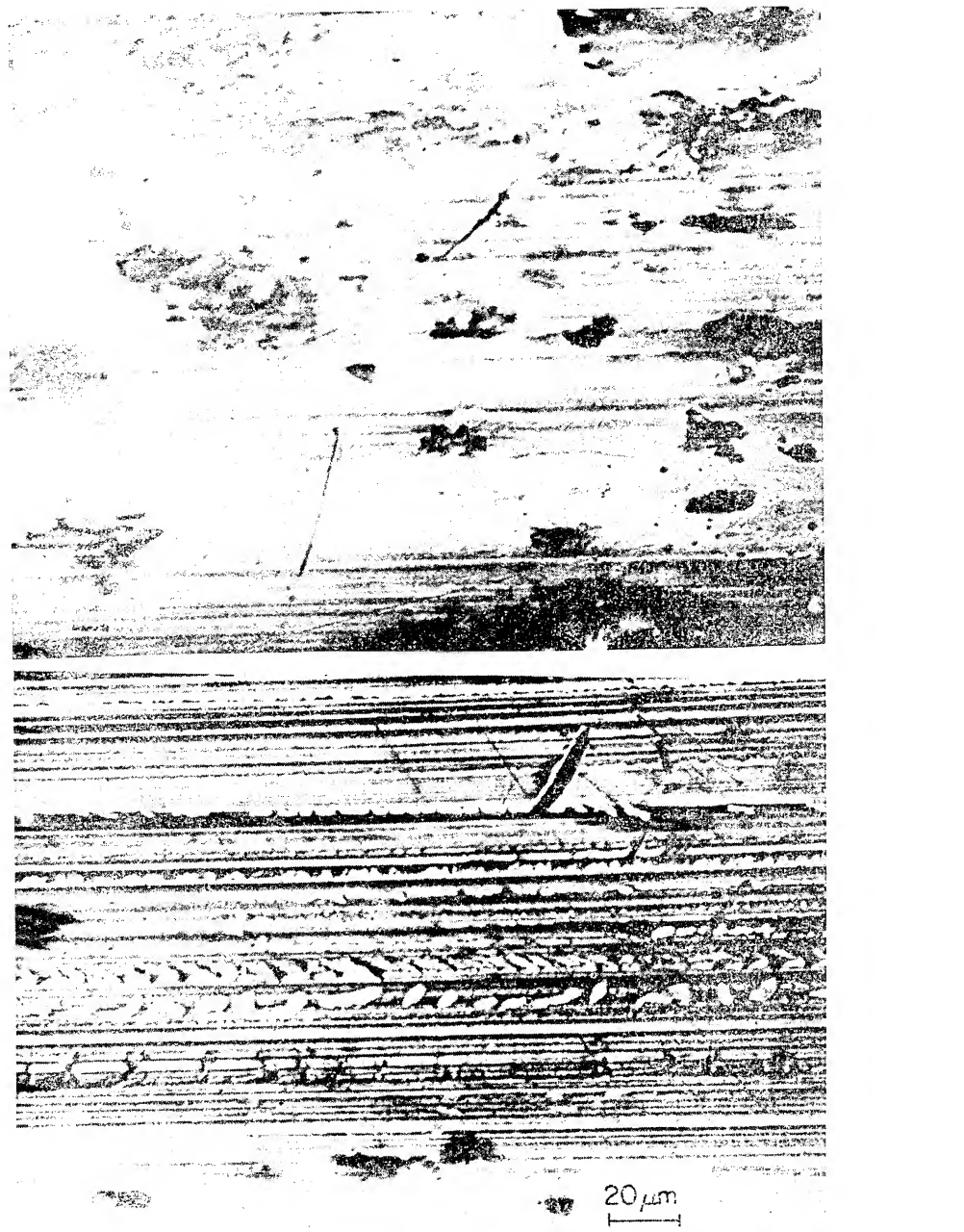
Fig.3. Appearance of surface of zinc-coated wire after 17 draws;
(a) electrolytic and (b) hot-dipped zinc coating (6).
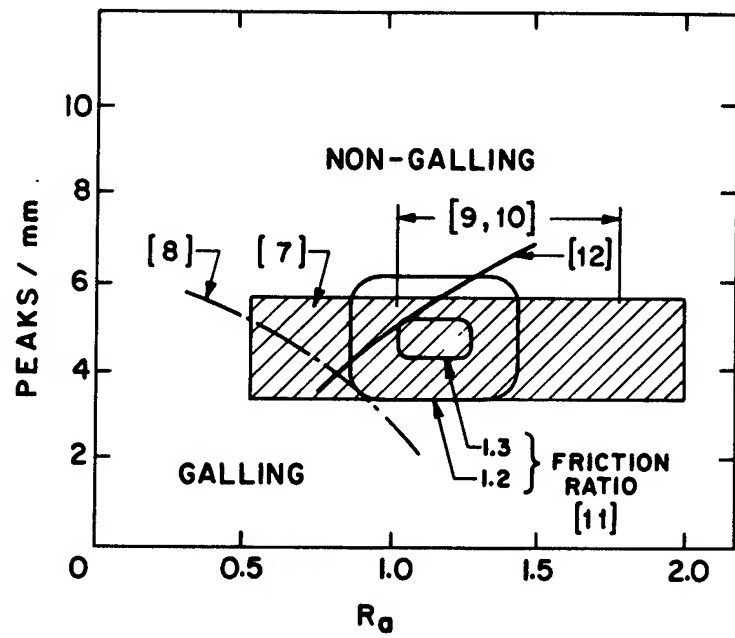
Fig.4. Surface roughness specifications for automotive sheet steel (2).

RESPONSE

Horst Czichos
Bundesanstalt fur Materialprufung
Berlin, Federal Republic of Germany

I like to thank Professor Sato for his interesting questions. The first question concerns the tribological behaviour of material pairings of hardness ratios of 300/600 HV and 600/600 HV. In the frist case (i.e. a soft stationary pin sliding against a hard moving disc under lubricated conditions) initially a pronounced running-in effect at the soft stationary pin takes place. Thus the interacting surfaces can "adjust themselves" leading to self-accomodation and a low steady state wear rate. Because of the lubrication, mild adhesive/tribo-oxidative processes prevail.

In the other case (i.e. a hard stationary pin sliding against a hard moving disc under unlubricated conditions) abrasive mechanisms dominate. Due to the high hardness and the martensitic microstructure of the steels severe adhesive processes - which are observed for pairings of low hardness - are avoided and a comparably low steady state wear rate is observed. (It must be noted, however, that the wear of the unlubricated 600/600 HV pairing is at least one order of magnitude higher than that of the lubricated 300/600 HV pairing).

The second question concerns conditions for the transition from mild wear to severe wear. As can be seen from Figure 13 "severe wear" was observed for pairings of 200/200 HV and 300/300 HV whereas "mild wear" was observed for pairings of 450/450 HV and 600/600 HV. SEM studies showed that in the mild wear regime abrasive mechanisms dominate whereas

in the severe wear regime adhesive mechanisms prevail. Generally
speaking, severe (adhesive) wear processes are more likely to
occur for sliding steels of a homogeneous ferritic-perlitic
microstructure (i.e. "soft" steels) rather than for steels with
a heterogeneous martensitic microstructure (i.e. "hard" steels).
Another aspect is that a transition from severe wear to mild
wear may occur if tribochemical reaction layers are formed
which reduce the effect of severe interfacial adhesive wear
mechanisms. Such reaction layers (e.g. iron oxides) have a low
wear rate if the ratio of the oxide hardness to the hardness
of the bulk metal has a value of about 1. Because, for example,
Fe_3O_4 has a hardness of appr. 400 HV the hardness of the bulk
steel should be higher than that value in order to obtain
a transition from severe wear to mild wear.

I appreciate Dr. Schey's contribution which, for the field
of metal working, is a good addition and extension of the
systematic consideration of parameters relevant to friction
and wear behaviour. The basic parameter groups of tribological
systems as compiled in a very simplified manner in Figure 22
are discussed by Dr. Schey with respect to metalworking in
detail. This has led to the complex parameter chart of his
Figure 1. Whereas the similarity of the basic important
parameters is obvious, it is also interesting to note the
"dual nature" of tribology in metal working: On one hand,
the tribological processes at a tool/workpiece interface
must create - as a "use-output" - the required surface finish
and product quality of the workpiece. On the other hand,
the same tribological processes are responsible for the
"loss-outputs" of frictional energy and tool wear. Clearly,
the optimization of this dual nature of tribology in manu-
facturing requires a systematic approach as outlined by
Dr. Schey in his contribution.

FUTURE DIRECTIONS OF RESEARCH IN ADHESION AND FRICTION

Status of Understanding

David Tabor
Cavendish Laboratory
Cambridge, England

This review covers four main classes of materials: metals, ceramics, elastomers and polymers. In dealing with adhesion a distinction is drawn between adhesion (which often involves thermodynamic concepts) and the observed adhesive strength, here designated as the "pull-off" force.

With metals our level of understanding of the interfacial bond is well understood theoretically and has been elegantly studied experimentally. However the role of surface roughness and especially ductility needs to be incorporated into an overall view of metallic adhesion. The effect of contaminant films has not gone far beyond purely descriptive language. The friction of metals is understood in terms of surface topography, adhesion and deformation and there are now promising solutions using slip-line-field theory. These do not however, cope very satisfactorily with work hardening. For surfaces sliding at higher speeds there are now good models which deal with asperity instabilities produced by frictional heating.

With ceramics our understanding of surface interactions is less unequivocal and there is need for critical theory and careful experiment. Generally it appears that the interfacial bond is weaker than bonding in the bulk so that sliding may occur truly at the interface, though the details of interface failure are not fully established. The sliding mode implies negligible adhesive wear although cracking and fatigue may be important. However at higher sliding speeds interfacial temperatures generated by friction may both increase the interfacial strength and increase ductility. Metal-ceramic interaction raises a number of fascinating theoretical problems as well as important practical issues.

With elastomers the adhesion is generally due to van der Waals forces and may be expressed in terms of surface energies. However the observed pull-off force may be 100 or 1000 times greater than the thermodynamic energy of adhesion on account of viscoelastic losses. On the other hand surface roughnesses can greatly reduce the pull-off force. Both these effects are now well understood. Adhesion results obtained with rubber can be extrapolated to explain the low pull-off forces often observed with clean hard elastic solids. The friction of soft rubbers involves the generation of a ruck or buckle which passes through the interface, the overall movement resembling the motion of a caterpillar. It is not yet clear whether these "waves of detatchment" vanish for rubbers of very high modulus.

With polymers the adhesion is again a function of surface energies and dissipative processes. Chemical treatments can greatly modify the adhesive action and there are now satisfactory theories to explain the behaviour. The frictional mechanism resembles that of metals except that softening and flow occur at much lower temperatures: and some polymers may show markedly brittle behaviour. There is considerable scope for examining frictional behaviour in terms of the chemical structure and morphology of polymers. The paper concludes with a rather speculative model of polymer friction

in terms of surface energy, atomic spacing, compressibility and a thermally activated crank-type rotation.

1. INTRODUCTION

If two clean bodies are brought into intimate atomic contact bonds may be formed across the interface. The energy involved may be expressed in terms of surface energies (thermodynamic adhesion) or in terms of bond-energies. However in practice the strength of the junction is usually measured in terms of the force to pull the surfaces apart, and depends not only on bond strength but on certain mechanical and strength properties of the adherends. For this reason (although I do not approve of multiplying scientific jargon) it seems to me desirable to give it a specific name. Dr. Maugis (ref. 1) suggests the word "adherence" but I prefer the more direct transparent term "pull-off-force" which clearly distinguishes it from the thermodynamic adhesion.

2. ADHESION OF CLEAN METALS

We now have ample evidence, not least from NASA that clean metals if pressed together can adhere very strongly indeed (ref. 2). The pull-off-force clearly depends on the strength of the interfacial bond: but it also depends on the applied load, the surface geometry (both macroscopic and microscopic), the loading time and on the ductility of the metals. There is no doubt, as Buckley and his group have shown, that with similar metals the pull-off-force and the friction fall off very rapidly the larger the amount of d-bonding. This has been interpreted in terms of reduced bond-strength. However a simple measure of the effective bond strength is the absolute melting point and this parameter show no systematic correlation with the amount of d-bonding. Further, our own experiments suggest that the pull-off-force often depends crucially on the ductility of the metal (ref. 3). This is because in the unloading part of the loading cycle released elastic stresses can stretch the junctions: their viability then clearly depends on their ductility. As we shall see below with purely elastic solids the criterion for strong adhesion can be expressed by a parameter which includes the surface roughness, the surface energy and the elastic modulus. With metals it is possible to provide an equivalent criterion (ref. 4), but this area needs further exploration. Again in the adhesion of similar metals which have a hexagonal structure the pull-off-force depends on the c/a ratio as has been shown very elegantly at NASA. Here again it would be interesting to know if the physical property involved is the ductility which is closely linked to the number and mutual orientation of the relevant slip planes.

A simple method of separating ductility from the bond-strength, crystalline structure and geometry would be to study the adhesion of similar metals under standardised conditions at temperatures sufficiently low to "freeze out" the ductility. The metals should be chosen from those which do not undergo phase changes. Similar experiments could be carried out in the sliding of clean surfaces.

With dissimilar metals the strength of the interface depends on electronic properties, lattice misfit, mutual orientation. Some of these factors have been studied in some beautiful experiments using the field ion microsocope (ref. 2). One of the most interesting conclusions is that interactions at the interface are not the same as those in bulk so that pairs of metals which do not form bulk alloys may well form a monomolecular alloy interface. In some experiments the surfaces do not separate at the interface but within the weaker of the two bodies. In such cases the pull-off-force is a measure of the strength of the yielding body and one can only state that the interface is stronger than this. The intrinsic strength of the bond

between dissimilar metals has been studied theoretically (ref. 5, 6) and the treatments now availaibe show considerable advance on the earlier work. This must be pursued further.

3. SURFACE ASPERITIES

One of the difficulties of analysing the adhesion between extended surfaces is that the behaviour may be greatly affected by surface roughness and the deformation properties of the asperities involved. For this reason we have been studying in U.H.V. the adhesion between surfaces using the geometry of a very fine tungsten tip, representing a single asperity (tip radius about 1 μm) loaded against a nickel (111) single crystal (ref. 7). The surfaces are characterised in situ using scanning electron microscopy and Auger sepctroscopy. This lacks the resolution and elegance of Buckley's field ion microscope but the arrangement provides greater flexibility in that the joining load and pull-off-force can cover a range of 1 to 1000 μN while electrical resistance measurements enable the area of contact to be monitored during the whole of the loading-unloading cycle. The results show, as expected, that for clean surfaces there is strong adhesion. In addition the electrical resistance measurements show that as the pull-off-force is applied the contact area remains almost constant until the force approaches the final pull-off value (Figure 1). The material in and around the contact behaves like a ductile notched tensile specimen. One of the most interesting results is that in the absence of any normal applied load surface forces alone may be sufficient to initiate plastic flow in the contact zone (ref. 8). Indeed for normal forces below 1 μN (10^{-4} g force) the behaviour is dominated by these forces (Figure 2). Similar conclusions concerning plastic initiation by surface forces have been drawn by Pollock (ref. 9) and by Maugis (ref. 10). The latter carried out some fascinating experiments in a transmission electron microscope and was able to infer that dislocations were generated during contact. However both of these studies were carried out on poorly characterised surfaces. Further work is needed to establish whether such surface forces can play any significant part in the adhesion of extended surfaces under extremely small loads, for example in lightly loaded electrical contacts. These experiments also provide a means of studying the deformation of very small volumes of solids and in due course should be applied to the sliding of surfaces.

4. EFFECT OF CONTAMINANT FILMS

Practically all published work agrees that extremely small amounts of contaminants, especially oxygen, can greatly reduce the adhesion between metals (ref. 2, 11). At the same time a contaminant film on one surface may be transferred to another. The extent to which contaminant films reduce the pull-off-force depends on the nature of the film, the geometry of the surface and whether surface deformation is sufficient to produce penetration of the film. In our own work where contact is between a fine stylus and a nickel flat we have studied the effect of two monolayers of oxide on the nickel surface. We find that over a wide load range where oxide film appears to remain intact, the pull-off-force is reduced by a factor of 3 or 4 while the electrical resistance is increased a hundred fold or more (ref. 8). In this delicate load range it appears that surface forces from the oxygen - covered surface are by no means negligible. If an oxide film 40 - 50 Å thick is formed on the nickel the adhesion decreases further while, so long as penetration of the oxide film does not occur, the electrical resistance increases by an enormous factor. In this load range the loading-unloading cycle is more nearly reversible and the behaviour resembles that of an elastic system (ref. 7). At higher loads the oxide is penetrated and the behaviour resembles that of clean metals. These experiments need to be extended to sliding surfaces.

121

The effect of surface films has its parallel in the effect of interfacial films formed, by the diffusion of minor constituents or of adventitious impurities to the grain boundaries. This often leads to a marked reduction in strength and often to embrittlement. The effect has been attributed to atomic misfit at the boundary, to a reduction in surface energy, to a weakening of bonds, to the inhibition of dislocation movement (ref. 12, 13, 14). The mechanism still needs critical examination. The simplest descriptive explanation, when marked embrittlement occurs, is that a grain boundary is formed lacking ductility.

Another aspect of this problem is the effect of molecular or polymolecular surface films on the mechanical properties of the underlying metal. Finally we may note that in the contact of metals with non-metals a monolayer of oxygen may <u>increase</u> the bond strength: this will be discussed in a later paper by Dr. Pepper in this session.

5. THE FRICTION OF METALS

The mechanism of metallic friction is fairly well understood at a descriptive level in terms of the area of real contact, junction growth, breakdown of contaminant films, adhesion, shearing and ploughing (ref. 11). Quantitatively the picture is less satisfactory. The area of contact can now be calculated using various topographical treatments but on account of the difficulty of choosing the correct lateral sampling length the quantitative results are not very reliable. The behaviour of the surfaces during sliding is even more problematical. First of all, with clean metals, there will be appreciable junction growth due to the combined effect of the normal and tangential stresses. Analytical expressions for this are largely qualitative. If the surfaces are somewhat contaminated junction growth may be unimportant but other problems arise. On the one hand the asperities may be deformed or torn so that the overall topography may be changed. On the other the asperities will be work hardened in a way that is not easy to quantify. What does seem clear is that whereas initial contact may involve plastic deformation of the asperity tips, repeated sliding, if interfacial shear forces are not too large, leads to a shake-down condition and subsequent elastic contact.

The adhesion of clean surfaces is fairly well understood. However the behaviour of oxide coated surfaces, the adhesion of the oxides, the break-up of the oxide films, the adhesion of the mixed oxide-metal interface, the influence of surface deformation on the structure and mechanical properties of the surface layers are all too difficult to be treated analytically. In fact we still need better physical pictures of these processes before they can be further analysed. As mentioned in another context, the break-up of surface films is still in the realm of hand waving!

The shearing process raises interesting problems as to whether shear sliding occurs or whether there is a tearing of the interfacial junctions (ref. 11). Some theoretical models on this issue provide an interesting approach: but work hardening is still a difficult complication.

Finally the ploughing or deformation of one surface by a harder asperity on the other has been tackled in terms of slip-line field theory. A striking conclusion is that even in the absence of interfacial adhesion the hard asperity raises a plastic mound of metal ahead of it which it may then "iron-out" (ref. 15). This is shown schematically in Figure 3. Consequently the surface geometry is scarcely changed but the surface layers are subjected to extremely high shear strains. This may play an important role in surface fatigue. In some cases depending on geometry and/or the strength of interfacial adhesion the raised mound may be cracked off, or removed as in a microcutting operation. These models are extremely helpful and it would be

interesting to know if any radical changes will emerge, if work-hardening is incorporated into the model. A far more difficult problem, which is now receiving the attention it deserves is the break-up of the surface and subsurface structure of the metal as a result of repeated sliding (ref. 16). Rigney's work suggests that there must be reasonably large surface tractions but it would seem that adhesion must not be too strong if a steady-state is to be achieved. In practice particularly in the presence of lubricants or oxide films many metal-metal systems operate in this domain. This probably means that the fragmented surface layers incorporate a certain amount of oxide and other contaminants.

In high speed sliding appreciable frictional-heating is generated. There are some excellent models for this. For example Barber (ref. 17) has shown how one higher asperity taking most of the load will expand thermally and so withdraw contact from other asperities. This will continue until the single asperity carries all the load: it then wears away until the load is supported by the next highest asperity. The former asperity then cools, contracts, and withdraws from contact. Here the effect of frictional heating can be treated quantitatively. Of course there is an under-lying problem which has not yet been fully resolved: – the location of the heat source. Most analyses assume that the heat source is generated at the interface at a rate given by the product of the velocity and the measured frictional force. Clearly the heat must be generated in some finite volume of the material being deformed or sheared during sliding. For example in a classical paper on the rolling of polymer discs over one another Archard showed that the main heat source was below the surface in the region of maximum shear stress (ref. 18). It would be useful to know how far our calculations of surface temperatures are changed if volume deformation is taken into account.

At high speeds there is surface softening and, in the limit, surface melting (ref. 11). The broad features are understood but the application to practical situations is tricky and challenging. High temperatures favour oxidation and there is now a whole field of study devoted to oxidational wear. This will be dealt with in another session but my own impressions are that more effort has been expended on calculating heat flow and oxidation rates than on clarifying the detailed processes that occur during sliding.

6. ADHESION OF CERAMICS

Our understanding of the adhesion of ceramics to one another is far poorer than that of metals. If the ceramic is mainly ionic the bonding forces across the inter-face are primarily Coulombic and are accessible to calculation. However if the bonding within the ceramic is covalent we cannot define the state of atoms at the free surface with any certainty. The evidence for dangling bonds at a free surface is still contentious and in any case depends on the particular system under consider-ation. If the dangling bond is fully available for interaction with a similar bond on another contacting surface the interfacial bond will be strong and calculable. But it seems to me that in many cases the dangling bond will link up with a neighbour on its own surface, or rehybridise, or back-bond (see Figure 4). In that case do such bonds need thermal activation before they can take part in bond-formation with another surface? In the sintering of ceramic powders the process is carried out at elevated temperatures to increase rates of diffusion, ductility and flow. Does the high temperature also play a part in activating surface bonds? Of course in engineering systems the surface is probably covered with strongly adsorbed films of oxygen and water vapour but this does not mean that the basic problem of interfacial bonding can be ignored.

123

7. FRICTION OF CERAMICS

Bond formation across ceramic interfaces may also have an important bearing on the friction and wear behaviour of these materials. If chemical bonds are not easily formed the interaction across the interface will be mainly the result of van der Waals' forces with perhaps some ionic contribution. These bonds will be weaker than the chemical bonds within the body of the ceramic itself. Consequently sliding will necessarily take place at the interface: the friction will not be high and, in principle, there will be no adhesive wear. If wear does occur it will be due to cracking or surface fatigue. In practical situations the presence of adsorbed films of oxygen and/or water vapour will further reduce the strength of the interfacial bond. On the other hand the sliding process itself may distort the surface structure and facilitate the formation of strong covalent bonds.

New ceramics of increasing toughness are now appearing as potential engineering materials (ref. 19). A systematic study of the adhesion, friction and wear of clean ceramics in terms of their structure and bond-type would be extremely valuable and timely. I presume that this will be discussed in Dr. Eiss's contribution.

An associated problem concerns the way in which the interface fails during sliding. Although the formation of cracks in and around the contact zone is now well understood the contact zone itself is under high hydrostatic pressure. As a result it may show some plasticity during shearing. The overall destruction of the surface is of course responsible for the wear.

8. ADHESION OF ELASTOMERS

Elastomers consist of long chain organic molecules linked together at various points by chemical bonds. The greater the number of cross-links the higher the elastic modulus. The free surface of an elastomer consists almost entirely of saturated carbon-hydrogen groups. The surface energy is very small, of order 30 m J m^{-2}: so that the surface is not wetted by water and probably does not even adsorb oxygen from the atmosphere. Consequently even if the experiments are carried out in the laboratory air, rubber consistitutes a very convenient material for studying the adhesion of clean elastic solids. Further since the forces between two rubber surfaces are limited to van der Waals forces the interaction across the interface will be less than the bonding within the bulk of the rubber where strong chemical cross-links exist. Thus in adhesion experiments separation occurs truly at the interface. (Similar considerations apply to the sliding of rubber over smooth surfaces). Of course if two rubber surfaces are kept in contact over a prolonged period diffusion across the interface may occur. It will be limited because of the chemical cross-links which restrict the freedom of movement of individual parts of the molecular segments. However such diffusion, as Voyutsky showed can greatly increase the strength of the interface (ref. 20).

If γ_1 is the surface energy of a rubber specimen and it is placed in contact with another surface of surface energy γ_2 and if γ_{12} is the interfacial energy, the thermodynamic energy of adhesion per unit area of atomic contact is

$$\Delta\gamma = \gamma_1 + \gamma_2 - \gamma_{12} \tag{1}$$

If no other factors are involved the work required to peel apart unit area of interface would be $\Delta\gamma$. There are two complicating factors: visco elastic losses which increase the work of separation and surface roughenss which reduces it.

It is clear that if viscoelastic losses are involved as the surfaces are pulled apart the <u>work</u> of separation will be greater than $\Delta\gamma$. This leads to an increase in the peel <u>force</u> as was shown many years ago in Gent's pioneering studies (ref. 12). The connection between the peel-<u>work</u> and the peel-<u>force</u> is however rather subtle. It has recently been exposed in a very elegant way by treating the peeling process as a problem in fracture mechanics (ref. 22). Peeling is then considered to be equivalent to the spreading of a crack through the interface (Figure 5b). For two identical surfaces in contact the classical crack-shape is parabolic (Figure 5c). However this involves infinite stresses at the crack-tip: according to Barenblatt the crack tip must acquire a shape shown in Figure 5d where the surface forces fall-off from their maximum value at A to zero at gap regions further out than B. The curve AB then merges with the classical parabola BC, BD. The region AB is that over which the surface or interfacial forces operate and the integrated value of these forces over the area AB exactly balances the external peeling force F. For typical elastomers AB has a length of not more than a few $\overset{o}{A}$. If now we allow for the viscoelasticity of the material we find that the shape of the opening crack lags behind the equilibrium shape: the length AB over which interfacial forces operate is greatly increased (Figure 5e). Consequently the peeling force is correspondingly increased. The length AB may still be too small to be detected optically, say 1000 $\overset{o}{A}$, but it will correspond to an increase in the peel force of several hundred fold. We may note that for each unit increase of interface that is opened up the <u>surface</u> work done is still the thermodynamic energy $\Delta\gamma$: the vast increase in peeling energy derives from the viscoelastic losses. This analysis explains why the peeling force depends on peel-rate and temperature since it reflects the rate and temperature dependence of the viscoelastic properties of the solids (ref. 1). Derjaguin and his colleagues have shown that in systems where charge transfer is a major source of interfacial adhesion the effect of peel-rate on peel-force is due to the rate at which surface charges leak away (ref. 23). However charge separation often contributes only a very small part to the adhesion: with rubber-on-rubber it cannot play any significant role.

The role of surface roughness is best understood in terms of the adhesion of an individual asperity assumed to resemble a portion of a sphere of radius R. We do not need to discuss the detailed nature of the contact shape: it has been dealt with in a series of papers and is now more-or-less resolved (ref. 24, 25a, 25b). We present here a highly simplified version. The main conclusion is that the pull-off-force F_a between a hard sphere of radius R and an elastomeric surface is

$$F_a = K R \Delta\gamma \tag{2}$$

where K lies between $(3/2)\pi$ and 2π depending on contact conditions. The lower asperities, if they make contact with the elastomer, pull the surfaces together: the higher asperities penetrate the elastomer and experience an elastic resistance pushing the surfaces apart. For a sphere of radius R penetrating a depth σ into an elastomer of Young's modulus E the resisting force, according to Hertz, is of order

$$F_r \backsim \sigma^{3/2} E R^{\frac{1}{2}} \tag{3}$$

There is thus a competition between the attractive force F_a and the repulsive force F_r (Figure 6). Thus the ratio F_r/F_a expresses the extent to which adhesion is reduced. The crucial parameter, which is dimensionless, is

$$\theta = \frac{\sigma^{3/2} E R^{\frac{1}{2}}}{R \, \Delta\gamma} \tag{4}$$

125

where we identify R as the asperity-tip radius and σ as the mean deviation of the asperity heights. A model experiment has been described in which a clean smooth rubber sphere of large radius of curvature is brought into contact with a hard polymeric surface. The latter is initially smooth but can be roughened by various amounts so that R and σ can be varied. The pull-off-force of the roughened surface may be expressed as a fraction of the pull-off-force for the initial smooth surface. A typical result is shown in Figure 7 and it is seen that for quite small roughnesses (σ ≈ 1 μm) the adhesion ratio falls to a very small value. It turns out, using the full parameters of the surface, that if θ exceeds a value of about 10 the adhesion is negligible (ref. 26, 27).

This has an interesting bearing on the adhesion of very hard elastic solids. With these materials the surface energy is up to 100 times greater than that of rubber. However the elastic modulus may be as much as 10^5 times greater. Simple arithmetic (assuming the asperity tip radius to be roughly constant) shows that for the hard solid the pull-off-force could fall to zero (θ ≈ 10) for a value of σ one-hundred times smaller than the roughness observed with rubber. In the example quoted here this would correspond to a surface roughness less than 100 Å. Although the analysis given here is extremely crude more sophisticated treatments confirm that with hard elastic solids the pull-off-force may be very small on account of surface roughnesses hardly greater than a few atomic spacings. Thus the pull-off-force of clean WC to itself in U.H.V. is very small. By contrast the adhesion of clean WC to copper (which is just as rough) is large. This is primarily because the copper is ductile and junctions subjected to the forces exerted by higher asperities pushing the surfaces apart can be accommodated by plastic flow (ref. 3).

The adhesion of elastomers is relevant to the friction of rubber, to the functioning of materials such as Scotch tape as well as to the fabrication of automobile tyres. In the latter case chemical bonding is widely used.

9. THE FRICTION OF ELASTOMERS

If a smooth clean hemispherical specimen of a soft elastomer is slid over a clean smooth hard surface it is found that, although the friction may be high, there is virtually no transfer of rubber to the harder surface. If the hard surface is transparent (say glass or Perspex) the interface may be studied while sliding occurs. It is then observed that as a result of the shear stresses developed at the interface, an instability occurs and a ruck or buckle is formed in the rubber (ref. 28). The ruck travels through the interface, the movement of the rubber thus resembling the motion of a caterpillar (Figure 8). There is no true sliding. The frictional process which is often referred to as the generation of Schallamach waves, involves a continuous laying down and peeling apart of the rubber on the substrate. The frictional work is thus related to the surface energies and the hysteretic loss properties of the rubber (ref. 29). In most systems, as mentioned in a previous section, bonding across the interface is weaker than that within the bulk of the rubber itself. Only with the very softest rubbers where there is very little cross-linking is there some transfer.

If the rubber is more highly cross-linked both the modulus and the mechanical strength are greatly increased. On the other hand the interfacial forces are still dominated by van der Waals interactions. Thus the strength of the interface remains roughly constant while that of the bulk increases. Under these conditions the size of the Schallamach waves decreases and it is probable (though by no means proven) that at some critical ratio of interfacial strength to elastic modulus they vanish

126

altogether. In these cases true sliding will occur. In principle hard rubbers should show even less transfer than soft. However in practice it appears that the shear process at the interface produces bond scission and the formation of low molecular-weight products which smear and adhere to the counterface.

If rubber slides over a clean rough surface the deformation of the rubber by the surface asperities will make a relatively small contribution to the friction. However in the presence of a lubricant the adhesion component may be reduced to a negligibly small value and in that case the greater part of the friction will be due to deformation losses in the rubber. This has led to the use of high hysteresis-loss rubbers in the tread of automobile tyres as a means of increasing skid resistance on wet or greasy road surfaces (ref. 30). Of course the deformation process may involve fatigue or tearing of the rubber involving relatively heavy wear.

10. THE ADHESION OF POLYMERS

The adhesion of polymers resembles that of elastomers involving surface energy concepts, electrical charge separation, interfacial diffusion, surface roughness and deformation losses. The surface energy is generally higher than with elastomers but not by a large factor so that the thermodynamic energy of adhesion is rarely greater than a few tenths of a $J\ m^{-2}$. However, interfacial diffusion between two polymers, which has been studied recently as an example of molecular reptation, can greatly increase the energy of interaction as a result of chain entanglement (ref. 31). When placed in contact with metals and especially semi-conductors marked charge separation can occur. It is indeed possible to modify the interaction by irradiation with U.V., which can activate various donor-acceptor levels (ref. 23). With some polymers lower molecular weight fractions may migrate to the free surface producing a relatively weak surface layer (ref. 32). An extreme example of this is the deliberate addition of short chain amphipathic molecules to the melt: these diffuse to the surface and act as an "anti-adhesion" or blocking agent.

11. ADHESION BETWEEN POLYMERS AND OTHER SURFACES

The thermodynamic work of adhesion of polymers to other solids can be estimated by a number of semiempirical relations which combine the polar and non polar parts of the surface energies of each solid. This is discussed very clearly in Wü's book (ref. 33). In most cases the interface is stronger than one of the adherends and separation occurs in the weaker material.

In static contacts adhesion may be greatly enhanced by applying the principle of acid-base bonding. For example if the surface of PE is sulphated it becomes anionic. This forms a strong chemical bond with a basic material such as Fe_2O_3 (a common oxide on ferrous materials). Some workers however suggest that the enhanced adhesion is due to electrostatic forces since Fe_2O_3 carries a positive surface charge and SO_4 a negative charge. (This is not simply a matter of semantics). Similarly imine treatment of PE leaves the surface in a cationic condition and the adhesion to Fe_2O_3 is reduced (ref. 33).

During the last few years Andrews and his colleagues have studied the adhesion of polymers cast against rigid surfaces and have examined the effect of changing the interfacial thermodynamic energy of adhesion $\Delta\gamma$ by suitable chemical treatments (ref. 34). They find that the observed work of adhesion, i.e. the pull-off work, is proportional to $\Delta\gamma$ but enormously greater, due to deformation losses in the polymer (ref. 35). The behaviour thus resembles the adhesion of elastomers except that the

127

dissipative processes are associated with flow of the polymer rather than hysteresis losses. So far there has been no analytical model which links the increased pull-off work with the increased pull-off force to parallel the treatment described above for elastomers.

12. FRICTION OF POLYMERS

The friction of polymers involves adhesion and deformation as well as cracking at and below the surface. The behaviour resembles that of metals except that there is little evidence for junction growth and the deformations occurring during sliding are more dependent on temperature and shear rate. Because of their poor thermal conductivity and low melting points softening and melting can occur fairly readily as a result of frictional heating. Once surface melting takes place heat generation appears to occur by viscous dissipation in the molten layer (ref. 36).

We may summarise some specific aspects of polymer friction under the following headings.

(a) In slow-speed sliding against a smooth counterface where frictional heating is unimportant polymers appear to fall into two main groups (i) those that slide truly at the interface: these include cross-linked polymers, and glassy polymers such as polystyrene and P.M.M.A. below their glass-transition temperatures. Here the polymer is "stronger" than the interface. (ii) those that lay down a thin film of highly oriented polymer apparently by a process of cold drawing aided perhaps by some adiabatic shear: these include semicrystalline polymers such as PTFE and high density PE which have "smooth" molecular profiles. Here the interface is "stronger" than the polymer (ref. 37, 38). With this group of polymers the interaction of the polymer with the transfer film has interesting consequences if the polymer slider is rotated about its axis while sliding takes place since orientation of the slider will periodically be unfavourable for easy drawing (ref. 39). In linear sliding (without rotation) the shear process changes if the sliding speed exceeds a low but critical value; it then becomes easier to rupture the polymer and pull out a fragment than to draw out a molecular film: there is an increase in friction and a large increase in wear (lumpy transfer).

(b) If the counterface is rough and the asperities penetrate fully into the polymer the interface appears to be strong enough to shear off the polymer at an angle to the surface. These shear angles correlate with the energy-to-rupture of the polymer (ref. 40). This paper does not deal with wear mechanisms in polymers but it may be noted that most workers in the field accept the view that the wear rate is very largely dependent on the energy-to-rupture or some similar failure criterion (ref. 41).

(c) An enormous amount of effort has been expended on the development of filled polymers that will combine the favourable frictional properties of certain polymers (especially PTFE) with low wear rates, low creep rates and good thermal conductivity. Some of the mechanisms are understood at least at a descriptive level. Another development is the use of irradiation to produce cross-linking in an otherwise semicrystalline thermoplastic (ref. 42).

The friction (and wear) of polymers is often affected by liquids which may plasticise the surface layers or penetrate more deeply. Generally the effects are most marked the larger the solubility parameter of the liquid. These tribological changes are associated with a reduction in the fracture toughness of the polymer (ref. 43).

ADHESION: SOME FINAL COMMENTS

The adhesion between two bodies brought into atomic contact depends on the strength of the bond formed at the interface. Most bond-types are now well understood though with covalent solids there are still problems to be solved. In some systems charge transfer may occur across the interface and this may be regarded as an additional type of bond. The adhesion may be expressed in terms of these bond energies or equivalent surface energies and may be treated as part of the broader field of thermodynamics. However this approach presupposes reversibility and probably never applies to real situations. The system which is nearest to the ideal is the contact between mica surfaces covered with an adsorbed layer capable of preventing tearing of the mica surface. For virtually all other systems irreversible processes are involved and the adhesion can be usefully described only in terms of the pull-off-force or the pull-off energy.

With clean surfaces factors which increase the pull-off energy are dissipative processes in the contact region: with metals, ductility; with elastomers, visco-elasticity; with polymers, flow. Factors which reduce adhesion are contaminant films and surface roughness. Contaminant films usually weaken the strength of the inter-facial bond though this is not always the case. With metal-ceramic contacts oxides may provide a strong bridge between the surfaces. Again with polymers specific surface treatments may provide a chemical or ionic bond which is stronger than the usual van der Waals bond. Surface roughness reduces the pull-off-force because it reduces the area of true contact, provides high asperities which tend to prize the surfaces apart and introduces discontinuities in the interface which can act as sources of stress concentration. In the practical application of liquid adhesives, surface roughening produces a cleaner surface and a larger surface area so that, if good wetting occurs adhesion is probably improved. With solids, however, surface roughness reduces adhesion except perhaps in those rare cases where mechanical entanglement may occur.

THE LAWS OF FRICTION

Ever since the time of Coulomb it has been recognised that the frictional force F is not always proportional to the normal load N and that a more realistic relation may be written in the form:-

$$F = \mu N + b \tag{5}$$

Coulomb attributed the first term to the interaction of asperities (the "engineering", or Coulombic friction) and the second to adhesion. The first atomic model to explain this was due to Derjaguin who, nearly 50 years ago, derived an equation

$$F = \mu(N + P) \tag{6}$$

where the attraction P was the pull-off-force in static contact and was assumed to augment the normal load (ref. 44). Delicate experiments for example by Skinner and Gane at loads of the order of 10^{-2} gm have indeed demonstrated a behaviour consistent with this and finite frictional forces at negative loads and an appropriate static pull-off-force have been observed (ref. 45).

There are, of course, other models which lead to relations resembling equation (5) and these may be more applicable to practical situations. For example, Bowden and Tabor expressed the frictional force as the sum of a ploughing term and a term

129

for the shearing of adhesional junctions. Again in a long series of experiments Briscoe and others have shown that the shear strength τ of organic solids and inorganic crystalline materials increases with contact pressure p in a roughly linear (symbatic!) way (ref. 46, 47).

$$\tau = \tau_o + \alpha p \qquad (7)$$

Kragelsky reports a similar behaviour for metals (ref. 48). Consider now the contact between a hard smooth surface and the solid under discussion. If the normal load is N the true area of contact A, whatever the nature of the deformation process, will be given by

$$A = N/p \qquad (8)$$

If there is strong adhesion at the interface so that during sliding shearing occurs in the solid under consideration, the frictional force will be

$$F = A\tau = (N/p)(\tau_o + \alpha p) = N(\tau_o/p + \alpha) \qquad (9)$$

so that the coefficient of friction is

$$F/N = \tau_o/p + \alpha \qquad (10)$$

This relation holds particularly well for polymers and other solids where junction growth is not important. In many such systems the first term is very small and the coefficient of friciton is dominated by the term α (ref. 49). Thus we may measure the shear properties of very thin films of a solid between rigid plattens as a function of confining pressure and so determine the pressure coefficient α of the shear strength. This then provides a fairly reliable measure of the coefficient of friction of the solid. Experiments of this type have proved very convenient in determining the friction of explosive materials (ref. 50).

With metals the area of real contact for both concentrated and extended surfaces is roughly proportional to the load. With elastic and polymeric materials the area of contact increases less rapidly than the load so that the contact pressure p increases. Consequently if the friction is dominated by adhesion and shearing the coefficient of friction will decrease as the load increases (see equation (10)). This is generally observed. A very detailed analysis of the friction between solids in terms of surface roughness, deformation properties, and interfacial shear strength has been developed by Kragelsky and his colleagues (ref. 48).

An interesting aspect of the friction of non-polar polymers and similar organic materials is that in the relation

$$\tau = \tau_o + \alpha p \qquad (7)$$

the actual values of τ_o and α do not vary by more than a factor of two for materials ranging from PE, PTFE, paraffin wax, metallic soaps, to oriented monolayers of fatty acids. The common feature appears to be that for all these materials the surface energies do not vary by more than a factor of about two (15 to 30 m J m^{-2}) and the bonding is dominated by van der Waals forces. This has led to a very simple molecular model which reproduces equation (7) qualitatively and semi quantitatively (ref. 51). The parameters involved are the surface energy, the atomic spacing and the compressibility of the solid. The model also includes the concept of a crank-type motion.

Of course there is always the underlying uncertainty involved in deriving strength properties from molecular or atomic forces: this applies particularly to the role of dislocations. Naturally this could not have been considered in Derjaguin's 1934 paper. However the limited information that is available indicates that τ is of order (shear modulus)/30 so that τ approaches the theoretical strength: dislocation mechanisms may thus be ignored. These ideas concerning the friction of van der Waals solids are highly speculative but are not out of place in a paper which attempts to review our present state of understanding of adhesion and friction.

REFERENCES

1. Maugis, D. and Barquins, M. "Fracture Mechanics and the Adherence of Viscoelastic Solids". J. Phys. D: Appl. Phys. 11, 1978, pp. 1989-2023.

2. Buckley, D.H. "Surface Effects in Adhesion, Friction, Wear and Lubrication". 1981, Elsevier.

3. Gane, N., Pfaelzer, P.F. and Tabor, D. "Adhesion between Clean Surfaces at Light Loads". Proc. Roy. Soc. London. A340, 1974, pp. 495-517.

4. Johnson, K.L. "Adhesion at the Contact of Solids" in "Theoretical and Applied Mechanics". Ed. Koiter, 1976, North-Holland Publishing Co.

5. Ferrante, J. and Smith, J.W. "A Theory of Adhesion at a Bi-metallic Interface: Overlap Effects". Surface Sci. 38, 1973, pp. 77-92.

6. Inglesfield, J.E. "Adhesion between Al Slabs and Mechanical Properties". J. Phys. F: Metal Phys. 6, 1976, pp. 687-710.

7. Pethica, J.B. and Tabor, D. "Contact of Characterised Metal Surfaces at Very Light Loads: Deformation and Adhesion". Surf. Sci. 89, 1979, pp. 182-188.

8. Pashley, M.D. and Tabor, D. "Adhesion and Deformation Properties of Clean and Characterised Metal Micro-contacts". Vacuum, 31, 1981, pp. 619-623.

9. Pollock, H.M., Shufflebottom, P. and Skinner, J. "Contact Adhesion between Solids in Vacuum: I Single Asperity Experiments". J. Phys. D. Appl. Phys. 10, 1977, pp. 127-138.

10. Maugis, D., Desalos-Andarelli, G., Heurtel, A. and Courtel, R. "Adhesion and Friction of Aluminum Thin Foils Related to Observed Dislocation Density". ASLE Trans. 21, 1978, pp. 1-19.

11. Bowden, F.P. and Tabor, D. "The Friction and Lubrication of Solids". Part I, 1950: Part II, 1964, Clarendon Press, Oxford.

12. Hondros, E.D. and McLean, D. "Cohesion Margin of Copper". Phil. Mag. 29, 1974, pp. 771-795.

13. Seah, M.P. "Segregation and Strength of Grain Boundaries". Proc. Roy. Soc. London, A349, 1976, pp. 535-554.

14. Seah, M.P. "Surface Science in Metallurgy". Surf. Sci. 80, 1979, pp. 8-23. see also: "Comment on the Quasi-chemical Model of Interface Decohesion". Scripta. Met. 15, 1981, pp. 457-460.

15. Challen, J.M. and Oxley, P.L.B. "An Explanation of the Different Regimes of Friction and Wear Using Asperity Deformation Models". Wear, 53, 1979, pp. 229-243.

16. Heilmann, P., Clark, W.A.T. and Rigney, D.A. "Orientation Determination of Sub-surface Cells Generated by Sliding". Acta. Met. (in Press), see also Rigney, D.A. and Shewmon, P.G. "Wear and Erosion of Metals", in 'Metallingical Treatise", 1981, AIME, pp. 621-641.

17. Barber, J.R. "Thermoelastic Instabilities in the Sliding of Conforming Solids". Proc. Roy. Soc. London, A312, 1969, pp. 381-394: see also Trans. ASME, 47, 1980, pp. 871-874.

18. Wannop, G.L. and Archard, J.F. "Elastic Hysteresis and a Catastrophic Wear Mechanism for Polymers". Proc. Instn. Mech. Engrs. 187, 1973, pp. 615-623.

19. Marmach, M., Servent, D., Hannink, R.H.J., Murray, M.J. and Swain, M.V. "Toughened PSZ Ceramics: their Role as Advanced Engine Components". Soc. Automotive Engrs. Phoenix Arizona, Conference March 1983.

20. Voyutskii, S.S. "Autoadhesion and Adhesion of High Polymers". (translated by S. Kaganoff) 1963, Interscience Publishers.

21. Gent, A.N. and Petrich, R.P. "Adhesion of Viscoelastic Materials to Rigid Substances". Proc. Roy. Soc. London, A310, 1969, pp. 433-448.

22. Greenwood, J.A. and Johnson, K.L. "The Mechanism of Adhesion of Viscoelastic Solids". Phil. Mag., A43, 1981, pp. 697-711.

23. Deryagin, B.V., Krotova, N.A. and Smilga, V.P. "Adhesion of Solids". (Translator, Johnson, R.K.), 1978, Consultants Bureau, N.Y.

24. Johnson, K.L., Kendall, K. and Roberts, A.D. "Surface Energy and the Contact of Elastic Solids". Proc. Roy. Soc. London, A324, 1971, pp. 301-313.

25a. Tabor, D. "Surface Forces and Surface Interactions". J. Colloid and Interface Sci., 58, 1977, pp. 2-13.

25b. Muller, V.M., Yushchenko, V.S. and Derjaguin, B.V. "On the Influence of Molecular Forces on the Deformation of an Elastic Sphere and its Sticking to a Rigid Plane". J. Colloid Interface Sci, 77, 1980, pp. 91-101.

26. Fuller, K.N.G. and Tabor, D. "The Effect of Surface Roughness on the Adhesion of Elastic Solids". Proc. Roy. Soc. London, A345, 1975, pp. 327-342.

27. Briggs, G.A.D. and Briscoe, B.J. "Effect of Surface Roughness on Rolling Friction and Adhesion between Elastic Solids". Nature, 260, 1976, pp. 313-315. See also J. Phys. D: Appl. Phys. 10, 1977, pp. 2453-2466.

28. Schallamach, A. "How does Rubber Slide?" Wear, 17, 1971, pp. 301-312.

29. Briggs, G.A.D. and Briscoe, B.J. "The Dissipation of Energy in the Friction of Rubber". Wear, 35, 1975, pp. 357-364.

30. Tabor, D., Giles, C.G. and Sabey, B.E. "Friction between Tyre and Road". Engineering, 186, 1958, pp. 838-846.

31. de Gennes, P.G. "The Behaviour of Polymer-Polymer Junctions". in "Microscopic Aspects of Adehsion and Lubrication". Ed. Georges, J.M. 1982, pp. 335-367, Elsevier.

32. Sharpe, L.H. and Schonhorn, J. "Contact Angle, Wettability and Adhesion". Adv. Chem. Ser. No. 43, Ed. F.J. Gould, 1964.

33. Wu, S. "Polymer Interface Adhesion". 1982, Marcel Dekker, N.Y.

34. Andrews, E.H., Pingsheng, He, and Vlachos, C. "Adhesion of Epoxy Resin to Glass". Proc. Roy. Soc. London. A381, 1982, pp. 345-360.

35. Andrews, E.H. "Generalised Fracture Mechanics". J. Materials Sci. 9, 1974, pp. 887-894.

36. Tanaka, K. and Uchiyama, Y. "Friction, Wear and Surface Melting of Crystalline Polymers", in "Advances in Polymer Friction and Wear". Ed. Lee, L.H., A5, 1974, pp. 499-530, Plenum, N.Y.

37. Briscoe, B.J. and Tabor, D. "The Sliding Wear of Polymers: a Brief Review", in "Fundamentals of Tribology". Ed. Suh, N.P. and Saka, N., 1980, MIT Press.

38. Briscoe, B.J. "Wear of Polymers: an Essay on Fundamental Aspects". Tribology International, Aug. 1981, pp. 231-243.

39. Briscoe, B.J. and Stolarski, T.A. "The Influence of Linear and Rotating Motions on the Friction of Polymers". Trans. ASME, J. Lub. Technology, 103, 1981, pp. 503-508.

40. Warren, J.H. and Eis, N.S. "Depth of Penetration as a Predictor of the Wear of Polymers on Hard Rough Surfaces", in "Wear of Meterials". Ed. Glaeser, W.A., Ludema, K.C. and Rhees, S.K. 1977, pp. 494-499, ASME, N.Y.

41. Lancaster, J.K. "Friction and Wear". Chap. 14, in "Polymer Science, a Materials Science Handbook". Ed. Jenkins, A.D., N972, North Holland Publishing Co.

42. Briscoe, B.J. Private Communication, 1983.

43. Lancaster, J.K. and Atkins, A.G. Private Communication, 1983.

44. Beryagin, B.V. "Molecular Theory of Friction and Sliding". (in Russian) Zh. Fiz. Khim. 5, 1934, pp. 1165-1171.

45. Skinner, J. and Gane, N. "Sliding Friction under a Negative Load". J. Phys. D: Appl. Phys. 5, 1972, pp. 2087-2094.

46. Amuzu, J.A.K., Briscoe, B.J. and Tabor, D. "Friction and Shear Strengths of Polymers". ASLE Trans. 1977, 20 (40), pp. 354-358.

47. Briscoe, B.J. and Tabor, D. "Shear Properties of Polymeric Films". J. Adhesion. 9, 1978, pp. 145-155.

48. Kragelsky, I.V., Dobychin, M.N., Kombalov, V.S. "Friction and Wear - Calculation Methods". 1982, Pergamon, U.K. see also:- Kragelsky, I.V. and Alisin, V.V. "Friction, Wear, Lubrication: Tribology Handbook, Vols. 1, 2, 3, (In English) Mir Publishers, Moscow.

49. Briscoe, B.J. and Tabor, D. "Shear Properties of Thin Organic Films". ACS Preprints, 21(1), 1976, pp. 10-25.

50. Amuzu, J.m Briscoe, B.J. and Chaudhri, M. "Frictional Properties of Explosives". J. Phys. D: Appl. Phys. 9, 1976, pp. 133-143.

51. Tabor, D. "The Role of Surface and Intermolecular Forces in Thin Film Lubrication", in "Microscopic Aspects of Adhesion and Lubrication", Ed. Georges, J.M., 1982, pp. 651-682, Elsevier.
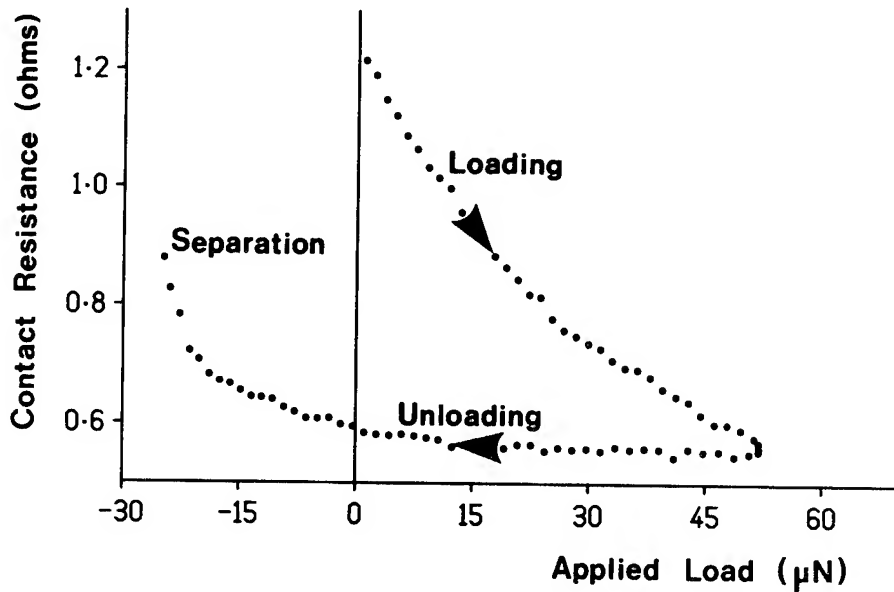
Figure 1.   Contact between a clean tungsten tip (radius 1 μm) and a clean nickel(111)
surface.   On decreasing the load the contact resistance is almost constant
until the surfaces begin to pull apart.   Separation resembles the failure
of a ductile notched specimen.
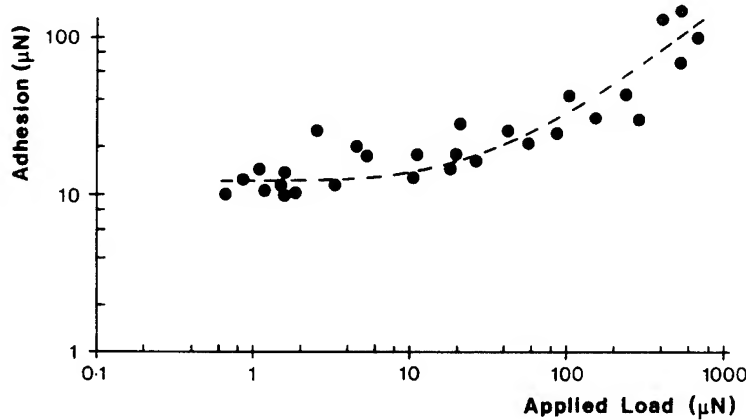
Figure 2.   Adhesion between a tungsten tip and a clean nickel(111) surface.   The
pull-off force remains constant at very small joining loads suggesting
that in this range plastic deformation is due primarily to surface forces.
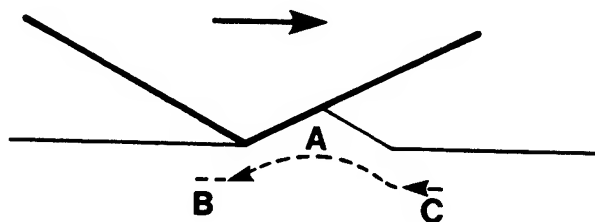

Figure 3.   A wedge-shaped asperity forms a protrusion which is then ironed out.   The
surface remains unchanged in shape but the surface layers are heavily
sheared.

136
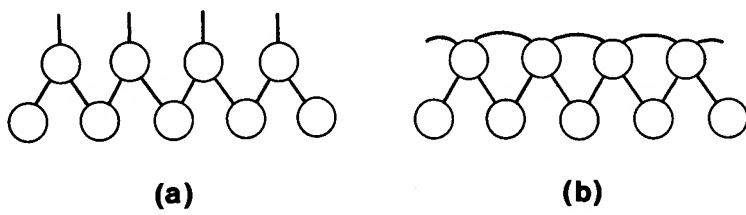
Figure 4. Surface bonds (a) dangling, (b) interlinked.
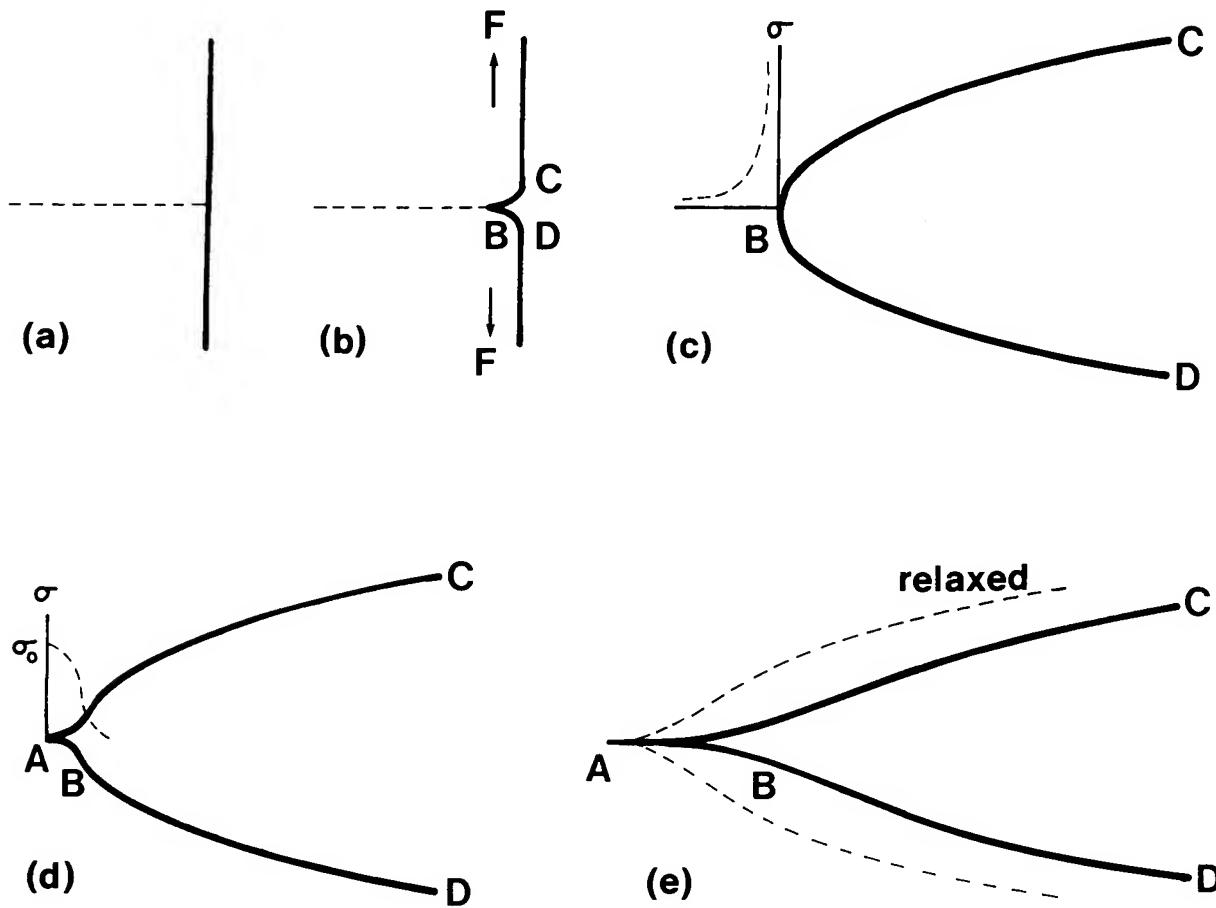
Figure 5. (a) Adhesion of two slabs of clean rubber, (b) separation begins at B as tensile force F is applied, (c) magnified view of region BCD according to classical fracture mechanics: this involves infinite stresses at B, (d) Barenblatt correction which allows for finite atomic forces over region AB, merging with classical behaviour beyond B: the surface forces over AB balance the pull-off or peeling force (e) with viscoelastic materials, separating surfaces lag behind the classical shape so that atomic forces operate over a much greater length AB.

Modulus E
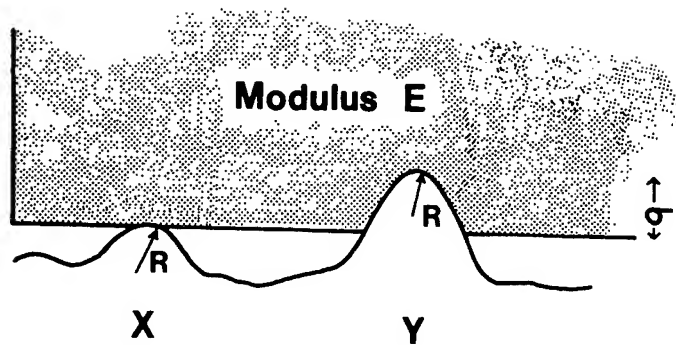
At **X** adhesive attraction = $KR\Delta\gamma$

At **Y** elastic repulsion = $\sigma^{3/2}ER$

Figure 6. Competition between the repulsion forces due to the higher asperities and the attractive forces due to the lower asperities.

Youngs Modulus
$A = 24 \times 10^5\ Nm^{-2}$
$B = 6.8 \times 10^5\ Nm^{-2}$
$C = 2.2 \times 10^5\ Nm^{-2}$
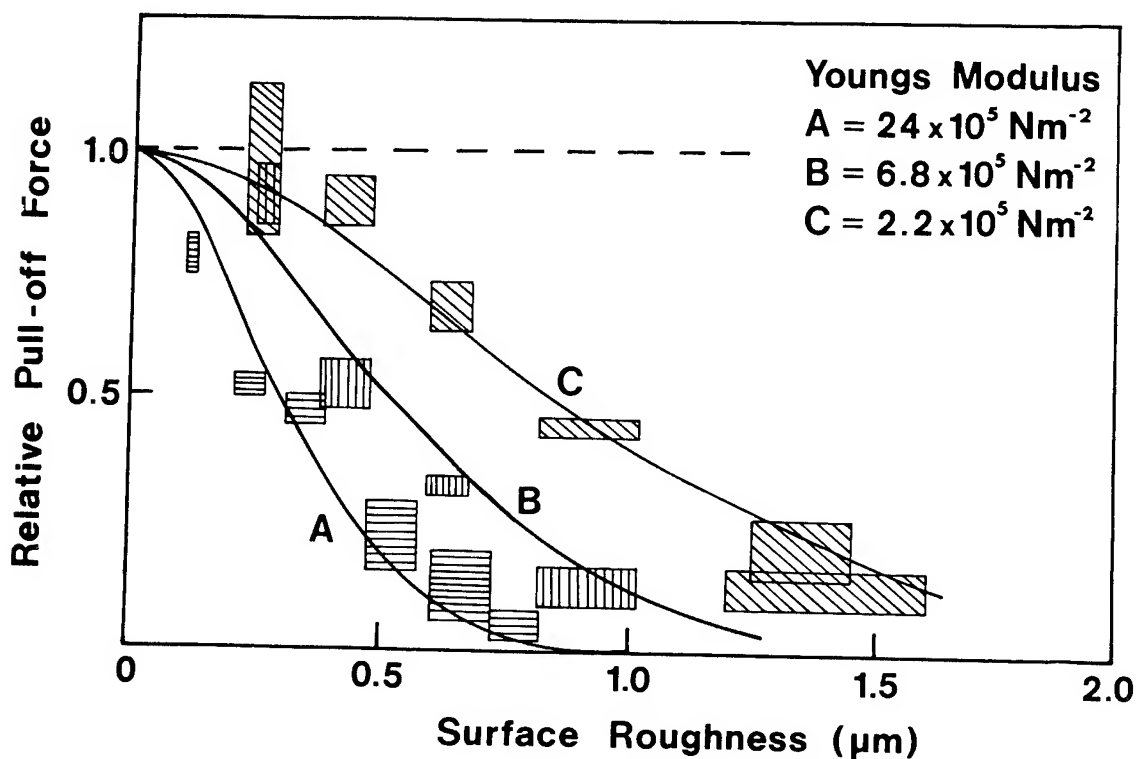
Figure 7. Adhesion of a smooth rubber sphere on a PMMA surface as a function of the roughness of the PMMA.

138
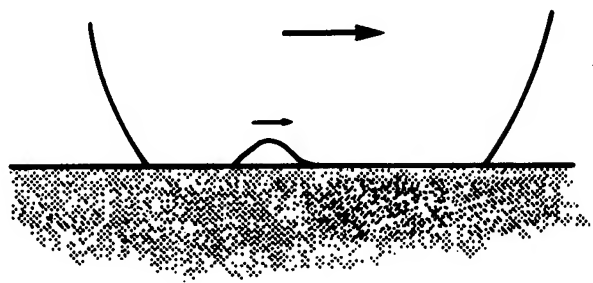
Figure 8. The movement of a ruck at the interface enables rubber to move over a smooth surface by a process of adhesion and dehesion.

DISCUSSION

Yoshitsugu Kimura
The University of Tokyo
Tokyo, Japan

The discusser would like to begin his discussion with a tribute to
Professor Tabor, as he began his plenary lecture at the ASME-ASLE Inter-
national Lubrication Conference held in 1980 with a tribute to Coulomb.
In collaboration with the late Professor Bowden, Professor Tabor has
made the most comprehensive contribution to our fundamental ideas about
friction in this century. Furthermore, it is our pleasure he is still
making it energetically.

We often say 'friction and wear' as a pair of words. However,
there is a marked difference in the present states of our understanding
of them. In the case of wear, even the most basic mechanisms are still
controversical. On the other hand, the adhesion theory afforded a
sound foundation on which our understanding of friction has grown by
steady steps. In particular, it should be appreciated that Professor
Tabor gave a beautiful explanation of frictional behavior in terms of
the junction growth concept.

Now, the discusser will take the liberty of pointing out a problem
of practical importance, which should be studied further. It is curious
that, in spite of all our understandings of the basic mechanisms of
friction, we cannot predict friction in a specific case to sufficient
accuracy. It seems that tribologists place no confidence in the tables
of coefficients of friction often seen in handbooks. Indeed, we know
general means of lessening friction by appropriate lubrication, but it

is still difficult to afford guarantee for a sliding system to have the coefficient of friction in a certain specified range. The possible predictions remain still qualitative, if not empirical.

In the discusser's opinion, the reason can be found in a fact that the states of the surfaces, with which we study friction, are not fully characterized, and this prevents the results to be generalized quantitatively. For example, it is well known that metals covered by the monolayer of fatty acids show lower friction if the longer-chain acids are used. However, the exact values of the coefficient of friction differ from experiment to experiment, mainly depending upon the difference in preparation of the metal surfaces on which the monoloayer is deposited.

Of course, there are some experimental results which were obtained with the surfaces well characterized by AES, LEED or other analytical tools, but these tools are only applicable to characterize the surfaces which are extraordinarily clean in the engineering sense. What is needed is to characterize 'contaminated surfaces.' It is a very difficult task indeed; if a surface is clean its state is unique, but if not surfaces can be contaminated in a great number of ways.

Once OECD published a glossary of terms and definitions in the field of friction, wear and lubrication. They defined 'dry sliding' as an imprecise term frequently used to indicate sliding under nominally unlubricated conditions. Nevertheless, innumerable studies of friction have been conducted with dry sliding, and many important conclusions have been derived from them. Moreover, the values of the coefficient of dry friction are required in engineering practices. It is desired to fortify the quantitative aspect of tribology by extending our basic understandings.

RESPONSE

David Tabor
Cavendish Laboratory
Cambridge, England

I agree with Professor Kimura. It would be marvellous if we could characterise "contaminated surfaces" in such a way that their tribological behaviour would become predictable. I think this is a very difficult task.

METALLIC ADHESION AND BONDING

John Ferrante
National Aeroanutics and Space Administration
Lewis Research Center
Cleveland, Ohio

John R. Smith*
General Motors Research Laboratories
Warren, Michigan

and

James H. Rose**
Ames Laboratory (U.S. Department of Energy)
Iowa State University
Ames, Iowa

Although metallic adhesion has played a central part in much tribological speculation, few quantitative theoretical calculations are available. This is in part because of the difficulties involved in such calculations and in part because the theoretical physics community is not particularly involved with tribology. In the present paper we summarize the calculations currently involved in metallic adhesion and show that these can be generalized into a scaled universal relationship. We also show that relationships exist to other types of covalent bonding, such as cohesive, chemisorptive, and molecular bonding. A simple relationship between surface energy and cohesive energy is offered.

INTRODUCTION

An important aspect of friction and wear of metals is the nature of the adhesive force between the surfaces. Tabor (ref. 1) has used adhesion between metals to explain parts of the friction and wear process. Of particular interest in these processes is the physical nature of the forces in dissimilar metal contacts. There have been numerous attempts to postulate the nature of these forces, but few model calculations. For example, adhesion between dissimilar metals was explained in terms of solubility (ref. 2), but without accompanying model calculations. Buckley (ref. 3) has shown that metals with low mutual solubility can have higher adhesion than those with high solubility.

In order to deal with evaluating the effects of adhesion in metal-metal contacts, the problem must be viewed from several aspects. A real metal-metal contact is a physical situation with considerable complexity. In a real contact, surfaces are not flat; therefore, surface topography must be considered. Next, mechanical properties of the solid are important, e.g., ductility or brittleness; therefore, the nature of deformations which occur in the contact, e.g., elastic or plastic and elastic recovery, once the load has been removed are important. In addition, the effects of surface films and adsorbates on the binding forces and the mechanical properties of the interface must also be considered. Extensive consideration of these matters has been given by Tabor (ref. 1) and Pollock (ref. 4). An example of the behavior of a stress-strain curve for an adhesive contact with differing material properties is shown in figure 1.

Considering the complexity of the physics of real metal contacts, it is necessary to break the problem into its component parts with the hope of gaining some unity once the various components are understood.

The one aspect of the problem that has received the least attention is the metallic bonding force. This has occurred for two reasons. First, the theoretical techniques needed to treat this problem properly have only recently been developed (ref. 5), and second, the physics community, which is most appropriately able to tackle this problem, is not particularly aware of the field of tribology. Only a limited amount of fundamental theory has been attempted in this area. That of Ferrante and Smith (refs. 6 and 7) has treated the problem of simple metals in contact in great detail. Yaniv (ref. 8) and Allan, Lannoo, and Dobrzhynski (ref. 9) have treated the problem of transition metals in contact qualitatively. Rose, Ferrante, and Smith have recently shown that the simple metal results may be more general than first anticipated and may indeed be relevant to the case of transition metals in contact (refs. 10 to 14). In fact, they have shown that certain features in covalent bonding are universal.

In this paper, we will summarize the calculations of Ferrante, and Smith, and Rose, Ferrante, and Smith, and we will allude to the results of Yaniv and Dobrzhynski, Allan, and Lannoo.

FORMULATION OF THE PROBLEM

We will now describe an adhesion calculation on its most rudimentary level by considering two perfect surfaces in contact and the binding energy of this system as we pull them apart. No consideration will be given to deformation of materials in the subsurface region. The intent is to explore the bonding forces which exist in this type of contact. In examining this situation we see strong analogy to the surface energy. A possible definition of surface energy is the amount of energy per unit area required to separate a solid along a plane from zero to infinite separation. However, in this case we will extend this idea to two different metals in contact. A schematic diagram of such a model is shown in figure 2. The Kohn-Sham formalism (ref. 5) and the work of Lang and Kohn (refs. 15 and 16) will be used as guides in this calculation.

USE OF KOHN-SHAM FORMALISM FOR ADHESION CALCULATIONS

The calculational formalism and methods used for obtaining self-consistent interface electronic structure are now presented. A more extensive description

(particularly of numerical techniques) is given in references 6, 7, and 9. The adhesive interaction energy E_{ad} between two metal surfaces is a function of the distance a between the two surfaces (see fig. 1). E_{ad} is defined as the negative of the amount of work necessary to increase the separation from a to ∞ divided by twice the cross-sectional area A. Thus,

$$E_{ad} = \frac{E(a) - E(\infty)}{2A} \qquad (1)$$

where E is the total energy. For identical metals, E_{ad} is the negative of the surface energy when a is at the energy minimum.

According to the density functional formalism of Hohenberg, Kohn, and Sham (ref. 4), the total energy is given by (atomic units are used throughout unless otherwise specified)

$$E\{n(\vec{r})\} = \int v(\vec{r})n(\vec{r})d\vec{r} + \frac{1}{2} \sum_{i \neq j} \frac{z_i z_j}{R_{ij}} + F\{n(\vec{r})\} \qquad (2)$$

$$F\{n(\vec{r})\} = T_s\{n(\vec{r})\} + \frac{1}{2} \iint \frac{n(\vec{r})n(\vec{r}')}{|\vec{r} - \vec{r}'|} d\vec{r}d\vec{r}' + E_{xc}\{n(\vec{r})\} \qquad (3)$$

where $v(\vec{r})$ is the ionic potential, and $n(\vec{r})$ is the electron number density. The first two terms in equation (2) are the electron-ion and ion-ion interaction energies, respectively. z is the ionic charge and R_{ij} is the distance between ion core nuclei (there is no ion core overlap in the systems considered here). $T_s\{n(\vec{r})\}$ is the kinetic energy of a system of noninteracting electrons with the same density $n(\vec{r})$, the next term is the classical electron-electron interaction energy, and E_{xc} is the exchange-correlation energy.

The contribution of crystallinity to the electron-ion interaction is included using pseudopotentials and first-order perturbation theory (ref. 5). For metals like Zn, Mg, Al, and Na, the jellium model (fig. 1) is a good zeroth-order approximation, and the difference between the total pseudopotential and the potential due to the jellium is small for the closest packed plane. Thus, for a given separation a, one obtains E to a first-order perturbation approximation as

$$E\{n(\vec{r})\} = A \int v_j(y,a)n(y,a)dy + \frac{1}{2} \sum_{i \neq j} \sum \frac{z_i z_j}{R_{ij}} + F\{n(y,a)\}$$

$$+ A \int \delta v(y,a)n(y,a)dy \qquad (4)$$

where v_J is the potential produced by the jellium, y the direction normal to the surfaces, and δv the average, over planes parallel to the surface, of the difference in potential between an array of pseudopotentials and jellium. Following Lang and Kohn (ref. 5), the Ashcroft pseudopotential is used:

$$v_{ps}(r) = \begin{cases} 0, & r < r_c \\ -z/r, & r > r_c \end{cases} \tag{5}$$

where r_c is determined empirically and is close to the ion core radius. The electron number density is obtained from a set of self-consistent equations:

Schroedinger equation:

$$\left[-\frac{1}{2}\frac{d^2}{dy^2} + v_{eff}(n;y) \right] \psi_k^{(i)}(y) = \frac{1}{2}\left(k^2 - k_F^2 \right) \psi_k^{(i)}(y) \tag{6}$$

where

$$v_{eff}(n;y) = \phi(y,a) + \frac{\delta E_{xc}\{n(y,a)\}}{\delta n(y,a)}$$

$$n(y,a) = n_L(y,a) + n_R(y,a)$$

$$n_L(y,a) = \frac{1}{4\pi^2}\int_0^{k_{FL}} dk \left| \psi_k^L(y) \right|^2 \left(k_{FL}^2 - k^2 \right)$$

and

$$n_R(y,a) = \frac{1}{4\pi^2}\int_0^{k_{FL}} dk \left| \psi_k^R(y) \right|^2 \left(k_{FR}^2 - k^2 \right)$$

Poisson's equation:

$$\frac{d^2\phi(y,a)}{dy^2} = -4\pi[n(y,a) - n_+(y)] \tag{7}$$

where $\phi(y,a)$ is the electrostatic potential, $n_+(y)$ the jellium density (fig. 1), k_F the Fermi wave vector magnitude, and $\psi_k^{(i)}(y)$ the wave function ($i = L, R$; i.e., left and right). The calculation is divided into two regions, below the conduction band of the less dense metal and above it. Above the bottom of the conduction band of the less dense metal the solutions are doubly degenerate.

It is useful to combine the first two terms of equation (4) with the classical electron-electron interaction term of $F\{n(y,a)\}$ as follows:

146

$$-\frac{1}{2} A \int \rho(y,a)\phi(y,a)dy + W_{int} \qquad (8)$$

where $\rho(y,a)$ is the net charge density of the zeroth-order jellium solution. W_{int} is the exact difference between the ion-ion and the jellium-jellium interaction. W_{int}/A is negligible unless the facing planes are in registry, i.e., commensurate (ref. 17). In this calculation, we assume incommensurate adhesion ($W_{int} = 0$), since registry is not obtained with dissimilar metals in contact without corresponding loss of energy due to strains in the lattice which would be difficult to evaluate.

The exchange-correlation energy E_{xc} is written in the local-density approximation (LDA):

$$E_{xc}\{n(\vec{r})\} = \int n(\vec{r})\epsilon_{xc}(n(\vec{r}))d\vec{r} \qquad (9)$$

where $\epsilon_{xc}(n(r))$ is the exchange-correlation energy of a uniform electron gas of number density $n(r)$. We use Wigner's interpolation formula for the correlation energy and the Kohn-Sham exchange energy.

The kinetic-energy functional of equation (3) is

$$T_s\{n(y,a)\} = A \int t_s\{n(y,a)\}dy \qquad (10)$$

where

$$t_s\{n(y,a)\} = \sum_{i=1}^{2} \sum_{\substack{k,k_x,k_z \\ (occ.)}} \left(k^2 + k_x^2 + k_z^2\right)\left|\psi_k^{(i)}(y)\right|^2$$

$$+ [\nu_{eff}(n;\pm\infty) - \nu_{eff}(n;y)]n(y,a) \qquad (11)$$

The sum is over all occupied states. The summation index i again refers to degenerate wave functions as in equation (6). In references 6 and 7, an expression for $T\{n(y,a)\} - T_s\{n(y,0)\}$ is presented which is based on kinetic-energy densities in the interface region. We find this approach more natural for our problem, as it is the interface region in which the large changes in kinetic energy density occur upon adhesion.

RESULTS

The results of the calculation for all dissimilar combinations of Al(111), Zn(0001), Mg(0001), and Na(110) are shown in figure 3. As can be seen, there is a wide variation of shapes and binding energies, and the curves look very similar to binding energy curves for diatomic molecules.

Table I shows the binding energy for an adhesive contact under two conditions, registry and nonregistry. The binding energy is defined as the depth of the well. Registry is defined as a perfect continuation of the lattice across the interface. Obviously, this situation can occur only in a perfect crystal where the two halves are rejoined in exactly the way they were sepa-

rated with no relaxation effects. In real contacts this situation can not be obtained and the nonregistry results are the ones that should be considered.

As was just pointed out, there is a great similarity in appearance between the various binding energy curves. The question arises as to how quantitative this similarity is. Can some generalizations be obtained from these curves?

Scaling Rules for Adhesive Energies

The calculations needed to obtain the results for figure 2 are quite difficult and time-consuming. It is of interest, therefore, to look for some similarities between these curves which may generalize the results. Rose, et al. (ref. 10), have found such scaling laws. It will now be shown that the curves for figure 2, as well as those of the identical metal contacts (refs. 6 and 7) (Al(111) - Al(111), etc.), can be simply scaled into a universal curve. This scaling is motivated by the expectation that metals having shorter screening lengths would have adhesive energy curves which rise faster with separation; that is, the metals would screen the disturbances caused by creating the surface over a shorter distance. This suggests that for identical metal contacts the separation is scaled by the Thomas-Fermi screening length $\lambda = (9\pi/4)^{1/3} r_s^{1/2}/3$ (atomic units), where the bulk electron density $n_+ = 3/4\pi r_s^3$. When we encounter bimetallic contacts as represented in figure 1, a length scaling appropriate to both metals must be considered. In that case, we chose to scale by an arithmetic average, $(\lambda_1 + \lambda_2)/2$. The energy amplitude was scaled by its equilibrium value $\Delta E \equiv E_{ad}(a_m)$ where a_m is the equilibrium separation. Explicitly,

$$E_{ad}(a) = \Delta E E_{ad}^{\star}(a\star) \tag{12}$$

where $E_{ad}^{\star}(a\star)$ is the universal adhesive energy function and $a\star = 2(a - a_m)/(\lambda_1 + \lambda_2)$.

Figure 3 shows the results of scaling the calculated adhesive energies. An analytical fit is given by

$$E_{ad}^{\star} = -(1 + \beta a\star) \exp(-\beta a\star)$$

with $\beta = 0.90$. The universality of the scaled adhesive energy curve is truly remarkable. The results for all ten bimetallic contacts lie very close to the universal curve. This is true even though the bulk metallic densities in the various metals vary by a factor of eight.

It is important to understand how the fortunate result of a universal energy curve comes about. In the following, we attempt to provide a plausibility argument within the jellium model. First, we have found that solid-vacuum denisty distribution $n(y)$ (ref. 11) scale rather accurately with λ. In other words, there is, to a good approximation, a universal number denisty distribution $n\star(y - a/2)$ where

$$n(y - a/2) = n_+ n\star[\lambda^{-1}(y - a/2)] \tag{13}$$

Here $a/2$ is the coordinate of the jellium surface. There is a similar scaling for the Kohn-Sham effective one electron potential:

$$V_{eff}(y - a/2) = v_B v_{eff}^{\star}[\lambda^{-1}(y - a/2)] \tag{14}$$

148

We were motivated to look for this scaling by the fact that the Thomas-Fermi equation scales (refs. 18 and 19) exactly with y in units of λ. Secondly, we have found (refs. 6 and 7) that the total number density in the bimetallic interface is given to a fair accuracy by a simple overlap of the corresponding solid-vacuum distributions. This, and the stationary property of $E[n]$, indicates that it would be a good approximation to use overlapping solid-vacuum number density and potential distributions.

Thus, in a first-order perturbation approximation, we have for identical metal contacts

$$E_{ad}(a) \cong (1/A) \int_{-\infty}^{\infty} n(y - a/2)v_{eff}(y + a/2)dy \tag{15}$$

Combining equations (3) to (5), we have

$$E_{ad}(a) \cong (1/A)(n_+v_B) \int_{-\infty}^{\infty} n^*(y - a^*/2)v_{eff}^*(y + a^*/2)dy \tag{16}$$

The integrand in equation (16) is independent of r_s. The constants in front of the integral are independent of a, and thus equation (16) scales exactly as we scaled the adhesive energy curve to give figure 4. Although our plausibility agrument is restricted to jellium interfaces, we note that the calculated adhesive energies include the ion-ion term exactly for a rigid lattice model and the electron-ion term in first-order perturbation theory.

DISCUSSION

There are several topics of importance in metallic adhesion: the nature of the attractive forces, the range of such forces, and finally, any generalizations that can be found. The work of Ferrante and Smith (refs. 6 and 7) indicates that electron sharing similar to covalent bonding in molecules is sufficient to give strong bonding. They also determine the magnitudes of such forces for several simple metals (table I). These results also establish that an approximate range for the forces is an interplanar spacing. Finally, Rose, Ferrante, and Smith (ref. 10) have found scaling laws which generalize these results.

In metallic adhesion of real surfaces, further considerations come to mind. First, real surfaces are not flat, and consequently, how important are the strong forces compared to the weaker, long-range van der Waals forces Next, the results of these theoretical calculations represent ideal strengths. Real contacts fail at conditions lower than at ideal strengths. Finally, metals used in most engineering applications are either transition metals or alloys.

Inglesfield (ref. 20) examined the problem of van der Waals versus strong interaction forces using the calculations of Ferrante and Smith (ref. 17). He concluded that, even though the strong forces only dominate at the positions of asperity contact, these strong interaction forces dominate the strength of the contact.

The fact that the strength of real contacts is dominated by defect struc-
tures and the mechanical properties of the solids is an issue that ultimately
must be addressed. Also, these results apply only for brittle fracture; how-
ever, metals will undergo ductile extension before fracture. Since adhesion
and other contact processes are complicated combinations of physical and mech-
anical properties, each part of the process must be understood independently.
This study has been carried out in this spirit. The results of table I, how-
ever, contain some aspects of these considerations. A question of interest is
whether the binding energies of a dissimilar metal contact is weaker, stronger,
or between that of the same metal. The first column in table I (labeled
$W_{int} = 0$) gives the binding energy of a contact when perfect registry is not
obtained. Perfect registry can only be obtained when the same crystallo-
graphic planes of the same metal are in contact. A more complete discussion
of this issue is given in reference 17. The second column gives the binding
energy in the ideal case of perfect matching of planes, which does not occur
in a real contact. An examination of table I reveals that the interfacial
energy is slightly lower than or comparable to the bulk energy except for the
case of Na where the interface between Na and any of the other metals is
clearly stronger than the bulk. In a real contact, the two surfaces would
probably distort in an attempt to come into registry with the formation of
defect chains to accommodate the distortions, thus modifying the interfacial
energy. In general, the interfacial binding energy is comparable to the
energy of the weaker partner in the different metal contacts examined.

A final concern with these results is the limitations of the calculations.
The quasi-three-dimensionality of the adhesion calculations limits the reli-
ability of the calculations to the densest packed planes of the simple metals.

Most engineering materials are transition metals. To properly handle
transition metals would theoretically require extensive three-dimensional
calculations which are now in progress. Yaniv (ref. 8) and Allan, Lannoo, and
Dobrzhinski (ref. 9) have applied the tight-binding approximation to the tran-
sition metal problem. Although these calculations probably give accurate
trends, the approximations used make quantitative results questionable.

The question arises concerning whether the results are more general than
for the simple metals examined. Recently, theoretical binding energy curves
have become available for several bulk metals (Carlsson, et al. (ref. 21),
(Mo, K, and Cu) and unpublished data from J.F. Herbst for calculations of Sm
and Ba (Sm^{+2}, Sm^{+3}, and Ba)(In this case, r_s was determined from the electron
density at the cell boundary.)). These total cohesive energy curves were cal-
culated as a function of the separation between atoms for a uniformly dilated
lattice. We characterize the density of the lattice in terms of the Wigner-
Seitz radius $r_{ws} = (3/4\pi n_A)^{1/3}$ where n_A is the atom density. As shown in
figure 5, these quite disparate cohesive energy curves can be approximately
scaled into a universal function E_c^*, which is also defined in equation (12)
if we replace E_{ad} by E_c everywhere. ΔE is the cohesive energy at the
equilibrium spacing r_{wsm} and $a^* = (r_{ws} - r_{wsm})/\lambda$ where λ is again the
Thomas-Fermi screening length. The value of r_s used to determine λ was
determined by the equilibrium interstitial electron density (ref. 21 and Herbst's
unpublished data). The binding energies of Mo, K, Ba, $Sm[4f (5d,6s)^2]$, and
$Sm^{+3}[4f^2(5d,6s)^3]$ fall closely on a single curve with $\beta = 1.16$ where we have
used the same analytic form as for the adhesive energies. The value of β
differs from that appropriate for adhesive energies presumably, in part,
because all atoms change their positions in the bulk cohesive energy calcula-

tions while the adhesive energy curves assume that atomic planes are moved rigidly. The results for Cu have the same shape, but a somewhat different β than the other metals. We do not understand this variation.

The cohesive energy calculations for Carlsson, et al. (ref. 21) (ASW density functional theory), and Herbst (unpublished data) (relativistic Hartree-Fock) are quite different from each other and from the perturbative-density functional results of references 6 and 7 for E_{ad}. The nature of cohesive bonding in these metals is quite varied. Ba is a divalent band overlap metal; Sm is an f-electron metal; Mo and Cu have important d-band interactions; while K is a simple metal. That such different metals calculated in quite different ways fall on a single curve indicates the generality of the scaling relations. We note that the "tail" region of the screening charge distribution around metal ion cores can be represented by electron gas parameters. The screening charge density and potential in this region scale as $r_s^{1/2}$ to a fair approximation (ref. 23). Then the agrument of equations (13) to (15) applies to the long-range interaction of screened bulk ions with $\pm a/2$ referring to the relative lattice positions and y replaced by $\vec{r}$.

The use of the electron density at r_{ws} is reminiscent of the approach of Miedema, et al. (refs. 24 and 25), whose work complements our own. They calculate equilibrium energies (e.g., heats of formation). We, on the other hand, use similar equilibrium quantities to determine the form of the binding energy-distance relation.

The plotted energies of figure 4 were computed for the same electronic configuration at all atomic separations as were the interface calculations. The adhesive energy scaling was illustrated for simple metals. However, the appearance of an analogous scaling relation for the bulk energy of transition metals indicates that the adhesive energy scaling may well extend beyond simple metals.

As can be seen from the scaled curves, the quality of the fit for cohesive energies is not as close as for the adhesive energies. This occurs because the screening length for the varied types of bonding for the metals considered is not well defined. As a consequence, another type of scaling is chosen which is suggested because of the success of the screening length scaling. The second derivative of the binding energy at the minimum is used to define the scaling length (ref. 12). In figure 6 we show the result of this scaling for the adhesive energy. As can be seen, the quality of the fit is equally good. Using this technique for scaling the cohesive energy (fig. 7) greatly improves the quality of the fit, giving even stronger support for the extension of the adhesive energy universality. A more remarkable result occurs if we ask whether there is some universality of covalent bonding in general. In figure 8 we show a plot of molecular, chemisorptive, adhesive, and cohesive bonding using the second derivative scaling technique. As we can see, all types of covalent bonding have the same universal shape. This is a stronger result regarding universality because the binding energy curve for H_2^+ is exact and is not dependent on some calculational mode. Knowing the universality of shape for these types of binding has important further implications with regard to obtaining interrelationships between physical properties. We present two possibilities, the vibration spectra of chemisorbed atoms and the relationship between surface energy and cohesive energy, the support our assertions.

Relation of Surface and Cohesive Energies

As an example of relationships that can be derived from the knowledge that universality exists, we look for a relationship between surface energies σ and cohesive energies E_{coh}. Using the stated scaling laws,

$$\left[\frac{d^2E(a)}{da^2}\right]_{a_m} = \frac{\Delta E}{\ell_{TF}^2}\left[\frac{d^2E^*(a^*)}{da^{*2}}\right]_0 \tag{17}$$

For adhesion, expression (17) can be approximated in terms of C_{11}', the elastic stiffness constant associated with the direction perpendicular to the interface as

$$\frac{2\sigma}{\ell_{TF}^2}\left[\frac{d^2E_{ad}^*(a^*)}{da^{*2}}\right]_{a_m^*} = \frac{C_{11}'}{d} \tag{18}$$

where d is the interplanar spacing. Similarly, for uniform dilation of a bulk metal,

$$\frac{E_{coh}}{\ell_{TF}^2}\left[\frac{d^2E^*(a^*)}{da^{*2}}\right]_{a_m^*} = 12\pi Br_{ws} \tag{19}$$

where B is the bulk modulus.

Combining equations (18) and (19) gives

$$\frac{\sigma}{E_{coh}} = \left\{\left[\frac{d^2E^*(a^*)}{da^{*2}}\right]_{a_m^*} \middle/ \left[\frac{d^2E_{ad}^*(a^*)}{da^{*2}}\right]_{a_m^*}\right\}\frac{C_{11}'}{2d}\left(\frac{1}{12\pi Br_{ws}}\right) \tag{20}$$

Because of the universality, the ratio of the second derivatives in the brackets is independent of the metal considered. From figures 6 and 7 one can evaluate them, and

$$4\pi r_{ws}^2\sigma = 1.7\frac{C_{11}'}{2d}\frac{r_{ws}}{3B}E_{coh} \tag{21}$$

As will be discussed, the term $\dfrac{C_{11}'}{2d}\dfrac{r_{ws}}{3B}$ is a constant within ± 20 percent for a wide range of metals. Thus, we find

$$(4\pi r_{ws}^2)\sigma \propto E_{coh} \tag{22}$$

152

This is a well known empirical result. We see now that a simple proportionality relation between a metal's cohesive and surface energies per atom is due to universal behavior exhibited by the binding energy relations.

For the (111) face of an fcc metal, equation (23) can be rewritten as

$$\sigma \approx 0.25 \; \frac{(C_{11} + 2C_{12} + 4C_{44})}{C_{11} + 2C_{12}} \; \frac{E_{coh}}{a^2} \tag{23}$$

For the (110) face of a bcc metal,

$$\sigma = 0.24 \; \frac{(C_{11} + C_{12} + 2C_{44})}{C_{11} + 2C_{12}} \; \frac{E_{coh}}{a^2} \tag{24}$$

For the (0001) face of a close-packed hcp metal,

$$\sigma = 0.17 \; \frac{C_{33}}{C_{11} + 2C_{12}} \; \frac{E_{coh}}{a^2} \tag{25}$$

Here the C's are the elastic constants and a is the lattice parameter for the fcc and bcc metals. Equations (17) to (22) show that the energetics of cleavage are entirely controlled by the energetics of the bulk solid within the approximations to universality which we have made. The details for establishing constants are found in reference 13.

Subsequently we will test the accuracy of our expressions for the surface energy. In figure 9 we plot the left side of equation (17) against the right side and obtain a 45° straight line. This represents the theoretical predictions. We have also plotted the experimental values of the same quantities. Deviations of experimental values from the theoretical estimate indicate either experimental error or inaccuracies in the theoretical prediction. In figure 9 we see that the experimental values for the cubic metals agree with the theory to within ±20 percent which is comparable to the experimental accuracy to which the surface energy of the densest faces is known for these metals. Similar agreement can be obtained for hcp metals.

Chemisorption on Transition Metals

A further example of the utility of the relations given in the last section deals with chemisorption. Given the perhaps surprising accuracy of the scaling relations of adsorbates on jellium, one might well ask if a similar relation exists for adsorbates on crystalline transition metals. In this case a number of complexities arise with respect to the results shown for the jellium surface. First, in the relatively open structure of the crystalline solid, an adsorbate in, say, the fourfold symmetric site may penetrate between the surface atoms. It is hard to imagine that a scaling length simply related to local electron density would describe the binding of an adsorbate in that case as well as an adsorbate located far from the surface. Secondly, the nature of the bonding is rather different, depending on the surface geometry

at the adsorbate's site (e.g., the on-top, the twofold, or the fourfold symmetric site).

We have met the first difficulty by considering only adsorbates which bond in the exponential tail region of the substrate electron density. Those adsorbates which penetrate so far into the metal surface as to lie between surface atoms are neglected. The fact that the relationship between the electron density and the scaling length varies from site to site can be used to advantage. Here the variation will aid in deciding on the site for a given observed adsorbate.

In order to test this extension of the universal scaling hypothesis, we will derive the simple relation which it implies between the adsorbate-substrate vibrational stretch excitation energy ω and its desorption energy ΔE. Then we will test this relation for a variety of adsorbates on Ni(100). From the scaling relations,

$$\omega = \left[\frac{1}{M} \frac{d^2 E(a)}{da^2} \right]_{a_m}^{1/2} = \left[\frac{\Delta E}{M \ell^2} \frac{d^2 E^*(a^*)}{da^{*2}} \right]_{a_m}^{1/2} \tag{26}$$

We ignore modes in which the vibration of the substrate atoms is important.

Here M is the mass of the adsorbate. One might hope to determine $(d^2 E^*/da^{*2})_{a_m}$ by scaling $E(a)$, which gives a universal shape. In fact, no such curves of $E(a)$ are available for transition metal surfaces. However, one can eliminate $(d^2 E^*(a^*)/d^2 a^*)_{a_m}$ by considering only ratios of vibrational stretch frequencies for different atomic adsorbates, all at the same site. The vibrational energy of one adsorbate, ω_2, given that of another adsorbate is

$$\omega_2 = \omega_1 \left[\frac{\Delta E_2}{\Delta E_1} \frac{M_1}{M_2} \frac{n_2^{1/3}(a_m)}{n_1^{1/3}(a_m)} \right]^{1/2} \tag{27}$$

Here we have used the local density result for the screening length. The densities are given by the bare metal surface.

One can test equation (27) in the following way. Upton and Goddard (ref. 26) have used the generalized valence bond method to treat chemisorption of gas atoms on a 20-atom Ni cluster, yielding values of ω and ΔE for various adsorption sites on the cluster. The clean surface electron densities $n(a_m)$ are obtained from a self-consistent local-orbital calculation for a Ni(100) film (ref. 27). While some differences are expected between the cluster and film substrates, this provides an approximate test. For the one-fold or on-top site of Ni(100) the results are given in table II(a). The reference adsorbate was taken to be Cl, although the choice is arbitrary and does not affect the test. The agreement on adsorbate vibrational frequencies is rather good, considering the large range between H and Na. Apparently the mixture of s-, p- and d-symmetries is not a severe complication here. For this site the adsorbate equilibrium positions are relatively far from the surface. For the twofold and fourfold sites, the H equilibrium positions are quite close to the surface, and the penetration problem discussed previously is severe. Vibrational frequencies for H from equation (27) are two to three

154

times too large for these sites. The results are generally good for the other adsorbates, however, as shown in table II(b) and II(c). Here the reference adsorbate was taken to be S. For O there are two chemisorbed states in the twofold site and only one for the fourfold site. In every case, there is reasonably good agreement, with the lone exception of Cl on the Ni(1000) two-fold site. We have no explanation for the one Cl result at this time. The results for the other sites and adsorbates do suggest that universality approximately extends to chemisorption on cyrstalline transition metals, provided that the adsorbate does not penetrate the surface atomic layer.

We suspect that equation (27) may be of use to experimentalists who are looking for a rough check of their vibrational or desorption energy results. In that connection, it is perhaps important to note that equation (27) applies only to adsorbates on the same symmetry site. One gets quite inaccurate results, for example, if adsorbate 1 of equation (27) is on a onefold site and adsorbate 2 is on a fourfold site. This difference may be useful in experimentally determining the adsorbtion site. For example, if a set of measured desorption energies and vibrational frequencies scales nicely using equation (27) for one particular site (say the onefold site) but not for the others, then one has some indication that the site is, in fact, onefold symmetric. The determination of relative vibrational frequencies depends on knowing the electron number density for the clean substrate and the adsorbate's position. Such clean substrate densities may be either obtained from the overlapping atom approximation or from first principles calculation (ref. 27), as in our example.

Since the dependence on the density is weak ($n^{1/6}$), equation (27) can be roughly approximated as

$$\omega_2 \approx \omega_1 \left(\frac{\Delta E_2}{\Delta E_1} \frac{M_1}{M_2}\right)^{1/2} \tag{28}$$

While equation (28) is not as accurate as equation (27), it may nevertheless be useful in correlating experimental data. The vibrational frequency trends listed in tables II(a) to II(c) are preserved when equation (28) is used.

In conclusion, we have discovered scaling relations which map adhesive energies onto a universal binding energy curve. Similar scalings for cohesive energies for a wide range of metals suggest that this relation may apply to more than just the simple metals. Finally, a simple analytic energy-separation scaling relation is provided which may be of use in practical analysis of contacts.

REFERENCES

1. Tabor, D.: Interaction Between Surfaces – Adhesion and Friction. Surface Physics of Materials, vol. 2, J.M. Blakely, ed., Academic Press, 1975, pp. 476-529.
2. Rabinowicz, E.: Friction and Wear of Materials. Wiley, 1965.
3. Buckley, D.H.: The Metal-to-Metal Interface and its Effects on Adhesion and Friction. J. Colloid Interface Sci., vol. 58, 1977, pp. 36-53.
4. Chowdhury, S.K.R.; et al.: Adhesion Energies at a Metal Interface – the Effects of Surface Treatments and Ion Implantation. J. Phys. D, vol. 13, 1980, pp. 1761-1784.

5. Kohn, W.; and Sham, L.J.: Self-Consistent Equations Including Exchange and Correlation Effects. Phys. Rev. Sec. A, vol. 140, 1965, pp. 1133-1138.

6. Ferrante, J.; and Smith, J.R.: Theory of Metallic Adhesion. Phys. Rev. Sec. B, vol. 19, no. 8, 1979, pp. 3911-3920.

7. Ferrante, J.; and Smith, J.R.: Theory of Metallic Adhesion. Bull. Am. Phys. Soc., vol. 26, 1981, p. 428.

8. Yaniv, A.: Electronic Properties of a Simple Metal-Metal Interface. Phy. Rev. Sec. B, vol. 17, no. 10, 1978, pp. 3904-3918.

9. Allan, G.; Lannoo, M.; and Dobrzynski, L.: Simple Self-Consistent Theory of Adhesion at a Bimetallic Interface. Philos, Mag., vol. 30, 1974, pp. 33-45.

10. Rose, J.H.; Ferrante, J.; and Smith, J.R.: Universal Binding Energy Curves for Metals and Bimetallic Interfaces. Phys. Rev. Lett., vol. 47, no. 9, Aug. 1981, pp. 675-678.

11. Smith, J.R.; Ferrante, J.; and Rose, J.H.: Universal Binding-Energy Relation in Chemisorption. Phys. Rev. Sec. B, vol. 25, no. 2, Jan. 1982, pp. 1419-1422.

12. Ferrante, J.; Smith, J.R.; and Rose, J.H.: Universal Binding Energy Relations in Metallic Adhesion. Microscopic Aspects of Adhesion and Lubrication, J.M. Georges, ed., Elsevier (Amsterdam), 1982, pp. 19-30.

13. Rose, J.H.; Smith, J.R.; and Ferrante, J.: Universal Features of Bonding in Metals. Phys. Rev. B, vol. 28, no. 2, July 1983.

14. Ferrante, J.; Rose, J.H,; and Smith, J.R.: Diatomic Molecules and Metallic Adhesion, Cohesion and Chemisorption - A Single Binding-Energy Relation. Phys. Rev. Lett., vol. 50, no. 18, May 1982, pp. 1385-1386.

15. Lang, N.D.; and Kohn, W.: Theory of Metal Surfaces - Charge Denisty and Surface Energy. Phys. Rev. Sec. B, vol. 1, no. 12, 1970, pp. 4555-4568.

16. Monnier, R.; and Perdew, J.P.: Surfaces of Real Metals by the Variational Self-Consistent Method. Phys. Rev. Sec. B, vol. 17, no. 6, 1978, pp. 2595-2611.

17. Mrowka, B.; and Rechnagel, A.: Theory of Metals According to the Thomas-Fermi Method. Physik. Z., vol. 38, 1937, pp. 758-765.

18. Ying, S.C.; Smith, J.R.; and Kohn, W.: Self-Consistent Screening of Charges Embedded in a Metal Surface. J. Vac. Sci. Technol., vol. 9, 1972, pp. 575-578.

19. Inglesfield, J.E.: Adhesion Between Al Slabs and Mechanical Properties. J. Phys. F., vol. 6, no. 5, 1976, pp. 687-701.

20. Ferrante, J.; and Smith, J.R.: A Theory of Adhesion at a Bimetallic Interface-Overlap Effects. Surf. Sci., vol. 38, no. 1, July 1973, pp. 77-92.

21. Carlsson, A.E.; Gelatt, C.D., Jr.; and Ehrenreich, H.: An ab initio Pair Potential Applied to Metals. Philos. Mag. A, vol. 41, no. 2, 1980, pp. 241-250.

22. Moruzzi, V.L.; Janak, J.F.; and Williams, A.R.: Calculated Electronic Properties of Metals. Pergamon Press, 1978.

23. Raimes, S.: The Wave Mechanics of Electrons in Metals. Interscience Publishers, 1961, Eq.10,85, pp. 305.

24. Miedema, A.R.; Boom, R.; and DeBoer, F.R.: On the Heat of Formation of Solid Alloys. J. Less-Common Met., vol. 41, 1975, pp. 283-298.

25. Miedema, A.R.: The Heat of formation of Alloys. Phillips Tech. Rev., vol. 36, no. 8, 1976, pp. 217-231.

26. Upton, T.H.; and Goddard, W.A., III.: Chemisorption of Hydrogen, Chlorine, Sodium, Oxygen, and Sulfur Atoms on Nickel(100) Surfaces - A Theoretical Study Using Nickel (Ni20) Clusters. CRC Crit. Rev. Solid State Mater. Sci., vol. 10, no. 3, 1981, pp. 261-296.
27. Arlinghaus, F.J.; Gay, J.G.; and Smith, J.R.: Self-Consistent Local-Orbital Calculation of the Surface Electronic Structure of Ni(100). Phys. Rev. Sec. B, vol. 21, no. 6, Mar. 1980, pp. 2055-2059.
28. Kittel, C.: Introduction to Solid State Physics. 4th Ed., Wiley, 1971.
29. Simmons, G.; and Wang, H.: Single Crystal Elastic Constants and Calculated Aggregated Properties. 2nd Ed., MIT Press, 1971.
30. Tyson, W.R.; and Miller, W.A.: Surface Free Energies of Solid Metals - Estimation from Liquid Surface Tension Measurements. Surf. Sci., vol. 62, 1977, pp. 267-276.
31. Tyson, W.R.: Surface Energies of Solid Metals. Can. Metall. Q., vol. 14, 1975, pp. 307-314.

TABLE I. - BINDING ENERGY COMPARISON[a]

Metal combination	Binding energy	
	$W_{int} = 0$, ergs/cm^2	Perfect registry
Al(111)-Al(111)	490	715
Zn(0001)-Zn(0001)	505	545
Mg(001)-Mg(0001)	460	550
Na(110)-Na(110)	195	230
Al(111)-Zn(0001)	520	
Al(111)-Mg(0001)	505	
Al(111)-Na(110)	345	
Zn(0001)-Mg(0001)	490	
Zn(0001)-Na(110)	325	
Mg(0001)-Na(110)	310	

[a]All energy values taken from the minimum in the adhesive energy plots (see figs. 3 and 4).

TABLE II. – COMPARISON OF ADSORBATE-SUBSTRATE VIBRATIONAL STRETCH MODE FREQUENCIES COMPUTER FROM EQUATION (27) WITH THOSE OF REFERENCE 26

(a) One-fold site on Ni(100)

Absorbate	Vibrational frequencies, meV	
	Reference 26	Equation (27)
H	283	242
Cl	43.6	-----
Na	19.3	22.7

(b) Two-fold site on Ni(100)

Absorbate	Vibrational frequencies, meV	
	Reference 26	Equation (27)
Cl	32.4	59.9
Na	16.9	22.9
S	48	----
O	65	56.1
O	68	72.9

(c) Four-fold site on Ni(100)

Absorbate	Vibrational frequencies, meV	
	Reference 26	Equation (27)
Xl	30.4	31.8
Na	16.9	13.8
S	37	----
O	46	50.7
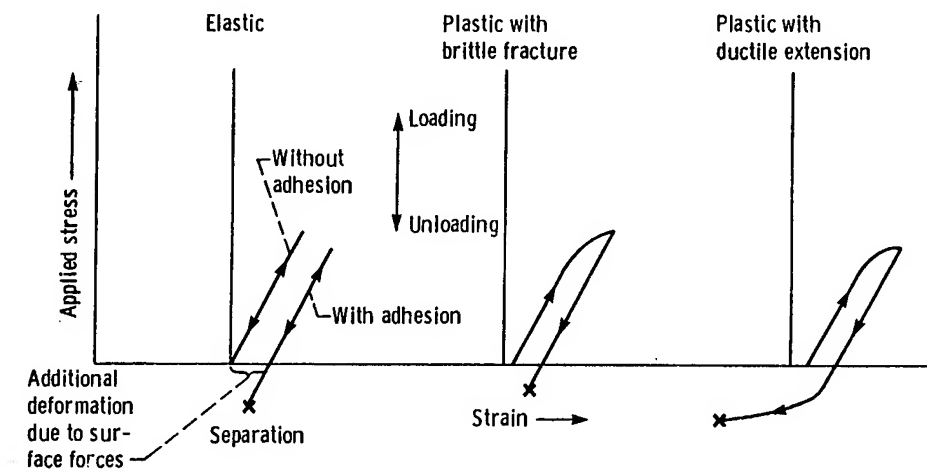
Figure 1. - Loading and unloading stress-strain curves with adhesion (idealized single contact) (ref. 4).
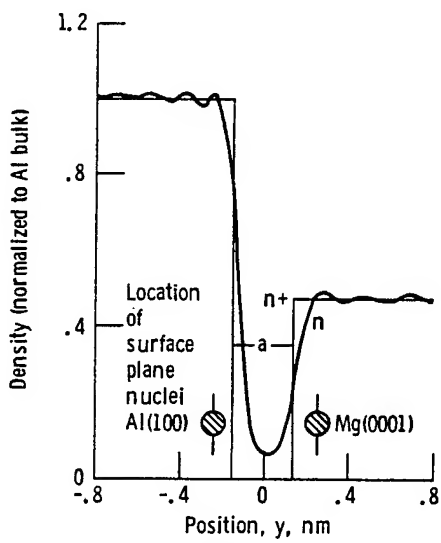

Figure 2. - Electron number density n and jellium ion charge density n_+ for an Al-Mg contact.

159
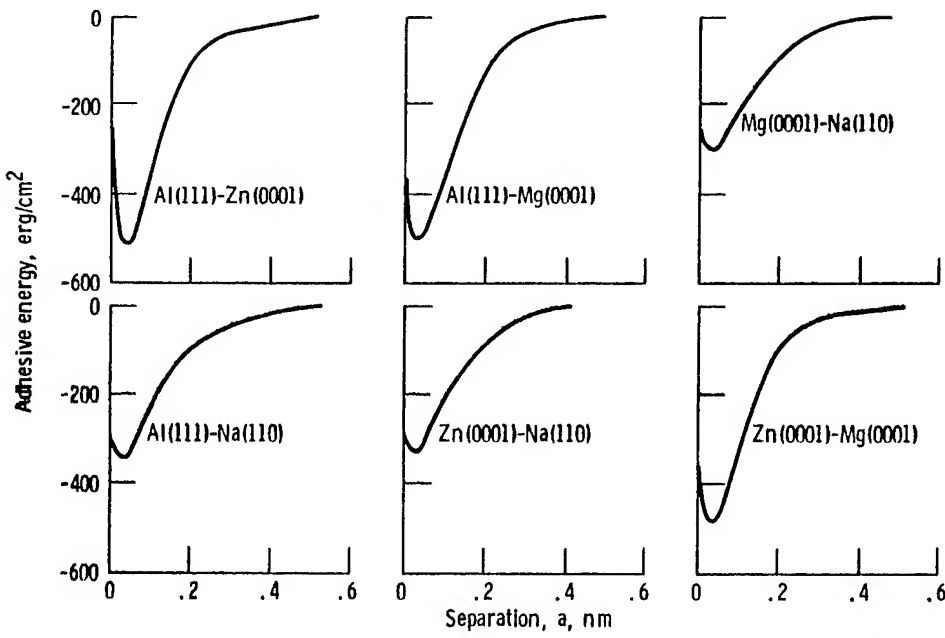
Figure 3. - Adhesive binding energy versus the separation a between the surfaces indicated.
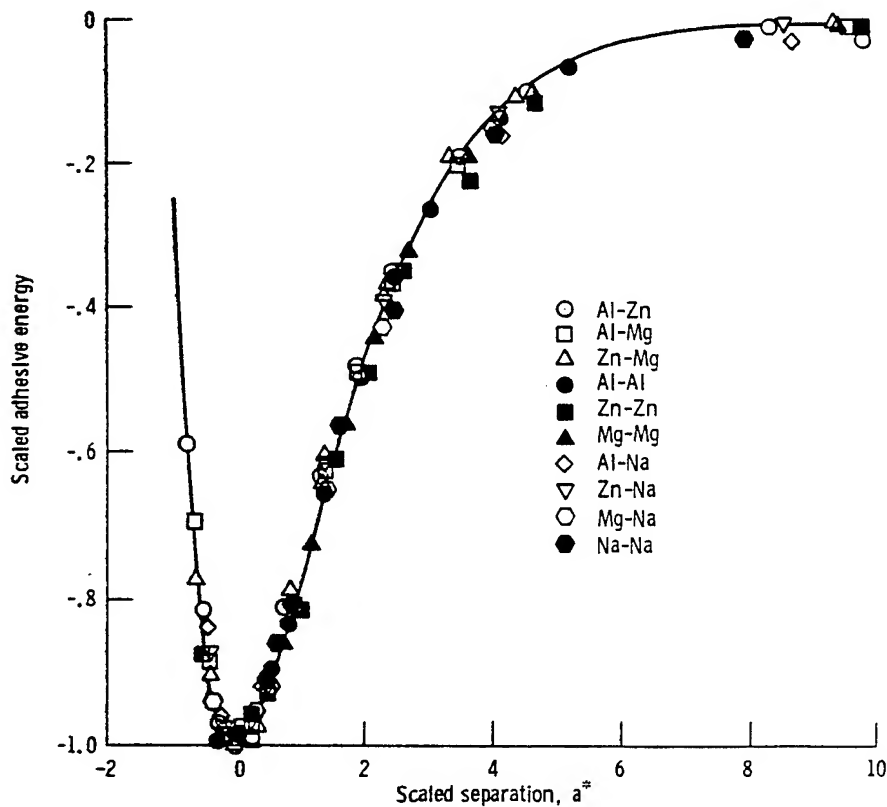
Figure 4. - Scaled bimetallic adhesion energy versus separation using screening
length for separation scaling.

160
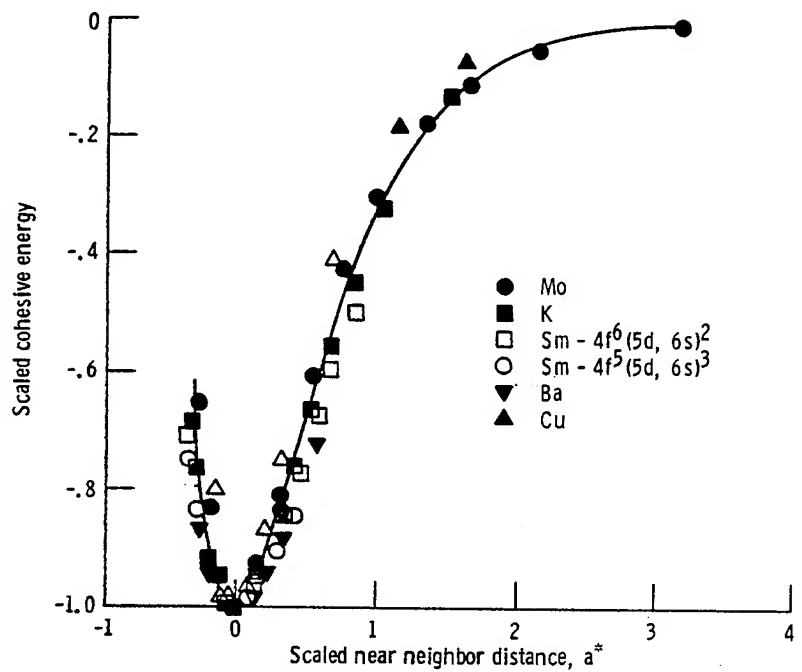
Figure 5. - Scaled cohesive energy versus scaled nearest neighbor distance using the screening length for nearest neighbor scaling.
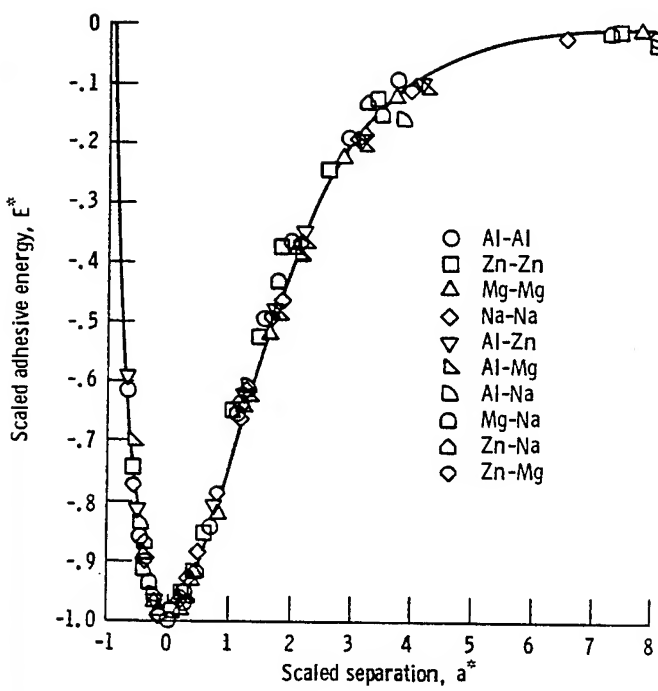
Figure 6. - Scaled adhesive energy versus separation using second derivative at minimum to define scaling length.
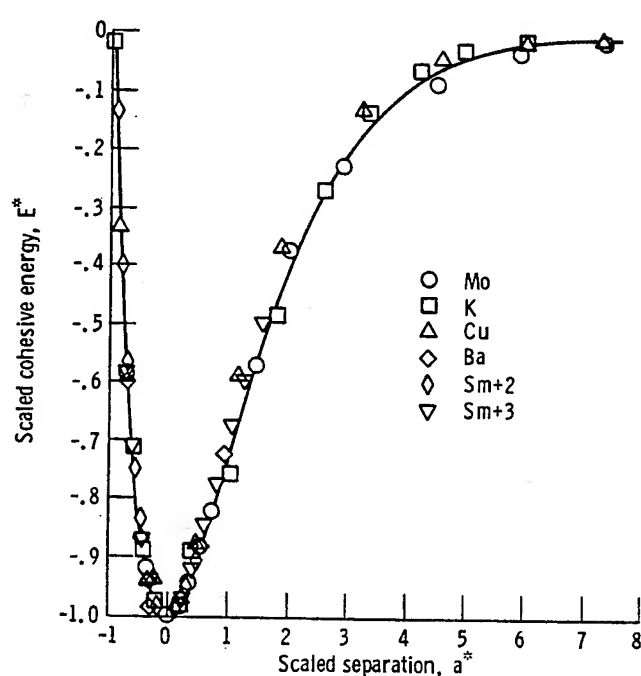

Figure 7. - Scaled cohesive energy versus separation using second derivative at minimum to define screening length.

161
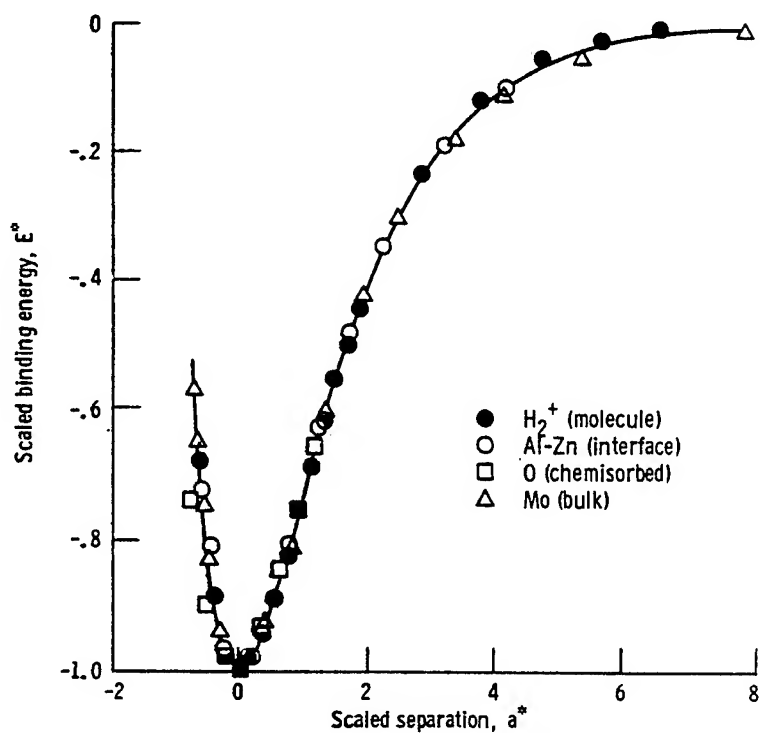
Figure 8. - Scaled binding energy versus separation for different types of covalent bonding using the derivative at the minimum to define scaling length.
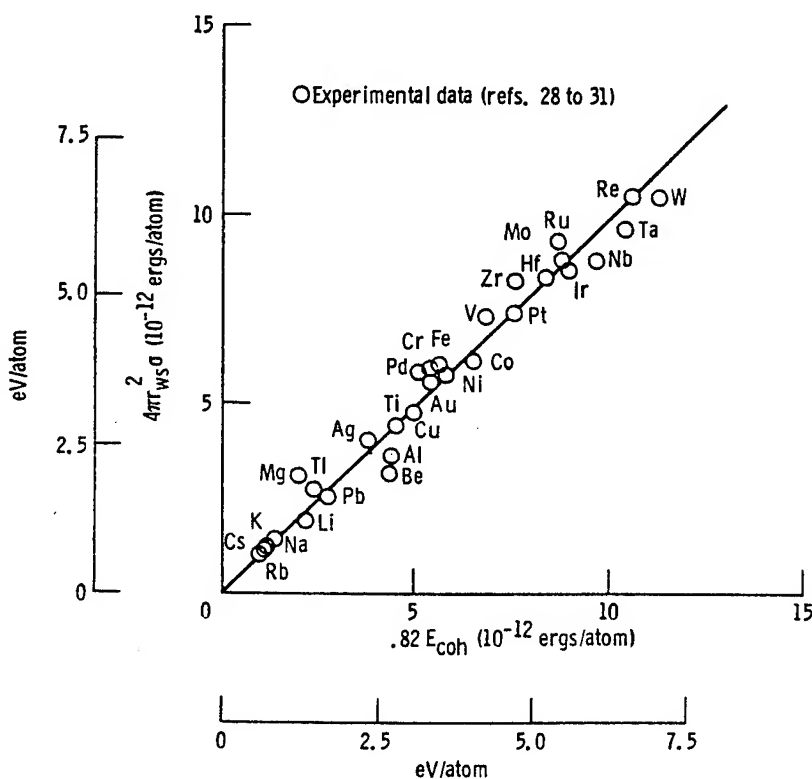

Figure 9. - Plot at left side of equation (24) versus left side yielding straight line.

162

DISCUSSION

Lieng-Huang Lee
Xerox Corporation
Webster Research Center
Webster, New York

Dr. Ferrante should be congratulated in undertaking this fundamental study about metal adhesion. Indeed, adhesion is one of the fundamental phenomena involved in friction and wear of materials, and its magnitude depends on the distance between the two counterbodies, or the interacting members discussed in this paper.

I would like to hear the author explain the following questions:

(1) What is jellium?
(2) Why the jellium model is only good for Na, Zn, etc.?
(3) What is the screening length of metal?
(4) Why your scaling fit in most cases of metal adhesion?
(5) How does electron orbital overlapping explain the metal-bonding?

I also would like to suggest that the author include a list of notations in the final manuscript.

THE STRENGTH OF THE METAL - ALUMINUM OXIDE INTERFACE

Stephen V. Pepper
National Aeronautics and Space Administration
Lewis Research Center
Cleveland, Ohio

The strength of the interface between metals and aluminum oxide is an important factor in the successful operation of devices found throughout modern technology. One finds the interface in machine tools, jet engines, and microelectronic integrated circuits. The strength of the interface, however, should be strong or weak depending on the application. The diverse technological demands have led to some general ideas concerning the origin of the interfacial strength, and they have stimulated fundamental research on the problem. This paper reviews the present status of our understanding of the source of the strength of the metal - aluminum oxide interface in terms of interatomic bonds. Some future directions for research are suggested.

INTRODUCTION

Tribology is the study of friction and wear of sliding systems. Our current understanding of the physical basis for the friction force is that it is due, at least in part, to the adhesion between the sliding bodies (ref. 1). Thus, the strength of an interface is of fundamental interest in tribology and it may be through the study and understanding of interfacial strength that some aspects of tribological systems may be understood.

The strength of an interface is a fundamental physical property of a system and as such may be considered the province of the physicist to explore and understand the sources of strength. The metal-metal interface has been treated in just such a way by Ferrante and collaborators (refs. 2 and 3). They modeled the system in terms of the free electrons in the solid, and the adhesive strength of the interface was found to be due to the overlap of the free electrons that spilled out of the solid a little ways into the vacuum. In fact, the source of interfacial adhesive strength was found to be the same as the source for internal cohesion of a metal - the interaction of the free electrons.

When one asks for the source of strength of a metal-nonmetal interface, the approach that generally proves useful for the metal-metal interface fails because of the lack of free electrons in the nonmetal. In fact, the class of nonmetals is too varied to even consider the possibility of such a very general approach. After all, the nonmetals span the range of solid types from the very ionic alkali halides to the completely covalent diamond and include the mixed cases of polymers. Each class of nonmetals may be expected to interact differently with metals to establish an interfacial strength so one must be more specific and concentrate on a particular subclass or even a particular material to make progress.

After the choice of a nonmetallic material is made, then a way to understand interfacial strength must be found - the first, a theoretical approach as for the metal-metal case, or the second, an experimental approach to gather evidence regarding the nature of the interfacial forces. The former approach requires insight into the nature of the interfacial forces before a theory can

165

be developed. Such as approach was provided by Ferrante for metal-metal adhesion. The other approach, an experimental one to poke and prod the interface to elicit information concerning the source of its strength, is the one I will describe here.

The nonmetallic material considered is aluminum oxide and the metals are just about all that can be used (and referenced). The reason for this choice is simple – the aluminum oxide – metal interface is found throughout an extraordinary range of technologies, and its strength is important from the small clean world of the microelectronic integrated circuit to the big dirty world of the industrial machine shop. Considering the wide range of technical applications for this interface, there is ample reason to search for the fundamental source of strength. And yet, if one looks in the literature, one finds almost nothing. Certainly nothing to rival the consideration given to understanding the metal-metal interface.

Thus, the approach here is to describe what the technologies – and experiments done within a technology – have to tell us about the nature of the interaction between metals and aluminum oxide that leads to interfacial strength. In essence, it is an attempt to gather those places where one finds the metal – aluminum oxide interface and ferret out those aspects of the technology that give insight to interfacial strength.

However, it is important to emphasize that finding evidence of interfacial strength is almost never straightforward. The reason is that the system strength (which is the endpoint in the technology) is not just the result of interfacial strength but also involves the properties (mechanical, physical, chemical) of the partners making up the interface as well as the precise method of formation of the interface (temperature, time, environmental conditions). All these latter aspects of system strength can mask the role of interfacial strength. Thus, one benefit of making a broad survey of the technologies is the promise that the interfacial strength will remain a constant of the motion (so to speak) while the properties of the partners and the history of the interface change. Hopefully the common aspect of interfacial strength will be persuasively revealed. We will then list those aspects of interfacial strength that require a fundamental explanation and present their current state of understanding. Finally, some suggestions will be made for research, both theoretical and experimental, in this rather poorly understood area.

THE TECHNOLOGIES

From the point of view of this conference there is a natural division when considering the technologies of interest – on the one hand, there are static interfaces in which maximum strength is desired, and on the other, there are the dynamic interfaces of interest to tribology where the strength of the moving (sliding or spinning) interface is to be minimized. This division of technologies is depicted in figure 1. As can be seen, there are many subdivisions even within the static and dynamic technologies, illustrating the wide-spread occurrence of this interface. These technologies will be considered in order, starting with the thin-film static system and ending with the dynamic systems. Aside from the main point of understanding the sources of interfacial strength, it will also be seen just how close a connection there really is between static interfacial strength and real friction and wear – a connection that should be gratifying to those tribologists familiar with the adhesion theory of friction.

166

By far the greatest application of thin metal films on oxide substrates in general and aluminum oxide in particular has been in the electronics industry. The metallization of thermal silicon dioxide is the area of greatest application with the metallization of aluminum oxide not far behind. The thickness of the films is of the order of 0.1 to 1 micrometer, and the films are deposited in vacuum by evaporation or sputtering. The adherence of the film to the substrate is required for the reliability of the integrated circuits.

A recent review by Mattox offers a good survey of this technology (ref. 4). The emphasis of the review is on thin-film adhesion, and there is a good discussion of the many factors that can determine adhesion beside interfacial strength. However, some interfacial strength factors are discussed. It is pointed out that those metals that oxidize easily, or, to put it another way, form strong bonds with oxygen, are more adherent to the oxide substrate (either SiO_2 or Al_2O_3) than are the more noble metals. Of course, in the modern solid-state electronics industry great emphasis is placed on extreme cleanliness of the deposition conditions, and this has led to the phenomenon of being "too clean." There is a loss of adhesion if the deposition system is too clean so a little water vapor or oxygen may be desirable. However, this beneficial effect is not widely recognized in the electonics literature. This effect has been attributed to processes other than the establishment of strong interfacial bonds, such as nucleation phenomena (ref. 5). Thus, it is not possible to draw firm conclusions regarding this mechanism regarding interfacial strength. It is noted here and returned to later. It is, however, a good illustration of the difficulty of drawing conclusions from observations of system strength regarding the microscopic mechanism for the observation.

When we turn to the thin aluminum oxide films on superalloy turbine blades containing aluminum the difficulty is even greater. The thin oxide films grow naturally on the blade surfaces in the high temperature turbine environment. The mission of these oxide "scales" is to protect the blade from continuous oxidation during operation. To be effective the scales must adhere to the blade. In fact, the adherence may be considered a life or death affair because catastrophic failure of an engine may be associated with the loss of a blade by excessive oxidation. The development of these superalloys that produce controlled aluminum oxide films in the turbine environment was absolutely necessary to operate modern jet engines. This is an active area of research at Lewis, and it is an area in which Lewis continues to make significant contributions. A comprehensive review of adhesion mechanisms in this technology is given by Whittle and Stringer (ref. 6).

As important as adhesion is to this technology, a look at the field reveals that almost no conclusions concerning the fundamentals of interfacial forces can be drawn. The interfacial forces are even considered irrelevant compared to simple mechanical interlocking or keying (pegging is another word used) of the film into the substrate as a mechanism for adhesion. However, the technology is still developing, and the Lewis group continues to investigate scale adherence mechanisms, mainly because of the great advantage to be gained in blade life from more adherent scales. Perhaps further developments in this field will deal with interfacial forces also.

The third technology with a static interfacial strength considered here is that of ceramic-metal composites (CERMETS). These structures consist of a ductile metal matrix reinforced by a strong ceramic filler. The fillers may be either fine particles (<0.1-μm diameter (dispersion-strengthened composite)), intermediate sized particles (~1-μm diameter (particle-strengthened composite)), or rods or fibers (fiber-strengthened composite). In the last case, the fibers bear the load and the matrix transmits the load to the

167

fiber. The matrix-fiber interface must be strong for the load to be transferred and the structure to be useful. The technological promise of these materials has prompted a number of studies on the strength of the Al_2O_3 metal interface. These studies (reviewed by Signorelli, Petrasek, and Weeton of Lewis Research Center, ref. 7; see also ref. 8) have been concerned with wetting the ceramic by the molten metal, since this is an intrinsic step in the fabrication of the structures. More complete wetting indicates a stronger interaction between ceramic and molten metal and a higher interfacial bond strength in the solid state. One conclusion of these studies is that reactive elements (with respect to oxygen) form stronger bonds than do less reactive elements. This finding agrees with that of the thin-film adhesion studies. Additional studies by Chakladar and coworkers (refs. 9 and 10) using sessile drops in controlled atmospheres indicated that oxygen in the bond-forming environment enhanced the bond strength. This conclusion on the effect of oxygen is in agreement with those of thin-film adhesion studies, although the experimental conditions are very different. In thin-film formation the metal atoms are in the form of a vapor and have access to the oxygen atoms in the deposition ambient environment on their way to the sapphire substrate. In the sessile drop experiments, the liquid metal drop is always in direct contact with the substrate and the oxygen must migrate through the liquid to reach the interface in order to be effective. In spite of these experimental differences the final effect is the same, indicating a common mechanism for the strengthening effect of oxygen.

Turning now to the technologies in which the interface is in constant motion, termed here dynamic interfaces, the first to be considered is the use of alumina tools to cut metal. The use of these tools is reviewed by King and Wheildon (ref. 11). The strength of the interface is a factor in determining the cutting forces of the workpiece on the tool and also in determining tool wear. In this technology a weak interface is desired in order to minimize friction and wear on the tool. Some basic studies relevant to this technology have been performed with the coefficient of kinetic friction as the indicator of the strength of the interface - higher friction indicating a stronger interface. It has not been possible to draw conclusions from these friction studies on the effect of different metals on the strength of the interface - the coefficient of kinetic friction is dominated by bulk material properties. The best one can do in this technology concerning the effect of the metal is to assess (1) the compatability of alumina to cut different metals from the tool lifetime and (2) the quality of cut. Machining experience (ref. 11) shows that chemically reactive metals like titanium and beryllium are not as compatible with alumina tools as is the less reactive nickel. This is in line with the previous conclusion regarding the strength of reactive metal-alumina interfaces in that strong interfaces would lead to tool wear and metal tearing.

As far as environment goes, the change in friction due to changing the atmosphere in which sliding takes place has confirmed the role of oxygen as an interface strengthener. Experiments in simple sliding were initiated by Coffin (ref. 12), and Tabor and coworkers continued sliding experiments by measuring the forces on sapphire tools cutting metal (refs. 13 and 14) and, most recently, by incorporating surface analysis in a highly controlled vacuum chamber (refs. 15 to 17).

The technology of grinding metals with alumina wheels presents a situation in which material properties such as hardness or ductility play dominant roles in grinding wheel lifetime. There are, therefore, no direct conclusions regarding interfacial strength that can be drawn from experience in this field. Research in this field has, however, produced one very interesting observation relevant to our purposes. If ferrous metals are ground with

168

alumina in air and the wear debris is examined by X-ray diffraction, there is evidence of iron alumina spinel, $FeAl_2O_4$ (ref. 18). Evidently, the iron oxidizes to form FeO which reacts with alumina to form the spinel

$$FeO + Al_2O_3 \rightarrow FeAl_2O_4$$
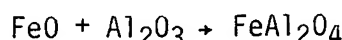
Thus, alumina is removed from the surface of the abrasive particles, and this reaction is considered to be a chemical mechanism for wear of the abrasive. It is also considered to be a source of wear for alumina tools cutting metal. The reaction of two single oxides to form a complex mixed oxide is a generally observed phenomenon. All the common metals such as iron, nickel, copper, and cobalt exhibit a tendency to oxidize and to form the mixed oxide with alumina. Thus, the chemical mechanism of wear should be of quite general validity.

At this point it is possible to summarize the results from the technologies and consider their implication for the atomic basis of interfacial strength. There are two major effects:

(1) The effect of the particular metal species is such that base metals – those that tend to oxidize – form stronger interfaces than more noble metals.

(2) The interface formed in an environment containing oxygen is stronger than one formed in the absence of oxygen.

Before we proceed further, we note a point of interest to tribologists. These two major results hold for both static and dynamic interfaces. The modern theory of friction holds that the friction force arises (at least in part) from the strength of adhesive bonds formed at the interface and thus links the static interfacial strength with the dynamic aspects of friction and wear. The finding of completely similar effects for both dynamic and static technologies is thus a nice illustration of the adhesion theory of friction in this system.

Now, when considering the implication of these two findings for the source of interfacial strength a problem is presented. Since the metals that form stronger interfaces oxidize more easily and oxygen increases interfacial strength, it may be that the oxygen in the ambient (where the interface is formed) is generating metal oxide which adheres strongly to the aluminum oxide – the ranking of the metals in terms of interfacial strength may simply reflect the ability of these metals to form an oxide. We are thus led to ask whether the clean metal – aluminum oxide interface exhibits the previous ranking in strength and whether there is any intrinsic strength to this interface at all. This is difficult to answer with the information from the technologies alone because adequate care may not have been taken to rigorously exclude oxygen from the ambient. To answer this question one must have chemical control and characterization of the interface as well as a method of assessing its strength under these controlled conditions. We are thus led to discuss our experiments on this fundamental question.

EXPERIMENTAL APPROACH

In order to determine the role of oxygen and oxide films on interfacial strength one must have both (1) control and characterization of the elements at the interface and be able to vary this chemistry and (2) be able to assess the strength of the interface as a function of these conditions. The approach we have devised to satisfy these requirements is the following. The experiment is carried out in an ultrahigh vacuum chamber with a base pressure of $<1 \times 10^{-10}$ torr. This low pressure allows a clean metal surface to remain free of adsorbed species for at least 1 hour and satisfies the first require-

ment of control of the environment. The metal – aluminum oxide interface is formed by the contact of two solids whose surfaces may be prepared atomically clean – the metal sphere by argon ion bombardment and the sapphire flat by heating to 1200° C. The interface may thus be prepared in a clean state or, if the metal is exposed to various gases before contact, with interfacial species present. The requirement of characterization is satisfied by using Auger electron spectroscopy to analyze the surfaces to be brought into contact. Thus, any oxygen present on the metal can be assessed, at least in a semiquantitative way. Interfacial strength is assessed by measuring the coefficient of static friction of the interface formed by bringing the metal sphere onto the sapphire flat under a load. A higher coefficient of friction implies a stronger interface. This technique is most reliable in assessing the effect of interfacial species on interfacial strength by simply keeping the specimens – metal sphere and sapphire flat – the same and varying the surface chemistry of the metal (e.g., by exposing it to oxygen). One may assess the effect of metal species on interfacial strength by comparing the static friction on sapphire of one clean metal with another. Although not as reliable a comparison as changing the surface chemistry by chemisorption because the mechanical properties of one of the partners of the friction couple is changed, it may still provide useful information. The experimental technique and results now summarized have been presented in a series of publications (refs. 15 to 17).

There are three main results of this experimental approach:

(a) When atomically clean, oxidizable metals do form stronger interfaces with aluminum oxide than do noble metals.

(b) Oxygen at the interface strengthens the interface, even for monolayer coverage of the metal. The metal need not be oxidized.

(c) (Nitrogen/chlorine) on copper (strengthens/weakens) the interface.

Result (a) confirms the suspicion from the technologies that base metals are more adherent than noble metals on aluminum oxide. Even though such clean interfaces may not be easily prepared or of great importance in the technologies, their strength is considered here to be the first order of business to be understood because they involve the interface in its simplest form. Such "simple" systems are considered to be appropriate for attack by quantum-chemical methods as will be discussed. Result (b) is a confirmation of the technological evidence that interfacial oxygen strengthens the interface and extends this result to cover the case of oxygen present on the metal simply as chemisorbed atoms, prior to oxide nucleation. This result on chemisorbed oxygen may also be considered a system simple enough to be attacked by quantum chemistry, although this has not yet been attempted. Result (c) shows that interfacial atoms other than oxygen can be active in changing interfacial strength: chlorine acts as a lubricant (no surprise to tribologists) whereas nitrogen on copper is an adhesive. Thus, oxygen has lost its privileged position as an interface strengthener. Both results (b) and (c) are obviously important technologically in modifying the strength of a system whose component materials are fixed, leaving only the interface to be dealt with.

DISCUSSION

We see from the evidence reviewed that there are two sources of inter-facial strength – an intrinsic one due to the contact of clean metal with aluminum oxide and an extrinsic one due to interfacial species between the metal and the aluminum oxide. We shall first discuss the atomic mechanisms

that may be responsible for the intrinsic interaction and then we will briefly consider the source of the extrinsic contribution to interfacial strength.

The idea of an intrinsic interaction has, of course, been around for some time. The basic idea is that of a direct chemical bond between the interfacial metal atom and the interfacial oxygen anion of the aluminum oxide. The strength of this "bridging" interfacial bond is considered to be proportional to the (negative) free energy of formation of the metal oxide. Metals that are more oxidizable have higher heats of oxide formation, form stronger metal-oxygen bonds, and thus form stronger interfacial bonds with the oxygen anions at the interface. Thus, base metals should adhere more strongly to aluminum oxide than noble metals. This idea seems to have originated with Kingery and Kurkjian (ref. 19) and elaborated somewhat by McDonald and Eberhart (ref. 20).

There are, however, objections that may be raised to this idea of a direct chemical bond. In the first place, the oxygen with which the interfacial metal atom is interacting is not free oxygen but an anion in the aluminum oxide surface. It does not seem appropriate to use the free energy of metal oxide formation, which involves free oxygen molecules, to describe the strength of a bond between metal and the oxygen already oxidized in the aluminum oxide. In the second place, the metal oxide is not formed at the interface: the heats of reaction do not allow nickel, for example, to reduce the aluminum oxide to make nickel oxide. It is simply not obvious that a metal atom can be brought up to the surface of aluminum oxide and form a chemical bond with an oxygen anion already chemically bonded within the aluminum oxide lattice. Thus, in spite of the successful correlation of metal adherence with the metal-oxide bond strength, the concept of the interfacial chemical bond lacks an adequate theoretical foundation.

An attempt has recently been made by K. H. Johnson and the author to establish a theoretical justification of such a direct chemical bond (ref. 21). The calculation is based on a molecular-orbital theory of a cluster of atoms to represent the metal - aluminum oxide interface. The principle theoretical method was the self-consistent field X-alpha scattered wave (SCF X-α SW) formalism developed by Slater and coworkers to calculate the electronic structure of molecules (ref. 22). The method has since been extended to calculate the electronic structure of solids and interfaces. Several different configurations were used to model the metal - aluminum oxide interface, the simplest of which was a single metal atom on the surface of a seven atom cluster AlO_6, with the aluminum in the center, representing the aluminum oxide. Thus, the metal atom was in the immediate vicinity of the oxygen anion. The different models yielded qualitatively the same results that are summarized in figure 2. The energies of the molecular orbitals are indicated on the vertical scale for different configurations representing bulk sapphire and the metal-sapphire interface.

The primary interaction at the metal-sapphire interface, as revealed by these studies, occurs between the metal d orbitals and otherwise nonbonding p orbitals of the oxygen ions at the surface of the sapphire crystal, i.e., the nonbonding p orbitals at the top of the valence band. Indeed, figure 2 shows that the d-orbital energies of the isolated metal atoms, as determined by this method, are in close proximity to the sapphire valence band, and the position of the atomic level relative to the top of the valence band changes systematically through the series iron, nickel, copper, and silver. The metal-sapphire contact interaction produces at the interface manifolds of spatially localized occupied metal(d) - oxygen(p) bonding molecular orbitals of energies near the bottom of the sapphire valence band and metal(d) - oxygen(p) antibonding molecular orbitals of energies near the top of the sapphire valence band. For iron and nickel, the antibonding orbitals are only partially occupied and are

171

located well above the valence band within the band gap. For copper and silver, the antibonding orbitals are fully occupied and are located close to the top of the valence band. In addition to these covalent bonding and anti-bonding interactions between the metal and sapphire substrate, there is an ionic component associated with metal-to-oxygen charge transfer at the metal-sapphire interface. These results on covalent and ionic interactions indicate that (1) a chemical bond is, in fact, established between metal atoms and the oxygen anions on the sapphire surface and (2) the ionic component of bonding is proportional to the metal(d) and oxygen(p) orbital electron negativity difference.

We can now comment on the strength of this bond. It is well known from the most elementary principles of quantum chemistry that the occupation of antibonding molecular orbitals tends to cancel the effects of occupied bonding orbitals, and it reduces the net chemical bond strength in comparison to the situation where only bonding orbitals are occupied. Therefore, the increase in occupancy of the metal-sapphire antibonding orbitals through the series iron, nickel, copper, and silver should lower the net metal-sapphire chemical bond strength, which correlates with the significant reduction in metal-sapphire contact strength measured through this series. The relatively small shear strengths of copper and silver are consistent with the fact that the fully occupied antibonding orbitals shown in figure 2 essentially cancel the covalent contributions of the bonding orbitals, leaving only small residual ionic and van der Waals contributions.

This cluster model of the metal – Al_2O_3 interface appears to lead to a new understanding of the source of interfacial strength. However, the model also leads to predictions of the electronic structure of the interface and thus may be testable by modern methods of experimental surface science. For example, one might be able to deposit partial monolayers of a metal on sapphire (to fulfill the geometric requirements of the cluster model) and then to measure the occupancy and symmetry of the interfacial molecular orbitals by photoelectric emission. Such an approach is used in understanding the electronic structure of the metal-semiconductor interface. It is important to verify as many features of a detailed model (such as the cluster model) by such methods because the measurement of interfacial strength can rarely be interpreted as simply due to interfacial chemical bonding. One must also contend with the mechanical properties of the materials constituting the couple. For the same reason, one must also be aware that a successful test of the electronic structure predictions of such a model does not necessarily prove its validity as a source of interfacial strength.

Thus far the discussion has dealt with the clean metal – aluminum oxide interface. Some comment can also be made on the effect of foreign interfacial species on interfacial strength, although they are not as yet supported by detailed quantum-chemical calculations. It was noted previously that the oxygen in the environment can generate a metal oxide which reacts with aluminum oxide to produce the mixed oxide of spinel structure. This reaction has been considered to be the source of increased adhesion and friction due to oxygen in the environment (refs. 12, 15, and 16). That oxygen in the environment increases interfacial strength is beyond dispute, but the previous mechanism must be questioned for the following reasons. First, interfacial strength has been increased by chemisorbed oxygen atoms, without the presence of metal oxide (ref. 17). Thus, the reaction of two oxides is not a necessary condition for increased interfacial strength. Second, increased interfacial strength results from chemisorbed nitrogen. Whether the chemisorbed nitrogen forms a nitride of copper and if so whether this nitride reacts with aluminum oxide are still very open questions. It appears to the author that the basic

172

quantum chemical reasons for increased interfacial strength due to these species are still unknown. For that matter, the reasons for the reduction of interfacial strength due to chlorine is as open a question as is the increase due to oxygen.

We might conclude this discussion by noting that heretofore any interfacial species was considered to be dirt or contamination that would interfere and reduce interfacial bonding and strength. This attitude probably arose from experience with metal—metal interfaces where this indeed appears to be the case. However, the strengthening effects noted here show that this is simply not always the case, and thus, we are forced to reappraise the role of interfacial species on interfacial strength. In the fundamental sense, there is no such thing as dirt or contamination. Each interfacial species has its own role to play at the interface and may form stronger or weaker interfacial bonds than those it replaces. At present, since one cannot predict from basic principles whether a particular species strengthens or weakens any particular system, the situation presents a fruitful area for basic research in solid-state physics.

CONCLUDING REMARKS

This survey of the source of strength of the metal – aluminum oxide interface has focused on the basic aspects of interfacial bonding. However, the point of departure has been from the existence of a highly successful array of technologies that has developed without waiting for the fundamental mechanisms to be uncovered. Such a situation is not uncommon – catalysts were recognized and used well before the basic surface science now used to investigate catalytic mechanisms was developed. Basic science playing catchup to technology thus has precedence, and, although it may be rather humbling, provides a backdrop of solid experience against which the basic scientist must pit his laboratory results. The future will hopefully see the loop closed and instead of the technology providing clues to the scientist, the scientist will understand the mechanisms and feed back information to further improve the technology of the metal – aluminum oxide interface.

REFERENCES

1. Bowden, F. P.; and Tabor, D.: The Friction and Lubrication of Solids. Clarendon Press (Oxford), 1950.
2. Ferrante, J.; and Smith, J. R.: Theory of Metallic Adhesion. Phys. Rev., vol. B19, no. 8, Apr. 1979, pp. 3911-3919.
3. Ferrante, J.; and Smith, J. R.: A Theory of Adhesion at a Bimetallic Interface-Overlap Effects. Surf. Sci., vol. 38, 1973, pp. 77-92.
4. Mattox, D. M.: Thin Film Metallization of Oxides in Microelectronics. Thin Solid Films, vol. 18, 1973, pp. 173-186.
5. Mattox, D. M.: Influence of Oxygen on the Adherence of Gold Films to Oxide Substances. J. Appl. Phys., vol. 37, no. 9, 1966, pp. 3613-3615.
6. Whittle, D. P.; and Stringer, J.: Improvement in Properties – Additives in Oxidation Resistance. Philos. Trans. R. Soc. London, Ser. A, vol. 295, 1980, pp. 309-329.

7. Signorelli, R. A.; Petrasek, D. W.; and Weeton, J.: Interfacial Reactions in Metal–Metal and Ceramic–Metal Fiber Composites. Modern Composite Materials, L. J. Broutman and R. H. Krock, eds., Addison–Wesley Publishing Company, 1967, pp. 146–171.

8. Mehan, R. L.; and Noon, M. J.: Nickel Alloys Reinforced with α–Al_2O_3 Filaments. Metallic Matrix Composites, K. G. Kreider, ed., Academic Press, 1974, pp. 159–227.

9. Chaklader, A. C. D.; Armstrong, A. M.; and Misra, S. K.: Interface Reactions Between Metals and Ceramics: IV. Wetting of Sapphire by Liquid Metals. J. Am. Ceram. Soc., vol. 51, no. 11, Nov. 1968, pp. 630–633.

10. O'Brien, T. E.; and Chaklader, A. C. D.: Effect of Oxygen on the Reaction Between Copper and Sapphire. J. Am. Ceram. Soc., vol. 57, no. 8, Aug. 1974, pp. 329–332.

11. King, A. G.; and Wheildon, W. M.: Ceramics in Machining Processes. Academic Press, 1966.

12. Coffin, L. H.: Fundamental Study of Synthetic Sapphire as a Bearing Material. ASLE Trans., vol. 1, no. 1, Apr. 1958, pp. 108–114.

13. Doyle, E. D.; Horne, J. G.; and Tabor, D.: Frictional Interactions Between Chip and Rake Face in Continuous Chip Formation. Proc. R. Soc. London, Ser. A, vol. 366, 1979, pp. 173–183.

14. Wright, P. K.; Horne, J. G.; and Tabor, D.: Boundary Conditions at the Chip–Tool Interface in Machining: Comparisons Between Seizure and Sliding Friction. Wear, vol. 54, 1979, pp. 371–390.

15. Pepper, S. V.: Shear Strength of Metal–Sapphire Contacts. J. Appl. Phys., vol. 47, no. 3, Mar. 1976, pp. 801–808.

16. Pepper, S. V.: Effect of Adsorbed Films on Friction of Al_2O_3–Metal Systems. J. Appl. Phys., vol. 47, no. 6, June 1976, pp. 2579–2583.

17. Pepper, S. V.: Effect of Interfacial Species on Shear Strength of Metal–Sapphire Contacts. J. Appl. Phys., vol. 50, no. 12, Dec. 1979, pp. 8062–8065.

18. Brown, W. R.; Eiss, N. S.; and McAdams, H. T.: Chemical Mechanisms Contributing to Wear of Single-Crystal Sapphire on Steel. J. Am. Ceram. Soc., vol. 47, no. 4, Apr. 1964, pp. 157–162.

19. Kurkjian, C. R.; and Kingery, W. D.: Surface Tension at Elevated Temperatures. III. Effect of Cr, In, Sn, and Ti on Liquid Nickel Surface Tension and Interfacial Energy with Al_2O_3. J. Phys. Chem., vol. 60, July 1956, pp. 961–963.

20. McDonald, J. E.; and Eberhart, J. G.: Adhesion in Aluminum Oxide–Metal Systems. AIME Trans., vol. 233, Mar. 1965, pp. 512–517.

21. Johnson, K. H.; and Pepper, S. V.: Molecular-Orbital Model for Metal–Sapphire Interfacial Strength. J. Appl. Phys., vol. 53, no. 10, Oct. 1982, pp. 6634–6637.

22. Slater, J. C.: The Self-Consistent Field for Molecules and Solids. Vol. 4, McGraw–Hill, 1974.
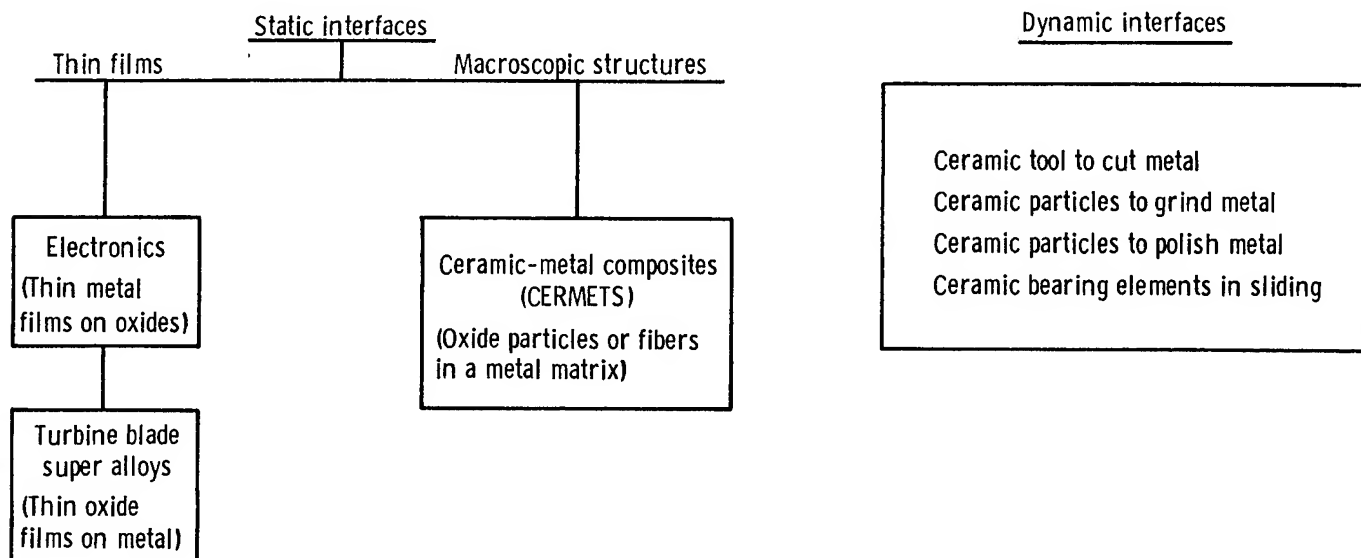
Figure 1. - Metal - aluminum oxide technologies.
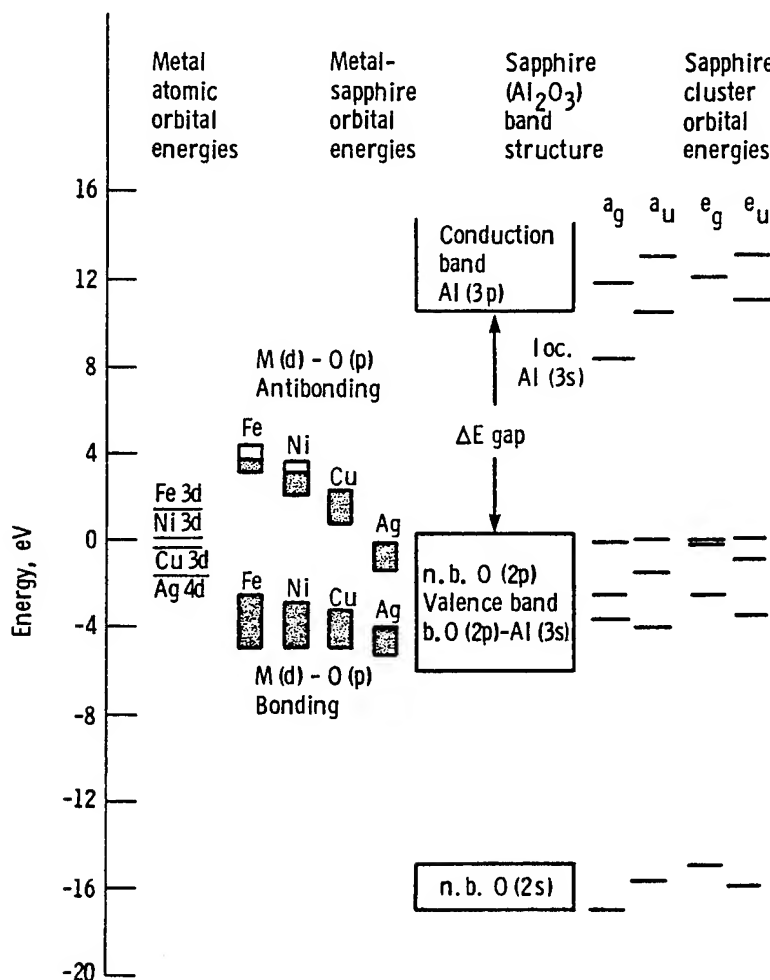
Figure 2. - Molecular-orbital energies, as determined by the self-consistent-field X-alpha scattered wave method, for clusters representing bulk sapphire and metal-sapphire interfaces (ref. 17).

175

DISCUSSION

N. Ohmae
Osaka University
Osaka, Japan

An in situ field ion microscopical study of adhesion and friction is being carried out at the discussor's laboratory in Osaka University. Field ion microscopy provides the investigation into the change in the arrangement of atoms before and after adhesion experiments. Furthermore, the depth of induced damage can be examined using a field evaporation technique. This discussion paper deals with the effect of oxygen adsorption on the adhesion property between a tungsten tip and a gold plate.

SLIDE 1

Slide 1 shows FIM photographs of clean tungsten tip before and after an adhesion contact to gold at an applied force of 0.43µN. The righthand side FIM photograph was taken after a field evaporation of several atomic layers from the original surface. Even at this very low applied force, adhesion contact induces a disturbance in atom arrangement on the upper left (111) plane. This lattice defect was analyzed to be caused by the slip on the (01$\bar{1}$) plane. The defect-free surface was obtained after a field evaporation of approximately 20 atomic layers on the (011) plane.

SLIDE 2

Slide 2 shows the results of adhesion experiments using an oxygen adsorbed tungsten tip, the oxygen exposure in this case being 16 L. The adhesion-induced lattice defect is visible near the upper (001) plane. An analysis using a computer simulation showed that the defect was caused by the slip on the (101) plane. The defect-free surface was obtained after a field evaporation of approximately 10 atomic layers on the (011) plane. It should be noted that at a relatively high applied force of 5.8µN adsorbed oxygen prevents real metal to metal contact and that reduces adhesion-induced damage.

SLIDE 3

Slide 3 summarizes the discussor's recent results of FIM study on adhesion. The influence of oxygen on adhesion is quite profound. In future, the intrinsic nature of adhesion and friction can be investigated on tha atomic scale or on the much finer scale.

THE INFLUENCE OF SURFACE TOPOGRAPHY ON POLYMER FRICTION

Norman S. Eiss, Jr.
Professor of Mechanical Engineering
Virginia Polytechnic Institute and State University
Blacksburg, Virginia

Current friction models for polymers are examined to determine their applicability in predicting the effects of roughness on friction. The two-component, adhesion-deformation model of friction predicts the variation of friction with the change in the sliding direction with respect to the lay direction on anisotropic rough surfaces. The two-component model does not predict the change in friction with changes in roughness. It is suggested that a combination of an energy based model and a slip line deformation model may provide a friction model which could better represent measured friction.

INTRODUCTION

The increasing use of polymers as components in sliding systems has resulted in research directed toward the modeling of friction and wear mechanisms. Such models could then be used to predict tribological performance and to suggest modifications in the components of sliding systems to improve tribological performance. Surfaces in sliding contact are usually not smooth and therefore the models developed must include the influence of the roughness of either or both surfaces on the friction and wear mechanisms. As a result of wear and transfer of material the surface roughnesses change with time of sliding and these changes are reflected by the friction phenomena.

It is the purpose of this paper to determine the role that surface roughness has in the models of polymer friction as described in recent reviews (ref. 1,2). Some experimental results will be described in which the various components of friction are shown to be related to the surface roughnesses. Finally, some suggestions for future research on the influence of roughness on polymer friction will be given.

MODELS

There have been two approaches to modeling friction, one based on energy and one based on forces. In energy based models the frictional work is equated to the energy dissipated in the materials. The energy based models can be directly related to the heat generated during sliding since all of the energy dissipated is assumed to appear as thermal energy. In the force based models, the friction force is equated to the tangential forces generated in the interface. The force based models are directly related to the mechanical properties of the materials since the forces are assumed to be generated by shearing and plastic deformation. Examples of these models will be given below.

Energy Based Models

Energy models for polymer friction have been applied mainly to elastomers. The

177

frictional work has been related to the energy dissipated in hysteresis losses in the material, where these losses have been assumed proportional to the loss tangent of the polymer measured at the deformation frequency (ref. 3). Ludema and Tabor (ref. 4) attempted to relate sliding friction to loss tangent for polyoxymethylene (POM), polychlorotrifluoroethylene (PCTFE), polypropylene (PP), and nylon and found no correlation. However, they did find a correlation between rolling resistance of a steel roller on polytetrafluoroethylene (PTFE) and the loss tangent. The authors suggested that the lack of correlation in sliding resulted because the strain rates in sliding are orders of magnitudes higher than in conventional tests to measure loss tangent.

Heilmann and Rigney (ref. 5) have proposed an energy based model of friction in which the frictional work is equated to the energy dissipated in plastic deformation. The model is based on two assumptions: first, the mechanical properties are constant with time, i.e. the effects of work hardening and recovery balance each other; second, the generation of wear particles is considered as discrete localized events which superimpose a noise on the steady state friction versus time curve. (A similar view was expressed by Archard (ref. 6) who considered all contacts contributing to friction but only a small fraction producing wear particles in a given time interval.)

This energy based friction model does not predict friction values. Rather, it gives insight into the dependence of the coefficient of friction on structural parameters. In addition, the model was derived primarily considering metals but could also be adapted to consider layered systems, e.g. bonded coatings, reaction products, and transferred layers on metallic substrates. They concluded that the model could be extended to any combination of materials in which plastic deformation is the dominant dissipative mechanism.

The model does not include any surface roughness parameter. The sliding interface is assumed to be flat. Adhesive bonds are considered to be the mechanism by which the sliding motion generates a shear stress on the surfaces of the contacting components.

Force Based Models

The force-based models of friction which dominate the literature are usually stated: the friction force is equal to the sum of the force due to adhesion and the force due to deformation. This model was originally developed for friction of metals (ref. 7) and it was assumed that the adhesion term dominated for most practical systems. This assumption was questioned by Kragelskii (ref. 8) who claimed that for metals both terms were significant. There is also general agreement that for polymers both terms are important (ref. 9).

The adhesion component of friction consists of shear force developed at the contact areas. Thus, the shear strength and the area being sheared are the important components of the adhesion component of friction. The shear strengths of polymers measured in conventional tests are considered to be not representative of shear strengths in contacts because the strain rates in the latter are estimated to be orders of magnitude higher than in the former. Therefore, the shearing of thin films by sliding has been used to measure shear strengths (ref. 10). In these experiments, thin films of polymers ca. 100 nm thick coated on a glass plate are sheared by sliding a glass sphere over the film. Using the area of contact calculated by Hertzian theory of a glass sphere on a glass plate, the measured tangential force is converted

178

to a shear stress and the normal load is converted to a pressure. The calculated shear stress was found to be a linear function of the pressure. A similar relationship was also obtained by placing polymer films 40 to 70 μm thick between steel slabs and measuring the force required to shear the films as a function of normal force on the steel slabs (ref. 11).

Most investigators acknowledge that estimation of the real area of contact is still restricted to simple static contact models. Either elastic contact is assumed and the area is calculated using Hertzian contact theory or plastic contact is assumed and the area is calculated by dividing the load by the hardness of the material. For contact between rough surfaces, various plasticity indices have been developed (ref. 12,13) to determine whether the contacts are predominantly elastic or plastic. Halliday (ref. 14) has estimated that for similar roughnesses polymers are more likely to undergo elastic deformation than metals. The relation between the area of contact during sliding and that in static contact requires further investigation.

The most frequently cited model for the deformation component of friction is that of a rigid asperity indenting a softer polymer. The deformation force is that required to displace the polymer as the asperity moves through it. Thus, the projected area of the asperity normal to the direction of motion times a pressure required to displace the polymer is the value of the deformation force. Experimental determination of the deformation component is complicated by the movement of the displaced material which may pile up in front of the slider and by the presence of adhesive forces at the contact area.

Originally, the adhesion and deformation components of friction were considered as independent. However, if one considers that the principal source of energy dissipation is in plastic deformation, then the adhesion component of friction must, in some way, result in deformation losses in the material. Johnson (ref. 15) has presented a model of friction in which the adhesion component of friction serves to increase the plastic strains involved in deformation. The model is based on an asperity moving through an ideally plastic material and classical slip line analysis is used to predict the stresses and displacements resulting from the application of tangential forces. One of the conclusions derived from the model was that, with no adhesion, the coefficient of friction is determined by the surface topography and, in general, was less than 0.15. The model also predicted a theoretical limit of 1.0 for the coefficient of friction regardless of topography.

RELATIVE MAGNITUDES OF ADHESION AND DEFORMATION FRICTION

Various techniques have been used to measure the relative magnitude of adhesion and deformation components of friction. The classic experiment for metals (ref. 16) used sliders with different contact areas and the same ploughing area. (It should be noted that forces were measured just prior to the commencement of motion in these tests). For polymers the change in friction when sliding with and without lubrication has been used (ref. 17). In these tests a steel sphere was slid against the polymers and the force measured without lubrication was assumed to be the sum of adhesion and deformation components and the force measured with lubrication was assumed to be the deformation component only. The ratio of adhesion to deformation components was found to be 0.025 for PTFE and 0.032 for polyethylene (PE).

The experiment of a rigid sphere sliding on a polymer is an attempt to model a contact between a hard asperity and a polymer. This experimental model cannot simu-

179

late load sharing between multiple asperity contacts and the contact area is orders of magnitude higher than contact areas at actual asperities. With the availability of surface profile meters and computer programs to calculate any desired parameter describing the topography, investigators have the ability to estimate the geometry of contacts of real asperities. In addition, rough surfaces which are anisotropic can be used to detect differences in friction resulting from the relative contributions of the adhesion and deformation components of friction.

In several experimental programs in which the wear of polymers as a function of surface roughness was studied (ref. 18-22) it was noted that the friction of a polymer pin on a rotating ground steel disk varied from a maximum when the pin was sliding perpendicular to the lay of the disk to a minimum when sliding parallel, as shown in Figure 1. Since the load is constant, the contact area must be constant regardless of the orientation of the lay of the topography with the sliding direction. Hence, the adhesion component must be constant. Therefore, the deformation component must be changing as the disk rotates.

If the friction force, F, is modeled by:

$$F = As + A^1 p \tag{1}$$

where

    A is the real contact area,
    s is the shear strength of the polymer,
    A^1 is the projected area perpendicular to sliding direction, and
    p is the pressure required to displace the polymer;

then as the disk rotates, A, s, and p remain constant but A^1 varies. Then a second equation can be written

$$F^* = As + A^{1*} p \tag{2}$$

where the * indicates measurements made with sliding parallel to the lay whereas in equation 1 measurements are made with sliding perpendicular to the lay.

By estimating A, A^1, and A^{1*}, the values of s and p and the relative contributions of adhesion and ploughing can be calculated.

In one of these experiments, the wear and friction of low density PE (LDPE) and the surface topography of the steel disks were measured (ref. 21). It was assumed that the real area of contact A could be calculated using W/3Y where W = normal load (2.7 N) and Y is the yield strength of LDPE (5.7 MPa). The ratio of the real area to the apparent area of the polymer pin (3.12 mm dia) defined the bearing area ratio (BAR). Using surface profiles of the steel disks, the BAR was used to calculate how many asperities contacted the pin at any instant of time, the depth of penetration of each asperity, and the curvature of each asperity (Fig. 2). The areas A^1 and A^{1*} shown on figure 3 are calculated as follows. The value of A^1 is determined by

$$A^1 = n \, \overline{h} \, \overline{d} \tag{3}$$

where

    n = number of asperities contacting the polymer pin,

180

$\overline{h}$ = average penetration depth of each asperity, and

$\overline{d}$ = average length of the contacting asperities. (The asperities are modeled as ridges, thus each asperity is assumed to contact the pin along the entire length of a chord.)

The value of A^{1*} is determined by

$$A^{1*} = n \, R^2 \, [\theta - B(1 - B^2)^{1/2}] \qquad (4)$$

where

R = average asperity radius (inverse of average curvature),

$B = \dfrac{R - \overline{h}}{R}$, and

θ = arc cos B.

The data from the first rotation of the disk in two experiments are given in Table 1 along with the calculated values of the parameters in equations 1 and 2.

The tensile strength of LDPE was 5.7 MPa, so the values of shear strength and deformation pressure appear to be reasonable. Since friction forces vary considerably from test to test, appropriate statistical confidence limits would have to be calculated for the values of s and p before any detailed interpretation of the results were attempted. The interesting aspect of the results is that the deformation area A^{1*} is insignificant compared to A^1. This means that the deformation force when sliding parallel to the lay is negligible compared to the adhesion force. The data also show that for Disk D, the ratio of the adhesion component to the deformation component was 2.0 and for disk E, the ratio was 4.1.

The above experiment indicates that anisotropy in surface topography can be used to estimate the relative contributions of the adhesion and deformation components of friction and provide estimates of the material parameters governing shear and deformation processes.

SURFACE ROUGHNESS AND FRICTION

On very smooth surfaces (R_a less than 0.05 micrometers), PTFE has a coefficient of static friction of 0.17 which immediately drops to 0.06 when sliding commences. Similar behavior was observed for high density PE (HDPE). However for rough surfaces (R_a above 0.10 μm) the friction coefficient of these materials remained constant at their static values (ref. 23). Other fluorocarbons, Teflon FEP and PCTFE, had kinetic frictions which were independent of roughness over a range of roughness values from 0.01 to 1.0 μm. In general, the friction of polymers appears to be relatively insensitive to changes in surface roughness.

Eiss and Vincent (ref. 19) measured the friction of rigid polyvinylchloride (PVC) pins sliding on ground steel surfaces with R_a roughnesses of 0.15, 0.51, and 1.27 μm at a sliding speed of 0.1 m/s. The coefficients of friction were 0.34, 0.27, and 0.32, respectively. The surface profiles were analyzed and the ploughing areas A^1 were calculated to be in the following ratio for the three roughnesses 1:2.8:6.8. Since the normal loads were the same for all three roughnesses, the real areas of contact were the same and thus the adhesion components of friction would be the same. The two component model of friction would then predict that the

181

coefficient of friction should rise with increasing roughness. The fact that the coefficient of friction remains relatively constant as a function of roughness suggested that the two component friction model is not in agreement with the measured data.

Eiss and Bayraktaroglu (ref. 18) measured coefficient of friction of LDPE at two roughnesses 0.065 and 1.16 micrometers R_a at 0.32 m/s in a pin on disk experiment. On the smoother surface, the friction coefficient at the start of the experiment was 0.79 and it gradually decreased to about 0.48 after 10^5 cycles of sliding. Transfer films were evident on the steel surfaces. On the rougher surface the friction coefficient was 0.52 at the start and throughout the experiment.

Eiss and Smyth (ref. 20) also noted that the coefficient of friction of LDPE measured at the start of an experiment was higher for smooth surfaces than for rough surfaces; $\mu = 0.81$ on surfaces with $R_a = 0.06$ μm, and $\mu = 0.52$ on surfaces with $R_a = 0.23$ and 0.91 μm. On the same surfaces the coefficients of friction for PVC and PCTFE showed a slight tendency to increase with roughness. The coefficient of friction of nylon pins sliding on steel disks at velocities from 0.01 to 0.2 m/s also showed a tendency to decrease as the roughness increased (ref. 24).

This cursory looks at friction data as a function of roughness indicates that the two component friction model is unable to predict the trends observed in the friction-roughness relationship. Clearly, factors such as transfer and the relationship of polymer ductility to transfer influence the degree to which the polymer friction depends on roughness.

SUMMARY AND FUTURE DIRECTIONS

The two component model of friction, while it predicts the changes in friction that occur when a polymer pin slides perpendicular to or parallel to the lay on the contacting disk, it does not predict the friction changes observed for overall roughness changes. The model predicts that as the roughness increases, the ploughing component should increase and thus so should the overall friction coefficient. However, the experiments indicate that the friction decreases with increasing roughness (LDPE), or stays the same or increases slightly with increasing roughness (PVC, PCTFE, FEP).

The two component model of friction does not address the mechanism of energy dissipation directly although it is implied in the interfacial shear and in the deformation. The energy model of friction (ref. 5) does address the energy dissipation but surface roughness is not included in the model. It appears that a combination of the slip line model (ref. 15) with the energy model may provide the basis for further friction models.

The topography of rough surfaces used in experiments to study friction must be thoroughly characterized so that the details of the contacts can be examined. While the surface topography is very important at the beginning of a test, as transfer occurs the topography becomes modified. This phenomenon may be responsible for the relative insensitivity of friction to surface roughness after steady state friction values have been reached.

REFERENCES

1. Briscoe, B. J., "The Friction of Polymers: A Short Review," in Friction and

Traction, ed. by Dowson, D., et. al. Westbury House, Guildford, England 1981, pp. 81-90.

2. Bartenev, G. M., and Lavrentev, V. V., Friction and Wear of Polymers, edited by Lee, L. H., and Ludema, K. C., Elsevier Scientific Publishing Company, New York, 1981, Chapter 3.

3. Moore, D. F., and Geyer, J., "A Review of Hysteresis Theories for Elastomers," Wear, Vol. 30, 1974, pp. 1-34.

4. Ludema, K. C., and Tabor, D., "The Friction and Viscoelastic Properties of Polymeric Solids," Wear, Vol. 9, 1966, pp. 329-348.

5. Heilmann, P., and Rigney, D. A., "An Energy-Based Model of Friction and Its Application to Coated Systems," Wear, Vol. 72, 1981, pp. 195-217.

6. Archard, J., "Wear Theory and Mechanisms," in Wear Control Handbook, edited by Peterson, M. B., and Winer, W. O., ASME, New York, 1980, p. 63.

7. Bowden, F. D., and Tabor D., Friction and Lubrication of Solids, Oxford University Press, London, 1954, Chapter V.

8. Kragelski, I. V., Friction and Wear, Butterworths, Washington, D.C., 1965, pp. 145-152.

9. Lancaster, J. K., "Basic Mechanisms of Friction and Wear of Polymers," Plastics and Polymers, Vol. 41, 1973, pp. 297-306.

10. Amuzu, J. A. K., Briscoe, B. J., and Tabor, D., "Friction and Shear Strength of Polymers," ASLE Trans., Vol. 20, 1977, pp. 354-358.

11. Bartenev, G. M., and Lavrentev, V. V. loc. cit., p. 82-83.

12. Greenwood, J., and Williamson, J. B. P., "Contact of Nominally Flat Surfaces," Proc. Royal Soc., Vol. A295, 1966, pp. 300-319.

13. Whitehouse, D. J., and Archard, J., "The Properties of Random Surfaces of Significance on their Contact," Proc. Royal Soc., Vol. A316, 1970, pp. 97-121.

14. Halliday, J. S., "Surface Examination by Reflection Electron Microscopy," Proc. Institution Mechanical Engineering, Vol. 169, 1955, p. 777.

15. Johnson, K. L., "Aspects of Friction," in Friction and Traction, loc. cit. pp. 3-12.

16. Bowden, F. P., Moore, A. J. W., and Tabor, D., "The Ploughing and Adhesion of Sliding Metals," Jl. Applied Physics, Vol. 14, 1943, pp. 80-91.

17. Bartenev, G. M., and Lavrentev, V. V., loc. cit. p. 70-71.

18. Eiss, N. S., Jr., and Bayraktaroglu, M. M., "The Effect of Surface Roughness on the Wear of Low Density Polyethylene," ASLE Trans, Vol. 23, 1980, pp. 269-278.

19. Eiss, N. S., Jr., and Vincent, G. S., "The Effect of Molecular Weight, Surface

Roughness, and Sliding Speed on the Wear of Rigid Polyvinylchloride," <u>ASLE Trans.</u>, Vol. 25, 1982, pp. 175-182.

20. Eiss, N. S., Jr., and Smyth, K. A., "The Wear of Polymers Sliding on Polymeric Films Deposited on Rough Surfaces," <u>ASME Jl. Lub. Tech.</u>, Vol. 103, 1981, 266-273.

21. Eiss, N. S., Jr., and Milloy, S., "The Effect of Asperity Curvature on Polymer Wear," in <u>Wear of Materials 1983</u>, edited by Ludema, K. C., ASME, New York, New York, 1983.

22. Eiss, N. S., Jr., and Warren J. H., "The Effects of Surface Finish on the Friction and Wear of PCTFE Plastic on Mild Steel," Society of Manufacturing Engineers, Paper No. IQ75-125.

23. Pooley, C., and Tabor, D., "Friction and Molecular Structure, The Behavior of Some Thermoplastics," <u>Proc. Roy. Soc.</u>, Vol. A329, 1952, pp. 251-274.

24. Vroegap, P. H., Vermeulen, H. H., and Bosma, R., "The Influence of Temperature, Speed and Roughness on the Dry Sliding Friction and Wear of Nylon 6.6 Against Steel," in <u>Friction and Traction</u>, loc. cit. pp. 93-98.

Table 1. Estimates of Shear Strengths and Flow Pressure

	Disk D	Disk E
Friction (perpendicular to lay), $F(N)$	1.84	1.52
Friction (parallel to lay), $F^*(N)$	1.23	1.22
Number of Asperities in Contact, n	26	25
Average penetration of asperities, $\bar{h}(\mu m)$	0.52	0.57
Average radius of asperities, $R(\mu m)$	3.53	4.46
Real Area of Contact $A(m^2)$	$0.15(10)^{-6}$	$0.15(10)^{-6}$
Average Asperity Length, $\bar{d}(mm)$	2.45	2.45
Projected Area (sliding $\perp$ lay), $A^1(m^2)$	$3.31(10)^{-8}$	$3.49(10)^{-8}$
Projected area (sliding ‖ lay), $A^{1*}(m^2)$	$3.38(10)^{-11}$	$4.20(10)^{-11}$
Interfacial shear stress, s (MPa)	8.2	8.13
Ploughing pressure, p (MPa)	18.4	8.61
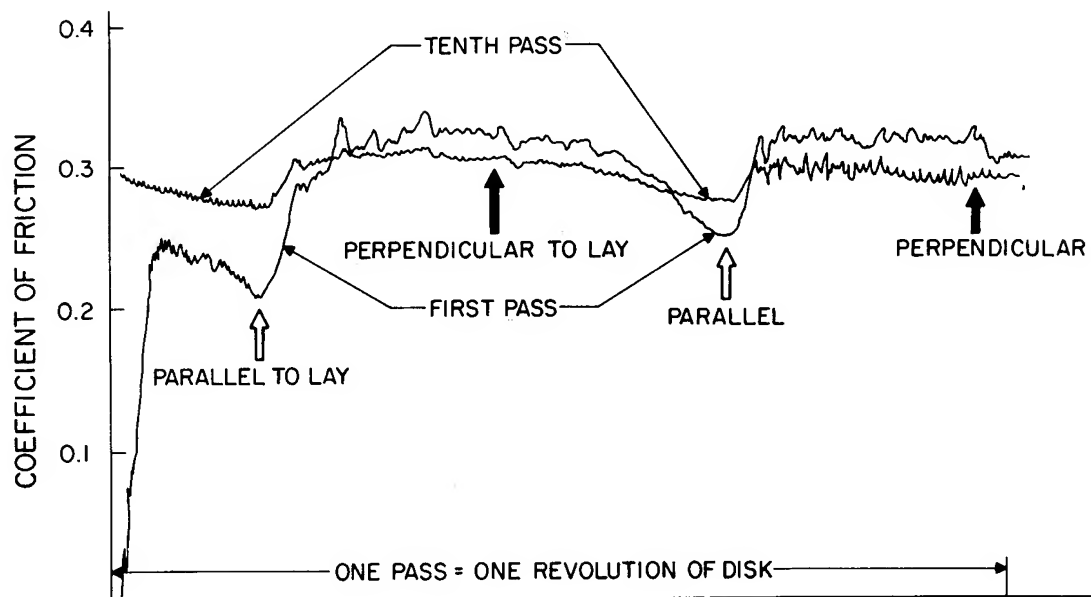
Figure 1. Coefficient of friction of PCTFE on a ground 1018 surface, $R_a = 0.68$ μm, 0.2 cm/s
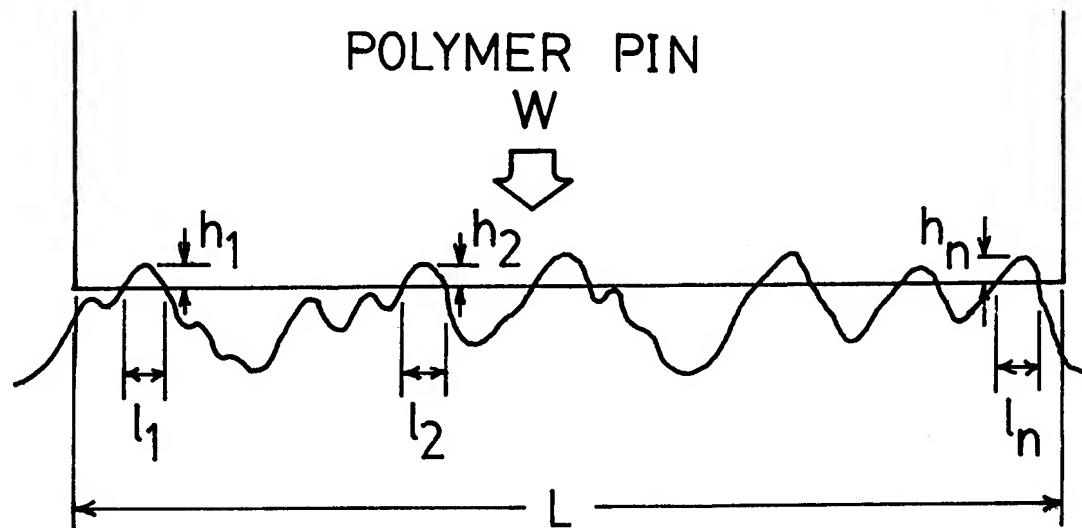
$$BAR = \frac{1}{L} \Sigma l_i \qquad \rho = \frac{1}{n} \Sigma \rho_i$$

$$\bar{h} = \frac{1}{n} \Sigma h_i \qquad R = \frac{1}{\rho}$$

Figure 2. Identification of penetrating asperities from surface profiles

185
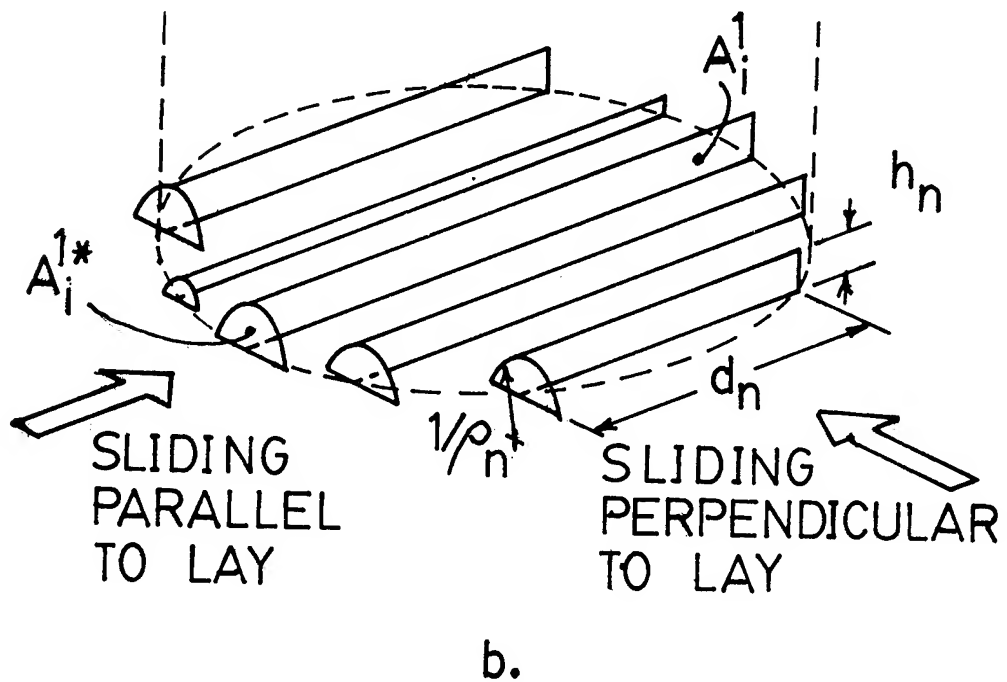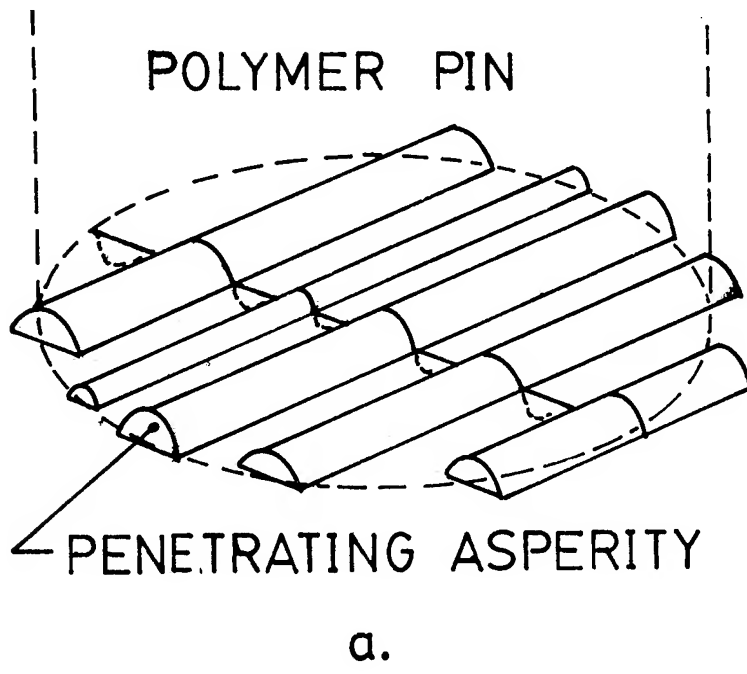
Figure 3. Modeling the ploughing component of friction
a. geometry of penetrating asperities
b. projected areas for sliding perpendicular to lay, A^1, and parallel to lay, A^{1*}

DISCUSSION

S. Bahadur
Iowa State University
Ames, Iowa

I commend the author for dealing with a topic which has its basis in the mechanisms of friction that rely upon concepts which have not yet lended to direct measurements and verification. The following problems are perceived with the author's approach:

1. Application of the concepts of abrasion (or abrasive wear) to friction which distorts the understanding of the deformation component of friction.

2. Consideration of plastic deformation in the polymer substrate due to loading of asperities.

3. Neglect of strain rate dependent deformation in the contact zone.

4. Modeling of asperities as ridges.

These points are discussed below in the order mentioned.

According to the "force-based model" (a terminology used by the author), the contribution to friction is derived from adhesion and deformation where the latter pertains to the loss of energy that occurs in ploughing of hard asperities into a softer polymer substrate. It should take into account the energy expended in deforming the material ahead of the asperities as well as the energy recovered due to the viscoelastic deformation (or recovery) of polymer from unloading behind the asperities. The correlation between sliding friction under lubricated conditions (which eliminates the adhesion contribution) and tan δ for several plastics bears testimony to this aspect (1).

I do not think that it is realistic to consider plastic deformation in the polymer at asperity contact points. It is because of this assumption that the author ends up with a contact area being independent of the lay of topography because then it depends only upon the normal load. I would like to draw the attention of the author to our paper (2) which considers elastic deformation and provides an equation for real area of contact in terms of the surface parameters. Since the latter have different values for different lays, the contact area values will also be different. This will also provide different values of adhesion component of friction in different lay directions. Further-more, there will also be changes occurring in the shear strength in equations (1) and (2) due to the variation in contact pressure.

The deformation in a sliding contact zone is highly strain rate dependent (3-5). Such a dependency must be considered while expressing the coefficient of friction or the real area of contact in terms of the mechanical properties. The author seems to ignore this aspect altogether.

The assumption in the derivation of equation (4) that asperities act as ridges and contact the pin along the entire length of a chord is rudimentary. The number of asperities taking part in a contact zone would depend upon the statistical distribution of asperity heights.

The failure of the proposed model due to unrealistic assumptions is evidenced by the calculated values in Table 1. The shear strength values (as calculated) are about 44% higher than the ultimate strength and the ploughing pressures for the same material differ by a factor of 2 for the two disks used. I wonder if there is any physical connection between the ploughing pressure and a commonly measured mechanical property.

The author is correct in recognizing that the transfer films play a strong role in governing the friction behavior. It is so because surface films affect the surface topography of the metal counterface (6).

References

1. Bueche, A. M. and Flom, D. G., "Surface Friction and Dynamic Mechanical Properties of Polymers," Wear, 2, 168 (1959).

2. Jain, V. K. and Bahadur, S., "Development of a Wear Equation for Polymer-Metal Sliding in Terms of Fatigue and Topography of Sliding Surfaces," Wear, 60, 237 (1980).

3. Grosch, K. A., Proc. Roy. Soc., A274, 21 (1963).

4. Ref. 4 of paper.

5. Bahadur, S. and Ludema, K. C., "The Viscoelastic Nature of the Sliding Friction of Polyethylene, Polypropylene and Copolymers, Wear, 18, 109 (1971).

6. Jain, V. K. and Bahadur, S., "Surface Topography Changes in Polymer-Metal Sliding-II, Paper #82-Lub-15, ASME/ASLE Joint Lubrication Conference, Washington, D.C., October 5-7, 1982.

DISCUSSION

Brian Briscoe
Imperial College
London, England

The friction of clean polymers when they are slid against rough clean counterfaces is a neglected area of study. There have been many studies of abrasive wear and many features of this type of wear process are understood in general terms. Ratner, Lancaster and Schallamach as well as Dr. Eiss have made useful observations and correlations. However as Dr. Eiss points out we may see relatively large changes in abrasive wear for many polymers but virtually no variation in the frictional work. The PTFE's and linear polythenes are an exception as are a number of poly(etheretherketones). (They are however special reason for these observations).

Dr. Eiss's approach to this problem is interesting and it touches upon an aspect of friction which many investigations have sought to avoid; the neat distinction of two non-interacting mechanisms in the classical two term model of friction. The non-interacting model serves to make an intractable system of this sort at least amenable to a cursory analysis. One does however have to concede that K.L. Johnson (Ref.15 of Eiss) is entirely correct when he reminds us that the two term non-interacting model is conceptually inadequate (see also ref.1 of Eiss). The analysis presented by Dr. Eiss seeks to abstract the two components using the classical means of measurements with and without efficient lubrication. He assumes that the adhesive component will not modify the magnitude of the deformation component (the basis of the classical two term model) and finds that this is not consistent

with experiment. Prof. Johnson would probably say that this is to be expected. It is interesting however to see that this is indeed the case. However as Dr. Eiss indicates there are probably many other factors which contribute to its indifferent predictive capacity. To include this comment I would like to ask Dr. Eiss if he feels that rather poor agreement between theory and experiment is due to a weakness in the non interacting notion or simply the fact that the term separation cannot be carried out with sufficient precision.

Finally I would like to indicate that the interface shear yield stress parameter (S, equation 1) can be regarded as an interfacial rheological parameter akin to a viscosity. The adhesion model then becomes "Energy Based". This is cheating of course as we still cannot specify the molecular or microscopic nature of the friction process: we just say that it is a process which is comparable to continuous bulk flow with a few interesting features such as a very high rate of strain and an imposed quasi hydrostatic stress.

DISCUSSION

D.G. Flom
General Electric Corporate Research and Development
Schenectady, New York

Professor Eiss has presented a concise and well-written review of prevailing friction models. This discussor finds little with which to take issue. Rather, comments are offered which, it is hoped, will motivate Professor Eiss and his students to pursue these studies further with additional carefully planned experiments.

The failure of investigators to find correlations between sliding friction and loss tangent in polymers is not universal. The author is referred to an early paper by Bueche and Flom in which a clear correlation between friction and dissipation factor (i.e., loss tangent) was found for sodium stearate-lubricated sliding of steel on polymethyl methacrylate[1]. The trends of both of these measured quantities with temperature and frequency of stress were in good agreement. Since other lubricants gave results independent of sliding speed and temperature, we cannot conclude that shearing forces were absent. However, experiments on various polyethylene specimens, in addition to those on polymethyl methacrylate, clearly demonstrated the importance of dynamic mechanical properties. As is well known and pointed out by Professor Eiss, the predominant role of dynamic mechanical properties in rolling friction has been well corroborated over the past 20 years.

The relationship between friction and surface roughness continues to be a subject for study and will probably be so for decades to come. As Professor Eiss concludes, the two-component model is inadequate for predicting changes in friction with increasing roughness. It is highly likely that any model which predicts a strictly linear relationship between friction and roughness will suffer the same fate. There have been numerous observations of friction being high on very smooth surface and on very rough surfaces and a minimum within an intermediate range of roughness. A recent empirical model in the field of cutting tool wear has been proposed on the basis of such observations.[2].

In the case of polymer friction it may well be that an energy model combined with a slip line model, as suggested by Professor Eiss, will predict the correct relationship between friction and roughness. This discussor, for one, encourages Professor Eiss to pursue this line of investigation further.

1. A.M. Bueche and D.G. Flom, "Surface Friction and Dynamic Mechanical Properties of Polymers", WEAR, 2, 168-182 (1959).

2. S.M. Pandit and S. Kashou, "Variation in Friction Coefficient with Tool Wear", WEAR, 84, 65-79 (1983).

RESPONSE

Norman S. Eiss, Jr.
Virginia Polytechnic Institute and State University
Blacksburg, Virginia

I would like to thank the discussors for their encouraging remarks and provocative questions. As a preface to my response to their questions the analysis of some additional friction data is presented and discussed below.

Since this paper was written the friction data for experiments described in Ref. 20, have also been analyzed using the model described by Eq. 1 and 2. In these experiments, PVC, LDPE, and PCTFE pins were rubbed against rotating steel disks with R_a roughness of 0.06, 0.23, and 0.91 μm. Only PVC and PCTFE sliding on the rougher disks had friction variations similar to that shown in Fig. 1. The calculated values for s and p', are given in Table 2.

Table 2

Calculation of Shear Strengths s and Ploughing Pressure p' for PVC and PCTFE

Polymer	s MPa		p' MPa		
	Mean	Std. Dev.	Mean	Std. Dev.	Strength MPa
PCTFE	27.5	2.7	215	68	23.1
PVC	108	38.4	1221	654	103

*Based on 8 samples

While one may question the absolute values of these shear strengths because of the dependency of shear strength on strain rate and contact pressure as noted by Bahadur in his discussion the model predicts the relative magnitudes of the shear strengths quite well. LDPE does not respond to the roughness variation as the disk rotates because it transfers in a more ductile mode than PVC or PCTFE, a phenomenon which is discussed in Ref. 20 and also mentioned by Bahadur. On the smoothest disks, the roughness variation as the disk rotated was not sufficiently large enough to cause a significant change in the ploughing component of friction.

The author thanks Dr. Flom and Prof. Bahadur for reference to the work of Bueche and Flom which shows the correlation between sliding friction and the loss tangent. These investigators did consider the relative strain rates in the sliding and loss tangent tests and concluded that they were similar.

Bahadur questions the assumption of plastic deformation in calculating area of contact and referred to his fatigue model in which elastic deformation was assumed. The author agrees that elastic deformation is the predominant mode of deformation in steady state wear for which fatigue is the major mode of wear particle generation. However, for the calculations in Tables 1 and 2 the friction data was taken on the first pass over the rough surface. In this circumstance, plastic flow is more likely since the polymer will be transferring to the sharpest and highest asperities which it contacts.

Bahadur suggests that the real area of contact is a function of the direction of sliding relative to the lay direction. His basis for this suggestion is that surface topography parameters for an anisotropic surface have different values when measured perpendicular to and parallel to the lay and the real area of contact for elastic deformation is a function of these parameters. If the surface parameters are used to predict the real area of contact, a model for the asperity geometry is necessary. In Jain and Bahadur's fatigue model, they adopt the Greenwood and Williamson model (ref. 12) of a spherical asperity. However, if one applies a spherical asperity model to an anistropic surface, the curvature of the asperities calculated from the profile measured perpendicular to the lay will be greater than that calculated from the profile measured parallel to the lay. Hence, different real areas of contact will be calculated.

However, the asperities in an anisotropic surface are not spherical, their geometries are ellipsoidal (and in the limit, cylindrical). Thus to predict the area of contact, the profile measurements perpendicular and parallel to the lay should be used to calculate the dimensions of an ellipsoidal asperity model. The Hertzian equations could then be used to estimate the area of contact.

It is certainly possible that the real area of contact may change as a function of sliding direction relative to the lay. However, this change would be more likely due to the viscoelastic response of the polymer to the different deformation rates (as Dr. Bahadur has noted) experienced then sliding perpendicular or parallel to the lay.

The asperities were modeled as cylinders in this paper. Scanning electron microphotographs show that there is variation in the asperity height parallel to the lay direction. When the ploughing area was calculated for sliding parallel to the lay, the area was assumed to be the area normal to the lay direction of the portion of the asperity penetrating the polymer. This implies that when sliding parallel to the lay, there must be a variation in the height of the asperity ridge equal to the penetration depth.

Since the ploughing term in Eq. 1 represents forces associated with deformation of the polymer in a three dimensional stress field, the

calculated ploughing pressure, should be different for polymers with different strengths. In Table 2 the results for p' do reflect the difference in strengths of PVC and PCTFE. However, the specific relationship between the calculated ploughing pressure and a mechanical property such as yield strength is unknown.

In response to Dr. Briscoe's question, the agreement between the friction model given by Eqs. 1 and 2 and experiment is best for single traversal sliding. There appears to be a critical roughness level (probably best characterized by the asperity curvature) below which no cyclic variation of friction force on an anisotropic surface is observed. This roughness level will not be the same for all polymers. For example, ductile polymers like LDPE would have a higher level of critical roughness than more brittle polymers like PVC or PCTFE because of the differences in transfer characteristics as discussed in ref. 12.

In steady-state, multiple-pass sliding the model predicts increasing friction with increasing critical counterface roughness which is contrary to the observations that friction remains constant as the roughness increases. At steady state considerable transfer has occurred and the effect of transfer is to decrease the asperity curvature (see ref. 6 of Bahadur's discussion). The different roughnesses require that different amounts of polymer be transferred until the effective asperity curvatures are such that steady state sliding can occur. Thus, at steady state the transferred polymer has masked the initial roughness and the friction tends to be independent of this roughness.

FUTURE DIRECTION OF RESEARCH IN WEAR AND WEAR RESISTANT MATERIALS

Status of Understanding

T. Sasada
Tokyo Institute of Technology
Tokyo, Japan

The adhesion of materials is one of the most popular interactions occuring between mating solid surfaces in contact, and has been regarded as a key factor in wear process. However, because the adhesion is not a separation factor but a joining factor for mating materials, it is not easy to show a general plot of the formation process of wear particles through adhesion. In this paper, the author show a new idea on the mechanism of formation of wear particles in adhesive wear. The wear particles are not separated from their mother surfaces directly as their final form, but minute adhered fragments are assembled and piled up to form a big particle which should be called as a wear particle after it is removed out of the rubbing system. From this proposed mechanism the author will interprete many other phenomena related to wear.

INTRODUCTION

One of the most important problems in the study of the mechanism of wear is the production process of wear particles. In previous studies, the author has proposed a new model for the formation process of wear particles, in which small fragments called "transfer elements" adhere to the rubbing surfaces and combine to grow in size to be finally removed as a loose wear particle. This mutual transfer and growth model for the formation process of wear particles has been published firstly on 1972 in Japanese (ref.1) and 1975 in English (ref.2).

The author's idea about the formation mechanism of wear particles mentioned above is still unchangeable fundamentally nowadays. But the number of facts backing up the theory has been increased and many related phenomena which can be understandable only through the theory have been discovered for the last ten years. Here, the author wish to summerize a current study on this formation process of wear particles in the author's laboratory and to discuss a meaning of the "wear resistance" of rubbing materials in dry adhesive wear.

POSE A PROBLEM

As has been well known widely, the classical theory of adhesive wear is based on a premise that wear results from the shearing of junctions formed between contacting solid surfaces. According to the modern theory of solid friction, the real contact of two solids is performed by the plastic deformation of isolated asperities of solid surfaces named junctions, as shown in Fig.1.

For the shearing process of a junction, a classical model has been proposed, as

197

shown in Fig.2, by Bowden and Tabor (ref.3), Rabinowicz (ref.4) and Archard (ref.5). In this picture, the rubbing solids contact each other in a plane XX, which forms the real area of contact. According to this model, if the junction is sheared off along the contact interface XX by a frictional motion, no material loss should occur, even thouth a frictional resistance is generated by the shearing resistance in XX plane. When the shear strength at the interface between the two intimate solid surface XX is stronger than that of the bulk solids —— though it is not always realized —— , the sharing crack is formed in the softer material as shown YY in Fig.2. Then a portion of XXYY is removed as a particle from the rubbing system.

This classical interpretation for the formation process of a wear particle is somewhat unconvincing. The shearing fracture in the junction, as shown in Fig.2, does not cause a separation of the wear particle XXYY from the solid I but merely a transfer of the softer material portion XXYY to the harder surface XX, because the materials I and II adhere tightly each other in the interface XX. That is, this classical model by itself is inadequate for the production of loose wear particles. Even if the statement that XXYY in Fig.2 is removed from the rubbing system as a wear particle is true, the following feature must be observable in adhesive wear. That is, a volumetric loss should occur only in the softer solid and any wear particle must be solely composed by the softer solid. Moreover, the particle size must be the same order of the real area of contact.

According to the author's observations, as would be mentioned later, any phenomena appeared in the adhesive wear has made a denial of the above predictions. This clearly proves the inadequency of the classical model shown in Fig.2 in explaining the mechanism of adhesive wear.

BACKGROUND

Before considering the formation process of wear particles, the author would like to mention some of the characteristic phenomena in adhesive wear which might be of significant influence on the mechanism of wear particle formation.

The first is on the size of the wear particle. The particle size predicted from the model illustrated in Fig.2 should be of the same order of the real area of contact formed between the intimate surfaces, that is, about $10^{-3} - 10^{-2}$ mm. The real size of wear particles observed by the author is, however, distributed over a wide range, from 10^{-5} mm which is far smaller than a real contact area to 10^{-1} mm which is far larger than a junction. Typical wear particles are shown in Fig.3.

Next is the mutual material transfer between the rubbing surfaces. Fig.4 and Fig.5 show the X-ray microanalytic structures of Cu and Ni surfaces which are rubbed together repeatedly under an unlubricated condition. It is seen that not only the softer cu (Hv 113) is transferred onto the harder Ni (Hv 175) surface, but that Ni is also found on the Cu surface.

The third phenomenon to be pointed out is the fact that every wear particle is a composition of the two materials rubbed together. Fig.6 shows the appearance of the wear particles produced in Cu-Ni rubbing, under the same rubbing conditions as those in Fig 4 and Fig.5. It is seen that a particle is composed of a fine mixture of Cu and Ni.

These three typical phenomena pointed out here are also observed in the other

metal-metal, metal-polymer, ceramics-ceramics, metal-ceramics and polymer-ceramics combinations in dry rubbing, and metal-metal rubbing combinations in oil lubricating conditions. Some examples of the XMA photographs for mutual transfer and mixing structure of wear particles are shown in Fig.7 - Fig.12.

The facts mentioned in this section show clearly that the shearing of the junction does not occur only in the softer of mating materials, and the fragments sheared off are not yet formed as wear particles These are all contrary to the predictions of the model illustrated in Fig.2.

WEAR MODEL

Mutual Transfer and Growth Process

With the above mentioned facts as background, the formation process of a wear particle perceived by the author is as follows:

Firstly, the real area of contact must be consider because wear might occur only on the contacting portion of the intimate solids. As the real contact area is formed by the mutual geometric interference among the asperities of the two surfaces, the transverse symmetrical junction like that shown in Fig.2 is scarecely found even in a static contact. In almost all cases, it might be reasonable to suppose the contact to be made at the slope of the asperities, as illustrated in Fig.13(1). Through this oblique contact, it is highly possible for fractures to occur in the interior of either of the bulk even if the shear strength at the interface XX is weaker than in the bulk.

Now, the interface XX in Fig.13(1) formed between the slopes of asperities never has an uniform shear strength. A small portion of the real contact area might be a direct solid contact, but the majority of the remainder might be made between adsorbed molecular films. When the system is put into sliding action, a bulk shearing fracture occurs only near the direct contact portion (Fig.13(2)). Hence a small fragment is produced, transferred and adhered onto the opposite surface as Fig.13(3). In this case, though it might be more natural for the softer solid to be sheared off more, it is not impossible for shearing to occur in the harder one, as the junctions are not necessarily symmetrical. The author would like to call this small transferred piece as the "transfer element".

Then, this element itself makes a new asperity on the opposite surface. This may form a new junction in the course of further sliding as Fig.13(4). When shearing occurs, resulting a material transfer from the upper surface to the lower, as in Fig.13(5), or from lower to the upper, a "transfer particle" is formed with the merger of the two transfer elements, and this particle adheres upon any one surface. Through repeating of such accumulating process, as shown in Fig.13(4) and (5), the transfer particle gradually grow up into a considerable size as shown in Fig.13(6). After this big particle removes from the surface by an impingement against some asperity of the opposite surface with a relatively small resistance. it must be called the "wear particle".

Press-slide Flattening

The formation process of wear particles proposed here can satisfactorily ex-

plain three fundamental facts pointed out in former section, *i. e.*, the size of wear particles, the mutual material transfer to each intimate surface and the mixing structure of wear particles. But the model needs a slight modification and extention taking into account of the load supporting mechanism.

In the model illustrated in Fig.13, only one transfer particle supports the total contact load. If the particle is only hardened by work hardening or oxidizing during the friction process, the solid or cubic particle shown in Fig.13(6) can be formed. If the material properties do not change during sliding, on the other hand, the particle between the mating surfaces must be depressed until the contact pressure becomes equal to the flow pressure of the material to support the total load. (See fig.14(1) and (2).) In addition, with this friction procedure, the particle is not only depressed normally by the contact load but also extended longitudinally by the shearing action. As a result, a transfer particle with press-slide flattened shape is formed adhering to the rubbing surface as illustrated in Fig.14 (3). The final stage of the formation process of a wear particle must be the accumulation and the piling up of these "press-slide-flatteded" transfer particles. The largest of these particles adhering to one surface supports the total normal load so the contact is only between the bottom of the largest particle and the opposite surface. The particle then grows quickly to large size entangling the transfer elements or particles dotted on the opposite surface into itself, and finally removing them from the rubbing system to make a flake-like wear particle (Fig.14(4)). (ref.6)

An *in-situ* observation for the metallurgical structure of an interposed transfer particle is carried out for the rubbing system. The wear test apparatus is stopped at a point where a growing particle is interposed between the sliding surfaces. After the rubbing system is bonded with acrylic resin, a cut is made through the specimen-particle-specimen. Fig.15 shows the XMA photographs of the cut section of Zn-Cu rubbing system in which a flake-like large particle is observed between Zn and Cu surfaces. The interposed particle has hairline mixing structure of Zn and Cu, which shows evidently the press-slide flattening action should be proceeded to form the particle between the rubbing interface. The fact that the wear particle and transfer particle have a hairline mixed structure of both materials is observed not only in the Zn-Cu system illustrated in Fig.15 but also in many other cases.

The hairline mixing structure of the transfer particle shown in the cut section of the rubbing system (Fig.15) is not in consistent with the irregular mixing appearance of wear particles shown in Gig.9. Because the photograph shown in Fig.9 is looked from unspecified outside observational direction, the hairline structure might not be observed clearly.

The model for formation process of wear particles proposed by the author has been described in this section. According to this model, it is easy to understand that the size of wear particles, mutual material transfer and the mixing structure of wear particles. The most remarkable point in this theory is that a raw fragment removed from its mother surface is not a wear particle just as it is, but a wear particle is made from many raw fragments after they are assembled and piled up to form a big size.

DIRECT OBSERVATIONS

In the forgoing section, a model for formation process of wear particles has been shown. Though this model is highly reasonable for understanding some basic

200

basic features of wear phenomena, it is no more than a model. To secure this idea, it is necessary to observe the formation process of wear particles directly.

The direct observation of the growing process of a wear particle can be carried out through recording the transverse movement of a rubbing parts during sliding. If the fragments originating from each of the rubbing surfaces are piled up to grow between the mating surfaces and are removed from there, the surface must move transversally according to the origin, growth, and removal of the fr-gments. Then it is possible to know the behavior of transfer particles and the formation process of wear particles from the record of this movement.

The principle of the method derived to measure the transverse movement of a rubbing specimen is shown in Fig.16 and Fig.17. On a pin-rotating disk apparatus, a datum plane is located parallel to the disk surface and distance w between the top of the pin specimen and the datum is measured. If the wear proceeds linearly (as is commonly believed) as in Fig.16(1), the length of the pin diminishes with the sliding distance l linearly, so that the relation between w and l will be shown as ABC in Fig.17. If a fragment produced during the friction process is interposed between the mating surfaces and enlarges on the other hand, the pin will be lifted up inversely to the direction of its wear loss and will then be returened to the disk surface suddenly by the removal of the fragment. Then the w-l curve will be shown as a saw tooth during a repetition of this process (ADEF in Fig.17). (ref.6)

Typical example of the chart recording the variation of the gap between sliding surfaces (transverse movement of the pin specimen) is shown in Fig.18 for Zn-Zn rubbing. As seen in this picture, the linear wear progresses with violent intermittent transverse movement of the pin specimen. The phenomenon is seen more clearly in the partially enlarged chart of Fig.18 shown in Fig.19.

The intermittent lift up of the pin specimen appears at every 0.5 — few meters of sliding distance, but this interval can change. Following some small vibrational movements (A) in Fig.19, the pin tends to appart from the disk surface (D). After the lift up reaches in the order of 10^{-1} mm (E), the pin falls suddenly onto the disk surface (F = A). This cycle of pin movement (A) — (F) is repeated throughout the pin sliding. These facts obviously mean that the transverse movement of the pin specimen is caused by the origin and growth of the transfer particle interposed between mating surfaces which is not still removed from the rubbing system.

Fig.20 shows the photographic records of the gap between the mating surfaces of Cu-Zn rubbing in the wear process. (1),(2)—(4), and (6) in Fig.20 correspond to the stages shown in (A), (D), (E), and (F) in Fig.19, respectively. This series of photographs shows the wear process in which a transfer particle is generated, grows, and becomes a wear particle, and is suddenly removed, thus closing the gap. The wear particles produced here have the same thickness as the lift up of the pin.

The gap variation during the wear process is limited to the adhesive wear. In abrasive wear, as shown in Fig.21, though the abrasive surface has high asperities, the elevation of the pin specimen is not observed. This phenomenon means that the wear particles(that is, cutting chips) are removed directly from the clearance among the abrasives and that the metal and the particles are not compressed between the metal and the abrasive paper during abrasive wear.

Now the author will try to explain some of the outstanding experimental facts using the above proposed model. The first problem is that what is the criterion for removal of the transfer particles from the rubbing system to become to wear particles. For this question, the author will point out that the criterion is ambient atmosphere or lubricant —— in wide sense.

If the atmosphere around the sliding system is rich, the wear particles would leave the system at an early stage of growth, as the adhesive force between the particle and the surface is minimized by the chemical action of the gas molecules on the sheared surfaces. An excessive case is so-called mild wear, in which very fine wear particles are produced. On the contrary, in high vacuum, the growth of the transfer particle would be unlimiting, with some big particles removed to make loose wear particles. The poor lubricating effect of the surrounding atmosphere, the larger is the average size of the wear particles. Fig.22 shows the experimental relation between the wear particle size and the surrounding atmospheric pressure.

The mechanical rubbing conditions such as sliding velocity and load give the same effect sa ambient atmosphere. The lower the sliding velocity or the average contact pressure the better is the lubricating condition, because the mean free time of a sheared junction during which the surrounding gas molecules would attack its naked surface is inversely proportional to the sliding velocity or the contact pressure (ref.7). Fig.23 shows the experimental relation between the particle size and sliding velocity in Ni-Ni rubbing systems. Fig.22 and Fig.23 indicate that the average size of the wear particles is inversely proportional to the surrounding gas pressure and proportional to the sliding velocity. This tendency is easily apprehensible with the model mentioned in the forgoing section.

Polar molecules or EP additives in lubricating oil acts samely as the ambient gas molecules mentioned above. Shown in Fig.24 is the wear particles produced under the same condition as shown in Fig.3(2) except that it is lubricated with purified spindle oil. Though the particle size in Fig.24 is somewhat smaller than that in Fig.3(2) produced under the dry condition, the size is yet large. Wear particles produced under the lubrication with spindle oil containing tricresyl phosphate is, on the contrary, very fine as shown in Fig.25, which seem like as mild wear particles shown in Fig.3(1).

A typical effect of polar molecules in lubricating oil on the growing process of transfer particles is shown in Fig.26. Shown in Fig.26(1) is the chart in which the variation of the gap between Cu-Zn rubbing surfaces is recorded under lubrication with purified kerosene. As seen in this chart, the transverse movement of the pin specimen is not yet diminished with the application of kerosene. On the contrary, the lubricant with the addition of 0.5% stearic acid makes to eliminate markedly the transverse movement of the pin specimen as shown in Fig.26(2).

LARGE-SMALL SIZED RUBBING PART

In practical rubbing systems, it is the most popular that a smaller component rubs repeatingly on a larger component. In such a case, according to empirical knowledge, the larger component wears out more rapidly than the smaller one. This phenomenon is easy to be interpreted using the author's wear model.

As seen in Fig.20, the surface of smaller component is protected by the adhered big transfer particle. The particles which are adhering onto the surface of the larger component are, on the contrary, teared off and joined to the former particle during repeating run. So the contact is made between the big transfer particle and the surface of the larger component in the most period during rubbing. This is the reason why the larger component wears more rapidly than the smaller.

RUBBING VIBRATION

The wear process interpreted here, in which the sliding component repeats the transverse movements owing to the formation process of wear particles, means that the wear is not a phenomenon without any vibrational movement of its rubbing component. It has been believed hitherto that the rubbing vibration has a bad influence to the result of the wear test and that the vibration must be eliminated to give a "correct result" of the experiment.

According to this study, however, it is obvious that the prevention of relative movement of the order which equals to the dimention of the wear particles is impossible. In the other words, rubbing vibration is not a cause but it is a result of the wear.

WHICH IS MORE WEAR IN DIFFERENT METAL COMBINATIONS

When wear proceeds in accordance to the classical junction model shown in Fig.2, only softer solid would be worn off in the different metal combinations. In practice, however, many cases have been reported that wear was also observed in the harder metal. Moreover, it has even been observed sometimes that the harder solid has worn off more than the softer. The author would explain these phenomena as follows.

Though the shearing fracture near the direct contact portion occurs, as mentioned above, mainly in the softer of mating materials, it is not impossible to occur in the harder material, because the junction is not necessarily symmetrical. The surface activity of a transfer element (produced by the shearing) can be neutralized by the adsorption of surrounding gas molecules. As the affinity for chemisorption of transition metals (usualy harder metals) is greater than that of non-transition metals (usualy softer metals) in general (ref.8), the surface energy of the fresh harder metal surfaces formed after shearing declines abruptly. Therefore, it is more difficult for particles of hard metals to adhere onto the metal surfaces. On the other hand, though the junctions easily break off from the side of the softer metal, the discreted particles readily adhere with one another as well as with their parent metals. As a result, the harder metal is sometimes severely worn off in different metal combinations.

Let me present an interesting evidence. In Cu-Fe rubbing under natural atmospheric conditions, the softer Cu was worn away more than the harder Fe. In a 10^{-6} torr vacuum, on the contrary, Cu was not worn off: instead, the harder Fe was transferred onto the Cu surface. This can be considered to be due to the thin atmosphere of 10^{-6} torr, which was insufficient to destroy the surface activity of Cu but sufficient for the more active Fe. (ref.2 and ref.9).

Here, an additional comment on the antiwear property of metals must be given.

203

To produce a small wear particles it is necessary to accept chemically any ambient gas or lubricant molecules on the solid surface. As the most popular chemical action to reduce the surface energy of solids is chemisorption, transition metals are highly effective for this purpose. That is, the d-electron vacancy, which characterize the transition metals, is the fundamental origin of gas chemisorption activity (ref.8). From this reason mild wear (producing very fine wear particles) in dry rubbing occurs only in the metal combinations in which the transition metal is used for either rubbing component at least (ref.6 and ref.7).

SEIZURE OF METALS

In practice, it is believed commonly that the seizure results a sudden increase of frictional resistance owing to the break down of a lubricating oil film. Nevertheless, when seizure occurs the frictional resistance in the rubbing system reaches usually to a value higher than that of dry friction. From this reason, it is evident that seizure is not a merely disappearance of the lubricant from between the rubbing interface.

From the study carried out by the author's group recently, the seizure is only a special case of growing of transfer particles (ref. 10). If, for iexample, a transfer particle is originated and developed at the bottom of a journal bearing as illustrated in Fig.27, the bearing gap would be filled up by the grown transfer particle. After the particle cloggs in the gap, the actual normal load becomes greater, then the growing of the particle becomes more accelerated until the driving motor would be stopped.

Fig.28 is a cut section of a seized portion in Cu-Ni rubbing system. It is seen that a big, flake-like shaped particle with hairline mixing structure of Cu and Ni is interposed between the rubbing interface. This transfer particle is clearly formed throgh press-slide flattening as mentioned above.

CONCLUSIVE REMARK

As mentioned in forgoing sections, formation process of wear particles is highly dependent to mutual adhesion of rubbing materials. The main points of the process proposed in this paper are as follows:
What separated from the bulk solid by the frictional shearing may be considerably small particles. Though these small particles transfer onto the mating surface through further shearing, they do not leave the system as wear particles easily. these particles repeat such migrations in the course of sliding and grow into large sized particles. After the press-slide-flattening process, it falls off depending on the strength of its adherence, and becomes a loose wear particle.

This model is very useful in explaining the many phenomena; that is, the mutual transfer phenomena, the size and structure of wear particles, the effect of atmosphere and lubricants, large-small sized rubbing parts, rubbing vibration, wear phenomenon found in different metal combinations and the seizure of metals.

204

REFERENCES

1. Sasada, T.; Frictional Damage of Solid Surfaces, Journal of Japanese Society of Mechanical Engineers, vol.75, no.641, June 1972, p. 905 (in Japanese).

2. Sasada, T., Norose, S.; The Formation and Growth of Wear Particles Through Mutual Material Transfer, Proc. JSLE-ASLE International Lubrication Conference, Elsevier, 1976, p.82.

3. Bowden, F.P., and Tabor, D.: The Friction and Lubrication of Solids, Part I, Oxford Univ. Press, 1954, p.285.

4. Rabinowicz, E.; Friction and Wear of Materials, John Wiley & Sons, 1964, p.137.

5. Archard, J. F.; Contact and Rubbing of Flat Surfaces, J. of Appl. Physics, vol. 24, no.8, Aug. 1953, p.981.

6. Sasada, T., Norose, S. and Mishina, H.: The Behavior of Adhered Fragments Interposed between Sliding Surfaces and the Formation Process of Wear Particles, J. of Lubrication Technology, Trans. ASME, vol.1o3, Apr. 1981, p.195.

7. Soda, N. and Sasada, T.; Mechanism of Lubrication by Surrounding Gas Molecules in Adhesive Wear, J. of Lubrication Technology, Trans. ASME, vol.100, Oct. 1978, p.492.

8. Trapnell, B.M.W.; Chemisorption, Butterworths Sci. Pub., 1955, p.153.

9. Sasada, T., Norose, S. and Nagai, J.; Wear in Different Metal Combinations in Vacuum, Proc. of the 21st Japan Congress on Mater-als Research, The Society of Materials Science, Japan, Kyoto, 1978, p.112.

10. Mishina, H. and Sasada, T.; Observation of Micro-structure in Seized Portion and Mechanism of Seizure, International Conference on Wear of Materials 1983, ASME, in press.
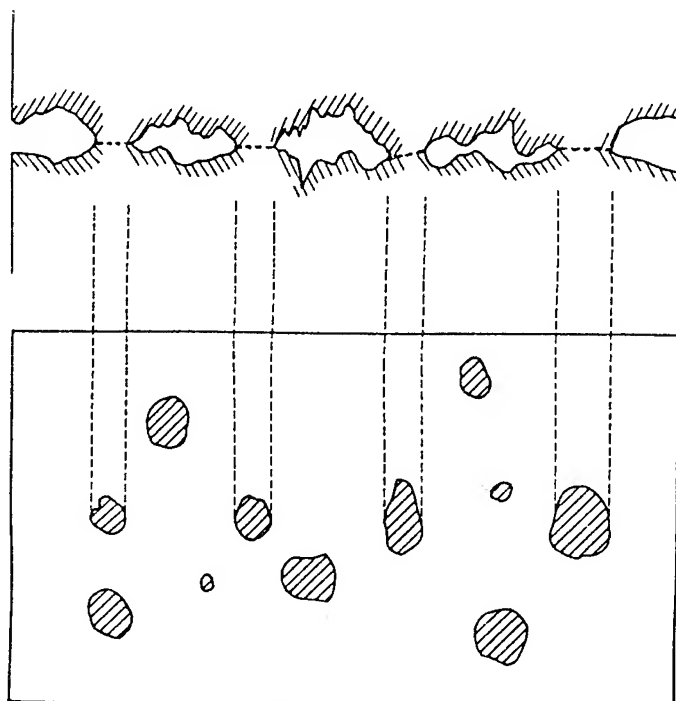
Figure 1
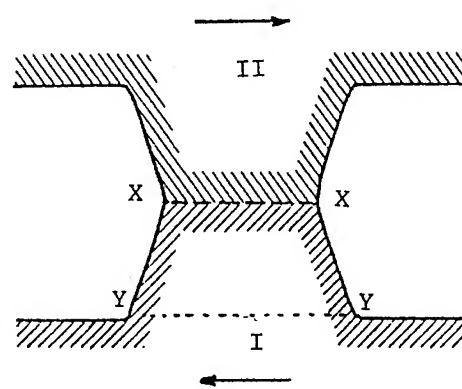
Figure 2

TYPICAL WEAR PARTICLES

Hardened Steel - Hardened Steel in Dry Rubbing

(1) Fine Particles
P = 75 N, v = 1 m/s.

(2) Big Particles
P = 75N, v = 4m/s.

Figure 3

206
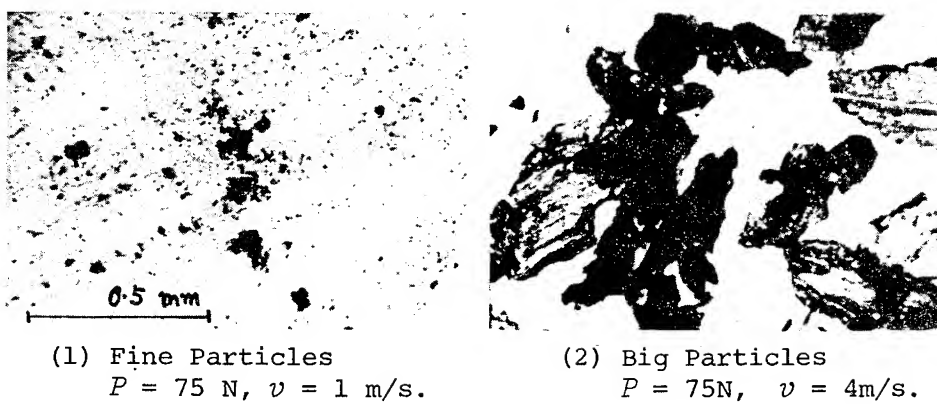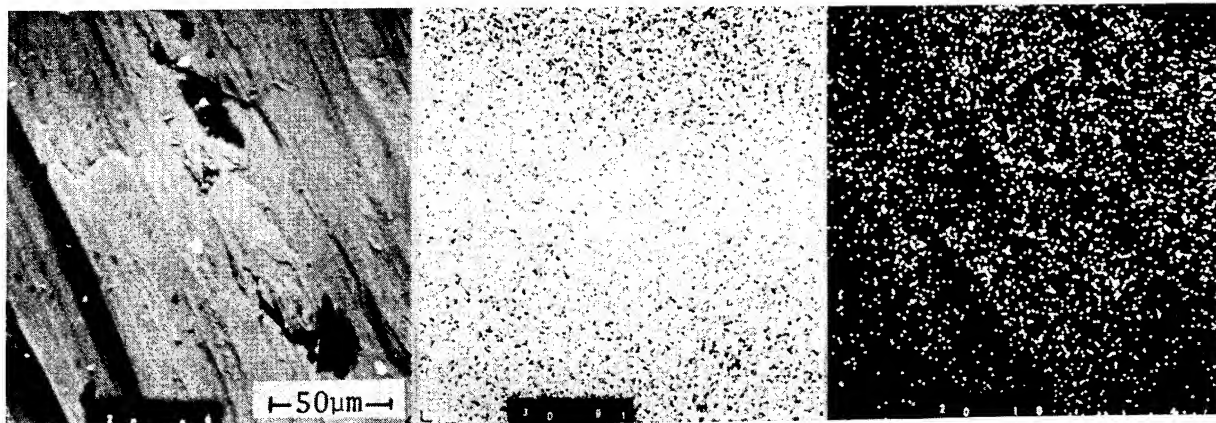
Back Scatter Electron Image.   Cu *K*α X-Ray Image.   Ni *K*α X-Ray Image.

Figure 4.   XMA PHOTOGRAPHS: Cu Surface Rubbed Against Ni in Dry.
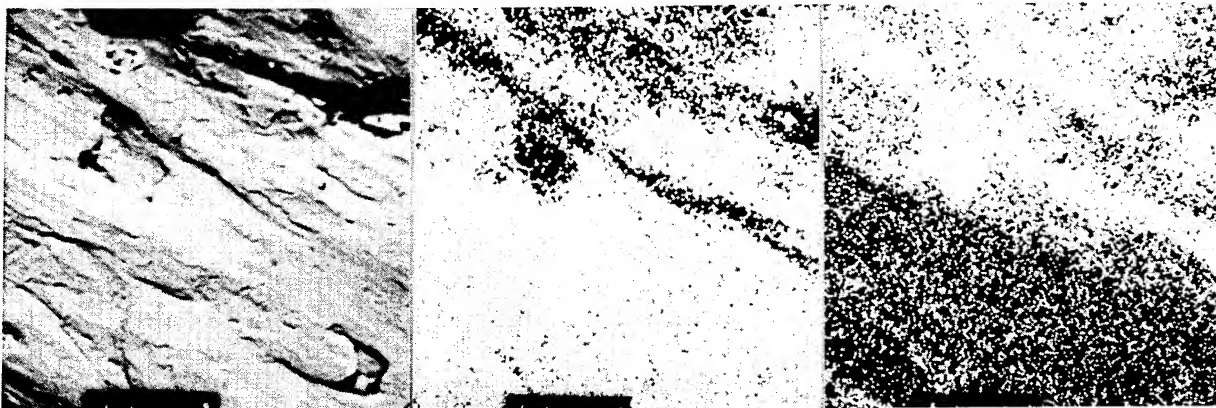
Back Scatter Electron Image.   Cu *K*α X-Ray Image.   Ni *K*α X-Ray Image.

Figure 5.   XMA PHOTOGRAPHS: Ni Surface Rubbed Against Cu in Dry.
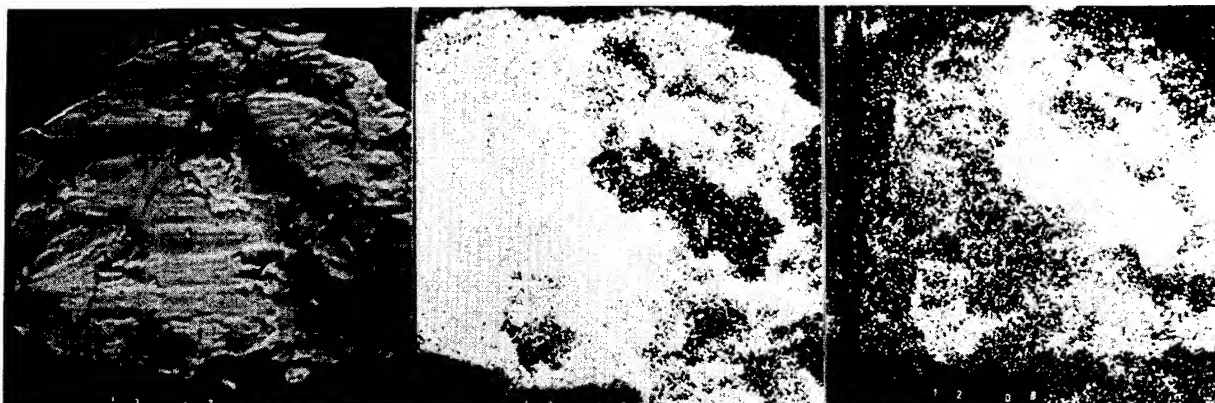
Back Scatter Electron Image.   Cu *K*α X-Ray Image.   Ni *K*α X-Ray Image.

Figure 6.   XMA PHOTOGRAPHS: Wear particles Produced by Cu-Ni Rubbing in Dry.

207

Secondary Electron Image.   Si *K*α X-Ray Image.   Al *K*α X-Ray Image.

Figure 7.   XMA PHOTOGRAPHS: SiC Surface Rubbed Against Al$_2$O$_3$ in Dry.
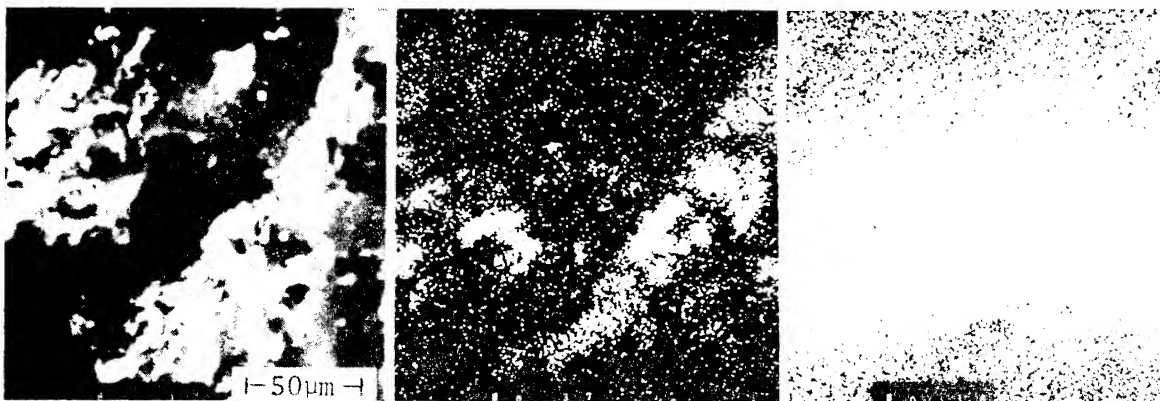
Secondary Electron Image.   Si *K*α X-Ray Image.   Al *K*α X-Ray Image.

Figure 8.   XMA PHOTOGRAPHS: Al$_2$O$_3$ Surface Rubbed Against SiC in Dry.
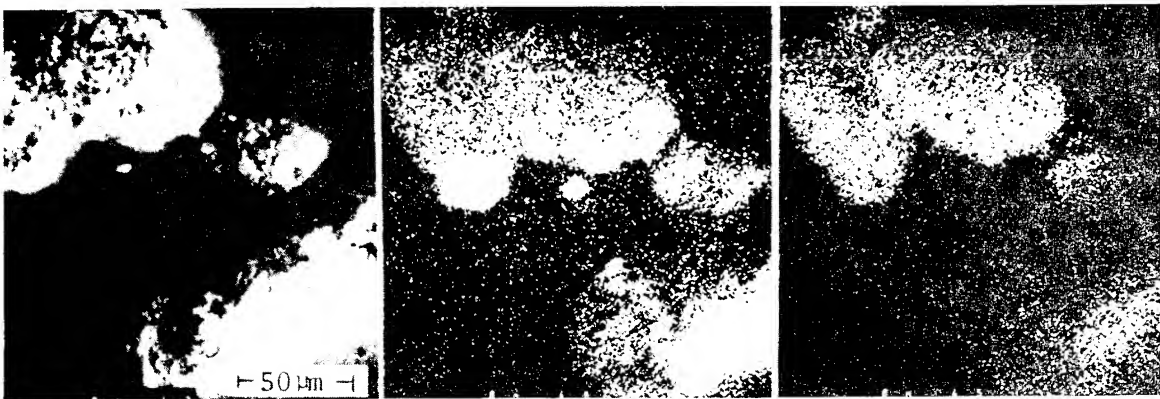
Secondary Electron Image.   Si *K*α X-Ray Image.   Al *K*α X-Ray Image.

Figure 9.   XMA PHOTOGRAPHS: Wear Particles Produced by SiC-Al$_2$O$_3$ Rubbing in Dry.

208

Secondary Electron Image   Cu *K*α X-Ray Image   Fe *K*α X-Ray Image
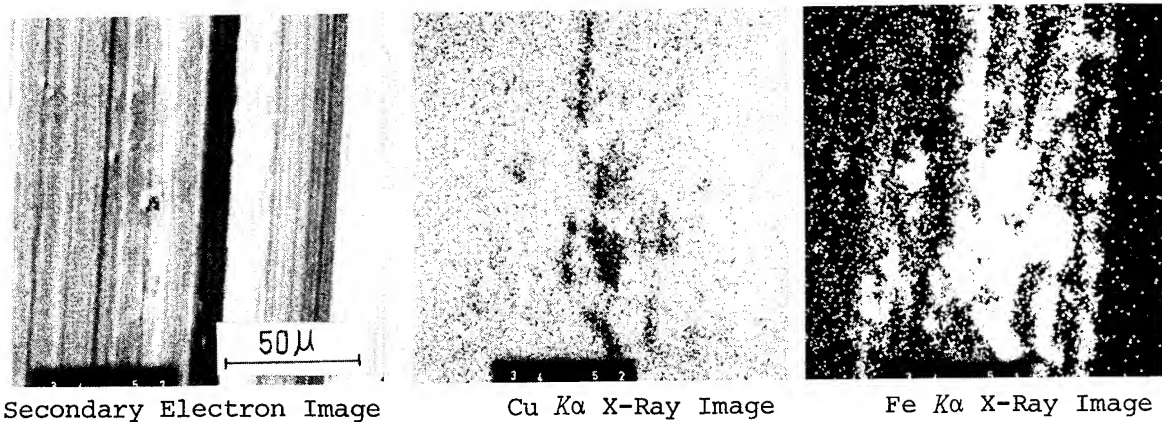
Figure 10. XMA PHOTOGRAPHS: Cu Surface Rubbed Against Fe in Lubricant Oil.
(Purified Base Oil)

Secondary Electron Image   Cu *K*α X-Ray Image   Fe *K*α X-Ray Image
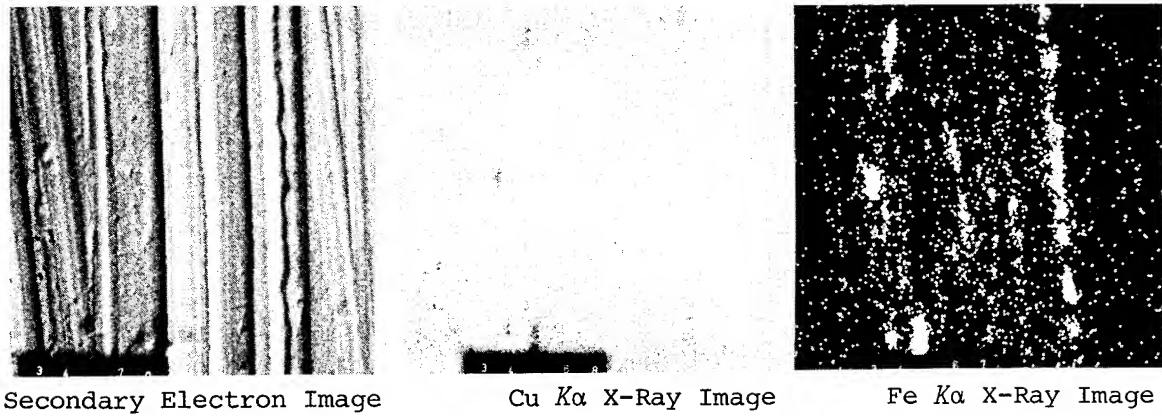
Figure 11. XMA PHOTOGRAPHS: Fe Surface Rubbed Against Cu in Lubricant Oil.
(Purified Base Oil)

Secondary Electron Image   Cu *K*α X-ray Image   Fe *K*α X-ray Image
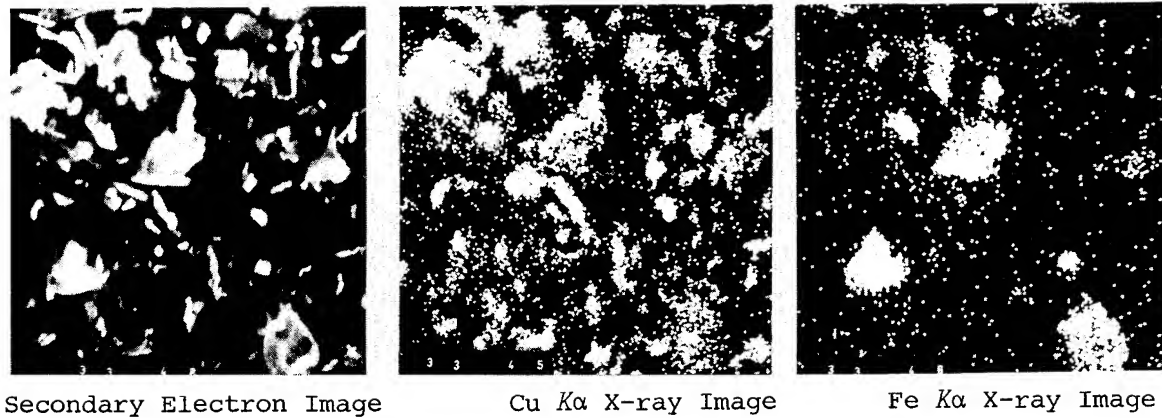
Figure 12. XMA PHOTOGRAPHS: Wear Particles Produced by Cu-Fe Rubbing in Lubricant
Oil. (Purified Base Oil)

209

THE MODEL FOR FORMATION OF WEAR PARTICLE
(ref. 2)

(1) Contact of
Asperities

(2) Breakdown in
Junction

(3) Formation of
Transfer Element

(4) Contact on Second
Chance

(5) Merger of Two
Transfer Elements

(6) Transfer Particle
Just Before Its Removal
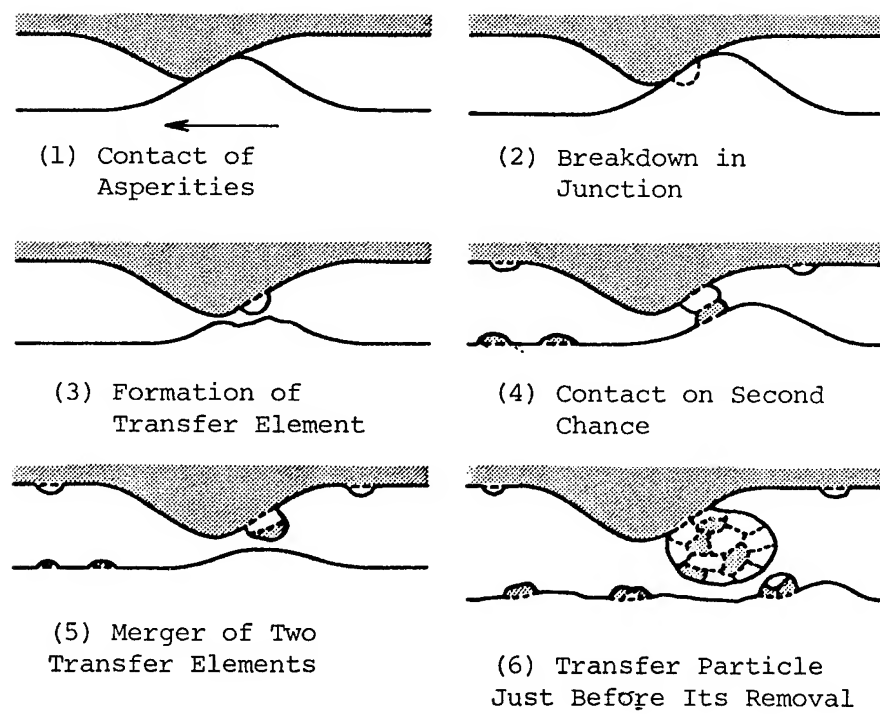
Figure 13

PRESS-SLIDE FLATTENING OF THE TRANSFER
PARTICLE   (ref. 6)
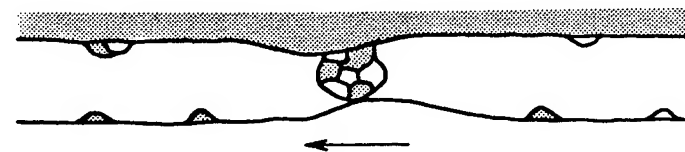
(1) Transfer Particle Growing Enough to
    Support the Total Load
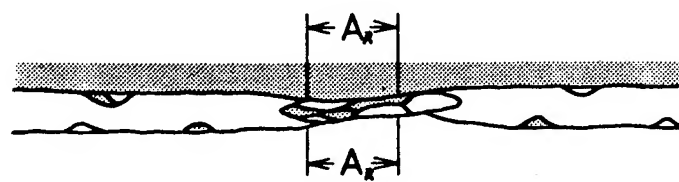
(2) Depressed Transfer Particle Contacting
    with Area A_R Determined by the Flow
    Pressure
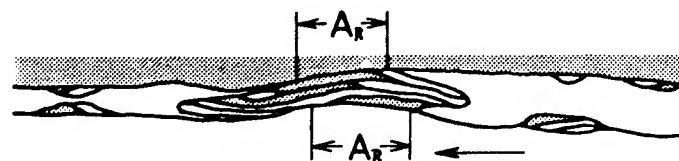
(3) Press-slide Flattening Through
    Frictional Motion
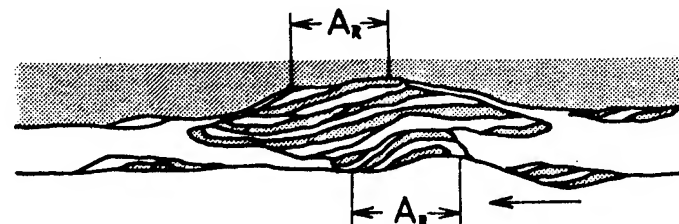
(4) Grown Transfer Particle Just Before
    Removal

Figure 14

XMA PHOTOGRAPHS: CUT SECTION THROUGH RUBBING SYSTEM,
Zn-Cu Rubbed in Dry   (ref. 6)
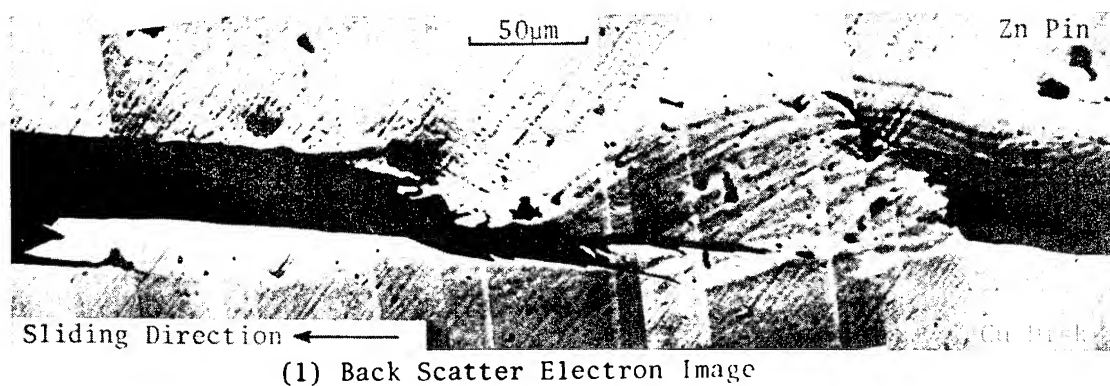
(1) Back Scatter Electron Image

(2) Zn-$K\alpha$ X-ray Image

(3) Cu-$K\alpha$ X-ray Image

Figure 15

212

TRANSVERSE VARIATION OF PIN POSITION
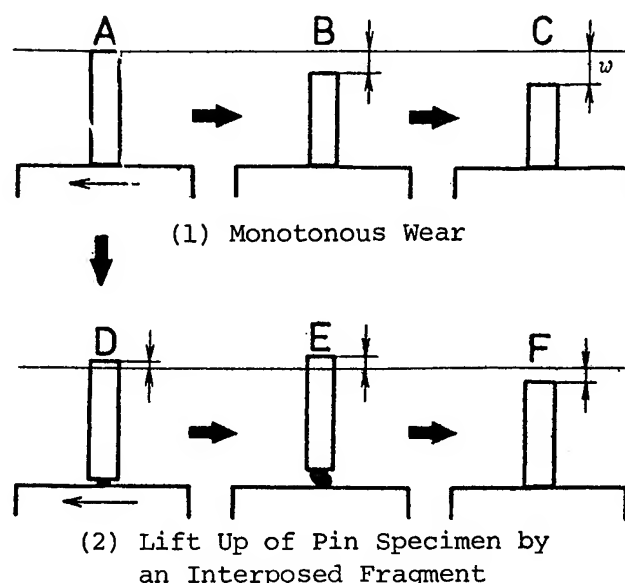
PIN POSITION - DISTANCE CURVE

(1) Monotonous Wear

(2) Lift Up of Pin Specimen by an Interposed Fragment
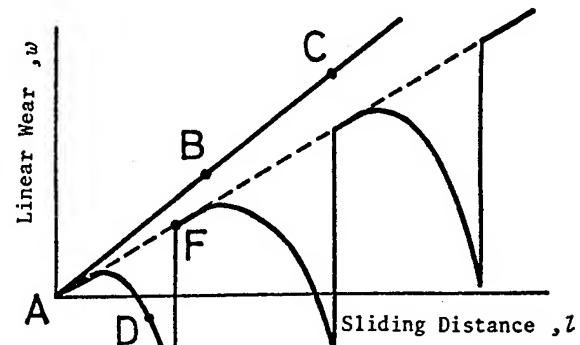
Figure 16

Figure 17

VARIATION OF GAP BETWEEN MATING SURFACES, Zn-Zn (Partially Enlarged from Figure 18)
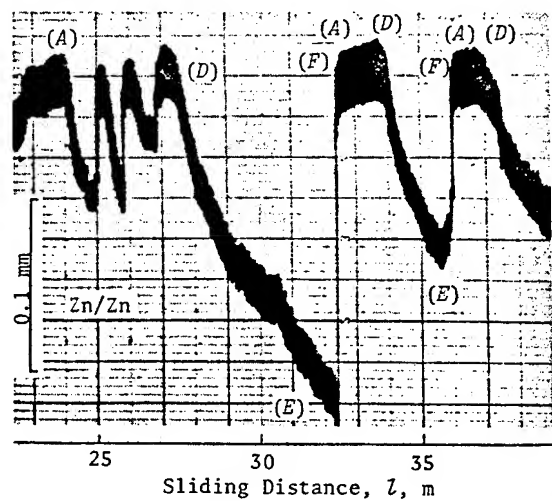
Figure 19

Variation of Gap Between Mating Surfaces and Linear Wear. Zn-Zn, in Dry. (ref. 6)

Figure 18

213
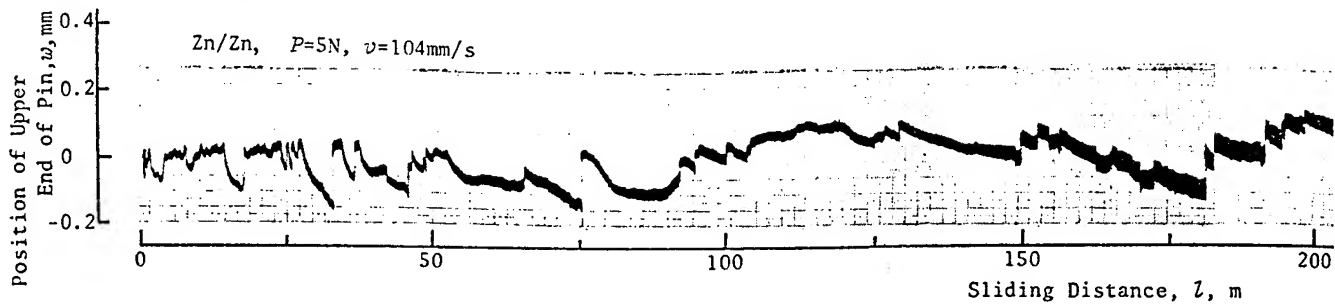
BIRTH, GROWTH AND REMOVAL OF A TRANSFER PARTICLE.
(Cu Pin with 1.5mm in Diameter) - (Zn Disk),
Under Dry, P=5N, v=10.4mm/s.   (ref. 6)
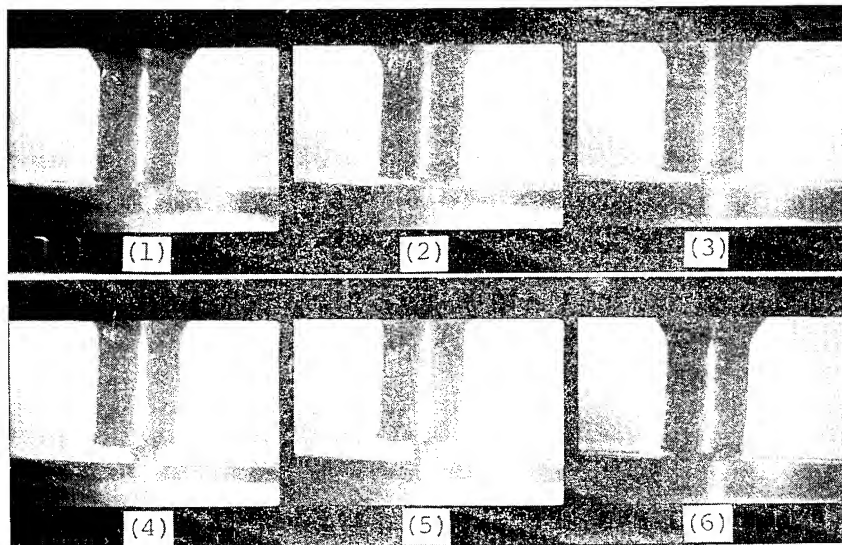
Figure 20

VARIATION OF GAP BETWEEN MATING SURFACES AND LINEAR WEAR.
(Cu Pin with 1.5mm in Diameter) - (600# Abrasive Paper), (ref. 6)

Figure 21

214
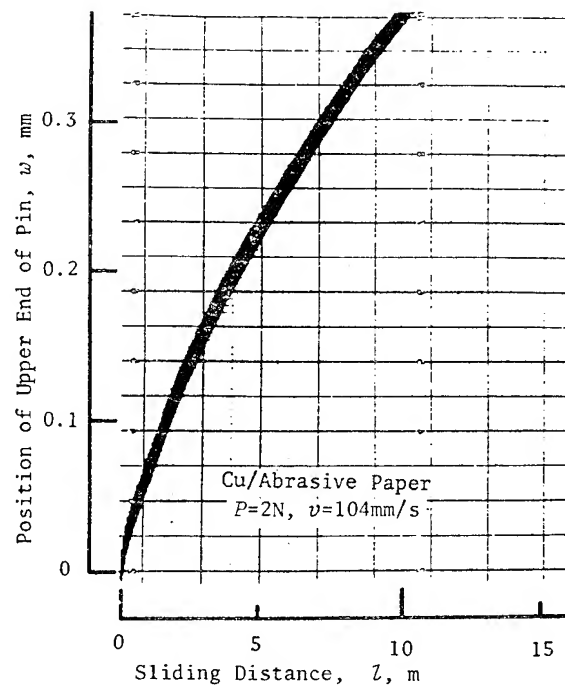
EFFECT OF AMBIENT ATMOSPHERIC PRESSURE
ON THE MEAN SIZE OF WEAR PARTICLES
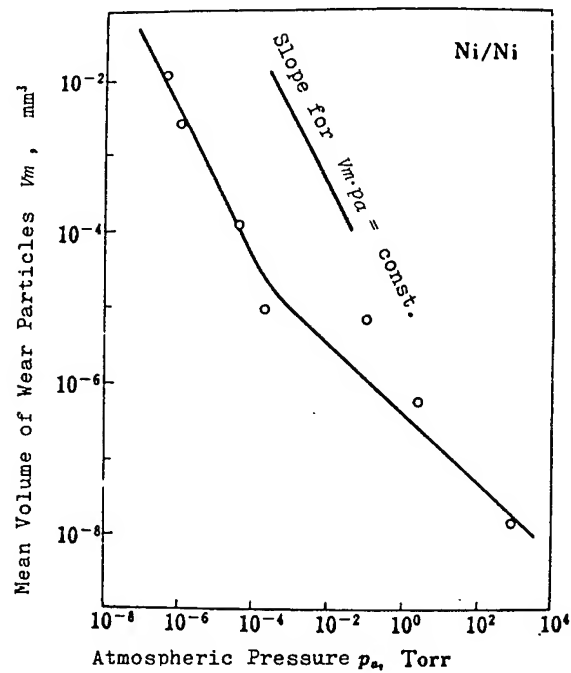
EFFECT OF SLIDING VELOCITY ON THE
MEAN SIZE OF WEAR PARTICLES
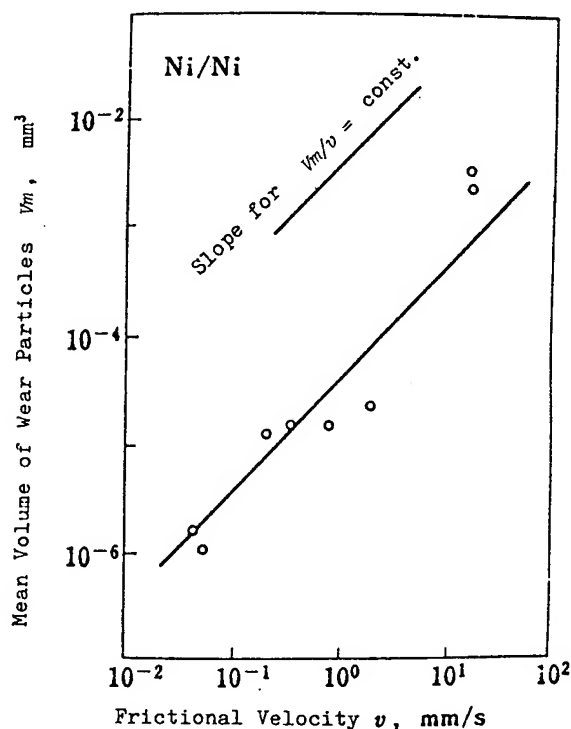
Figure 22

Figure 23

TYPICAL WEAR PARTICLES
Hardened Steel - Hardened Steel
Lubricated with Purified Base Oil
$P = 75$ N, $v = 4$ m/s.
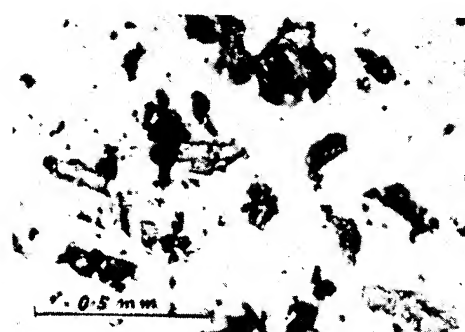
Figure 24

TYPICAL WEAR PARTICLES
Hardened Steel - Hardened Steel
Lubricated with Base oil Containing
1.5% Tricresyl Phosphate,
$P = 75$ N, $v = 4$m/s.

Figure 25

215

EFFECT OF LUBRICANT OIL ON VARIATION OF
GAP BETWEEN MATING SURFACES
Cu-Zn.

(1) Cu/Zn
$L = 500\,\text{g}$
$V = 10.4\,\text{mm/s}$
Kerosine
$1.5\,\phi\,\text{pin}$

0.02 mm

10 laps

5 m   10 m   15 m

Position of Upper End of Pin Specimen

(2) Cu/Zn
$L = 500\,\text{g}$
$V = 10.4\,\text{mm/s}$
Kerosin + Stearic Acid
$1.5\,\phi\,\text{pin}$

10 laps

0.02 mm

5 m   10 m   15 m

Frictional Distance
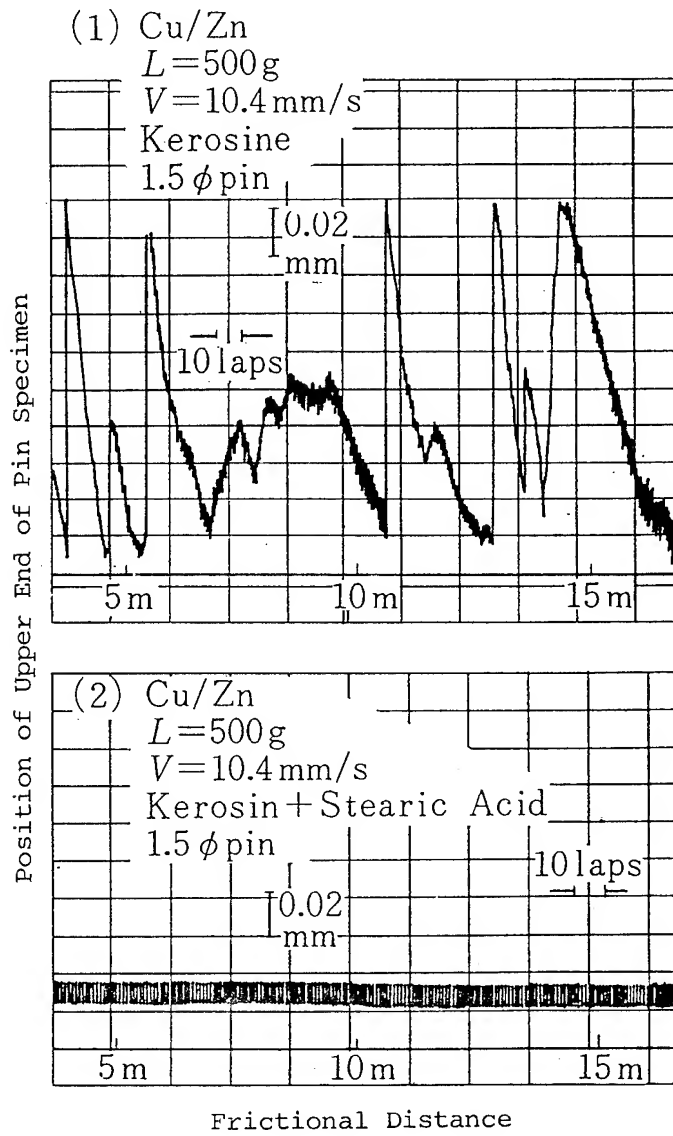
Figure 26

SEIZURE OF JOURNAL BEARING

P

Transfer Particle

Figure 27

216
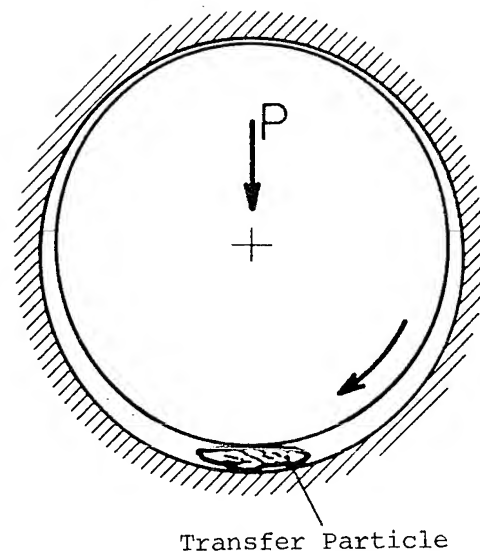
XMA PHOTOGRAPHS OF SEIZED PORTION OF Cu-Ni RUBBING SYSTEM.
Dry rubbing.
Note: Rubbing surfaces are connected by a flattened large transfer
particle of which structure is the lamellar mixture of the
sliding metals. (ref. 10).

(1) Sketched Illustration
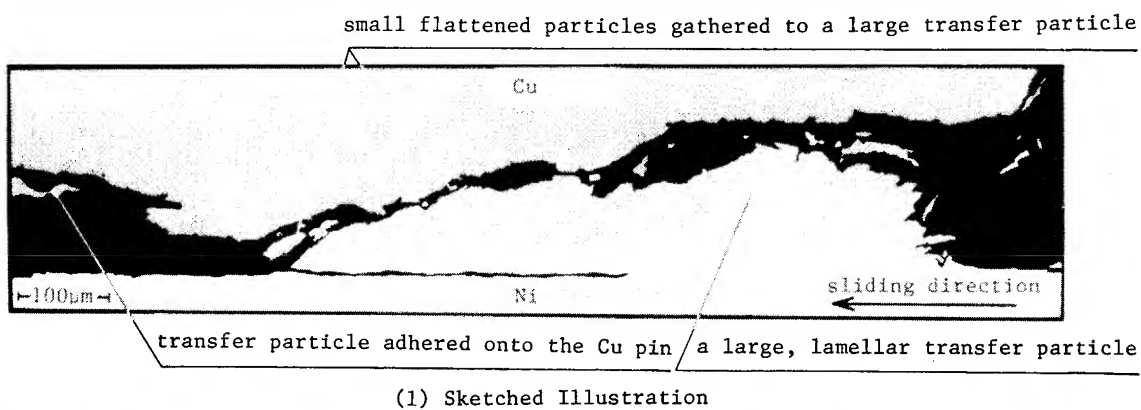
(2) Composite Image
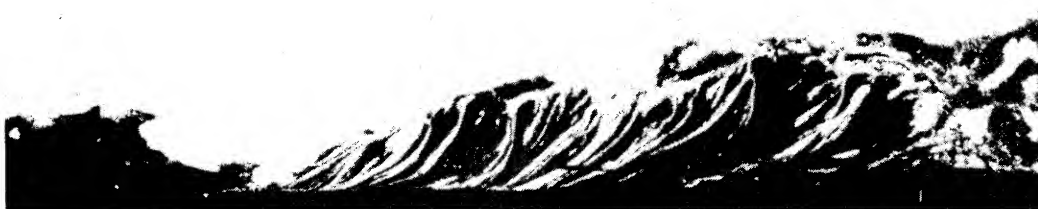
(3) Cu Kα X-ray Image

(4) Ni Kα X-ray Image

Figure 28

217

DISCUSSION

David Tabor
Cavendish Laboratory
Cambridge, England

In Professor Sasada's paper on the Status of Understanding of Research in Wear we heard a brilliant and elegant account of the type of wear fragments generated between sliding surfaces. Based largely on his own research he has drawn attention to the marked difference between the compacted micro-fragments formed in the presence of air (or oxygen) and those larger fragments formed between relatively clean metals. However, in a Conference intended "to assess the best understanding of basic mechanisms" I feel that some comment is called for concerning other types of wear mechanisms that are engaging the attention of dedicated tribologists. Because of Professor Sasada's vast experience in wear research it would surely be of value to hear his critical views of other wear processes. I would welcome for example brief penetrating comments on delamination, oxidational wear, mutual solubility, surface energy, etc.

MICROSTRUCTURES ASSOCIATED WITH WEAR[*]

W. A. Glaeser
Battelle Columbus Laboratories
Columbus, Ohio

High strain associated with wear of metals is discussed. Both macroscopic and fine microscopic aspects are referred to. Several mechanisms for the production of debris are discussed, including extrusion of microfurrows, and adhesive transfer, and fragmentation. The structure of near surface deformation zones, including a thin transfer layer, is also discussed. The similarity among the size of fine wear debris particles, the structure of the transfer layer, and large wear flakes is shown. Differences in microstructure associated with dry wear and lubricated wear are pointed out. Some parallels and differences for classic high strain deformation and wear microstructures are discussed.

INTRODUCTION

Since the development of the scanning electron microscope (SEM) there has been a proliferation of its use in characterizing wear microtopography. This has happened as the advantage of depth of focus and later the incorporation of EDAX and WDX elemental analysis capabilities made possible new understanding of the microscopic aspects of wear. Not that microscopy (TEM) has been ignored in wear studies prior to the availability of the SEM. In fact, the use of surface replication and transmission electron microscopy goes back at least 35 years. An example of this approach to wear microscopy is shown in Figure 1. This is part of a study on failure mechanisms in babbitt journal bearings done in 1946[1]. The photomicrograph shows details of surface deformation, micropitting and debris-caused gouging. The white particles are loose debris (unidentified) picked up by the replica. The process was much more time consuming than SEM techniques and, therefore, its use was much more limited. Of course replication is still used and is valuable for the study of surface features beyond the resolution of conven-

tional scanning electron microscopes. An example of the more recent use of surface replication and TEM is shown in Figure 2. This is fine scratch detail from a precision ball bearing.

Attempts at studying the defect structures developed in alloys subjected to wear or rolling contact have introduced a whole new microstructure concept. The excellent transmission micrographs of near surface structures by Ives[2], Heilmann[3] and Ohmae[4] have given new insights into substrate deformation processes produced in near-surface and extra-surface regions during wear. Many different deformation microstructures have been reported in association with wear. Probably there are still many more to be reported. It seems appropriate, nevertheless, that a good look be taken at the current state of wear microstructure so that further speculation can be made on the origin of wear debris.

FIGURE 1. PHOTOMICROGRAPH OF WORN TIN BABBITT BEARING SURFACE. TRANSMISSION ELECTRON MICROSCOPE IMAGE FROM SHADOWED PLASTIC REPLICA (Circa 1946)

20,000X   └──┘ 0.5 μm
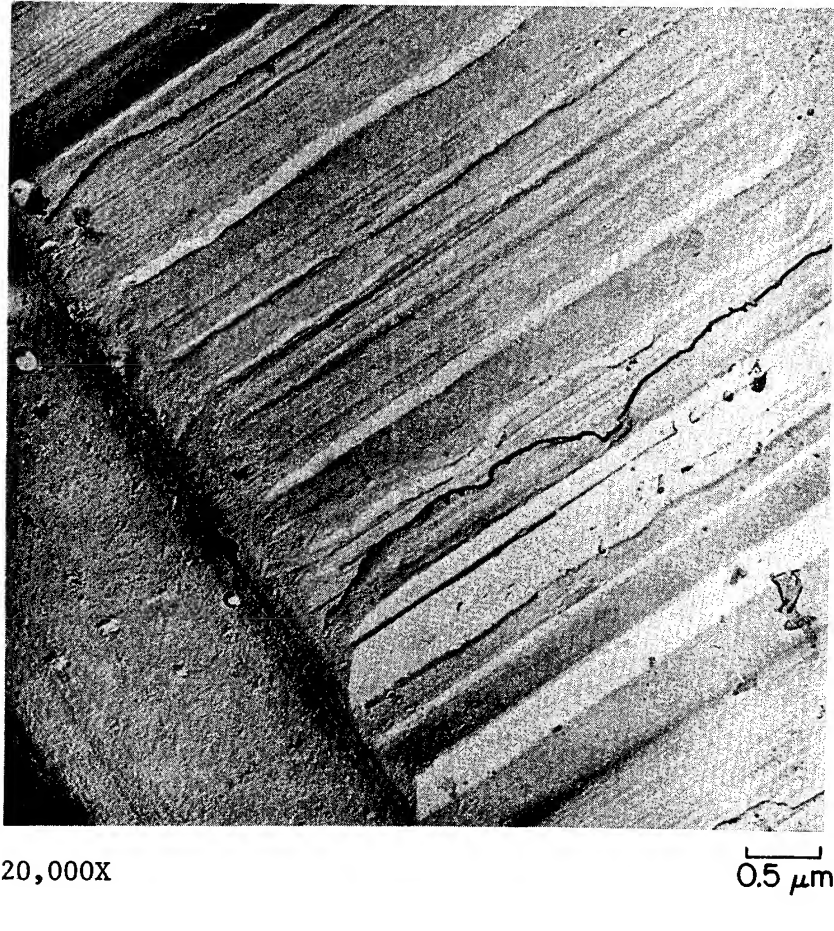
FIGURE 2.   HIGH RESOLUTION TEM MICROGRAPH OF AN AISI 52100 STEEL
            BEARING RACE SURFACE FROM A SHADOWED PLASTIC REPLICA
            (Circa 1978)

MACRO DEFORMATION

        Dimensional changes associated with wear can occur by several means.
Loss of material from the surface in the form of particulate debris is the most
familiar means.   Transfer of material from one surface to another without debris
formation is another means.   Gross plastic deformation and accumulation of plastic
strain (especially during "wear-in") is another means that is often overlooked.
This kind of deformation can often be seen with the naked eye.   Deformation of
rails from heavy freight traffic is one example.   Usually the formation of debris
and some transfer occur concurrently with deformation.   The initial "wear-in"
deformation can also be accompanied by changes in friction characteristics.   The
LFW-1 ring and block tester exhibits this type of behavior.   As the initial
cylindrical impression into the wear block proceeds, friction changes until an
equilibrium deformation conditions exists.   This characteristic is repeatable and

221

often has a "signature" for a given block material. Blau[5] has studied the progressive variation of friction during wear-in for various surface conditions (water immersion, dry air, humid air) and found that changes in microstructure accompanying wear-in deformation appear to influence friction behavior.

Wear of chain is often accompanied by heavy deformation. Two examples illustrate this fact. The first one is from a chain used to secure oil tankers when loading or unloading. The links in these chains are made of AISI 1024 steel. A metallographic section taken through one link of a worn chain from a chain test is shown in Figure 3. Contact conditions between links cause material flow from the edges of the contact into the center producing a hard lump in the center of contact. The extent of deformation and the direction of flow can be seen in the curvature of the original wire drawing texture. The results are readily visible to the naked eye.

Even in chain hardened by carburization the characteristic flow pattern in the link contact area is easily seen in metallographic section. Figure 4 shows a composite micrograph with flow lines directed to the center of the contact area. Note also that subsurface fissures are associated with the flow lines. The fissures appear to be generated at sites of hard inclusions and follow the texture lines or lines of inclusion concentration. We have observed this type of exfoiliating or delamination in hardened steels having a certain amount of inclusion content.

One other example of macro deformation in contact wear is wire rope. The wire rope used in excavating machinery (drag lines, hoists, clam shell scoops, etc) have internal notches and flats caused by heavy contact pressures between wires and strands in the rope construction. An example of this kind of deformation is shown in Figure 5. Both notches and flats are produced in the manufacture of the wire but they increase in dimension during field service and the outside diameter of the wire decreases partly because of this internal deformation. Removal of material from the internal wire surfaces by fretting also occurs but the major change in dimension can be shown to be plastic deformation. This deformation and "extrusion" is shown in a metallographic section of a wire pictured in Figure 6.

All of these illustrations serve to remind us that we must regard wear as a deformation process as well as a debris-produced-by-microfracture process.
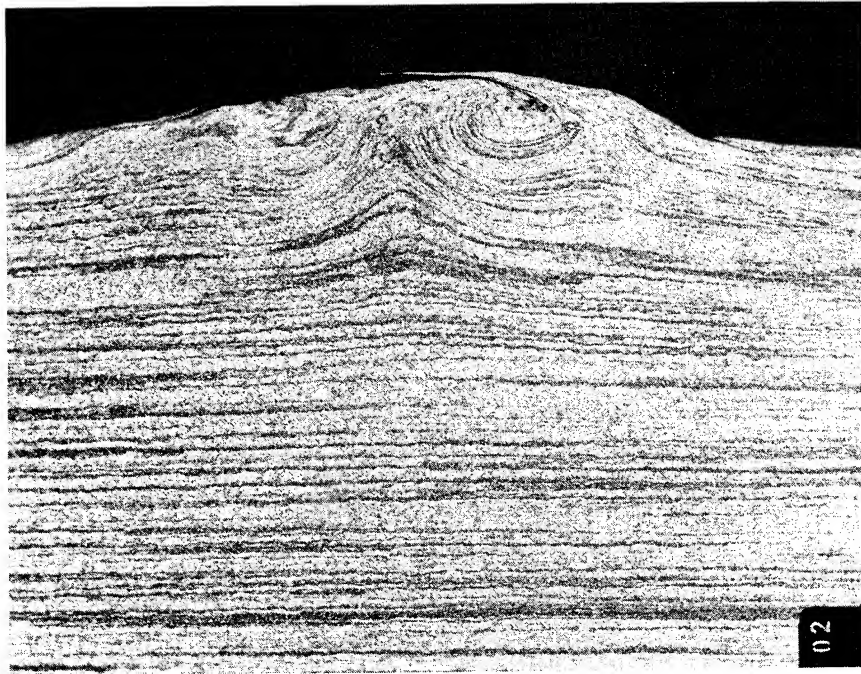
25X

FIGURE 3.   SECTION THROUGH A CHAIN LINK (AISI 1024 STEEL) SHOWING
HEAVY WORKING AND FLOW TOWARD THE CENTER OF THE CONTACT

10 μm
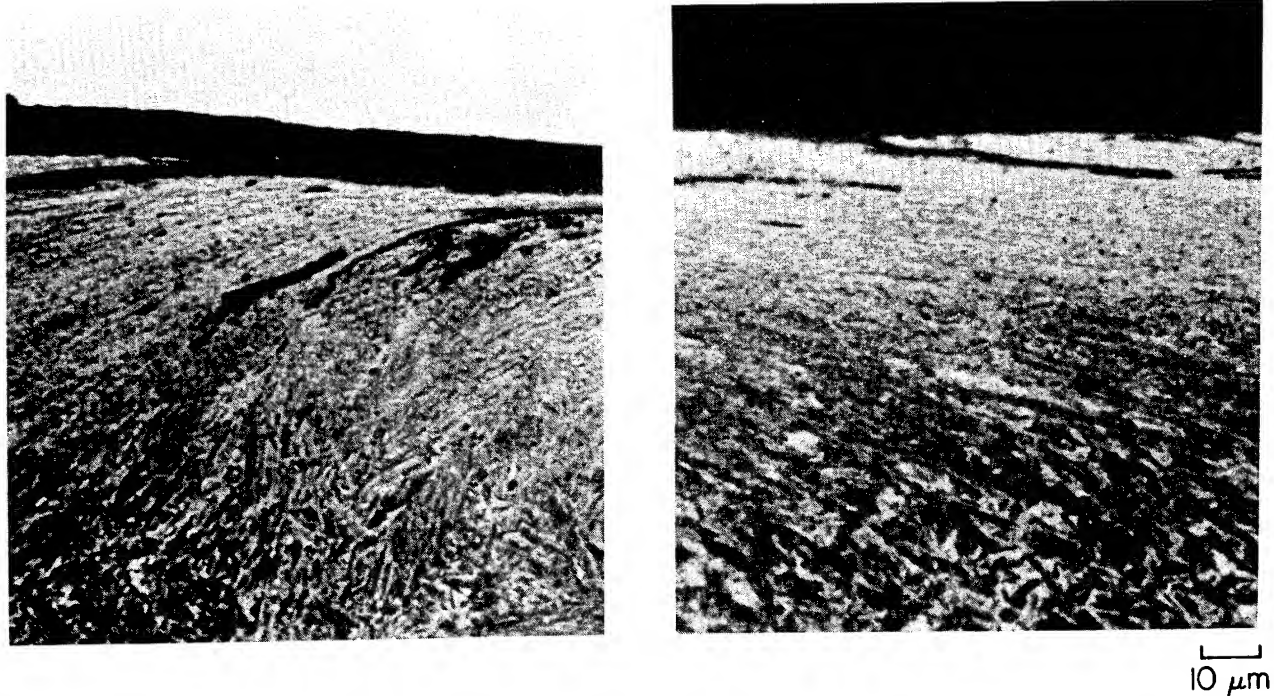
FIGURE 4.   COMPOSITE OF CONTACT ZONE IN CARBURIZED CHAIN LINK
SHOWING DEFORMATION AND FLOW TOWARD CONTACT

223

FIGURE 5. DEFORMATION AND NOTCHING OF CORE WIRES FROM A WIRE
ROPE USED ON A LARGE DRAGLINE EXCAVATOR
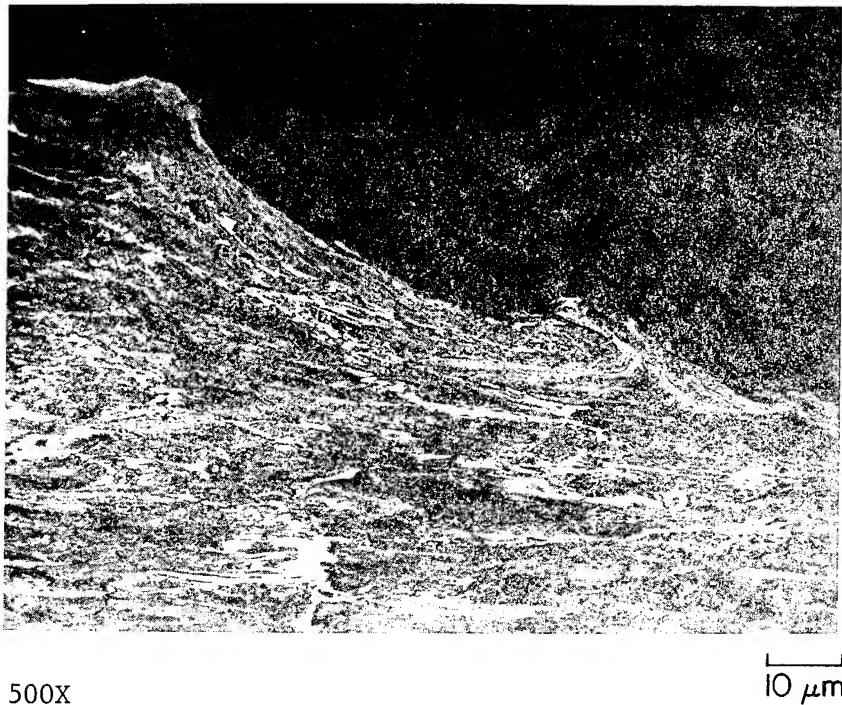
500X

10 μm

FIGURE 6. SECTION THROUGH A "NOTCH" IN A WIRE FROM A WIRE ROPE
USED IN A DRAGLINE EXCAVATOR

224

A number of people investigating the microstructure of wear[6,7] have suggested a characteristic near-surface structure composed of 3 zones:

1. grain deformation
2. highly deformed zone (cells, subgrains, twinning)
3. transfer layer.

A schematic representation of this condition is shown in Figure 7. Before we go into the details of the near surface microstructure let us first look at the worn surface as seen by high resolution microscopy.

Light microscopy, using the metallographic microscope, shows a rounded surface with a directionality – grooves or scratches in the direction of sliding. It also shows surface deposits as distinguished by color or by different responses to illumination or polarized light. The SEM reveals the microtopography in much greater detail.

Sterescopic SEM micrographs are particularly revealing. Here, one can see the microgrooving as well as minute extrusions, lip formations, and surface tearing. The details of the process of ridge formation, ridge flattening, extrusions and tear off of extrusions are explained in other papers[8,9].
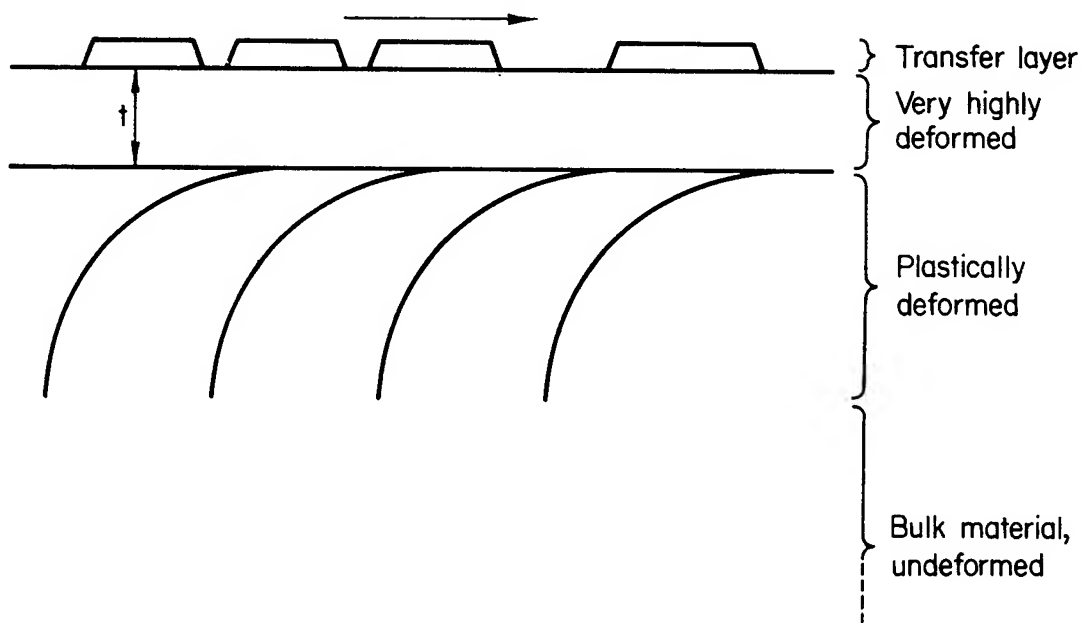

FIGURE 7.   LONGITUDINAL SECTION OF A WEAR SPECIMEN;
            THE CURVED LINES INDICATE STRAIN AND THE ARROW
            INDICATES THE SLIDING DIRECTION

225

However, it is clear that some wear debris can originate from micro extrusion and tearing. An example is shown in Figure 8. Another removal process involves micromachining and it occurs when a hard asperity traverses the surface with the correct cutting angle.

Asperity contact between moving surfaces produces localized deformation in the form of scratches, furrows, grooves, etc. The overall contact stress, if higher than the criterion for subsurface shear, results in a gradient of strain seen in elongated and bent over subsurface grains. In the scratch zone however, extreme deformation takes place as ridges are produced, ironed out and produced again. This process varies with materials and with the frequency of sliding contact. Some of the microgrooves and surface tearing can be associated with asperity welding. This action is difficult to diagnose since most of the features (long scratches) appear to be caused by asperity plowing. The act of asperity welding and shear-off occurs less frequently than the plowing and therefore is difficult to observe. An example of both processes is shown in Figure 9. An iron pin has been in sliding contact with a copper-nickel flat. The iron welded to the copper nickel at an asperity contact and the localized deformation produced a permanent abberation which caused the plowing mark following the welding event.
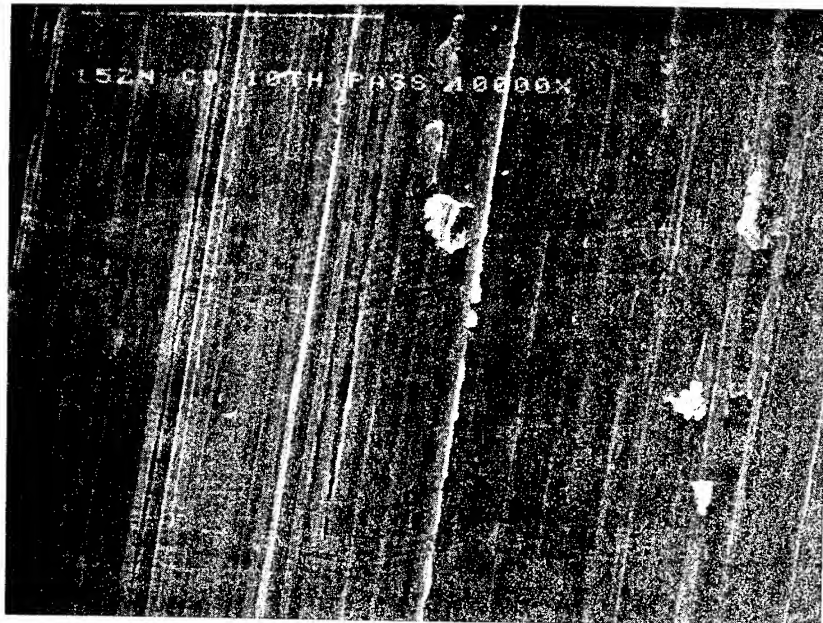
300X

FIGURE 8.   SEM MICROGRAPH OF WEAR SCAR ON COPPER SURFACE SHOWING
            FLATTENING OF PLOWED RIDGES, EXTRUSION AND TEARING

226
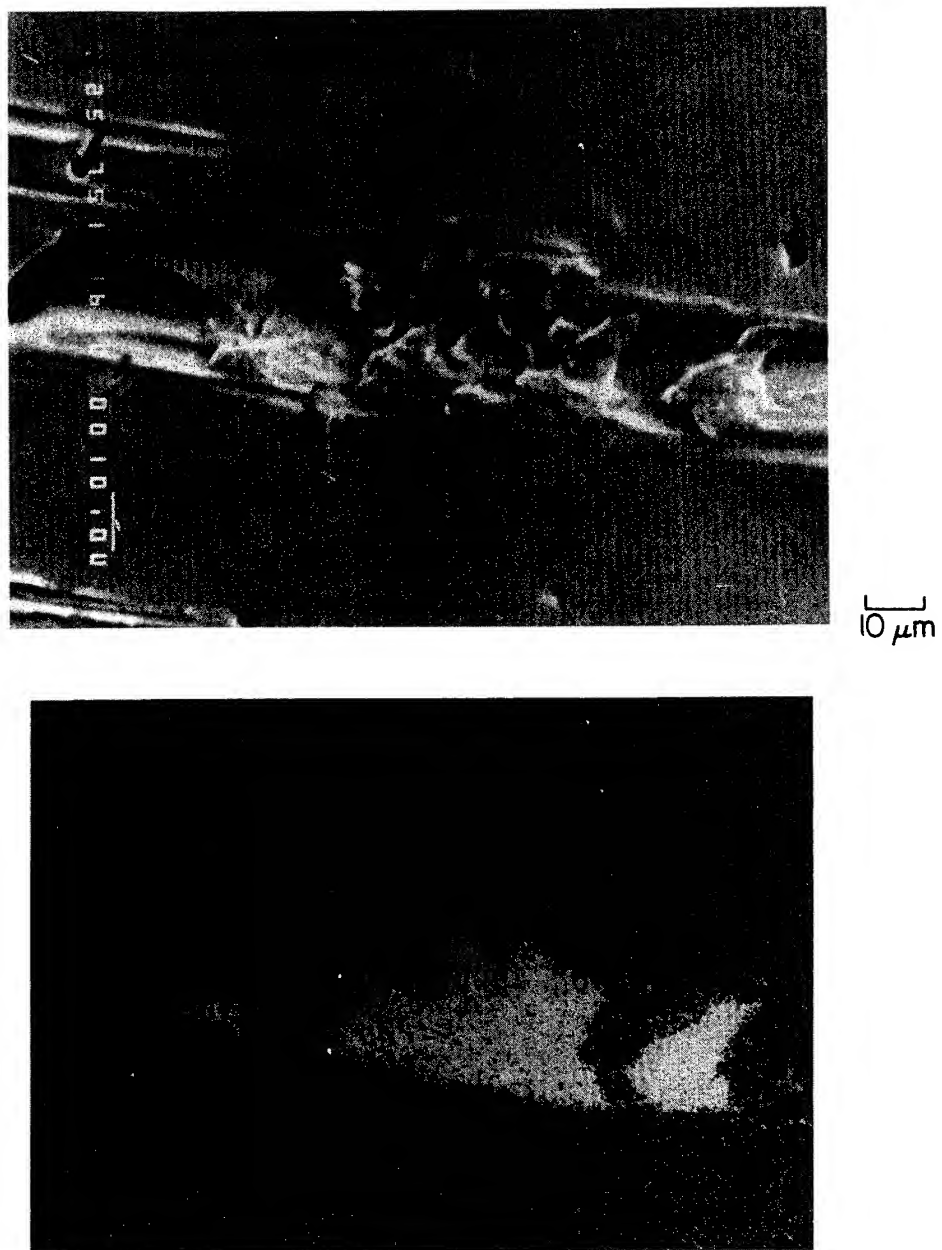
FIGURE 9. PLOWING DAMAGE ON A NI-CU ALLOY SURFACE CAUSED BY ADHESION
AND TRANSFER OF IRON FROM AN IRON PIN (From Chen, The Ohio
State University)

This process has been analyzed by Landheer and Zatt[10]. Further passes over the origin of the mark flattened out the weld point but did not obliterate it. However, in the flattening process the lump of material can be seen to fragment as shown in Figure 10.

227
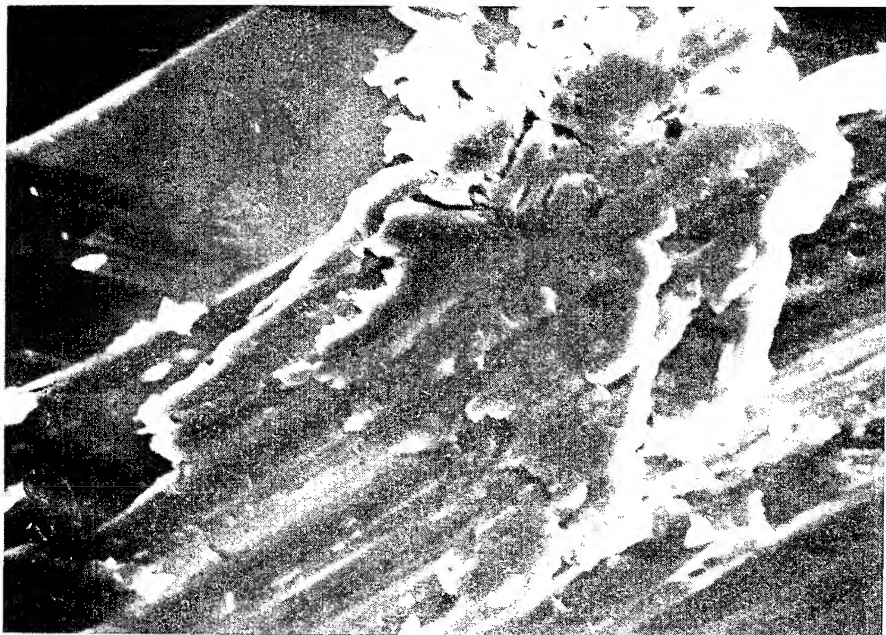
1000X

10 μm

FIGURE 10.   SEM MICROGRAPH OF LOCALIZED TRANSFER IN THE PROCESS
OF FRAGMENTATION AFTER SEVERAL SLIDING CONTACTS

When a wear scar is sectioned, the directionality of the topography has
a significant influence on what is perceived in the section. If the section is in
the direction of sliding (as many are to bring out the elongation and bending of
grain boundaries) one can cut along the bottom of a groove, along a ridge, or in
and out of both. Deformation is likely to be much more concentrated in the ridge
section, and the probability of hitting an adhesion initiaton is very low. In
addition, the type of deformation in an adhesion generated furrow (or sheared off
prow) should be more chaotic than in an adjacent scratch caused by plowing or
micromachining. Sections made crosswise and lengthwise probably define the near
surface wear microstructure more accurately. Examples of this approach will be
shown.

A large body of TEM micrographs made of thin foil sections from wear
scars is developing together with excellect definition of structural phases and
orientation of structural elements. Soon we should begin to develop wear micro-
structural characteristics for classes of materials, and perhaps for generating
conditions such as shear rate and temperature.

228

Examples of the microstructures analyzed are shown in Figures 11, 12 and 13. In Figure 11, a section was made parallel with the sliding direction in a copper specimen. It demonstrates the three zones: grain deformation, high strain (cells), and transfer layer. Note how the grains elongate and bend over in the direction of sliding. The strain can be estimated from the amount of grain boundary rotation. Grain structure gives way to a cell structure first with large cells and diffuse boundaries with little mismatch in orientation from cell to cell, then, closer to the surface, smaller cells and much sharper cell boundaries. In the sharp cell boundary region, greater misorientation is found. This is expected as the strain level increases. The highest strain then is found just under the surface - possibly in a ridge zone where considerable latteral flow has occurred. Cell size near the surface is very small - often on the order of several hundred angstroms. The transfer layer can be seen with a sharply defined boundary line between it and the substrate. There is no indication of diffusion bonding. The structure of the transfer layer in this case appears to be very small particles, some as small as 100 Å. The composition for this type of transfer obtained with a steel ring sliding unlubricated on a copper block is copper, iron, and copper oxide. In addition, the iron appears in layers sandwiched between copper layers. Auger analysis of such transfer layers also reveals layers as the structure is sputtered off.

Figure 12 shows a section made transverse to the sliding direction. This is from recent work done by Don[11] in which he shows that in materials with a substrate that does not work harden rapidly the transfer material often imbeds in the surface, filling grooves (and perhaps producing grooves). Materials with hard substrates produce a transfer layer which sits on top of the surface and does not imbed.

Under lubricated conditions, transfer still occurs, but is much less in amount. This is shown in Figure 13, a section through a copper-aluminum alloy which had been run against a steel ring with stearic acid - octadecane lubricant[12]. The transfer materials in Figure 13 can barely be detected because the layer is so thin, however, its structure is very similar to the transfer in Figures 11 and 12, being composed of very small particles. Void space between particles is larger in the lubricated condition presumably because of lubricant reaction product (metal soap) associated with the particles.

5 μm

FIGURE 11. TRANSMISSION ELECTRON MICROGRAPH OF A FOIL MADE
OF A SECTION THROUGH A WEAR SCAR ON COPPER.
SUBSTRATE CELL ZONE AND TRANSFER LAYER ARE SHOWN
(From Heilmann and Rigney)[3]

50 μm
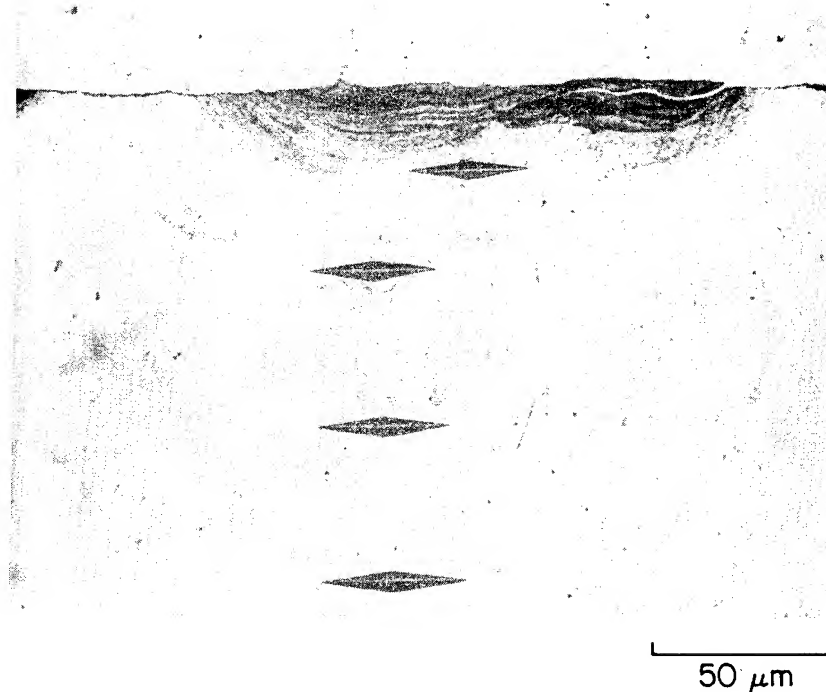
FIGURE 12. METALLOGRAPHIC SECTION THROUGH A COPPER-BERILLIUM ALLOY
TRANSVERSE TO THE SLIDING DIRECTION SHOWING PENETRATION
OF HARD TRANSFER MATERIALS (From Don[11])

230

1 μm

FIGURE 13.   TEM MICROGRAPH OF A FOIL MADE FROM A SECTION THROUGH A
WEAR SCAR ON COPPER-ALUMINUM SUBJECTED TO WEAR UNDER
LUBRICATED CONDITIONS

The structure of the transfer layer seems to make sense when one
examines the wear debris from the same experiments. Debris separated from the
lubricant in lubricated experiments is composed of very small metal particles
(100-500 $\overset{\circ}{A}$ diameter) imbedded in a gel or metal soap. Larger flakes are also
found. A detailed description of debris from lubricated wear experiments will be
found in other papers[13]. Debris from dry wear experiments is found to be
chiefly flake-like. Sectioning of these flakes show them to be composed of very
small particles - the same structure as found in the transfer layer. An example
is shown in Figure 14[14].

It appears that the transfer layers shown in the above examples are
compacted wear debris. Very small particles, submicron in size, are dragged into
the contact region and compressed and possibly sintered together in a continous
layer. This transfer is often layered, containing alternating compositions of
counter surface and substrate material. It is assumed that the larger flakes come
from detachment of transfer layers by fracture at the contact boundary with the
substrate.

231

CONCLUSIONS

Studies of the microstructures associated with wear show that the strain rates can be very high owing to the small volume being strained. The microstructures are similar in morphology to large strain microstructures developed in metal working. The magnitude of the strains involved are probably greater than 10 (a value associated with hydrostatic extrusion). Wear microstructures have their own characteristic in that the large strain or cell zone is highly localized at the surface and very often there is a patchy transfer layer of very fine particle structure on the surface. The structures produced in the wear process should be subject to the same controlling parameters as found in metal working[15]. Workhardening rates would be expected to be influenced by crystal habits, temperature, and precipitates and hard phases present in the alloy. It has been shown that copper base alloys develop a well defined cell structure in near surface regions in the wear affected zone. Since the work hardening rates of copper-tin and copper-zinc alloys are much higher than for pure copper, one would expect this sensitivity to strain rate to cause suppression of cell formation. Twinning might be more likely. This has not been found as yet. Instead, increasing strain
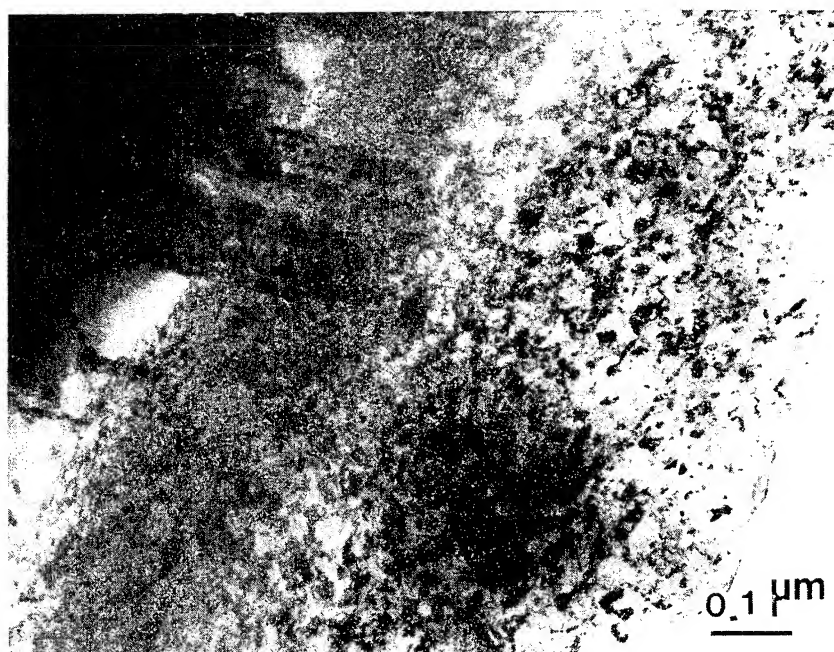

FIGURE 14. TEM MICROGRAPH OF LARGE DEBRIS FLAKE FROM
DRY WEAR EXPERIMENT. MATERIAL IS Al_2O_3
DISPERSION HARDENED COPPER

232

(assumed to be a factor of the closeness to the surface) produces sharper cell walls with greater misorientation between the cells. It is interesting that the workhardening rate for pure iron when cell formation is taking place is almost the same as the hardening rate of their alloys which tend to develop no cells or just rudimentary cells[15]. It appears that the local state of stress developed in rubbing contact is such that cell structures are favored. Since low temperature and low stacking fault energy (SFE) tend to suppress cell formation, these factors might be investigated. Low SFE, so far, has not appeared to influence this microstructural effect. The author knows of no attempts to evaluate the effect of low temperature as yet.

Studies of large strain structures formed during metal working shows that one should expect the following sequence as strain accumulates:

- Rapid rise in dislocation density
- Dislocation tangles develop into rough 3 dimensional cell structure
- At a strain of about 10 percent a well defined cell structure has developed
- With further strain accumulation cell size decreases, cell walls sharpen and misorientation between cells increases
- Finally cell wall annihilation can occur and formation of subgrains
- For materials with low SFE, twinning on all slipplanes develops with fracture developing at twin intersections.

One can conclude from the work of Heilmann[3,7] that much of this process does occur during wear and that the change in microstructure as one proceeds toward the surface reflects an increase in accumulated strain. The maximum occurs just at the surface. Subgrain development or extensive twinning have not been found as yet in microstructures associated with wear. (Some twinning has been found at depths where strains are not as great as in the cell region.)

The effect of strain rate has not been investigated as yet. Even in metal working studies, little is known about strain rate effects. It is suspected that high strain rates will decrease the work hardening rate in metal alloys. The same is true for increased temperature. Strain rate in wear deformation processes is very difficult to measure or even estimate. In addition, frictional heating can complicate the process. This is an area, however, that should provide interesting research opportunities.

Wear microstructures not only include part of the near surface morphology caused by contact stress but also include transfer layers. The "transfer layers" are an important part of the wear process and their structure provides some clues as to the origin of wear debris. Aside from the relative large particles torn from lips and extrusion in the surface ridges of ductile materials, there are collections of very fine particles (some as small as 50 angstroms) layered into the surface. These particles are usually a mixture of materials from both sliding surfaces and appear to be sintered into continuous layers. These layers can debond and come off as flakes. The analysis of wear debris has revealed flakes made up of individual particles. Recent studies at Ohio State University and Battelle have shown that adhesive transfer from one surface to another occurs in early stages of wear and that the particulate layers come after loose wear debris has begun to accumulate and is swept through the contact zone. High resolution scanning auger analyses of surface features on both dry and lubricated copper-aluminum alloy sliding against steel have shown iron-copper-aluminum in the zones recognized as transfer layers while a little iron has shown up at scattered sites in wear grooves after dry sliding. Much greater concentrations have been found at transfer overlayers covering wear grooves. In the case of lubricated wear, iron has been associated only with zones containing carbon and oxygen, remnants of the lubricant. This seems to correlate with observations of wear debris extracted from lubricant. The wear debris in this case is usually imbedded in organic reaction products (gels or soaps).

The study of near surface and debris microstructure associated with wear is difficult and at times tedious. That makes progress very slow. However, the amount of this type of research is on the increase and techniques are being refined and improved. In the future, we should expect the results of this work to provide new insights into the mechanisms of wear debris formation.

REFERENCES

(1)   Report title unknown. Authors were R. W. Dayton and C. M. Allen, Battelle
       Columbus Laboratories (Now retired).

(2)   Ruff, A. W., Ives, L. K., and Glaeser, W. A., "Characterization of Wear
       Surfaces and Wear Debris", Fundamentals of Friction and Wear of Materials,
       1980 ASM Materials Seminar, D. A. Rigney, Editor, pp 235-289.

(3)   Heilmann, P. and Rigney, D., "Running-in Processes Affecting Friction and
       Wear", Leeds-Lyon Conference Proc., September 1981, Edit. Grodet and Dowson.

(4)   Ohmae, N., "Transmission Electron Microscope Study of the Inter-Relationship
       Between Friction and Deformation of Copper Cyrstals", Fundamentals of
       Tribology Proceedings, MIT, June 1978, pp 201-222.

(5)   Blau, P. J., "Observations on the Wear-in Process During the Sliding of
       Several Copper Alloys Against 52100 Steel", Proceedings, Wear of Materials
       Conference (ASME), 1981, pp 69-74.

(6)   Goreger, J. H., Wayne, S. F., Nowatny, H., Rice, S. L., "Wear of Copper
       Alloys Under Repetitive Impact Sliding", Materials Science & Engineering, 49
       (1981) pp 249-255.

(7)   Heilmann, P., Clark, W.A.T., Rigney, D. A., "Orientation Determination of
       Subsurface Cells Generated by Sliding".

(8)   Glaeser, W. A., "Wear Experiments in the Scanning Electron Microscope",
       Wear, 1981, pp 371-386.

(9)   Zum Gar, R. H., "Abrasive Wear on Metallic Materials", Metallurgical Aspects
       of Wear, 1981 DGM, (Germany), pp 73-104.

(10)   Lundheer, D. and Zatt, J. H., "The Mechanism of Metal Transfer in Sliding
       Friction", Wear, 27 (1974), 129-145.

(11)   Don, J., "Unlubricated Friction and Wear in the Cu-Be System", Thesis for
       Doctor of Philosophy, Ohio State University, 1982.

(12)   Glaeser, W. A., - unpublished data.

(13)   Glaeser, W. A., "The Nature of Wear of Debris Generated During Lubricated
       Wear-in" ASME-ASLE Lube Conference 1982 preprint # 82-LC-3B-1.

(14)   Sun, T. C., "Unlubricated Friction and Wear in Dispersion Hardened Systems",
       Thesis for Doctor of Philosophy, The Ohio State University, 1983.

(15)   Sevillano, L. G., Van Houtte, P., and Aernoudt, E., "Large Strain Work
       Hardening and Textures", Progress in Materials Science, Pergamon, 1981, Vol.
       25.

DISCUSSION

I. M. Hutchings
University of Cambridge
Cambridge, England

This paper provides a welcome survey of some recent metallographic studies of wear (1). In this discussion I should like to focus on two aspects of the work reported in the paper.

First, I would like to comment on the microstructures illustrated in Figures 3 and 4, and draw a parallel between those and the structures found after erosion by solid particle impact under certain conditions. Figures 3 and 4 show extensive plastic flow in the material close to the worn surface, and the formation of a laminar structure caused by material folding over on to the surface and being pressed out into sheets. Similar structures have been found in impact wear experiments carried out under laboratory conditions (2-4). In these cases, thin plate-like wear debris was also formed. I should like to point out the similarity of this type of deformation pattern to that generated in normal impact erosion by very small spherical particles. Under these conditions, where the individual impacting particles may be 100 μm or so in diameter and the impact velocity of the order of 100 ms^{-1}, very similar subsurface regions have been identified in several different metals (5-7); in these cases also, the wear debris is flake-like. It is suggested in the present paper that this subsurface structure, and the exploitation of the surface layers, is enhanced by the presence of inclusions in the steel. It is worth pointing out that in the case of the similar structures arising in erosion, pre-existing inclusions in the metal do not seem to be necessary. There is ample evidence (7) that fragments from the impacting particles (even if only a very small number fracture on impact), or surface oxide from the particles (e.g. iron oxide from steel shot), or even oxide from the eroded surface itself, become incorporated into the surface layers, inhibit rewelding of the material after it has been raised up by a nearby impact and battered down on to the surface again, and thereby contribute markedly to the development of the lamellar subsurface structure. A similar role has been suggested for surface oxide in the impact wear of copper (4), and it seems possible that the mechanical incorporation of oxide into the surface plays an important part in the development of the structures shown in Figures 3 and 4.

The second point to which I would like to refer briefly concerns the strain rates obtaining under sliding wear conditions. As the author points out, the strain rates in sliding wear are difficult to estimate, and little attention has been paid to the possible influences of strain rate on deformation mode. Since there is always a strain gradient associated with sliding wear, measurements of which have been well reviewed in reference 8, strain rate will in any case not be a uniquely-defined quantity; it should be possible, however, to make some estimates of the relevant quantities. Attempts have been made to examine strain rate effects in two-body abrasive wear, the strain rate being estimated by analogy with machining (9); estimates of strain rate have also been made for erosion by solid particle impact (10). Further study of the effects of strain rate in the response of materials to all these types of wear will probably be profitable, although it is sometimes difficult to separate the effects of strain rate from those of local temperature rise, which at high sliding speeds may have a dominant effect (e.g. in the sliding wear of brass, 11).

REFERENCES

1. Readers may also find relevant some of the papers on the microscopy of wear presented at the session on Erosion and Wear at MICRO 82, London, 1982, to be published in Journal of Microscopy, 1983.

2. K. Wellinger and H. Breckel, Wear 13, (1969), 257-281.

3. S.L. Rice, H. Nowotny and S.F. Wayne, Wear 74, (1981), 131-142.

4. E.B. Iturbe, I.G. Greenfield and T.W. Chou, Wear 74, (1981), 123-129.

5. R. Brown and J.W. Edington, Wear 72, (1981), 377-381.

6. R. Brown, E.J. Jun and J.W. Edington, Wear 70, (1981), 347-363.

7. A.K. Cousens and I.M. Hutchings, in Wear of Materials 1983, 382-389, A.S.M.E., New York, 1983.

8. D. Kuhlmann-Wilsdorf, in Fundamentals of Friction and Wear of Materials, ed. D.A. Rigney, 119-186, A.S.M., 1980.

9. J. Larsen-Basse and P.A. Tanouye, Wear of Materials 1977, 194-198, A.S.M.E., New York, 1977.

10. I.M. Hutchings, J. Phys. Appl. Phys. 10, (1977), L179-184.

11. W. Hirst and J.K. Lancaster, Proc. Roy. Soc. Lond. A 259, (1961), 228-241.

DISCUSSION

Kohji Kato
Tohoku University
Sendai, Japan

Dr. Glaeser made an important and new analysis for the microstructures associated with wear. In relation to his viewpoint, I would like to make some comments and questions.

Although we can observe many types of wear debris some of wich are composed of homogeneous bulk material and others of various fine particles, flake-like wear debris may be one of the most popular and principal type.

Such flake-like wear debris might some times be formed by the mechanism of slip-tongue [1] which is controlled by the accumulated plastic flow and adhesive fracture and seems to be the same as the extrusion in his expression.

The flake-like wear debris of this type is composed of homogeneous bulk material, and it will drop out immediately from the interface in some cases, but in another cases it will remain at the interface and be crushed to fine particles in the process of successive sliding. Crushed fine particles will repeat transfer and back transfer and will form the transfer layers.

But if we consider the fine cell structure formed at the surface on the other hand, the each cell might be expected as the unit of adhesive transfer to form the transfer layer.

So, I would like to ask whether the extrusion could be expected to form the flake-like wear debris in the same manner as that of slip-tongue or not and what would be expected as the origin of the fine particle size in the transfer layer.

[1] T. Kayaba and K. Kato;"The Adhesive Transfer of the Slip-Tongue and the Wedge", ASLE Transactions, Vol. 24, 2, (1981), pp 164 - 174.

DISCUSSION

Jorn Larsen-Basse
University of Hawaii
Honolulu, Hawaii

The ultimate goal of wear research is to develop sufficient understanding of the mechanisms of material removal so that wear performance can be predicted from three sets of information:

(1) The microstructure of the materials involved
(2) The properties of the materials as determined by simple standard tests
(3) Some parameters which define the tribological system

In order to move towards this understanding it is most certainly necessary to study the microstructure formed due to wear - in the worn surface, in the subsurface regions, and in the wear debris.

Traditionally, instrument capabilities have limited the resolution that one could obtain of the very fine features associated with wear. Bill Glaeser has nicely illustrated the flurry of excitement and research activity which follows each new development in the instrumentation field - first and foremost the SEM which allowed us to see worn surfaces and, recently, high resolution TEM which has allowed us to resolve some of the very fine microstructures that form immediately below worn surfaces. Undoubtedly, future advances will allow us to see even finer detail and change our views of many wear processes.

My own interests in the wear area are focussed on abrasion and abrasive wear. In that field the immediately needs are probably less for high resolution than for a systematic, broad approach. The remainder of my remarks will address that issue.

ABRASIVE WEAR

It is generally accepted that abrasion of ductile metals by hard abrasives takes place by cutting of chips and extrusion of material to the sides of the grooves. We are beginning to understand for the simplest cases why and how the amounts of material which partition into chip, groove ridge, and general surface flow depend on basic material properties and the shape of the abrasive (refs. 1 and 2). The models need considerable refinement and correlation with the properties of real abraded surfaces.

The chip forms by a plastic deformation process which involves shear strains of 400-650 percent as estimated from wear test data and a suitable model (refs. 3 and 4). The resistance to abrasion can be represented by the area under the true stress - true strain curve up to that strain. The rate of straining appears to have a modest effect on abrasion resistance (ref. 4) as it does on the stress-strain curve. However, at this stage too little is known about the behavior of materials at the very high strains and strain rates encountered in abrasion to allow even semiquantitative correlations to be drawn between abrasion resistance and stress-strain - strain rate properties.

During the metal removal process the immediate surface sample is heavily deformed. The maximum strains probably reach 400-600 percent, similar to the values estimated for metal-metal wear (ref. 5). Judging from some recent wear

data (ref. 6) it would appear that the thickness of the heavily deformed layer depends strongly on the applied load and the method of force transmission between the grit and the surface. The layer apparently may become quite thick in highly stressed 3-body abrasion. Below the surface layer the strain is 25-35 percent and drops to zero at some depth below the surface. A cutting grit may penetrate deeply enough to see an average strain of around 25 percent, as has been estimated for simple 2-body abrasion of copper (ref. 7), or it may possibly see mainly the heavily deformed layer; and then the effects of original bulk hardness on wear rate will have disappeared, as in some recently reported results for very high stress abrasion (ref. 6).

As the complexity of the abrading alloy increases so does the complexity of the deformation behavior while, at the same time, our knowledge of the wear performance and the effect of microstructure decreases. Finely distributed carbides or other hard particles may anchor the dislocation cell walls and thus affect work hardening and wear resistance (refs. 3 and 8) and possibly also wear debris formation. As the carbides increase in size and amount they begin to provide part of the contact path for the sliding abrasive, and then relative hardness, coherence with the matrix, brittleness, inter-particle distance, etc., become additional factors which must be taken into account. Near one end of the spectrum of compositions are located the cemented carbides which contain 85-95 percent of the hard phase. These alloys also abrade by groove formation due to gross plastic deformation (ref. 9). The total strain may be less than for ductile metals because of the low ductility – the "chip" fragments before it can take on the typical chip shape. The removed material consists of WC grain fragments and bits of smeared cobalt binder. Occasionally cobalt rich debris is found.

When cemented carbides are abraded by relatively soft abrasives, such as quartz, the deformation behavior changes drastically and the wear rate drops. Material is removed by gradual binder extrusion, followed by WC grain fragmentation. The binder extrusion starts at the first contact and continues gradually until the near-surface material has a basically lower binder content than the material below. As the binder is extruded the compressive stresses that it maintained in the carbide grains are relaxed and these grains begin to fragment in response to the repeated loading from the contacting abrasives. It was estimated that each contacting grain removed 1-2 Å of material (ref. 10). This obviously points to a contact fatigue or similar type of loading about which little is known.

The whole question of the role of fatigue, or repeated loading/strain accumulation, in abrasive wear is one which must be resolved. Kragelskii (ref. 11) has suggested that chips do not form in real abrasive situations but that material is removed only by fatigue of the material extruded to the groove sides. Other researchers (ref. 12) have found a relationship between wear rate and stacking fault energy which basically is opposite to the relationship one would expect if fatigue dominated as a wear mechanism. Nevertheless, much repeated loading and deformation does take place, and if the abrasives are not sharp or if they are softer than the metal then substantial fatigue cracks appear (ref. 13). Whether this cracking actually contributes to the wear is not known at this stage.

CONCLUSIONS

The above summary has illustrated how much remains to be done before we have a good understanding of the abrasion process and how much of this work must be in the form of carefully conducted study of microstructures. We need

to define the microstructures which develop in and around wear scars and in wear particles as a function of starting material and wear conditions. And we must compare these microstructures with microstructures formed due to fatigue and to high strain and high strain rate deformation.

And herein lies a challenge for the materials scientist/tribologist for the 80's.

REFERENCES

1. M. A. Moore and P. A. Swanson, "The Effect of Particle Shape on Abrasive Wear: A Comparison of Theory and Experiment," in Wear of Materials 1983, K. C. Ludema (ed.), ASME 1983, 1-11.
2. K. H. ZumGahr and D. Mewes, "Severity of Material Removal in Abrasive Wear of Ductile Metals," ibid, 130-139.
3. J. Larsen-Basse, "The Abrasion Resistance of Some Hardened and Tempered Steels," Trans. AIME 236 (1966), 1461-66.
4. J. Larsen-Basse and P. A. Tanouye, "Strain Rate Effects in Low Speed Two-Body Abrasion," J. Lub. Technol., 100 (1978), 181-184.
5. W. J. Salesky, R. M. Fisher, R. O., Ritchie and G. Thomas, "The Nature and Origin of Sliding Wear Debris from Steels," in Wear of Materials 1983, op.cit. (1), 434-445.
6. R. J. Dawson, J. E. Pritchard and R. A. Beland, "Silica Abrasion of Ferrous Castings," ibid, 97-106.
7. J. Larsen-Basse, "Abrasion Mechanisms-Delamination to Machining," in Fundamentals of Tribology, N. P. Suh and N. Saka (eds.), MIT Press 1980, 679-689.
8. J. Larsen-Basse, "Abrasion of Some S.A.P.-Type Alloys at Room Temperature," Wear 12 (1968), 357-368.
9. J. Larsen-Basse, C. M. Shishido and L. K. Salem, "Abrasion of Some Cemented Carbides by SiC Papers," in Advances in Hard Material Tool Technology, R. Komanduri (ed.), Carnegie-Melon University, 1976, 231-243.
10. J. Larsen-Basse and E. T. Koyanag, "Abrasion of WC-Co Alloys by Quartz," J. Lub. Technol., 101 (1979), 208-212.
11. I. V. Kragelskii and E. A. Marchenko, "Wear of Machine Components," J. Lub. Technol., 104 (1982), 1-7.
12. J. J. Wert, S. A. Singerman and S. G. Caldwell, "An X-ray Diffraction Study of the Effect of Stacking Fault Energy on the Wear Behavior of Cu-Al Alloys," (oral presentation at Wear 83), Wear (in press).
13. J. Larsen-Basse and B. Premaratne, "Effect of Relative Hardness on Transitions in Abrasive Wear Mechanisms," in Wear of Materials 1983, op. cit. (1), 161-166.

DISCUSSION

Tavashi Yamamoto
Tokyo University of Agriculture and Technology
Tokyo, Japan

This paper gives us an interesting viewpoint for investigating the wear mechanism of metal. The discussor agrees with the author's opinion that we must regard wear as a deformation process as well as a debris-produced-microfracture process. The discussor has presented a paper of wear mechanism in collaboration with Dr. D. H. Buckley, NASA Lewis Research Center (ref. 1). In our paper we pointed out that the wear theory based on adhesion, which is successful in explaining friction behaviors, does not yet offer a suitable mechanism of wear fragment formation. Proponents of the theory have a tendency to discuss it from an atomistic viewpoint. In most practical problems, however, contact occurs over a finite area larger than the atomic scale. Therefore, a good deal of knowledge is needed for larger areas as well as atomic size contact. It is necessary to establish the boundary conditions for the large-scale contact and to determine how the fundamental information obtained from the atomic scale can be applied. Such an investigation should assess the morphological behavior of the contact region. The discussor wanted to discuss the wear mechanism based on our experimental results (ref. 2).

Experiments were conducted with the rider specimen of Al_2O_3 loaded against the disk surface of 304 stainless steel in vacuums of 10^{-6} Pa and 5×10^{-4} Pa of chlorine gas using the apparatus shown in figure 1. As the disk was rotated, the rider scribed a circular sliding track on the flat surface of the disk. Then the surfaces were analyzed using the optical microscope and SEM. A typical portion of the sliding wear track after sliding some distance in a vacuum of 10^{-6} Pa is shown in figure 2. The height and depth of the surface profiles are indicated in the photographs as measures of the distance from the initial level of the disk surface. Two types of characteristic protuberances are observed on the sliding track. One is isolated as an island and the other is intermittently scattered on the track. Substantially similar results were observed in a 5×10^{-4} Pa chlorine gas environment as shown in figure 3. On all the disk surfaces, characteristic trapezoid-shaped or step-shaped protuberances are found during the initial stages of sliding contact. Slip marks are visible on most upper surfaces of the protuberances.

From these observations, we suggest the following mechanism for the formation of the step-shaped protuberances. When surface interaction occurs between disk and rider, the surface layer of the disk suffers shearing deformation by the tangential movement of the rider in the sliding process. There are many asperities of the rider so inclined as to engage each other across the interface in the sliding direction at early stages of the sliding process. Even when the contact changes into the metal-metal contact owing to material transfer to the aluminum oxide rider, the interface brought about in this manner is apt to be inclined in a similar way as is indicated by Cocks as shown in figure 4 (ref. 3). In either case, adhesion is developed preferentially in these areas because the normal component of the sliding force is superimposed in the areas. On the other hand, since the material involved in the adhesion process suffers plastic deformation, the material existing near the interface is generally work hardened. Furthermore, an interfacial adhesion bond, which

occurs in the contact zone is generally stronger than the cohesive bond in the cohesively weaker of the two materials. Based on those considerations, the shearing force necessary to separate the interface is usually larger than that of the material located below the interface. Therefore, the surface layer once adhering to the rider surface is sheared at a certain depth below the interface.

Real contact areas, incidentally, are generally scattered randomly in the apparent contact area. When an infinitesimal part of the surface layer deforms plastically within the real contact area, the deformation can not extend to infinity in the tangential direction but is concentrated to a limited area. In other words, the deformation must be compensated for by the elevation of the localized surface layer. Therefore, the volume of material involved in the contact behavior expands in both the tangential and vertical directions. These phenomena usually occur randomly in the apparent contact area, taking on different sizes and shapes. The rate of development in the vertical direction generally varies, depending on the area elevated. Therefore, elevated areas will be separated by the vertical movement caused by the elevation at other arears. This process is illustrated schematically in figure 5. The formation of characteristic modes of protuberances and slip marks observed on surfaces can be understood with the use of these mechanisms. The contact area where the specific contact stress exceeds a critical value will be pressed out and flattened on the "parent" surface by the rider during the sliding process. In this manner, the disk surface, initially smooth, will become rougher with repetitions of the process, and the surface layer with a plateau-shaped con-figuration (which is referred to later) will be formed in subsequent sliding processes.

Next, the separation process of the wear particles is discussed. The surface contour of the sliding track observed after some sliding repetitions is shown in figure 6. The nonsliding area and isolated protuberances are observed on the surface under both environments. The protuberances exist in the contacting regions of the sliding surfaces and do not exist in the unslid portion of the wear track. Results obtained under both conditions indicate that the surface layer is gradually torn off and the surface takes on a char-acteristic geometry. A typical topographical representation of a sliding track is illustrated as shown in figure 7. This is based on the top photograph of figure 7. The topography of the sliding track has indications that wear frag-ments are separated from the edge of surface plateau, that the grooves develop, and that the plateau becomes smaller. The formation process of characteristic configuration is explained as follows.

It is generally difficult for any particle of material to move out of the inside of the plateau as illustrated in figures 8(a) to (c) or from the lead-ing edge of the plateau. On the contrary, if the plateau is shaped as illus-trated in figures 8(d) and (e), particles in the surface layer can be taken off the edges of the plateau more easily than from inside the contact area. Therefore, these situations can be modeled as shown in figure 9. In all cases, no surface layer exists to oppose the detachment of particles. If the shape of the particle is assumed ideally to be a rectangular parallelepiped, the relationship among the shear strength of the interface between the rider and the surface, the shear strength at the depth h from the surface, and the average tensile strength of the surface layer are obtained from the simple balance of forces allowing the detachment of a particle from the corner of a plateau. For example, the required critical condition for the balance of forces can be described as follows:

$$\tau_0 ab > \sigma_t ah + \tau_h ab + \left(\frac{\tau_0 + \tau_h}{2}\right) bh \qquad (1)$$

$$\left[(\tau_0 - \tau_h)a - (\tau_0 + \tau_h)\frac{h}{2}\right] b > \sigma_t ah \qquad (2)$$

The left term must be positive to have a physical meaning. Then

$$(\tau_0 - \tau_h)a > (\tau_0 + \tau_h)\frac{h}{2} \qquad (3)$$

Again for equation (3) to have physical meaning,

$$\tau_0 > \tau_h \qquad (4)$$

Therefore, requirement (3) is reduced to

$$a > \left(\frac{\tau_0 + \tau_h}{\tau_0 - \tau_h}\right)\frac{h}{2} \qquad (5)$$

and requirement (1) is reduced to

$$b > \left[\frac{\sigma_t}{(\tau_0 - \tau_h)a - (\tau_0 + \tau_h)\frac{h}{2}}\right] ah \qquad (6)$$

where

τ_0 shear strength of interface between rider and surface layer
τ_h shear strength at depth h from surface
σ_t average tensile strength of surface layer

The same fundamental equation as (4) can be reduced from cases (b) and (c):

$$\tau_0 > \tau_h$$

This equation means that the shear strength between the initial rider and disk surface should be larger than the shear strength at the depth h from the surface. This characteristic phenomena is certified by Dr. D. H. Buckley and Dr. J. Ferrante. That is, the interfacial adhesion bond is generally stronger than the cohesive bond in the cohesively weaker of the two materials. In our example, the cohesive bond of the 304 stainless steel disk is weaker than that of the aluminum oxide rider. Taking into account the schematic geometry of figure 8, initial configurations should have a tendency to change gradually into a final stable profile that is more parallel with respect to the sliding direction as shown in figure 10. Observation results of the sliding surface

244

can be consistently explained based on our wear mechanism and models taking into account the deformation and fracture behavior.

REFERENCES

1. Yamamoto, T. and Buckley, D. H.: Wear Mechanism Based on Adhesion. NASA TP-2037.
2. Yamamoto, T. and Buckley, D. H.: Plastic Deformation at Surface During Unlubricated Sliding. NASA TP-2036.
3. Cocks, M.: Shearing of Junction Between Metal Surfaces. Wear, vol. 9, 1966, pp. 320-328.
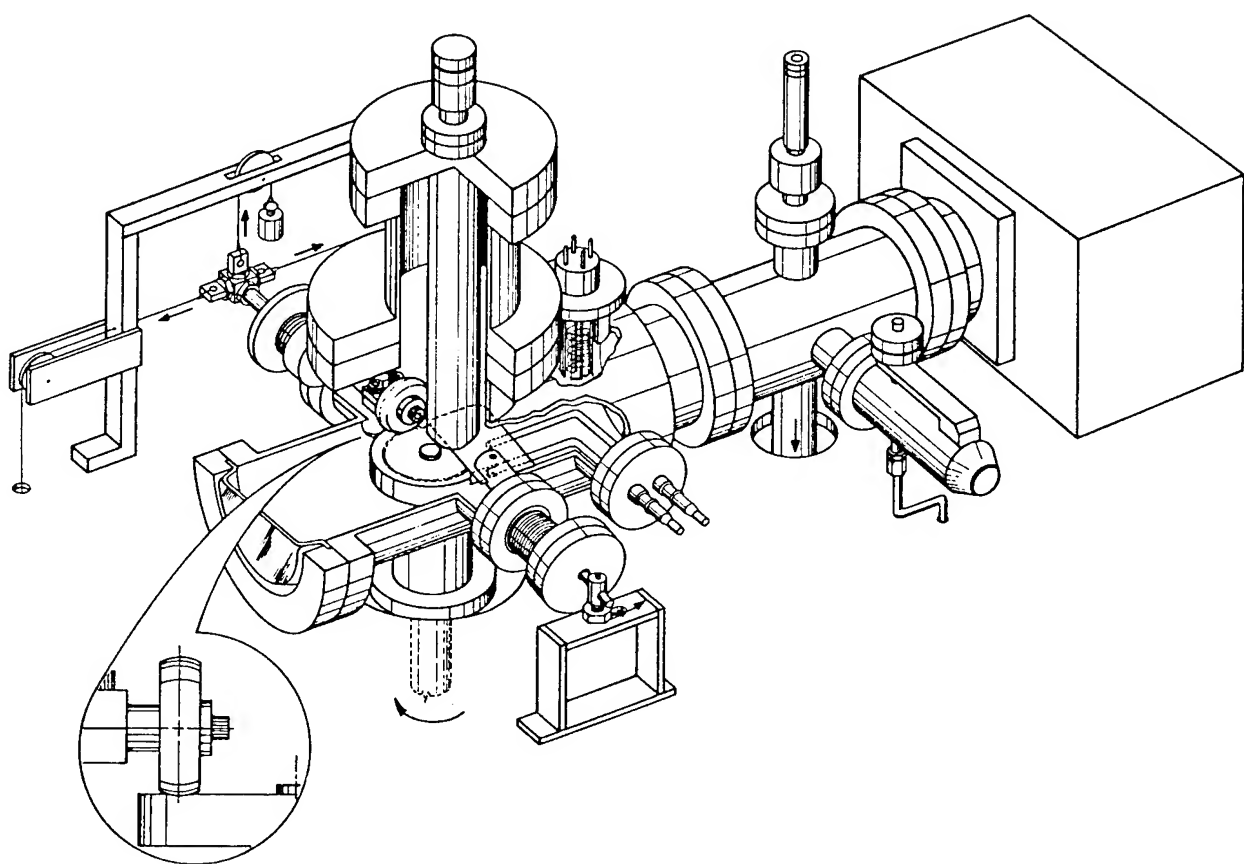
·CD-81-12631

Figure 1. - Sliding and rolling contact apparatus with Auger spectrometer.
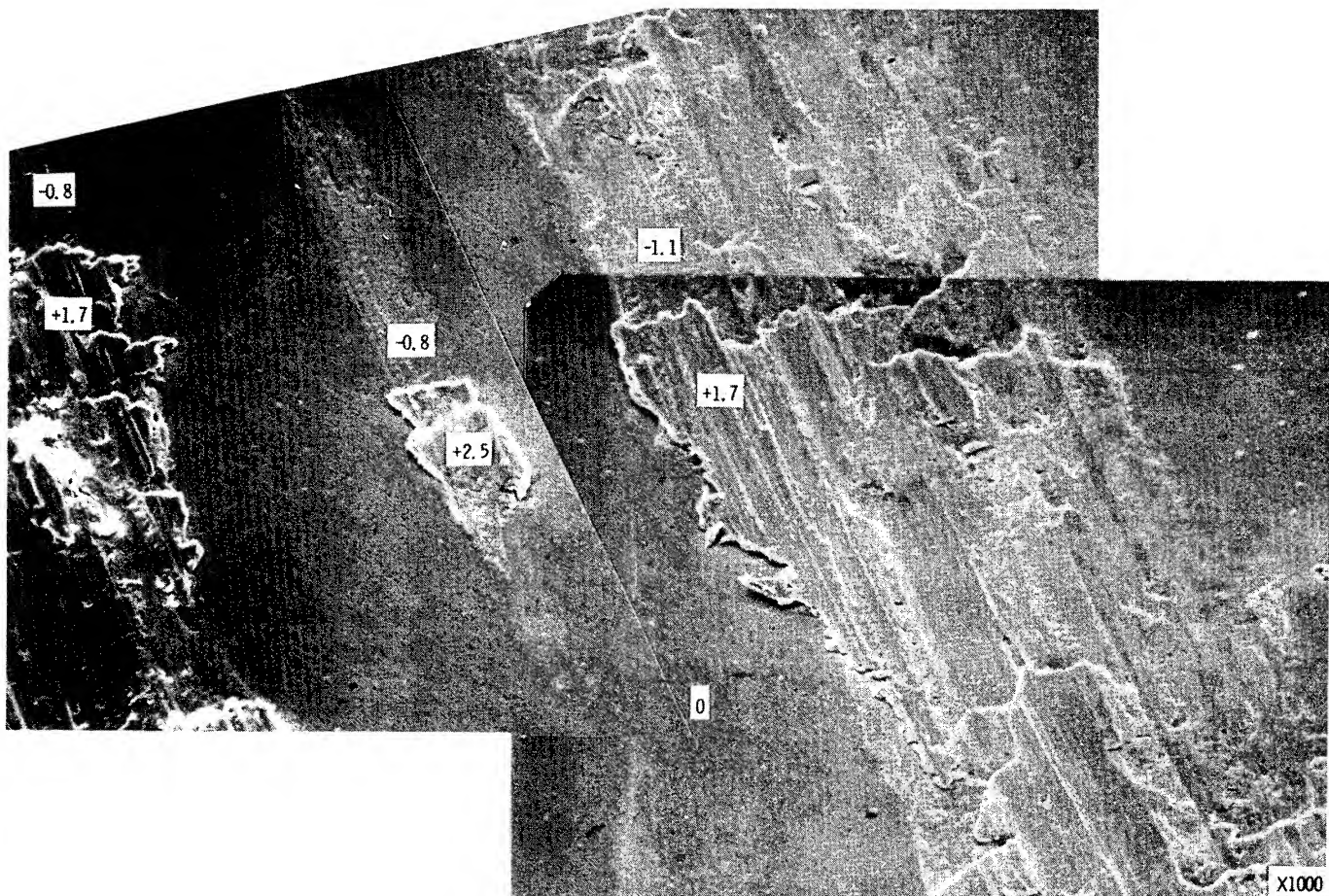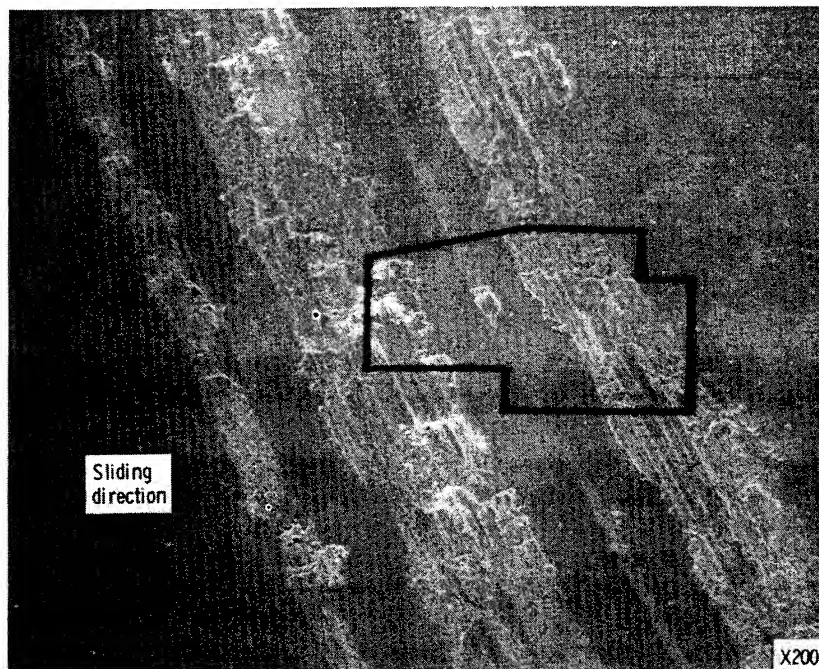
Figure 2. – Plastic deformation on disk surface (II). Later stage of one-pass sliding in 10^{-6}-Pa vacuum. Figures denote distance (in µm) from initial height of disk surface.
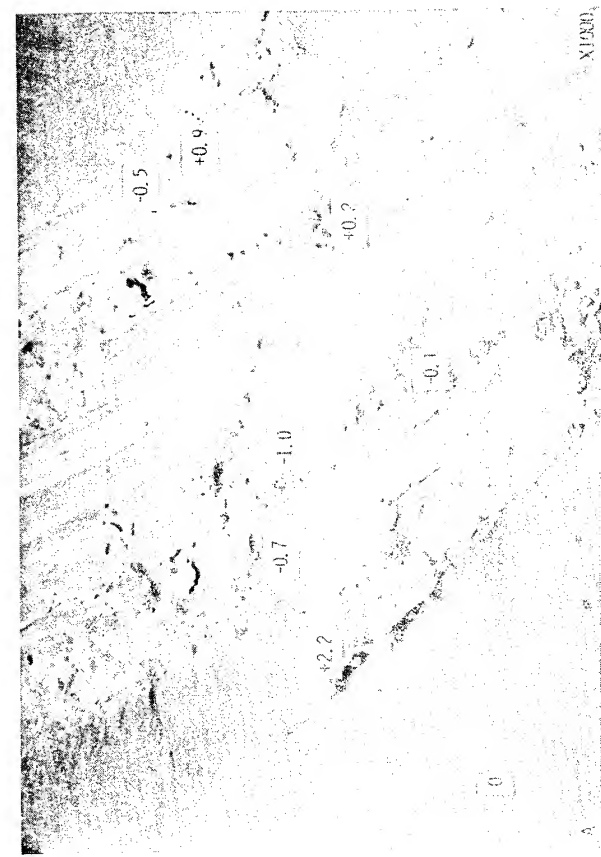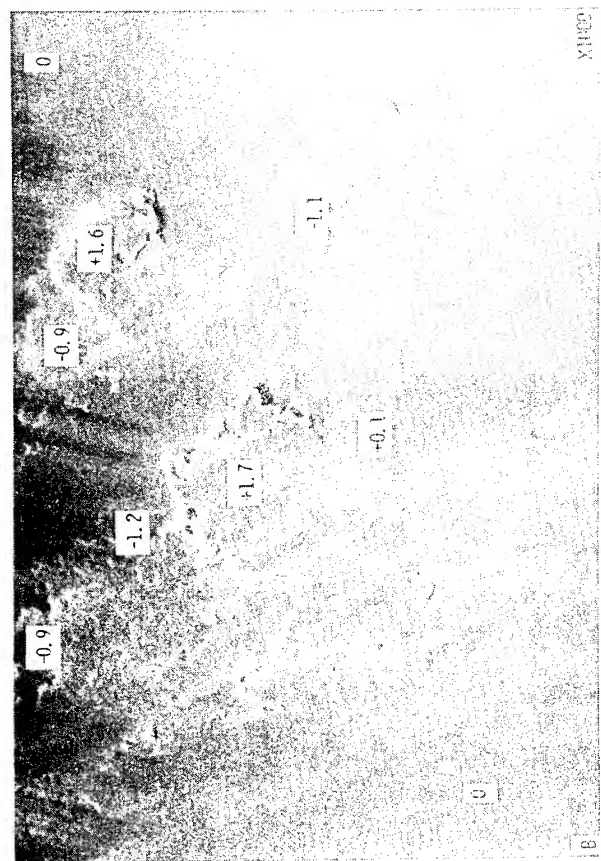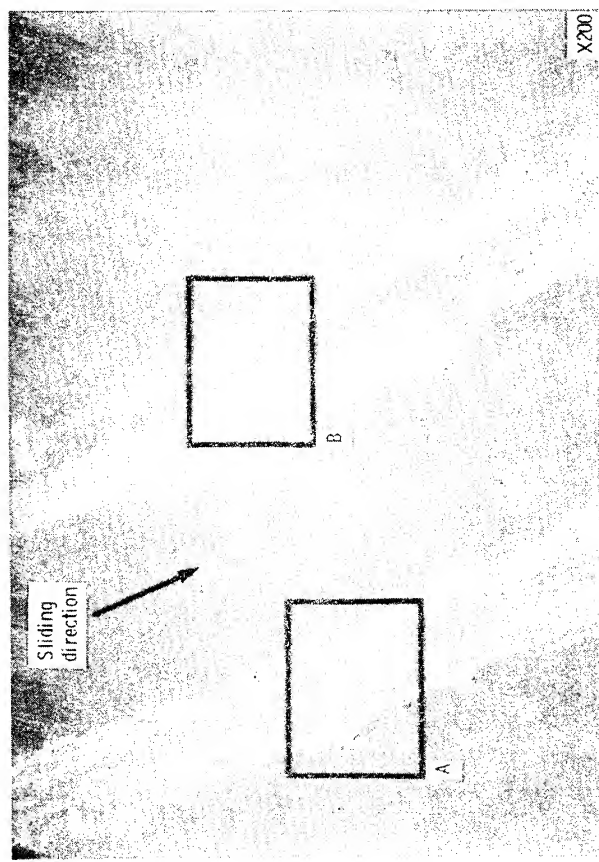
Figure 3. – Plastic deformation on disk surface (V). Later stage of one-pass liding in 5x10⁻⁴-Pa chlorine gas. Figures denote distance (in μm) from initial height of disk surface.

248

(a) Configuration of interface after a very
short sliding distance.
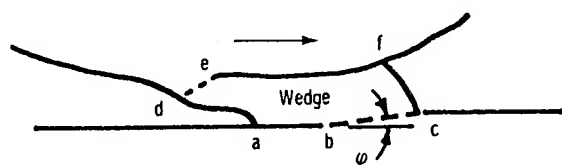
(b) Wedge formed between contacting surfaces during subsequent
sliding.

Figure 4. - Wedge formation between contact surfaces by Cocks

(1) - (2) Accumulation process
(3) - (4) Separation process
(4) - (5) Accumulation process
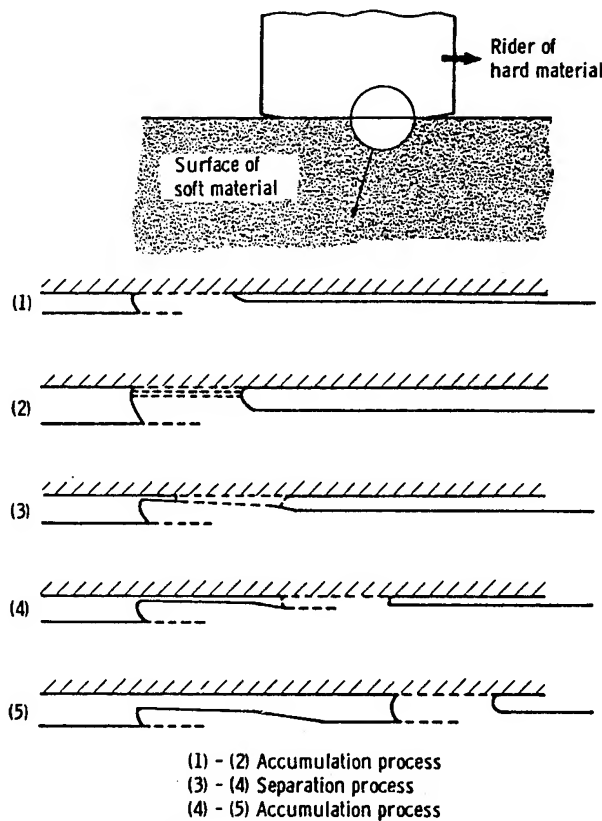
Figure 5 - Formation process of protuberance.

249

(SEM)

(a) 10^{-6}-Pa vacuum.

(b) 5×10^{-4}-Pa chlorine gas.
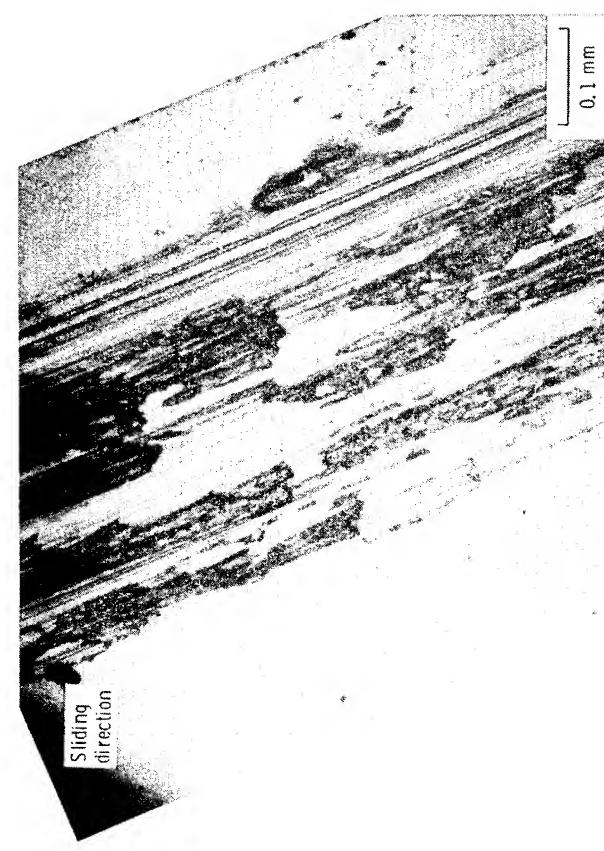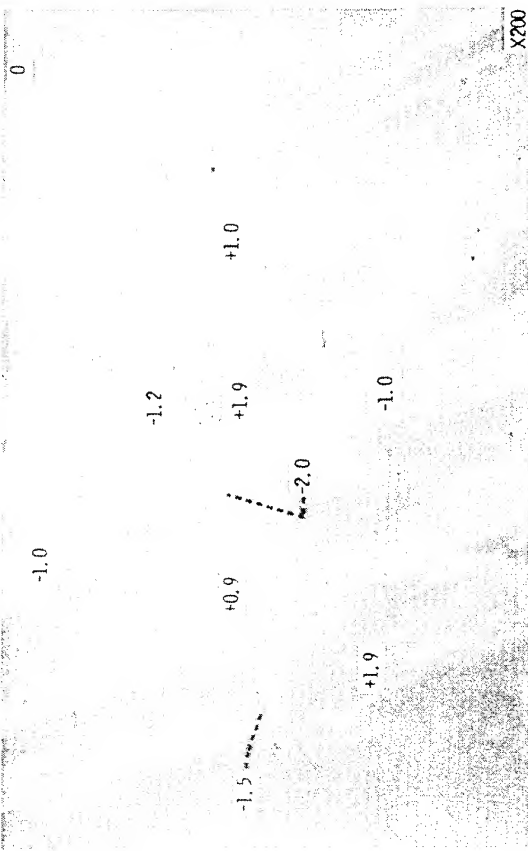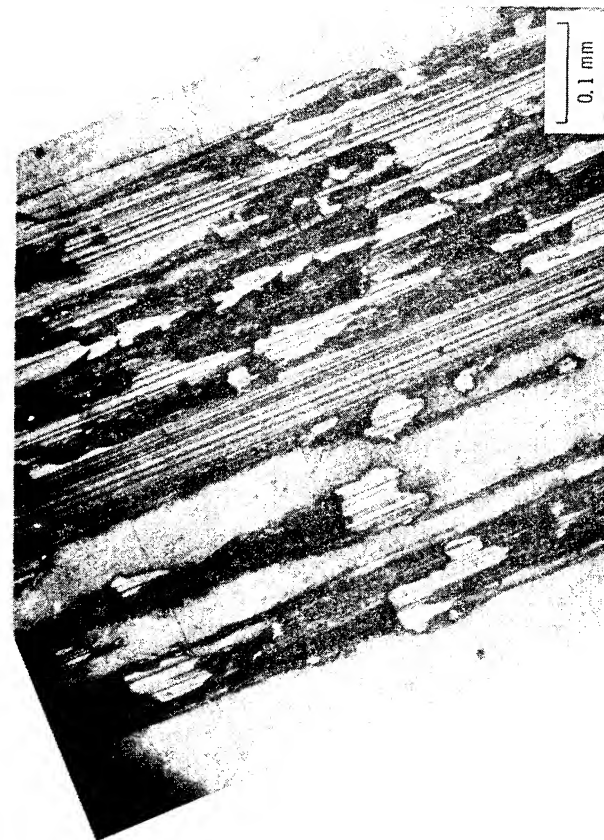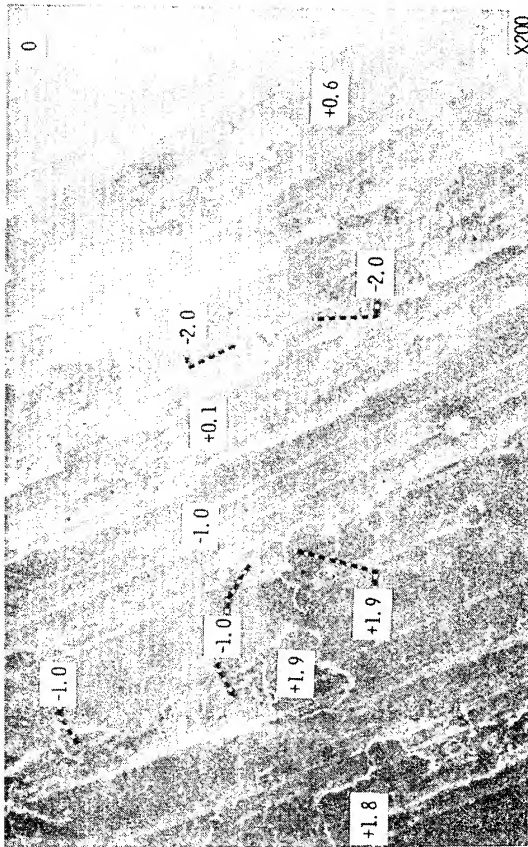
Figure 6. – Comparison of sliding tracks on disk surfaces after 50 passes. Figures denote distance (in μm) from initial height of disk surface.
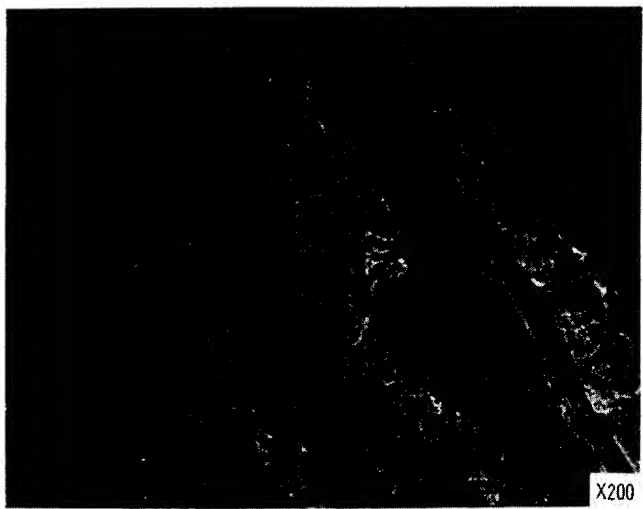
(a) Typical sliding track.
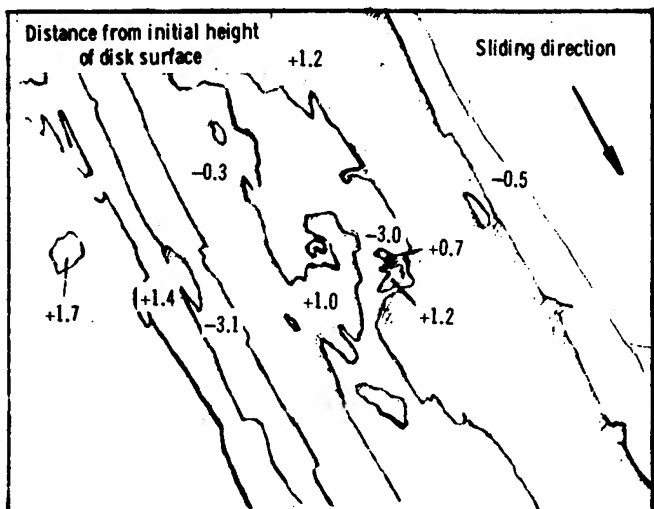
(b) Topographical representation of sliding track.

Figure 7. - Typical contour of sliding track.

(a) - (c) Contours where lumps are not easily removed.

(d), (e) Contours where lumps are easily removed.
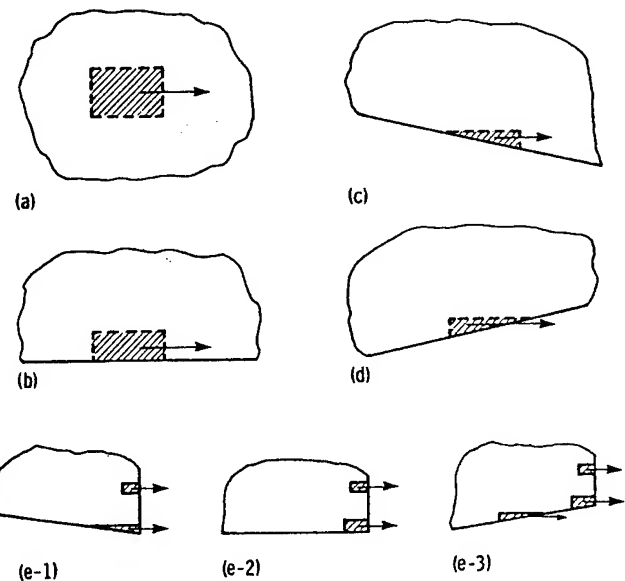
Figure 8 - Illustrations of various contours on sliding track, where particles are removed from the surface layer.

(a) Detachment from corner of plateau.

(b) Detachment from trailing edge of strip-shaped plateau.

(c) Detachment from trailing-edge inside plateau.
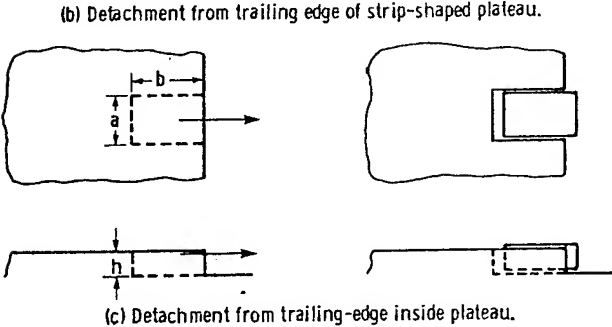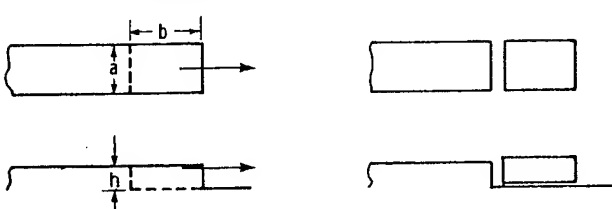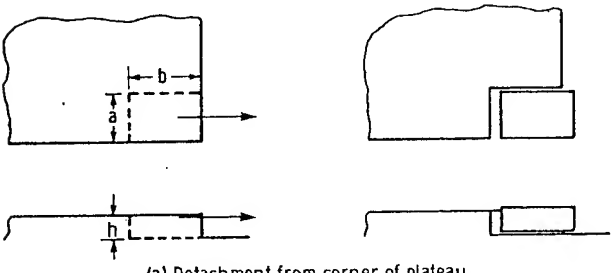
Figure 9 - Three models for detachment of particles from a plateau.
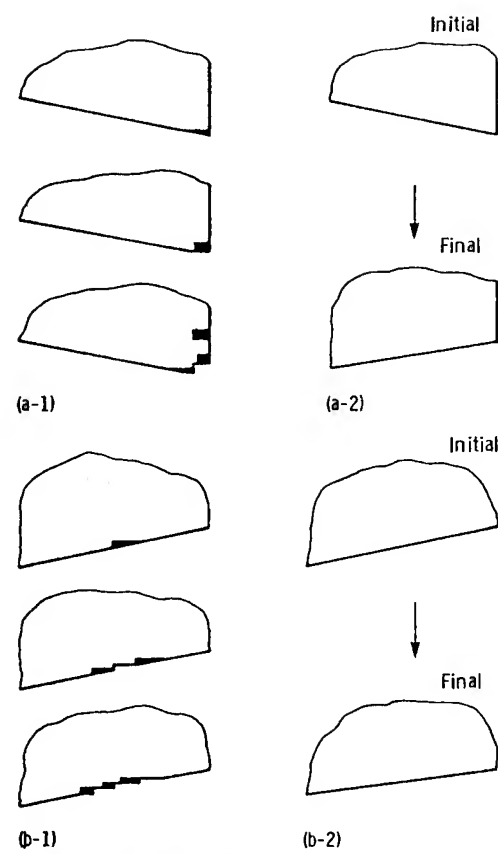
Figure 10 Two types of transformation of initial contours into stable ones on sliding tracks.

STRUCTURES AND PROPERTIES OF POLYMERS IMPORTANT TO THEIR WEAR BEHAVIOR

Kyuichiro Tanaka
Kanazawa University
Kanazawa, Japan

The experimental results obtained in the present author's laboratory for the wear and transfer of various semicrystalline polymers sliding against smooth steel or glass surfaces are outlined. On the basis of the results, the effects of structures and properties of polymers on their wear behavior are discussed. The high wear characteristics of PTFE were found to be due to the easy destruction of the banded structure of PTFE. The size of spherulites and the molecular profile were closely related to the magnitude of wear rates of typical semicrystalline polymers. The effects of these factors on the wear rate are discussed on the basis of the destruction or melting of spherulites at the frictional surface. The tensile strength and melting point of polymers appeared to be of little importance to the adhesive wear of polymers. Although the fatigue theory of wear indicates that some mechanical properties are important to wear behavior, it is shown that the theory does not always explain the experimental result obtained on a smooth surface.

INTRODUCTION

From the technological point of view, the control of wear is the most important object of wear research. Unfortunately, a powerful law for controlling wear does not exist in our present status of knowledge of polymer wear, although some factors controlling polymer wear have been found. Scientific approaches to clarify the mechanism of polymer wear may be the best way to find a law for controlling wear. Of these approaches, it may be best to clarify the wear mechanisms on the basis of the molecular and morphological structures of polymers, since these structures generally determine the physical, mechanical, and other properties thought to be important to polymer wear. There are many difficulties in this approach, because the relationships among the structures and the properties have not yet been completely resolved. In the present status of understanding, it may be most useful to discuss polymer wear from the structural point of view.

In this paper, a part of the results in the works carried out in the wear and transfer of polymers at the present author's laboratory is outlined, and the structures and properties of polymers important to their wear behavior are discussed in light of these results. In our experiments, the wear of typical semicrystalline polymers sliding against a smooth steel or glass surface was generally studied under a load of 10 N using a pin-disk-type apparatus. The flat ends of polymer pins with 3-mm diameters were generally rubbed on the first rotating disks. In addition, the wear rate described in this paper was obtained in the steady wear state. The mechanical properties of polymers important to their wear behavior are also discussed on the basis of the fatigue theory of wear developed by mainly Russian workers.

WEAR CHARACTERISTICS OF SEMICRYSTALLINE POLYMERS

Wear Rate of Polymers Sliding Against a Hard, Smooth Surface

at Various Sliding Speeds

Figure 1 (ref. 1) illustrates the variation in wear in terms of the decrease in length of the pin (wear depth) h and the coefficient of friction μ at various sliding speeds as functions of the number of disk revolutions N for polytetrafluoroethylene (PTFE), high-density polyethylene (HDPE), and low-density polyethylene (LDPE) sliding against the smooth steel surface with a roughness less than 0.02 μm center line average (c.l.a.). The polymers except PTFE exhibited a low wear rate after an initial transient wear state with a much higher wear rate. PTFE behaves differently from the others. Its steady state of wear rate follows an initial state of lower wear rate, particularly at a speed of 0.01 m/s. The coefficient of friction generally varied with the number of disk revolutions in the transient wear state. With LDPE, however, the friction in the initial wear state decreased as the number of revolutions increased at any speed. This is in marked contrast to the frictional behavior of other polymers. It was noted that the initial transient wear state does not always correspond to the initial transient friction state.

Figure 2 presents the specific wear rates obtained for various polymers rubbed against steel under a condition similar to that in the case of figure 1. It should be noted that PTFE exhibits a much higher wear rate than other polymers, and the wear rate at a speed of 0.01 m/s for the polymers except PTFE generally is considerably higher than that at higher speeds. With the polymers except PTFE, the difference among the wear rates at speeds of 0.01 and 0.1 m/s generally is much greater than that among the wear rates at both speeds of 0.1 and 1 m/s.

The relationship between the wear rates and sliding speed was obtained from the rubbing experiments of PTFE at various speeds and temperatures on a glass disk. The results are presented in figure 3, where the temperature of the glass disk is taken as a parameter (ref. 2). It is noted that the wear rate versus speed curves have peaks of wear rates, and the peaks shift to higher speeds as the temperature is increased. The coefficient of friction becomes smaller with increasing speed. A master curve was derived from the experimental results in figure 3 by translating the curve obtained at a temperature T horizontally by an amount log a_T to fit the reference curve at temperature T_0. The temperature dependence of log a_T could not be expressed by the William-Landel-Ferry equation but rather in the Arrhenius form. However, the value of activation energy of about 7 kcal/mol was deduced by using the temperature dependence of log a_T.

The effect of sliding speed on the friction and wear of several polymers having spherulite structures (i.e., HDPE, LDPE, polyacetal-homopolymer, nylon 6, and polypropylene) sliding against the smooth steel and glass surfaces was studied over the range of speed from 0.1 to 3 m/s (ref. 3). With the polymers on glass, the wear rates were somewhat dependent on speed up to the critical speeds and rapidly increased in the range beyond these critical speeds. The critical speed did not appear for the polymers on steel, except for LDPE. Figure 4 indicates the variation in the specific wear rate with sliding speed for HDPE sliding against steel and glass. The results for the other polymers

were generally similar to HDPE. As will be described, surface melting of polymers due to frictional heating occurred at any speed in the steady wear state. It is noted that the difference between the wear rates on steel and glass at lower speeds is relatively small, while the thickness of molten surface layer is much greater in the case of rubbing on glass because of lower heat conductivity.

Effect of Temperature on the Wear Rate of Polymers

PTFE exhibits very little flow at temperatures above the melting point (ca. 327° C) and allows measuring the wear rate over the high temperature range. Therefore, the effects of temperature and sliding speed on the friction and wear of PTFE were studied in the rubbing on a stainless steel disk over the temperature range of 280° to 380° C (ref. 4). Friction showed little variation with temperature, whereas an abrupt increase in wear rate occurred at the melting point. The variation of specific wear rate with temperature is shown in figure 5. The abrupt increase in the wear rate suggests that an amorphous polymer shows higher wear than does a crystalline polymer. It is interesting that the wear rate decreases as the temperature increases in the range of temperatures above the melting point.

The friction and wear of recently developed heat-resistant polymers (i.e., polyimide (PI: m.p., higher than 520° C), polyamide-imide (PAI: T_g, 275° C), polyphenylene-sulfide with glass fibers of 40 wt. % (PPS: m.p., 290° C; T_g, 88° C), polyether-ether-keton (PEEK: m.p., 334° C; T_g, 143° C), and polyether-sulphone (PES: T_g, 225° C) sliding at a speed of 0.1 m/s against the stainless steel disks heated to various temperatures) were studied. PES is an amorphous polymer and PAI is nearly amorphous, and both polymers have a high glass transition temperature. The polymers except PI flow at a high temperature and thereby allow injection molding. PAI and PEEK exhibited relatively low coefficients of friction (ca. 0.2) at temperatures above 200° C. PI developed a friction peak at about 150° C, and the coefficient of friction at temperatures above 200° C was about 0.4. On the other hand, the coefficient of friction for PPS and PES was about 0.6 at temperatures above 105° C. The temperature dependencies on wear rate for the heat resistant polymers are presented in figure 6. In figure 6(a), the schematic temperature distribution in the steady wear state of polymers pins sliding against the heated disk is also presented, where T_a is the ambient temperature. It is noted that a characteristic of the temperature dependence of wear rates for PPS, PEEK, and PES is somewhat similar to that of the speed dependence on wear rate for HDPE sliding against a glass surface shown in figure 4. The wear rate for these heat-resistant polymers begins to increase rapidly with increasing the disk temperature above a certain critical temperature, and the higher the melting point the higher the critical temperature. It should be noted that the specific wear rates of the heat-resistant polymers at room temperature are generally higher than those for HDPE, polyacetal, and nylon 6. The high wear rate of PES suggests that an amorphous polymer generally exhibits a higher wear rate than does a semicrystalline polymer.

PI and PAI show the wear peaks at about 200° and 105° C, respectively, while the wear rate of PAI is much higher than that of PI over a wide temperature range. The wear rate of PI was also measured at a speed of 1 m/s, and

this result indicated that the wear peak shifted to a lower temperature with increasing speed.

TRANSFER CHARACTERISTICS OF SEMICRYSTALLINE POLYMERS

Transfer in a Single Pass of Polymers on a Glass Surface

at a Very Low Speed

The friction and transfer of typical semicrystalline polymers were studied in the experiments in which the cylindrical surface of polymers was slid on a glass plate at a speed of 0.18 mm/s (ref. 5). Figure 7 shows the electron micrographs of the transferred materials for various polymers after the first traverse. Although a large lump is seen in the case of HDPE, the transfer of such a large lump is very rare in HDPE and is considered to be produced in the surface finish process of the specimen. It is seen that the transferred material of PTFE is a very thin film with a thickness which appears to be below 5 nm and is very different from that of other polymers. The transfer of HDPE and polypropylene is generally in short streaks and that of LDPE is in relatively thick lumps. The thickness of the transferred streaks seems to be of the order of 10 nm with polypropylene and less than 10 nm with HDPE. It was also found that the transfer of PTFE occurred successively on previously transferred PTFE film. Electron microscopic examinations of the polymer surfaces indicated that long films were produced on PTFE and HDPE frictional surfaces. The experiments carried out at very low speed indicate that the transfer characteristics of polymers are closely related to whether or not the molecular profile is smooth. The molecules of PTFE and HDPE have a smooth profile, while those of polypropylene and LDPE have a bulky profile. The transferred material for the polymers of a smooth molecule is very thin films or streaks and that for the polymers of a bulky molecule is thick streaks or lumps. In addition, Pooley and Tabor (ref. 6) have reported that HDPE and PTFE produce very thin transfer films.

Transfer in Multiple Passes of Polymers on Smooth Steel

Surface at Various Sliding Speeds

The present author developed a new technique for measuring the thickness of a polymer layer transferred to a smooth metal surface using electrical capacitance (ref. 7). It should be noted, however, that the thickness obtained from this technique is the thickness reduced to the electrical capacitance and generally is not equal to the thickness in a normal meaning. Therefore, the thickness obtained by the electrical capacitance technique is designated to be the reduced thickness. Figure 8 presents the variation in the reduced thickness of the transferred polymer layer for PTFE, HDPE, and LDPE at various sliding speeds with the number of disk revolutions (ref. 1). There was a great variation in the reduced thickness obtained at different positions over the frictional track on the steel disk. The average reduced thickness is plotted, and the range of the reduced thickness obtained is also presented in the bars of figure 8. With PTFE and HDPE, the reduced thickness

at 10^4 revolutions is slightly dependent on the speed, while that for LDPE increases considerably with increasing speed. The increase of the reduced thickness with the number of disk revolutions is relatively small at the higher speeds, after 10^3 revolutions. The reduced thickness at 10^3 revolutions at 0.01 m/s is generally smaller than that at the higher speeds, and this is very clear for PTFE and LDPE. In addition, the experiments carried out at a speed of 0.1 m/s under loads of 10 and 50 N indicated that the reduced thickness for a greater number of revolutions was slightly dependent on the load. Many lumps of polymer were generally scattered over the transferred layer for PTFE and LDPE.

Optical microscopic examinations indicated that the thickness of transferred layer at 0.01 m/s was generally smaller than that at 1 m/s, and the transferred layer of HDPE was very thin compared with those of other polymers. Figure 9 illustrates electron micrographs of frictional tracks at speeds of 0.01 and 1 m/s after 10^3 revolutions. With PTFE and LDPE, it is clearly seen that the thickness of a transferred layer at 1 m/s is much thicker than that at 0.01 m/s, and this is consistent with the result of the reduced thickness measured. The appearance of a transferred layer for LDPE at 1 m/s is very different from that for other polymers at the same speed. This suggests that the mechanism of transfer for LDPE at higher speeds is considerably different from that for other polymers. Figure 10 shows an electron micrograph and diffraction pattern for the transferred film adhered to the replica taken from the frictional track of steel disk rubbed against an LDPE pin at a speed of 1 m/s. It is seen that long films with oriented molecules are produced for multiple passes of LDPE on the smooth steel surface.

Effect of Temperature on the Transfer of Polymers

In the case of multiple passes of polymers on a heated steel disk, it seems that the higher the disk temperature the thicker the transferred layer. However, it was found that the temperature dependence of the transfer for PAI was considerably different from that of other polymers. Figure 11 presents optical micrographs of the frictional track on the disks rubbed against PAI at disk temperatures of 100°, 150°, and 200° C. The transfer at 150° C is very small compared with those at other temperatures, and this must be related to the fact that PAI exhibits the wear peak at about 150° C as shown in figure 6(b).

Figure 12 is an electron micrograph of a frictional track on the stainless steel disk rubbed against PTFE at a speed of 1 mm/s and a temperature of 330° C (ref. 4). Many clear parallel white lines can be distinguished, and their widths are similar. The white lines result from shadowing the replica surface. The appearance of the white lines with similar widths suggests that the transferred films adhering to the frictional track has a layerlike structure and that the thickness of each layer is almost constant. From the shadowing angle used, the thickness of the layer is estimated to be about 25 nm, which is comparable with that of the films produced on the frictional surface of the PTFE pins. Electron microscopic examinations of the PTFE frictional surfaces and the frictional tracks also indicated that (1) very long films (about 25 nm thick) are produced on the frictional surface during the wear process, (2) the film transfers to the countersurface, and (3) the film is formed by the lateral connection of long fibers. The characteristics of

such wear behavior of PTFE above the melting point are similar to those obtained in the wear processes at lower temperatures (ref. 2).

CHANGES OF THE STRUCTURES IN THE SURFACE LAYER OF

SEMICRYSTALLINE POLYMERS DURING SLIDING

Destruction of the Banded Structure of PTFE

Electron microscopic examinations of the frictional surface of PTFE rubbed against a glass surface at various speeds and temperatures indicated that long films (about 30 nm thick) were produced on the frictional surface. This must be due to the destruction of the banded structure (ref. 2). The long films sometimes adhered to the replica taken from the PTFE frictional surface, and the electron microscopic examinations of the films indicated that the film was formed by the lateral connection of long fibers in which molecular orientation occurred. Figure 13 is an electron micrograph of the frictional surface. It is seen that a very thin film (shown by the arrow) remains after the relatively thick film has been separated. This, therefore, demonstrates that the separation of the film occurs not just over the banded structure but also inside the film.

Surface Melting of the Polymers Having Spherulite Structure

It is well known that many typical semicrystalline polymers have a spherulite structure. At the end of wear testing when the pins of some typical polymers having spherulites were rubbed against the smooth steel and glass surfaces and the wear rates were determined in the steady-state wear states, the polymers pins were abruptly separated from the countersurfaces without halting the disk. As a result of this abrupt separation, the surface layer of the pin must be quenched in the air if surface melting of the pin has occurred during the wear process. Since the quenching of molten polymer suppresses the growth of spherulites during the solidification process, an examination of the surface layers of abruptly separated pins will give information regarding surface melting. In order to examine the surface layer, the thin sections were cut normal to the frictional surface and parallel to the sliding direction by means of an ultra-microtome and were examined under a polarizing microscope with crossed-Polaroids (ref. 3). The examination indicated that surface melting had occurred during the sliding of polymers on steel and glass over the sliding speed range studied (0.1 to 3 m/s).

Figure 14 presents examples of polarizing micrographs of the sections of the surface layers of polymers. When the section is rotated under a polarizing microscope with crossed-Polaroids, the surface layer becomes bright at a certain position of rotation and changes to dark at a position 45° from the bright position. This is shown in figure 14(a). No spherulites remain in the surface layer, and this indicates that melting due to frictional heating has occurred in the surface layer of the polymer pin and that the orientation of polymer chains has become parallel to the sliding direction. The bright surface layer must correspond to the molten layer produced in the polymer pin during the wear process. It is noted that the surface melting occurs even

258

when the polymers are rubbed against a steel surface at a speed of 0.1 m/s. With LDPE, no molten layer was detected under any rubbing condition. However, it is reasonable to conclude that surface melting also occurs during sliding of LDPE because of its lower melting point.

Destruction of the Spherulite Without the Surface Melting

When some typical semicrystalline polymers were rubbed against a steel surface at a speed of 0.01 m/s, a polarizing microscopic examination of the surface layer in the polymer sections indicated that surface melting generally does not occur. In the wear process under such a sliding condition, a destruction of spherulites is supposed to occur because of a large deformation of the radial fibrils in spherulites at the frictional surface of the polymers. Figure 15 shows the electron micrograph of polypropylene fibrils adhering to a smooth steel surface at a sliding speed of 0.01 m/s. It is seen that many fibrils are produced, and short fibrils connecting long fibrils are also produced. The fibrils must be due to the large deformation of the radial fibrils in the spherulites and may be composed of many microfibrils.

EFFECTS OF THE STRUCTURES AND PROPERTIES OF THE

SEMICRYSTALLINE POLYMERS ON THEIR ADHESIVE WEAR

Formation Ability of the Transfer Film During Sliding

Although PTFE has an excellent film formation ability, other polymers can also produce a transferred film on the countersurface during sliding in the initial transient wear states, and this generally reduces the wear rate. It is noted, however, that the transferred layer of PTFE does not always reduce the wear rate as seen in figure 1(a). We may consider that the wear of polymers generally occurs on the similar polymer in the case of a smooth countersurface. The result of the reduced thickness of the transferred polymer layer indicates that the thickness does not always increase when surface melting occurs, and it does not always remain constant during sliding in the steady wear state. In other words, the wear rate in the steady wear state seems to have little dependence on the thickness of the transferred layer. It is interesting that HDPE produces the thinnest transferred layer while its wear rate is the lowest.

The result for the wear of PI and PAI sliding against the heated steel disk suggests that their transferred layer reduces greatly the wear rate at high temperatures.

At first, the fact that the wear of polymers occurs on the transferred film of similar polymers may seem strange. When the transfer of polymers occurs on the countersurface, it is reasonable to consider that a small defect is produced in the subsurface and thus a localized weak portion is generated. Such a mechanism may explain the transfer of similar polymers.

259

Banded Structures Characteristic of PTFE

The morphology of PTFE is not yet completely understood. It is known that PTFE forms extended chain crystals similar to those of polyethylene grown at elevated pressure and the lamellae spray apart in spherulitic fashion (ref. 8). Figure 16 is an electron micrograph of a fracture surface of PTFE used as the specimen in our work. The banded structure is clearly seen, and the width of the bands (i.e., lamellae length) seems to be approximately 0.3 μm and relatively small, indicating that the lamellae are not composed of the completely extended chain crystals because the length 0.3 μm corresponds to the extended chain molecule of PTFE with a molecular weight much less than that of PTFE with a normal molecular weight. Speerschneider and Li (ref. 9) have reported that the bands are composed of crystalline slices about 20 nm thick and oriented normal to the length of band; slippage between the individual slices can easily occur. This model for PTFE morphology was applied to explain the transfer characteristics by Makinson and Tabor (ref. 10) and also the high wear of PTFE by the present author (ref. 2). At present, however, it is more reasonable to consider that the crystalline slice in the model should be replaced with the rodlike lamellae as shown in figure 17(a). The lamellae thickness seems to be about 20 nm based on the number of striations in the bands shown in figure 16. From the temperature dependency of the wear rate versus sliding speed curve for PTFE, an activation energy of about 7 kcal/mol was obtained. This suggests that the slipping of lamellae occurs easily as reported by Speerschneider and Li with respect to the crystalline slices. As a result of the easy slipping of the lamellae, the destruction of the banded structure occurs easily without melting of the sliding surface, and a film of 20 to 30 nm thick is produced on the surface. Since the film detaches easily from the surface, PTFE reveals a very high wear rate as seen in figure 2.

According to the results of the transfer experiment carried out at a very low speed, it may be considered that PTFE molecules are easily withdrawn from the lamellae at the frictional surface, because the PTFE molecule is very rigid and smooth. As a result of this, a very thin film can be transferred to the countersurface.

Spherulite Structure Characteristic of Typical Semicrystalline Polymers

Figure 18 shows polarizing micrographs of the sections of various polymers used in our work. The polymers are arranged in order of increasing size of spherulites as follows: HDPE, LDPE, nylon 6, polyacetal, polypropylene. It seems that the spherulites of LDPE are somewhat larger than those of HDPE, although their spherulites can not be seen clearly in the micrographs. On the other hand, the polymers are arranged in order of increasing specific wear rate at a speed of 0.01 m/s as follows: HDPE, polyacetal, nylon 6, polypropylene, LDPE. It should be noted that the order of the specific wear rate at the speed of 0.1 m/s when surface melting occurs is similar to that at the speed of 0.01 m/s when no surface melting occurs.

The molecular profile of polyacetal is relatively smooth and that of HDPE is even smoother. The melting point and tensile strength of HDPE are much lower than those of polyacetal. Therefore, a comparison of the wear rates for the previously mentioned polymers suggests that the size of spherulites plays an important role in the magnitude of the wear rate. The polymers having

smaller spherulites exhibit lower wear rates. On the other hand, the melting point and tensile strength of nylon 6 are much higher than those of polyacetal, while the polyacetal molecule is much smoother than the nylon molecule. However, nylon 6 shows a much greater wear rate in the wear process without surface melting than does polyacetal. Therefore, the comparison between the wear rates of nylon 6 and polyacetal suggests that the polymers with the smoother molecules exhibit lower wear rates. A comparison between the wear rates for HDPE and LDPE also suggests that a lower wear rate appears in the case of the smoother molecule. From these results, it may be concluded that the wear rate of polymers is strongly controlled by the size of the spherulites and whether the molecular profile is smooth or bulky. The smaller the spherulites and the less bulky the molecule the lower the wear rate. In addition, the tensile strength and melting point do not seem to control the wear rate very much. In fact, surface melting occurs in the steady wear state at an engineering speed for typical semicrystalline polymers, and the melting point is meaningless in the wear process where surface melting has occurred, while the wear rate generally is lower for rubbing without melting.

The wear rate of polypropylene is much higher than that of nylon 6 and polyacetal, and this must be due to its bulky molecule and very large spherulites. LDPE also shows a high wear rate at sliding speeds where surface melting occurs, and its wear rate in the wear process without melting is also very much higher. With LDPE, it was found that shearing occurred at a distance from the frictional surface as soon as melting occurred and a film, as shown in figure 10, was laid down on the countersurface on a large scale (ref. 3). This suggests that the shear strength at high temperatures near the melting point plays an important role in the wear rate and must be high in order to suppress the high wear rate at the speeds when surface melting occurs. The wear rate of LDPE in the wear process without melting is very high; this must be due to the characteristics that the massive lumps are transferred to the countersurface, as seen in the transfer experiment at a very low speed (fig. 7). The LDPE molecule has many chain branches in its main chain. The chain branches are much longer than the side group, CH_3, in the polypropylene molecule and are flexible; also, they undergo many entanglements with adjacent molecules, resulting in the transfer of massive lumps.

Russian workers have also pointed out that the wear is lower in the case of smaller spherulites and the morphological structure is important in wear. They have shown that transcrystalline growth in the surface layer of a molded polymer reduces the wear rate (ref. 11).

Consider the relationship between the destruction of the spherulite structure at the frictional surface and the wear rate. The main component of the spherulite is the radial fibril shown in figure 19(a) (ref. 12). Kakudo and Kasai (ref. 13) studied the destruction of the crystal region in the spherulite during the necking process of polyethylene, and they have shown that a fiber structure was produced after necking (fig. 19(b)). Peterlin (ref. 14) has shown that the structural unit of the ordered chain folded crystalline domains in a synthetic fiber is a microfibril (fig. 19(c)). According to these facts, the microfibrils must be produced at the frictional surface as the result of the large deformation of the radial fibrils in the spherulites when rubbed on the countersurface. This is also suggested from our electron microscopic examination of the polypropylene frictional surface (fig. 15). Furthermore, Komoto, et al., have found that the materials having

the structure similar to a synthetic fiber are produced on the HDPE surface rubbed against a steel sphere (ref. 15).

Figure 20 shows the schematic representation for the wear process where no surface melting occurs. In the case of polymers having small spherulites, many spherulites will deform as show in the figure, while the deformation of a part of spherulite near the frictional surface will only occur in the case of polymers having large spherulites. An accumulation of the microfibrils produced due to the destruction of radial fibril transfers occasionally on the countersurface composed of the transferred layer during rubbing. If you assume the transferred unit has a length a and a thickness b, the larger the spherulite the greater the length a; also, the smoother the molecule, the smaller the thickness b. The wear rate may be assumed to increase as the product ab increases. From this concept, the observed effects of molecular profile and size of spherulites on the wear rate are explained qualitatively, although it must be recognized that the probability of occurrence of transfer events contributes to the wear rate.

Figure 21 is a schematic representation of the wear process when surface melting occurs. When the molten polymer layer is thinner than about 20 μm, the wear rate is generally very low; this case is indicated schematically in figure 21(a). The temperature distribution in the polymer pin is also shown schematically in the figure. It should be noted that the temperature distribution in this case is very different from that in the polymer pin sliding against a heated countersurface as indicated in figure 6(a). Figure 21(b) reveals the wear process for LDPE. Figure 21(c) indicates the wear process in which the thickness of the molten layer becomes considerably greater. It is observed in the rubbing of polymers on a glass plate at speeds greater than a critical speed. In this case, the outflow of a molten polymer layer through the rear edge of the polymer pin occurs, resulting in a very high wear rate.

It was observed that the order of increasing wear rate for various polymers at 0.1 m/s was similar to that for polymers at 0.01 m/s. This suggests that the size of spherulites and the molecular profile play an important role even in the wear process where surface melting occurs. The distribution of the number of molecular chains in the direction perpendicular to the frictional surface in the molten layer may be similar to that in the surface layer without melting because of the difficulty of migration of the molecules in the direction perpendicular to the sliding direction in the molten layer. Furthermore, the temperature dependence of the molecular profile may be small. Therefore, it is reasonable that the order of wear rate is somewhat dependent on whether or not surface melting occurs.

The ultra high molecular weight polyethylene shows a considerably lower wear rate than does normal HDPE (ref. 3). This indicates that molecular weight is an important factor in the wear of polymers. Some molecular structural parameters such as the degree of crystallinity, lamellae thickness, and the interlamellae distance may also be important in wear.

Chemical Reaction Polymer Wear

The sliding friction studies conducted in vacuum with PTFE and PI indicated that their decomposition products were generated with increasing sliding speed, as the result of a scission of polymer chains due to the frictional heat generated (ref. 16). Such decomposition contributes to the wear rate of

polymers. However, the quantitative estimation for the contribution of decomposition of polymer chains to the wear rate has not yet been clarified.

PI and PAI showed the wear peak at a certain disk temperature (fig. 6(b)). With PAI, the wear peak was particularly great, and its transfer to the countersurface was very small at the temperature corresponding to the wear peak. This seems to indicate a remarkable effect of chemical reaction occurring at the polymer frictional surface on wear. To make the imide bond in the synthesis process of PAI, the chemical reaction shown in figure 22 may be assumed to occur. The imide bond is formed at state (b) and at the same time the H_2O vapor is generated. However, certain amounts of the unreacted material, which is represented in state (a), are considered to remain in the molecular chains of the molded PAI that is used for engineering purposes. It is known that the COOH group existing in state (a) decomposes easily at a high temperature and generates CO_2 gas. The chain scission of the main chains of PAI will occur easily at the unreacted sites at a high temperature. On the other hand, the formation of imide bonds at the unreacted sites may also occur and generate H_2O vapor at the sliding interface. The wear peak and high wear near the peak may be due to such a chain scission and generation of gases such as CO_2 or H_2O in the wear process. A small amount of transferred PAI at the temperature corresponding to the wear peak may be due to the influence of such gases. Similar phenomena may occur in the case of PI. The decrease of wear rate with increasing disk temperature above the temperature of the wear peak may be due to the wear suppression action of the very thick transferred film formed at high temperature. From the forgeoing it may be concluded that the after-cure treatment for PI and PAI may be very important to reduce the wear peak at elevated temperatures.

Various Properties Supposed to be Important in Polymer Wear

The wear rate must be related to many properties of polymers. In some types of wear, the properties important to wear are presently known. For example, the stress and strain at breaking are important in abrasive wear. Unfortunately, the adhesive wear which generally appears in many sliding components is related to various kinds of properties (i.e., physical, chemical, mechanical, and others). The wear rate of polymers may increase with increasing surface energy of polymers because of increasing adhesive forces, while it may decrease with increasing shear and tensile strengths, the strain at break, the cohesive energy, and the activation energy for thermal degradation. The elastic moduli may be related to wear due to an increase in the real area of contact. However, the influences of these quantities on the wear rate are not independent but generally interrelated. Although the expression of wear rate derived in the fatigue theory of wear developed by the Russian workers includes only the mechanical properties of materials, it indicates that the factors composed of some properties affect the wear rate. In the present author's view, therefore, it is very useful to study the morphological and molecular characteristics important to polymer wear because of the close relationship between the wear rate and characteristics such as the size of the spherulites and the molecular profile.

263

IMPORTANT MECHANICAL PROPERTIES OF POLYMERS

PREDICTED FROM THE FATIGUE THEORY OF WEAR

Lancaster (ref. 17) has shown that the important factor in the wear of polymers on a rough surface is the work of fracture, which is approximately proportional to the product of the stress and strain at fracture of polymers, although it is not clear whether the main mechanism of the wear process studied by him is abrasive or fatigue. Jain and Mahadur (ref. 18) developed the wear equation for polymer – metal sliding in terms of the fatigue and topography of the sliding surfaces. The wear equation indicates that the wear rate increases with increasing elastic modulus and volume of wear particles, and it decreases with increasing tensile strength. According to the expression for volume they derived, the volume increases with increasing elastic modulus, surface energy, and coefficient of friction and decreasing yield strength. The wear equation also indicates that the index in the Wohler's equation for fatigue plays an important role in the wear rate. Jain and Bahadur (ref. 19) have shown that the computed steady-state wear rates on the basis of their equation are in excellent agreement with the experimental wear rates for the three polymers tested. Since the elastic modulus depends on the time scale measurement and this was not taken into consideration for the derivation of the wear equation, further experimental verification may be needed for the wear equation.

The fatigue theory of wear has been developed most intensively by Russian workers under the direction of Kragelsky. The theory seems to be widely used in the Soviet Union to calculate the wear rates of practical machine components. Kagelsky, et al., (ref. 20) state that the results of calculating wear rates in various sliding pairs by their method show a satisfactory agreement with experimental data and, to our surprise, the maximum possible discrepancy between the theoretical and experimental wear rates is about one order of magnitude. From the theory of Kragelsky, et al., the linear wear rate (i.e., the wear depth per unit sliding distance) I of polymers rubbed on a rough, hard surface without waviness under the elastic contact condition is expressed as follows:

$$I = KK_{t\nu}\alpha(0.5)^{(t-1)-1/2\nu}2^{1/2\nu}p_a^{(1+t)/(2\nu+1)}E^{2\nu t/(2\nu+1)-1}\Delta^{\nu t/(2\nu+1)}\left(\frac{k\mu}{\sigma_0}\right)^t \qquad (1)$$

where

K	factor determined by geometric shape and height of individual asperities (commonly, $K = 0.2$)
$K_{t\nu}$	coefficient determined by t and ν
k	factor characterizing contact stress condition; factor depends on nature of material (for highly elastic material $k = 3$)
α	ratio of real area of contact to apparent area of contact
ν	parameter of bearing-area curve for hard surface
Δ	parameter determined by surface topography of hard surface
p_a	nominal contact pressure
μ	adhesion component of coefficient of friction

E   elastic modulus of polymer

t   index in Wohler fatigue curve (i.e., $n = (\sigma_0/\sigma_{eff})^t$ where σ_{eff} and σ_0 are effective and ultimate tensile stresses at single elongation cycle, respectively, and n is number of cycles to fracture)

Kragelsky, et al., show the values of t and σ_0 obtained in the frictional fatigue experiments for various materials, and they show that σ_0 and t can also be obtained from a bulk fatigue experiment (ref. 20). The values of σ_0 for PTFE and nylon are 63 and 180 MN/m^2, respectively, and the values of t for both polymers are 5 and 2, respectively, according to references 20 and 21. The values of σ_0 are much higher than these of tensile strength normally obtained in PTFE and nylon. This may be due to the fact that σ_0 is determined by the extrapolation of the experimental results carried out in a limited range of the number of stress cycles to failure.

The values of the roughness parameters Δ and ν for the smooth steel surface used in our wear experiments may be estimated as 4×10^{-4} and 1.4, respectively, according to reference 20. In the following, compare the ratio for the linear wear rate of PTFE to that of nylon 6 using the above values for σ_0, t, Δ, and ν and the values of the coefficient of friction and of p_a in our experiments at a speed of 0.01 m/s from which the data shown in figure 2 were obtained. In addition, the values of K, α, and k are assumed to be the same as those in the case of both polymers. The linear wear rates are calculated as follows:

$$I_{PTFE} = Const. \left[(2 \times 0.5^{3.64}) p_a^{2.32} E^{2.68} (4 \times 10^{-4})^{1.84} \left(\frac{3 \times 0.17}{6.3} \right)^5 \right]$$

$$= Const. (1.4 \times 10^{-13}) \qquad (2)$$

$$I_{nylon} = Const. \left[(1.6 \times 0.5^{0.643}) p_a^{1.53} E^{0.474} (4 \times 10^{-4})^{0.736} \left(\frac{3 \times 0.6}{18} \right)^2 \right]$$

$$= Const. (2.3 \times 10^{-5}) \qquad (3)$$

where 42 and 2700 MN/m^2 are taken as the values of the elastic modulus for PTFE and nylon 6 on the basis of the data published by the manufacturer of polymers and $P_a = 1.4$ MN/m^2 in our experiments. This calculation indicates that the wear rate of PTFE is much smaller than that of nylon 6, and this is not consistent with the experimental result.

Therefore, equation (1) does not seem to estimate the wear rate of polymers sliding against a smooth steel surface, although the equation may apply to the wear of polymers on a rough steel surface. It should be noted that equation (1) indicates approximately zero wear in the case of a extremely smooth surface with approximately a zero value of Δ. Also, it does not take into account the transfer of polymers on the countersurface. However, the fatigue theory of wear suggests that the wear rate increases with an increasing elastic modulus and fatigue parameter t, and with a decreasing tensile strength, as shown by Jain and Bahadur, when the wear of polymers

originates from fatigue. An exact theory for fatigue wear of polymers should account for the viscoelastic nature of the mechanical properties of polymers.

CONCLUDING REMARKS

The effects of the structures and properties of semicrystalline polymers on their wear rates were discussed on the basis of the results obtained in experiments in which the polymers were rubbed against a smooth steel or glass surfaces. The high wear rate characteristic of PTFE is due to easy destruction of the banded structure of PTFE. For typical polymers having the spherulite structure, the wear rate increases as the size of spherulites increases and the bulkiness of polymer molecules increases. HDPE, having very small spherulites and very smooth molecules, exhibits a much lower wear rate than do nylon 6 and polyacetal; however, HDPE's tensile strength and melting point are relatively low compared with other polymers. Therefore, the tensile strength and melting point do not seem to be important factors in the adhesive wear of polymers. The wear rate is generally higher in the wear process without the surface melting due to frictional heating compared with the wear process where surface melting occurs. Although the fatigue theory of wear indicates that some mechanical properties are important to wear, the theory does not always explain the result of wear rates obtained in the rubbing of polymers on a smooth countersurface.

Since the adhesive wear of polymers is related to various kinds of polymer properties and is very complex, the scientific approach to the basis of the morphological and molecular structures seems to be very useful in finding a law to control polymer wear.

REFERENCES

1. Tanaka, K.; and Yamada, Y.: Effect of Sliding Speed on Transfer and Wear of Semicrystalline Polymers Sliding Against Smooth Steel Surface. Wear of Materials-1983, Ludema, K. C., ed., ASME, 1983.
2. Tanaka, K.; Uchiyama, Y.; and Toyooka, S.: The Mechanism of Wear of Polytetrafluoroethylene. Wear, vol. 23, 1973, pp. 153-172.
3. Tanaka, K.; and Uchiyama, Y.: Friction, Wear and Surface Melting of Crystalline Polymers. Advances in Polymer Friction and Wear, vol. 5B, Lee, L. H., ed., Plenum, 1974, pp. 499-530.
4. Tanaka, K.; and Ueda, S.: The Mechanism of Wear of Polytetrafluoroethylene Above the Melting Point. Wear, vol. 39, 1976, pp. 323-333.
5. Tanaka, K.; and Miyata, T.: Studies on the Friction and Transfer of Semicrystalline Polymers. Wear, vol. 41, 1977, pp. 383-398.
6. Pooley, C. M.; and Tabor, D.: Friction and Molecular Structure - The Behaviour of Some Thermo-Plastics. Proc. Roy. Soc., London, Ser. A, vol. 329, no. 1578, 1972, pp. 251-274.
7. Tanaka, K.: Transfer of Semicrystalline Polymers Sliding Against a Smooth Steel Surface. Wear, vol. 75, no. 1, 1982, pp. 183-199.
8. Wunderlich, B.: Macromolecular Physics. Vol. 1. Academic Press, 1973.

9. Speerschneider, C. J.; and Li, C. H.: Some Observation on the Structures of Polyterafluoroethylene. J. Appl. Phys., vol. 33, no. 5, 1962, pp. 1871-1875.

10. Makinson, K. R.; and Tabor, D.: The Fricton and Transfer of Polytetrafluoroethylene. Proc. Roy. Soc., London, Ser. A, vol. 281, no. 1384, 1964, pp. 49-61.

11. Bely, V. A.; et al.: Friction and Wear in Polymer-Based Materials. Pergamon Press, 1982.

12. Samuels, R. J.: Structured Polymer Properties. John Wiley & Sons, Inc., 1974.

13. Kakudo, M.; and Kasai, N.: X-Ray Diffraction by Polymers. American Elsevier, 1972.

14. Peterlin, A.: in Properties of Solid Polymeric Materials. Part A. Schultz, J. M., ed., Academic Press, 1977, p. 229.

15. Komoto, T.; et al.: Morphological Study of the Wear of Crystalline Polymers I: High Density Polyethylene. Wear, vol. 75, 1982, pp. 173-182.

16. Buckley, D. H.: Friction, Wear, and Lubrication in Vacuum. NASA-SP-277, 1971.

17. Lancaster, J. K.: Abrasive Wear of Polymers. Wear, vol. 14, 1969, pp. 223-239.

18. Jain, V. K.; and Bahadur, S.: Development of a Wear Equation for Polymer-Metal Sliding in Terms of the Fatigue and Topography of the Sliding Surface. Wear, vol. 60, 1980, pp. 237-248.

19. Jain, V. K.; and Bahadur, S.: Experimental Verification of a Fatigue Wear Equation. Wear, vol. 79, 1982, pp. 241-253.

20. Kragelsky, I. V.; and Alisin, V. V., eds.: Friction, Wear, Lubrication - Tribology Handbook. Vol. 1. Min Publishers, Moscow, 1982, pp. 241-253.

21. Kragelsky, I. V.; Dobychen, M. N.; and Kombalov, V. S.: Friction and Wear - Calculation Methods. Pergamon Press, 1982.
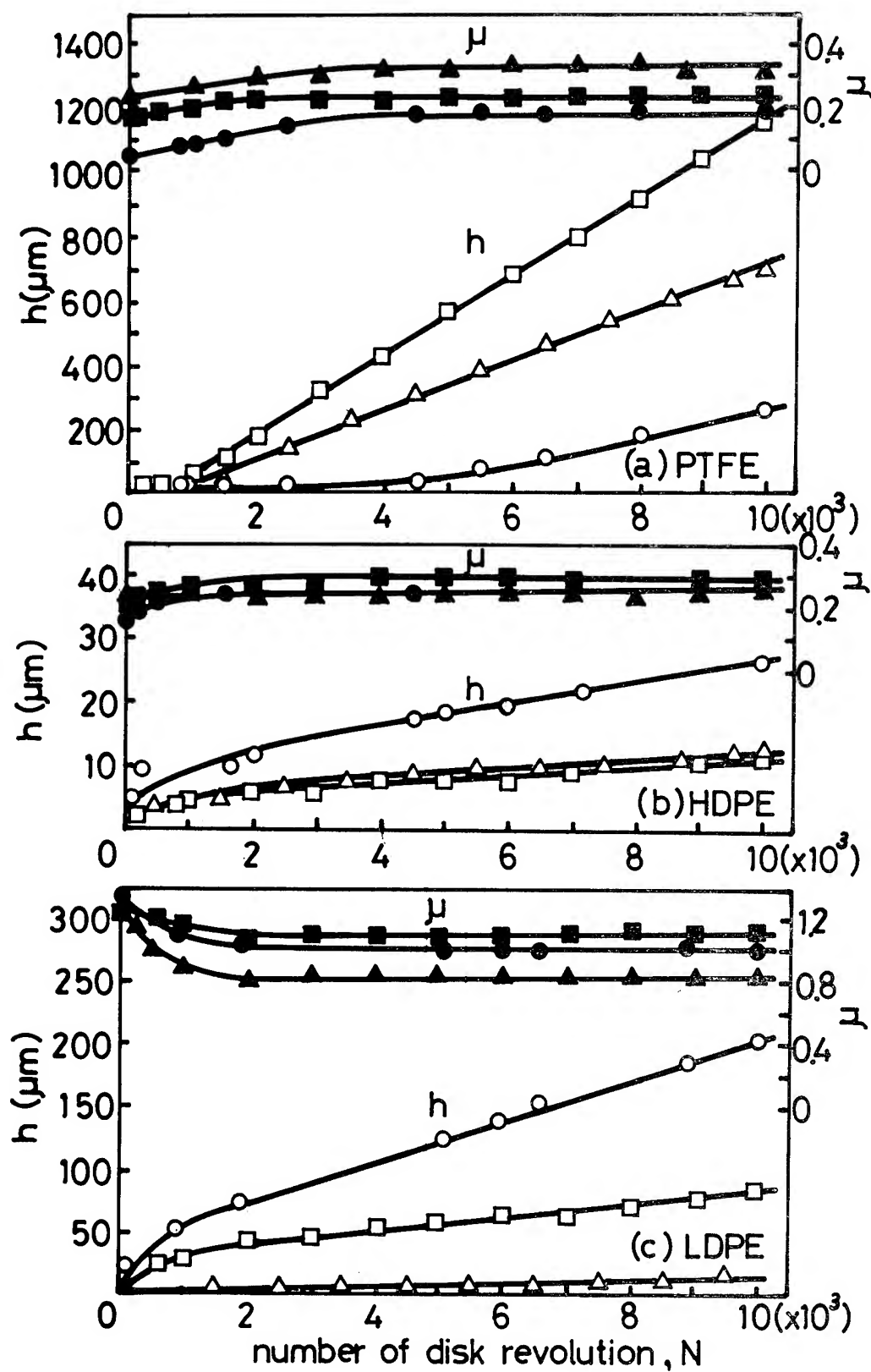
Figure 1.- Variation in wear depth h and coefficient of friction μ for various polymers at various sliding speeds with the number of disk revolutions N. load, 10 N; diameter of frictional track, 5 cm. (○,●), 0.01 m/s;(□,■),0.1 m/s (△, ▲), 1 m/s.
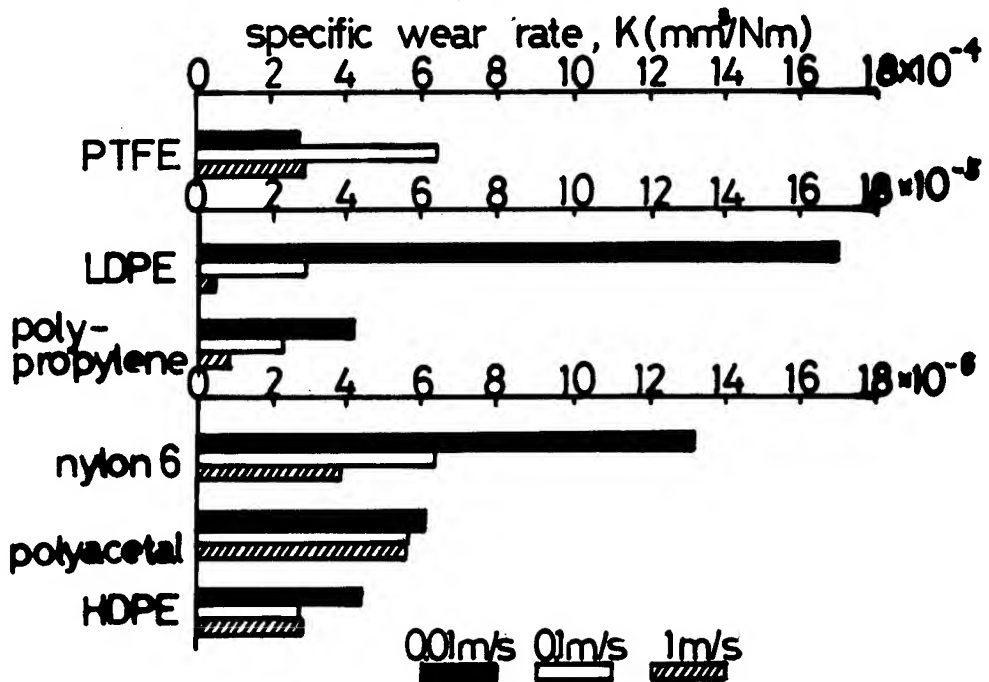
Figure 2. - Specific wear rate K for various polymers sliding against
a smooth steel surface at various sliding speeds.
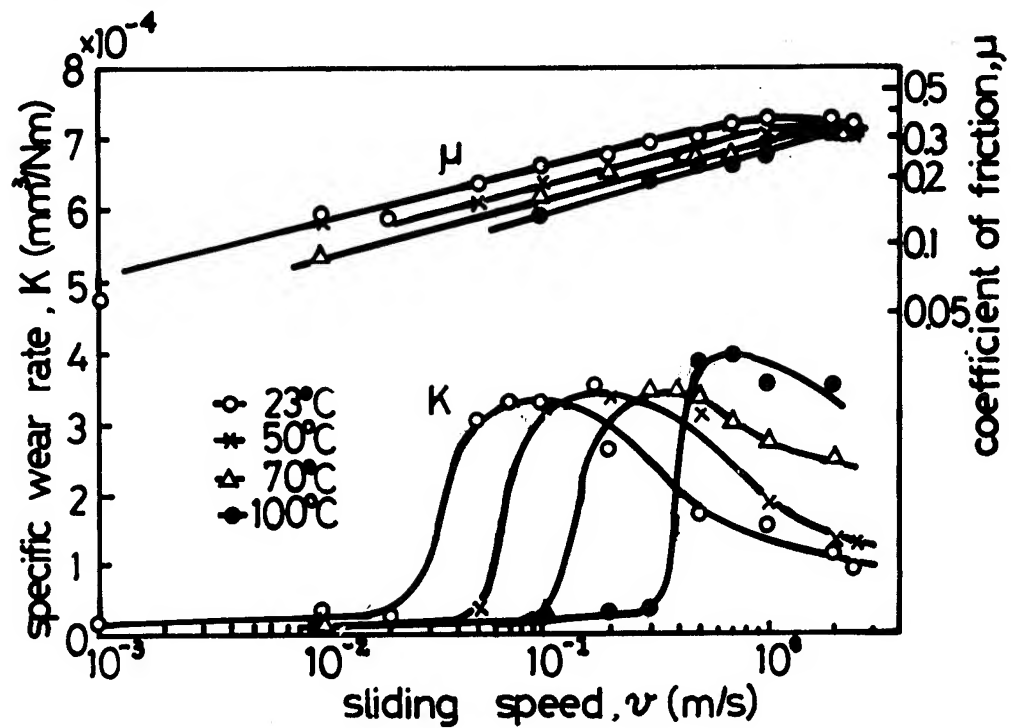
Figure 3. - Variations in specific wear rate K and coefficient of friction μ
for PTFE sliding against glass surface at various temperatures with sliding
speed.
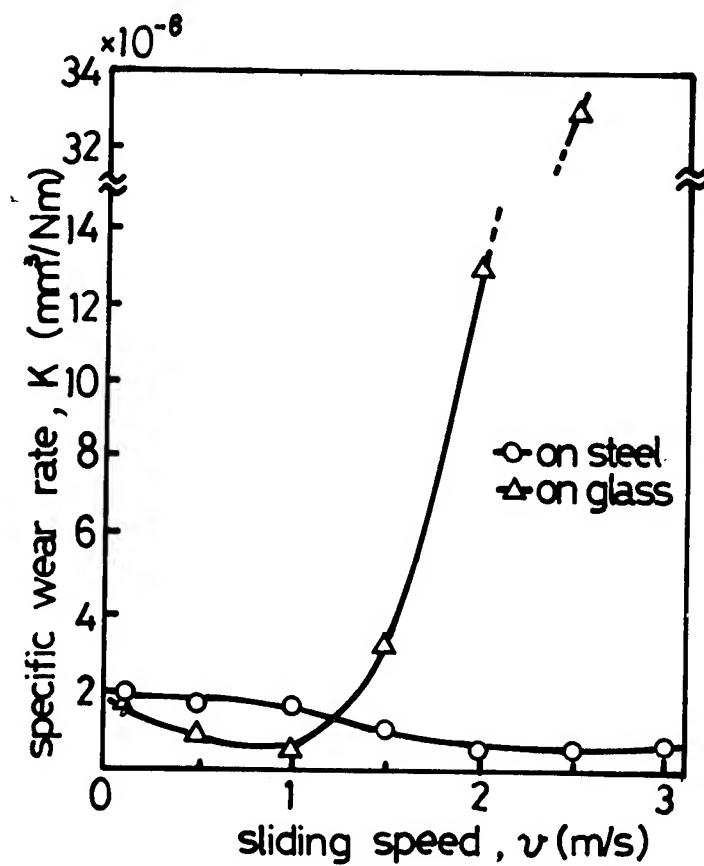
Figure 4. - Effect of sliding speed on the specific wear rate of HDPE.
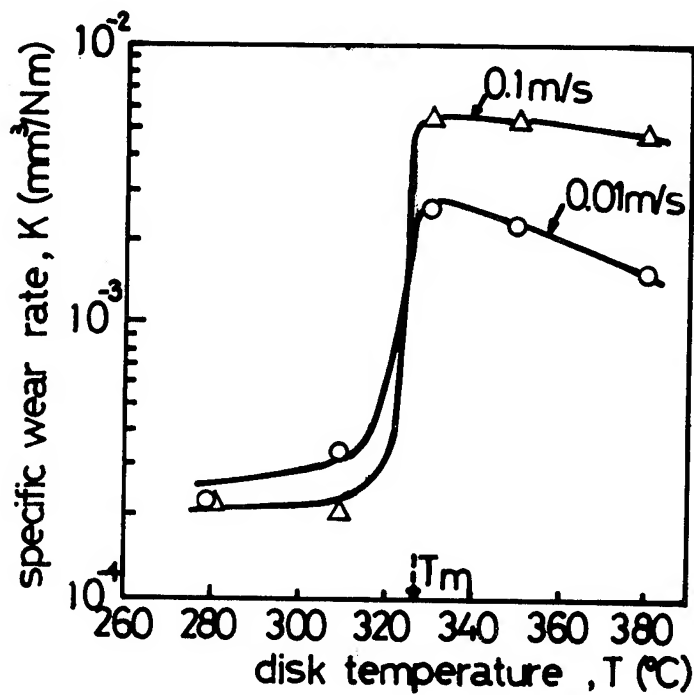
Figure 5. - Effect of temperature on the specific wear rate of PTFE at the high temperatures.
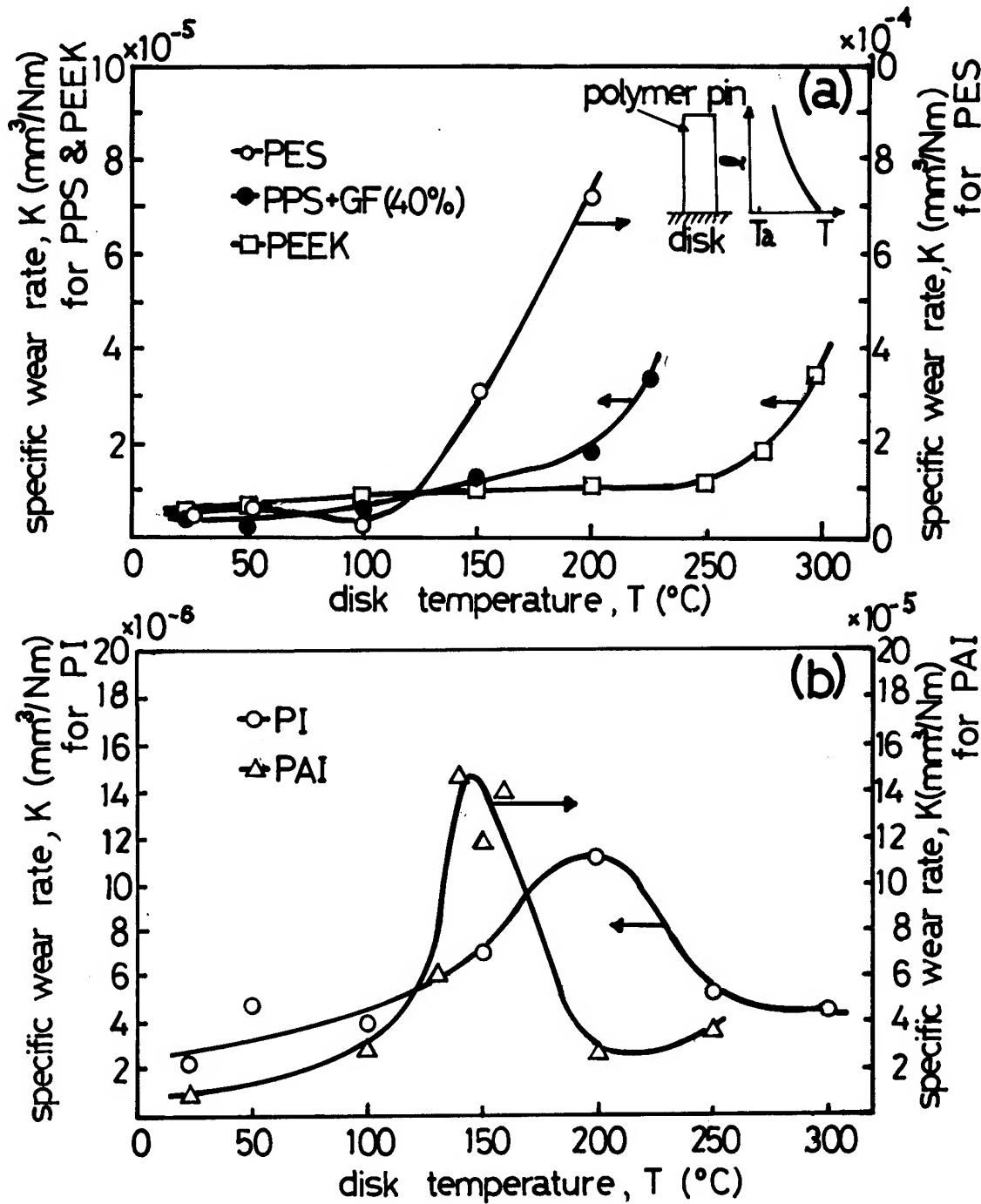
Figure 6. - Effect of temperature on the specific wear rates of various heat resistant polymers.

PTFE   1μm   HDPE
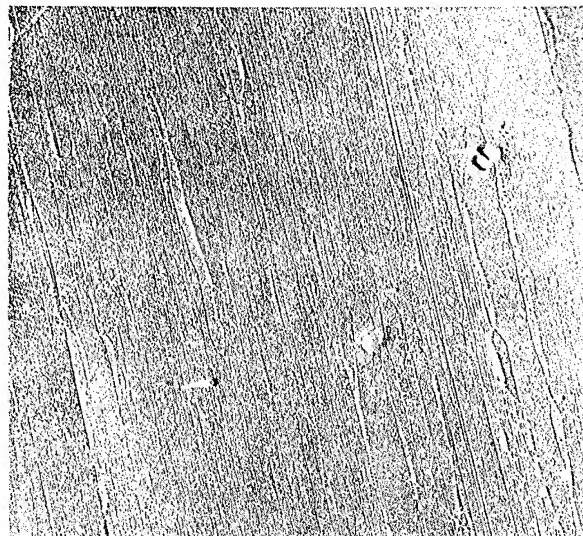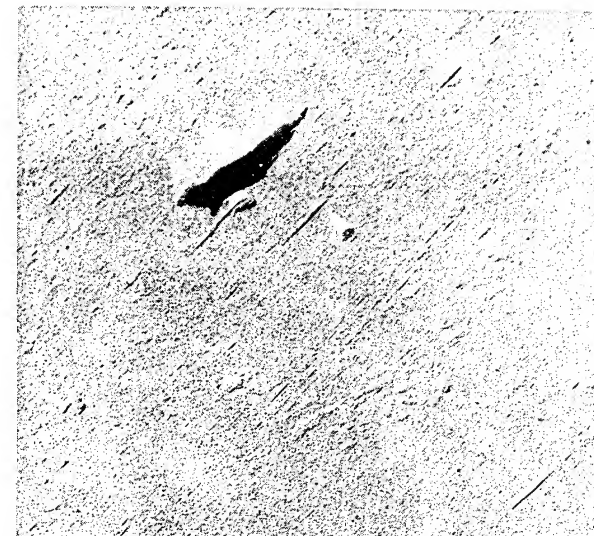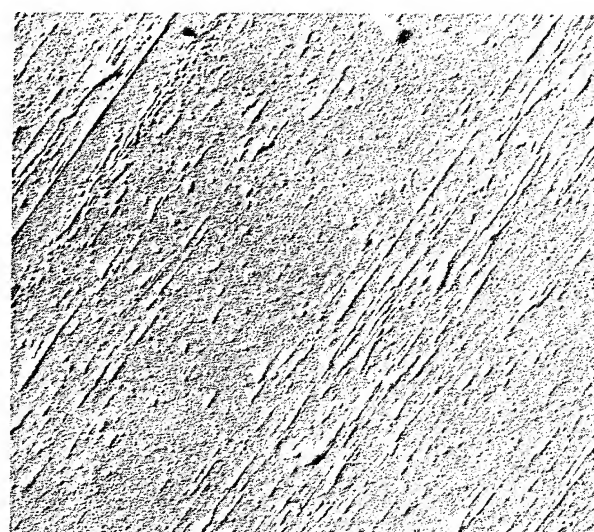
LDPE   0.5μm   polypropylene

Figure 7. - Electron micrographs of the transferred materials after the first traverse of various polymers on a glass surface.
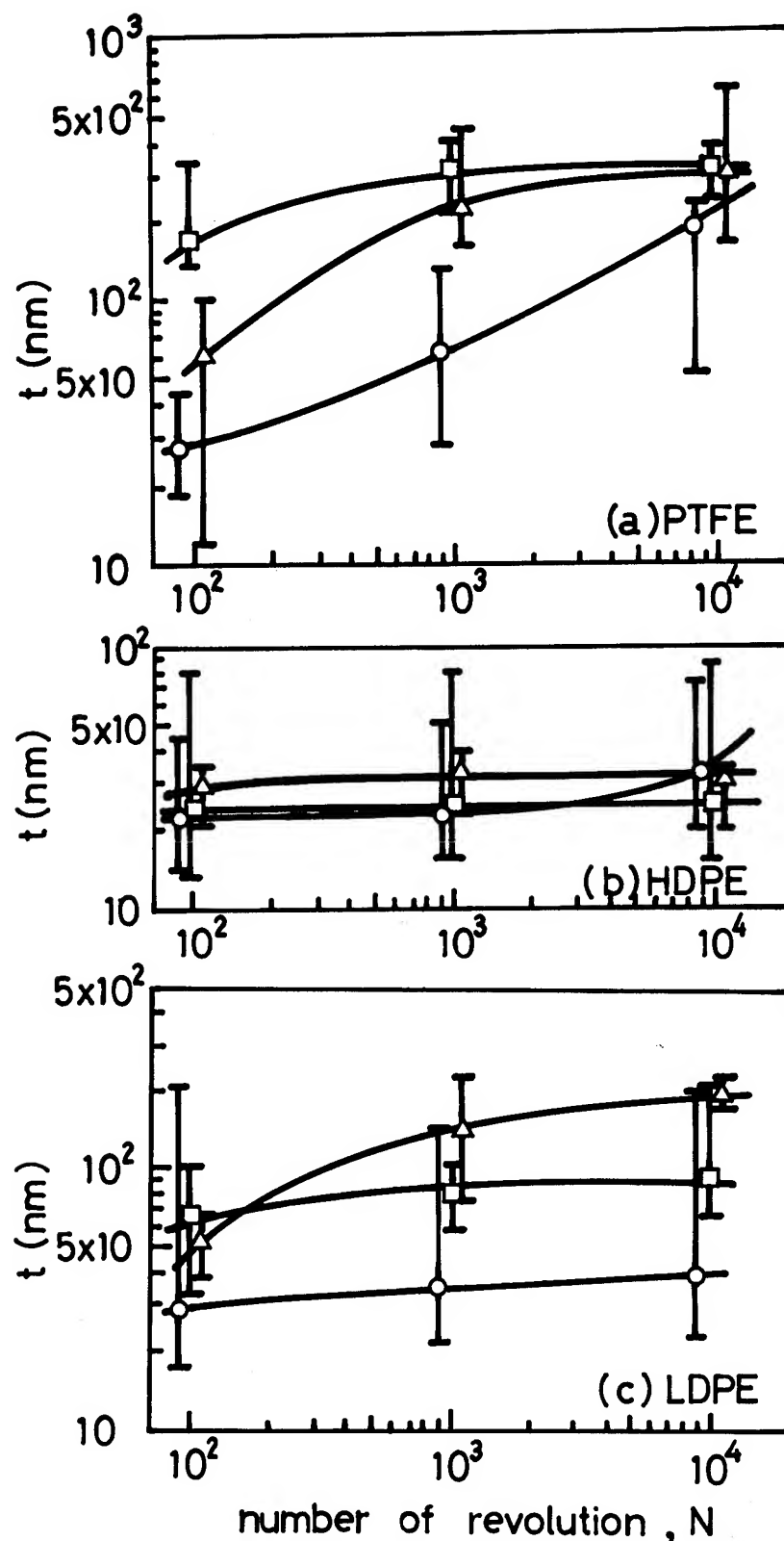
Figure 8. - Variation in the reduced thickness t of the transferred polymer layers at various sliding speeds with the number of disk revolutions N.
o , 0.01 m/s;□ , 0.1 m/s;△ , 1 m/s.
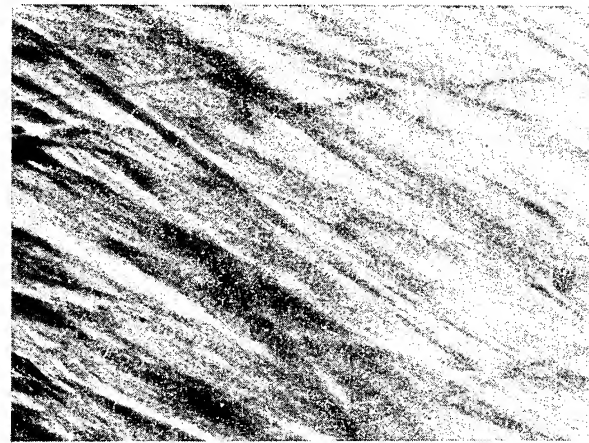
PTFE
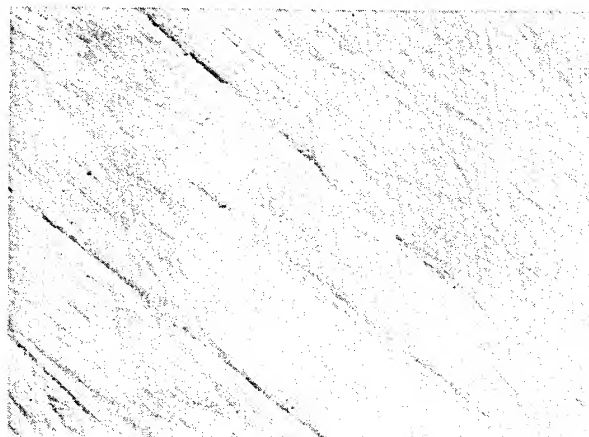
HDPE
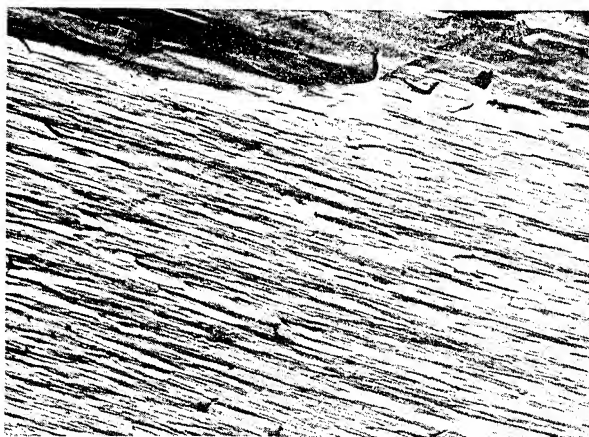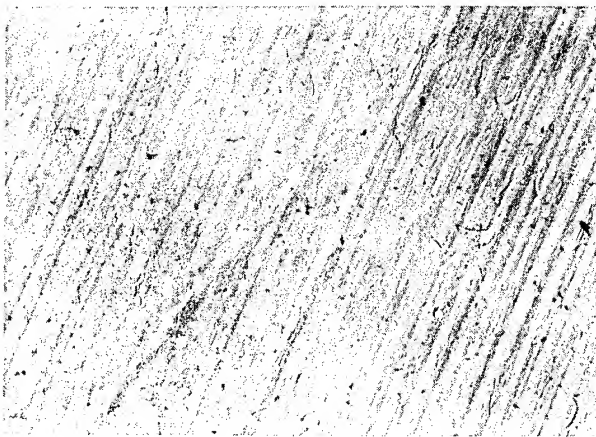
LDPE

$\underline{2\,\mu m}$

Figure 9. - Electron micrographs of frictional tracks rubbed on various
polymers for a disk revolutions of 1000.
left, 0.01 m/s ; right, 1 m/s.

Figure 10. - Electron micrograph and diffraction pattern of LDPE film adhering to steel disk. sliding speed , 1 m/s.
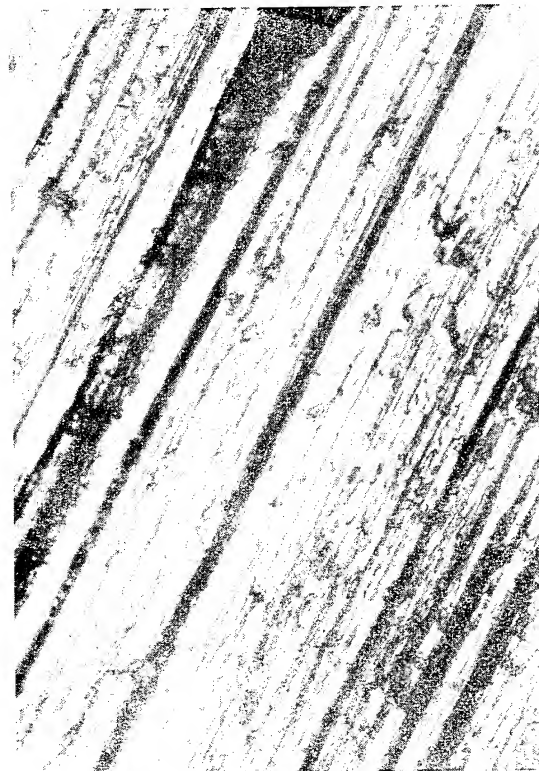
100 °C

150 °C
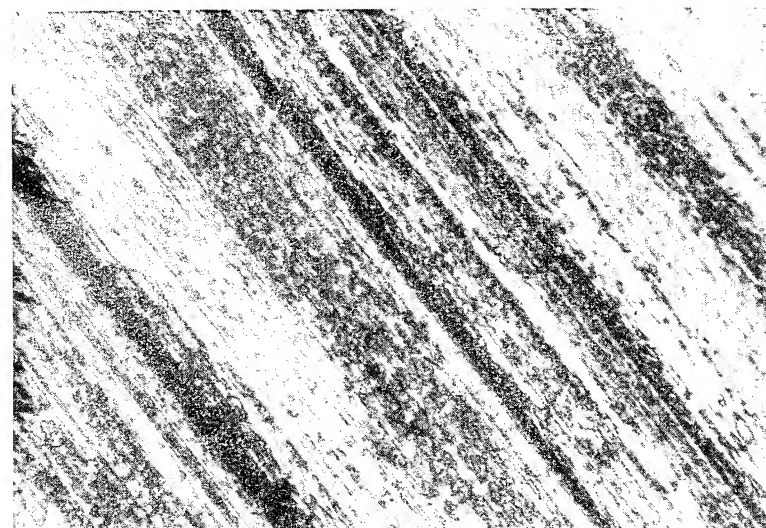
200 °C

50μm

Figure 11. - Optical micrographs of frictional tracks rubbed against polyamide-imide at various temperatures.
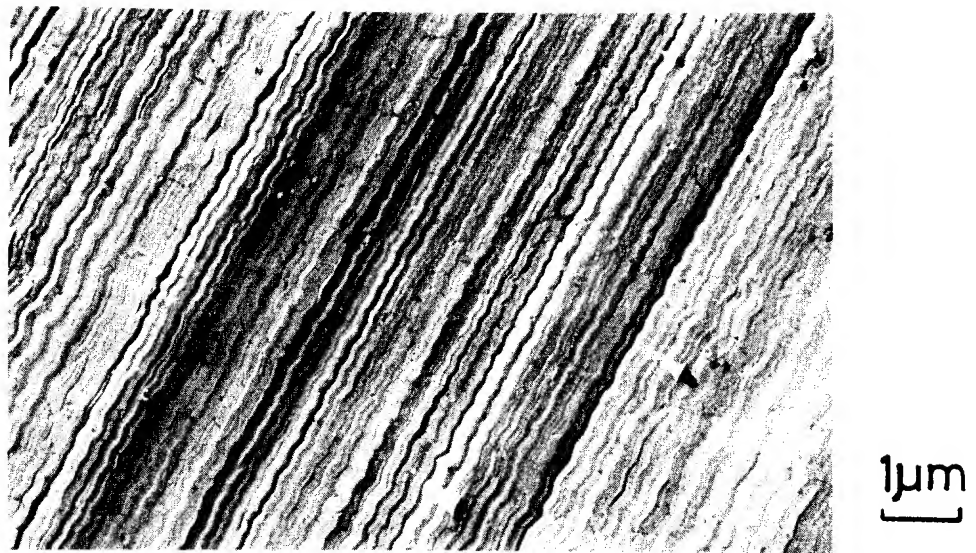
Figure 12. - Electron micrograph of frictional track rubbed against PTFE at a temperature of 330 C and a speed of 1 mm/s.
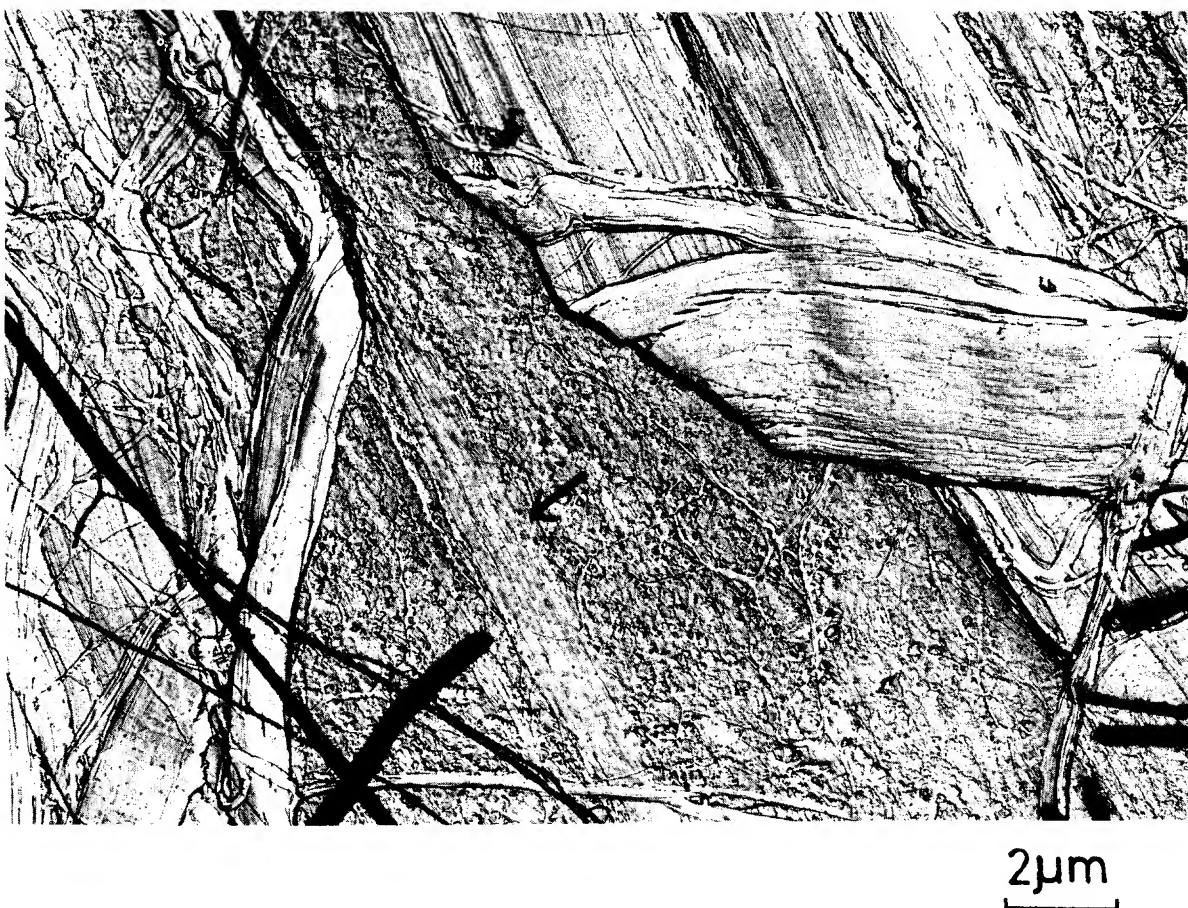
Figure 13. - Electron micrograph of the worn surface of PTFE rubbed against glass surface.
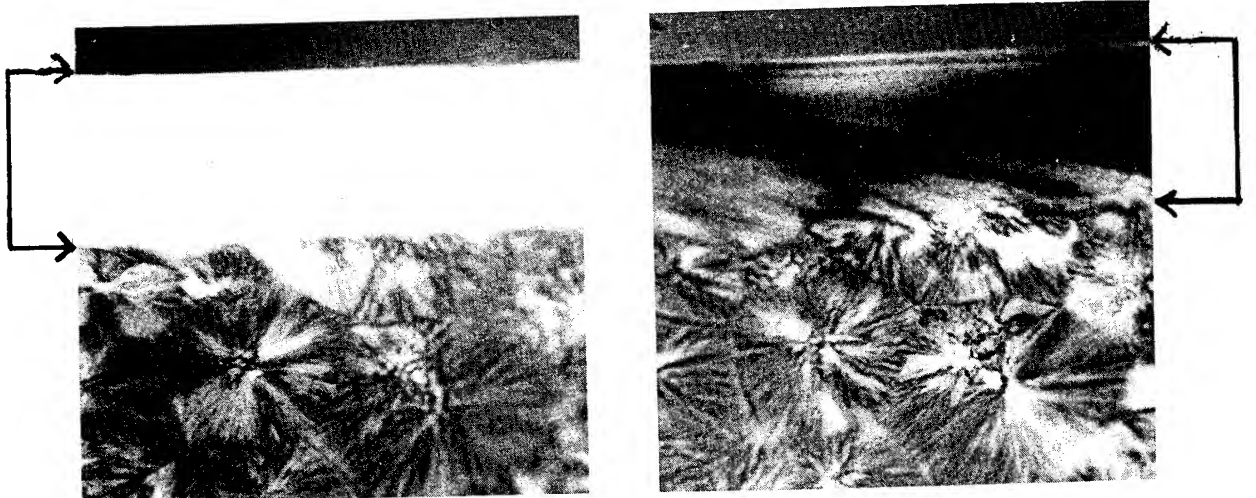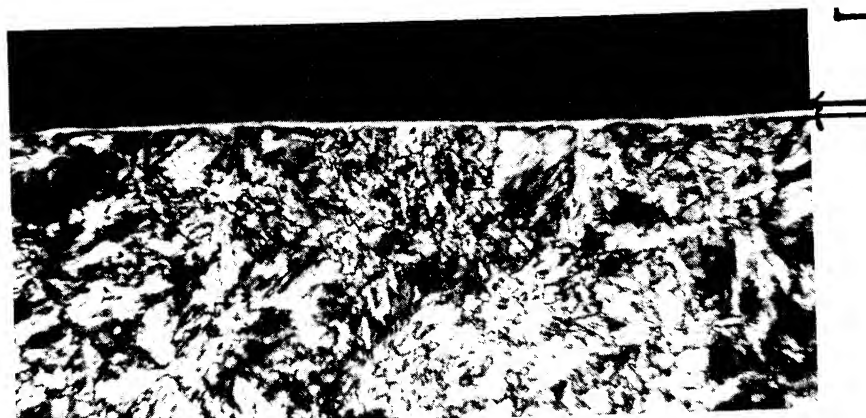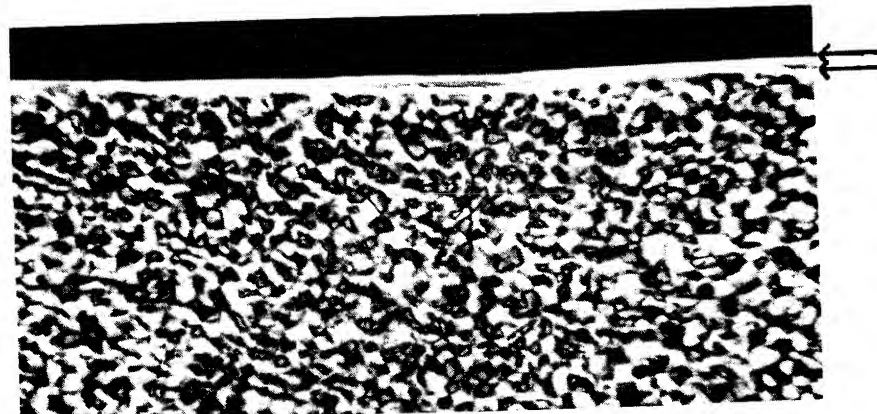
Figure 14. - Polarizing micrographs of sections of surface layer of various polymers. The arrows show the molten surface layer. (a) polypropylene rubbed on glass at 1 m/s. In the right figure, the section is turned by 45 degrees from the position in the left figure. (b) polyacetal rubbed on steel at 0.1 m/s. (c) nylon 6 rubbed on steel at 0.1 m/s.
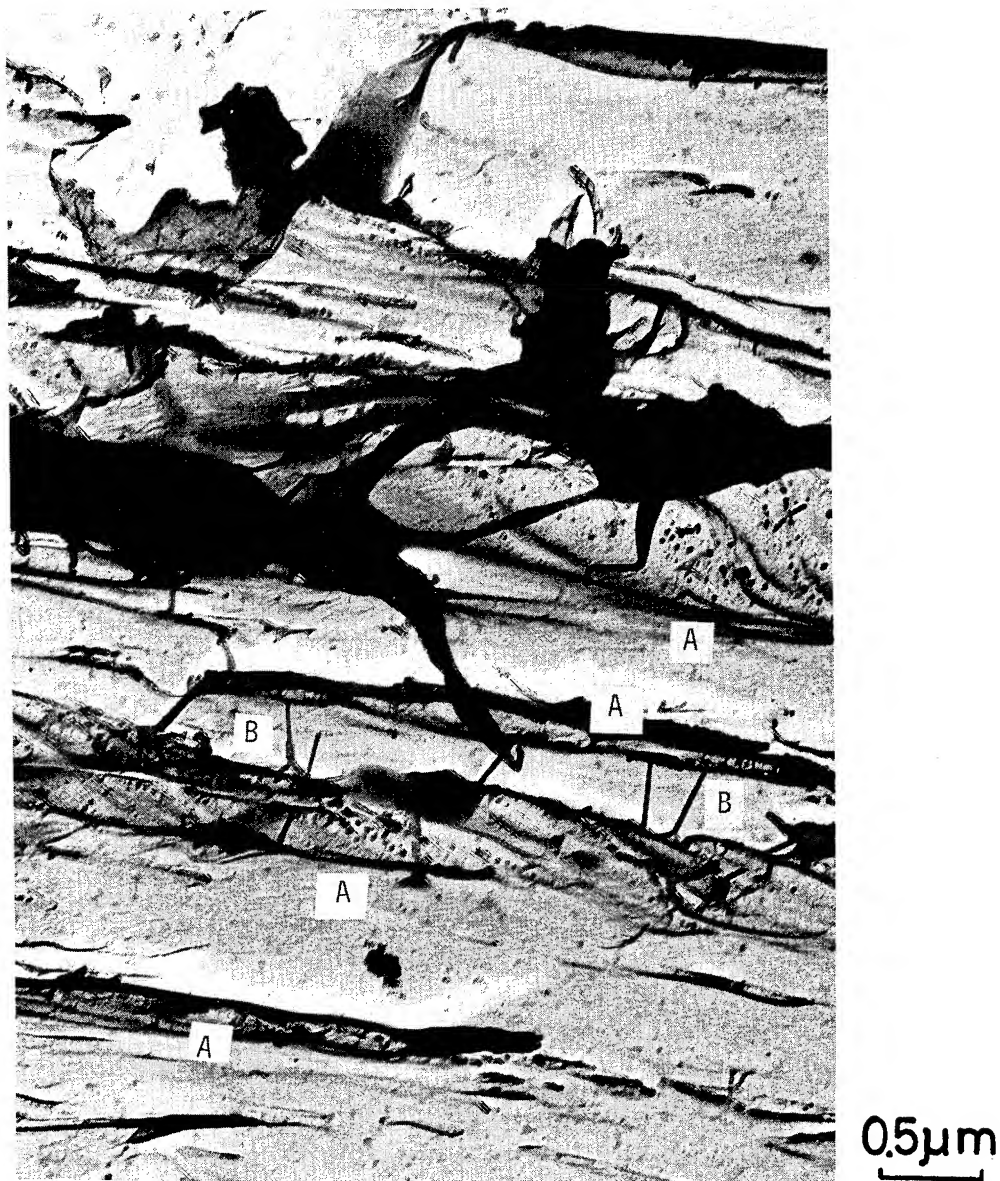
Figure 15. - Electron micrograph of polypropylene fibrils
   adhering to steel disk. (sliding speed, 0.01 m/s)
   A, fibril ; B, interconnected tie fibril.

279
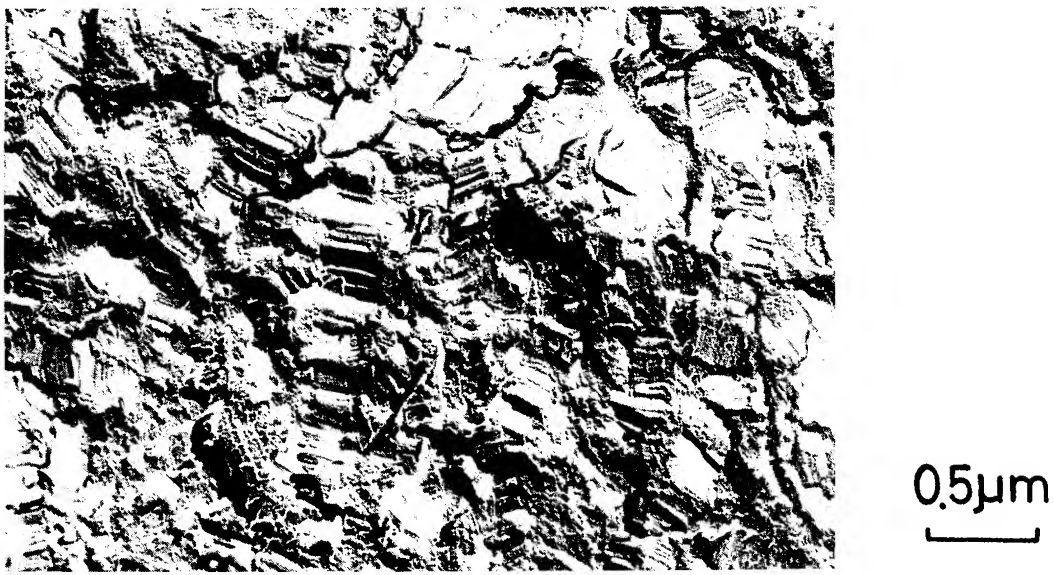
Figure 16. - Electron micrograph of a fractured surface of PTFE.
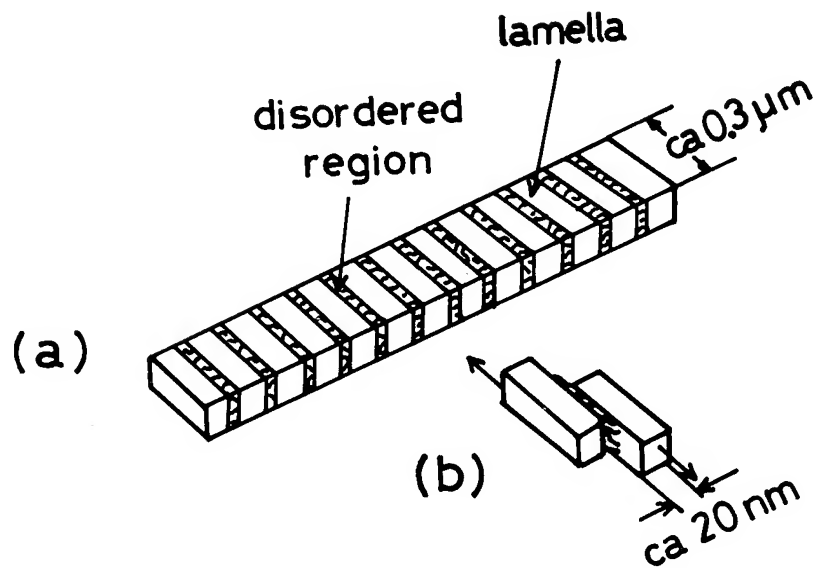
Figure 17. - Schematic representations of the banded structure of PTFE and the slipping of lamellae.

HDPE

LDPE

nylon 6

polyacetal

50μm
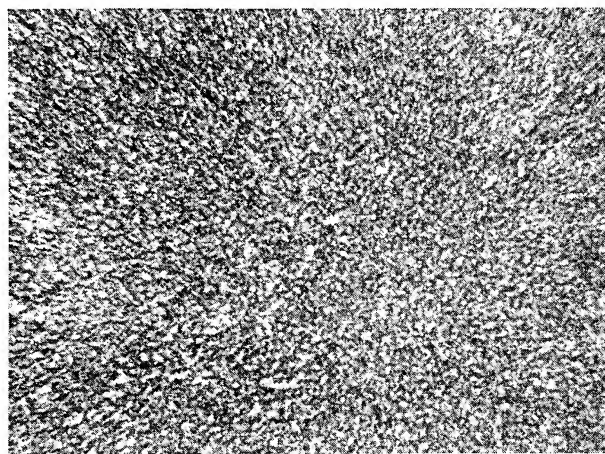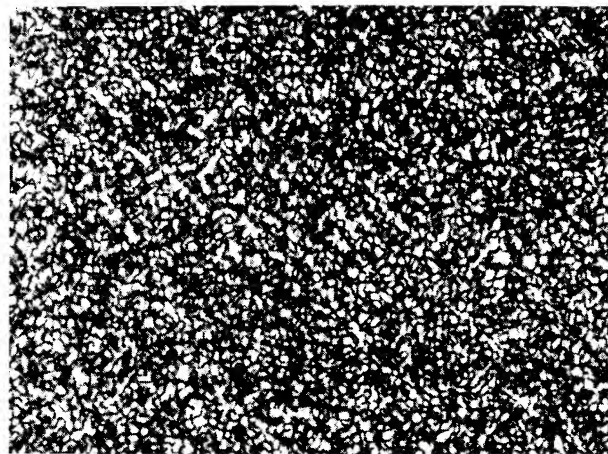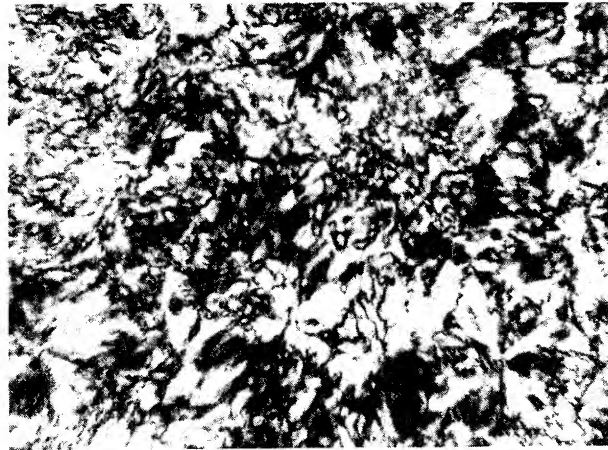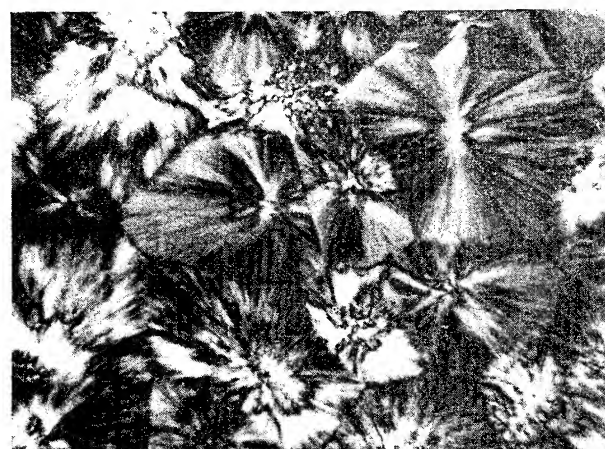
polypropylene

Figure 18. - Polarizing micrographs showing the spherulitic structures of various polymers.
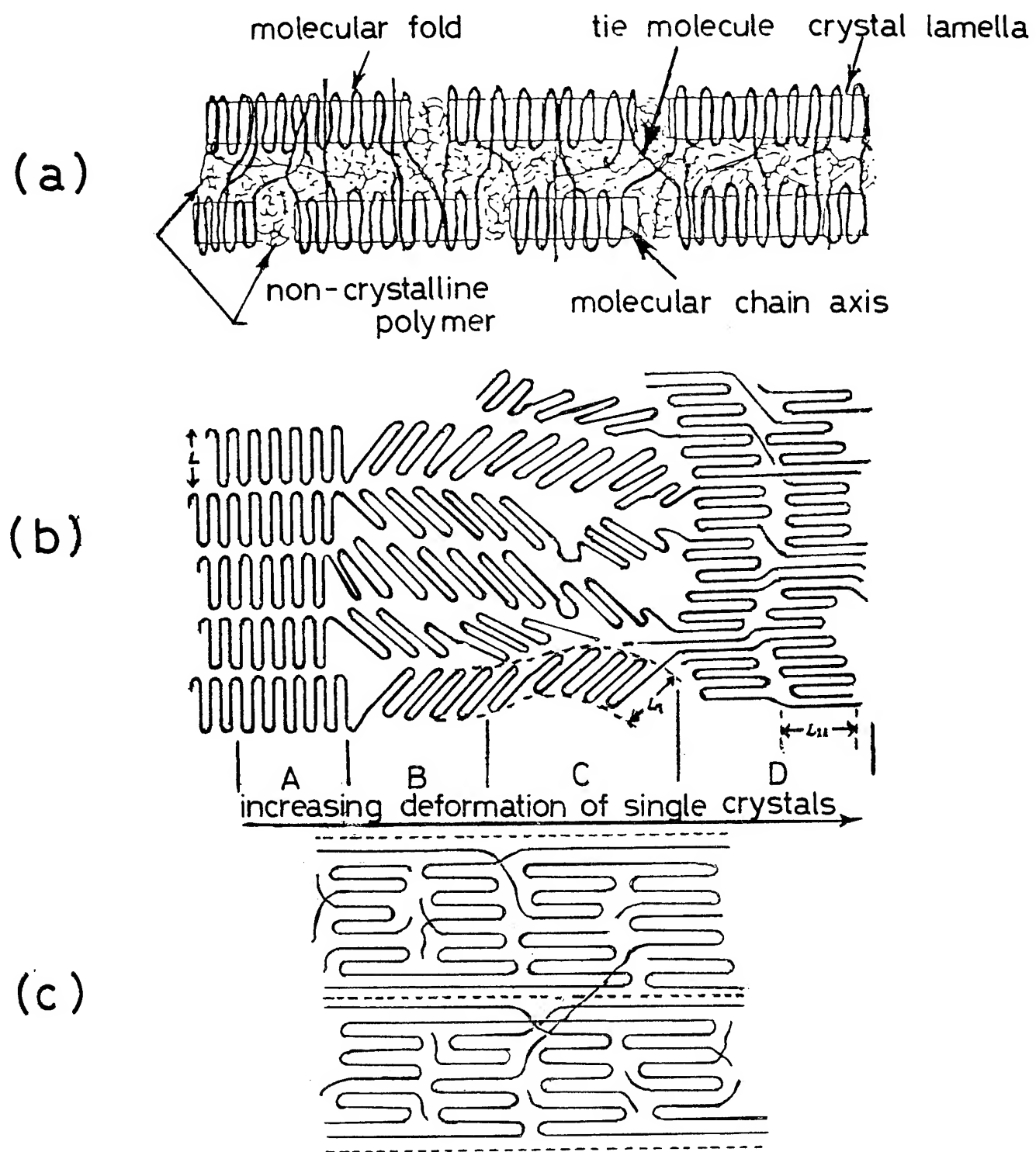
Figure 19. - Schematic representations of the structural components in a spherulite and the deformations. (a) radial fibril, (b) deformation process occurring in the necking of polymers, (c) microfiblillar model showing ordered chain-folded crystal domains and interconnected tie molecules in a polymer fiber.

282
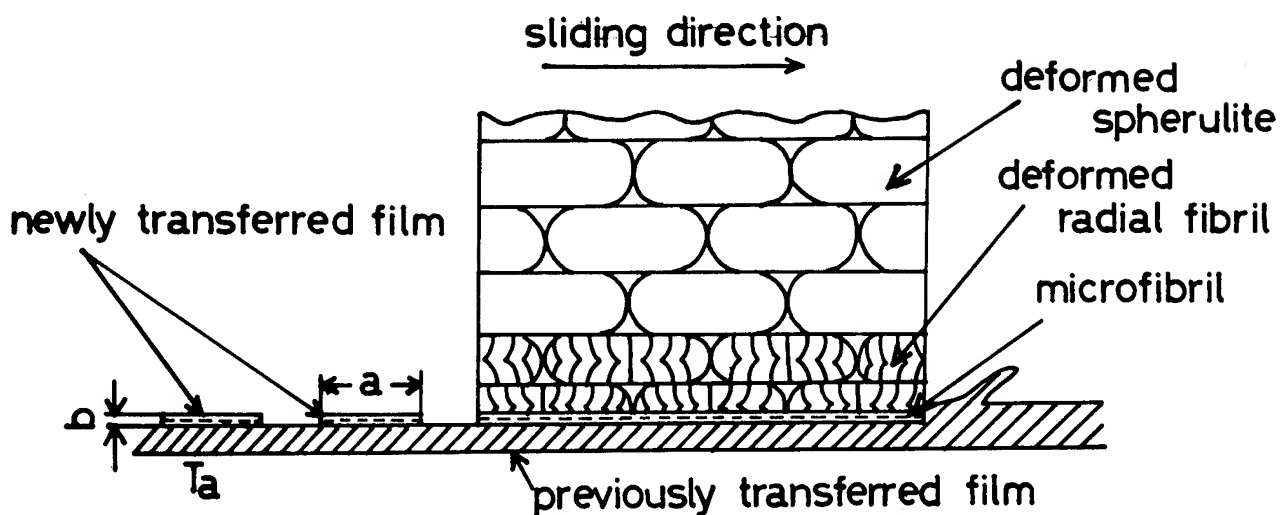
Figure 20. - Schematic representation for a wear process of
polymers having spherulitic structure.
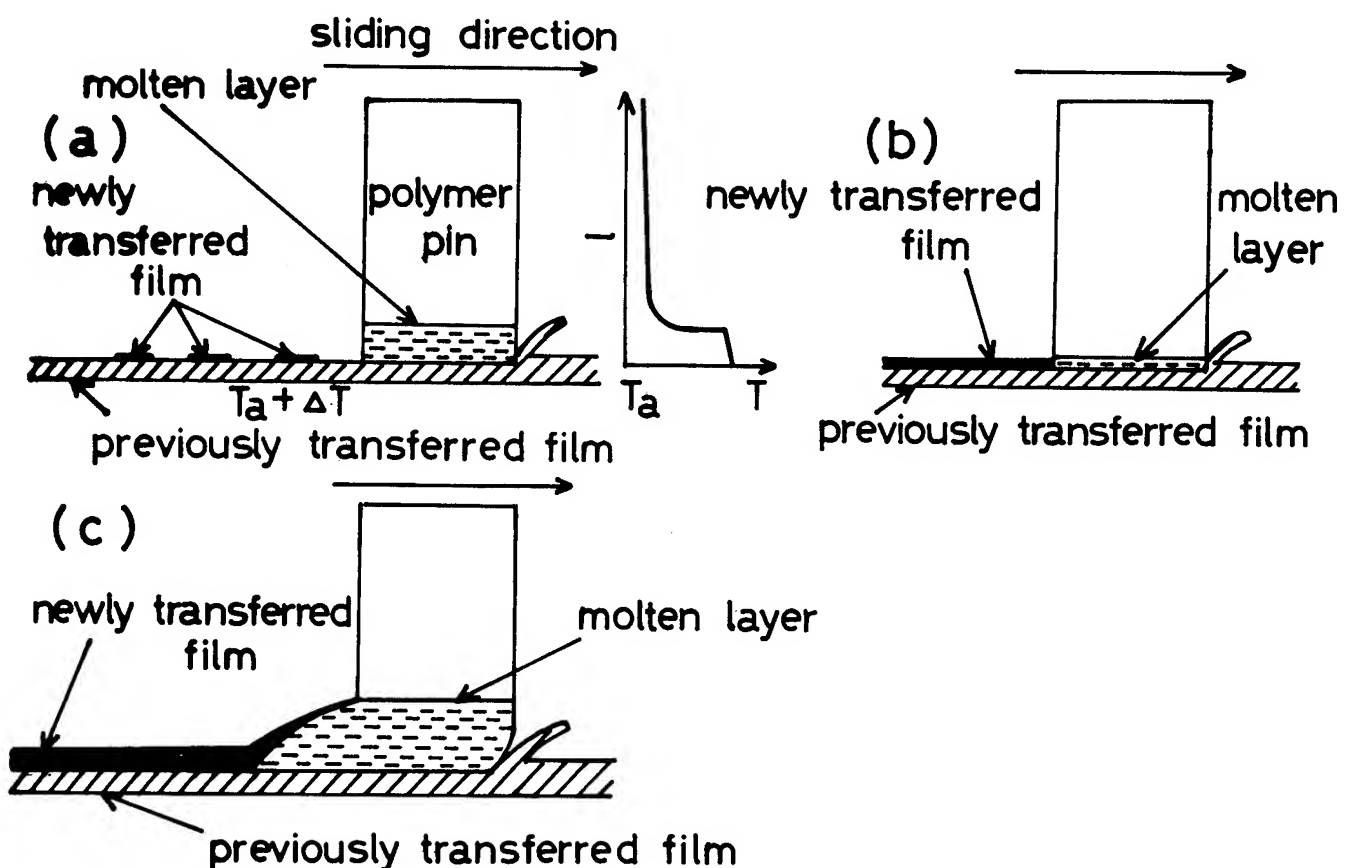
Figure 21. - Schematic representations for the wear processes in which
the surface melting occurs. (a) thin molten layer in many polymers,
(b) thin molten layer in LDPE, (c) outflow in thick molten layer.
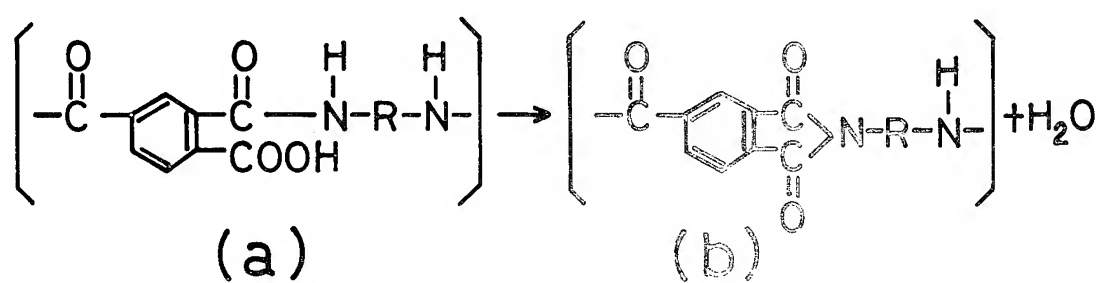
Figure 22. - Chemical reaction in the formation of
   polyamide-imide.

284

DISCUSSION

Brian Briscoe
Imperial College
London, England

Dr. Tanaka's review concenrates upon the adhesive modes of wear
and contains many excellent electron micrographs of transferred films.
Transfer wear processes are poorly understood and Prof. Tanaka has
introduced a number of new ideas. In particular his argument that
spherulite size may be related to the rate of wear is of interest.
The "cold transfer" model he proposes to account for this correlation
does however focus only upon one element of the overall the process;
the thickness of the transfer layer. The total wear process contains
several other aspects such as the adhesion of transfer film the
subsequent removal of transfer film from the counterface and perhaps
of more importance the displacement of loose debris from the contact
zone. I would be interested to hear Dr. Tanaka's comments upon the role
of molecular organisation in these processes.

I would also like to invite Dr. Tanaka's comments upon the recent
work by Hu and Eiss and also by Ni and myself (Wear '83, Reston)
upon the influence of molecular weight and crystallinity upon transfer
wear in PTFE. There seems little doubt that the degree of crystallinity
has a very marked effect upon the rate of transfer wear. The higher the
crystallinity the lower the rate of wear. The evidence also suggests
that high molecular weight also produces lower wear. It may be of
course that high overall crystallinity and high molecular weight also
produce small "ordered" structures. Has Dr. Tanaka observed these
trends in PTFE?

We cannot make such general comments on other organic polymers but it is my feeling that the rate of transfer, as opposed to transfer wear, is largely controlled by the matrix strain softening due to surface tractions. This is seen in an extensive way with the "smooth molecular profile" polymers such as the PTFE's and the linear poly-ethylenes. The first important question is whether a polymer will transfer at all then how readily and in what form. Interface zone shear softening in the matrix provides the locus for cohesive rupture and hence transfer. I can see how the spherulite size might define the internal shear plane but I am not sure that this automatically ensures rupture takes place in this plane. Could Dr. Tanaka comment upon this point?

Finally I would like to make mention of what I see as a major fundamental problem; the transition between "transfer" wear and "abrasive" wear. We know that a rather indiscriminate application Ratner-Lancaster correlation is quite successful in the abrasive regime. In these cases there is a good correlation between the rate of wear and the inverse of the tensile toughness or even the inverse of the strain at tensile rupture. An interesting point emerges. When does transfer wear become abrasive wear as the counterface is roughened and indeed may the size of the spherulites influence this transition? We may then wonder if the difference between the two regimes is just a question of the scale and uniformity of the transferred material. The extent of both processes involve the work or local strain required to remove material from the surface of the polymer be it in a "unit" or "fatigue" process. Again we may conjecture that the scale of the surface molecular organisation may be influential in both processes.

DISCUSSION

Lieng-Huang Lee
Xerox Corporation
Webster Research Center
Webster, New York

(1) Since LDHE is an amorphous polymer, it should have no melting point. Why did you observe the crystalline-spherulitic structure?

(2) Is an amorphous polymer always weaker than crystalline polymer of the same kind (e.g., PE)? If so, why?

(3) Why does PTFE wear slower above its melting point?

Dr. Tanaka's work on the wear of polymer has always been carefully developed. This paper gave an excellent overview of macroscopic and microscopic structures of polymers and their subtle effects on wear. This kind of experimental work is generally more important than those developed by the Russian researchers who constantly apply many parameters in their equations.

DISCUSSION

K. L. Mittal
IBM Corporation
Hopewell Junction, New York

This is an interesting paper and contains some useful information. However, I would like to make the following comments. Apropos, this paper would benefit from improvement in language at certain places.

On p.3 you have calculated 7kcal/mol activation energy (from the temperature dependence of log a_T) for PTFE and this suggests that the slipping of lamellae occurs easily which results in destruction of the banded structure and consequently a high wear rate. Has the activation energy (in a similar fashion) been determined for other polymers, and if yes, then can the magnitude of activation energy be a useful parameter for predicting the wear rate?

On p. 3 what is thickness reduced to the electrical capacitance? How does it relate to the real thickness? A few comparative values would be very helpful.

On p.5 you mention that the transferred material of PTFE is a very thin film whose thickness appears to be below 5nm. How did you determine this thickness? Did you use some chemical spectroscopic method? Is this average thickness, i.e., how uniform is this film?

On p. 5 what is meant by "long films"?

On p.13 you discuss the effect of molecular weight on wear rate. In the case of thermoset polymers, what is the effect of degree of curing or crosslinking on the wear rate? Has this sort of study been carried out? Also in polymeric coatings the internal strains (stresses) are found to be very important with respect to their adhesion to the underlying substrate (see, e.g., S.G. Croll in Adhesion Aspects of Polymeric Coatings, K.L. Mittal, Editor, Plenum Press, April 1983 and references therein) . I presume the stresses should be important in the wear behavior of polymeric coatings. Has the work been carried out to relate stresses with wear rate, and if yes how does annealing of stresses affect the wear rate?

On p.14 you mention the importance of surface energy of polymers in their wear behavior. Recently there has been a great deal of interest in the acid-base characteristics of polymers and other materials (see, e.g., F.M. Fowkes in Physicochemical Aspects of Polymer Surfaces, K.L. Mittal, Editor, Vol.2, pp. 583-603, Plenum Press, March 1983 and references therein). I think it would be very instructive to explore the relevance of acid-base interactions in the wear of polymers, i.e., the role of polymer and sliding metal(oxide) acidity or basicity on the wear rate.

Some other general comments.

Has anybody looked at the wear rate of a plasma deposited polymer(coating) vis-a-vis that deposited by conventional technique? For example it has been reported that the plasma deposited tetrafluoroethylene has different surface energy than the conventional   PTFE(and it may be true for other polymers also)so it would be very informative to study the wear behavior of plasma deposited coatings.

Can you comment on the wear behavior of polymer blends? Can the wear rate of a blend be predicted from the wear behavior of its components?

RESPONSE

Kyuichiro Tanaka
Kanazawa University
Department of Precision Engineering
Ishikawa, Japan

The following are in response to Dr. Lee's comments.

(1) LDPE is generally a semicrystalline polymer, while its crystallinity is lower than that of HDPE.

(2) It seems to be the general concept that an amorphous polymer is weaker than a semicrystalline polymer of the same kind, because the crystalline region is much stronger than the amorphous region and also prevents the mutual slippage of molecules.

(3) As shown in figure 5, the wear rate shows considerable increase abruptly when the steel disk temperature exceeds the melting point, while it does not increase in the temperatures above the melting point. The abrupt increase of wear at the melting point must be due to the increase of transfer rate of PTFE onto the countersurface which is caused by the disappearance of crystallites. On the other hand, the wear behavior in the temperatures above the melting point is considered to be due to the fact that the viscosity of a molten PTFE is extremely high.

CONSIDERATIONS IN FRICTION AND WEAR

Kazuhisa Miyoshi and Donald H. Buckley
National Aeronautics and Space Administration
Lewis Research Center
Cleveland, Ohio 44135

Recent work on the friction and wear properties of ceramics that arise primarily from adhesion between sliding surfaces in contact is reviewed. The role of chemical bonding in adhesion and friction and the influence of surface films, temperature, and crystallographic orientation effects on tribological response with respect to adhesion, friction, and wear are discussed. Also, many investigators have examined the abrasion and friction behavior of ceramic materials and inorganic crystals over the last 30 years. This paper will deal briefly with the subject of abrasion of ceramic materials. Because of the complex interaction of various deformation and fracture mechanisms in ceramics, the effect of crystallographic orientation on abrasion, friction, and fracture behavior will be primarily addressed.

INTRODUCTION AND BACKGROUND

The principal concern of this paper is a fundamental understanding of the tribological properties (adhesion, friction, and wear) as they relate to other material properties of crystalline ceramics. Like all material properties, tribological properties of ceramics are largely determined by their constituent atoms, their arrangement, and the bonding between them as well as those of the contacting counter surface.

The difficulty with studies of ceramic materials is generally that over one-third of the practically used ceramic materials will 5 years from now be those that currently are not available. Particularly with the tribological studies the conditions at and below the sliding surface of a ceramic material are extremely complex in most practical processes. It is, therefore, important to gain a better fundamental understanding of the physics and chemistry of ceramics involved in tribology so that ceramics, like metals and polymers, can be used in tribological applications where their properties can be used to the best advantage.

For the simplicity of discussion, the tribological properties of concern in the processes are separated into two major classes. The first class is that in which the friction and wear of ceramics arise primarily from the adhesion between sliding surfaces in contact and the shear force required to break the interfacial junctions. These forces arising from adhesion are primarily responsible for the frictional force and adhesive wear. The areas of primary concern are (1) the role of chemical bonding in adhesion and friction of ceramic materials sliding against themselves or metals, (2) the influence of surface films, and (3) the temperature effects. These parameters have been discussed with SiC, Al_2O_3, manganese – zinc and nickel – zinc ferrites, BN, and diamond as well as ionic solids by the present authors (refs. 1 to 15).

The second area of interest is where plastic deformation occurs in ceramics, much like metals, as a result of ceramics sliding against a hard material such as diamond. Diamond grits indent ceramics and plow a series of grooves or furrows. Plastic deformation was found to play a significant role, even though ceramic materials are normally brittle and fracture with little or

no evidence of plastic flow, except at a high temperature in bulk deformation experiments.

Steijn and others have measured the friction, deformation, and fracture properties of a host of different ceramic materials and inorganic crystals, including metallic halides, and have found that friction properties are generally anisotropic with these substances (refs. 16 to 27). They have established that the coefficient of friction is very highly dependent on not only the crystallographic plane of sliding but also the crystallographic sliding direction, as has been observed in the investigation of metals.

Anisotropy in the hardness of many metals and ceramics has also been firmly established since the original development of the Knoop hardness test (refs. 28 to 30). The anisotropic hardness behavior has been generally explained with resolved shear stress analyses whether based on tensile or compressive forces by Daniel and Dunn (ref. 31).

The microcracking which occurs in contact loading of ceramics or a brittle solid is a feature basic to a wide range of tribological phenomena. Fracture mechanics analyses of the indentation process and observations of microcrack patterns and fracture behavior in ceramics and other brittle materials have been conducted by many investigators. Lawn, et al., have intensively investigated the fracture mechanics of these materials (ref. 32). The scanning acoustic microscope and acoustic emission techniques used in the fundamental study of microfracture of brittle solids are of interest (refs. 33 to 35).

The presence of surface-active agents on nonmetallic materials, particularly on ionic solids, can influence the mechanical behavior of the surfaces of these solids. Surface-active films can influence the deformation behavior of ionic solids by various mechanisms. These include (1) strengthening by dissolution of the solid surface or the Joffe effect (ref. 36); (2) surface hardening, or the Roscoe effect (refs. 37 and 38); (3) surface softening, or the Rehbinder effect (ref. 39); (4) correlation between hardness and the zeta-potential (refs. 40 and 41); (5) the effect of adsorbed water on indentation creep (refs. 42 and 43); and (6) the formation of chemical compounds in the surficial layers (refs. 44 and 45). The significance of these effects to tribology has been recognized (refs. 46 to 51). Although considerable effort has been put forth in determining the environmental effects on the hardness of solids, neither the fundamentals of surface chemistry involved nor the tribological properties of the solid surfaces in a variety of environments are clearly understood. A number of mechanisms involved in causing the effects of surface-active agents on solids may be identified with the aid of analytical surface tools such as Auger electron and X-ray photoelectron spectroscopies.

ADHESION AND FRICTION

Chemical Bonding

The surfaces of ceramics usually contain, in addition to the constituent atoms, adsorbed films of water vapor, carbon monoxide, carbon dioxide, and oxide layers. For example, figure 1(a) presents an Auger electron spectroscopy spectrum of the single-crystal silicon carbide (0001) surface. A carbon contamination peak is evident as well as an oxygen peak. The carbon peak in the spectrum was similar to that obtained for carbon but not carbide. The presence of a silicon peak at 78 eV and an oxygen peak in figure 1(a) indicates that the surface is covered with silicon oxides as well as a simple adsorbed film of oxygen.

292

In a vacuum environment, sputtering with rare gas ions or heating surfaces to very high temperatures can remove contaminants that are adsorbed on the surface of ceramic materials, as demonstrated by the data in figure 1(b) and (c), respectively.

The Auger spectrum taken after the silicon carbide had been sputter cleaned clearly revealed the main silicon peak at 91 eV and a carbon peak at 272 eV as well as a small argon peak (fig. 1(b)). The oxygen peak is negligible. Moreover, the carbon peak is of the carbide type. The three carbide-type Auger peaks are labeled A_0 to A_2 in figure 1(b), where A is used to denote an Auger peak. The spectrum of the silicon carbide surface heated to 800° C was essentially the same as that obtained for an argon-sputter-cleaned surface. No argon peak, however, is seen in the spectrum, as shown in figure 1(c).

Removing adsorbed films from the surfaces of ceramics and metals results in very strong interfacial adhesion when two such solids are brought into contact. For example, when an atomically clean silicon carbide surface is brought into contact with a clean aluminum surface, the adhesive bonds formed at the silicon carbide – aluminum interface are sufficiently strong that fracture of the cohesive bonds in the aluminum and transfer of the aluminum to the silicon carbide surface result. This is indicated in the scanning electron micrograph and X-ray map presented in figure 2. In figure 2(a) the light area of the figure, where a lot of aluminum transfer is evident, was the contact area before sliding of the aluminum rider. It is the area where the surfaces of the aluminum and the silicon carbide were sticking together and where strong interfacial adhesion occurred. All the metals, to be subsequently discussed herein with reference to their friction properties, transferred to the cohesively stronger ceramics such as silicon carbide and the ferrites.

Clean ceramic to ceramic contacts also result in very strong interfacial adhesion when two such solids are brought into contact (ref. 7). Figure 3 indicates the adhesive bonds formed at the silicon carbide to silicon carbide interface are sufficiently strong that the cohesive bonds fracture. In figure 3 the flat, hexagon-shaped silicon carbide wear debris was observed to transfer to the flat specimen of silicon carbide. The formation of platelet hexagon-shaped wear debris is due to the cleavage of $\{10\bar{1}0\}$ planes, and the platelet flat is due to the cleavage of $\{0001\}$ planes. This is consistent with the results of a study in which sliding friction experiments were conducted with single-crystal manganese – zinc ferrite sliding against itself (ref. 10).

Pauling in 1948 formulated a resonating-valence-bond theory of metals and intermetallic compounds in which numerical values could be placed on the bonding character of the various transition elements (ref. 52). Since the d-valence bonds are not completely filled in transition metals, they are responsible for such physical and chemical properties as cohesive energy, shear modulus, chemical stability, and magnetic properties. The greater the amount or percentage of d-bond character that a metal possesses, the less active is its surface. While there have been critics of this theory, it appears to be the most plausible in explaining the interfacial interactions of transition metals in contact with ceramics as well as with themselves.

When a transition metal is placed in contact with a ceramic material in the atomically clean state, the interfacial bonds between the metal and ceramic that form are going to depend heavily on the character of the bonding in the metal.

The data in figure 4 indicate the coefficients of friction for some of the transition metals in contact with a silicon carbide surface as a function of the d-bond character of the metal. These data indicate a decrease in fric-

tion with an increase in d-bond character, as predicted from Pauling's theory. Titanium and zirconium, which are chemically very active, when in contact with silicon carbide exhibit very strong interfacial adhesive bonding to silicon carbide. In contrast, rhodium and rhenium, which have a very high percentage of d-bond character, have relatively low coefficients of friction. Thus, the d-bond character of the metal influences the adhesion and friction of metals in contact with other nonmetallic materials such as diamond, ferrites, and boron nitride just as it does for metals in contact with silicon carbide (ref. 2). The more active the metal, the higher the coefficient of friction.

As already mentioned, a clean metal in sliding contact with a clean ceramic material will fail either in tension or in shear because some of the interfacial bonds are generally stronger than the cohesive bonds in the cohesively weaker metal. It should, therefore, also be possible to determine such tribological properties as friction in terms of the physical and mechanical properties of these metals (ref. 53).

Figure 4 also presents the coefficients of friction as a function of the theoretical shear strength of the metallic bond. There generally appears to be a strong correlation between friction and the theoretical shear strength of metals. The higher the shear strength, the lower the friction. An estimate of the theoretical (ideal) shear strength τ_{max} for metals subjected to a simple shear mode of deformation was obtained from the repeat distance of atoms b in the direction of shear, shear modulus G, and interplanar spacing d of shearing planes (ref. 53); that is,

$$\tau_{max} = \frac{Gb}{2\pi d} \tag{1}$$

The coefficient of friction for metals was also found to be related to the theoretical tensile strength σ_{max} and actual shear strength of metals (ref. 53). The higher the strength of the metal, the lower the coefficient of friction. The theoretical strength σ_{max} is given by the well-known equation

$$\sigma_{max} = \sqrt{\frac{E\gamma}{d}} \tag{2}$$

where E is the appropriate Young's modulus, γ the surface energy per unit area, and d the interplanar spacing of the planes perpendicular to the tensile axis.

All the metals shown in figure 4 transferred to the surface of silicon carbide with sliding. The morphology of metal transfer to the ceramic material revealed that the metals that have low strength and a low percent d-bond character exhibit much more transfer than those having higher strength and a higher percent d-bond character.

For example, an examination of the wear tracks on the silicon carbide after single-pass sliding with titanium in vacuum revealed that very thin transfer films and lump particles of titanium transferred to the silicon carbide. On the other hand, an examination of the silicon carbide surface after multipass sliding with titanium indicated very thin transfer films, multilayer transfer films, very small particles, and a pile up of particles. Table I summarizes the metal transfer to silicon carbide observed after multiple passes sliding. Generally, metals farther to the right in table I have less chemical affinity for silicon and carbon and greater resistance to tensile and shear fracture and, accordingly, lower coefficients of friction. Therefore, with metals farther to the right in table I, less transfer to

silicon carbide was observed. Thus, the chemical affinity and activity of metal to ceramic materials, tensile strength, and shear strength play important roles in not only the adhesion and friction but also in the transfer and wear of metals contacting ceramic materials.

Today, virtually all the known elements are used to make ceramic materials and products. Probably, however, the most widely used class of ceramic materials is the oxides. The coefficients of friction were measured for such magnetic oxides as nickel – zinc ferrite and manganese – zinc ferrite in contact with various metals in vacuum. The coefficients of friction for the ferrites can be correlated with the free energy of formation of the lowest metal oxides as shown in figure 5. The correlation shown in figure 5 clearly indicates that the metal-ferrite bond at the interface is primarily a chemical bond between the metal atoms and the large oxygen anions in the ferrite surface. The strength of this bond is related to the oxygen–metal bond strength in the metal oxides (refs. 54 to 56). A similar correlation between the shear coefficients of the metal to sapphire contacts and the free energy of formation of the lowest metal oxide was also found (ref. 9).

Environmental Effects

Not only are the friction properties and the mechanical behavior of metals and polymers affected by the presence of surface films, but also those of ceramic materials in sliding contact with themselves or metals.

The surface activity related to the friction properties for a clean ceramic material contacting ceramics or metals is strongly affected by gas or liquid interactions with the surface, such as the adsorption of a specie (physically or chemically adsorbed material) or the chemical reaction of the surface with a specie.

Figure 6(a) presents the coefficients of friction for a clean silicon carbide surface and for a titanium pin in sliding contact with (1) a clean silicon carbide surface and (2) a silicon carbide surface containing a chemically reacted oxide film, as indicated by Auger spectra in figures 6(b) and (c), respectively. Figure 6(b) is the Auger spectrum taken after the silicon carbide surface had been argon sputter cleaned. The spectra clearly reveal the silicon and carbon peaks associated with silicon carbide. Figure 6(c) is an Auger spectrum for the silicon carbide which had been exposed to air at atmospheric pressure and $700°$ C for 10 minutes and subsequently argon sputter cleaned at a pressure of 1.3 pascals. The carbon peak is barely discernible in the spectrum leaving an oxygen peak and a chemically shifted silicon peak at 82 eV indicative of a chemical reaction product layer of SiO_2. The reacted oxide surface interacts with the silicon carbide surfaces to produce two effects: (1) the oxidation of silicon carbide to form a protective oxide surface layer, and (2) the resulting oxide layer increases the coefficients of friction for both silicon carbide to silicon carbide and silicon carbide to titanium contacts. The effects of oxygen when increasing the friction are related to the relative chemical thermodynamic properties of silicon, carbon, and titanium to oxygen. The more chemically active the surface, the greater the degree of oxidation and the higher the coefficient of friction. In such a situation oxygen tends to bond chemically to the surface.

Figure 7 presents the coefficients of friction for various metals in contact with nickel – zinc ferrite, in which both clean metal and ferrite specimens were exposed to 1000 Langmuirs (1×10^{-6} torr-sec) of oxygen gas.

Comparative data for clean metals in contact with clean nickel - zinc ferrite specimens are also presented in figure 7. Solid symbols denote clean metal-ferrite contacts. The data of figure 7 indicate the coefficients of friction as a function of the d-bond character of the metal. Again, the adsorption of oxygen on argon sputter cleaned metal and ferrite surfaces produces two effects: (1) the metal oxidizes and forms an oxide surface layer, and (2) the oxide layer increases the coefficients of friction for the ferrite to metal interfaces. The effect of oxygen adsorption on friction of nickel - zinc ferrite to metal contacts is the same as observed for metals in sliding contact with manganese - zinc ferrite.

Thus, the oxygen exposures did strengthen the metal to ferrite adhesion and increased the friction. The enhanced bond of the metal oxide to ferrite may be due to the formation of a complex oxide on establishing contact.

Temperature Effects

Surface chemistry. - An increase in surface temperature of a ceramic material tends to promote surface chemical reactions. These chemical reactions cause products to appear on the surface which can alter adhesion, friction, and wear (ref. 57).

Figure 8 presents the surface chemistry of silicon carbide analyzed by X-ray photoelectron spectroscopy. The as-received crystal was heated to various temperatures in a vacuum. The Si_{2p} photoelectron peak energies are associated with silicon carbide at various temperatures. The photoelectron lines for C_{1s} of the silicon carbide surface are split asymmetrically into double energy peaks. The results show a significant influence of temperature on the silicon carbide surface. The double energy peaks are due to distinguishable kinds of carbon: (1) a carbon contamination peak and a carbide peak at room temperature, and (2) the graphite and the carbide peaks at temperatures from 400° to 1500° C.

At room temperature and 250° C, the primary peaks were the adsorbed carbon contamination and carbide. For specimens heated to 400° C the carbon contamination peak disappears from the spectrum. Above 400° C both the peak heights of graphite and the carbide are increased with an increase of heating temperature. A large carbide peak was distinguished at 800° C. At 900° C the carbide peak height was smaller than that at 800° C, but the graphite peak height was larger. At 1000° C the height of the carbide peak decreased and became smaller than that of the graphite. At 1500° C the height of carbide peak became very small, but a very large graphite peak was observed. The results indicate that temperature affects the surface chemistry significantly and the surface of silicon carbide graphitizes.

Three questions arise as a result of the foregoing observations:
(1) How thick is the graphite layer formed on the silicon carbide?
(2) What is the graphitization mechanism for silicon carbide?
(3) Does the graphite affect the friction properties of silicon carbide?

Table II presents the estimated thickness of the graphite layer formed on the silicon carbide surface (ref. 1). The thickness of the outermost surficial graphite layer on the silicon carbide heated to 1500° C is 1.5 to 2.4 nm. This result suggests that the collapse of the carbon of two or three successive silicon layers after evaporation of the silicon is the most probable mechanism for the graphitization of silicon carbide surface (ref. 1).

A complete elemental depth profile analysis for the silicon carbide surface heated to 1500° C was conducted. The depth profiling indicated that

the depth of a mixture of graphite and silicon carbide was of the order of 100 nm (ref. 1).

Friction. – To answer the third question, sliding friction experiments were conducted with silicon carbide in contact with iron in vacuum (fig. 9).

As mentioned, the heating to 800° C removed contaminants that were adsorbed on the silicon carbide surface. After being heated to 800° C and cooling to room temperature, the silicon carbide specimen was reheated to 800° C. Silicon carbide surfaces after reheating at any temperature revealed the same Auger spectrum as a surface after preheating to 800° C as shown in figure 9(b).

As is generally known, both the Auger and XPS spectrums of an element depend strongly on the chemical bonding state. Therefore, the surfaces preheated to 800° C have nearly the same surface condition as those of specimens reheated to 800° C.

The friction properties of the silicon carbide {0001} surface in contact with iron at temperatures to 800° C after preheating to 800° C are indicated by the data in figure 9. The coefficient of friction generally increased with increasing temperature from about 0.5 in the {10$\overline{1}$0} sliding direction and 0.4 in the <11$\overline{2}$0> sliding direction at room temperature to 0.75 and 0.63, respectively, at 800° C. Although the coefficient of friction remained low, below 300° C, it increased rapidly with increasing temperature in the 300° to 600° C range with little further increase in friction above 600° C.

The rapid increase in friction at temperatures from 300° to 600° C may be due to an increase in the adhesion resulting from recrystallization of the iron. Iron normally recrystallizes at 200° to 300° C. The experiments herein were started with textured surfaces of polycrystalline iron because the surfaces were mechanically polished. Iron in contact with silicon carbide will recrystallize at 300° to 600° C. Recrystallized annealed iron surfaces are less resistant to deformation and adhesion than are textured surfaces. The general increases in friction at high temperatures are due to increased adhesion and increased plastic flow in the area of contact.

As already indicated, the heating to 1500° C graphitizes the silicon carbide surface. After being heated to 1500° C, the silicon carbide specimen was cooled to room temperature and then reheated to 1200° C. The surface of the silicon carbide after reheating at any temperature revealed the same Auger spectrum as that typically shown in figure 9(c). Friction experiments were conducted on the reheated surface of silicon carbide.

The friction properties of silicon carbide surfaces in contact with iron at temperature to 1200° C are shown in figure 9. The solid symbols denote the coefficient of friction for the silicon carbide preheated to 1500° C. When compared with the results for the silicon carbide preheated to 800° C (open symbols), the coefficients of friction are generally lower (solid symbols) with the silicon carbide preheated to 1500° C.

The low friction over the entire temperature range correlates with the graphitization of the silicon carbide surface. The coefficients of friction on this surface at the high temperatures are nearly the same as those on pyrolytic graphite in sliding contact with single-crystal iron in a vacuum of 10^{-8} Pa (ref. 58).

Furthermore, sliding friction experiments were also conducted in air with the surfaces of the silicon carbide specimens, which had been heated to 800° and 1500° C, sliding against various metals. The friction properties are shown in figure 10. The coefficients of friction for the graphitized surface of the silicon carbide specimen heated to 1500° C are generally twice as low as those for the surface heated to 800° C. The marked difference in friction shows the effect of graphitization of silicon carbide on the friction proper-

ties even in air. Figure 10 also indicates the marked difference in friction for the two environments. The coefficients of friction for various metals sliding on silicon carbide in air were much lower than those in vacuum.

Crystallographic Orientation Effects

Although considerable effort has been used to determine the anisotropic friction behavior of single crystals on a variety of crystallographic planes and directions, the anisotropic friction and wear arise primarily from non-adhesive processes such as abrasion, as will be discussed later. Very few studies of the anisotropic nature of friction and wear have been conducted from the consideration of adhesion between the sliding surfaces.

The data in figure 9 indicate that the adhesion and friction behavior of silicon carbide in contact with iron is highly anisotropic over the entire temperature range from room temperature to $800°$ C. Several slip systems have been observed in α-silicon carbide including the $\{0001\}$ $<11\bar{2}0>$, $\{3\bar{3}01\}$ $<11\bar{2}0>$, and $\{10\bar{1}0\}$ $<11\bar{2}0>$ (refs. 59 and 60). The preferred crystallographic slip direction, or the direction of shear for the basal $\{0001\}$ plane, is the $<11\bar{2}0>$ direction. Examination of the coefficient of friction on the basal plane indicates that it was lower in the $<11\bar{2}0>$ direction than in the $<10\bar{1}0>$ direction; that is, it was lower in the preferred crystallographic direction than in the $<10\bar{1}0>$ direction. The plastic deformation of crystalline substances can occur by means of translational slip, in which one part of a crystal slides as a unit across a neighboring part. The slip direction is almost always that along which the atoms are most closely packed; namely, the preferred crystallographic direction. The results of figure 9 revealed that the highest atomic density (most closely packed) direction exhibits the lower coefficient of friction. This indicates that direction is important in the friction behavior of crystalline substances.

The formation of graphite hexagon is possible, and an orientation of the formed graphite layer on the silicon carbide surface that was preheated to $1500°$ C seems probable. This orientation effect influences the friction behavior of the basal plane of silicon carbide, as shown in figure 9.

Figure 11 presents the coefficient of friction for single-crystal manganese – zinc ferrite in contact with itself in vacuum. In the results presented in figure 11 the $\{110\}$ rider slid on the flat surfaces of the $\{110\}$, $\{111\}$, and $\{211\}$ planes in the same crystallographic direction as that of the rider and in dissimilar crystallographic directions. Sliding in the same direction was in the $<110>$ directions on both rider and disk. When the sliding was in different directions, it was in the $<110>$ direction of the rider and the $<100>$ direction on the $\{110\}$ surface of the disk, in the $<211>$ direction on the $\{111\}$ surface of the disk, and in the $<111>$ direction on the $\{211\}$ surface of the disk. As expected, the differences in the coefficients of friction with respect to the mating crystallographic directions are significant. The coefficients of friction for the three matched crystallographic planes in dissimilar directions are generally higher than those in the same directions and vary according to the orientation of the surface of the disk.

The coefficient of friction is lowest with $\{110\}$ plane of the rider parallel to the interface, that is, at an angle of zero to the sliding mating surface. Thus, the mating of highest atomic density directions on matched crystallographic planes results in the lowest coefficient of friction, and the mating of higher atomic density planes may also result in lower coefficients of friction. These results indicate that mating the crystallographic direction can play a significant role in the friction behavior of ferrite. Sliding

298

along the direction which is most closely packed minimizes adhesion and friction.

WEAR UNDER ADHESIVE CONDITION

The sliding of a metal or ceramic rider on a ceramic surface results very locally in cracks along cleavage planes. For example, figure 12 presents scanning electron micrographs of the wear tracks generated by ten passes of rhodium and titanium riders on the silicon carbide {0001} surface along the <10$\bar{1}$0> direction. The cracks, which are observed in the wear tracks, primarily propagate along cleavage planes of the {10$\bar{1}$0} orientation. In figure 12(a), a hexagonal light area is the beginning of a wear track, and there is a large crack where cracks primarily along the {10$\bar{1}$0} planes were generated, propagated, and then intersected during loading and sliding of the rhodium rider on the silicon carbide surface. It is anticipated from figure 12(a) that subsurface cleavage cracking of the {0001} planes, which are parallel to the sliding surface, also occurs. Figure 12(b) reveals a hexagonal pit and a copious amount of thin titanium film around the pit. The hexagonal fracturing is primarily due to cleavage cracking along {10$\bar{1}$0} planes and subsurface cleavage cracking along the {0001} plane. The very smooth surface at the bottom of the hexagonal pit is due to cleavage of the {0001} planes.

Detailed examination of silicon carbide wear debris produced by ten-pass sliding of aluminum riders on the silicon carbide surface revealed evidence of multiangular wear debris particles of silicon carbide with transferred aluminum wear debris on the silicon carbide wear track. Such multiangular wear debris particles had crystallographically oriented sharp edges. They had shapes which were nearly hexagonal, rhombic, parallelogram, or square (ref. 7). These shapes may be related to surface and subsurface cleavage of {10$\bar{1}$0}, {11$\bar{2}$0} and {0001} planes.

Similar fracture pit and multiangular wear debris, having crystallographically oriented sharp edges, were also observed with single-crystal manganese – zinc ferrite in contact with itself or a metal (ref. 10). The fracture behavior of the ferrite crystal during sliding is significantly dependent on the cleavage systems of {110} planes. Not only does the fracture wear of ceramic materials depend on the cleavage systems, but it is also dependent on stress trajectories in a solid occurring during the sliding process.

Figure 13 presents a scanning electron micrograph of the wear track on the silicon carbide surface where the wear track was generated by a single-pass sliding of the iron rider at 800° C in a vacuum of 10^{-8} Pa. The wear track contained microfracture pits in very small areas in the sliding contact region. Two kinds of fracture pits were generally clearly observed in wear tracks: (1) pits with spherical debris and (2) pits with multiangular wear debris that have crystallographically oriented sharp edges and are nearly of a hexagonal platelet shape. These results revealed that a nearly spherical debris particle can exist in the fracture pit. In other words, a spherical fracture occurs in even single-crystal silicon carbide under the sliding surface with sliding friction contact.

The present authors have suggested a mechanism for generating a spherical wear debris particle (ref. 5). Briefly, the mechanism has two aspects involving (1) a stress concentration and (2) a circular or spherical fracture.

When two solid surfaces are in contact, stress concentration at the contact area may produce a small zone of inelastic deformation in the solid. Cracks will subsequently be initiated in the solid. The cracks develop stable

299

growth in a subsurface region and on the surface around the inelastic deformation zone during the loading and unloading processes.

The cracks also grow easily by application of shearing force during sliding. The cracks are generally circular, spherical, and radial.

The spherical cracks may be developed along circular stress trajectories (ref. 61) in solids. Although crystallinity is imposed on the crack geometries of anisotropic materials such as silicon carbide, it is possible that the cracks may grow and pile up in atomistic terms by the sequential rupture of cohesive bonds along the circular or spherical stress trajectories (ref. 61).

ABRASION AND FRICTION

Deformation and Fracture

Abrasion occurs if a hard particle or a hard asperity cuts or plows the surface of the ceramic materials. However, if the particle is smooth and has dull corners or edges, the process probably involves elastic deformation rather than plastic deformation. For example, with a diamond rider of radius of 0.3 mm in contact with silicon carbide in a load range up to 0.5 N, the sliding involves primarily elastic deformation. The coefficient of friction is not constant but decreases as the load increases, as shown in figure 14(a). The sliding truly occurred at the interface, and an elastic deformation occurred in both silicon carbide and diamond accounting for the low friction observed.

Over the entire load range, when an estimate is made, the mean contact pressure is about 150 to 350 kg/mm^2. The maximum pressure at the center according to Hertz will be about 230 to 490 kg/mm^2. Furthermore, to a first approximation for the load range investigated, the relation between coefficient of friction μ and load W is given by an expression of the form

$$\mu = KW^{c-1} \qquad (c - 1 \doteq -1/3)$$

The inverse minus 3 power may be interpreted most simply as arising from an adhesion mechanism, the area of contact being determined by elastic deformation herein (ref. 62). Bowden, et al., has found a similar friction characteristic for diamond on diamond in vacuum (ref. 64).

It should be noted further that, even at the high magnifications (up to 10,000 times) of the scanning electron microscope, no groove formation due to plastic flow and no cracking of silicon carbide with sliding were observed.

If a hard particle is smooth and sharp enough, most of the abrasion will be in the form of plastic grooves with very little removal of ceramic material. With riders having radii of 0.15 and 0.02 mm, the friction is not constant but increases as the load increases, as indicated by the data in figure 14(b). To a first approximation for this load range, the relation between coefficient of friction μ and load W is given by $\mu = KW^{c-1}$. The index c depends on the radius of curvature of the rider. The value of c is approximately 1.3 for riders having radii of 0.02 and 0.15 mm. The value of c indicates that friction is due to shearing and plowing of silicon carbide by the diamond rider. The surface replication electron micrographs of wear tracks generated by the diamond clearly indicate that

plastic deformation occurred primarily in silicon carbide, and permanent grooves with very small cracks in silicon carbide were formed during sliding (ref. 63). The calculated mean contact pressure, at a load of 0.5 N with a rider of radius 0.02 mm, is about 2000 kg/mm^2. The maximum pressure at the center would be approximately 3000 kg/mm^2, the yield pressure of silicon carbide.

Further sliding friction experiments were conducted with a hard particle having more sharp edges than that of the case conical diamond rider. The apical angle of the rider was 117° and the radius of curvature at the apex was less than 5 micrometers to provide a high contact pressure, that is, a high concentrated stress in the contact area. This friction process is accompanied by both gross surface cracking and plastic deformation.

Figure 15(a) shows a scanning electron micrograph of the wear track and wear debris before gross sliding. In this case, both loading and tangential forces were applied to the silicon carbide specimen, but no gross sliding was observed. In figure 15(a), the sector-shaped light area adjacent to and ahead of the wear track (plastic indentation) made by the rider is a large particle of wear debris which was generated during micro-sliding of the rider. A large number of small wear debris particles are also generated during loading and micro-sliding by the rider. It is anticipated from figure 15(a) that gross fracturing is primarily due to cleavage cracking along {10$\bar{1}$0} planes and subsurface cleavage cracking. Figure 15(b) shows a scanning electron micrograph of a wear track and the wear debris after gross sliding. Figure 15(b) reveals the wear debris has been separated by gross-sliding of the rider and the wear track is plastically deformed. Figure 15(c) indicates the third stage of the fracture process. One of the gross wear debris particles fractured, divided, and was ejected from the wear track. The track, from which the wear debris particle was ejected, reveals that the fracturing is the result of surface cracking. This cracking occurs as a result of cleavage of {10$\bar{1}$0} planes, and subsurface cracking occurs as a result of cleavage along {0001} planes. Dislodged gross wear particles can be observed near the wear track in figure 15(c).

Crystallographic Orientation Effects

The coefficient of friction and the widths of the permanent grooves in plastic flow accompanied by surface cracking were measured as functions of the crystallographic direction of sliding on the {0001}, {10$\bar{1}$0}, and {11$\bar{2}$0} planes of silicon carbide for the diamond rider in mineral oil. Mineral oil was used to minimize adhesion. Figure 16 indicates that the coefficient of friction and the groove width are influenced by the crystallographic orientation. The <11$\bar{2}$0> direction on the basal {0001} plane has the larger groove, primarily as a result of plastic flow, and it is the direction of high friction for this plane. The <0001> directions on the {10$\bar{1}$0} and {11$\bar{2}$0} planes have the greater groove width and are the directions of high friction when compared with the <11$\bar{2}$0> on the {10$\bar{1}$0} plane and the <10$\bar{1}$0> on the {11$\bar{2}$0} plane.

Figure 16 also represents the contact pressure calculated from the data of the groove width in figure 16(b) and the Knoop hardness obtained by Shaffer (refs. 65 and 66). The anisotropies of the contact pressure during sliding and Knoop hardness clearly correlate with each other. The anisotropies of friction, groove width, contact pressure, and Knoop hardness on the {0001}, {10$\bar{1}$0}, and {11$\bar{2}$0} planes of silicon carbide are primarily controlled by the slip system {10$\bar{1}$0} <11$\bar{2}$0> and are explained by a resolved shear stress calculation.

Figure 16 suggests that the $\langle 10\bar{1}0 \rangle$ directions on the basal plane of silicon carbide would exhibit the lowest coefficient of friction and greatest resistance to abrasion resulting from plastic deformation.

Figure 17 presents the coefficient of friction as a function of the crystallographic direction of sliding on the {100}, {110}, {111}, and {211} planes of manganese - zinc ferrite in sliding contact with a spherical diamond rider with a radius of 20 μm at a load of 1 N in laboratory air. The sliding involved primarily plastic flow as well as surface cracking in maganese - zinc ferrite. Figure 17 indicates that the coefficient of friction is influenced by the crystallographic orientation. The anisotropic friction and deformation of manganese - zinc ferrite may be controlled by the slip systems {110} <110>.

CONCLUSIONS

From the results of experiments on single-crystal and polycrystalline ceramic materials the following conclusions are drawn:

1. Friction characteristics of ceramic materials in sliding contact with metals can be related to fundamental physical and chemical properties of the metals. Both ideal tensile and shear strengths of metals correlate with observed friction behavior. The d valence bond character of elemental metals relates to observed adhesion and friction. The greater the degree of bond saturation, the lower the adhesion and friction. With the oxide ceramic-metal system the interfacial bond can be regarded as a chemical bond between the oxygen anion in the ceramic surfaces and metal atoms. The bonding strength, that is, the coefficient of friction, correlates with the free energy of formation of the lowest metal oxide.

2. There is a significant temperature influence on both the surface chemistry and friction properties. An increase in surface temperature tends to promote surface chemical reaction and to increase friction. The chemical reaction cause products to appear on the surface which can alter adhesion and friction. For example, when the surface of silicon carbide is heated above 800° C, the surface graphitizes and the coefficient of friction is dramatically lower.

3. The sliding on the highest atomic density (most closely packed) planes and directions can minimize the adhesion and friction.

4. Multiangular and spherical wear particles of ceramics are observed as a result of sliding friction under a high adhesive condition. Multiangular wear particles are produced by cleavage cracking. Spherical wear debris may be produced where a spherical-shaped fracture occurs along circular or spherical stress trajectories under the inelastic deformation zone in the contact area.

5. In the case that friction and wear of ceramics arise primarily from abrasion, the primary slip systems of ceramics can explain the anisotropy of friction and deformation observed. The anisotropic fracture during sliding is controlled by the surface and subsurface cracking along cleavage planes.

REFERENCES

1. Miyoshi, K.; and Buckley, D. H.: XPS, AES and Friction Studies of Single-Crystal Silicon Carbide. Appl. Surf. Sci., vol. 10, no. 3, 1982, pp. 357-376.
2. Miyoshi, K.; and Buckley, D. H.: Adhesion and Friction of Transition Metals in Contact with Non-Metallic Hard Materials. Wear, vol. 77, 1982, pp. 253-264.

3.   Miyoshi, K.; and Buckley, D. H.: Anisotropic Tribological Properties of SiC. Wear, vol. 75, 1982, pp. 253-268.

4.   Miyoshi, K.; and Buckley, D. H.: The Adhesion, Friction, and Wear of Binary Alloys in Contact with Single-Crystal Silicon Carbide. J. Lubr. Technol., vol. 103, no. 2, Apr. 1981, pp. 180-187.

5.   Miyoshi, K.; and Buckley, D. H.: The Generation and Morphology of Single-Crystal Silicon Carbide Wear Particles Under Adhesive Conditions. Wear, vol. 67, 1981, pp. 303-319.

6.   Miyoshi, K.; and Buckley, D. H.: Friction and Wear Behavior of Single-Crystal Silicon Carbide in Sliding Contact with Various Metals. ASLE Trans., vol. 22, no. 3, 1979, pp. 245-256.

7.   Miyoshi, K.; and Buckley, D. H.: Friction and Fracture of Single-Crystal Silicon Carbide in Contact with Itself and Titanium. ASLE Trans., vol. 22, no. 2, 1979, pp. 146-153.

8.   Buckley, D. H.: Friction and Wear Behavior of Glasses and Ceramics. Surfaces and Interfaces of Glass and Ceramics. V. D. Frechette, W. C. LaCourse, and V. L. Burdick, eds., Plenum Press, 1974, pp. 101-126.

9.   Pepper, S. V.: Shear Strength of Metal-Sapphire Contacts. J. Appl. Phys., vol. 47, no. 3, Mar. 1976, pp. 801-808.

10. Miyoshi, K.; and Buckley, D. H.: Friction and Wear of Single-Crystal Manganese-Zinc Ferrite. Wear, vol. 66, 1981, pp. 157-173.

11. Buckley, D. H.: Friction and Transfer Behavior of Pyrolytic Boron Nitride in Contact with Various Metals. ASLE Trans., vol. 21, no. 2, Apr. 1978, pp. 118-124.

12. Miyoshi, K.; and Buckley, D. H.: Adhesion and Friction of Single-Crystal Diamond in Contact with Transition Metals. Appl. Surf. Sci., vol. 6, no. 2, Oct. 1980, pp. 161-172.

13. Pepper, S. V.: Effect of Electronic Structure of the Diamond Surface on the Strength of the Diamond-Metal Interface. J. Vac. Sci. Technol., vol. 20, no. 3, Mar. 1982, pp. 643-646.

14. King, R. F.; and Tabor, D.: The Strength Properties and Frictional Behavior of Brittle Solids. Proc. Roy. Soc., London, vol. A223, no. 1153, 1954, pp. 225-237.

15. Steijn, R. P.: Sliding and Wear in Ionic Crystals. J. Appl. Phys., vol. 34, no. 2, Feb. 1963, pp. 419-428.

16. Steijn, R. P.: Friction and Wear of Single Crystals. Wear, vol. 7, 1964, pp. 48-66.

17. Steijn, R. P.: Friction and Wear of Rutile Single Crystals. ASLE Trans., vol. 12, no. 1, Jan. 1969, pp. 21-33.

18. Steijn, R. P.: On the Wear of Sapphire, J. Appl. Phys., vol. 32, no. 10, 1961, pp. 1951-1958.

19. Duwell, E. J.: Friction and Wear of Single-Crystal Sapphire Sliding on Steel. J. Appl. Phys., vol. 33, no. 9, 1962, pp. 2691-2698.

20. Bowden, F. P.; and Hanwell, A. E.: The Friction of Clean Crystal Surfaces. Proc. R. Soc. London, Ser. A, no. 295, no. 1422, 1966, pp. 233-243.

21. Brown, W. R.; Eiss, N. S., Jr.,; and McAdams, H. T.: Chemical Mechanism Contributing to Wear of Single-Crystal Sapphire on Steel. J. Am. Ceram. Soc., vol. 47, no. 4, 1964, pp. 157-162.

22. Bowden, F. P.; and Hanwell, A. E.: Friction and Wear of Diamond in High Vacuum. Nature, vol. 201, no. 4296, 1964, pp. 1279-1281.

23. Seal, M.: The Abrasion of Diamond. Proc. R. Soc. London, Ser. A, vol. 248, no. 1254, 1958, pp. 379-393.

24. Bowden, F. P.; and Brookes, C. A.: Frictional Anisotropy in Nonmetallic Crystals. Proc. R. Soc. London, Ser. A, vol. 295, no. 1442, 1966, pp. 244-258.

25. Tanaka, K.; et al.: Friction and Deformation of Mn–Zn Ferrite Single Crystals. Proc. JSLE–ASLE International Lubrication Conference, T. Sakurai, ed., Elsevier, Amsterdam, 1976, pp. 58–66.
26. Miyoshi, K.; and Buckley, D. H.: Friction and Wear of Single–Crystal Manganese–Zinc Ferrite. Wear, vol. 66, 1981, pp. 157–173.
27. Bowden, F. P.; Brookes, C. A.; and Hanwell, A. E.: Anisotropy of Friction in Crystals, Nature, vol. 203, no. 4940, 1964, pp. 27–30.
28. Sugita, T.; and Hashikawa, A.: The Roles of Brittle Microfracture and Plastic Flow in the Wear of MgO Single Crystals. Wear, vol. 72, 1981, pp. 295–303.
29. Knoop, F.; Peters, C. G.; and Emerson, W. B.: A Sensitive Pyramidal-Diamond Tool for Indentation Measurements. J. Res. Nat. Bur. Stand., vol. 23, 1939, pp. 39–61.
30. Winchell, H.: The Knoop Microhardness Tester as a Mineralogical Tool. Am. Mineral., vol. 30, 1945, pp. 583–595.
31. Thibault, N. W.; and Nyquist, H. L.: The Measured Knoop Hardness of Hard Substances and Factors Affecting its Determination. Trans. Am. Soc. Met., vol. 38, 1947, pp. 271–330.
32. Daniels, F. W.; and Dunn, C. G.: The Effect of Orientations on Knoop Hardness of Single Crystals of Zinc and Silicon Ferrite. Trans. Am. Soc. Met., vol. 41, 1949, pp. 419–442.
33. Lawn, B.; and Wilshaw, R.: Indentation Fracture: Principles and Applications. J. Mater. Sci., vol. 10, June 1975, pp. 1049–1081.
34. Yamanaka, K.; and Enomo, Y.: Observation of Surface Cracks with Scanning Acoustic Microscope. J. Appl. Phys. In process (1982).
35. Ikawa, N.; Shimada, S.; and Ono, T.: Microstrength of Diamond. Technology Reports of the Osaka University, vol. 26, no. 1298, 1976, pp. 245–254.
36. Ikawa, N.; and Shimada, S.: Microstrength Measurement of Brittle Materials. Technology Reports of the Osaka University, vol. 31, no. 1622, 1981, pp. 315–323.
37. Joffe, A. F.: The Physics of Crystals. McGraw–Hill Book Co., Inc., 1928.
38. Roscoe, R.: The Plastic Deformation of Cadmium Single Crystals. Philos. Mag., vol. 21, 1936, pp. 399–406.
39. Harper, S.; and Cottrell, A. H.: Surface Effects and the Plasticity of Zinc Crystals. Proc. Phys. Soc., ser. B, vol. 63, pt. 5, May 1950, pp. 331–338.
40. Rehbinder, P. A.; and Shchukin, E. D.: Surface Phenomena in Solids During Deformation and Fracture Processes. Progress in Surface Science, Vol. 3, S. G. Davison, ed., Pergamon Press, Inc., 1973, pp. 97–188.
41. Macmillan, N. H.; Huntington, R. D.; and Westwood, A. R. C.: Relationship Between Zeta–Potential and Dislocation Mobility. Philos. Mag., vol. 28, no. 4, Oct. 1973, pp. 923–931.
42. Macmillan, N. H.; and Westwood, A. R. C.: Surface Charge–Dependent Mechanical Behavior of Non–metals. Surfaces and Interfaces of Glass and Ceramics, V. D. Frechette, ed., Plenum Press, 1974, pp. 493–513.
43. Westbrook, J. H.; and Jorgensen, P. J.: Indentation Creep of Solids. Trans. Am. Inst. Min. Metall. Pet. Eng., vol. 233, no. 2, Feb. 1965, pp. 425–428.
44. Westbrook, J. H.; and Jorgensen, P. J.: Effects of Adsorbed Water on Indentation Hardness Anisotropy in Crystals. Anisotropy in Single-Crystal Refractory Compounds, Vol. 2, F. W. Vahldiek, and S. A. Mersol, eds., Plenum Press, 1968, pp. 353–360.
45. Miyoshi, K.; Ishigaki, H.; and Buckley, D. H.: Influence of Mineral Oil and Additives on Microhardness and Surface Chemistry of Magnesium Oxide {001} Surface. NASA TP–1986, Mar. 1982.

46. Ishigaki, H.; Miyoshi, K.; and Buckley, D. H.: Influence of Corrosive Solutions on Microhardness and Chemistry of Magnesium Oxide {001} Surfaces. NASA TP-2040, Aug. 1982.
47. Buckley, D.H.: Effect of Surface Active Media on Friction, Deformation, and Fracture of Calcium Fluoride. NASA TN D-5580, Dec. 1969.
48. Buckley, D. H.: Effect of Surface Films on Deformation of Zinc Single-Crystal Surface During Sliding. ASLE Trans., vol. 15, no. 2, 1972, pp. 96-102.
49. Ciftan, M.; and Saibel, E.: Rehbinder Effect and Wear. Wear of Materials, 1979, vol. 2, K. C. Ludema, et al., eds., American Society of Mechanical Engineers, 1979, pp. 659-664.
50. Ciftan, M.; and Saibel, E.: The Effect of Zeta Potential on Pitting. Wear of Materials, 1979, vol. 2, K. C. Ludema, et al., eds., American Society of Mechanical Engineers, 1979, pp. 653-658.
51. Wiederhorn, S. M.; and Roberts, D. E.: Influence of Normal Alcohols on the Abrasive Wear of Glass. Wear, vol. 32, no. 1, 1975, pp. 51-72.
52. Macmillan, N. H.; Huntington, R. D.; and Westwood, A. R. C.: Chemomechanical Control of Sliding Friction Behaviour in Non-metals. J. Mater. Sci., vol. 9, no. 5, May 1974, pp. 697-706.
53. Pauling, L.: A Resonating-Valence-Bond Theory of Metals and Inter-metallic Compounds. Proc. Roy. Soc., London, ser. A, vol. 196, no. 1046, Apr. 1949, pp. 343-362.
54. Miyoshi, K.; and Buckley, D. H.: Correlation of Tensile and Shear Strengths of Metals with Their Friction Properties. ASLE Preprint No. 82-LC-4B-1, Oct. 1982.
55. Kurkjian, C. R.; and Kingery, W. D.: Surface Tension at Elevated Temperatures - III Effect of Cr, In, Sn, and Ti on Liquid Nickel Surface Tension and Interfacial Energy with Al_2O_3. J. Phys. Chem., vol. 60, 1956, pp. 961-963.
56. McDonald, J. E.; and Eberhart, J. G.: Adhesion in Aluminum Oxide-Metal Systems. AIME Trans., vol. 233, 1965, pp. 512-517.
57. Smithells, Colin J.: Metals Reference Book. Volume 1, 4th. ed., Plenum Press, 1967.
58. Glassner, Alvin: The Thermochemical Properties of the Oxides, Fluorides, and Chlorides to 2500° K. Argonne National Laboratory, ANL-5750, 1957.
59. Peterson, M. B.; and Murray, S. F.: Frictional Behavior of Ceramic Materials. Met. Eng. Quart., vol. 7, no. 2, 1967, pp. 22-29.
60. Buckley, D. H.; and Brainard, W. A.: Friction and Wear of Metals in Contact with Pyrolytic Graphite. Carbon, vol. 13, 1975, pp. 501-508.
61. Amelinckx, S.; Strumane, G.; and Webb, W. W.: Dislocations in Silicon Carbide. J. Appl. Phys., vol. 31, no. 8, Aug. 1960, pp. 1359-1370.
62. Brookes, C. A.; O'Neill, J. B.; and Redfern, B. A. W.: Anisotropy in the Hardness of Single Crystals. Proc. Roy. Soc., London, vol. A322, no. 1548, 1971, pp. 73-88.
63. Miyoshi, K.; and Buckley, D. H.: Occurrence of Spherical Ceramic Debris in Indentation and Sliding Contact. NASA TP-2048, Aug. 1982.
64. Bowden, F. P.; and Tabor, D.: The Friction and Lubrication of Solids - Part II. Clarendon Press, Oxford, 1964, pp. 158-185 and p. 173.
65. Miyoshi, K.; and Buckley, D. H.: Friction, Deformation and Fracture of Single-Crystal Silicon Carbide. ASLE Trans., vol. 22, no. 1, Jan. 1979, pp. 79-90.
66. Shaffer, P. T. B.: Effect of Crystal Orientation on Hardness of Silicon Carbide. J. Am. Ceram. Soc., vol. 47, no. 9, 1964, p. 466.

TABLE I. – METAL-TRANSFER TO SINGLE-CRYSTAL SILICON CARBIDE {0001}

SURFACE AS A RESULT OF MULTIPLE PASS SLIDING

Form of metal transfer	Metals*										
	Al	Ti	Zr	Cu	Ni	Co	Cr	Fe	Re	Rh	W
Very small particle (submicron in size)	+	+	+	+	+	+	+	+	+	+	+
Piled-up particle (several microns in size)	+	+	+	+	+	+	+	+	–	–	–
Streak thin film	+	+	+	+	+	+	+	–	–	–	–
Multilayer film structure (piled up)	+	+	+	–	–	–	–	–	–	–	–
Lump particle (several microns in size)	(±)	(±)	(±)	–	–	–	–	–	+	+	+
Surface roughness of metal wear scar	← Rougher										
Chemical affinity of metal for silicon and carbon	Lesser →										
Resistance to shear and tear of metal	Greater →										

*Transferred after 10 passes sliding +; not transferred after 10 passes sliding – ; transferred after single pass sliding (+).

TABLE II. – VALUES FOR THE THICKNESS OF THE

GRAPHITE LAYER ON THE SILICON CARBIDE

SURFACE PREHEATED TO 1500° C

Element and photoelectron (Mg kα)	Electron inelastic mean free path, λ, nm	Thickness of layer, d, nm
Si_{2p}	4.7 3.9	2.0 1.7
C_{1s}	4.4	1.8
Graphite C_{1s}	2.1 3.1 3.4	1.5 2.3 2.4

(a) As-received specimen.
(b) Argon sputter cleaned specimen.
(c) Heat-cleaned specimen.
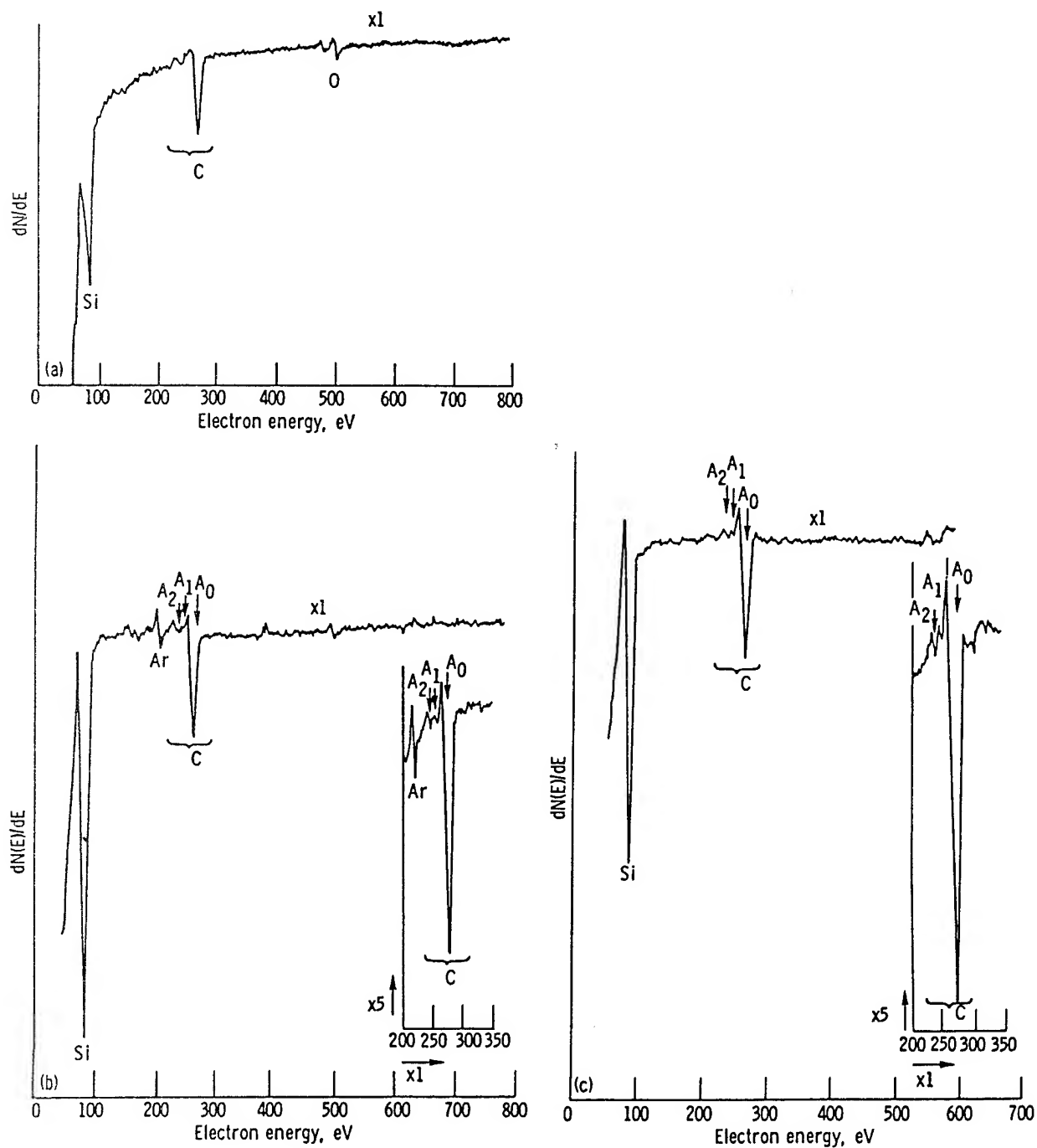
Figure 1. - Auger spectra of silicon carbide (0001) surface.
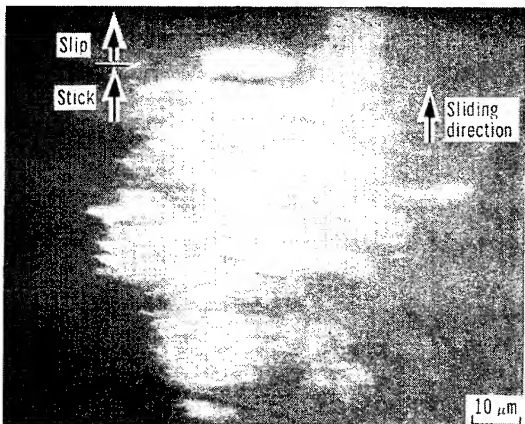
(a) Scanning electron micrograph.

(b) Aluminum K_α X-ray map; 1.5×10^4 counts.

Figure 2. – Aluminum transferred to single-crystal silicon carbide at commencement of sliding as a result of single pass of rider in vacuum. Silicon carbide (0001) surface; sliding direction $\langle 10\bar{1}0 \rangle$; sliding velocity 3 mm/min; load, 0.3 N; temperature, 25° C; vacuum pressure, 10^{-8} Pa.

308

(a) Nearly complete hexagon-shaped wear debris.

(b) Partially hexagon-shaped wear debris.

Figure 3. - Transfer of hexagon-shaped wear debris of single-crystal silicon carbide rider to disk (silicon carbide, itself). Scanning electron micrographs of a wear track on silicon carbide disk. Sliding velocity, 3 mm/min; load, 0.5 N; temperature, 25^0 C; and pressure, 10^{-8} N/m^2.
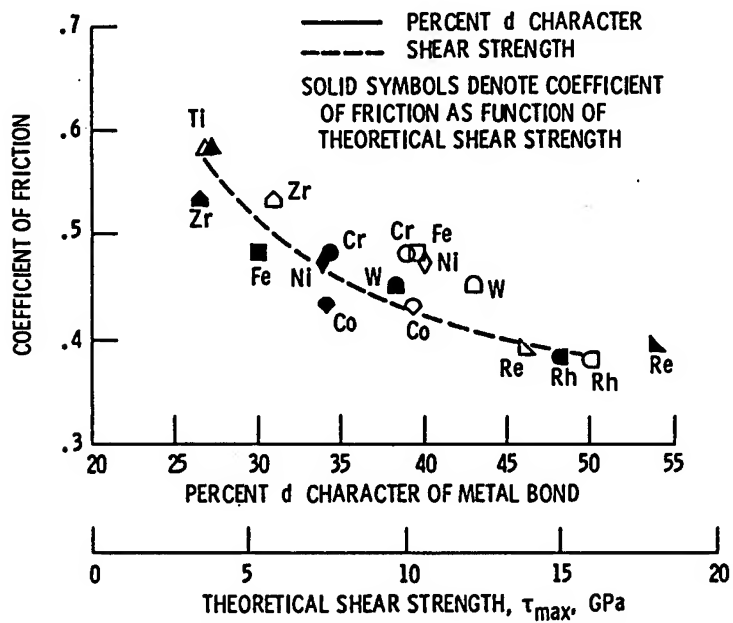
Figure 4. - Coefficients of friction as function of percent of metal d bond character and theoretical shear strength of metals in contact with silicon carbide {0001} surface in vacuum. Sliding direction, <$10\bar{1}0$>; sliding velocity, 3×10^{-3} m/min; load, 0.05 to 0.5 N; room temperature; vacuum pressure, 10^{-8} Pa.
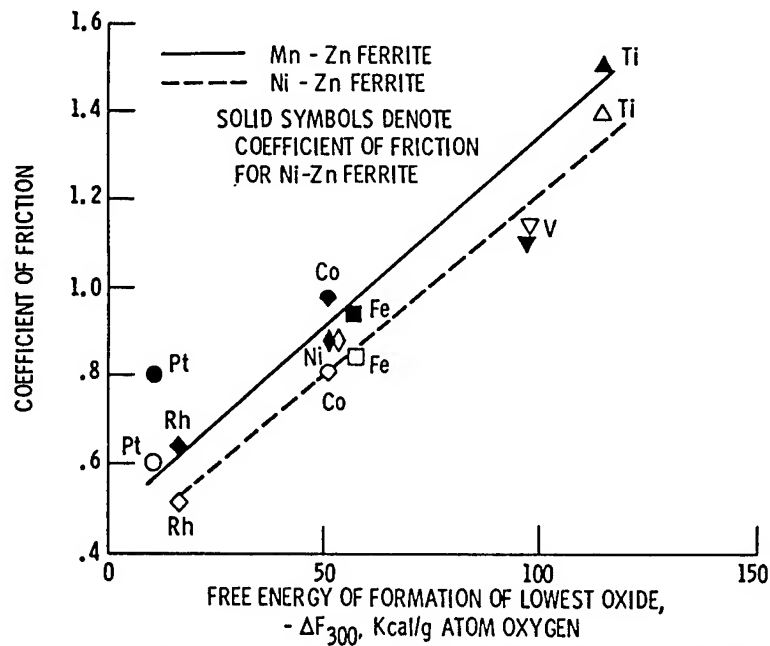
Figure 5. – Coefficients of friction for various metals in contact with ferrites as function of free-energy of formation of lowest oxide. Single pass sliding; sliding velocity, 3 mm/min; load, 0.05 to 0.2 N; vacuum, 3×10^{-8} Pa; room temperature.

(a) Coefficient of friction.
(b) Argon-sputter-cleaned surface of SiC.
(c) Argon-sputter-cleaned surface of SiC with reacted-oxides film.
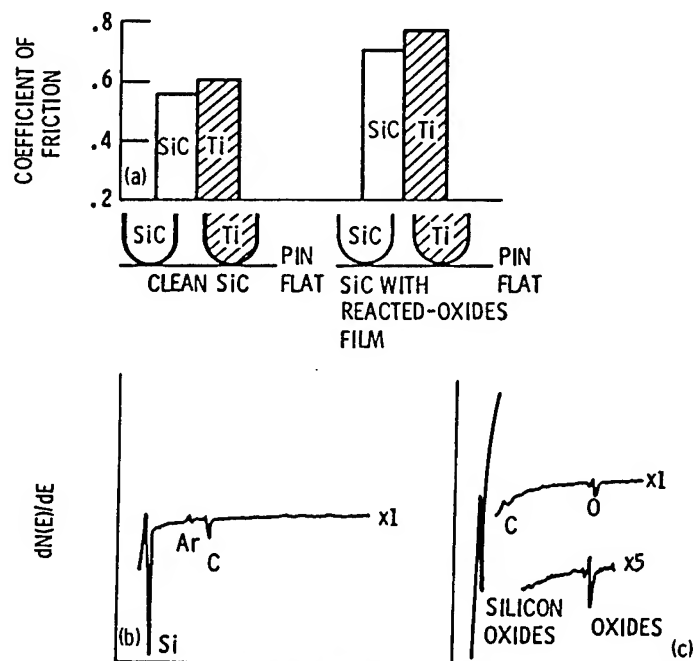
Figure 6. – Effect of oxygen on friction for silicon carbide in contact with itself and titanium. Auger spectra showing clean silicon carbide and silicon carbide with reacted-oxide film. Single pass sliding; sliding direction, $\langle 10\bar{1}0 \rangle$; sliding velocity, 3×10^{-3} m/min; load; 0.3 N; room temperature; vacuum pressure, 10^{-8} Pa.

310
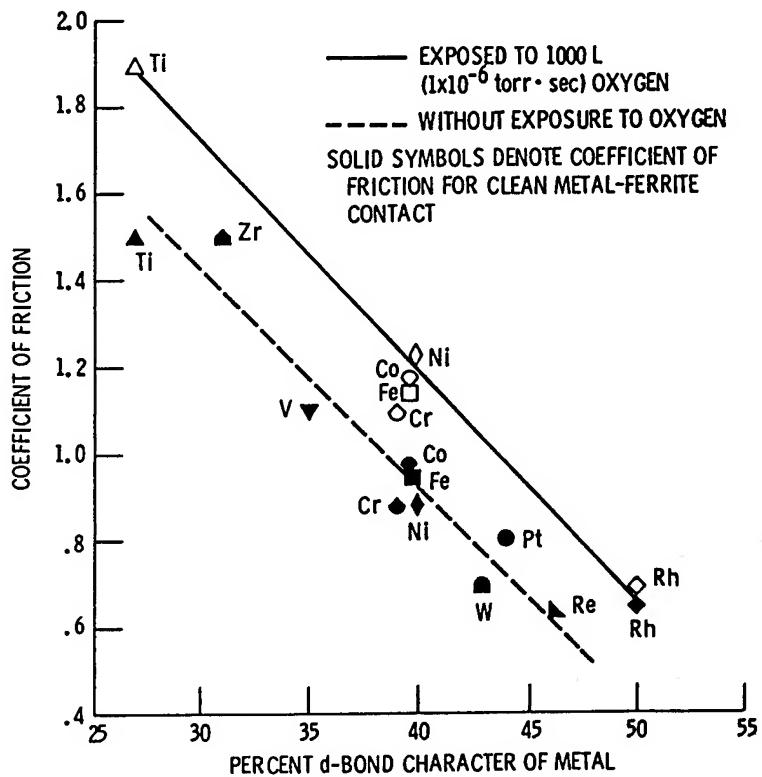
Figure 7. - Effect of adsorbed oxygen on friction for various metals in contact with the ferrites. Exposure, 1000 L in oxygen gas; sliding velocity, 3 mm/min; load, 0.05 to 0.2 N; vacuum. 3x10⁻⁸ Pa; room temperature.

Figure 8. – Representative Si_{2p} and C_{1s} XPS peaks on silicon carbide {0001} surface preheated at various temperatures to 1500° C.

312

AUGER SPECTRA SHOWING CLEANED
AND GRAPHITIZED SURFACES
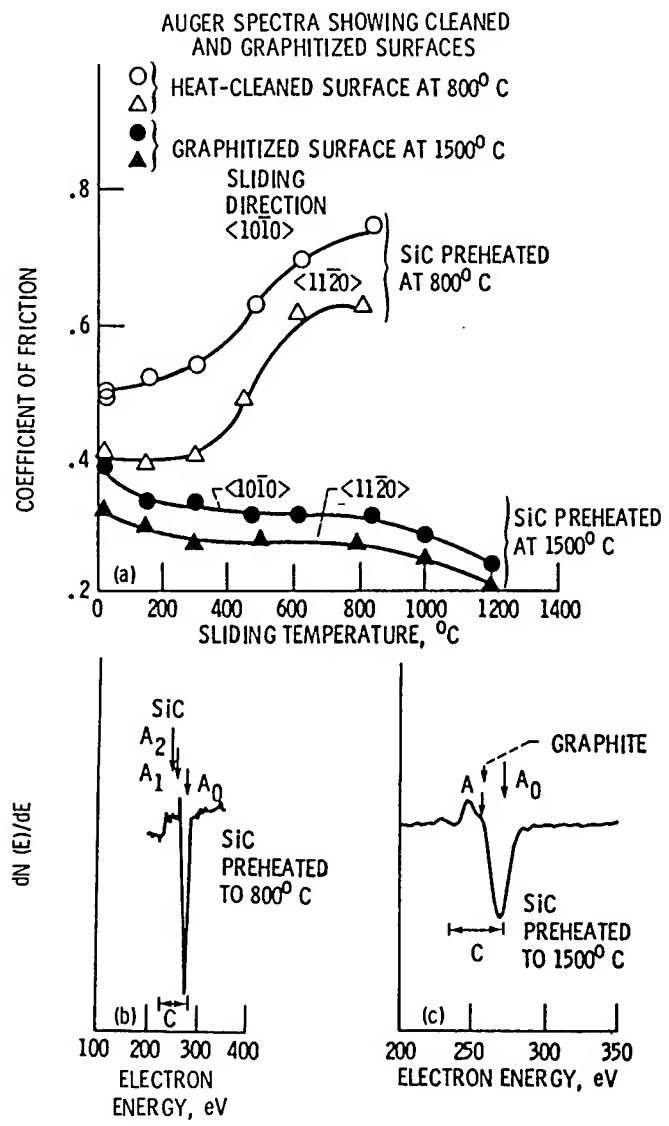
(a) Coefficient of friction.
(b) SiC surface.
(c) Graphitized surface.

Figure 9. - Effect of temperature and crystallographic orientation on friction for SiC |0001| surface sliding against iron rider (normal load, 0.2 N; pressure, 10^{-8} Pa).

313
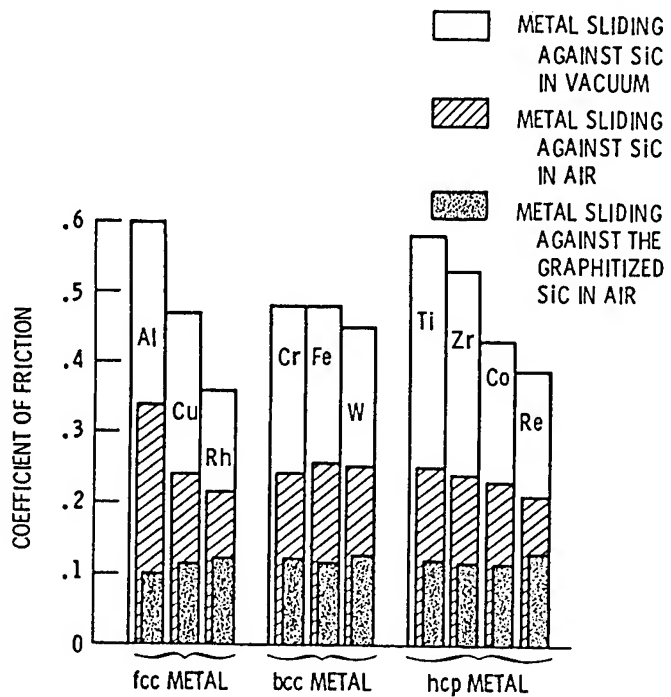
Figure 10. - Coefficient of friction for clean silicon carbide and graphitized silicon carbide in sliding contact with various metals in laboratory air and in vacuum. Single pass sliding, sliding velocity, 3 mm/min; load, 0.5 N; room temperature.

314
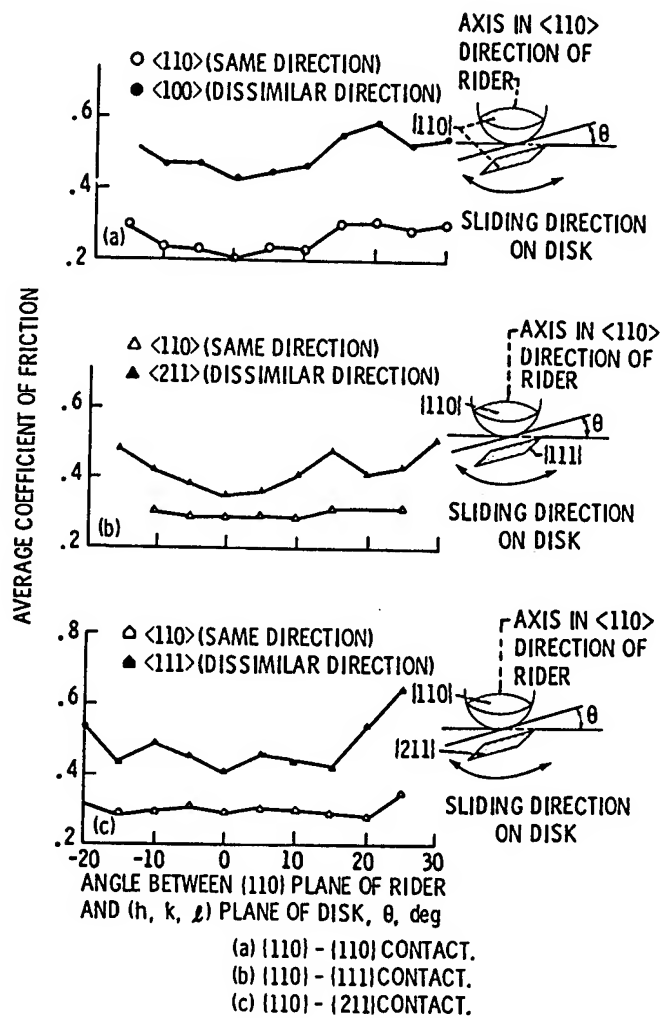
Figure 11. - Coefficients of friction for mating the same and different rider and disk directions (sliding direction of the rider, <110>; single-pass sliding; manganese-zinc ferrite riders and disks).

315
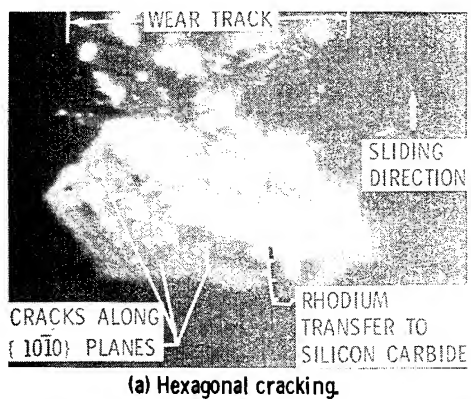
(a) Hexagonal cracking.
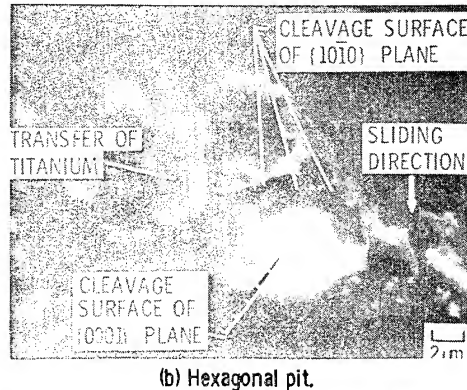
(b) Hexagonal pit.

Figure 12. - Scanning electron micrographs of wear tracks on the (0001) surface of single-crystal SiC in contact with rhodium and titanium as a result of ten passes of a rider in vacuum. Sliding direction, $<10\bar{1}0>$; sliding velocity, 3 mm/min^{-1}; load, 0.3 N; room temperature; pressure, 10^{-8} Pa.
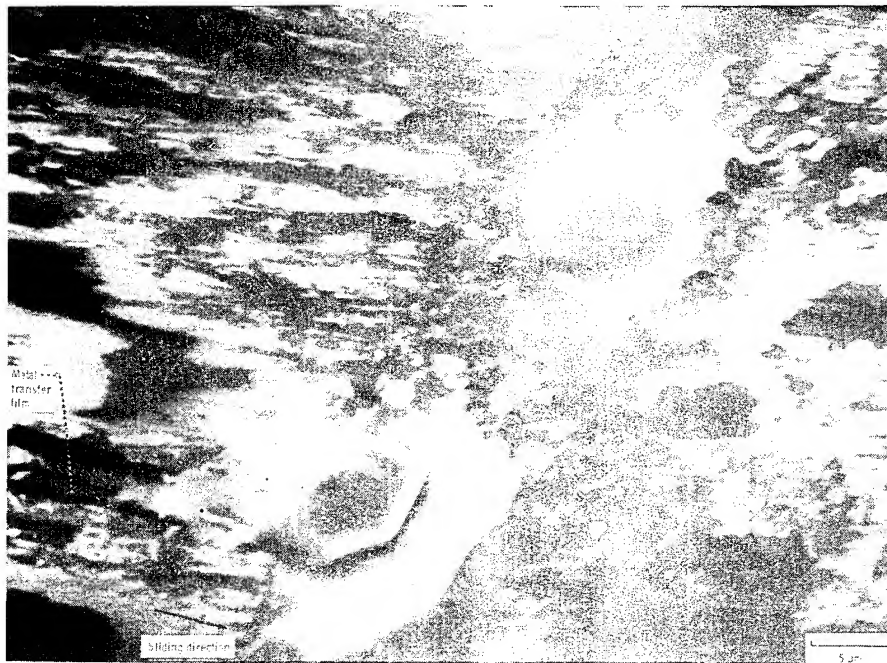
Figure 13. - Wear track with fracture pits on silicon carbide {0001} surface as a result of single-pass sliding of iron rider. Sliding velocity, 3 mm/min; load, 0.2 N; temperature, 800° C; vacuum, 30 nPa.

316
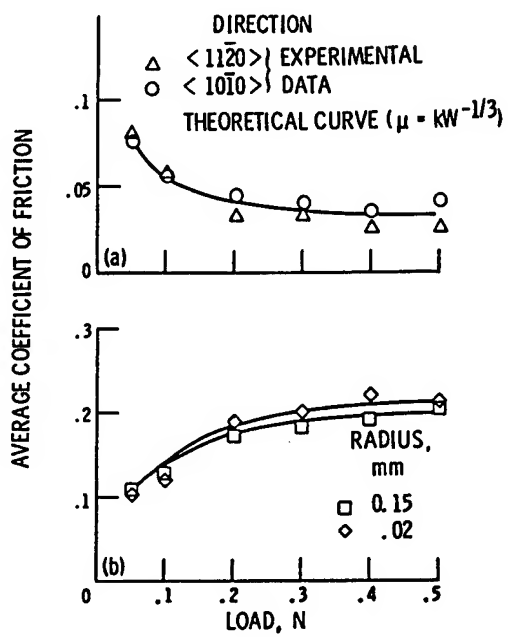
(a) Diamond radius, 0.3 mm
(b) Diamond radii, 0.15 and 0.02 mm.

Figure 14. - Average coefficient of friction as function of load for spherical diamond riders of different radii sliding on single-crystal silicon carbide (0001) surface. Sliding velocity, 3 mm/min; temperature, 25° C in argon at atmospheric pressure.
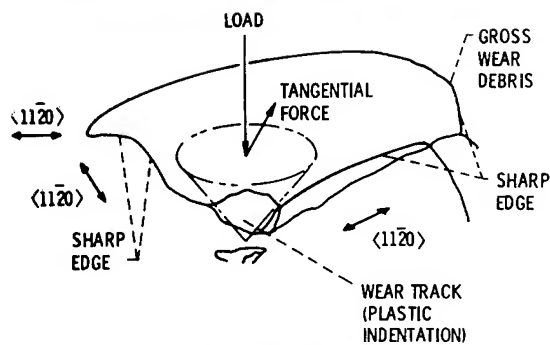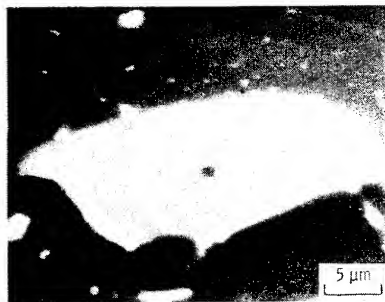
(a) First stage (before gross sliding).
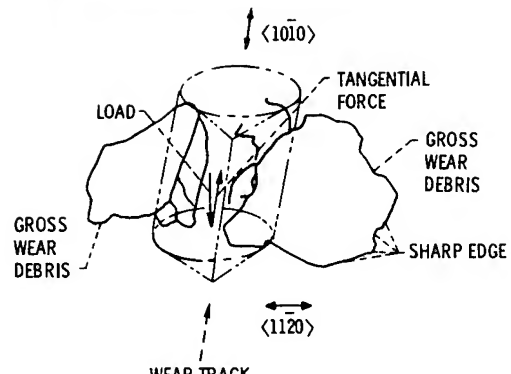
(b) Second stage (after gross sliding).
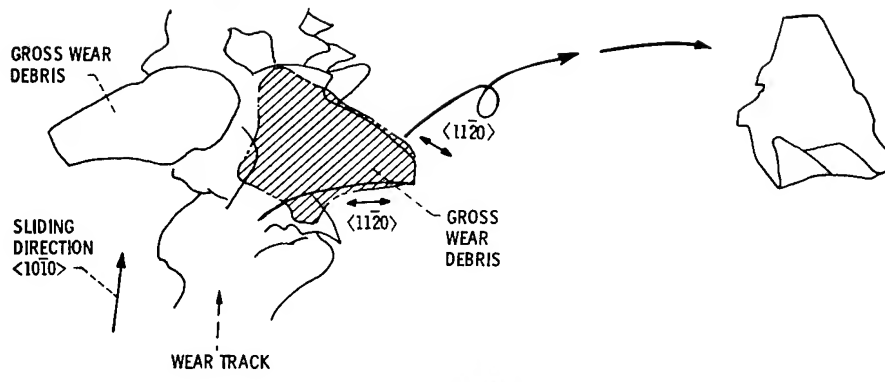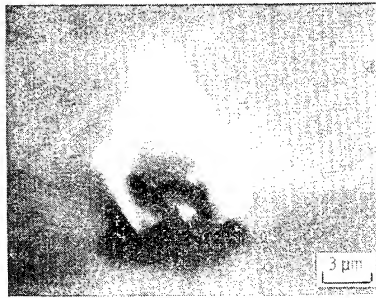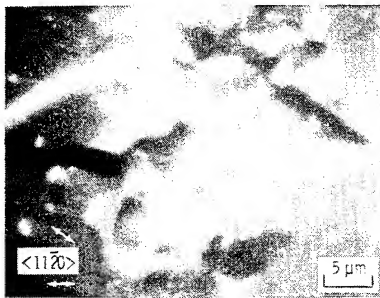
(c) Third stage.

Figure 15. – Mechanism of fracture. Single pass of conical diamond rider; sliding surface, (0001); sliding direction, ⟨10$\bar{1}$0⟩; sliding velocity, 3 mm/min; load, 0.3 N; temperature, 25° C in argon at atmospheric pressure.

318

SLIDING DIRECTIONS

(a) Coefficient of friction.
(b) Groove width.
(c) Contact pressure (load, 0.2 N).
(d) Knoop hardness (load, 1 N).
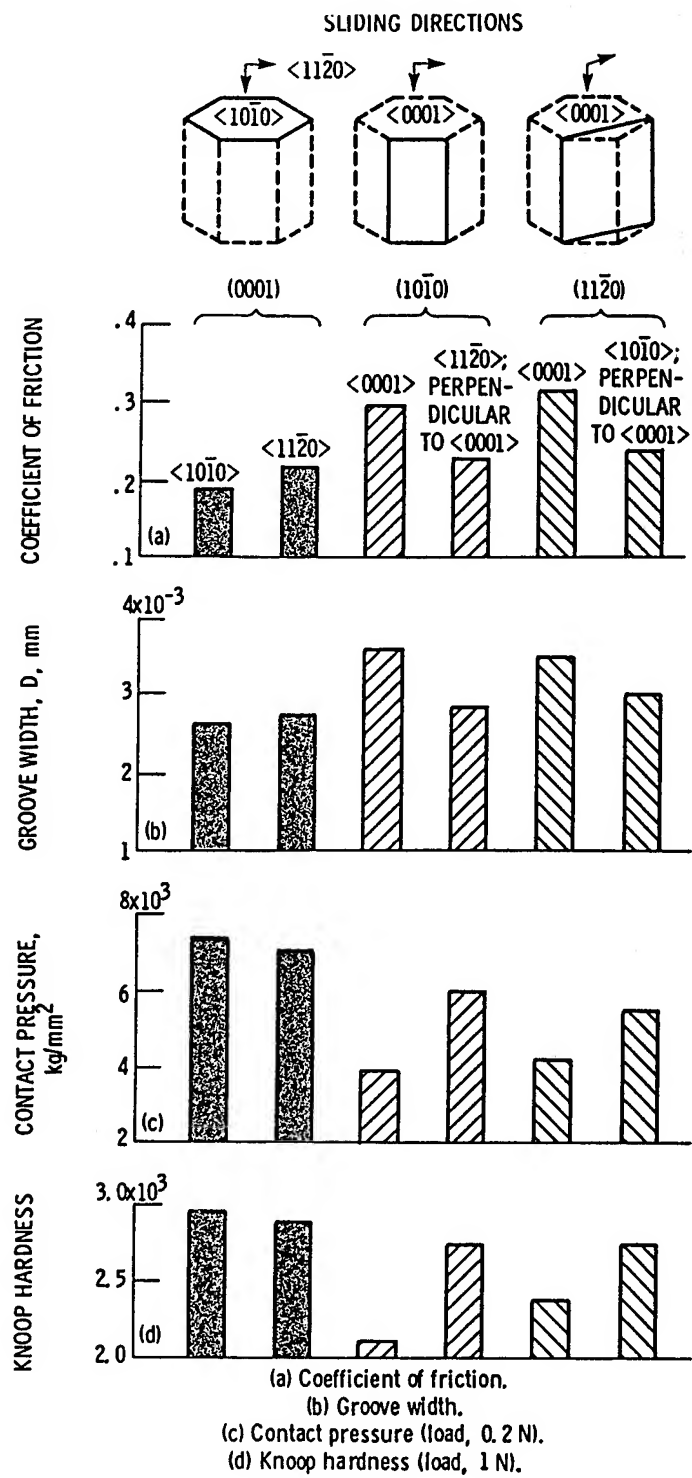
Figure 16. - Anisotropies on {0001}, {10$\bar{1}$0} and {11$\bar{2}$0} surfaces of SiC.

319
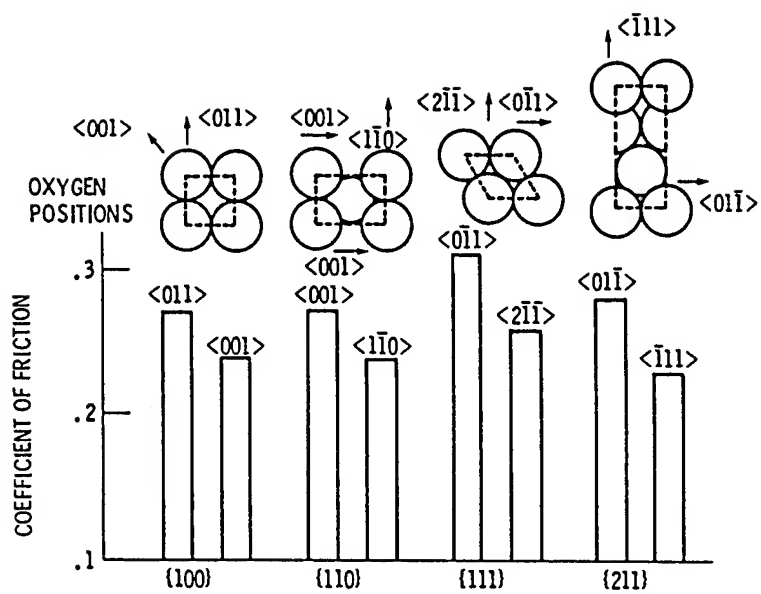
Figure 17. - Anisotropies of friction on {100}, {110}, {111}, and {211} surfaces of Mn - Zn ferrite in contact with spherical diamond rider (radius, 20 μm) sliding velocity, 3 mm/min; load, 1 N; laboratory air; room temperature.

320

DISCUSSION

Yuji Enomoto
Mechanical Engineering Laboratory
Namiki 1-2, Sakura-mura,
Niihari-gun, Ibaraki-ken, Japan

The authors have presented their valuable and very interesting results on fundamental properties of materials and surface chemistry determining the frictional and wear behavior of ceramics. The discussor realizes that in order to facilitate the determination of what happens on sliding surfaces, rather simplified system, single crystal and single pass sliding, is preferable. In connection with tribological application of ceramic, however, the most engineering system involves polycrystalline materials and multiple-pass sliding; grain boundary and repeated loading-unloading are also important factor affecting to material change in wear.

As an example how multiple-pass sliding enhance its effect on wear damage, Fig. 1 shows the secondary electron and the corresponding cathodoluminescence images of the wear damage of single crystalline MgO (001) face produced by the sliding of a 2 mm diameter WC ball after single to-and-fro traversal and 100 traversals. Luminescent slip bands on both $\{110\}_{90°}$ and $\{110\}_{45°}$ could be observed inside the track after single to-and-fro-traversal (Fig. 1c). Further multi-traversal of the ball rider generated enough slip bands to make the track completely luminescent. It is noted that around the center of the track where the contact stress is maximum, there are dark bands (cf. Fig.1d). The reason why the luminescence is absent around the center of the track is not attributed to recrystalization and/or reorientation but to very severely distorted structure of material with very high density of defects.[1]

321

We also observed similar behavior in polycrystalline MgO.

Some questions are concerned with effects of grain boundary properties and repeated sliding. Firstly, would you expect graphitazation in vaccum and oxidation in air at high temperature can effect on grain boundary behavior of sintered polycrystalline SiC. If any, does it bring any notable change in frictional and/or wear behavior between single and polycrystalline SiC? Secondly, I would like to ask them if crystallographic orientation effect on frictional (adhesive or abrasive) anisotropy was observed even after multi-pass sliding. In this connection, what type of anisotropy does it occur for SiC-SiC contact.

Reference

1) Y. Enomoto and K. Yamanaka, J. Materi. Sci. 17(1982)3288.
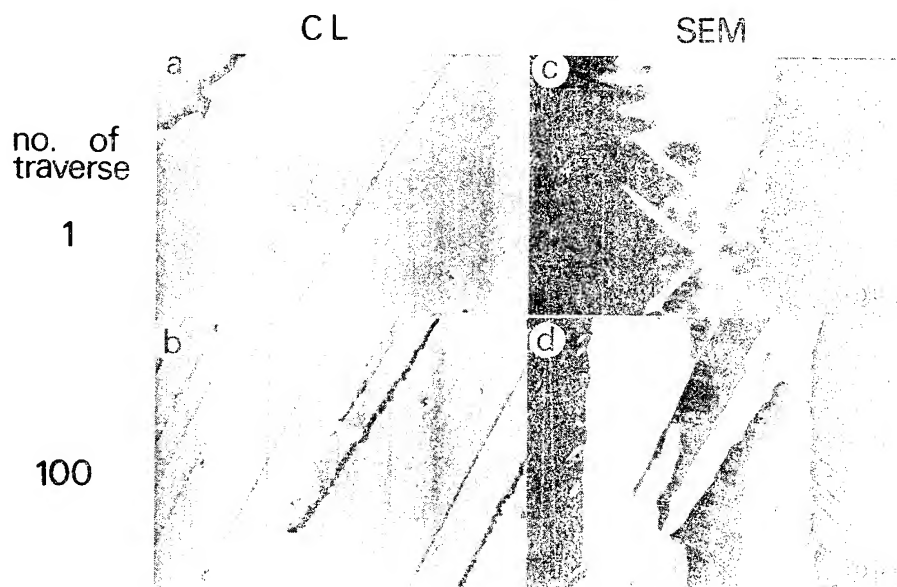
Figure 1. - Secondary electron ((a) and (b)) and cathodoluminescence ((c) and (d)) images of wear damage of MgO crystal produced by sliding of 2-mm single to and from traversal: (b) 100 traversals. Load, 7.8 N. Coefficient of friction, 0.12 for (a) and 0.14 for (b).

DISCUSSION

Alan G. King
Ferro Corporation
Independence, Ohio

Silicon carbide is becoming a material of increasing technological importance. The combination of high hardness, retention of physical properties at high temperature, and resistance to oxidation by the formation of a protective surface film is resulting in SiC's increased importance as a wear resistant material. The authors have added significantly to the knowledge of this material's tribological behavior in a fundamental way.

There is a similarity between tribological phenomena in sliding friction and in metal cutting, either by cutting tools or by abrasives. As the authors point out there is a correlation between friction and the fundamental physical and chemical properties of the metals. One relationship in particular is that the authors found the coefficient of friction correlates with the free energy of formation of the lowest metal oxide. In our own work we also found a correlation between the free energy of formation and wear rate on an alumina abrasive. When cutting metals with a range of negative free energies of formation of the oxide, wear rates on the abrasive span about three orders of magnitude.

It is often helpful to consider tribological processes as being related to mass transport. There are four transport processes: plastic deformation, diffusion, viscous flow, and fracture with kinetic displacement. The chemical reactions at the interface can affect these mass transport processes. For example, when machining a ferrous metal with an alumina tool bit, atmospheric oxygen reacts with the metal and ceramic to form a spinel with cubic symmetry. Spinel has sufficient slip systems available for volumetric plastic deformation.

323

Under the conditions of high pressure (2000-3000 N/m^2) and high temperature (1000-1200°C) at the interface we would expect the spinel to be readily wiped clean from the interface. The surface of the ceramic becomes highly polished where oxygen is available. In this case the mass transport process is plastic deformation. However, the rate controlling process is the chemical reaction, and both must be considered to explain wear under these conditions.

With most ceramics and metals it is difficult to eliminate adsorbed species on the surface. Equilibrium dissociation pressures of common metal oxides are for example much lower than vacuums which are available. Silicon carbide is an interesting material in this regard in that SiO has a relatively high vapor pressure and as the authors have shown, can be removed from the surface. Obtaining atomically clean surfaces is much more difficult on most metals or oxides.

Since surface graphitization of SiC lowers the coefficient of friction about three fold at 800°C, there could well be an interest as SiC in high temperature bearings operating in a vacuum. It will be of interest to see if the wear rate increases due to graphitization. The experience on cutting tool coatings would lead us not to take it for granted. A thin coating on a substrate can be durable.

DISCUSSION

N. H. Macmillan
The Pennsylvania State University
University Park, Pennsylvania

This is an interesting paper, which serves two functions. First, it provides a convenient summary of much of the recent work of Buckley and co-workers on friction and wear at ceramic-ceramic and ceramic-metal interfaces; and second, it provides a sufficient review of the work of others to enable the reader to set the conclusions reached by these researchers in their proper perspective. The organization of the material presented draws upon the idea, first proposed by Bowden and Tabor (1) many years ago, that the coefficient of friction μ is the sum of two terms -- an adhesion term and ploughing term, so that

$$\mu = F/N = (AS + P)/N \ ,$$

where F and N are the horizontal and vertical contact forces, A is the area of contact, S is the shear strength of the contacts, and P is the force required to produce ploughing. Clearly, the first term (AS) is more important when the ratio N/R, where R is the smallest radius of curvature in the contact region, is low; and equally obviously, the latter term (P) gains importance as N/R increases. In keeping with the interests of Buckley's group, the emphasis in the present paper is on the adhesion term.

It may, however, be useful to raise before the present audience the question of just how fundamental the separation of μ into these two components really is. Remember that the adhesion term arises from (i) the processes of making and breaking interatomic bonds over those portions of the nominal contact area where opposing asperities close to within a distance of about one atom spacing and (ii) the deformation of the asperities that accompanies these these processes. Then remember, too, that the ploughing process involves the deformation to some characteristic depth of one of the contacting surfaces by the other. Apparently, both terms involve plastic deformation (by dislocation glide and/or twinning) and crack propagation, and to that extent their separation might be deemed artificial.

There are, however, also likely to be significant differences between the flow and fracture behavior of a small (~ 1 μm) asperity and a bulk ($\gg 1$ μm) sample of the same material. In particular, because one half of the energy of a dislocation typically resides further than 1 μm from its core, the behavior of

dislocations in asperities will be markedly affected by dislocation-surface interactions. Indeed, there may be a tendency for dislocations to be attracted to the surfaces of asperities by these interactions, and hence to be lost from them. This would have the effect, in the case of a metal, of raising the yield stress of the asperity, because it is generally more difficult to nucleate dislocations (especially if the strained volume is small) than to propagate them. Conversely, it seems plausible that asperities on a ceramic surface would appear more ductile than the corresponding bulk ceramic -- partly because the small volume of the asperity makes it statistically unlikely that it would contain the critical flaw necessary to nucleate fracture, and partly because it becomes more difficult to satisfy Griffith's criterion for flaw propagation as the stressed volume decreases. The experiments of Gane et al. (2-9) throw interesting light on these conjectures.

Regardless of such differences, however, the important corollary to the preceding argument is that both the ploughing and the adhesion components of the coefficient of friction might intuitively be expected to correlate better with those defect properties (such as the Peierls-Nabarro stress or the work of fracture, for example) which characterize the mechanical behavior of a solid than with such properties of the perfect lattice as the nature of the d electron bonding or the theoretical shear strength (Figs. 4 and 7), or the free energy of formation (Fig. 5). Ultimately, of course, all the properties -- lattice or defect -- of any solid derive from its bonding, so there is no fundamental objection to the correlations reported. But, because lattice and defect properties do not, in general, correlate well between (as opposed to within) classes of materials (e.g., metals of different crystal structure) it is at first sight surprising that the correlations presented in Figs. 4, 5 and 7 are so successful. This is particularly the case for the correlation with theoretical shear strength presented in Fig. 4, because the approximation used to estimate this parameter is a very crude one (10-12). It would be most interesting to know if better correlations can be obtained with any defect properties.

Turning now to the question of the influence of environment on friction, it is again important to consider the question of scale. In particular, it is appropriate to ask what differences the electron or hole supplied by an atom or molecule seeking to chemisorb on a defect-riddled solid surface "sees" between a site made available by the advance of a kink a distance of one atom spacing along a dislocation line and a site made available by the

corresponding process at a crack front. Is it possible that on this scale the quantum mechanical electronic tunnelling processes that take place in the two deformation events are not too dissimilar? Likewise, is it possible that the differences between the mechanical responses of a crystalline ceramic and a glass of the same composition derive from differences in the degree of spatial correlation of succeeding unit processes of flow and fracture rather than from differences between the processes themselves? It is to be hoped that answers to such questions may come from combining the continuing progress being made in resolving the atomic structures of defects by high resolution transmission electron microscopy with the growing ability of the quantum chemists to model the behavior of clusters of atoms.

To close, one final point about environmental effects is perhaps also worth making -- namely, that there has in the past few years begun to emerge (notably from the work of Westwood and co-workers) a framework for unifying thinking about the variety of environmental effects that can affect the mechanical properties of the surficial region -- and hence the frictional behavior -- of a solid. The characteristic that relates all of the diverse phenomena listed on pages 3 and 4 of the present paper is that they take place in the electrical double layer that exists at any solid-liquid or solid-gas interface. Consequently, all such effects can be understood in terms of the same parameters -- the extent of the double layer on the solid and fluid sides of the interface, the movement of different charged and uncharged species into, out of and within both sides of this layer, and the way in which adsorption at the solid-fluid interface alters the distribution of the mobile species. There is neither time nor space to go into the details of Westwood's work here; nor is it necessary to do so, for a comprehensive review of the whole subject has recently been published (13).

References

1. F.P. Bowden and D. Tabor, The Friction and Lubrication of Solids, Part I, Oxford University Press, England (1954).

2. N. Gane and F.P. Bowden, J. Appl. Phys., 39, 1432 (1968).

3. N.H. Macmillan and N. Gane, J. Appl. Phys., 41, 672 (1970).

4. N. Gane and J.M. Cox. J. Phys., D3, 121 (1970).

5. N. Gane, Proc. Roy. Soc. A317, 367 (1970).

6. N. Gane and J.M. Cox, Phil. Mag., 22, 881 (1970).

7. N. Gane and J.M. Cox, Phil. Mag., $\underline{23}$, 229 (1971).

8. N. Gane, Phil. Mag., $\underline{25}$, 25 (1973).

9. J. Skinner and N. Gane, Phil. Mag., $\underline{28}$, 827 (1973).

10. N.H. Macmillan and A. Kelly, Mater. Sci. & Eng., $\underline{10}$, 139 (1972).

11. N.H. Macmillan, Can. Met. Qty., $\underline{13}$, 555 (1974).

12. N.H. Macmillan, The Ideal Strength of Solids, to be published in The Atomistics of Fracture, R.N. Latanision and J.R. Pickens, Eds., Plenum Press, New York (1983).

13. R.N. Latanision and J.F. Fourie, Eds., Surface Effects in Crystal Plasticity, Noordhoff, Leyden, Holland (1977).

DISCUSSION

David Tabor
Cavendish University
Cambridge, England

This is a very valuable paper. I have, however, one general comment.
In the sliding of Ti on SiC shear occurs in the titanium. Consequently, the
interface is stronger than the metal. In that case increasing the interfacial
adhesion by an environmental change should not, in principle, change the fric-
tional behaviour since it is limited by the shear strength of the metal itself.

RESPONSE

Kazuhisa Miyoshi and Donald H. Buckley
NASA Lewis Research Center
Cleveland, Ohio

The authors wish to express their appreciation to the discussors for taking time from their own busy schedules to prepare their discussions of our paper.

In response to Dr. King's comments, the authors believe that the study presented in this paper could lead to a better fundamental understanding of tribological phenomena in sliding friction and metal cutting by abrasives. This knowledge in turn could result in a reduction in the energy consumed by the thousands of daily industrial grinding operations. A better understanding could likewise reduce the wear to grinding, cutting, and drilling surfaces and the amount of charging that occurs to such surfaces which reduces their efficiency. The authors are particularly interested in the fundamental mechanisms of adhesive, abrasive, and corrosive wear and in the material aspects of these wear mechanisms. Adhesion, friction, wear, and lubrication are extremely dependent on the basic properties of solid surfaces - that is, the physical, chemical, mechanical, and metallurgical properties. The materials we are concerned with are metals and ceramics. In addition to crystalline metals and alloys, the materials include SiC, diamond, BN, MgO, Al_2O_3, ferrites, and TiB_2.

In response to Professor Macmillan's comment concerning the correlation between coefficient of friction and any defect properties, we also, to some extent, correlated the effect of lattice friction stress in binary alloys by solute atoms on friction (refs. A1 and A2). In reference A1, sliding friction experiments were conducted with various iron-base alloys. The alloying elements were Ti, Cr, Mn, Ni, Rh, and W in contact with a single-crystal silicon carbide (0001) surface in ultrahigh vacuum. Results indicated that atomic size misfit and concentration of alloying elements play a dominant role in controlling adhesion, friction, and deformation of iron-base binary alloys. Generally, the coefficient of friction increases with an increase in solute concentration. It also increases as the solute to iron atomic radius ratio increases or decreases from unity. The controlling mechanism of the adhesion and friction of alloys is raising the Peierls stress or increasing the lattice friction stress by increasing solute atoms and increasing solute to iron atomic radius ratio.

The friction related to abrasion (that is, plowing) also correlates with solute concentration and solute to iron atomic radius ratio. The controlling mechanism of the alloy properties also had an intrinsic effect involving the resistance to shear fracture of cohesive bonding in the alloy. The trends in friction behavior are, however, just the opposite. The coefficient of friction and the volume of groove plowed generally decrease with an increase in solute concentration of binary alloys. Friction and abrasive wear decrease as the atomic radius ratio increases or decreases linearly from unity.

In response to Dr. Enomoto, the authors have taken the position that we are, at this time, not able to analyze complex engineering systems. We are, however, expanding the research on practical materials, such as metallic glass, to gain a better understanding of material behavior in the field of tribology. The authors and Thomas P. Jacobson are continuing the tribological research of sintered polycrystalline silicon carbide at high temperature in an air atmo-

sphere. At this time, however, we can not provide any answers regarding the effect of graphitization on grain boundary behavior.

With regard to the crystallographic orientation effect on frictional anisotropy after multipass sliding, it would be interesting to know how such tribological properties as friction and wear correlate with any defect property, as indicated by Professor Macmillan's discussion.

On a crystalline surface the crystallinity and crystallographic orientation can be changed markedly by strain as a result of sliding, rolling, or rubbing. The higher the degree of strain, the lower the temperature for recrystallization. The reoriented surface reflects the effects of the mechanical, physical, and chemical parameters imposed on the surface (refs. A3 to A6).

On a noncrystalline surface (e.g., amorphous alloy) the surface can be crystallized during the sliding process at a critical condition. Crystallization of the wear surface of the amorphous alloy causes an increase in friction (ref. A7).

In response to Dr. Tabor, the authors agree with the comment that the interfacial bonds between titanium and the silicon carbide are stronger than the cohesive bonds in the titanium and shear takes place in the titanium. The shear strength of the metal accordingly dictates friction behavior. If the environment is such that species from that environment adsorb, absorb or react with either surface, the presence of these species could reduce the amount of metal to silicon carbide bonding or even eliminate it under certain conditions and shear could occur at the interface in which case the contribution of the shear strength of the metal to friction will be reduced considerably. The diamond-metal data of Dr. Pepper presented in this Conference indicates that something so simple as hydrogen from the environment on the diamond surface can do much to reduce interfacial interaction between two solids and effect friction.

REFERENCES

A1. Miyoshi, K.; and Buckley, D. H.: The Adhesion, Friction, and Wear of Binary Alloys in Contact with Single-Crystal Silicon Carbide. J. Lubr. Technol., vol. 103, Apr. 1981, pp. 180-187.

A2. Miyoshi, K.; and Buckley, D. H.: The Friction and Wear of Metals and Binary Alloys in Contact with an Abrasive Grit of Single-Crystal Silicon Carbide. ASLE Trans., vol. 23, no. 4, Oct. 1980, pp. 460-472.

A3. Scott, V. D.; and Wilman, H.: Surface Re-orientation Caused on Metals by Abrasion - Its Nature, Origin and Relation to Friction and Wear. Proc. Roy. Soc. London, vol. A247, no. 1250, Sept. 30, 1958, pp. 353-368.

A4. Goddard, J.; Harker, H. J.; and Wilman, H.: The Surface Re-orientation Caused by Uni-directional Abrasion on Face - Centered Cubic Metals. Proc. Phys. Soc. London, vol. 80, no. 3, Sept. 1962, pp. 771-782.

A5. Buckley, D. H.: Recrystallization and Preferred Orientation in Single-Crystal and Polycrystalline Copper in Friction Studies. NASA TN D-3794, Mar. 1967.

A6. Wheeler, D. R.; and Buckley, D. H.: Texturing in Metals as a Result of Sliding. Wear, vol. 33, 1975, pp. 65-74.

A7. Miyoshi, K.; and Buckley, D. H.: Sliding Induced Crystallization of Metallic Glass. NASA TP-2140, Mar. 1983.

COMPOSITES FOR INCREASED WEAR RESISTANCE: CURRENT ACHIEVEMENTS AND FUTURE PROSPECTS

J. K. Lancaster
Royal Aircraft Establishment
Farnborough, Hants., United Kingdom

A review is given of the various ways in which reductions in wear and/or friction can be achieved by the use of composite materials. The main emphasis is on reinforced plastics and it is shown that fillers and fibres reduce wear via several mechanisms additional to their role of increasing overall mechanical strength, eg preferential transfer, counter-face abrasion, preferential load support, or "third-body" formation on either the composite or its counter-face. Examples are given from recent work on thin-layer composites of the type widely used as dry-bearings in aircraft flight control mechanisms. Brief mention is also included of developments in metal-based composites and carbon-carbon composites for high energy brakes. Throughout the discussion, attempts are made to identify those aspects which would benefit by increased fundamental understanding and to indicate which types of composites appear to have greatest potential for further growth.

INTRODUCTION

Composites have a long and distinguished record as tribological materials, dating back to the dawn of history and the evolution of articulated, skeletal joints. The structure of such joints well illustrates the two primary requirements of any composite bearing material; the ability to support a load without undue distortion, deformation or fracture and the necessity to maintain low friction and wear over long periods without seizure. When the latter can be achieved by fluid lubrication, as in joints, it is the structural aspects of the composites which become the all-important consideration, eg mechanical strength, creep, stiffness, fracture toughness etc. It is not intended to discuss these aspects, per se, in the present paper. A voluminous literature is available on structural composites and it will be taken for granted that information and techniques exist, in principle or in practice, for optimizing structure and composition to achieve maximum load-carrying-capacity of a component. The topic of primary concern here is how the structure and composition of composites influence their friction and wear behaviour. Most of the discussion will be confined to plastics-based materials since these have received more attention, and developed further, during the past few decades than any other group.

COMPOSITES CONTAINING PTFE

Although low friction and high thermal stability combine to make PTFE a particularly attractive polymer for sliding applications, poor mechanical strength, excessive viscoelastic deformation under load and a high rate of wear usually necessitate some form of reinforcement. The addition of almost any type of reinforcing fibre or filler results in significant reductions in wear and improvements to mechanical properties. With increasing filler concentration wear usually decreases monotonically but strength and stiffness may exhibit a maximum as

shown, for example, by the results in figure 1 for PTFE-carbon fibre mixtures. The detailed behaviour must obviously depend on the particular filler involved and it is therefore pertinent to ask the question - what is the 'best' type of filler to choose for minimum wear?   Regrettably, there is no simple answer and to see why this should be so, it is necessary to examine some of the ways in which different fillers and reinforcing fibres influence wear.   There are two general explanations. The first is based on the fact that during interfacial shear, long fibrils or ribbons of PTFE are drawn out across the surface (ref 1).   It was originally thought that these fibrils originated from within the amorphous regions of the bulk structure which separate the crystalline bands (ref 2) but more recent work (refs 3, 4) concludes that they are derived from within the crystalline bands themselves. The suggestion has therefore been made that filler particles impede this drawing-out process and thus prevent destruction of the banded structure (refs 4,5).   This hypothesis is consistent with the fact that wear of PTFE is reduced by virtually any type of filler but does not readily explain why some fillers are so much better than others.

An alternative explanation is that the filler particles or fibres support the load preferentially by virtue of their greater strength and stiffness (ref 6).   The friction and wear behaviour can thus be influenced directly by the type of filler although, in fact, a strong dependence may be inhibited if the particles are masked by smearing or flow of the PTFE during sliding.   The extent of preferential load support will be influenced by particle size (smaller particles tending to be buried more easily than larger ones), shape (large aspect ratios being most effective, ref 4) and orientation.   There is an element of confusion in the literature about the effects of orientation of reinforcing fibres, some work indicating that wear is a minimum when the fibre ends are normal to the sliding interface (ref 6) whilst other work suggests the optimum orientation is with the fibres lying in the plane of the interface and parallel to the direction of sliding (ref 7).   Moreover, the size and shape of the reinforcement in the composite surface may also change with time as a consequence of wear or fracture during sliding (ref 8).

Third-Body Film Formation

Whichever of the above explanations is accepted, and in all probability both are likely to be relevant, the ultimate, steady-state rate of wear of a composite is seldom related directly to its bulk structure but depends on the surface condition generated by the sliding process itself.   Surface modifications during sliding have been formalized (ref 9) by introducing the concept of 'third-bodies' which differ in composition and structure from the original material and which can exist either on the composite surface and/or as a film transferred to the counter-face, usually metal.   A whole range of variables can influence third-body film formation including the geometrical sliding arrangement (refs 10,11), the imposed operating parameters such as load, speed, temperature, surface roughness and type of motion (refs 12,13) and the bulk structure of the composite (ref 14).   However, despite considerable experimental effort in recent years it has so far only proved possible to clarify a few specific aspects of third-body film formation with PTFE composites.

1.   The wear rates of composites are generally very sensitive to the topography of metal counterfaces (ref 15).   Reductions in the effective roughness of a counter-face by transfer film formation are thus likely to be an important mechanism of

wear reduction. Figure 2 shows a typical example of the way in which a transfer film from a PTFE/polyimide composite modifies the appearance of a steel counterface. Chain orientation within the PTFE films is also a significant factor and sliding arrangements which interfere with this, eg rotation combined with unidirectional motion, lead to increased wear (ref 16).

2.   PTFE transfer to a metal counterface is enhanced by the presence of copper and lead within the composite (ref 17). It was subsequently suggested that the copper catalysed a reaction between degradation products of the PTFE and the lead (ref 18) but exactly why this should lead to improved transfer films has never been fully explained. Attempts have also been made to look for other potentially reactive PTFE/metal combinations via differential scanning calorimetry (ref 19) but the results are conflicting. There seems to be no necessary correspondence between the existence of an exothermic reaction between PTFE and a metal at high temperatures and the ability of that metal to improve transfer and reduce wear.

3.   Wear of PTFE-containing composites during oscillatory motion tends to be less than in unidirectional sliding at the same loads and speeds (ref 13). The entrapment of wear debris during oscillatory motion leads to more uniform and coherent third-body films. Figure 3 shows an example.

4.   Analyses of the worn surfaces of multi-component composites after sliding against metals show that, in general, almost every element available in the system is likely to become incorporated within the third-body films (ref 13). The relative proportions, however, differ from those in the bulk materials. This leads to the conclusion that there can be no simple mechanistic process of film formation; debris must be transferred to and fro between the surfaces with particles being repeatedly deformed, degraded and reformed. It is tempting to speculate that the rate-controlling parameter in wear might be the rate at which debris particles are irretrievably lost from the contact zone and it is therefore pertinent to consider how these particles can move around in particular contact configurations (ref 20). Experimental effort on this aspect, however, has so far been confined largely to model systems (ref 21).

5.   Third-body film formation from PTFE-containing composites is almost wholly prevented in the presence of fluids (ref 22). Fluid lubrication can thus result in an increase in wear rate of such composites and examples are shown in figure 4. Although water is particularly deleterious, most other fluids including conventional lubricating oils give similar trends. It is believed that the fluids penetrate surface cracks or voids and disrupt any existing surface films via hydrostatic action. In addition, further film formation is prevented because adsorption of the fluid inhibits adhesion of the debris particles to the substrate and cohesion between them.

6.   In composites containing more than one solid lubricant, interference can arise during third-body film formation. The situation is somewhat analogous to that of additive interference in extreme pressure lubrication. For example, when high modulus carbon fibres are introduced in PTFE composites, the transfer films on a metal counterface are rich in carbon (ref 23). In contrast, transfer films produced from PTFE/glass fibre/MoS_2 composites, of the type widely used as self-lubricating cages for rolling bearings, appear to contain little or no MoS_2 (ref 24). The reasons for adding MoS_2 to PTFE composites remain rather obscure, although one suggestion has been made that the MoS_2 prevents the formation of too thick a transfer film of PTFE (ref 25).

335

In addition to their influence on third-body film formation, fillers and reinforcing fibres in polymers play another major role. Most of the materials commonly used to increase strength or stiffness are abrasive to a greater or lesser extent towards metal counterfaces. Table 1 shows some comparative data obtained in an arbitrary test involving the wear of a bronze ball sliding against various filled polymers. Similar data has recently been given by Anderson and Davies (ref 26). In view of the marked dependence of polymer wear rates on counterface topography, it is reasonable to envisage that small amounts of abrasion by fillers could be beneficial in reducing wear by generating smoother surfaces. This turns out to be so, and a good example is illustrated in figure 5; the wear of PTFE containing the weakly-abrasive, high-modulus, graphite fibres is much more sensitive to counterface roughness (figure 5a) than that of PTFE containing the more-abrasive, high-strength fibres (figure 5b). For composites containing largely non-abrasive fillers, the introduction of small amounts of conventional abrasives, such as Al_2O_3, can sometimes be beneficial, particularly in lubricated conditions where third-body films cannot form (ref 27). However, the choice of the optimum level of abrasiveness needed for minimum wear is by no means clear-cut. Whilst abrasiveness depends on such obvious factors as particle size and shape, hardness relative to the counterface, and the way in which the particles are broken down during sliding, the type of polymer in which they are incorporated also plays a part. The second half of table 1 shows that the abrasiveness of glass fibre depends quite strongly on the matrix polymer. Two aspects are important here; the elastic modulus of the polymer and the extent to which plastic deformation and flow may encapsulate the abrasive particles. Other things being equal, the lower the polymer modulus, the less is the probability of an abrasive particle remaining sufficiently exposed to damage a metal counterface (ref 28).

In PTFE-containing composites, the transfer film on the counterface will also be susceptible to abrasion by fillers. It should, therefore, be possible, in principle, to control the transfer film thickness by suitable adjustment of the type and concentration of abrasive filler. However, the relative roles of transfer and abrasion do not, unfortunately, depend solely on the composite composition; they also vary with the conditions of sliding. Figure 6 shows the general trends in the variation of wear rate with temperature for PTFE containing abrasive and non-abrasive films, and it can be seen that there are marked differences over the lower part of the temperature range. Evans (ref 29) has suggested that the overall tendency for third-body film formation to decrease as the temperature increases is enhanced by the abrasive fillers.

Although the 'intrinsic' abrasiveness of most of the fillers and fibres typically added to polymers is usually relatively low – with the notable exception of glass – carbons and graphites pose special problems. These materials can vary very widely in abrasiveness, depending on the source and type of the original raw material, the heat treatment and degree of graphitization and, for natural graphite, the purity. It has been suggested (ref 30) that variability in abrasiveness could be one of the main reasons for the widely-differing wear behaviour often encountered between nominally similar PTFE/carbon-graphite composites obtained from different manufacturers. It could therefore be useful to consider initiating some form of quality control on filler abrasiveness, possibly by means of the accelerated test procedure developed for assessing the abrasiveness of MoS_2 (ref 31).

OTHER THERMOPLASTICS

In comparison with PTFE, the wear rates of almost all other thermoplastics sliding against metals are either lower or appreciably lower. Additions of fillers or fibres to these materials are therefore intended mainly to improve properties other than wear, such as stiffness, impact resistance, thermal conductivity or friction. Additions of solid lubricants, such as graphite, PTFE, MoS_2 or, more recently, $(CF_x)_n$ usually degrade the mechanical properties but this can be offset by fibrous reinforcement. A vast range of polymer/solid lubricant/ fibre composites is now available, presenting the designer with a confusing choice since the properties of many of these composites tend to be very similar (ref 32). The present situation is somewhat reminiscent of the early days of developments in bonded solid-film lubricant technology and, by analogy, the time may soon be approaching when rationalization and 'compromize' formulations reduce the overall product range to more manageable proportions.

The performance of many thermoplastics and composites, other than those containing PTFE and lamellar solid lubricants, can frequently be improved by lubrication with conventional oils or greases. The lubricant may be introduced externally or dispersed throughout the material itself and liberated either by diffusion (ref 33) or as a result of wear (ref 34). With some polymers, even minute traces of fluid appear to be able to maintain low friction and wear for long periods (ref 35) and figure 7 shows some recent results of this type. The reasons for the marked differences in 'endurance' between the different polymers and fluids are not yet fully understood, but plasticisation of the surface layer is likely to play an important role. In very severe conditions of sliding, it has also been shown (ref 36) that a fluid lubricant can penetrate into surface cracks which then act as reservoirs for the continuous supply of fluid to the contact when all excess is removed. Fluid may also penetrate the interface between a fibrous reinforcement and the polymer matrix, or even into the fibre itself if sufficiently porous. The latter is, in fact, used as the basis for controlled lubrication of miniature gyroscope bearings incorporating porous fibre-reinforced resin retainers.

COMPOSITES FOR HIGH LOADS

Composites based on fibre-reinforced thermosetting resins have been used for many years as high load-capacity bearings in well-lubricated conditions where the fluid can provide both hydrodynamic support and cooling (ref 37). For unlubricated operation however, heat generation greatly restricts the maximum permissible speed to around 0.1 m/s or less, even when the coefficient of friction is minimized by solid lubricant additions. One type of high-load composite, which is widely used for aerospace dry-bearings, comprises a thin layer of a fabric-reinforced, thermosetting resin incorporating solid lubricants and adhesively bonded to a harder substrate. There are two main variants; the solid lubricant, usually PTFE, is dispersed throughout the resin matrix - figure 8a - or PTFE is present in filamentary form as part of the structure of the reinforcing fabric - figure 8b. Within each of these variants, a whole spectrum of possible alternative formulations exists by changing the type of weave, the type of reinforcing fibre, the resin matrix or the solid lubricant. However, the literature appears to offer few, if any, general guide lines from which to predict the effects of such changes on friction and wear performance. In an attempt to remedy this, a research programme was initiated several years ago to examine the influence of the structure and

composition of these thin liners on their friction and wear. Using an accelerated test procedure (ref 38) a great deal of specific information was obtained to aid further development (ref 39). Some examples are given in figure 9 which show that:

a. polyamide-imide weft fibres in a double plain weave with PTFE warp fibres lead to lower wear than either glass or polyester;

b. dispersed graphite fluoride in a phenolic resin reinforced with an aramid plain weave fabric is more effective than dispersed PTFE;

c. a phenolic resin leads to lower wear than other resin types in conjunction with a plain weave fabric of twisted PTFE/aromatic polyamide fibres.

The substitution of high temperature resins, such as polyimides or polybenzimidazoles, for the more usual phenolics should be an obvious route for improving high-temperature performance. However, it has not yet proved possible to establish any general trends between composite wear performance and specific resin properties, such as strength, stiffness or thermal stability. There are several possible reasons for this; for example, the intrinsic wear properties of the resins are likely to differ, or there may be marked variations in interfacial bonding with the reinforcing fabric. In addition, it is known (ref 40) that composite wear performance is extremely sensitive to the 'quality' of the resin impregnation, voids being particularly deleterious. Optimization of the composite fabrication procedure following any change in composition is therefore an essential requirement before any meaningful comparisons can be made.

The potential of carbon fibres as a reinforcement for high-strength, dry-bearing composites was recognised at an early stage following their availability. A helically-wound, bearing liner of twisted PTFE and carbon fibres was shown (ref 41) to be capable of supporting stresses exceeding 210 MPa with negligible wear during slow speed, oscillatory motion. This early promise, however, was not immediately followed up, largely because of the non-availability of continuous lengths of fibre with small numbers of filaments per tow. Subsequent developments concentrated on incorporating chopped carbon fibres into thermoplastics (refs 42,43) and thermosetting resins (ref 44), particularly polyimides (refs 45,46). For high-load spherical bearings, the greatest dynamic load capacity is obtained when the composite is present as a thin layer on the outer shell rather than when attached to the ball (ref 47). It would seem reasonable to suppose that further increases in load capacity could be obtained by using carbon fibre reinforcement in woven form, and this has recently been demonstrated by Gardos and McConnell (ref 48) using a 3D weave of high strength fibres. In conjunction with a polyimide matrix resin and various lubricating additives a dynamic load capacity of around 200 MPa was obtained at 316°C during slow speed oscillation. This performance appears to be the best so far achieved and must be nearing the limit of the maximum attainable with an organic-based composite.

In so far as the coefficient of friction of high-load composites is concerned, PTFE is usually more effective as a solid lubricant addition than MoS_2, provided that the temperatures remain less than about 250°C. $(CF_x)_n$, however, is also promising - figure 9b - but it is not clear whether this is directly related to its intrinsic lubricant properties or to the greater ease with which it can be dispersed in organic resins (ref 46). With PTFE, two aspects combine favourably to facilitate lubrication at high stresses (ref 49); the coefficient of friction decreases with increasing temperature as a consequence of the reduction in shear

strength - figure 10a - and the friction also decreases with increasing load - figure 10b. The latter trend is, presumably, a reflection of the classical mechanism of solid lubrication, a thin, third-body film being generated on the harder substrate by the sliding process itself.

Some of the ways in which third-body films influence the friction and wear of PTFE-containing composites have already been discussed. A major problem still remaining is to relate the type of films to composite structure and composition and this, in turn, necessitates obtaining more information to characterise these films. Numerous techniques are available including XPS, IR spectroscopy and pyrolysis-gas chromatography (for composition), SEM and STEM (for structure and uniformity), profilometry or capacitance probes (for topography and thickness) and micro-indentation methods (for mechanical strength and stiffness). However, considerable uncertainty exists in defining the most appropriate levels of sensitivity required. For example, how relevant to the wear process is the surface composition determined by XPS, or of what significance to wear is the fine-scale topographical detail observed in high-resolution SEM? These problems are analogous to that of 'functional filtration' in the quantitative analysis of surface profiles (ref 50).

Since the primary requirement from any third-body film is that of minimising friction and wear, a more pragmatic approach to film characterisation can be made by assessing its wear-reducing properties independently of those of the composite from which it is derived. A convenient way of doing this is to determine the wear rate of a 'probe' material sliding against a transfer film - figure 11a. Interference with the structure of the film is minimized by ensuring that the load on the probe is very much less than that on the composite itself. Some work of this type was undertaken several years ago to examine the potential of various carbon fibre-reinforced polymers as self-lubricating cages for rolling bearings. It was hypothesised that the most suitable composite would be the one exhibiting least wear of both the probe and the composite, and figure 12 demonstrates that in this respect a number of composites appear to be superior to the two varieties of PTFE/glass fibre/MoS$_2$ which are in current use. Although later work (ref 51) demonstrated that there was only poor correlation between composites assessed in this way and their performance as rolling bearing cages, the basic method remains of interest in that it provides information on overall properties of the third-body films which is unobtainable in any other way. For example, figure 11b curve a, shows the dependence of the endurance of a preformed transfer film from PTFE/25% wt high modulus carbon fibre as a function of the time of film formation. The decrease in endurance after long formation times is believed to be associated with a weakening of the film adhesion to its substrate. Incorporating 10% of lead into the composite eliminates the reduction - curve b - and it is known from earlier work (ref 52) that soft metals facilitate adhesion of lamellar solids during transfer to harder metals.

METAL-BASED COMPOSITES

The basic problem with incorporating lamellar solid lubricants, such as graphite or MoS$_2$, into metals is that the mechanical strength, particularly in tension, is significantly reduced. These solids are intended to reduce friction by third-body film formation and it is known that transfer of lamellar solids is an inefficient process (ref 53). It follows that the high lubricant concentrations needed to achieve low friction are likely to result in mechanically weak composites

giving high wear rates.   This inverse trend between friction and wear is
illustrated in the top part of figure 13.   More detailed studies of sintered
metal-lamellar solid mixtures by Tsuya (ref 54) have shown that some deviations
from this general trend exist and wear may decrease to a minimum at some optimum
lubricant concentration.   However, even at this optimum level, the wear rates of
all such binary mixtures remain much greater (10^{-4}-10^{-3} mm^3/Nm) than those typical
of filled or reinforced plastics (10^{-7}-10^{-6} mm^3/Nm).

Greater reductions in the wear of metal-lamellar solid mixtures can be obtained
from increasing the efficiency of transfer by incorporating PTFE as a 'film-former'
(discussion to ref 53).   However, an alternative route is to devise suitable
fabrication techniques which result in mechanically stronger composites.   Examples
include the use of refractory metals, together with carbon, to induce carbide forma-
tion (ref 55);   codeposition by plasma spraying (ref 56);   the provision of a pattern
of minute holes or recesses in a metal surface which are then filled with lubricant
(ref 57) or the infiltration of porous metals by solid lubricants (ref 58).
One particular material of the last type - a layer of porous bronze on a steel
substrate and filled with a PTFE-Pb mixture - has been available for over twenty
years and its performance as a dry bearing at moderate temperatures and stresses
(<250°C and <35 MPa) is still hard to beat.   Attempts to duplicate this construction
with metals other than bronze, eg cobalt (ref 59), or lubricant mixtures other than
PTFE-Pb, eg PTFE-MoS$_2$ (ref 60), do not appear to have been particularly successful.
For high temperature applications the most promising metal matrix composites are
those based on porous nickel alloys containing CaF$_2$/BaF$_2$ eutectic as a solid
lubricant (ref 58).   Optimum performance, however, is critically dependent on
careful attention to detail during surface preparation and heat-treatment (ref 61).
Plasma-sprayed, multi-component coatings, such as 30% Ni-Cr, 30% Ag, 25% CaF$_2$,
15% glass avoid this sensitivity and have been reported to exhibit friction
coefficients of around 0.2 over the wide temperature range from -100°C to +870°C
(ref 62).

Very little attention has so far been paid to fibre-reinforced metal composites.
Mixtures incorporating chopped carbon fibres were examined some years ago (ref 63),
but the preparative techniques available at the time were primitive, resulting in
poor mechanical properties.   Since then the demands for structural composites
have stimulated much more sophisticated fabrication methods, particularly with
boron fibres, and the time may now be opportune for a re-assessment of the
tribological prospects.   Another area of potential future interest lies in
materials produced by rapid solidification processing.   This technique offers the
possibility of making novel, wear-resistant composites, involving both metals and
non-metals and either as uniform mixtures or as two-phase structures (ref 64).

BRAKE MATERIALS

Composites for high energy brakes comprise a group of materials whose require-
ments differ in several ways from those intended for bearings, eg stability of the
friction coefficient with varying load, speed and temperature, high thermal
capacity, resistance to thermal shock etc.   Although low wear rates are, of course,
important, the values which can usually be tolerated in service tend to be somewhat
greater than those acceptable for dry-bearing applications.   One of the most
significant advances of recent years has been the development of carbon-carbon
composites for aircraft brakes (ref 65) and this has prompted a number of

340

investigations into the ways in which performance is influenced by the structure and composition of the materials (refs 66,67,68).   The two main problems appear to be the tendency for graphitic materials to undergo rapid wear at elevated temperatures (ref 69) and for non-graphitic materials to exhibit large fluctuations in friction - figure 14a.   Both of these problems can largely be overcome by the introduction of additives.   Rapid wear at high temperatures is associated with the disruption of the third-body films and additions of phosphorous-containing additives assist in maintaining these films (ref 70).   These additives also have the additional merit of reducing the rate of oxidation.   The stability of the friction coefficient with non-graphitic composites is to some extent dependent on their structure and comparison of figures 14b with 14a shows that composites based on carbon fibre cloth are less-susceptible to friction fluctuations than those based on random mats.   Additives are again likely to be beneficial - figure 14c.   It has been suggested (ref 71) that many of the inorganic additives which prevent the build-up of high friction in non-graphitic carbons do so because they are mildly abrasive and maintain the real contact area in a uniformly sub-divided state.   Only very small amounts of abrasive material can be tolerated, however;   too much leads to increased composite wear (ref 67).

Over the whole spectrum of brake materials - carbon-carbon composites, metal ceramics, and organic-based composites - there is a wealth of technology available which has so far remained largely untapped as a source for other applications. With some modifications, notably to reduce friction, many brake material formulations might be of interest as dry-bearings.   Carbon-carbon composites, with additives, could be of particular interest in this respect.

COMMENT

This survey of the various ways in which composite materials can provide low friction and wear has necessarily been somewhat selective and omitted reference to a number of material groups which are being discussed elsewhere in this Conference; ceramics, surface treatments and wear-resistant metals.   Nevertheless it is hoped that sufficient has been given to show that there have been significant advances over the past decade or so, both in the development of improved composites and in the understanding of some aspects of their friction and wear mechanisms.   For the future, progress is needed on three general fronts.

1.   Novel composite compositions.   This item is difficult to discuss in general terms because what is needed is an element of 'lateral thinking' (ref 72) to result in an inventive step.   A relevant historical example is the concept of the thin, dry-bearing liner comprising a resin-bonded fabric of interwoven PTFE and glass fibres (ref 73).

2.   New blends of existing materials to achieve synergism.   The likelihood of any radically new types of solid lubricants emerging in the forseeable future is now beginning to seem rather remote.   Moreover, whilst new polymers with improved thermal stabilities do still emerge from time to time, they tend to be increasingly expensive and intractable to process.   There remain, however, numerous possibilities for blending existing materials together in different ways.   A good example is the recent development of the high-load, high-temperature dry-bearing composite described by Gardos and McConnell (ref 48).

3.   Relationships between composite structure, composition and performance.   This
item offers major research opportunities.   To assist in the development of new
composite formulations, effort needs directing towards elucidating many of the
mysteries still associated with the generation of third-body films.   These films
are so important to the unlubricated friction and wear behaviour of so many
materials that until more is known about their production and properties progress
is likely to remain sporadic and largely empirical.

REFERENCES

1.   Steijn, R.P.:   The Sliding Surface of Polytetrafluoroethylene: an
      Investigation with the Electron Microscope.   Wear, vol. 12, 1968,
      pp. 193-212.

2.   Pooley, C.M.; and Tabor, D.: Friction and Molecular Structure: the Behaviour
      of some Thermoplastics.   Proc. Roy. Soc. Lond., Ser. A., vol. 329, 1972,
      pp. 251-274.

3.   Tanaka, K.;   Uchiyama, Y.;   and Toyooka, S.:   Mechanism of Wear of
      Polytetrafluoroethylene.   Wear, vol. 23, 1973, pp. 153-172.

4.   Tanaka, K; and Kawakami, S.:   Effect of Various Fillers on the Friction and
      Wear of Polytetrafluoroethylene-based Composites.   Wear, vol. 79, 1982,
      pp. 221-234.

5.   Arkles, B;   Gerakaris, S;   and Goodhue, R.:   Wear Characteristics of
      Fluoropolymer Composites.   In - Advances in Polymer Friction and Wear,
      Polymer Sci. & Tech., vol. 5b, 1974, pp. 663-688.

6.   Lancaster, J.K.:   The Effect of Carbon Fibre Reinforcement on the Friction and
      Wear of Polymers.   Brit. J. Appl. Phys. (J. Phys. D.), vol. 1, 1968,
      pp. 549-559.

7.   Ohmae, N.;   Kobayashi, K.;   and Tsukizoe, T.:   Characteristics of Fretting of
      Carbon Fibre Reinforced Plastics.   Wear, vol. 29, 1974, pp. 345-353.

8.   Gardos, M.N.:   Self-lubricating Composites for Extreme Environment
      Applications.   Tribology Int., vol. 15, 1982, pp. 273-283.

9.   Godet, M.;   and Play, D.:   Introduction to Tribology.   Coll. Int. du CNRS,
      No. 23, Polymères et Lubrification.   CNRS, Paris, 1974, pp. 361-376.

10.   Lancaster, J.K.:   Geometrical Effects on the Wear of Polymers and Carbons.
      Trans. A.S.M.E., Ser. F., J. Lub. Tech., vol. 97, 1975, pp. 187-194.

11.   Play, D.;   and Godet, M.:   Self-Protection of High Wear Materials.
      A.S.L.E. Trans., vol. 22, 1979, pp. 56-64.

12.   Lancaster, J.K.;   Godet, M.;   Play, D.;   Verrall, A.;   and Waghorne, R.:
      Third Body Formation and the Wear of PTFE Fibre-based Dry Bearings.
      Trans. A.S.M.E., J. Lub. Tech., vol. 102, 1980,

13. Lancaster, J.K.; Bramham, R.W.; Play, D.; and Waghorne, R.: Effects of Amplitude of Oscillation on the Wear of Dry Bearings containing PTFE. Trans. A.S.M.E., J. Lub. Tech., vol. 104, 1982, pp. 559-567.

14. Play, D.: Portance et Transport des Troisieme Corps en Frottement Sec. Thesis, Université Claude-Bernard, Lyon, 1979.

15. Hollander, A.E.; and Lancaster, J.K.: An Application of Topographical Analysis to the Wear of Polymers. Wear, vol. 25, 1973, pp. 155-170.

16. Briscoe, B.J.; and Stolarski, T.A.: The Influence of Linear and Rotating Motions on the Friction of Polymers. Trans. A.S.M.E., J. Lub. Tech., vol. 103, 1981, pp. 503-508.

17. Mitchell, D.C.; and Pratt, G.C.: Friction, Wear and Physical Properties of Some Filled PTFE Bearing Materials. Proc. I. Mech. E. Lub. & Wear Conf., 1957, pp. 416-423.

18. Pratt, G.C.: Plastics as Bearing Materials, with particular Reference to PTFE. Plastics Inst. (Lond.) Trans. & J., vol. 32, 1964, pp. 255-260.

19. Pocock, G.; and Cadman, P.: The Application of Differential Scanning Calorimetry and Electron Spectroscopy to PTFE-Metal Reactions of Interest in Dry Bearing Technology. Wear, vol. 37, 1976, pp.129-146.

20. Godet, M.; Play, D.; and Berthe, D.: An Attempt to Provide a Unified Treatment of Tribology through Load Carrying Capacity, Transport and Continuum Mechanics. Trans. A.S.M.E., J. Lub. Tech., vol. 102, 1980, pp. 153-164.

21. Play, D.; and Godet, M.: Visualization of Chalk Wear. Proc. 3rd Leeds-Lyon Symposium on the Wear of Non-Metallic Materials. MEP, London, 1978, pp. 221-229.

22. Bramham, R.W.; King, R.B.; and Lancaster, J.K.: The Wear of PTFE-containing Dry Bearing Liners Contaminated by Fluids. A.S.L.E. Trans., vol. 24, 1981, pp. 479-489.

23. Giltrow, J.P.; and Lancaster, J.K.: The Friction and Wear of Carbon-fibre reinforced PTFE. Proc. AFML-MRI Conf. on Solid Lubricants. AFML-TR-70-127, 1970, pp. 305-331.

24. Gardos, M.N.: Theory and Practice of Self-lubricated Oscillatory Bearings for High Vacuum Amplications. Part I - Selection of the Self-lubricating Composite. A.S.L.E. Prep. 80-LC-6B-1, 1980.

25. Todd, M.J.: Solid Lubrication of Ball Bearings for Spacecraft Mechanisms. Tribology Int., vol. 15, 1982, pp. 331-337.

26. Anderson, J.C.; and Davies, A.: Polymer Composite Abrasiveness in Relation to Counterface Wear. A.S.L.E. Preprint 82-LC-2B-3, 1982.

27. Evans, D.C.: The Influence of an Abrasive Filler on the Wear Properties of PTFE-based Composites. Proc. 2nd Int. Conf. on Solid Lubrication, A.S.L.E. SP-6, 1978, pp. 202-211.

28. King, R.B.; and Lancaster. J.K.: Wear of Metals by Elastomers in an Abrasive Environment. Wear, vol. 61, 1980, pp. 341-352.

29. Evans, D.C.: The Friction and Wear Properties of PTFE Composites at Elevated Temperatures. Proc. I. Mech. E. Tribology Group Convention, Swansea, April 1978, Paper C26/78.

30. Lancaster, J.K.: Contamination Effects in Solid Lubrication. J. Soc. Env. Engrs., vol. 19-4, 1980, pp. 13-19.

31. Lancaster, J.K.: An Apparatus for Measuring Small Amounts of Abrasion by Finely Divided Solids. Tribology, vol. 1, 1968, pp. 240-243. (U.K. DEF. STAN. 05-50/1 Method No. 37).

32. A Guide on the Design and Selection of Dry Rubbing Bearings. Eng. Sci. Data Item No. 76029. Eng. Sci. Data Unit, Lond., 1976.

33. Bowers, R.C., Jarvis, N.L.; and Zisman, W.A.: Reduction of Polymeric Friction by Minor Concentration of Partially-Fluorinated Compounds. Ind. Eng. Chem. Prod. Res. Devel., vol. 4, 1965, pp. 86-92.

34. Pascoe, M.W; and Dzhanakmedov, A.K.: The Wear Characteristics of Oil-Filled Plastics. Proc. 3rd Leeds-Lyon Symp. on the Wear of Non-Metallic Materials, MEP, London, 1978, pp. 60-64.

35. Pratt, G.C.: Plastic-based Bearings. Chap. 8 in Lubrication & Lubricants Ed. Braithewaite, E.R. Elsevier, Amsterdam, 1967, pp. 377-426.

36. Skelcher, W.L.; Quinn, T.F.J.; and Lancaster, J.K.: The Influence of Polydimethylsiloxane on the Friction and Wear of Polyphenylene Oxide under Boundary Lubrication Conditions. A.S.L.E. Trans., vol. 25, 1982, pp. pp. 391-399.

37. Hother-Lushington, S.: Water Lubricated Bearings. Tribology Int., vol. 9, 1976, pp. 257-260.

38. Lancaster, J.K.: Accelerated Wear Testing of PTFE Composite Bearing Materials. Tribology Int., vol. 12, 1979, pp. 65-75.

39. Lancaster, J.K.: Assessment of the Wear of Composite Coatings in Reciprocating Line Contact Conditions. In - Selection & Use of Wear Tests for Coatings, A.S.T.M. - STP 769, 1982, pp. 92-117.

40. King, R.B.: Wear Properties of Dry-Bearing Liners at Ambient and Elevated Temperatures. Wear, vol. 56, 1979, pp. 37-53.

41. Shepherd, J.V.: Bearings and Methods of Constructing Bearings. U.K. Patent 1 233 103, 1971.

42. Giltrow, J.P.; and Lancaster, J.K.: Carbon Fibre Reinforced Polymers as Self-Lubricating Materials. Proc. Instn. Mech. Engrs., vol. 182-3N, 1968, pp. 147-157.

43 Giltrow, J.P.; and Lancaster, J.K.: Carbon Fibres in Tribology. Proc. 3rd Conf. on Industrial Carbons & Graphite. Soc. Chem. Ind., London, 1970, pp. 483-490.

44. Giltrow, J.P.; and Lancaster, J.K.: The Role of the Counterface in the Friction and Wear of Carbon Fibre-Reinforced Thermosetting Resins. Wear, vol. 16, 1970, pp. 359-374.

45. Sliney, H.E.; and Johnson, R.L.: Graphite-Fiber-Polyimide Composites for Spherical Bearings to $340^{\circ}C$ ($650^{\circ}F$). NASA TN D-7078, 1972.

46. Sliney, H.E.; and Jacobson, T.P.: Some Effects of Composition on Friction and Wear of Graphite-Fiber-Reinforced Polyimide Liners in Plain Spherical Bearings. NASA - Tech. Paper 1229, 1978.

47. Sliney, H.E.; Jacobson, T.P.; and Munson, H.E.: Dynamic Load Capacities of Graphite-Fiber-Polyimide Composites in Oscillating Bearings to $340^{\circ}C$ ($650^{\circ}F$). NASA TN D-7880, 1975.

48. Gardos, M.N.; and McConnell, B.D.: Development of a High Load, High Temperature Self-Lubricating Composite. Part I - Polymer Matrix Selection A.S.L.E. Preprint 81-3A-3, 1981. Part II - Reinforcement Selection, A.S.L.E. Preprint 81 3A-4, 1981. Part III - Additives Selection, A.S.L.E. Preprint 81-3A-5, 1981. Part IV - Formulation and Performance of the Best Compositions, A.S.L.E. Preprint 81-3A-6.

49. Brentnall, A.B.; and Lancaster, J.K.: The Friction and Wear Behaviour of a Composite, Dry Bearing Liner Sliding against Itself. Int. Conf. on Wear of Materials, Reston, VA., April 1983.

50. Thomas, T.R.; and Sayles, R.S.: Some Problems in the Tribology of Rough Surfaces. Tribology Int., vol. 11, 1978, pp. 163-168.

51. Stevens, K.T.; and Todd, M.J.: Parametric Study of Solid-Lubricant Composites as Ball-Bearing Cages. Tribology Int., vol. 15, 1982, pp. 293-302.

52. Lancaster, J.K.: The Influence of Substrate Hardness on the Formation and Endurance of Molybdenum Disulphide Films. Wear, vol. 10, 1967, pp. 103-117.

53. Lancaster, J.K.: Lubrication by Transferred Films of Solid Lubricants. A.S.L.E. Trans., vol. 8, 1965, pp. 146-155.

54. Tsuya, Y.: Microstructure of Wear, Friction and Solid Lubrication. Tech. Rep. of Mech. Eng. Lab., Tokyo, No. 81, 1975.

55. VanWyk, J.: MoS_2 Solid Lubricant Composites. Proc. AFML-MRI Conf. on Solid Lubricants, Kansas City, MO. AFML-TR-70-127, 1970, pp. 290-304.

56. Sliney, H.E.: Wide Temperature Spectrum Self-Lubricating Coatings Prepared by Plasma Spraying. Thin Solid Films, vol. 64, 1979, pp. 211-217.

57. Kinner, G.H.; and Lancaster, J.K.: Improvements in or Relating to Bearing Materials. U.K. Patent, 1 596 279, 1981.

58. Sliney, H.E.: Self-Lubricating Composites of Porous Nickel and Nickel-Chromium Alloy Impregnated with Barium Fluoride-Calcium Fluoride Eutectic. A.S.L.E. Trans., vol. 9, 1966, pp. 336-347.

59. Ward, R.: Investigation of a Cobalt-Based Dry Bearing Material. Cobalt, vol. 2, 1975, pp. 43-48.

60. Efimov, A.I.; and Semenov, A.P.: Estimating the Life of Metal-Fluoroplastic Bearings. Russ. Eng. J. vol. 55(1), 1975, pp. 3-6.

61. Gardos, M.N.: Some Topographical and Tribological Characteristics of a CaF_2/BaF_2 Eutectic Containing Porous Nichrome Alloy Self-Lubricating Composite. A.S.L.E. Preprint 74-LC-2C-2, 1974.

62. Sliney, H.E.: Solid Lubricant Materials for High Temperatures – a Review. Tribology Int., vol. 15, 1982, pp. 303-315.

63. Giltrow, J.P.; and Lancaster, J.K.: Friction and Wear Properties of Carbon Fibre Reinforced Metals. Wear, vol. 12, 1968, pp. 91-105.

64. Ast, D.G.; and Zielinski, P.G.: Preparation of Metallic Glasses with Second Phase Particles. Proc. 3rd Conf. on Rapid Solidification Processing Principles and Technologies. Nat. Bur. Stands. Dec. 1982. To be published.

65. Weaver, J.V.: Advanced Materials for Aircraft Brakes. Aero. J., vol. 76, 1972, pp. 695-698.

66. Lancaster, J.K.: The Friction and Wear of Non-Graphitic Carbons. A.S.L.E. Trans., vol. 20, 1976, pp. 43-54.

67. Bill, R.C.: Friction and Wear of Carbon-Graphite Materials for High-Energy Brakes. NASA TN D-8006, 1975.

68. Chang, H.W.; and Rusnak, R.M.: Contribution of Oxidation to the Wear of Carbon-Carbon Composites. Carbon, vol. 16, 1978, pp. 309-312.

69. Lancaster, J.K.: Transitions in the Friction and Wear of Carbons and Graphites Sliding against Themselves. A.S.L.E. Trans., vol. 18, 1975, pp. 187-201.

70. Lancaster, J.K.: Additive Effects on the Friction and Wear of Graphitic Carbons. Proc. 3rd Leeds-Lyons Symp. on Wear of Non-Metallic Materials, M.E.P., London, 1978, pp. 187-195.

71. Lancaster, J.K.: Stabilization of the Friction and Wear of Non-Graphitic Carbons by Additives. Proc. 2nd Int. Conf. on Solid Lubrication, Denver, A.S.L.E. SP-6, 1978, pp. 176-188.

346

72. de Bono, E.: The Use of Lateral Thinking.   Jonathan Cape, London, 1967.

73. White, C.S.: Improvements Relating to Low Friction Elements and Materials
        Used in Making Them.   U.K. Pat. 845, 547, 1960.

TABLE 1.   COMPARATIVE ABRASIVENESS OF POLYMERS WITH
VARIOUS FILLERS AND FIBRES

COMPOSITE	ABRASRION RATE

Polymers alone

Nylon 6.6, Acetal copolymer, Polyethylene, PTFE, Polyester	<0.01

PTFE-composites

25% wt asbestos fibre	10
25% wt high strength carbon fibre	8
30% wt flake mica	3.1
25% wt coke	1.7
25% wt high modulus carbon fibre	0.2
40% wt bronze	0.08
33% wt graphite	0.05

Glass-reinforced polymers (30% wt)

Polyester	146
PTFE	62
Acetal copolymer	15
Nylon 6.6	7.3

Abrasion rate of a bronze ball, H ∼185 VPN sliding in epicyclic motion at a
load of 10N over the polymer composite surface.
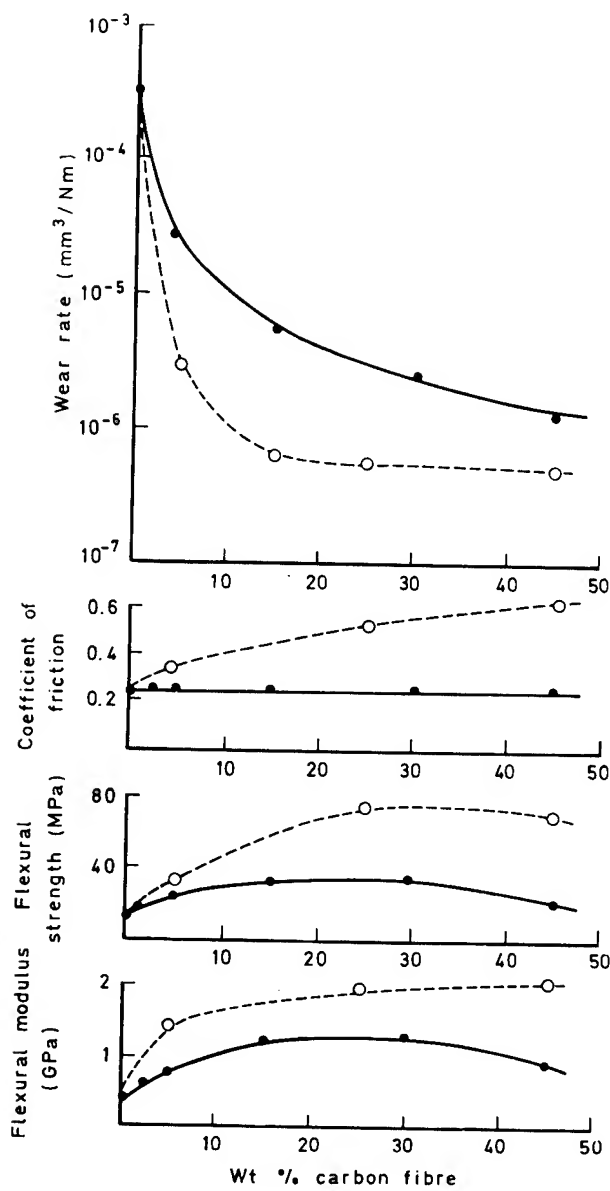
Figure 1.   Influence of carbon fibre concentration in PTFE on a. Wear
rate;   b. coefficient of friction;   c. flexural strength
and d. flexural modulus.
Full lines - high modulus fibres;   hatched lines - high
strength fibres.   Wear tested against low carbon steel,
0.15 μRa finish.
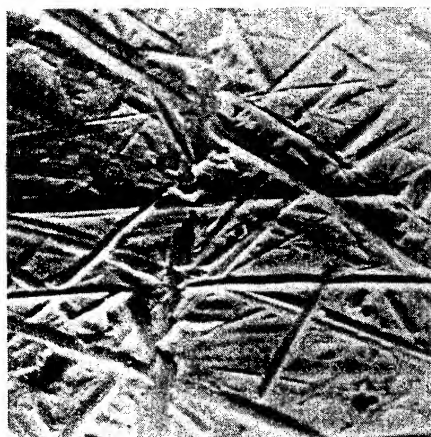
a
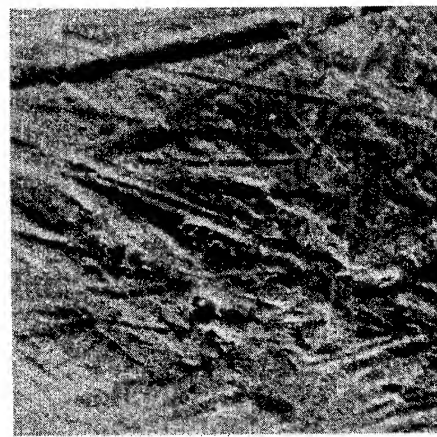
b

Figure 2.   Appearance of transfer film from PTFE/25% polyimide on low
carbon steel.   a. Original surface; b. film-covered.
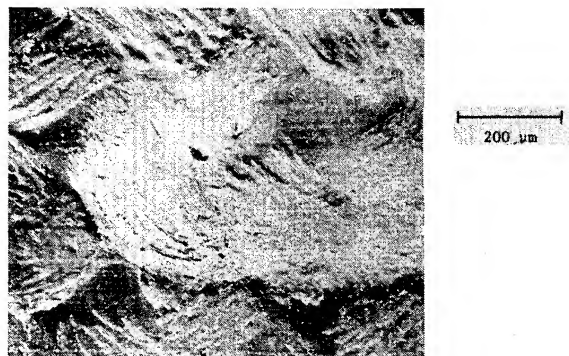
a
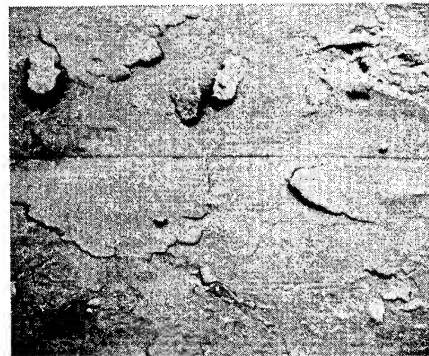
b

Figure 3.   Third-body surface films on a PTFE/glass fibre/resin
dry-bearing liner after a. Continuous rotation;
b. Oscillatory motion, amplitude 2.35 mm.
Load = 4.82 kN (mean stress = 15 MPa).

Figure 5. Influence of counterface roughness on the wear of carbon fibre-reinforced PTFE. a. High modulus fibres; b. High strength fibres.
Counterface; low carbon steel
Roughness; 1. 0.04 μm Ra, 2. 0.18 μm Ra, 3. 0.5 μm Ra.

Figure 4. Effect of introducing water on the wear of four PTFE composites. Counterface; stainless steel, 0.15 μm Ra.

350

Figure 7. Effects of traces of fluids on the friction of polymers.
a. Various polymers : mineral oil hydraulic fluid (OM15)
b. Acetal + various fluids
(Pin-disc tests against stainless steel with 0.5 µℓ of
fluid added after unlubricated running in. Load = 20 N,
Speed = 0.5 m/s.)

Figure 6. Variation of wear rate of PTFE composites with abrasive
and non-abrasive fillers.
Counterface; stainless steel, 0.15 µm Ra.

351
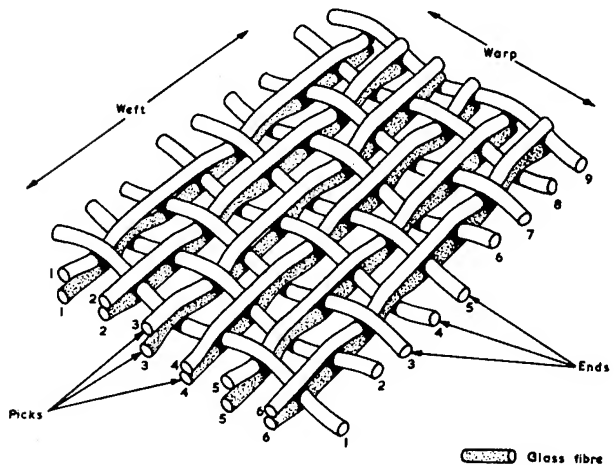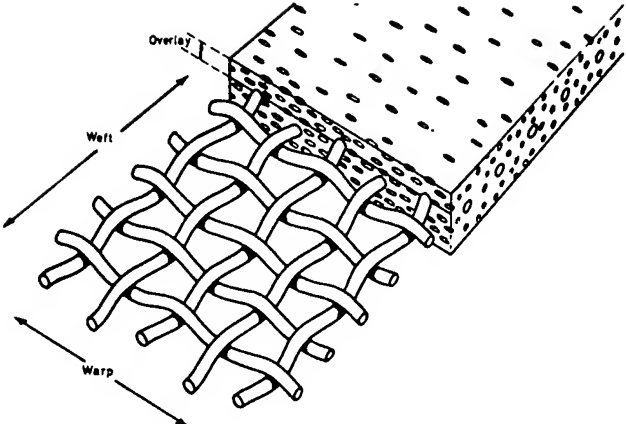
Figure 8.

Typical constructions of dry-bearing liners.
a. PTFE particles or flock dispersed throughout the resin.
b. PTFE fibre interwoven within the reinforcing fabric.
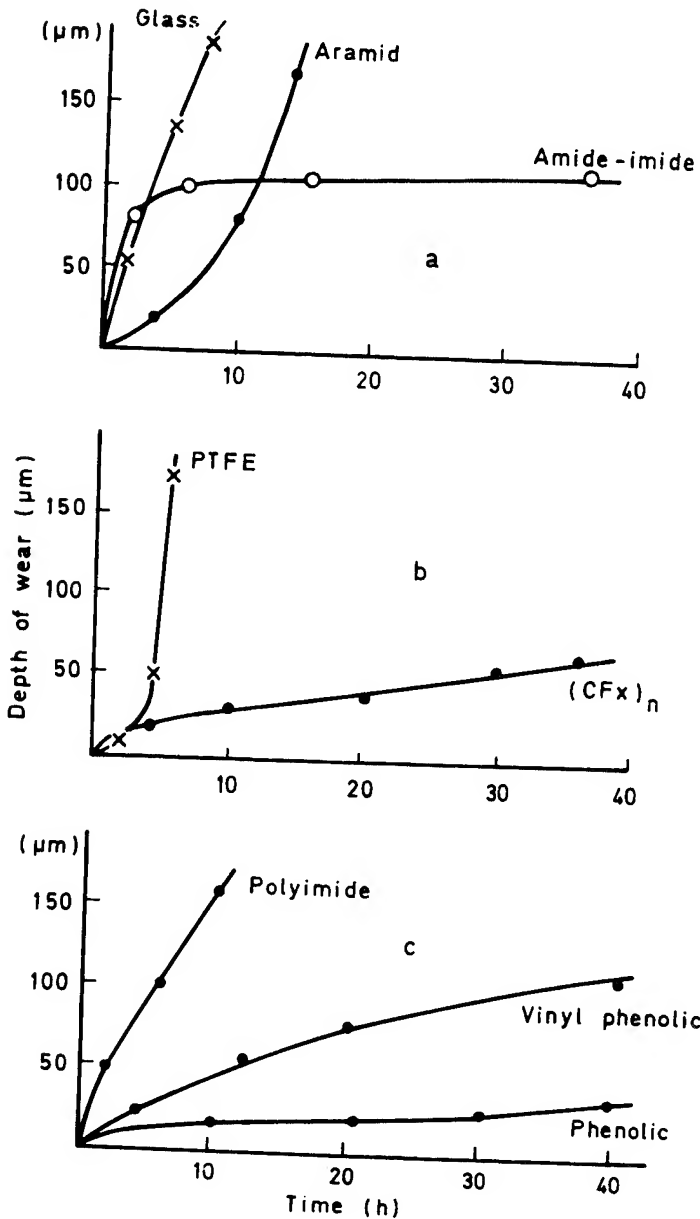
Figure 9.

Effect of various composition changes on the wear of thin, dry-bearing liners.
a. Different second fibres in a double weave fabric with PTFE warp fibres. Phenolic resin.
b. Solid lubricant additions (7% vol.) to the resin reinforced with an aramid plain weave fabric. Phenolic resin.
c. Different resin types with a matt weave fabric of twisted PTFE & aromatic polyamide fibres.
(Reciprocating line contact tests against 440C stainless steel; load = 450N.)

352

Figure 11. Wear of a low carbon steel probe sliding against a transfer
film on a steel ring.
a. Experimental arrangement
b. Endurance of transfer film v time of film formation
before removal of the composite
1. PTFE/25% high modulus carbon fibre
2. PTFE/25% high modulus carbon fibre/10% Pb.

Figure 10. Variation of friction with a. temperature and b. load for
a PTFE/glass fabric-reinforced dry-bearing liner.
1. Against itself
2. Against 440C stainless steel, 0.15 μm Ra.

353
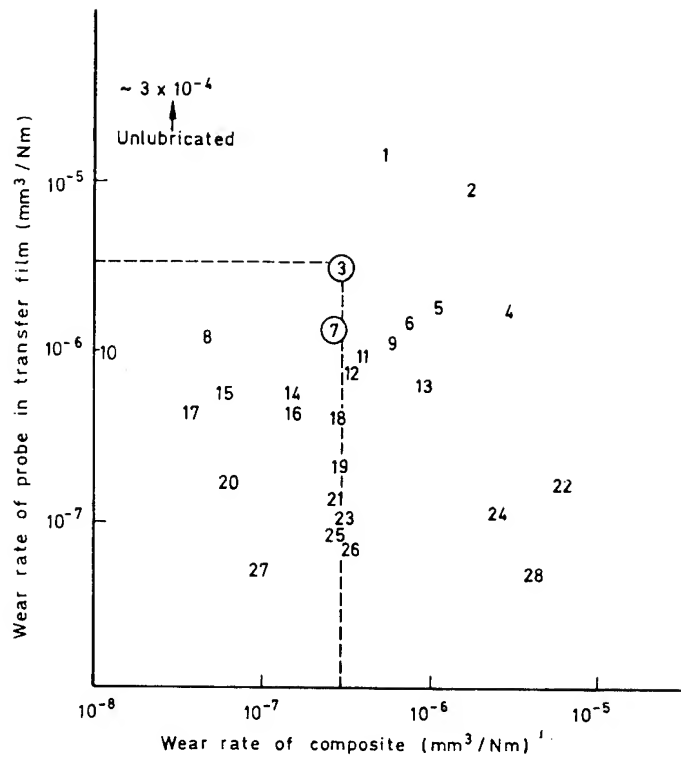
Figure 12. Variation of probe wear rate in transfer film with composite wear rate. Experimental arrangement as in Figure 11a. All films preformed for 4h and composite removed.
Materials.

1. Polyester/40% II cf
2. Acetal/25% I cf
3. PTFE/glass/MoS$_2$ (Type A)
4. Acetal
5. PTFE/15% II cf/10% MoS$_2$
6. PTFE/25% II cf
7. PTFE/glass/MoS$_2$ (Type B)
8. PTFE/20% II cf/20% Cu
9. PTFE/12$\frac{1}{2}$% I cf/12$\frac{1}{2}$% II cf
10. Polyimide/60% I cf

11. PTFE/24% I cf/7% Ag
12. PTFE/23% I cf/10% brass
13. PTFE/20% II cf/20% brass
14. Polyimide/15% graphite
15. Polyester/33% I cf/21% PTFE
16. PTFE/10% MoS$_2$
17. PPO/25% I cf
18. PTFE/25% graphite
19. PTFE/25% I cf
20. Polyphenylene/38% I cf

21. Polyester/60% I cf/10% Pb
22. PTFE/25% brass
23. PTFE/25% I cf/10% MoS$_2$
24. Polyimide/10% MoS$_2$
25. PTFE/25% I cf/10% Pb
26. PTFE/25% I cf/10% MoS$_2$/10% Pb
27. Polyester/40% I cf
28. PTFE/70% Ag/10% NbSe$_2$

354

Figure 14. Variation of friction with time for carbon composites sliding against non-graphitic carbon. Load = 22N, speed = 2 m/s.
a. Random mats of high strength carbon fibre densified in various ways
b. Carbon fibre cloth of various types Temperature ~75°C. Figures in brackets are the mean wear rates in 10⁻6 mm3/Nm.
c. Effect of various additives in non-graphitic carbon. Temperature ~200°C

Figure 13. Wear rate-coefficient of friction data for metal-solid lubricant mixtures, derived from various literature sources.

355

DISCUSSION

Brian Briscoe
Imperial College
London, England

Dr. Lancaster has presented some very interesting examples of "third-body" layers playing a vital role in defining the wear of composities. Could I ask whether this is generally important and also if the probable "lubricating" properties of these layers is considered during the formulation of confined bearings?

DISCUSSION

S. Frank Murray
Rensselaer Polytechnic Institute
Troy, New York

Dr. Lancaster has presented an excellent overview of the progress that has been made in developing reinforced or filled composites for improved wear resistance. Not too many years ago, typical PV limits (expressed as psi × sliding velocity in ft/min) for most of the better plastic bearing materials were generally in the range from 2000 to 5000. Today, thanks to the efforts of many investigators - including Dr. Lancaster and his associates - these PV limits have been substantially upgraded.

These advances have been the result of research along many lines, including: new resins, improved bearing designs, better reinforcements and fillers, and more awareness of the effects of the environment. In evaluating some of the newer high performance plastic composites, it is not unusual to find that the mechanical components of the test machines are oftentimes more temperature-sensitive than the plastic test specimens.

Dr. Lancaster has covered a wide spectrum of composites and operating variables in his presentation. However, my comments, which are more in the nature of questions, will be restricted to the concept of "third body formation" with plastic composites sliding against metal counterfaces.

In the Army Research Office Tribology program at RPI, we are particularly concerned with the mechanisms of "third body formation," and the durability of these surface layers. How is the transferred layer bonded to the counterface?

We have noted a definite "cycling" pattern in the sliding behavior of composite plastics during long term wear test evaluations. Initially, the sliding behavior is oftentimes very erratic for the first minute or so. Then, as the interface temperature rises, performance improves and smooth sliding is obtained for some period of time (perhaps several hours). However, periodically, even under steady state conditions, the

357

performance will suddenly deteriorate as manifested by noisy operation and a rapid temperature rise. This unstable period may only last for about 30 seconds; then, the test will run smoothly again and the temperature will decrease. We believe that this cycle is the result of "third body" film formation and subsequent disruption of both the surface layer on the composite and the transferred layer on the metal counterface. Figures 1A and 2A illustrate this effect. Figure 1A shows an SEM photomicrograph of the transfer from a graphite powder filled polyimide onto a lapped metal counterface. To the eye, the transferred film is smooth and highly polished, but at higher magnification, tiny mounds, which may be blisters, are visible. This film was formed by sliding at a velocity of $4 \text{ m} \cdot \text{s}^{-1}$ (13 ft/sec) under a stress of 137.9 KPa (20 psi) for about four hours. Figure 2A shows the condition of the transferred film after about 18 hours of sliding. The film had buckled and separated from both the plastic surface and the counterface, and the surface of the plastic composite underneath the film was very rough. These polished films will, however, reform with continued sliding. The films are extremely thin and fragile.

While this example is very specific for the test conditions that were used, it does set the stage for questions regarding the formation of these "third body" films. For instance:

1) Is the initial transfer the result of incipient melting of the plastic matrix followed by transfer to the metal counterface, or is there some chemical reaction taking place which promotes the initial formation and adherence of the transferred film? Buckley [1A] cited experiments in the field ion microscope which showed that when Teflon was loaded in contact with tungsten and then separated, a reaction occurred between the fluorocarbon and the tungsten surface. Reactions were also detected between a polyimide and tungsten. Has other evidence been reported on reactions between polymers and metal counterfaces as a result of sliding?

2) Is any consideration being given to charging [electrostatic effects] with plastics sliding on metals? Such charging effects are well documented [e.g., 2A], but are

358

rarely mentioned in studies on plastic bearings. Yet, such charging effects could promote chemical reactions.

3) Are there any general guidelines available on specifying the initial surface finish of the metal counterface? According to the data shown in Figure 5 of this paper, highly polished surfaces are optimal with the carbon fiber-reinforced Teflon. However, many investigations have recommended rougher surfaces to aid in the formation of adherent transfer films. It seems likely that the films shown in Figures 1A and 2A would behave very differently if the roughness of the counterface was increased, thus changing the stress pattern in the film.

In conclusion, the presentation by Dr. Lancaster has provided considerable food for thought. Many other points that he has raised in his paper, such as the effect of lubricants and the concept of counterface polishing by the use of mildly abrasive fillers would also be interesting topics for extensive discussion. In particular, his recommendation for a standard wear test to evaluate the abrasiveness of fillers or fibers would be a very worthwhile undertaking.

1A. Surface Effects in Adhesion, Friction, Wear, and Lubrication, D.H. Buckley, Tribology Series, 5 (1981) Elsevier Scientific Publ. Co., New York, pp.297-301.

2A. G.W. Sohl, J. Gaynor and S.M. Skinner, "Electrical Effects Accompanying the Stick-Slip Phenomenon of Sliding of Metals on Plastics and Lubricated Surfaces," Trans. ASME, Vol.79, No.8 (1957) pp.1963-1970.
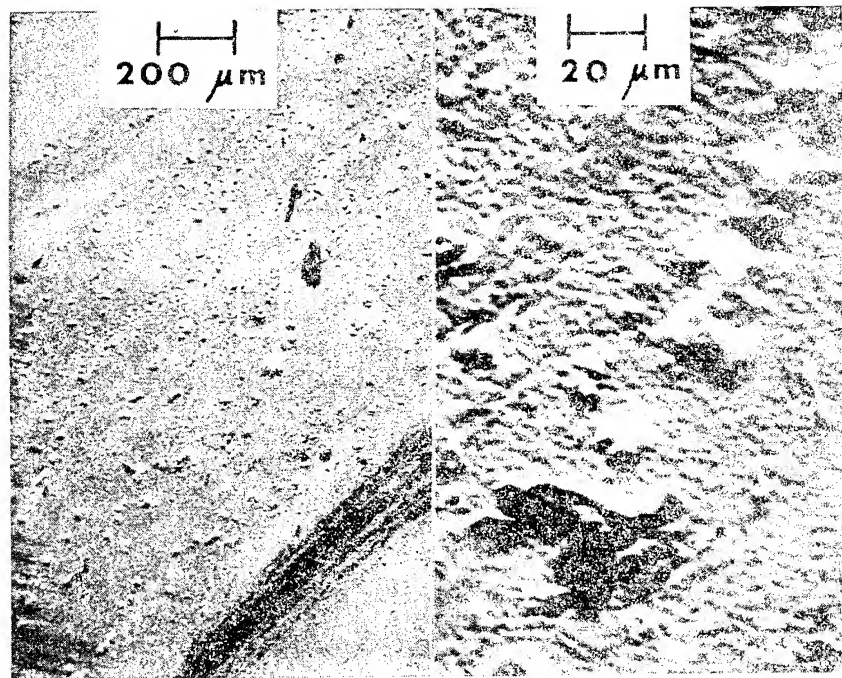
Figure 1A   SEM Photomicrograph of Transferred Film on Metal
Counterface After Four Hours of Sliding
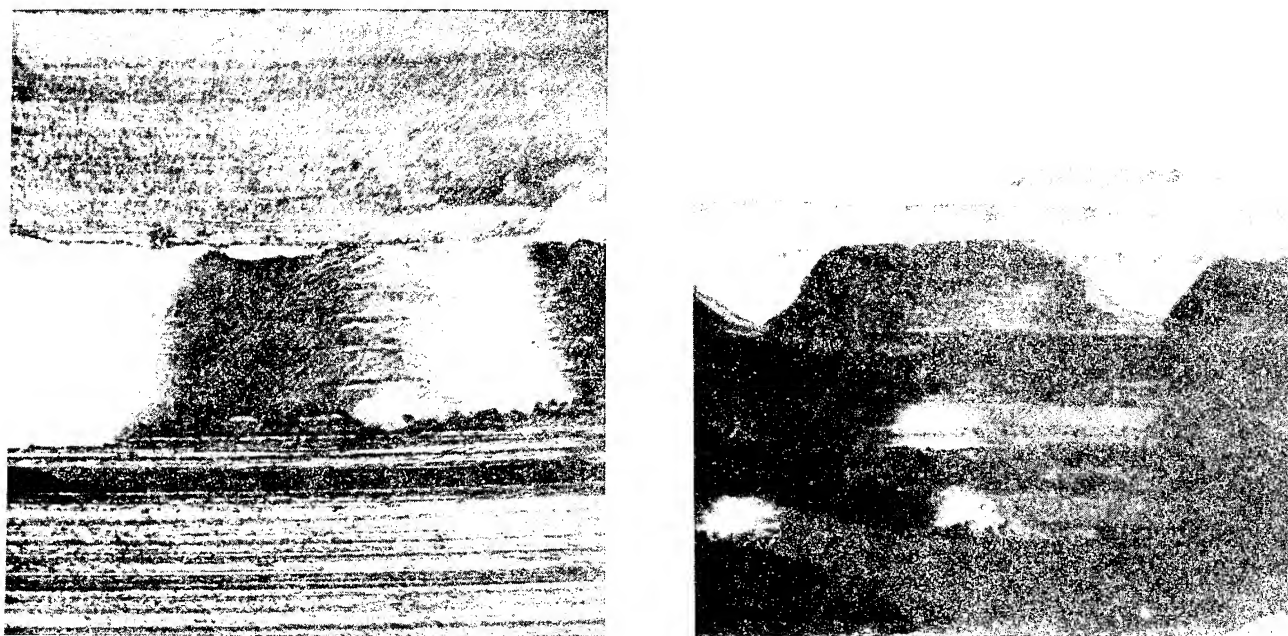
Figure 2A   Buckling of Third Body Film on Composite Substrate
After 18 Hours of Sliding

DISCUSSION

Olof Vingsbo
Uppsala University
Uppsala, Sweden

The paper mainly deals with bearing applications of composites. As to materials, there is strong emphasis on polymers, and PTFE dominates either as (reinforced) matrix material or as an additive. Composite materials in general encompass a wide class of applications, making use of a variety of materials and combinations. Certainly, however, one of the heaviest tribological applications is in bearing systems, and the author's review demonstrates the impact that plastics-based composites have had in this field.

Generally speaking the additions to the matrix material of a composite may serve two purposes:

(1) Contribute to the mechanical strength and stability of the component
(2) Provide (additional) raw material for the third-body film, i.e., effectively to lubricate the system

In terms of tribology, the second purpose is the more interesting. However, there are crosslinks between the two aspects:

(1) A "strengthening" additive may participate in the wear process by abrading the countersurface of the third-body film.
(2) A "lubricating" additive generally causes mechanical weakening of the matrix.

The relations between bulk mechanical properties and triboproperties vary widely from case to case, and the author describes for example the difficulties in selecting the "best" filler or optimizing the filler content in PTFE for minimum wear. For somebody who - like the present discusser - has mainly been working with metals, it is interesting to see that the search for a method or strategy to overcome the difficulties inherent in the selection process for metallic composites has lead to very similar solutions for such different fields as plastic bearings and, for instance, wear resistant steel for heavy mining equipment. In both cases the research effort has been concentrated to the surface region and particularly to the localized modifications generated by and during the triboprocess.

In the case of bearings, the surface phenomena are described in terms of the formation of a "third-body" film on one or both of the tribosurfaces, the structure and properties of which deviate from those of the bulk material. In the case of unlubricated wear of metals, the corresponding concept is the "active layer," developed in the surface region immediately at the beginning of sliding. The triboproperties of the system are determined by the properties of the modified material within the active layer. For obvious reasons, the latter can hardly ever be studied dynamically. It has, however, proved possible to work out a technique of deducing the structure and properties of the active layer from those of the "resulting layer" after testing, when sophisticated laboratory methods can be used.

Traditionally, lubricant-type (third-body) films have been studied with emphasis on chemical analysis, while resulting layers have been mapped with respect to microstructure. In the latter case, high space resolution information on features like grain boundaries, dislocation pattern or precipitates is necessary in the attempt to deduce events like phase transformations, plastic yield or dynamic recrystallization. An increasing interest is, however,

361

directed to chemical analysis with the aid of, for instance, X-ray micro-analysis or ESCA. Recently, analytical techniques also offering high space resolution, mainly scanning Auger microscopy, have been introduced.

The high resolution Auger analysis has the potential of becoming another bridge between studies of predominantly chemical or predominantly micro-structural character. The introduction of high spatial resolution (<100 nm) into chemical analysis appears very fruitful for third-body film studies. As an example, elemental diffusion between film and matrix material, enhanced at high service temperatures, might be possible to track by recording relevant concentration gradients along specimen cross sections.

In his concluding remarks the author suggests three lines of progress, with respect to improved friction and wear performance of composite materials:

(1) Novel compositions
(2) New blends of existing materials
(3) Relationships between structure, composition, and performance

This highlights the troublesome complexity of tribosystems in general, and supports the author's recommendation of, and wish for, "lateral thinking" in tribology. A step in this direction, when trying to improve the tribo-performance of materials - whether homogeneous or composite - is to remember that tribosystems are characterised by parameters from three categories:

(1) Design
(2) Material
(3) Atmosphere

Improving a system by focusing on its material may be the right thing to do, but it may also be just another example of "vertical" (traditional) thinking, which screens the lateral approach to question also the existing design (shape, mode of motion, applied loads, speed, etc.) or atmosphere (lubrication, air, vacuum, etc.). In dealing with all three categories, the number of parameters and variables involved may be large and difficult to handle. Further, vocabulary and "schools" may differ from engineering to chemistry to crystallography. To some extent these difficulties have been overcome (at least when dealing with metal/metal or metal/ceramic tribosystems) by emphasizing the study of operating wear mechanisms - i.e., the micromechanisms of material loss from the tribosurfaces - as a common element.

RESPONSE

J. K. Lancaster
Royal Aircraft Establishment
Farnborough, United Kingdom

The comments and questions raised by both of the discussers to the paper are much
appreciated. It is interesting to note from Professor Vingsbo's contribution of the
extent to which there has been a commonality of approach in studying the wear of
both metals and polymers. With the latter, however, elucidation of the composition
and microstructure in worn surface layers presents rather more difficult problems,
in that many of the sophisticated surface examination techniques widely-used for
metals are inappropriate. His final comment about the necessity for considering
all aspects of the system, rather than the materials alone is, of course, very valid.
Unfortunately, the ideal world has yet to come. All too often problems arise in
which the design of a component has, for a variety of reasons, become immutable and
the only realistic solution to a wear problem is either a change in materials or the
introduction of a 'magic fluid' as lubricant. The only way out of this situation is
to maintain a constant pressure on designers to recognize the necessity for a
systems approach at a very early stage in their thinking.

Dr Murray's observations of periodic instability in the friction and wear behaviour
of some composites are reminiscent of those noted many years ago by Midgely and
co-workers (1B) for non-graphitic carbons, and for which a broadly similar
explanation was invoked. They postulated that the consolidation of wear debris
gradually produced a very smooth surface topography, leading to an increase in the real
area of contact and, in turn, friction. The high friction disrupted the surface film,
produced a rougher surface, lower contact area and friction, and the whole cycle then
repeated.

With regard to the questions prompted by Dr Murray's experiments, however, there are
no simple answers; indeed one of the points made in the paper was that despite all
the research effort to date we are still unable to provide unambiguous answers to such
questions. In so far as bonding of transferred fragments to a metal are concerned,
there is evidence for both mechanical and chemical contributions. In some instances,
the volume of rapid, initial wear of a composite against a rough metal is approximately

commensurate with the volume of the surface depressions, thus supporting a mechanistic mechanism of transfer (2B). In other instances, however, strongly-bonded transfer films have been observed on very smooth metals, suggesting the existence of chemical effects. The best known example of the latter is with PTFE + Cu and Pb (or their oxides), as mentioned in the paper. Belyi and his co-workers (3B) have made extensive investigations into the role of polymer degradation, free-radical formation and chemical reaction during sliding, but it is very difficult to draw general conclusions; much depends on the polymer type and on the life-time of the radicals produced by degradation. There has also been Soviet work (3B) on the influence of electrostatic charging on transfer in which it is suggested that transfer occurs only for those polymers which acquire a positive charge during sliding against a metal, eg PTFE or polyethylene. Polymers which become charged negatively, eg polycaproamide, do not transfer. The relative importance of this mechanism to transfer, compared with mechanical interactions and chemical reactions, is difficult to evaluate at present.

Finally, on the question of whether or not there is an optimum, initial, counterface topography for minimum wear, there is again no really clear-cut answer. For unfilled polymers which transfer to a counterface, eg PTFE and polyethylene, a minimum in the wear rate-topography relationship has been reported on several occasions (4B, 5B, 6B) at roughnesses ranging from 0.1-0.4 μm Ra. Non-transferring polymers, however, do not show such a minimum (7B). When fillers are introduced it is no longer possible to predict any general trend because of the differing extents to which the fillers might be abrasive towards the metal counterface. For purposes of design guidance it now seems to be generally accepted that, with the notable exception of PTFE-fibre/resin liners for high load applications, there is little or no overall economic advantage to be gained by reducing counterface roughnesses below about 0.1-0.2 μm Ra.

References

1B Longley R.I; Midgley J. W; Strang A and Teer D.G: Mechanism of the frictional behaviour of high, low and non-graphitic carbon.
Proc. Inst. Mech. Engrs. Lub. and Wear Group Conv., 1964, pp 198-209.

2B Lancaster J. K: On the initial stages of wear of dry-bearing composites.
Proc. 8th Leeds-Lyon Symposium on "The running-in process in tribology", Butterworths, 1981, pp 33-43.

3B   Bely V. A; Sviridenok A. I; Petrokovets M. I and Savkin V. G: Friction and wear
      in polymer-based materials.

      Pergamon Press, 1982, pp 195-212.

4B   Lewis R.B: Rubbing contact evaluation of polymers. In "Testing of Polymers",
      eds. Schmitz J. V. and Brown W. E.

      Interscience, Vol. 3, 1967 pp 203-219.

5B   Buckley D. H: Advances in polymer friction and wear,

      Polym. Sci. and Tech. Plenum Press, Vol. 5B, 1974, pp 601-603.

6B   Dowson D; Challen J. M; Holmes K and Atkinson J. R: The influence of counter-
      face roughness on the wear rate of polyethylene.

      Proc 3rd Leeds-Lyon Symp on "Wear of Non-metallic materials". MEP Limited,
      1978, pp 99-102.

7B   Clerico M and Rosetto S: Influence of roughness on wear of thermoplastic on
      metal pairs: a Preliminary Analysis.

      Meccanica, Vol. 8, 1973, pp 174-180.

STATUS OF NEW DIRECTION OF LIQUID LUBRICANTS

E. E. Klaus
The Pennsylvania State Univeristy
University Park, Pennsylvania

Liquid lubricants continue to be the predominant form of lubrication for machinery. Petroleum base lubricants comprise a very high percentage of the liquid lubricants in use today. Currently, there is a significant movement toward synthetic lubricants driven by crude oil problems coupled with improved additive response, and low temperature performance for the synthetics.

Improvement of lubricant stability with oxidation inhibitors has increased in importance for most lubricant applications. Significant strides have been made in the understanding of how oxidation inhibitors function. Definition of the physical environment of lubricated bearings has been developed to the point where comparative methods of measurement and calculation of bearing temperatures are in good agreement. Bulk system temperatures tend to be in the range of 75 to 150°, while EHD and boundary lubrication temperatures tend to be in the range of 250 to 350°C.

Additives that provide adequate oxidation stability in the temperature range of bulk systems generally give only reduced oxidation rates under conditions of EHD and boundary lubrication. Convenient techniques have been developed to measure oxidation rates and the mechanisms of oxidation at bulk system and bearing temperatures with a minimum of interference from diffusion limitations. These studies shown that mineral oils, hydrocarbons, esters and a number of other synthetics oxidize through a carbon-carbon bond to form a peroxide which in turn forms a carbonyl as a primary oxidation product. The subsequent reactions of the primary oxidation products form condensation polymers which are precursors to sludge and deposits. The primary difference among the lubricant types are the rates of these reactions.

Metal surfaces, including wear debris, can interact at system temperatues to produce soluble organometallic compounds. These compounds can act as an inhibitor or a promoter for primary and/or subsequent oxidation reactions. The lubrication system metallurgy, as well as wear control additives in the lubricant can play a significant role in overall lubricant stability.

Thermal stability, metal corrosion, and oxidation of the lubricant at the temperatures and general environment of EHD and boundary lubrication may be the dominant source of lubricant breakdown in typical lubrication systems. These primary oxidation products can then undergo further condensaiton polymerization at bulk system conditions. These mechanisms of lubricant breakdown, which can be demonstrated under laboratory conditions, show good correlation with used lubricants taken from bearing tests and engines.

INTRODUCTION

Organic liquids continue to be the dominat form of lubricant used in machinery. Liquid lubricants are generally comprised of a base stock and smaller amounts of materials which are added to control certain functions of the finished lubricant. Additives are used to control such properties of the lubricant as:

  (a) Viscosity properties (polymers).
  (b) Low temperature fluidity (pour depressants).
  (c) Lubricant oxidation (antioxidants).
  (d) Lubrication (lubricity additives).
  (e) Metal corrosion (metal deactivators).
  (f) Deposit formation (detergents and dispersants).

The predominat mechanism by which oils degrade or wear out in use is oxidation. Most lubricants have a higher level of thermal stability than oxidative stability. Thermal stability is dependent primarily on the chemical structure of the base stock while oxidative stability is dependent primarily on the chemical structure of the base stock. Oxidative stability is generally obtained by the use of an additive. Thus, most liquid lubricants are more stable or exhibit a longer useful life in an inert atmosphere such as nitrogen than in an air atmosphere at comparable temperatures. Similarly, lubricants generally exhibit a longer useful life in a system that limits air availability or oxygen content in the atmosphere. These principles have been used in the design of automotive automatic transmissions, high temperature hydraulics, fluid heat transfer systems, etc.

The purpose of this paper is to discuss the state of the art of liquid lubricants. The current understanding of lubricant degradation mechanism will be included to provide some guidance in the selection of lubricant and additive types.

PHYSICAL PROPERTIES OF BASE STOCKS

The vast majority of base stocks used in liquid lubricants are obtained by physical separation techniques from crude oil. The present situation in the petroleum industry has made this source of base stocks less attractive and the properties more difficult to maintain. The current problems of mineral oil base stocks coupled with the increasing demands of lubricated devices are providing incentives for the development of improved refining techniques for mineral oils and the use of synthetics.

Hydrogen can be used to reduce S, N, and unsaturation in petroleum fractions. This product tends to show substantially improved additive response. Other ways of improving additive response is by producing synthetic hydrocarbons and organic esters. These materials are also produced from crude oil by indirect methods. However, such synthetics can also be prepared with appropriate molecular geometry to provide superior physical properties at both high and low temperatures.

Viscosity-temperature properties of synthetics and synthetic-polymer blends are shown on Table 1. These data demonstrate the superior viscosity properties that can be obtained with esters, synthetic hydrocarbons and ester-polymer blends. All of these fluids are free of wax problems at the low temperatures specified by

the respective aircraft and automotive lubricant specifications. They also have volatility properties superior to those of a typical SAE 30 mineral oil.

The volatility characteristics of fluids are related to viscosity-temperature properties by molecular geometry. This relationship is shown on Figure 1. Volatility can be related to viscosity through lines of constant viscosity index. Mineral oil and synthetic base oils are matched on Figure 1 with the appropriate set of physical properties. The combined data from Table 1 and Figure 1 show that certain esters and synthetic hydrocarbons offer very attrctive physical properties for the formultion of lubricants. The low viscosity level combined with low volatility (high flash point) allows for the use of more polymers to make the physical properties of the lubricant even more attractive without significant evaporation problems.

STABILITY OF BASE OILS

The stability of liquid lubricants against oxidation and metal corrosion is related to both the quality of the base oil and additives used to improve base oil stability. Thermal stability of liquid lubricants is related primarily to the structure of the molecules in the lubricant. Since liquid lubricants generally exhibit better thermal stability than oxidation stability or metal interaction (corrosion), the conditions causing the most serious stability problems will be treated first. Recent studies have demonstrated a large degree of commonality for the general mechanism of oxidation degradation. Thus, the discussion on oxidative degradation applies to a wide range of organic liquids where the C-C single bond in the molecule is vulnerable.

In general it has been shown that oxidative degradation of esters, mineral oils and synthetic hydrocarbons proceeds through the same general peroxy radical mechanism. The primary oxidation products resulting from this mechanism are generally molecules of the same general size as the starting material containing an alcohol aldehyde or ketone group. The primary oxidation products undergo further oxidation reactions to produce polymeric secondary reaction products which are the precursors of sludge and varnish-like deposits. From a lubrication point of view, these polymers have been referred to as friction polymers when formed in concentrated contacts. The rate of oxidation is controlled by temperature, oxygen availability, base stock purity and type, and oxidation inhibitors.

Oxidation Inhibitors. All automotive and aircraft lubricants are fomulated with oxidation inhibitors to prevent or reduce oxidation in use. These additives act to reduce peroxide formation or break the chain reaction associated with oxidation. Aromatic amines, hindered phenols and organic sulfides are typical additives used in commerical lubricant formulations. Metal coaters or deactivators represent another method of controlling oxidation in lubricants. Zinc dialkyl dithiophosphate and triciesyl phosphate are examples of effective metal coaters. It also appears that the addition of an excess of base to a lubricant not only limits the rate of increase of acid on oxidation but serves to increase the effectiveness of the inhibitors used to control oxidation.

The response of a lubricant to oxidation inhibitors appears to be related to the level of polar impurities present. Molecules containing C-C unsaturation are not inhibited to the same extent as saturated hydrocarbons. Similarly, polar compounds containing S and N tend to act as natural inhibitors but also may reduce

369

the effectiveness of the oxidation inhibitors added. In general, the small concentration of unsaturates and polar compounds in mineral oil base lubricants results in a less stable formulation than for synthetic hydrocarbons and esters using the same classes of oxidation inhibitors.

Oxidation of lubricants at bulk system conditions of 75 to 150° can be controlled adequately by the commercial inhibitor systems available. Lubricant temperatures ranging from 200 to >350°C are typical of concentrated contacts in gears and bearings in conventional machinery. The time the lubricant spends in these concentrated contacts is short but oxidation can and does occur in well inhibited formulations which would not react under bulk conditions. At the high temperatures existing in concentrated contacts the oxidation inhibitors produce a reduced oxidation rate but do not prevent oxidation. Recent studies have contributed significantly to the understanding of the role of inhibitors in preventing and/or reducing oxidation (1)(2)(3). Studies of oxidation stability in inhibited systems can be conducted in bulk systems during the induction period when little or no oxidation takes place. Under these conditions little oxygen is used and oxygen difusion limitation as a mechanism of supplying oxygen as a reactant is not a problem. After oxidation starts, due to higher temperatues or distruction of the inhibitor system, the reaction in a bulk system is severely diffusion limited.

Lubricant Oxidation. A number of thin film tests have been developed to eliminate or reduce oxygen diffusion as a problem in the study of lubriant oxidation (4)(5)(6)(7)(8). The Penn State microoxidation test has been used to study the kinetics as well as the basic mechanism of lubricant oxidation (9)(10). The general behavior of a well inhibited ester base lubricant is shown in Figure 2. The microoxidation tests have been described by Cvitkovic et al. (8). The analysis by gel permeation chromatography separates the reactants and reactions products by size and provides a semiquantitative analysis by refractive index and/or ultraviolet detectors. Since the ester used in this study is essentially a single compound and the oxidation inhibitors have a lower molecular size, the results shown in Figure 3 can be determined directly from the GPC detectors. The ester remains essentially unchanged until oxidation inhibitor concentration is reduced to less than 10 percent of the original. The primary oxidation product which is somewhat lower than that of the original ester starts to form at this point. However, the primary oxidation product undergoes further oxidation reactions to form a condensation polymer almost as fast as the primary oxidation product is formed. This reaction sequence is shown by the following reactions.

$$\text{Lubricant} + O_2 \xrightarrow{K_1} \text{Primary oxidation products} \xrightarrow{K_2}$$

$$\text{Condensation Polymer} \xrightarrow{K_3} \text{Further condensation polymerization}$$

$$\xrightarrow{K_4} \text{Solid or insoluble sludge and varnish.}$$
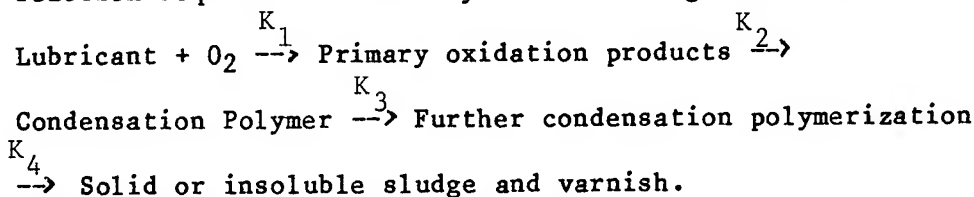
The primary oxidation described by reaction rate constant K_1 appears to be a first order reaction and the rate limiting step in the series. The primary oxidation products appear to undergo condensationpolymerization reactions with each other and with the resulting polymer as indicated by rate constants K_2, K_3, and K_4 until the final product is insoluble and is removed from the reaction system as sludge or varnish. The rate constants K_2, K_3, and K_4 are higher than those of the rate limiting stel K_1. For this reason, there is little build-up of primary oxidation product. The polymer products, sludge and varnish, continue to form even at low temperatures until all of the oxidized product becomes sludge and varnish.

370

A series of mineral oil, synthetic hydrocarbon, and ester base lubricants have been evaluted in the thin film oxidation test under the same test conditions. In all cases, the same basic degradation mechanism was noted and by spectrographic analysis of products the following chemical groupings were formed in every case.

$$OH$$
$$|$$
$$RCH-R$$

$$RCOOR$$

$$O$$
$$\parallel$$
$$RCH$$

$$O$$
$$\parallel$$
$$RC-R$$

$$O$$
$$\parallel$$
$$RC=C-CH$$

$$O$$
$$\parallel$$
$$RC=C-C=C-C-C$$
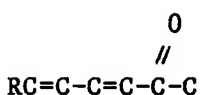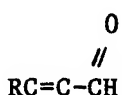
Alcohols, aldehydes, ketones, esters, conjugated unsaturation involving a carbon-carbon double bond with a carbonyl group and two carbon-carbon double bonds with a carbonyl group have been identified by Infra Red and NMR spectrometers.

The alcohol and carbonyl linkages appear to be characteristic of the primary oxidation products. The conjugated unsaturation involving two or three double bonds appears to be concentrated in the secondary reaction products (condensation polymer). The overall oxidation reaction, for all of the fluid types without an oxidation inhibitor or after the oxidation inhibitor has been consumed, proceeds by first order kinetics until essentially all of the original material has been reacted. This observation again confirms that the primary oxidation reaction is the rate limiting step. The subsequent reaction to form sludge and deposits proceeds at a much faster rate and will continue at temperatures typical of bulk lubrication systems. The primary oxidation reaction at concentration contact conditions with continued condensation polymerization can explain the presence of deposits in lubrication systems where the bulk of the lubricant does not show substantial oxidation degradation.

Effects of Metal on Oxidation Degradation. The general mechanism for oxidation degradation of lubricants will proceed in the absence of metal surfaces. However, the rate of primary oxidation and secondary condensation polymerization reactions can be influenced substantially by the presence of metal surfaces. The rate of primary oxidation of di-2-ethylhexyl sebacate as a function of metal surface on which the thin film test is run is shown on Figure 4. These data show the general conformance of the oxidative reaction to first order kinetics. Aluminum can be considered a nonreaction bearing surface in this study. On this basis, steel and stainless steel accelerate the oxidation rate while copper and brass reduce the reaction rate. Lead as a metal surface has no significant effect on

371

the primary oxidation rate. It appears that corrosion or reaction of the lubricant or its oxidation product cause the change in oxidation rate. The curves with copper and brass show a change in slope with reaction time indicating that soluble copper salts may act as an inhibitor. Thin film oxidation data for a super refined mineral oil are shown on Figure 5. These data exhibit the same general relationship for oxidation of a mineral oil with copper, iron, and aluminum as shown previously for di-2-ethylhexyl sebacate. The babbitt in this case contains both copper and tin. It is obvious in these data that both copper and babbitt with the super refined mineral oil and copper and brass with di-2-ethylhexyl sebacate appear to show a destinct change in oxidation behavior during the test. This change appears to be an inhibiting effect resulting from a build up of organo-metal compounds that are soluble in the oil. These soluble materials are a result of the fluid-metal interaction.

In Figure 6 the latter portions of the oxidation rate curve for copper is compared with a curve generated by the addition of 2000 ppm cu as copper naphthenate added to the lubricant. These data confirm the corrosion mechanism and suggest that metals affect oxidation reactions by homogeneous catalysis. These data also suggest that soluble copper salts are a very effective oxidation inhibitor when used in a high enough concentrtion.

Additional thin film oxidation data have been determined for di-2-ethylhexyl sebacate with zinc and tin as the metal test cups. These data on Figure 4 show that both zinc and tin exhibit the same behavior as copper. That is, after an initial high rate of oxidation during which metal-fluid interaction provides soluble metal-organic compounds the oxidation rate decreases dramatically. The slopes of the latter part of the oxidation rate curves for copper, zinc, and tin appear to be about the same.

Metals also appear to play a significant role in secondary oxidation reactions. Secondary oxidation reactions proceed at a much faster rate than the primary oxidation reaction. The results of these secondary and subsequent oxidation reactions is the formation of condensation polymers by a reaction similar to an aldol condensation. The comparative rate of formation of high molecular weight polymer for a super refined mineral oil on various metals is shown on Figure 7. The apparent asymptotic limit of the high moleculr weight product with time is a result of the formation of oil insoluble sludge or deposit and the lack of unreacted material for the primary oxidation. Since the secondary reactions are more rapid than the primary oxidation the relative build up of high molecular weight product, as anticipated, generally follows the rate of primary oxidation. One notable exception is lead which produces an oxidation rate for esters similar to that on aluminum. In this case, however, there is no build up of high molecular weight product with lead. Another view of high molecular weight product as a function of secondary oxidation is shown on Table 2. In this case, the same super refined mineral oil is oxidized under similar conditions to the same degree of oxidation. Under these conditions, about 50 percent more high molecular weight product is formed on copper than on steel. The test on copper took more than 5 times as long to achieve the same level of oxidation as the steel. In addition, the high molecular weight product formed on the copper surface was higher than that of the original lubricant but lower than the average of the high molecular weight product formed on the steel.

The effect of an optimum concentration of copper naphthenate on di-2-ethylhexyl sebacate and super refined mineral oil are compared on Tables 3 and 4 with an effective oxidation inhibitor package. In both cases the copper naphthenate is

372

as effective an additive as the best synthetic inhibitors available under conditions encountered in bearing areas of a conventional lubrication system.

Metals in bearings are generally considered to be relatively nonreactive with the lubricant under operating conditions. Thin film oxidation tests when oxygen diffusion is not a limiting factor and the bearing surface and fluid temperatues are in the range of 200 to 350°C show lubricant-metal interaction in a new perspective. A well inhibited ester with an aircraft gas turbine lubricant additive package including an effective metal coater has been used to obtain the lubricant-metal interaction data shown in Table 5. Comparable data are also shown for the unhibited ester. After 20 minutes at 225°F most of the soluble organic-metal reaction products have reached a maximum. These data indicate a high reaction rate under these relatively modest conditions. This suggests that it is difficult to control the metal catlytic effect on oxidation in a typical lubrication system with bearings lubricated in the elastohydrodynamic or boundary modes.

A series of thin film oxidation tests are available with automative crankcase oils, aircraft gas turbine oils, an a series of phosphate esters. Since oxygen diffusion is not a variable these materials can be compared directly to provide the relative stability or reactivity under the same general test conditions.

The data on Table 6 show that the oxidative behavior of a series of automotive crankcase oils tested under the same conditions give the same range in fluid degradation. The data on Table 7 shows the values for aircraft gas turbine lubricants and their base stocks under conditions similar to those for the automotive lubricants. The ester base stocks are severely degradaded under these test conditions. Similar behavior is noted for the mineral oil base stocks without additives. The formulated aircraft gas turbine oils show stability properties that are superior to automotive lubricants. Data at 245°C are shown for aircraft gas turbine lubricants and several non additive aromatic phosphate esters on Table 8. The aircraft gas turbine oils at 245°C show the levels of oxidation typical of the automotive lubes (mineral oil base) at 225°C. The typical aryl phosphate esters show relatively low levels of oxidative degradation after 20 to 25 minutes under these conditions while a diphenyl, ditertiarybutylphenyl phosphate ester shows essentially no oxidation after 6 hours. The data on Table 9 show the oxidative behavior of the aryl phosphate esters at 270°C in the thin film test. At 270°C the conventional aryl phosphate esters show excellent oxidation stability while the diphenyl, ditertiarybutylphenyl phosphate ester still shows essentially no oxidation after 3 hours. These data suggest that there are some liquid lubricants that have adequate stability to oxidation in the presence of a metal surface to function in EHD and boundary lubrication with a minimum of oxidative breakdown.

Thermal Stability. In general, organic liquids show better thermal stability than oxidative stability. It has been assumed that the thermal stability of the liquid is not measurably affected by the presence of metal surfaces. Recent studies by Ugwuzor (11) have shown that esters in a thermal sstability test under a nitrogen atmosphere show evidence of thermal degradation at temperatures as low as 200°C. Bulk thermal stability tests of dibasic acid esters in glass show incipient breakdown at 260°C while the polyol esters exhibit good thermal stability to about 310°C. Some evidence for the thin film chemical instability is shown on Figure 8 where the dashed line represents the anticipated evaporation loss based on an extrapolation of the data obtained at 150 and 175°C where the value of ester loss is the same on copper, aluminum, and steel. The actual losses on steel, aluminum, and cooper are all different and much larger than the predicted evaporation. These data may help to explain the better than expected cleanliness of the hot

373

metal surfaces in engines when esters are used instead of the conventional mineral oil lubricants. Since many of the original ester linkages exist in the new fluid and in the condensation polymer formed by oxidation, thermal instability may tend to reduce the amount of deposit on hot metal surfaces.

REFERENCES

1. Mahoney, L. R., Korcek, S. and Hamilton, E. J., Jr., "Time-Temperature of High Temperature Deterioration Phenomena in Lubricant Systems: Synthetic Ester Lubricants," Interim Report to the Air Force, Office of Scientific Research covering the work carriedout under the Contract #F4-4620-76-C-0097. For the period April 1976 to March 31,1977.

2. Sniegoski, P. J., "Selectivity of the Oxidative Attack of a Model Ester Lubricant," ASLE Trans., 20, 4, pp. 282-286 (1977).

3. Willermet, P. A., Mahoney, L. R. and Haas, C. M., "The Effects of Antioxidant Reactions on the Wear Behavior of a Zinc Dithiophosphate," ASLE Trans. 22, p. 301 (1979).

4. Diamond, H., Kennedy, H. C., and Larsen, R. G., "Oxidation Characteristics of Lubricating Oils at High Tempertures," Ind. Eng. Chem., 44, 8 (1952).

5. Brook, J. H. T., "A Circulatory Oxidation Test," J. Inst. Petrol., 48, 457, pp. 7-12 (1962).

6. Oberright, E. A., Leonard, S. J., and Hepplewhite, H. L., "Deposit-Forming Tendencies of High Temperature Lubricants," ASLE Trans., 7, pp. 64-72 (1964).

7. Cvitkovic, E., Klaus, E. E., and Lockwood, F., "A Thin-Film Test for Measurement of the Oxidation and Evaporation of Ester-Type Lubricants," ASLE Trans., 22, p. 395 (1979).

8. Cho, L. and Klaus, E. E., "Oxidative Degredation of Phosphate Esters," ASLE Trans, 24 No. 1, pp. 119-24 (1981).

9. Lockwood, F. E. and Klaus, E. E., "Ester Oxidation Under Simulated Boundary of Lubrication Conditions," ASLE Trans., 24 No. 2, pp. 276-84 (1981).

10. Shen, S. Y. and Klaus, E. E., "A Kinetic Study of Oil Oxidation in Concentrated Contacts," ASLE Preprint No. 83-AM-5A-3, April (1983).

11. Ugwuzor, D. I. K. A., "The Effects of Metals on High Temperature Degradation of Ester-Type Lubricants," M.S. Thesis, The Pennsylvania State University, University Park, PA (1982).

Table 1

PROPERTIES OF SYNTHETIC FLUIDS COMPARED WITH SAE GRADES

FLUID	SAE GRADE	VISCOSITY IN CENTISTOKES AT				FLASH PT. °C	VISCOSITY INDEX
		-17.8°C	37.8°C	98.9°C	149°C		
MIL-L-7808	5W	150	11.0	3.0	1.7	205	145
MIL-L-23699	5W	700	25.0	5.0	2.4	246	140
Olefin Oligomer	5W-20	890	33.8	6.0	2.8	246	133
PE Ester Blend	5W-20	892	31.8	5.75	3.3	260	130
PE Ester Blend	10W-30	2 200	63.0	10.0	4.2	260	150
PE Ester Blend	20W-40	4 100	96.2	13.3	5.5	260	140
Ester + Polymer*	5W-30	600	46.5	10.0	4.7	230	212
Ester + Polymer*	5W-40	800	67.7	13.0	6.0	230	211
Ester + Polymer*	5W-50	1 200	89.2	18.0	8.1	230	241

*Polymer used in these blends is more shear stable than those typically used in crankcase oils. Base stock is less volatile than a typical 10W-30 conventionally formulated crankcase oil.

Table 2

COMPARISON OF HIGH MOLECULAR WEIGHT PRODUCT FORMATION ON
DIFFERENT METALS AT EQUAL AMOUNTS OF DEGRADATION

Microoxidation Test Conditions include: Superrefined Mineral Oil
7828, 40 $\mu\ell$, and 225°C

METAL	TIME MIN.	UNREACTED WT. %	WT. % OXIDIZED PRODUCT	
			ORIGINAL MOL. WT.	HIGHER MOL. WT.
Fe	7.7	57	30	10.1
Al	8.5	57	29	6.5
Babbitt	10	57	21	6.5
Cu	40	57	13	15.4

Table 3

OXIDATION CHARACTERISTICS AT 225°C FOR
DI-2-ETHYLHEXYL SEBACATE

Penn State Microoxidation Test: 40 $\mu\ell$ sample on a low carbon steel
catalyst

FLUID ADD.%	TIME MIN.	WEIGHT PERCENT		
		UNREACTED	OXIDIZED	EVAPORATED
none	30	35	21	44
0.2 Cu Nap	30	71	8	21
2.0 Cu Nap	30	85	0	15
none*	30	81	3	16

*Run on a copper catalyst

Table 4

COMPARATIVE DATA FOR A CONVENTIONAL AUTOMOTIVE INHIBITOR PACKAGE AND
COPPER NAPHTHENATE IN A SUPERREFINED MINERAL OIL, PRL 7828

Microoxidation Test Conditions: 225°C, 30 min, 40 $\mu\ell$

| Basestock | Metal Catalyst | Quantity of Material as % of Original Oxidized Products | | |
		>Mol. Wt. Than Orig.	Same Mol. Wt. As Orig.	Unreacted Material
PRL 7828	Fe	31	27	16
	Al	19	39	28
	Cu	12	9	67
PRL 7828	Fe	1	7	81
+ 2.0% Cu Nap.	Al	0	3	80
	Cu	0	4	77
PRL 7828	Fe	1	5	81
+ 1.88% ZDP	Al	1	3	84
+ 0.5% PAN	Cu	4	11	82

2.0% Cu Nap. = 2000 ppm Soluble Cu

Table 5

METAL CONTENT OF LUBRICANTS AFTER MICROOXIDATION TEST

Test Conditions include: 225°C for 20 minutes with a 40 μℓ charge
of lubricant on the metal catalyst

| METAL | -CONCENTRATION OF DISSOLVED METAL IN PPM-- | |
	DEHS (1)	FULLY FORMULATED DEHS (2)
440 Stainless	195	25
Low Carbon Steel	863	40
Copper	1875	910
Zinc	1123	375
Lead	27340	22660

(1) Di-2-ethylhexyl Sebacate
(2) Di-2-ethylhexyl Sebacate + 0.5% Phenothiazine + 0.5%
Phenyl Alpha Naphthylamine + 2.5% Tricresyl Phosphate

Table 6

COMPARISON OF 3D REFERENCE OILS IN THE MICROOXIDATION TEST

Data Based on GPC Curves for the Original and Oxidized Sample
40 μℓ samples were used with a low carbon steel catalyst

CONDITIONS	TEST FLUID NBS NO. (HRS.)[1]	OXIDIZED PROD. >MOL. WT. THAN ORIGINAL	OXIDIZED AND UNREACTED MATERIAL AT ORIGINAL MOL. WT.	EVAPORATION LOSS
200°C, 2 HRS.	7048 (16)	7.4	72.4	20.2
	7044 (24)	4.5	58.6	36.9
	7046 (40)	13.6	55.1	31.3
	7047 (56)	11.1	59.1	29.8
	7045 (64)	6.3	65.0	28.7
225°C, 30 MIN.	7048 (16)	10.1	73.7	16.2
	7044 (24)	8.0	63.9	28.1
	7046 (40)	15.9	53.1	31.0
	7047 (56)	11.3	64.6	24.1
	7045 (64)	8.4	63.7	27.9

[1]Hours to failure in the 3D engine sequence test.

Table 7

OXIDATION CHARACTERISTICS OF ESTERS AT 225°C

Penn State Microoxidation Test: 40 μℓ sample on a low carbon
steel catalyst

	TIME MIN.	WEIGHT PERCENT		
		UNREACTED	OXIDIZED	EVAPORATED
MIL-L-7808	30	80	<5	15
MIL-L-23699	30	86	<3	11
Di-2-ethylhexyl Sebacate	30	3	80	17
Trimethylolpropane Triheptanoate	30	21	67	12
Tricresyl Phosphate	30	85	1	14

Table 8

COMPARATIVE OXIDATION STABILITY OF AIRCRAFT GAS TURBINE
LUBRICANTS AND PHOSPHATE ESTERS AT 245°C

Penn State Microoxidation Test: 40 μℓ sample on a low carbon
steel catalyst

FLUID	TIME MIN.	WEIGHT PERCENT		
		UNREACTED	OXIDIZED	EVAPORATED
MIL-L-7808	20	48	40	12
MIL-L-23699	25	58	30	12
Tricresyl Phosphate	30	57	3	40
Trixylyl Phosphate	30	65	4	31
Tertiarybutylphenyl Diphenyl Phosphate	360	77	<1	22

Table 9

OXIDATION CHARACTERISTICS OF PHOSPHATE ESTERS AT 270°C

Penn State Microoxidation Test: 40 μℓ sample on a low carbon
steel catalyst

FLUID	TIME MIN.	UNREACTED	OXIDIZED	EVAPORATED
Tricresyl Phosphate	15	60	5	35
Trixylyl Phosphate	15	55	6	39
Ditertiarybutylphenyl Diphenyl Phosphate	180	84	<1	15
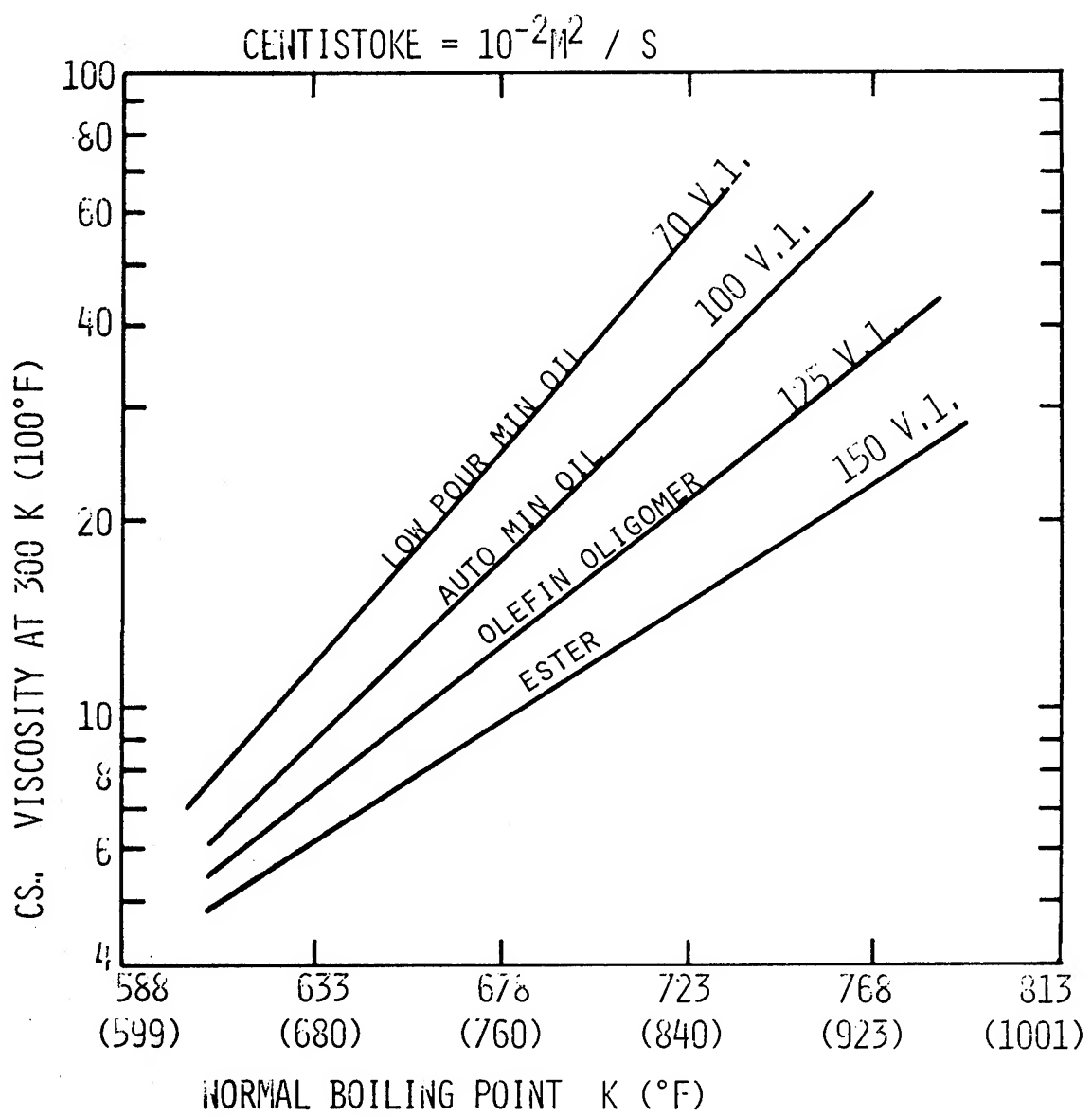
Figure 1. Viscosity-Volatility properties of some mineral oil and synthetic lubricant base stocks.

382
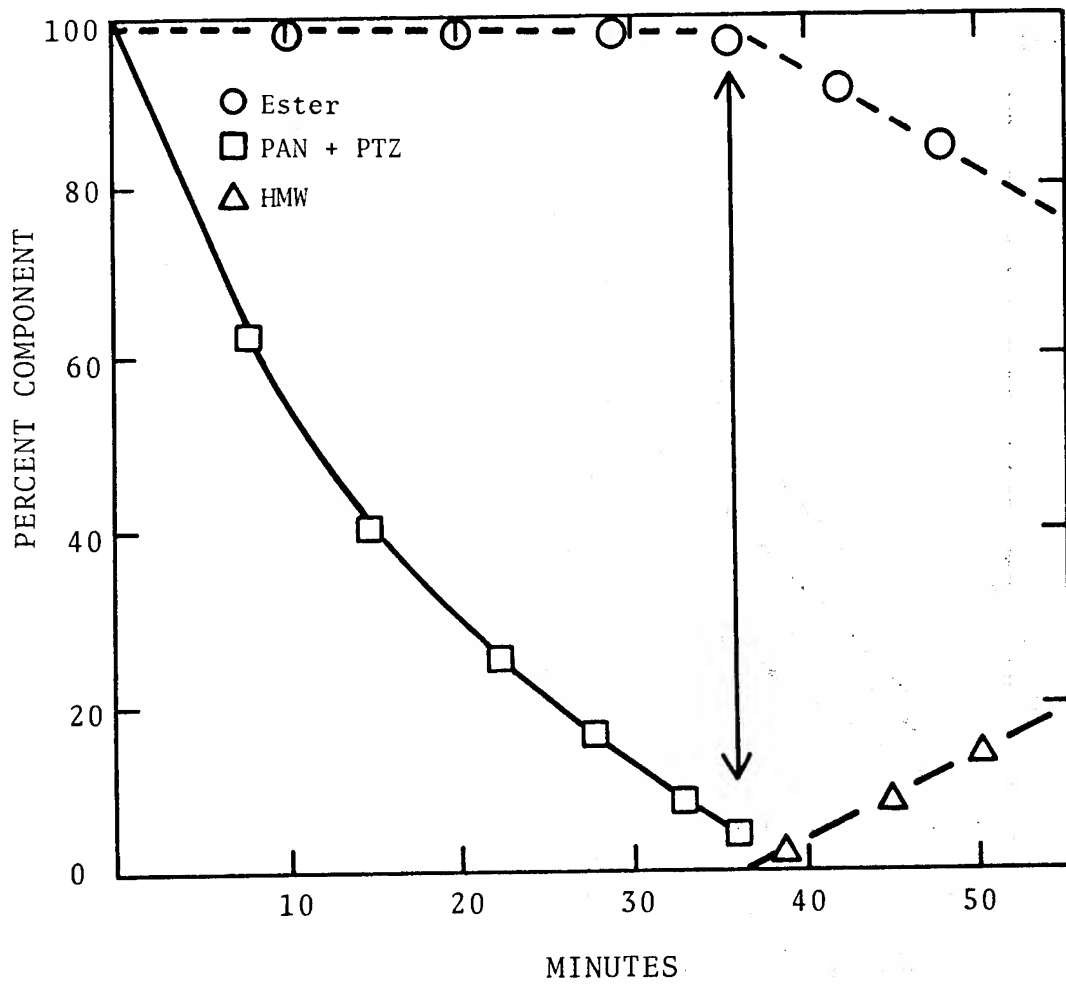
Figure 2. Behavior of a formulated di-2-ethylhexyl Sebacate base synthetic in the Penn State microoxidation test at 225 K.
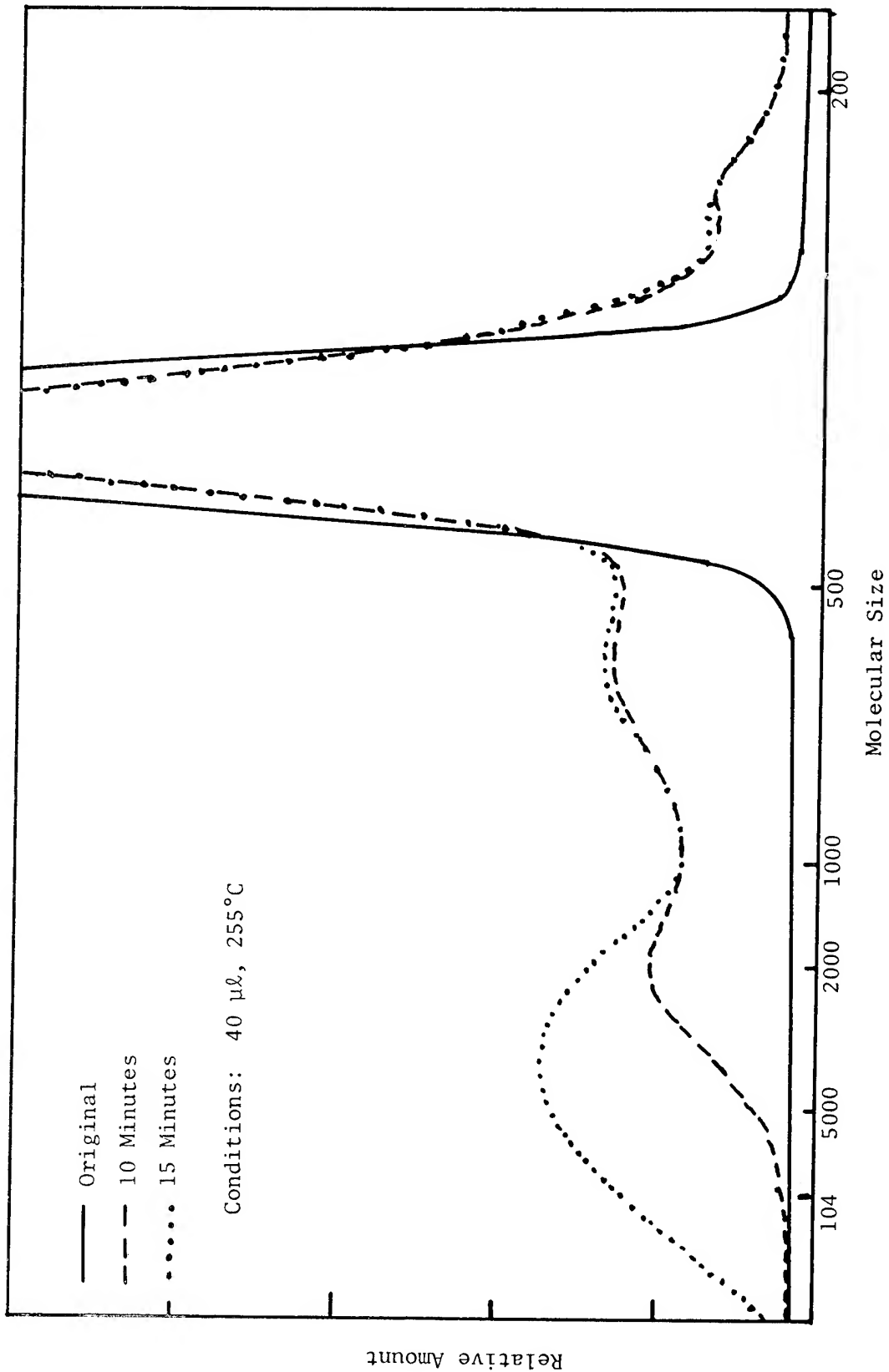
Figure 3. Gel Permeation Chromatograms Obtained for Oxidized Di-2-Ethylhexyl Sebacate From the Microreactor.

384
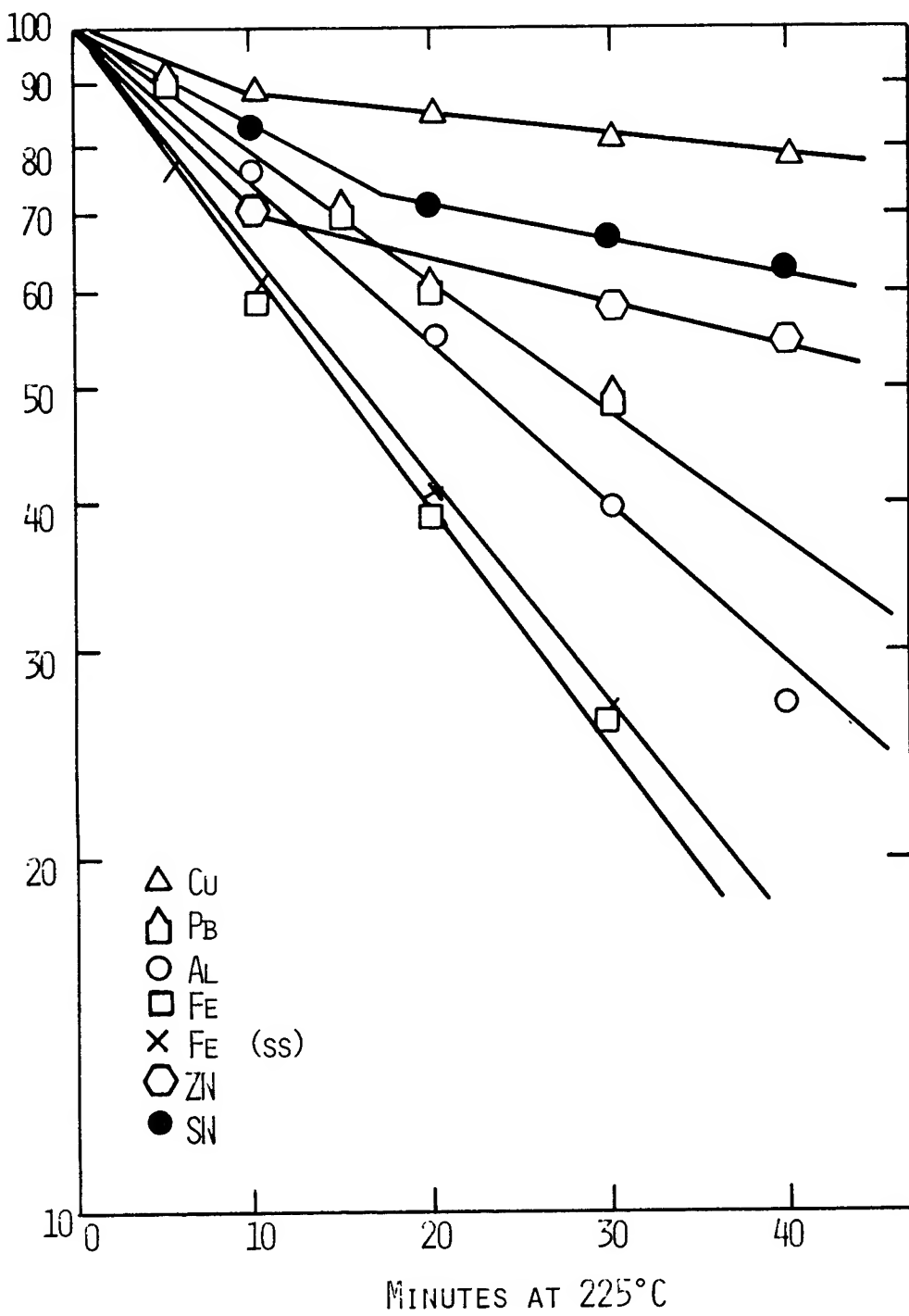
Figure 4. Effect of Metals on the Oxidation of Di-2-Ethylhexyl
Sebacate in the Penn State Microoxidation Test

Test conditions: 225°C
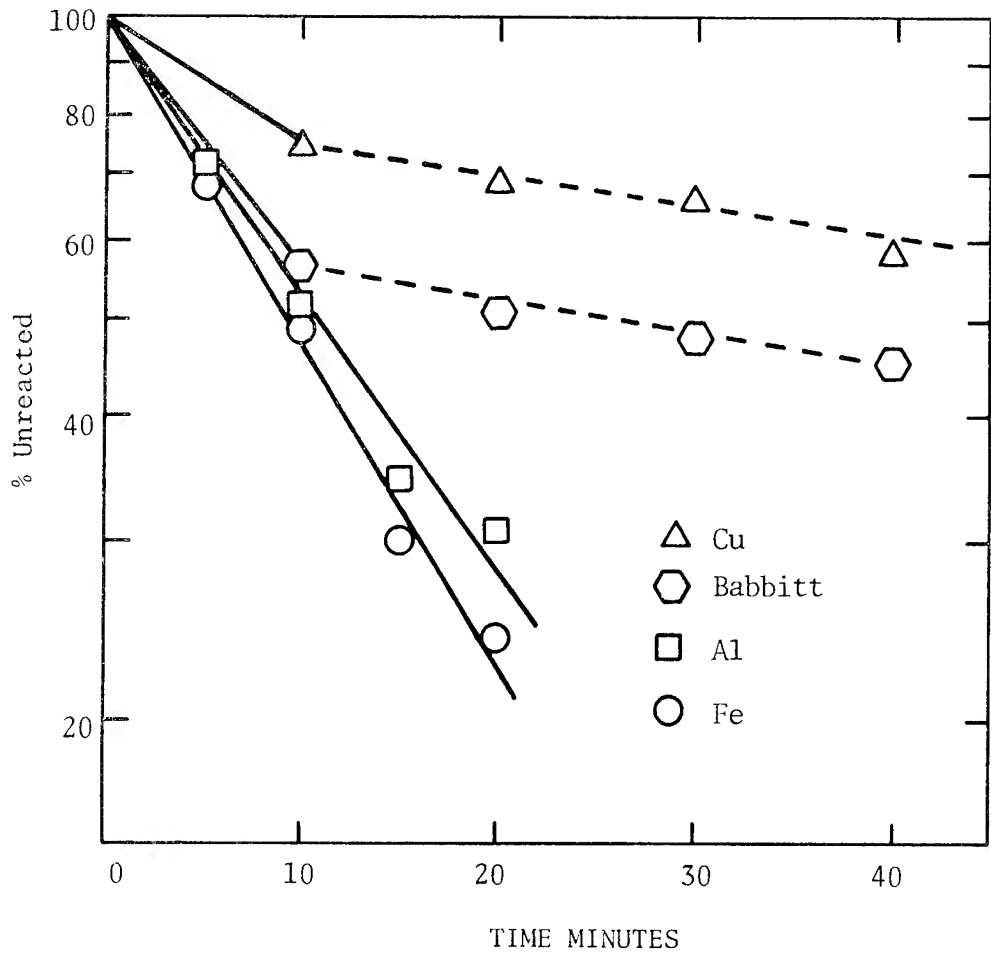
Figure 5. Effect of Metals on the Oxidative Degradation of a Superrefined Mineral Oil, PRL7828.

Microoxidation Test Conditions: 40 µℓ and and 225°C.
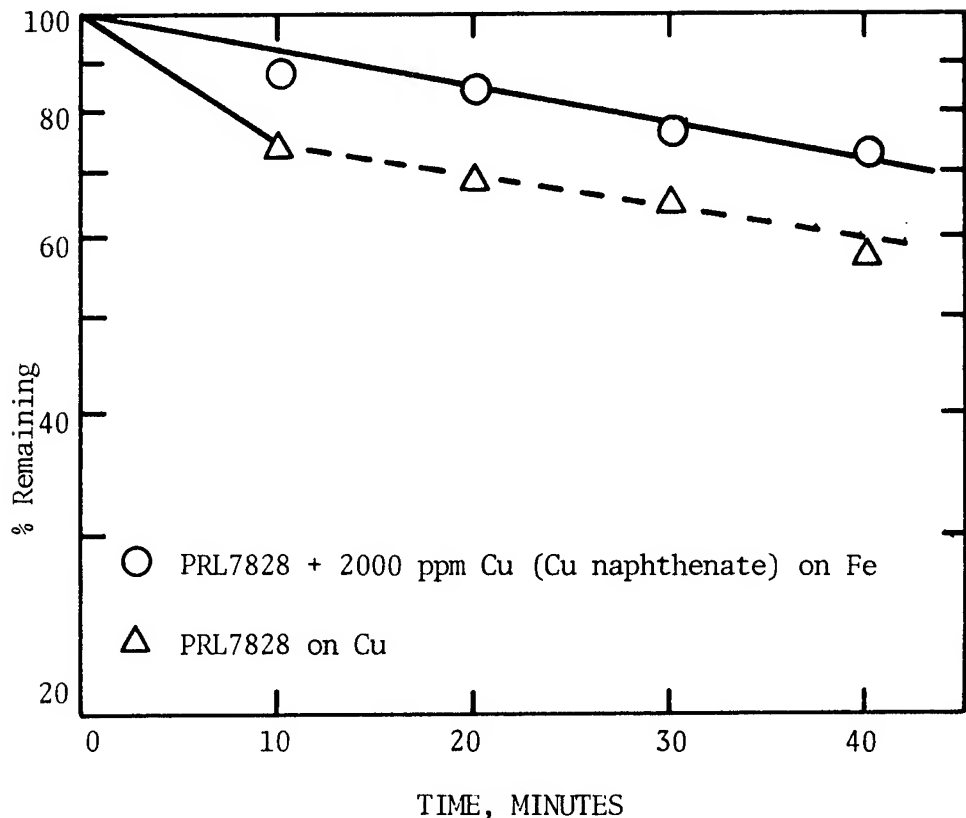
Figure 6. Comparative Effects of Copper Catalyst and Soluble Copper Naphthenate on the Oxidative Degradation of a Superrefined Mineral Oil, PRL7828.

Microoxidation Test Conditions: 40 μℓ and 225°C.
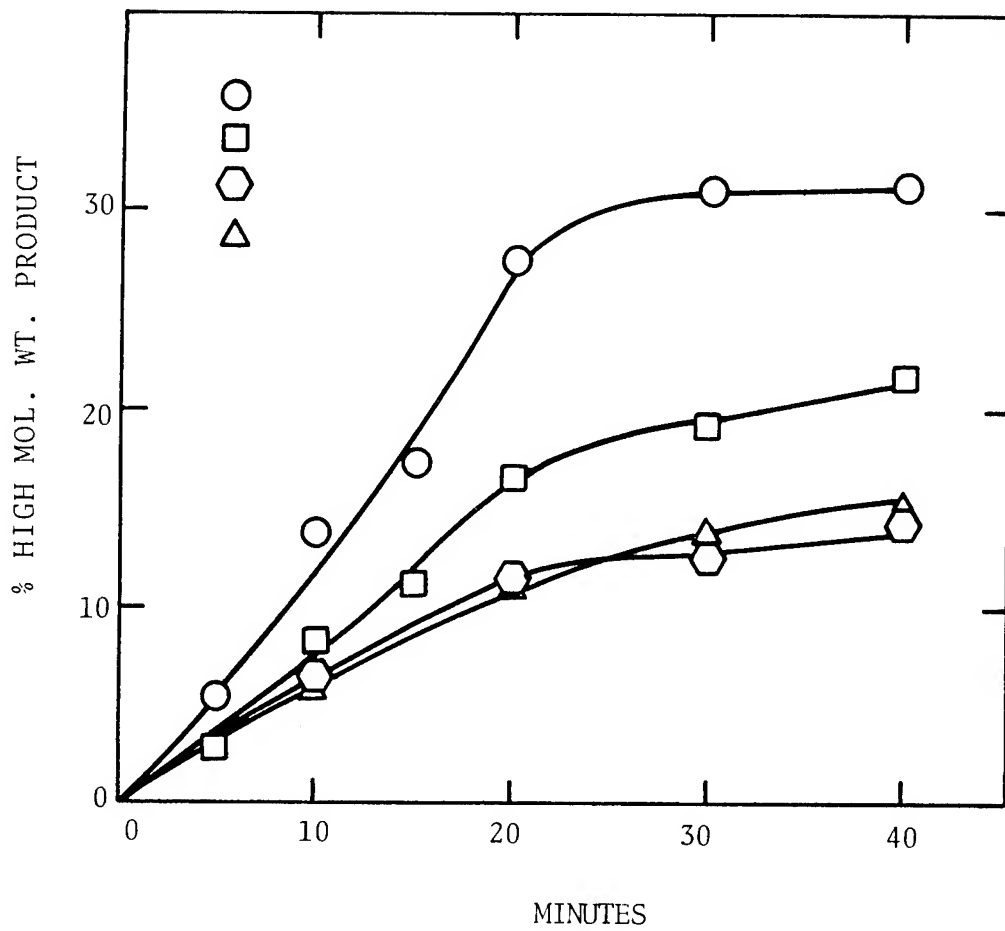
Figure 7. Effect of Metals on High Molecular Weight
Product Formation for a Super Refined Mineral
Oil at 225°C.

Microoxidation Test Conditions: 225°C,
40 μℓ
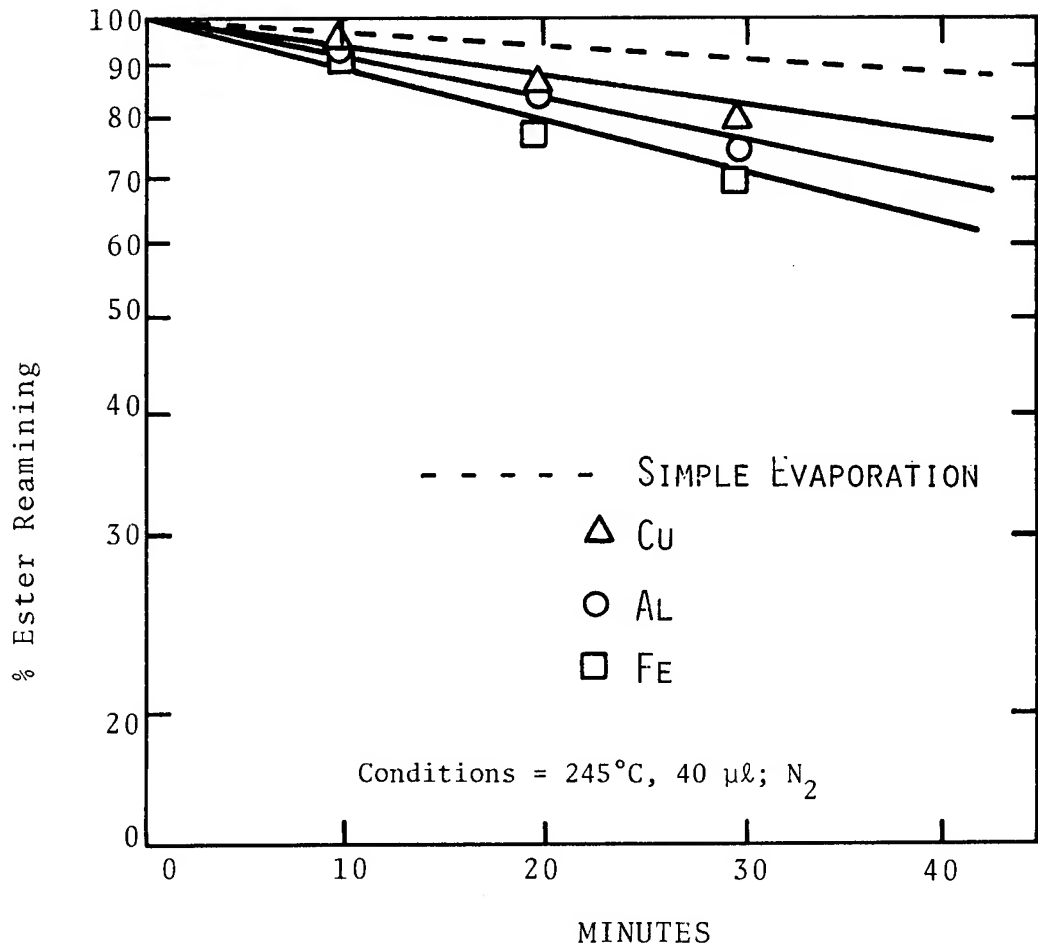
Figure 8. Thermal Behavior of Trimethylol Propane Tri-bystanoate in the Microreactor Under a Nitrogen Atmosphere.

ANTIWEAR ADDITIVE MECHANISMS IN SLIDING CONTACTS

B. A. Baldwin
Phillips Petroleum Co.
Bartlesville, OK 74004

This paper examines the possible mechanisms associated with wear in a sliding contact and how an oil and antiwear additive can mitigate wear or at least prevent catastropic seizure of the contacting parts. The various load and temperature regimes are examined and an attempt is made to determine which mechanisms are predominant under these conditions. The critical mechanism(s) depend on the test parameters, particularly load and temperature, although sliding speed is also a factor. Speculations on ways to improve the efficiency of antiwear additives are also made.

INTRODUCTION

The mitigation of wear in sliding contacts is a concern that dates back into antiquity (1-3). Much has been accomplished by improved mechanical design; for example, the replacement of the sled by wheeled carts, substitution of metal for wood, development of roller bearing elements and the hardening of metal surfaces. The development of lubricants paralleled and enhanced these mechanical improvements. For many years animal and vegetable fats and oils were the primary lubricants. With the expansion of petroleum resources in the late 1800s, mineral oil became the preferred lubricant. As mechanical design increased efficiency and reduced the size of the components it became necessary to include additives to achieve acceptable wear rates. As in most fields empirical development and field application came first followed by attempts to explain and understand the phenomena of wear mitigation. Although much has been accomplished we still do not know how antiwear additives function in all systems. The elements generally associated with antiwear activity are chlorine, phosphorus, and sulfur. This paper will address only sulfur compounds although there is reason to expect analogous mechanisms with the other elements. This paper will look at what has been learned, present a working model, and speculate on possible modifications of antiwear additives which would improve their efficiency.

EXPERIMENTAL

The wear test used for most of the results reported here consisted of a modified procedure using the standard Falex Test machine. The test was designed to simulate value train wear of an automotive engine and consisted of a 30 minute break-in at an applied load of 23 Kg followed by 3 hours of test-

ing at an applied load of 118 Kg. The test load corresponds to an initial Hertzian pressure of 0.63 GPa. For the non-temperature controlled tests the lubricant was heated to 79.5°C during break-in and allowed to reach an equilibrium temperature during testing, typically 75-85°C. Wear was measured as the distance which the two v-blocks moved toward each other to compensate for the material removed while maintaining constant load. The test specimen consisted of a SAE 3135 steel pin and SAE 1137 steel v-blocks. This test was found to give a correlation with laboratory engine wear (4).

Surface analysis was made of the pin using X-ray photoelectron spectroscopy, XPS. XPS was used to determine the types of elemental species and their oxidation state and when ratioed to iron as a semi-quantative indication of the relative surface concentrations (5,6). The ratioing was done primarily to correct for spectrometer throughput due to instrumental cleanliness and test specimen alignment.

Ferrographic analysis was carried out using standard techniques.

RESULTS AND DISCUSSION

To fully understand the mitigation of wear in a lubricated contact one must consider the base fluid, the antiwear additive(s), any other compound(s) present in the lubricant formulation, the mechanical and chemical properties of each of the above, and the effect of external variables, such as load and temperature, on each of the components and the various overall mechanical and chemical properties. This is a rather formidable list of topics to be covered. An early postulate was that boundary lubrication resulted from chemical films formed on the contacting surfaces (7-12). An impressive group of researchers used a variety of techniques in an attempt to elucidate the composition of the boundary lubricant films and the mechanism of their formation (13-21). The limitation of this work in defining the surface composition was the depth of analysis, 1000 nanometers or more. Because the actual surface film, ca 1 to 10 nanometers, was a small fraction of the total material analyzed, these previous studies have generally determined the bulk properties of the material in the wear scars and/or wear debris. With the advent of Auger spectroscopy and X-ray photoelectron spectroscopy, XPS, it became possible to analyze the first 1-4 nanometers of a test specimen (22-25). These latter techniques have allowed us to develop a better understanding of the composition of wear surfaces. However, one must always be cognizant of the earlier work because any mechanism proposed from surface analysis must be consistent with the more macroscopic observations found there.

First let us look at the proposed model then work back to explain the reasons which lead to this conclusion. A typical surface profile, even for a smooth engineering surface, looks like that shown in Fig. 1. With the steep slopes between the valleys and peaks the riding of asperities of one surface over another without severe wear does not seem possible until one notices that these typical profiles are presented with different scaling factors on the vertical and horizonal axes. A more realistic representation is shown in Fig. 2 where the average slope of an asperity is about 20 degrees (26). With this model one can visualize that stresses can be distributed so that an asperity

of one surface can slide over an asperity of the contacting surface without causing detectable damage provided that the point of contact contains some material in the interface which will prevent actual metallic contact. Fig. 3 illustrates what can happen in an unlubricated sliding contact. At a load in excess of that which the oxide layer can support, metal contacts metal. The combination of load and local temperature causes the two asperities to weld. For further movement of the two surfaces to occur this junction must be broken. The point of fracture may be the junction just formed or it may be at some weak point in the asperity. In this way metal can be removed from one surface and transferred to the second surface. In an unlubricated system wear is typically reduced by making the contacting parts of dissimilar metals to reduce these cohesive forces. By contrast, in a liquid lubricated contact the metallic surfaces can be separated by two basic mechanisms as shown in Fig. 4. The first is a mechanical property of the bulk lubricant; EHD on a microscopic scale. The second consists of boundary lubricant films formed from the various components of the lubricant, particularly the antiwear additives. These films can be further broken into sub-categories, adsorbed antiwear additive, reaction (polymeric?) films and inorganic films. The ability of these materials to separate the surfaces under increasing load is expected to increase in the order, bulk oil < adsorbed additive < reaction film < inorganic film.

It has been generally believed that fully flooded, highly loaded contacts, such as those used in these studies, were lubricated exclusively by boundary lubrication. The base oil was thought to be only the carrier of the antiwear additive and had little, if any, effect on wear. The potential effect of base oil was examined by wear testing with a series of super refined white mineral oils of varying viscosities, shown in Table 1, while holding the antiwear additive concentration constant. The results of such an experiment for two compounds, zinc dialkylththiophophate and di-t-butyldisulfide, are shown in Fig. 5 and 6, respectively. The absence of an antiwear additive resulted in immediate catastrophic failure. Two areas of viscosity effects are indicated by these results. The first shows little dependence of wear on viscosity. Upon reaching a critical minimum viscosity, about 5 cSt at 100°C, wear is dramatically dependent on viscosity increasing rapidly as viscosity decreases. The catastrophic failure of the di-t-butyldisulfide at the lower viscosities indicates that ZDTP is the better boundary lubricant. The sharp break in wear and the occurence of the break at the same viscosity for both compounds suggests a change in the wear mechanism. Abrupt breaks in wear have typically been associated with the transition from mild to severe wear. Ferrograms of the wear debris generated corroborate such an assignment (27). Generally such transitions are produced by varying the load and/or temperature. However, under the present test conditions load and temperature have been held constant. Similar effects have been reported to occur when the thickness of EHD films became comparable to the surface roughness (28,29), although unlike the present work they found the friction to undergo an abrupt increase at the break point. Calculated EHD specific film thickness, based on the original surface roughness, predict that there should be no contribution to wear control from the fluid properties. However, if the surface were to be polished during the wearing process the specific film thickness would increase. Scanning electron micrographs were made of worn surfaces. At low magnification the worn surface appears rough perpendicular to the direction of sliding, Fig. 7(a). At higher magnifications the tops of the ridges, the

393

points of contact between the two surfaces, are much smoother than the original surface finish, Fig. 7(b). In addition compounds similar to antiwear additives have been shown to increase EHD film thickness (30). The improved surface finish in the direction of sliding combined with enhanced rheological properties provided by the antiwear additive, could allow EHD lubrication to occur on a microscopic level.

The lack of a detectable change in the friction can be explained by examining the contributions of EHD and surface contact to the observed coefficient of friction, f, represented by Eq. 1, where f_c is the coefficient of friction for the surface in actual contact, f_{EHD} is the shear stress of the EHD films and A and A are the areas in contact and EHD, respectively,

$$f = f_c \frac{A_c}{A_{EHD} + A_c} + f_{EHD} \frac{A_{EHD}}{A_{EHD} + A_c.} \qquad 1)$$

Values for f_{EHD} are typically 0.06 (29) and f_c ranges from 0.1 to 0.8 (31). From Eq. 1 it can be seen that a transition from full EHD (A = 0) to partial EHD would produce a sizable change in f for a relatively small change in EHD film thickness. Because of the shape of asperities a small change in EHD film thickness, after partial EHD conditions are established, will produce only small changes in f. However these small changes in film height can significantly increase the stress on the contacting asperities and at some point cause the transition from elastic to plastic deformation. The latter leads to a different wear mechanism. One can thus predict several orders of magnitude change in wear and even a change in the predominate wear mechanism with no detectable change in friction.

Wear protection in lubricated, highly loaded, non-abrasive, fully-flooded, sliding contacts appears to consist of a mixture of localized EHD and boundary lubrication, loss of either results in excessive wear. The presence of the localized EHD is probably the result of a combination of surface polishing and rheological properties of the boundary lubricant films.

In an early attempt to analysis the 1-10 nm thick boundary lubricant film, Buckley et. al (23-25) used Auger Spectroscopy to determine the elements present in wear scars after testing. They found the elements of the additives and surface. However, in the early development of Auger Spectroscopy it was not possible to determine the chemical nature of the surface elements. XPS, on the other hand, was quite sensitive to the valance electrons and could readily determine the oxidation state or chemical nature of the surface material produced during wear. One of the first XPS observations was that a monometallic sulfide was produced during the wear process, both in laboratory tests and in automotive engines (5,32-34). The results in Table 2 show that for a wide variety of organosulfur compounds, with different initial sulfur environments, a single sulfur species was produced during wear testing. Since there is a factor of eight difference in the wear protection provided by these compounds one cannot assign good wear protection to a specific surface species and lesser wear protection to another surface species. A correlation was found between the relative amount of surface sulfide and wear, the higher the sulfide concentration the lower the wear (32). Figure 8 shows this correlation for the compounds in Table 2. The lower line represents fully formulated

oils while the upper line consists of the additives in a highly refined white mineral oil. The displacement will be discussed later. A similar plot was produced by varying the bulk concentration of a single additive in white mineral oil, as shown in Fig. 8. The slope of all three lines are within experimental error and the intercept of the two white mineral oil curves are also within experimental error of each other. Generating similar results by two different methods indicates that this is not just an experimental artifact. The surface sulfide concentration was found to be constant, for a given temperature, throughout the moderately loaded break-in period and the heavily loaded test period, but was different for each additive (32). The surface sulfide was constantly being removed during wear testing and had to be replaced by additives in the bulk to maintain a constant wear rate (32,35). The sulfide was found to oxidize to the thermodynamically preferred sulfite and sulfate upon exposure to the atmosphere (32).

One possible set of mechanisms which is consistent with the above experimental observations can be represented by Eqs. 2 through 7.

$$AA + SS \rightleftharpoons AA:SS \qquad 2)$$

$$AA:SS \longrightarrow S^{-2} + Byproduct \qquad 3)$$

$$AA + SS \longrightarrow S + Byproduct \qquad 4)$$

$$OA + SS \rightleftharpoons OA:SS \qquad 5)$$

$$S^{-2} \longrightarrow SS + Debris \qquad 6)$$

$$S^{-2} + O_2 \longrightarrow SO_3^{-2} + SO_4^{-2} \qquad 7)$$
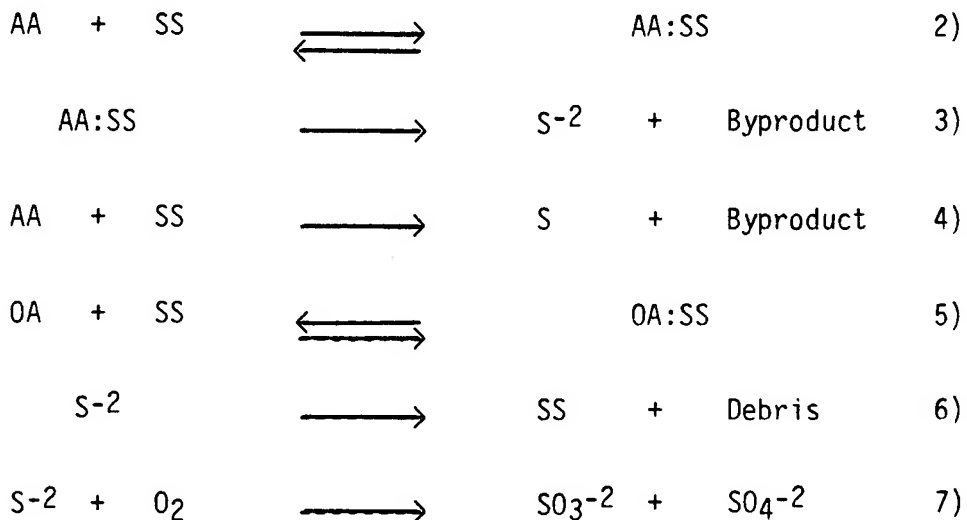
Where AA is the active antiwear additive, SS is a surface site available for interaction or reaction, AA:SS is the adsorbed antiwear additive, S^{-2} is the surface sulfide, OA is additives other than the antiwear additive, SO_3^{-2} is the surface sulfite and SO_4^{-2} is the surface sulfate. The byproducts in Eqs. 3 and 4 are not necessarily of the same composition and the debris will consist of all the preceeding plus the steel components. Eqs. 2 and 3 represent a process where the antiwear additive is first adsorbed reversibly on the surface then undergoes reaction. Most likely adsorption occurs during the portion of the cycle when the surface is not inside the contact zone and reaction of AA:SS occurs inside the contact zone as the result of the temperature and pressure produced. Eq. 4 represents a direct reaction between the antiwear additive and the surface site immediately upon collision of the additive molecule with the surface. Other additives, when present, will compete for surface sites and if successful can prevent some of the antiwear molecules from reaching the surface. However, these other additives are not always bad from

a wear viewpoint; some also contribute antiwear properties. This contribution is probably responsible for the displacement between fully formulated and white mineral oils in Fig. 8.

The selection of those chemical properties and structure which will produce a successful antiwear additive will depend on whether adsorption or reaction is primarily responsible for producing the boundary lubricant film. If the surface sulfide is the sole boundary lubricant species or if it is directly related to the boundary lubricant film components, as depicted in Eqs. 2 and 4, then one should be able to distinguish between adsorption and reaction as the major mechanism of surface interaction by examining the relative concentration of sulfide produced as a function of temperature. As temperature is increased the amount of adsorbed antiwear additive will decrease, decreasing the relative concentration of surface sulfide. Conversely, the rate of reaction will increase with temperature, increasing the relative concentration of surface sulfide (36-38). Based on the correlation between surface sulfide and wear, wear should increase with temperature if adsorption determines the antiwear properties and wear should decrease if direct reaction determines the antiwear properties. Of course, excessive reaction could lead to corrosive wear. The results shown in Fig. 10 indicate an increase in wear with temperature. The surface sulfide concentrations at the end of wear tests as a function of temperature are shown in Fig. 11. The most important feature of this data is that the surface sulfide concentration does not increase monotonically with temperature as would be expected if only direct reaction were occurring. The initial decrease in Fig. 11 can be fit to an exponential decrease as expected if adsorption were the limiting factor in the formation of the boundary lubricant film. The increase at the higher temperatures has been ascribed to an increase in direct reaction, one test appeared to have undergone the transition from normal to corrosive wear (38). At first these results appear to be at odds with the polymeric films observed by others (39,40), however it seems very likely that the mechanisms described by Eq. 2-7 could be easily expanded. For example the polymer films probably did not form from direct reaction of the additives otherwise they would be found on other parts of the test machine or equipment. Most probably the additives were adsorbed and underwent polymerization during the conditions experienced inside the contact zone. In a contact zone the temperature are not homogeneous throughout. For example the highest temperature will be obtained only on the tips of the asperities with temperature decreasing rapidly as one goes further from the point of actual contact. These various conditions will promote a variety of products, however the limiting case appears to be that the surface films are composed of those components of the lubricant that are on the surface as it goes into the contact zone.

It appears that primarily sulfide is formed on the surface during testing rather than the thermodynamically preferred sulfate because of kinetic factors inside the contact (41). The sulfide has only been observed under wear conditions and in a static test at higher temperatures where the oxygen bulk concentration was very low due to solubility (42). It has been proposed that the pressure inside the contact increases the viscosity (43,44) possibly to the point where oxygen will not readily diffuse through the bulk oil, thereby limiting oxidation (41).

396

One unanswered question centers on the actual role of the surface sulfide, is it the sole component of the boundary lubricant film, is it merely debris resulting from the decomposition of the actual boundary lubricant and thus inadvertently proportional to antiwear efficiency, or is it one component of several which make up the boundary lubricant film? If adsorption of the antiwear additive is the primary process in determining antiwear efficiency and the adsorbed additive film solely provides the boundary lubrication then one should not need one of the convention antiwear elements, S, P or Cl, in the additive. To test for the role of the sulfur, several compounds differing only in the replacement of a methylene, -CH2-, with a sulfide group, -S-, were tested. The results are summarized in Table 3. The wear values are generally lower when sulfur is present. Even more significant is the appearance of the surface as shown in Fig. 12. With the absence of sulfur the surface, Fig. 12a, shows evidence of localized welding and incipient galling, although overall wear was not too high. The lack of catastrophic failure can be ascribed to the presence of the adsorbed additive. When sulfur was present, Fig. 12b even in a very innocuous form, the surface appeared almost unworn. The difference can be ascribed to the prevention of welding at the closest approach of two asperities. At this point the local temperature is so great that an inorganic film is formed. The sulfide can then prevent metallic contact and welding through a eutectic (45).

The relationship between wear and bulk antiwear additive concentration, as shown in Fig. 13 and 14, gives some further indication of the processes involved in wear mitigation. These two figures indicate four possible wear regimes. At a high bulk concentration corrosive wear occurs, this is shown in Fig. 14 and has also been observed at about an order of magnitude higher concentration than shown in Fig. 13 for ZDTP. The physically observed response is high wear but the worn specimen appear smooth with no evidence of galling or seizure. The second regime exhibits the lowest wear. This mild wear is independent of concentration and produces the smoothest appearing surfaces. It appears that corrosion is minimal but enough additive is present to form the films which provide boundary lubriction. As concentration is further decreased, there is an abrupt break from mild to severe wear. This severe wear, although high, still appears to be controlled, concentration independent over a narrow range and of a similar absolute value for the two additives tested. The dramatic jump suggests a change in wear mechanism. The final regime, at the lowest concentrations, is characterized by catastrophic wear, severe galling, seizure and mechanical failure of the test specimen. At these low bulk concentrations the antiwear additive apparently cannot produce sufficient boundary lubricant to prevent metallic contact. These data also provide further evidence that the surface sulfide is not the sole component of the boundary lubricant film. If the sulfide was the boundary lubricant species then the break between mild and severe wear should occur at the same relative surface sulfide concentration, independent of which antiwear additive was being tested. The sulfide concentration at the break is shown in Table 4 for both of the compounds in Fig. 13 and 14. These results show about a factor of three difference between the two compounds. This indicates that the ZDTP provides a more effective boundary lubricant film than the DTBS.

The observations and suggested mechanisms given above generally explain the composition of boundary lubricant films and how they might be formed, but

397

even with these films wear occurs. One possible explanation for wear in a lubricated contact is based on the effects of diffusion of surface impurities into the grain boundaries of the contacting metal parts. Embrittlement and subsequent fracture of metals generally occur at or along grain boundaries (46,47). A shift of the embrittlement temperature, $\Delta\ T_t$, is effected by the inclusion of a number of elements, as shown in Eq. 8 for dilute solutions in iron (48).

$$\Delta\ T_t\ =\ 0.28\ P\ +\ 0.38\ Sb\ +\ 0.16\ Sn\ +\ 0.48\ As\ +\ 1700\ S$$

$$-\ 0.85\ Be\ -\ >20\ B\ -\ 21\ C. \tag{8}$$

This equation shows sulfur to be approximately 1000-fold more effective than any other element for increasing $\Delta\ T_t$ (48). It has been reported that sulfur is able to produce significant embrittlement at concentrations as low as 5 ppm (49). At higher concentrations the embrittlement temperature can reach the estimated surface temperatures of sliding parts in a highly loaded contact. Because of the small area of actual contact and the rapid disipation of heat the area subject to thermal embrittlement and fracture will be small.

If the wear in lubricated contacts is produced by thermal embrittlement and fracture on a microscopic basis the wear debris could not be smaller than a single crystallite. A wear test using benzyl mercaptan as the antiwear additive was selected as a check of this possible mechanism. The extremely high wear and ferrographic analysis of the wear debris indicates that benzyl mercaptan functions by a corrosive wear mechanism which should produce the smallest wear particles. The average crystallite diameter, as determined by X-ray diffraction, for a new test specimen and the wear debris were identical at 12.0 ± 1.0 nm. Although these data do not exclude wear on an atomic scale they demonstrate that even in a very corrosive test all wear is not due to atom-by-atom removal of the surface.

The mild wear regime probably consists of conditions where enough additive is present to form effective boundary lubricant films but not enough to aggrevate grain boundary fracture. However, when a wear particle is generated it still appears that separation occurs at the grain boundaries. The transmission electron micrograph in Fig. 15 shows several wear debris particles at an original magnification of 1000,000. A wear particle from ZDTP test was selected for this examination because it represented typical mild wear which is currently being achieved. The wear debris is much larger than a single crystallite. Close inspection of the particle edges reveals a rough but regular structure, see arrows on the micrograph. The size and shape of these edge features are comparable to that expected for an individual crystallite in the test specimen, ca 12 nm. The overall size of a wear debris particle would be related to the local stresses and the depth of sulfur diffusion into the test specimen. These micrographs are consistent with wear debris being produced by fracture along grain boundaries, even for mild wear, and could explain the similarity in shape and size of normal wear particles.

At low additive concentration, where high wear is obtained, there may not be enough additive to form or maintain an effective boundary lubricant film. Metallic contact probably occurs under these conditions on a local basis.

Severe galling and macroscopic seizure, however, are not produced, possibly because the limited amount of sulfur present still diffuses into the grain boundaries and limits the maximum size of a wear particle. The higher temperature resulting from increased frictional heating would accelerate the diffusion of sulfur into grain boundaries and could partially compensate for the reduced surface sulfur concentration.

At the lowest bulk concentrations tested there is not enough additive or sulfur present to prevent direct metallic contact or limit the size of the wear particles. Thus severe galling and macroscopic welding occur with subsequent catastrophic failure.

The observations and discussion presented here are consistent with the wear model represented by Fig. 4 for wear mitigation in a lubricated contact. Over much of the surface the two contacting parts are separated by EHD on a localized basis. When an asperity on one surface approaches an asperity on the second surface the EHD film can be penetrated. When this occurs the prevention of metallic contact is first prevented by adsorbed additives and reacted surface films. As the load further increases inorganic sulfide films, presumably formed on earlier passes prevent metallic contact. The sulfur can diffuse into the surface and through temperature embrittlement cause fracture at the grain boundaries when local stresses and temperatures are high enough.

With these observations and proposed mechanisms in mind what can one speculate would be needed to improve antiwear efficiency. An improved additive would need to contain sulfur, or one of the other wear reducing elements, P or Cl for example, but it needs to be present in such a chemical state that it does not contribute to corrosion. This would generally mean that the element should be in the backbone portion of the structure or in a sterically hindered position. The additive needs to form a tenacious bond not only with the surface but also with the other adsorbed additive molecules to form a boundary lubricant film which is held tightly and is difficult to rupture. However, the functional groups which interact with the surface cannot corrode or solubilize the surface. Multiple functional groups on a single additive molecule could increase the molecular interaction with the surface without making any one bond too active. Of course one must be cautious about making the projected surface area too large which would reduce the cross molecular interaction thus reducing the film strength. Alternately, compounds which form polymers on the surface could increase multiple surface interactions and at the same time increase the film strength of the boundary lubricant. This latter approach has been tried with some success (50). The major trick, with in-situ polymerization, is to develop a molecule which will readily polymerize on the surface but not in the bulk.

CONCLUSIONS

From this work the following conclusions can be drawn.

1. The mechanism of surface-antiwear additive interaction is most consistent with an equilibrium adsorption of the antiwear additive followed by reaction of the adsorbed material, most likely inside the contact zone.

2. The formation of a surface sulfide rather than the sulfate is probably the result of kinetic limitations which produce a 'reducing atmosphere' inside the contact zone.

3. The effect of viscosity indicates that even under boundary lubrication conditions part of the load and surface separation is provided by EHD on a microscopic, localized basis.

4. The boundary lubricant film is composed of adsorbed additive, reaction product and inorganic sulfide films.

5. A mechanism of producing wear debris during lubricated sliding when anti-wear additives are used was proposed. This process results from the diffusion of sulfur, or other active elements, into grain boundaries followed by subsequent fracture. This mechanism appears to be consistent the experimental observations over a range of antiwear additive concentration which produces different wear phenomena.

REFERENCES

1. D. Dowson, "History of Tribology", (Longman Inc., New York, 1979).

2. C. St. C. Davison, "Wear Prevention in Early History", Wear 1, 155 (1957/58).

3. C. St. C. Davison, "Wear Prevention between 25 B.C. and 1700 A.D.", Wear 2, 59 (1958/59).

4. B. A. Baldwin and J. E. Lee, "An Automated Laboratory Lubricant Test to Simulate Valve Train Wear", Wear 84, 139 (1983).

5. B. A. Baldwin, "Chemical Characterization of Wear Surfaces Using X-ray Photoelectron Spectroscopy", Lub. Eng. 32, 125 (1975).

6. D. R. Wheeler, Discussion of Ref. 42, ASLE Trans. 26, 37 (1983).

7. M. Kuhn, "Boundary-Friction Lubricants", Stahl und Eisen 72, 1212 (1952).

8. M. J. Furey, "Film Formation by an Antiwear Additive in an Automotive Engine", ASLE Trans. 2, 91 (1959).

9. R. C. Wiquist, S. B. Twiss and E. H. Loeser, "Distribution of an EP Film on Wear Surfaces", ASLE Trans. 3, 40 (1960).

10. J. Hickman and K. Middleton, "Some Surface Chemical Aspects of Lubrication", Advan. Sci. 26, 438 (1970).

11. S. Singhal, "Asperity Welding-An Aspect of Scuffing of a Lubricated Sliding Contact", Wear 24, 391 (1973).

12. P. Studt, "Lubricating Oil Additives for High Contact Pressures and Their Effectiveness", VDI-Berichte 156, 19 (1970).

13. D. Godfrey, "Chemical Changes in Steel Surfaces During Extreme Pressure Lubrication", ASLE Trans. 5, 57 (1962).

14. C. N. Rowe and J. J. Dickert, Jr., "The Relation of Antiwear Function of Thermal Stability and Structure for Metal O, O-Dialkylphosphorodithioates", ASLE Trans. 10, 85 (1967).

15. K. G. Allum and E. S. Forbes, "The Load-Carrying Mechanism of Organic Sulfur Compounds-Application of Electron Probe Microanalysis", ASLE Trans. 11, 162 (1968).

16. E. S. Forbes, K. G. Allum and H. B. Silver, "Load-Carrying Properties of Metal Dialkyl Dithiophosphates: Application of Electron Probe Microanalysis", Proc. Inst. Mech. Engrs. 183 (pt 3P), 35 (1968/69).

17. R. C. Coy and T. F. J. Quinn, "An Application of Electron Probe Micro-Analysis and X-Ray Diffraction to the Study of Surfaces Worn under Extreme Pressure Lubrication", Proc. Inst. Mech. Engrs. 186, 62 (1972).

18. F. L. Kolensichenko and P. V. Trushko, "Formation of Boundary Layers during Friction in the Presence of Sulfur", Poroshkovaya Metallurgiya 96 (12), 47 (1970).

19. D. V. Keller, Jr., "Adhesion, Friction, Wear and Lubrication Research by Modern Suface Science Techniques", J. Vac. Sci. Technol. 9, 133 (1972).

20. E. S. Forbes and A. J. D. Reid, "Liquid Phase Adsorption/Reaction Studies of Organo-Sulfur Compounds and Their Load-Carrying Mechanism", ASLE Trans. 16, 50 (1973).

21. P. Studt, "Lubricating Oil Additives for High Contact Pressure and Their Effectiveness", Verein Deutscher Ingenieure-Berichte 156, 19 (1970).

22. K. Siegbahn, C. Nordling, A. Fahlman, R. Nordberg, K. Hamrin, J. Hedman, G. Johansson, T. Bergmark, S. E. Karlsson, I. Lindgren, and B. Lindbert, "ESCA: Atomic, Molecular and Solid State Structure by Means of Electron Spectroscopy", Almqvist and Wilsells, Uppsala Sweden, 1967.

23. D. H. Buckley and S. V. Pepper, "Elemental Analysis of a Friction and Wear Surface during Sliding using Auger Spectroscopy", ASLE Trans. 15, 252 (1972).

24. D. H. Buckley, "Friction-Induced Surface Activity of Some Simple Organic Chlorides and Hydrocarbons with Iron", ASLE Trans. 17, 36 (1974).

25. D. H. Buckley, "Oxygen and Sulfur Interactions with a Clean Iron Surface and the Effect of Rubbing Contact on These Interactions", ASLE Trans. 17, 206 (1974).

26. R. E. Reason, "Progress in the Appraisal of Surface Topography during the First Half-Century of Instrument Development", Wear 57, 1 (1979).

27. B. A. Baldwin, "The Effect of Base Oil Viscosity on Simulated Valve Train Wear", ASLE Trans. 24, 42 (1981).

28. W. R. Jones, H. S. Nagaraj, and W. O. Winer, "Ferrographic Analysis of Wear Debris Generated in a Sliding Elastohydrodynamic Contact" ASLE Trans. 21, 181 (1978).

29. H. S. Nagaraj, D. M. Sanborn and W. O. Winer, "Asperity Interaction in EHD Contacts", ASME Preprint No. 77-Lub-19.

30. R. J. Parker and J. W. Kannel, "Elastohydrodynamic Film Thickness Between Rolling Disks with a Synthetic Paraffinic Oil to 589 K (600 F)" NASA TN D-6411 (1971).

31. J. F. Archard, "Single Contacts and Multiple encounters", J. Appl. Phys. 32, 1420 (1961).

32. B. A. Baldwin, "Relationship between Surface Composition and Wear: an X-Ray Photoelectron Spectroscopic Study of Surfaces Tested with Organosulfur Compounds", ASLE Trans. 19, 335 (1976).

33. R. J. Bird and G. D. Galvin, "The Application of Photoelectron Spectroscopy to the Study of E.P. Films on Lubricated Surfaces", Wear 37, 143 (1976).

34. E. N. Haeussler, "Tribological Studies of Wear Surfaces using the Combined ISS/SIMS Technique", Vide, Couches Minces 201, L135 (1980).

35. R. Holinski, "Dynamics of Boundary Lubrication", Lub. Eng. 36, 530 (1980).

36. H. A. Spikes and A. Cameron, "Scuffing as a Desorption Process-An Explanation of the Borsoff Effect", ASLE Trans. 17, 92 (1974).

37. H. A. Spikes and A. Cameron, "A Comparison of Adsorption and Boundary Lubricant Failure", Proc. Royal Soc. Lond. A336, 407 (1974).

38. B. A. Baldwin, "Effect of Temperature on Simulated Valve Train Wear", Presented at the 1982 ASME/ASLE Lubrication Conf., Washington D.C., Oct. 1982. To be published in ASLE Trans.

39. J. M. Georges, J. M. Martin, T. Mathia, Ph. Kapsa, G. Meille and H. Montes, "Mechanism of Boundary Lubrication with Zinc Dithiophosphate", Wear 53, 9 (1979).

40. A. Tonck, J. M. Martin, Ph. Kapsa and J. M. Georges, "Boundary Lubrication with Anti-wear Additives: Study of Interface Film Formation by Electrical Contact Resistance", Trib. Int. 12, 209 (1979).

41. B. A. Baldwin, "Wear Mitigation by Antiwear Additives in Simulated Valve Train Wear", ASLE Trans. 26, 37 (1983).

42. D. R. Wheeler, "X-Ray Photoelectron Spectroscopic Study of Surface Chemistry of Dibenzyl Disulfide on Steel Under Mild and Severe Wear Conditions", Wear 47, 243 (1978).

43. M. Alsaad, S. Bair, D. M. Sanborn and W. O. Winer, "Glass Transitions in Lubricants: Its Relation to Elastohydrodynamic Lubracation (EHD)", J. Lubr. Tech. 100, 404 (1981).

44. E. Drauglis and R. J. Jakobsen, "Solidification of Boundary Lubricant Films", Tech Report AFAPL-TR-78-111 (Dec. 1978).

45. R. C. Watkins, "The Antiwear Mechanism of ZDDP'S Part II", Trib. Int. 15, 13 (1982).

46. J. O. Arnold, "The Physical Influence of Elements on Iron", J. Iron Steel Inst. 45, 107 (1894).

47. H. P. Philpot, "Some Experiments on Notched Bars", Proc. Inst. Auto Eng. 12, 235 (1917/18).

48. M. P. Seah, "Interface Adsorption, Embrittlement and Fracture in Metallurgy", Surface Sci. 53, 168 (1975).

49. P. Jolly, "Elimination of Oxygen Induced Intergranular Brittleness in Iron by Addition of Scavengers", Met. Trans. 2, 341 (1971).

50. M. J. Furey, "The Formation of Polymeric Films Directly on Rubbing Surfaces to Reduce Wear", Wear 26, 369 (1973).

TABLE I

VISCOSITIES, SULFUR AND NITROGEN CONCENTRATIONS FOR

SEVERAL WHITE MINERAL OILS

Oil	Viscosity 38°C (cSt)	100°C (cSt)	VI	S (ppm)	N (ppm)
A	8.33	2.3	104	2.8	<1
B	13.3	3.1	102	2.2	<1
C	20.5	4.0	101	<1	<1
D	27.6	4.8	103	---	--
E	34.7	5.1	74	---	--
F	39.8	5.8	94	1.2	<1
G	45.9	6.2	87	<1	<1
H	78.7	8.3	78	<1	<1

TABLE 2

SULFUR SPECIES AND WEAR PRODUCED BY TESTING

A VARIETY OF ORGANO-SULFUR COMPOUNDS

COMPOUND / OIL	BINDING ENERGY S(2p), (ev)	WEAR (μm)
A. ZINC DIALKYLDITHIOPHOSPHATE/A	162.3	16
B. " " " /B	162.1	34
C. ' " " /C	162.4	30
D. t-NONYLSULFENYL-N,N-DIMETHYL-DITHIOCARBAMATE /A	162.0	27
E. " " " /B	161.8	45
F. " " " /C	162.4	93
G. t-BUTYLSULFENYL-N,N-DIMETHYL-DITHIOCARBAMATE /B	161.8	68
H. " " " /C	162.1	120
I. 2-BENZOTHIOYL-t-NONYLDISULFIDE/B	162.0	25
J. 2-MERCAPTOETHYLOCTADECYLETHER/B	162.0	21
K. DIALKYL-2,5-DIMERCAPTO-1,3,4-THIADIZOLE /B	162.1	34
L. PHENYLSULFIDE /A	161.7	86
M. BENZYLMERCAPTAN /B	161.8	71
N. OCTADECYLMERCAPTAN /B	162.0	27
O. n-DODECYLBENZYLMERCAPTAN /B	161.9	21

TABLE 3

WEAR OF SULFUR AND NON-SULFUR ANALOGS, INDIVIDUAL COMPOUNDS

DIFFER ONLY BY THE REPLACEMENT OF A METHYLENE BY A SULFIDE

Additive	Wear (μm)
A - sulfide	3.5 ± .7
A - methylene	31 ± 3
B - sulfide	29 ± 4
B - methylene	60 ± 5
C - sulfide	29 ± 1
C - methylene	37 ± 8
D - sulfide	65
D - methylene	Fails

TABLE 4

RELATIVE SURFACE SULFIDE AT THE BREAK BETWEEN MILD

AND SEVERE WEAR IN FIG. 13 AND 14

Additive	Mild to Severe Wear Break (I_{S-2}/I_{Fe})	
	Max.	Min.
Zinc dialkyldithiophosphate	0.195	0.148
Di-t-butyldisulfide	0.072	0.051

405
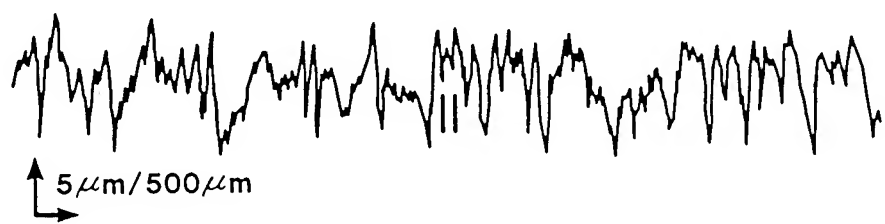
Fig. 1 SURFACE PROFILE OF A GROUND SURFACE AS
NORMALLY PRESENTED
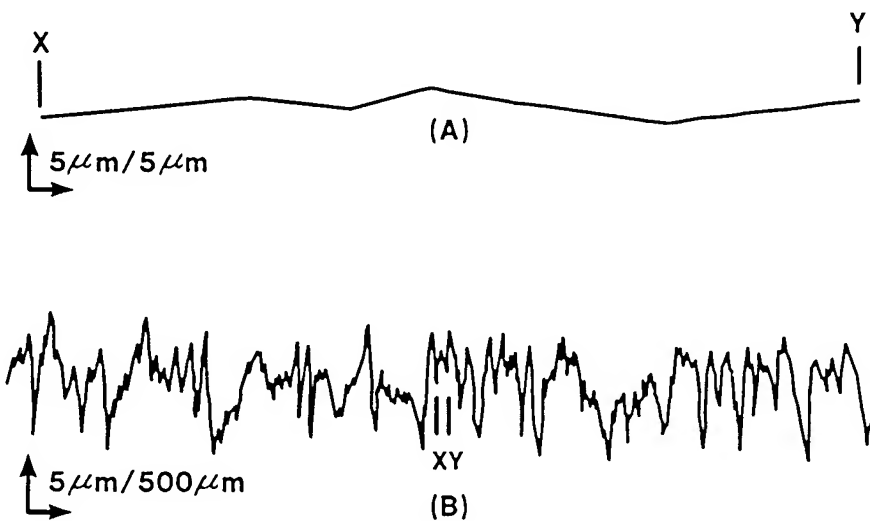
Fig. 2 SURFACE PROFILE USING EQUAL SCALING ON BOTH
AXES (A) FOR THE REGION X-Y IN FIG.1 (B)
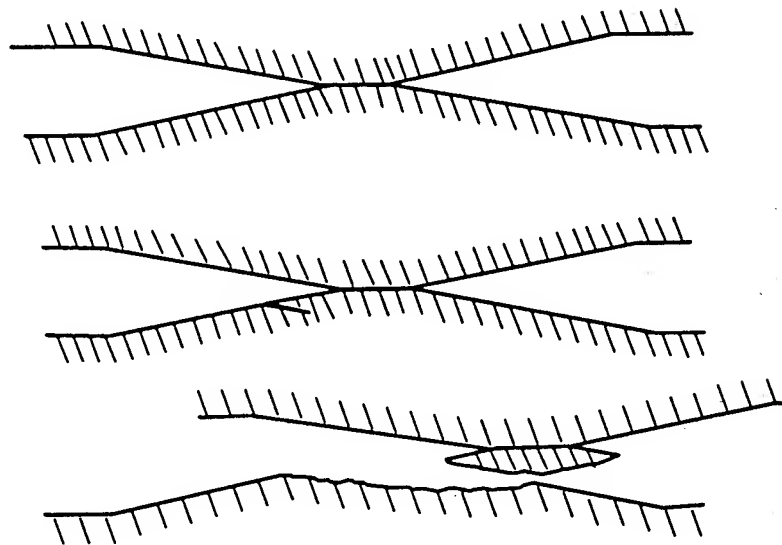
Fig. 3 ASPERITY CONTACT AND WEAR PARTICLE GENERATION
IN AN UNLUBRICATED SLIDING CONTACT
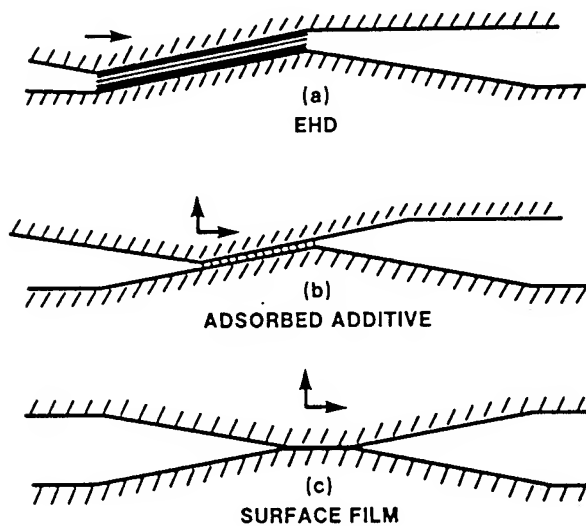
Fig. 4 MODEL FOR ANTIWEAR PROTECTION IN A LUBRICATED
SLIDING CONTACT; a) ELASTRHYDRODYNAMIC LUBRICATION
b) ADSORBED ADDITIVE FILMS OR SURFACE POLYMER
c) INORGANIC FILM

407
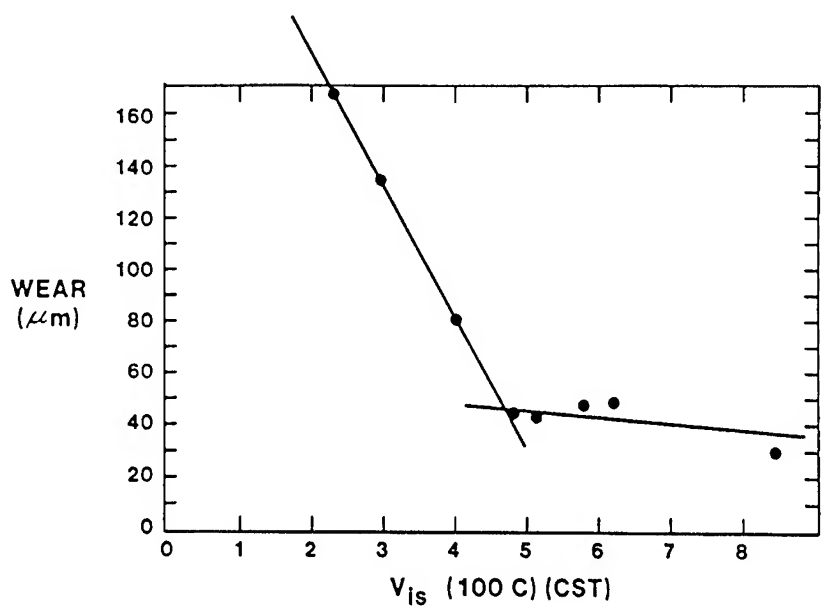
Fig. 5 WEAR OF 1 WT% ZINC DIALKYLDITHIOPHOSPHATE IN WHITE
MINERAL OILS AS A FUNCTION OF 100 C VISCOSITY
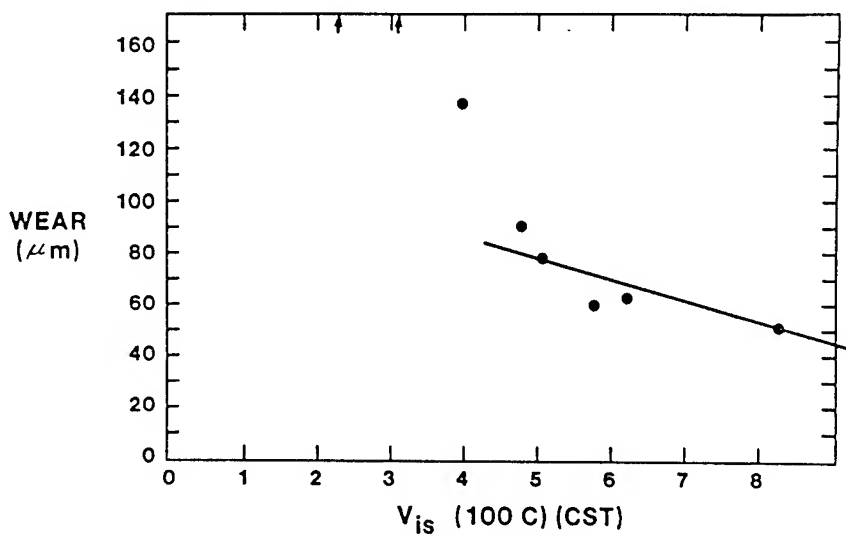
Fig. 6 WEAR OF 0.62 WT% DI-T-BUTYLDISULFIDE IN WHITE
MINERAL OILS AS A FUNCTION OF 100 C VISCOSITY

A $\overline{10\ \mu m}$ B $\overline{500\ nm}$
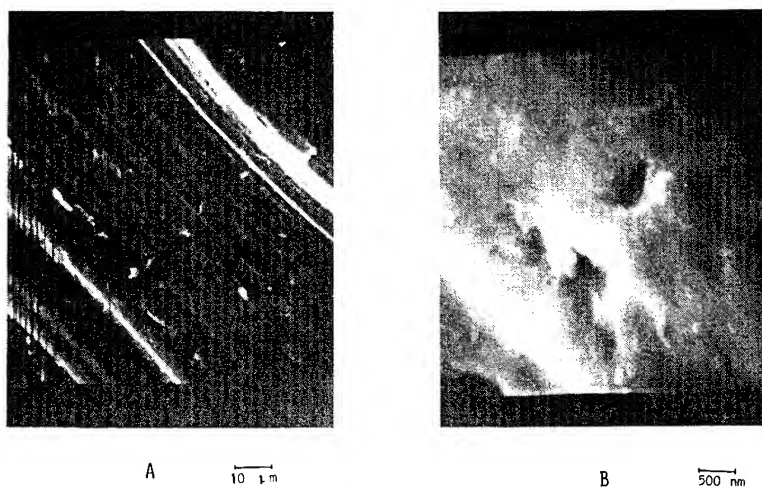
FIGURE 7 SURFACE APPEARANCE OF A FALEX PIN AFTER WEAR TESTING IN ZDTP A) LOW MAGNIFICATION   B) HIGH MAGNIFICATION
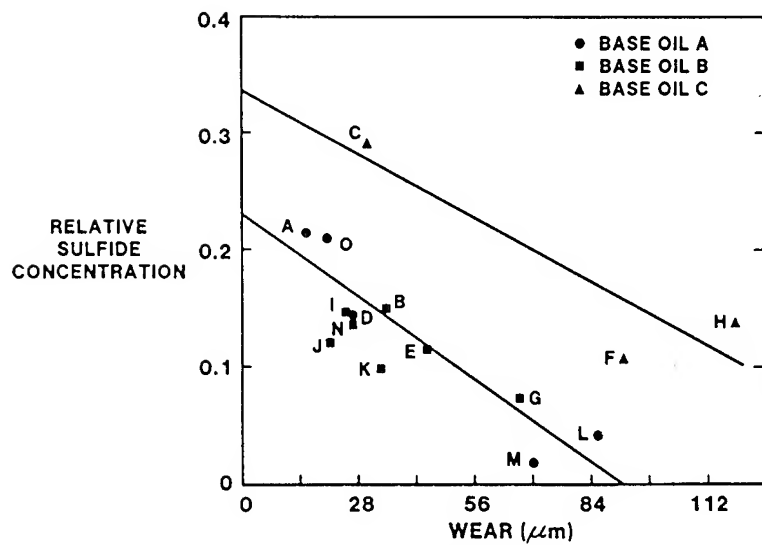
Fig. 8 WEAR AS A FUNCTION OF SURFACE SULFIDE AT THE END OF THE FALEX TEST FOR THE COMPOUNDS IN TABLE 2
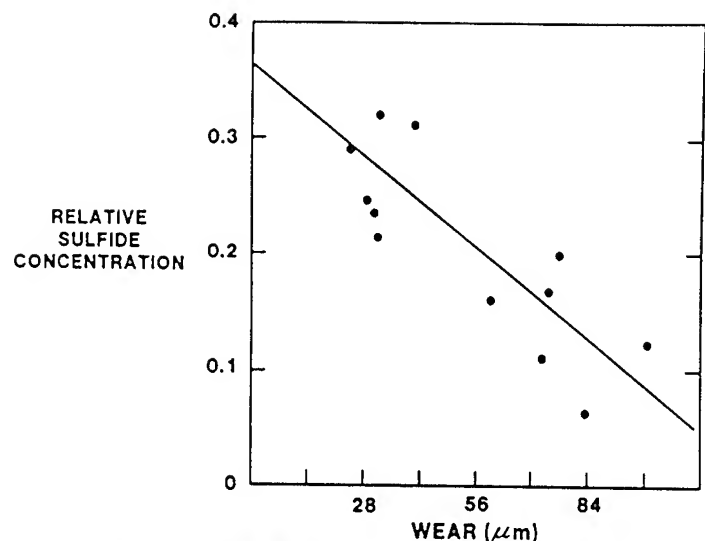
Fig. 9 WEAR AS A FUNCTION OF SURFACE SULFIDE CONCENTRATION
PRODUCED BY VARYING THE CONCENTRATION OF ZDIP
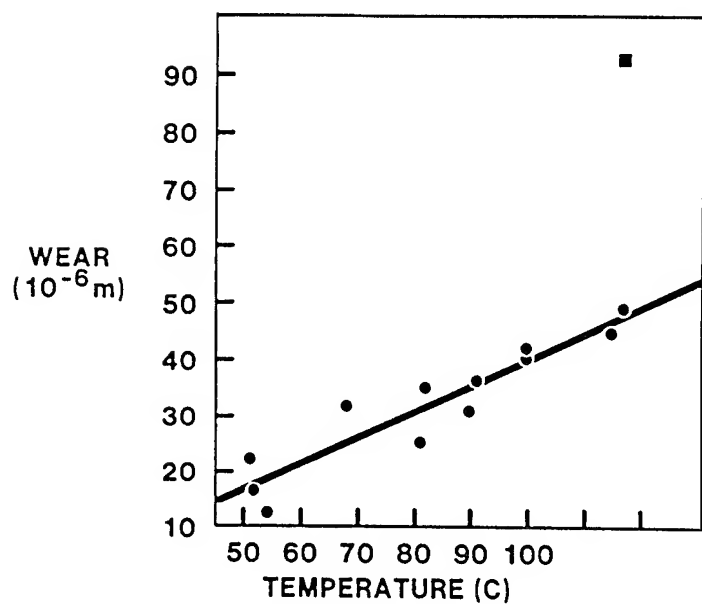
FIGURE 10   TEMPERATURE DEPENDENCE OF WEAR
AT A CONSTANT VISCOSITY OF 5.7 cSt

410
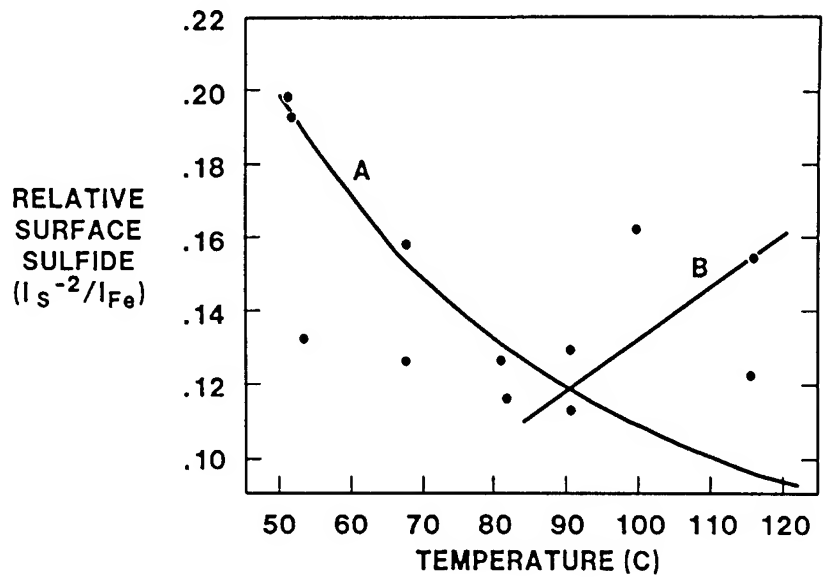
FIGURE 11   RELATIVE CONCENTRATION OF SULFIDE ON THE
FALEX PINS AT THE END OF EACH WEAR TEST AT
THE DIFFERENT TEMPERATURES
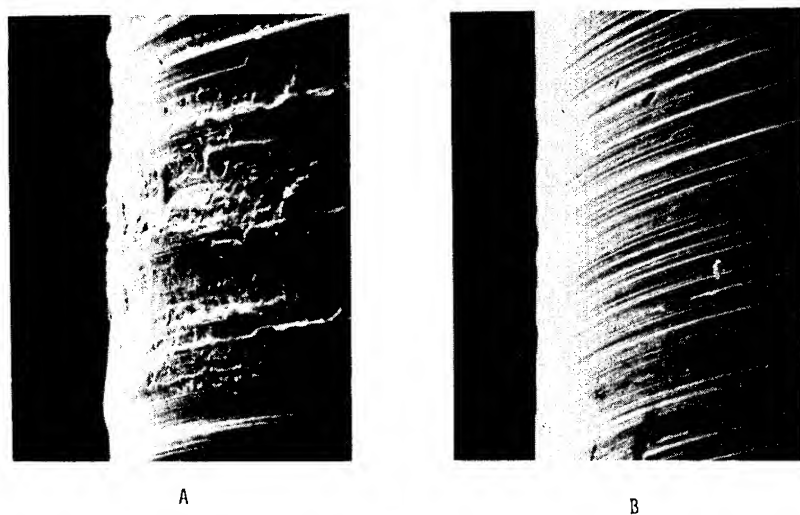
FIGURE 12   SURFACE APPEARANCE OF FALEX PINS TESTED WITH
A) NON-SULFUR AND   B) SULFIDE CONTAINING
ALALOGS MAGNIFICATION 200X
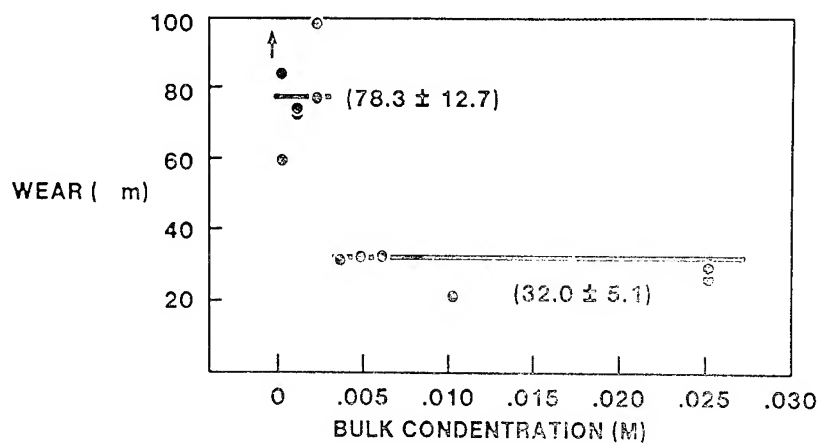
FIGURE 13 WEAR AS A FUNCTION OF ZINC
DIALKYLDITHIOPHOSPHATE CONCENTRATION
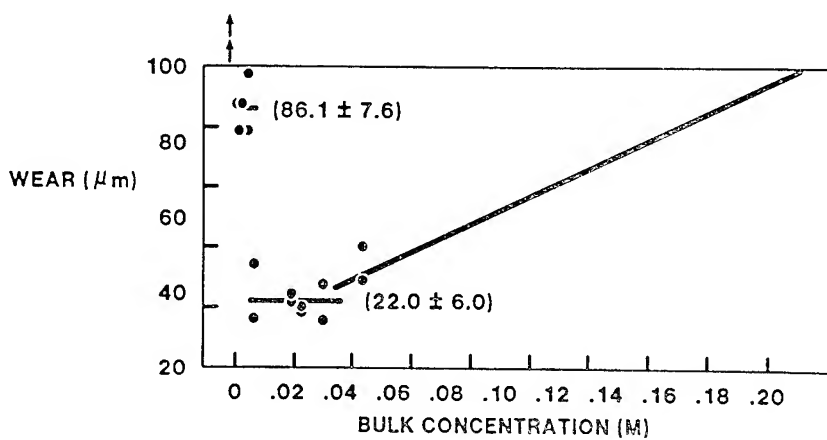
FIGURE 14 WEAR AS A FUNCTION OF
DI-t- BUTYLDISULFIDE CONCENTRATION

412

**FIGURE 15 ELECTROR TRANSMISSION MICROGRAPH OF
WEAR DEBRIS FROM MILD WEAR REGIME OF
ZDTP TEST BAR REPRESENTS 100 NM**

DISCUSSION

I. L. Goldblatt and S. Jahanmir
Exxon Research & Eng. Co.
Linden, New Jersey

The author is to be commended for his interesting and very provocative paper. We would appreciate it if the author would elaborate on several points in his paper.

Based upon the information provided in Table 1, it is expected thet the solubility parameter of oils A through H would increase from about 7.7 to about 9 or more (1). Such a large change in solubility parameter would have a profound effect upon the dissolution of wear products and/or adsorbed films. Hence, increased wear such as that demonstrated in Fig. 10 may be explained by changes in solubility. Would the author please discuss this point?

Would the author please clarify a point concerning the sulfide concentration? Figures 13 and 14 suggest that the minimum level of wear for both ZDTP and DTBS are essentially equivalent, about 32 μm for ZDTP and 22 μm for DTBS. It is suggested that the sulfide levels differ by about 3-fold. Doesn't this suggest that the surface sulfide concentration is not important in determining the antiwear effectiveness of the additive? How is this observation consistent with the embrittlement mechanism? Shouldn't the higher surface sulfide concentration be associated with greater depth of sulfur penetration? In particular, shouldn't the depth of penetration by sulfur be greater for the DTBS?

Have any studies been carried out using several additives having the same chemical functionality which demonstrate the proposed mechanism unequivically?

Fig. 13 suggests that above 0.005M ZDTP, there is no change in wear. Presumably the sulfide concentration is similar. The data below 0.005M also appears to give a single value. The sulfide concentration measurements for these runs all appear to be equivalent. This suggests that there are only two data points in Fig. 9. Alternatively, it suggests that the sulfide concentration measurements are not very significant. Might the author discuss the significance of the surface sulfide concentration measurements?

Would the author please comment on the significance of a zero value for the sulfide concentration shown in Fig. 8? Why are these differences in sulfide concentration which appear to depend upon base stock? Is base stock solubility important? Should the data be treated differently?

(1) C. Hansen and A. Beerbower, Solubility Parameters, Encyclopedia of Chemical Technology, Supplement Volume, pp 889-910, John Wiley (New York, 1971).

The author's suggestion that the reaction rate would increase and the adsorption rate decrease if the temperature is increased is plausible. However, the data in Fig. 11 are too scattered to be used as a support of this proposal. Can the author provide data on other compounds or an explanation for the scatter? Has Dr. Baldwin plotted wear vs. temperature in Fig. 11 rather than relative surface sulfide vs. T?

The mechanism of wear and the action of antiwear additives depend to a great extent on the test conditions. Has the author considered other test conditions and/or other test geometries?

The conclusion that wear is, in part, due to embrittlement has been suggested previously by others. The evidence has not always been thoroughly convincing in this regard. The author suggested that wear in boundary lubrication, especially in presence of S antiwear additives, occurs by S diffusion along the grain boundaries and embrittlement of the grain structure. In this process one would expect the wear particles to be on the same order of magnitude as the grain size. Has the author measured the grain size of his steel specimens? The average grain size of steel alloys is approximately 5 μm or 5000 nm, whereas the size of the wear particles measured by Dr. Baldwin is 120 nm. Small wear particles, i.e. about 100 nm, have been observed (2) even in the absence of any lubrication, therefore S embrittlement is not necessary for formation of small wear fragments. If the S embrittlement wear mechanism is correct then how does the author explain the wear process with P and Cl containing anti-wear additives?

(2)   P. Heilmann, J. Don, T. C. Sun, W. A. Glaeser & D. A. Rigney, "Sliding Wear & Transfer", Int. Conf. on Wear of Materials, K. C. Ludema (ed.), pp 414-425, ASME, New York (1983).

DISCUSSION

Frances Lockwood
Martin Marietta Laboratories
Baltimore, Maryland

In this paper, Dr. Baldwin brings together his previous work on sulfur-containing antiwear additives and presents several ideas which are a step toward explaining their antiwear behavior.

His first and most general point is that elastohydrodynamic (EHD) effects may occur on a microscopic or local level in contacts which have previously been thought to be lubricated exclusively by boundary mechanisms. I agree with this assertion, and I anticipate that the elastohydrodynamicists will soon respond to the challenge of predicting such local effects.

Dr. Baldwin's other major points relate specifically to sulfur containing antiwear additives. He has consistently found via XPS that sulfur-containing additives produce metallic sulfides on the wear surfaces with a correlation between the amount of sulfide produced and the wear reduction. This finding is justified based on his experimental data and is generally consistent with several other published reports (1a-2a). But the generality of a direct relationship between sulfide concentration and wear is questionable, particularly with respect to the effect of contact zone metallurgy and temperature. Other investigations with several sulfur containing additives have found that the relative proportions of the elements S,P,O and Zn in the wear area varies (3a,4a). For example, Bird et al. (4a) found evidence of two types of film; a thiophosphate film (Zn:P:S, 0.8:1.0:0.2) formed in the wear area, with ferrous sulfide being found in score mark regions. Dr. Baldwin, himself, I believe, demonstrated in his presentation that other compounds besides the sulfides play a role in wear reduction. He has shown that the surface concentrations of sulfide needed to obtain low wear with ZDTP were significantly lower than with DTBS. This argues for other compounds besides sulfides being active anti-wear agents. For example, Mills, et al. (5a) have suggested that EP-additives could act by producing the sulfide surface on which polar components, such as carboxylic acids, can adsorb. If this is the case, one would expect that the dominance of sulfide concentration in controlling wear would depend on the contact zone conditions.

Concerning sulfide concentration, those who have used surface analysis on wear surfaces recognize that problems with repeatability and sampling can be formidable. The Falex test itself is not highly repeatable; moreover, the films in the wear area are usually not continuous but very patchy. How was sampling of the wear scar areas handled? How many areas were examined on each pin and what was the XPS beam size?

I believe that some of these experimental difficulties are reflected in the figures. In Figure 8, the slopes being compared appear to have rather large experimental error, whereas in Figure 11, the sulfur to iron ratio versus temperature could perhaps be better represented by a band rather than lines. This would make the ratio dependence on temperature less obvious. It would

have also been interesting to see more data in the corrosive wear regime, for example in Figure 14, and also the outlying point in Figure 10 might reflect a transition to the corrosive regime.

The mechanistic discussion is very speculative but interesting nevertheless. The hypothesis that sulfur diffuses into the grain boundaries to cause embrittlement seems reasonable. Does Dr. Baldwin plan to test this hypothesis and by what experiment?

In regards to the adsorption and reaction mechanism, the seemingly decreasing sulfur/iron ratio with increasing temperature in the low temperature region of Figure 11 does, as Dr. Baldwin says, suggest additive adsorption as the limiting factor in this regime. Does Dr. Baldwin have any other data or experience which corroborates this?

1a. Coy, R.C. and Quinn, T.F.J., "The Use of Physical Methods of Analysis to Identify Surface Layers Formed by Organosulfur Compounds in Wear Tests," ASLE Trans. Vol. 18, 3, 163-174.

2a. Kawamura, M. and Fujita, K., "Organic Sulfur and Phosphorus Compounds as Extreme Pressure Additives," Wear 72 (1981) 45-53.

3a. Buckley, D.H., "Auger Spectroscopy Analysis of Lubrication with Zinc Dialkyldithiophosphate of Several Metal Combinations in Sliding Contact," NASA Technical Paper TP-1489, July 1979.

4a. Bird, R.J., Coy, R.C. and Hutton, J.F., "The Preparation and Nature of Surface Films from Zinc Dialkl dithiophosphate," ASLE Preprint No. 78-LC-1C-3.

5a. Mills, T.N. and Cameron, A., "A New Lubricant Test Device," ASLE Preprint No. 80-AM-40-1, 1980.

THERMAL AND OXIDATIVE STABILITIES OF LIQUID LUBRICANTS

William R. Jones, Jr.
National Aeronautics and Space Administration
Lewis Research Center
Cleveland, Ohio

The fundamental processes occurring during the thermal and oxidative degradation of hydrocarbons is reviewed. Particular emphasis is given to various classes of liquid lubricants such as mineral oils, esters, polyphenyl ethers, C-ethers, and fluorinated polyethers. Experimental techniques for determining thermal and oxidative stabilities of lubricants are discussed. The role of inhibitors and catalysis is also covered.

INTRODUCTION

Liquid lubricants are being subjected to ever-increasing thermal stresses. The role of the lubricants thermal and oxidative stabilities is becoming an important factor in the ability of lubricants to survive at high temperatures in oxidizing environments. Maximum fluid temperatures have been estimated to be in excess of 260° C for many applications (refs. 1 to 8). State-of-the-art fluids (esters, hydrocarbons, silicones, fluorinated polyethers, C-ethers, and polyphenyl ethers) have one or more deficiencies which limit or prevent their use above 260° C. Some of these deficiencies are related to physical properties, such as pour point or volatility, but for many, poor chemical stability at these high temperatures is the weak link.

This paper reviews the fundamentals of the thermal and oxidative breakdown processes occurring in liquid lubricants. In addition, the probable mechanisms of lubricant breakdown are reviewed for several chemical classes (hydrocarbons, esters, C-ethers, polyphenyl ethers, and fluorinated polyethers).

THERMAL STABILITY

It is unfortunate that the literature is often not explicit concerning the term thermal stability. It is sometimes used interchangeably with thermal-oxidative stability. However, the proper definition is reserved for processes occurring in the <u>absence</u> of oxygen.

Mechanism

In the case of hydrocarbons and most other fluid classes, thermal decomposition or pyrolysis proceeds through a free-radical chain reaction process yielding many products. Free radicals are organic fragments containing an unpaired electron, and are produced by homolysis (breaking) of C-C bonds. These radicals can be generated by radiation, mechanical processes, and thermal energy (ref. 9).

The production of free radicals from a hydrocarbon by a thermal process (refs. 10 and 11) is illustrated by

$$R-CH_2-CH_3 \rightarrow R\bullet + R-CH_2-\overset{\bullet}{C}H_2 + R-\overset{\bullet}{C}H-CH_3 \qquad (1)$$
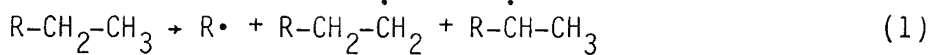
These radicals are highly reactive and start reaction chains by abstracting hydrogen atoms (H) from the parent hydrocarbon. The chainlike abstraction reaction arises from a simple mathematical principle — the sum of an even plus an odd number is always an odd number. When a radical (odd number of electrons) attacks a nonradical (even number of electrons) one of the resulting species must have an odd number of electrons. Therefore, it is a radical itself and also capable of attacking a nonradical. Attack by this second radical (possibly different than the initial radical) will produce a third radical. Abstraction reactions are illustrated by

$$R\bullet + R-CH_2-CH_3 \longrightarrow RH + R-CH_2-\overset{\bullet}{C}H_2 \qquad (2)$$
$$\searrow RH + R-\overset{\bullet}{C}H-CH_3$$
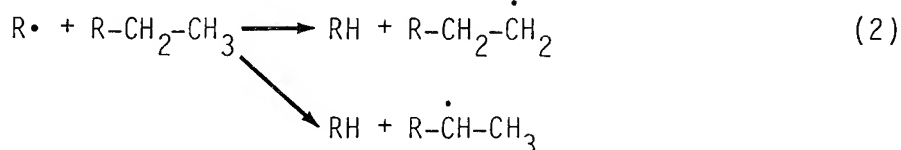
This chain sequence will continue until the radicals are destroyed or all the reactants are consumed. Hence, a single radical can bring about changes in thousands of molecules. Radicals may be destroyed by recombination,

$$R\bullet + R\bullet \rightarrow R-R \qquad (3)$$

or through disproportionation reactions (transfer of an atom from one radical to another),

$$R\bullet + H-CH_2-\overset{\bullet}{C}H_2 \rightarrow RH + CH_2 = CH_2 \qquad (4)$$
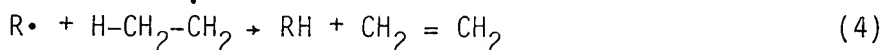
Radicals themselves may also fragment producing new radicals and unsaturated species:

$$R-CH_2-\overset{\bullet}{C}H_2 \rightarrow R\bullet + CH_2 = CH_2 \qquad (5)$$
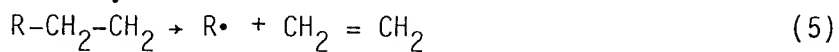
These reactions are analogous to industrial cracking.

Although higher molecular weight products may be produced in this series of reactions, the most general change in properties of the lubricant is an increase in the vapor pressure of the system. This is brought about by cleavage of large molecules into smaller, more volatile, gaseous fragments. This gaseous evolution can be utilized to quantitate the thermal stability of organic compounds.

Arrhenius Rate Law

The rate of thermal decomposition usually varies with temperature according to the empirical Arrhenius rate law (ref. 12) as shown in

$$k = Ae^{-E/RT} \tag{6}$$

where k is the rate constant, A the frequency factor or preexponential factor, E the activation energy, R the gas constant, and T the absolute temperature. According to this equation, a straight line should be obtained when log k is plotted as a function of the reciprocal of the absolute temperature. It has been shown (ref. 12) that, for most organic compounds, log dp/dt versus 1/T is also a straight line. Then, by analogy,

$$\frac{dp}{dt} = A'e^{-E'/RT} \tag{7}$$

Using this equation, one can define the rate constant for thermal decomposition by measuring the isothermal rate of vapor pressure rise at several temperatures. However, it is more convenient to have a single parameter for thermal decomposition rather than to tabulate values of A' and E' which actually define the rate constant.

An arbitrary thermal decomposition temperature (T_D) is defined as the temperature at which the isothermal rate of vapor pressure rise is 1.85 Pa/sec (50 torr/hr). The decomposition points for a series of organic compounds are the temperatures at which all have identical isothermal rates of vapor pressure rise. This technique is used in the standard test method (ASTM D2879) (ref. 13) for measuring the initial decomposition temperature of liquids. This test uses a constant volume device (the isoteniscope) which can also be used to measure vapor pressure as a function of temperature.

Tensimeter

An automated device (the tensimeter), based on the same principle, (ref. 14) also yields thermal decomposition temperatures and vapor pressure data. A schematic representation of the tensimeter appears in figure 1. The sample cell is made of ordinary borosilicate glass and has a volume of about 5 ml (5×10^{-6} m^3). Three to four milliliters (3×10^{-6} to 4×10^{-6} m^3) of test fluid are placed in the sample cell. The sample is then degassed and refluxed under a vacuum. The cell is placed in a temperature-programmed oven and heated to an initial temperature about 50° C below the suspected decomposition temperature. After a 5-minute stabilization period, the increase in vapor pressure, if any, is recorded as a vertical bar during a fixed time interval. Then the programmer automatically raises the temperature by a preset amount (usually 5° C) and the process is repeated. A typical thermal decomposition curve for a synthetic hydrocarbon is shown in figure 2. This figure shows a plot of the logarithm of the isothermal rate of vapor pressure increase as a function of reciprocal absolute temperature. A straight line is drawn connecting the tops of the recorded bars. The intersection of this line with the temperature axis is T_D. In addition, the activation energy for decomposition (E') can be calculated from the slope of this line.

Generalizations

Blake et al. (ref. 12), reported on the thermal decomposition of a variety of different chemical structures. From their data and that of others (refs. 15 to 20) one can make the following generalizations:

421

(1) The maximum thermal stability of a straight chain hydrocarbon or other compounds containing such groups is about $350°$ C.

(2) Branched chain hydrocarbons are less stable than straight chain hydrocarbons due to steric effects and the fact that free radicals of greater stability are formed.

(3) Steric crowding around larger central atoms such as tin and silicon actually increases the thermal stability.

(4) Aromatic bonds (C-H and C-C) have higher dissociation energies due to resonance. Therefore, these compounds are much more stable than their aliphatic analogs. Maximum stabilities of this class approach $450°$ C.

(5) Esters of alcohols having β-hydrogens decompose through a low energy transition state with maximum T_D's near $280°$ C.

(6) Esters not containing β-hydrogens have the low energy reaction path blocked and therefore exhibit stabilites approaching hydrocarbons ($320°$ to $340°$ C).

(7) Substitutions on an aromatic ring decrease its stability. Increasing the number of substituents continually decreases stability. Increasing the chain length also decreases stability until it approaches that of aliphatic hydrocarbons.

(8) Saturated ring compounds are more stable than their straight chain analogs.

(9) Completely replacing hydrogen with fluorine sometimes increases the thermal stability of an organic compound (aromatics and esters are exceptions).

Bond Dissociation Energy

The preceding generalizations arise from the fact that thermal decomposition occurs at the weakest link in the compound. Therefore, thermal decomposition should be a function of the weakest bond dissociation energy (E_{DIS}) in that compound. Table I tabulates T_D and E_{DIS} values for a variety of compounds. The thermal decomposition temperature is plotted as a function of the bond dissociation energy in figure 3. The general trend of increasing T_D with increasing E_{DIS} is apparent in the figure.

Degradation Products

In general, two types of thermal degradation are observed with organic fluids. One type is random degradation in which a great number of decomposition products are produced. A saturated straight chain hydrocarbon is an example. A second type is called chain depolymerization (or unzipping). Here the compound reverts to its monomer. Polyolefin fluids are examples. Polymers have analogous decomposition routes with polytetrafluoroethylene behaving in an unzipping mode while polyethylene exhibits a random degradation or chain scission (ref. 21). Both processes proceed by free radical mechanisms.

However, many fluids exhibit a combination of these mechanisms. Two factors that are important for chain depolymerization to occur are (1) the reactivity of the depropagating radical and (2) the availability of a reactive hydrogen atom which could allow chain transfer. For example, all polymers having α-hydrogens (such as polyacrylates) yield little monomer. On the other hand, polymers such as polymethacrylates give high yields of monomer because of the blocking action of the α-methyl group. Polytetrafluoroethylene also depolymerizes due to the resistance of the C-F bonds to chain transfer.

Catalytic Thermal Decomposition

Blake et al. (ref. 12), have reported that the thermal stability of most chemical classes is not affected by the presence of metal surfaces. One exception is esters, which yield decreases in T_D from 35° to 60° C in the presence of steel (ref. 12) or iron powder (ref. 15). Klaus has also shown that a number of hydrocarbons were not affected by the presence of various catalyst coupons (ref. 20). However, recent work (ref. 22) with two esters (DES and TMPTH) has yielded interesting results for evaporation tests performed in nitrogen. At temperatures below 180° C, evaporation losses are unaffected by metals. However, above 180° C, the rate of evaporation is increased and is different for different metals. This effect, which is shown in figure 4 (ref. 22), suggests that thermal degradation is being catalyzed by the metals yielding lower MW products which increase the evaporation rate.

OXIDATION STABILITY

The oxidation of an organic compound with molecular oxygen is usually referred to as autoxidation. As was the case with thermal decomposition, oxidations usually proceed through a free radical chain mechanism (ref. 23). However, with the additional participant (oxygen) the reactions can become exceedingly complex. The importance of hydroperoxides in the oxidation process was shown by Criegee (ref. 24).

Mechanism

The liquid–phase oxidation of organic compounds and liquid lubricants has been studied by many investigators (refs. 25 to 56). In general, the basic mechanism is thought to proceed as follows (ref. 57):

$$In_2 \xrightarrow{R_i} 2 \ In\cdot \tag{8}$$

$$In\cdot + RH \rightarrow InH + R\cdot \tag{9}$$

An initiator (In) produces free radicals (In·) at reaction rate (R_i) which abstracts a proton from the hydrocarbon and produces an alkyl free radical (R·). This highly reactive species reacts with oxygen in the propagation step of the chain reaction:

$$R\cdot + O_2 \rightarrow RO_2\cdot \tag{10}$$

This propagation step produces a peroxy radical ($RO_2\cdot$) which in turn reacts with the parent hydrocarbon (RH) to produce a hydroperoxide (RO_2H):

$$RO_2\cdot + RH \xrightarrow{k_p} RO_2H + R\cdot \tag{11}$$

423

This reaction regenerates an alkyl free radical (R·) which propagates the chain.

The chain reaction can be terminated by radical coupling of two peroxy radicals (RO_2·),

$$2RO_2\cdot \xrightarrow{2k_t} RO_4R \longrightarrow \text{nonradical products} \qquad (12)$$
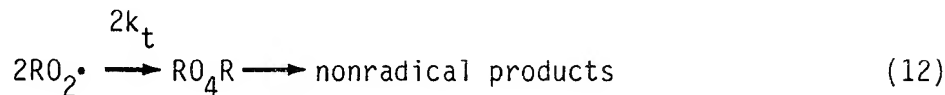
or by cross termination of an alkyl radical (R·) and a peroxyradical (RO_2·),

$$R\cdot + RO_2\cdot \rightarrow RO_2R \qquad (13)$$
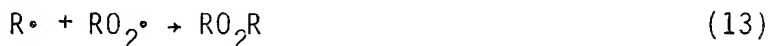
A third possibility is the termination reaction of two alkyl radicals (R·),

$$2R\cdot \rightarrow R-R \qquad (14)$$

Rate Equations

For normal oxygen concentrations where $[RO_2\cdot] \gg R\cdot$, reactions (13) and (14) can be neglected. Therefore, the rate of oxidation of hydrocarbon R-H can be expressed as

$$\frac{-d[R-H]}{dt} = k_p[R-H]\left(\frac{R_i}{2k_t}\right)^{1/2} \qquad (15)$$

The rate of oxidation is then directly proportional to the hydrocarbon concentration and to the square root of the rate of chain initiation. This relationship is illustrated in figure 5, which shows the rate of oxidation of ethyl linoleate (initiated by benzoyl peroxide) as a function of its concentration. For other types of chain termination, different rate of consumption equations will be obtained. Some of these relationships appear in reference 58.

Oxidizability

The ratio $k_p/(2k_t)^{1/2}$ which appears in equation (15) is referred to as the oxidizability. For a specific rate of initiation, the autoxidation of a hydrocarbon (R-H) is then determined by the values of k_p and k_t. The rate of chain propagation (k_p) can be estimated if the bond energy for the weakest C-H bond is known (ref. 59). The termination rate constant k_t can also be estimated. Thus, in theory, the oxidizability should be predictable for any pure hydrocarbon. Table II (ref. 60) contains a list of oxidizabilities for various hydrocarbons. This list illustrates the wide range of oxidation rates for different hydrocarbon structures. However, this simple relationship (eq. (15)) breaks down at high conversions (>20 percent). Complications are caused by the accumulation and reaction of secondary products such as aldehydes and ketones.

Chain Initiation

As mentioned earlier, chain initiation can be effected by the deliberate addition of an initiator. Typical initiators are azo compounds and peroxides. This circumvents the long and sometimes irreproducible induction periods (time before oxygen absorption begins).

Initiation can also take place by direct reaction with oxygen:

$$RH + O_2 \rightarrow R\cdot + HO_2\cdot \tag{16}$$

However, this reaction is thermodynamically and kinetically unfavorable. Initiation in the absence of added initiators is probably due to peroxidic impurities.

A common source of free radicals is the thermal decomposition of the alkyl hydroperoxides producing an alkoxy and a hydroxy radical:

$$RO_2H \rightarrow RO\cdot + \cdot OH \tag{17}$$
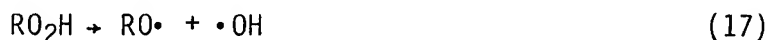
These radicals can then react with the parent hydrocarbon (RH) to produce water, alcohols, and alkyl radicals:

$$RO\cdot + RH \rightarrow ROH + R\cdot \tag{18}$$

$$\cdot OH + RH \rightarrow HOH + R\cdot \tag{19}$$

These reactions are referred to as chain branching.

Chain Propagation

As indicated, the reaction of an alkyl radical $(R\cdot)$ and O_2 (in itself a biradical) proceeds very rapidly. The rate controlling step is then hydrogen abstraction by the alkylperoxy radical in equation (11). The alkylperoxy radicals $(RO_2\cdot)$ are more stable than are the alkyl radicals $(R\cdot)$. They are quite persistent and selective. They preferentially abstract only the most labile hydrogen atom (weakest C-H bond). A group of H-bond energies appears in table III (ref. 57). It is obvious that phenols, thiols, aromatic amines, and phosphines have the most labile hydrogen atoms. It is also clear that the relative attack for primary, secondary, and tertiary bonds should be in the following order: tertiary (90 kcal) > secondary (94 kcal) > primary (103 kcal). Indeed, this has been shown to be the case for 2-methylpentane where the order is 1:30:300 (ref. 61) for primary, secondary, and tertiary bonds, respectively.

The propagation rate is also dependent on the type of hydrogen abstracting alkylperoxy radical. In order to correlate rates with C-H bond energies, rate constants for a series of hydrocarbons (R-H) should be compared for the same alkylperoxy radical. Table IV (ref. 57) shows rate constants for a series of hydrocarbons against their own peroxy radicals (k_p) and against t-butylperoxy radicals (k_p'). Obviously, reactivities are very structurally dependent. For example, the benzoylperoxy radical is 40,000 times more reactive than the t-butylperoxy radical toward benzaldehyde. Comparing only C-H bond energies (table III) would lead one to conclude that aldehydes and alkylaromatic compounds would oxidize at similar rates. However, aldehydes oxidize at appreciably greater rates than the alkylaromatics due to the strong electron withdrawing effect of the carbonyl group.

Chain Termination

As previously mentioned, the normal termination reaction is

$$2RO_2\cdot \rightarrow RO_4R \tag{12}$$

which is a tetroxide. The decomposition of tetroxides is also highly dependant on the nature of the R-group. For example, secondary and primary alkylperoxy radicals undergo disproportionation to an alcohol and a ketone:

$$RO_4R \rightarrow R_2CO + R_2CHOH + O_2 \tag{20}$$
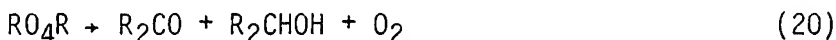
Tert-alkylperoxy radicals yield a different mechanism resulting in the formation of dialkyl peroxides and O_2. The dialkyl peroxides undergo further decomposition. Therefore, primary and secondary alkylperoxy radicals yield much higher termination rates than tert-alkylperoxy radicals.

The oxidation rate of a hydrocarbon is determined by both the propagation rate (k_p) and the termination rate (k_t) as indicated in equation (15). This illustrates why a reactive hydrocarbon such as toluene ($C_6H_5-CH_2-H$), which has a C-H dissociation energy of only 85 kcal/mole, has a rather low autoxidation rate. This is due to the high termination rate of its primary alkylperoxy radicals.

Inhibition of Autoxidation

Autoxidations can be inhibited by the addition of scavengers which break the chain reaction by forming stable free radicals:

$$RO_2\cdot + XH \rightarrow RO_2H + X\cdot \tag{21}$$

An example is in the use of substituted phenols (2,6-di-t-butyl-4-methylphenol) that would yield stable phenoxyl radicals (ArO$\cdot$) which are far less reactive than the $RO_2\cdot$ radical or the R$\cdot$ normally formed by hydrogen abstraction from the parent hydrocarbon.

A second type of inhibitor causes the destruction of hydroperoxides (RO_2H). Here the inhibitor (X) reacts with the hydroperoxide (RO_2H) yielding nonradical products:

$$RO_2H + X \rightarrow ROH + XO \tag{22}$$

An example of this type of inhibitor is phenothiazine (PTZ).

Metal coaters (such as tricresylphosphate) can sometimes be considered as a third type of inhibitor. Here their action is to prevent catalytic effects by coating metal surfaces.

Chain Branching

From the introductory material it might appear that, at least for pure component systems, predictions of reaction rates and product distributions should be relatively easy to make. At sufficiently low temperatures ($<100°$ C) and low conversions (<10 percent) this is probably true for many simple hydrocarbon systems. Above $100°$ C there is an increasing tendency for the primary

oxidation products (alkylhydroperoxides) (RO_2H) to decompose homolytically into alkoxy and hydroxy radicals as previously shown:

$$RO_2H \rightarrow RO\cdot + \cdot OH \tag{17}$$

These reactive species can further react with the parent hydrocarbon RH to produce more alkyl radicals:

$$RO\cdot + RH \rightarrow ROH + R\cdot \tag{18}$$

$$\cdot OH + RH \rightarrow HOH + R\cdot \tag{19}$$

These branching reactions can greatly accelerate the oxidation (autocalalysis) and complicate the reactions. Another complication is that the increased reaction rate may drive the system out of the kinetic region (i.e., into a region where oxygen diffusion becomes a limitation). Therefore, this must be taken into account in high-temperature oxidations.

EXPERIMENTAL METHODS

Reaction kinetics of liquid-phase oxidation processes must be studied in the kinetic region; that is, the reaction must not be oxygen diffusion limited. Most standard oxidation-corrosion tests developed in the past have been bulk tests. Air or oxygen is passed over a static fluid, bubbled through the fluid, or passed over a constantly agitated fluid. An example of a macrooxidation cell is shown in figure 6. It is not within the scope of this paper to describe these macrotests, many of which are diffusion limited. Reference 25 discussed various types of these reactors. Other standard tests are discussed in the literature (refs. 62 and 63).

Oxygen Diffusion

Oxygen transport into the liquid-phase involves three processes:

(1) Diffusion of oxygen in the gas phase to the liquid-gas interface
(2) Dissolution of oxygen into the liquid at the gas-liquid interface
(3) Diffusion of the dissolved oxygen into the liquid phase

Process (1) is very rapid and not a limiting factor. Process (2) is related to the partial pressure of oxygen and Henry's law. Process (3) depends on the interfacial surface area, rate of agitation, and the oxygen concentration gradient. To determine oxygen diffusion, the amount of fluid or oxygen can be varied and agitation rates can be changed. If the rate of oxidation is altered, then the reaction is not taking place in the kinematic region.

Kinetic Curves

The most common parameter measured in most oxidation studies is the absorption of oxygen. If this parameter is plotted as a function of time, four different kinetic curves are observed (ref. 25) (fig. 7). Curve a shows an autocatalytic effect sometimes observed with mineral oils of low aromatic content. Curve b is autoretarding; an example of it is highly aromatic

mineral oils. Curve c is linear and is neither autocatalytic nor auto-
retarding; a polybutene is an example of it. And finally, curve d shows mixed
behavior; an example of it is n-hexyldecylbenzene.

Microtests

Because of diffusion problems, many investigators have designed new
experiments involving small quantities of fluid. Several thin film tests have
been developed (refs. 64 to 66). One is that developed by Klaus and his
coworkers (refs. 30 and 67). In this test, which is illustrated in figure 8,
a very small quantity of lubricant (40 to 100 μl) is injected onto the surface
of a catalyst after the entire apparatus has been equilibrated at test tem-
perature. A constant flow of air is maintained through the air entry tube.
Volatile oxidation products can be trapped for analysis. At the conclusion of
the test, which could be a few minutes or a few hours depending on test tem-
perature, the apparatus is removed from the oven or bath and quenched to room
temperature. The degraded lubricant remaining on the catalyst surface is then
dissolved in an appropriate solvent. This solution can be analyzed by a
variety of techniques, some of which will be highlighted later. From this
analysis a rate of oxidation can be determined.

This apparatus has a number of advantages. It is simple, requires little
test sample, has good reproducibility, and tests are not long. Also, surface
area does not vary during the test. An infinite variety of catalysts can be
studied and each can be recycled. There are, however, some limitations
inherent in the device.

The thin film test is a batch process and is subject to evaporation as
well as oxidation. This usually can be taken into account by running identi-
cal tests in nitrogen. However, some highly stable materials require higher
temperatures for reasonable reaction rates to take place. Sometimes the
original charge disappears well before the conclusion of the test. This can
be alleviated by running tests above atmospheric pressure as has been done by
others (ref. 25). Another problem caused by the thin films is rapid loss of
additives from formulated fluids. Even with thin film tests diffusion
limitations can occur, especially at high temperatures, where local oxygen
consumption is great. In addition, these tests are usually run to high con-
version (up to 50 percent). At high conversions the chain branching reactions
which take place can greatly complicate the reactions. Under such conditions
many products are formed, and chemical analysis and kinetic treatment of the
data become difficult if not impossible. In spite of these limitations,
however, this technique has been successful in reproducing high-temperature
oxidation degradation from bearing tests (ref. 56) and gas turbine engine
tests (ref. 68), and it has contributed to the fundamental understanding of
the degradation of esters and hydrocarbons (ref. 69).

Stirred Flow Reactor

The thin film test just described is an example of a batch process. A
single charge of material is used. In a continuous process, a constant flow
of material to be oxidized is fed to the reactor. The stirred flow reactor is
an example of a continuous process (ref. 34). It has been shown that the
instantaneous reaction rate in the stirred flow reactor can be determined by
balancing the reaction rate with the flow rate (ref. 70). This essentially
maintains steady-state conditions.

The material to be oxidized is fed into the reactor having a constant volume in which thorough agitation take place producing a homogeneous mixture. This mixture is removed at the same flow rate as the input of oxidizable material. Eventually, steady-state conditions prevail and all reactants, intermediates, and final products have constant concentrations. The rate of consumption or formation of any product, intermediate or reactant, can then be calculated from

$$\frac{d(X)}{dt} = \frac{(X)_\tau - (X)_0}{\tau} \tag{23}$$

where $d(X)/dt$ is the rate of consumption or formation of substance X, $(X)_\tau$ the concentration of X in the effluent at steady-state at residence time τ, and $(X)_0$ the concentration of X in the entering fluid. This equation is valid for any species regardless of the complexity of the reaction. This is obviously a plus for kinetic studies. An empirical rate law can then be determined by finding a relationship that describes the rate of formation of a species as a function of its concentration in the reactor.

An example of a stirred flow microreactor is shown in figure 9. It consists of two pyrex spheres A and B. The inside sphere (B) is perforated. The hydrocarbon (R-H) enters at the top and is mixed with a stream of oxygen. This mixture passes through the perforated sphere into sphere A. Theoretically, ideal mixing of the reactants, oxygen, and products occurs. The outlet is on the upper right.

This technique also has some limitations. Since a continuous flow of reactants is necessary, a much greater quantity of test material is required than in the thin film test. In addition, reactant purity must be stringently controlled. Furthermore, it is not clear how a catalytic surface could be incorporated, although soluble metal catalysts could be incorporated in the reactant.

This type of apparatus has been used in kinetic and mechanistic studies of n-hexadecane (refs. 34 and 35) and pentaerythrityl tetraheptanoate (PETH) (ref. 36). In addition, the mechanisms of two common antioxidants, 4,4-diatyldiphenyl amine and 4,5-methylenebis (2,6-di-tert-butylphenol) (ref. 71), have been studied.

Microoxidation Corrosion Apparatus

Another microapparatus for batch operations is shown in figure 10. It is a modified version of the type reported by Snyder and Dolle (ref. 46). It consists of a pyrex decomposition tube and rod assembly. Metal catalysts may be positioned on the rod assembly. In a typical experiment, fluid is introduced into the decomposition tube. The system is evacuated and backfilled with oxygen to a know pressure. The tube is then placed in a preheated furnace for the specified test time. At test conclusion, the system is cooled and connected to a vacuum system. The liquid nitrogen noncondensibles are collected quantitatively, measured, and analyzed by various chemical means. The liquid nitrogen condensibles as well as the fluid residue are also analyzed. The rate of degradation is calculated from the amount of liquid nitrogen condensibles and is usually reported as milligrams of condensible product per gram of original fluid per hour of test.

This type of device has been used in a variety of studies on unbranched (ref. 52) and branched fluorinated polyethers (ref. 53). A similar device (only using flowing oxygen) was used to study a branched fluorinated polyether

and a perfluoropolyether triazine (ref. 49). This apparatus suffers from the same disadvantages as other batch reactors. Conditions must be chosen so as to eliminate oxygen depletion or diffusion problems.

Electronic Gas Sensor

As previously mentioned, both thermal and oxidative processes are accompanied by the evolution of gaseous hydrocarbon products. Ravner and Wohltijen (ref. 72) have taken advantage of this fact to develop a rather simple technique for monitoring the oxidative breakdown of lubricants. They used a solid-state metal oxide semiconductor gas sensor originally developed to detect explosure conditions. The system is diagrammed in figure 11. Correlation of the detected gas evolution with classical indicators of lubricant oxidation (such as viscosity and acid number changes) has been obtained.

ANALYTICAL TECHNIQUES

During testing or at test conclusion, a chemical analysis of the resulting products is necessary. A variety of common chemical analytical techniques is used for these analyses. They include high-pressure liquid chromatography (ref. 73), ultraviolet-visible spectroscopy (ref. 74), infrared spectroscopy (ref. 74), nuclear magnetic resonance (ref. 74), electron paramagnetic resonance (ref. 75), and gas chromatography (ref. 76).

OTHER EXPERIMENTAL TECHNIQUES

Chemiluminescence (CL) is simply light emitted from a chemical reaction. It was first observed in biological sources such as the firefly (ref. 77). If a reaction is to produce light several criteria must be met: (1) sufficient energy for excitation, (2) a species capable of forming an excited state, (3) an emitter to give off excitation energy, (4) a rapid chemical reaction, and (5) a reaction-coordinate system favoring production of an excited state over direct ground state formation.

For many years CL has been associated with many oxidation processes (ref. 78). If we refer back to the sequence of reactions in the autoxidation of hydrocarbons, it is believed that equation (12) is responsible for the observed CL:

$$2RO_2\cdot \longrightarrow ROH + R_2C=O + O_2 \qquad\qquad (12)$$
$$\searrow (R_2C=O)^*$$
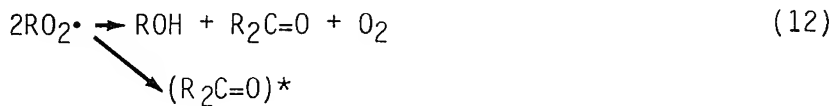
This disproportionation reaction produces a small amount of excited states $(R_2C=O)^*$. For most hydrocarbons, only one photon is emitted for each 10^8 to 10^{10} termination reactions. This inefficiency is caused, in part, by quenching reactions between the excited ketone with oxygen and other species:

$$(R_2C=O)^* + Q \rightarrow R_2C=O + Q \qquad\qquad (24)$$

$$(R_2C=O)^* \rightarrow R_2C=O + h\nu \qquad\qquad (25)$$

The intensity of the emitted radiation (hν) is directly proportional to the square of the concentration of peroxy radicals $[RO_2\cdot]^2$. This dependence is the basis for determining the concentration of peroxy radicals and thus the kinetics of hydrocarbon oxidation. The advantages of CL are (1) it is extremely sensitive, (2) it is noninvasive, (3) it provides a continuous monitor of peroxy radicals, and (4) only small samples are required. A number of investigators have used CL in oxidation studies (refs. 79 to 81). An example of a CL apparatus appears in figure 12. A thorough review of CL appears in reference 82, and a recent review concerning its applications to fuels and lubricants appears in reference 83.

CLASSES OF LUBRICANTS

Hydrocarbons

Most conventional automotive lubricants are mineral oils which are complex mixtures of hydrocarbons. Although some fundamental studies (refs. 20, 33, and 69) have examined these materials, others (refs. 34, 35, 38, 43, 44, 45, and 84) have opted to study a pure component.

Jensen and coworkers (refs. 34 and 35) have performed a series of elegant experiments with pure n-hexadecane. Autoxidation with molecular oxygen was carried out at 120° to 180° C using a stirred flow reactor. Initial studies concentrated on identifying the primary oxidation products at 120°, 160°, and 180° C. These primary products included mono-, di-, and trihydroperoxides, hydroperoxyketones, cyclic peroxides, and some trifunctional products. Negligible amounts of esters or acids were formed in these low conversion studies.

The hydroperoxides are formed by both interhydrogen and intrahydrogen abstraction reactions. Furthermore, it appeared that a high percentage of hydrogen abstractions were taking place by hydroxy radicals (·OH). It was felt that the intramolecular abstractions should play a role in the auto-oxidation of all n-alkanes larger than n-butane.

In a continuation of this work (ref. 35), secondary or clevage products of the autoxidation of n-hexadecane were determined. Products observed at low conversion (2 percent or less) included methylketones, alkanoic acids, hydrogen peroxide, aldehydes, ethers, carbon dioxide, and carbon monoxide. At higher conversions (<16 percent) esters and γ-lactones are formed.

The basic mechanism proposed by the authors to account for the observed products is now summarized. Chain initiation occurs via homolysis of hydroperoxides forming alkoxy (RO·) and hydroxy (·OH) radicals which subsequently abstract protons producing alkyl radicals (R·). The alkyl radicals (R·) react with oxygen producing peroxy radicals ($RO_2\cdot$) which in turn abstract hydrogens intra- or intermolecularly producing mono-, di-, and trihydroperoxides. Chain termination occurs via bimolecular reactions of chain carrying peroxy radicals ($RO_2\cdot$). Methyl ketones (CH_3COR) and alkanoic acids (RCO_2H) are formed by clevage reactions of α,γ-hydroperoxy ketones (HOOR=O). Excess acid and other clevage products are derived from reactions of alkoxyl radicals (RO·).

Esters

Most esters in use today as lubricants are gas turbine engine lubricants. Present formulations meeting military specifications MIL-L-23699 or

MIL-L-7808 are either based on trimethyolpropane or pentrerythritol. These alcohols, which contain no β-hydrogens, are estrified with various acids to produce the final ester products. In practice these lubricants contain a mixture of compounds.

However, as in the case of hydrocarbons, utilizing a pure compound for oxidation studies is advantageous. Hamilton, et al. (ref. 36), have studied the mechanism of the autoxidation of pentaerythrityl tetraheptanoate at 180° to 220° C. This study was analogous to their work with n-hexadecane previously discussed. The proposed reaction scheme for PETH is very similar to that reported for n-hexadecane and is reproduced in figure 13. Again it consists of initiation by hydroperoxide decomposition forming reactive free radicals (1), formation of monohydroperoxides by intermolecular hydrogen abstraction (3), and formation of dihydroperoxides and hydroperoxyketones by intramolecular abstractions (4 and 4*). Chain termination proceeds via peroxy radical recombination (6). Secondary products of acids and methylketones are formed from hydroxyketones (7). In addition, high MW carboxy and acetyl substituted tetraesters will be formed.

A kinetic analysis comparing rate constants for the two systems (PETH and n-C$_{16}$) showed a remarkable similarity for most reaction steps. This would indicate that indeed both compounds appear to be reacting by a similar mechanism. Continuing research over the last few years has also led to a fundamental understanding of the thermal-oxidative reactions taking place in ester based systems (refs. 27 to 32).

Bulk oxidation tests to 260° C (500° F) on di-2-ethylhexyl sebacate (DES) and trimethyolpropane triheptanoate (TMPTH) were reported by Czarnecki (ref. 28). At 260° C, tests with these esters were autoretarding (see fig. 7(b)). It was felt that this was due to the in situ formation of inhibiting materials. However, there were obvious oxygen diffusion limitations since an approximate 30 C° rise in test temperature only doubled the reaction rate. Reaction products for both tests were analyzed by gas chromatography and mass spectroscopy. For DES, a half acid ester and a high boiling fraction (>510° C) were reported. For TMPTH, a diester and smaller fragments were reported as well as a high boiling fraction. No definitive reaction scheme was theorized, but a condensation reaction was proposed for the formation of the high boiling (i.e., high molecular weight) fractions.

Ali (ref. 85) reported further on the chemical degradation of esters (diesters, TMPTH, and PETH) using a bulk oxidation technique. Oxidized products were separated by gel permeation chromatography. A chromatogram for di-2-ethylhexyl sebacate is shown in figure 14. Typically, all the esters produced three fractions of low, intermediate, and high MW. The individual fractions were isolated and further analyzed by IR, UV, and NMR techniques. It was deduced that, initially, a low molecular weight product is formed which eventually polymerizes to a high MW sludge (fraction 3). Spectroscopic analysis indicated that the polymerized fraction (up to MW of 50,000) contained carbonyl groups conjugated with one or more double bonds (-C=C-C=O).

Cvitkovic (ref. 30) described the development of the microoxidation test discussed previously. Ester oxidation was represented by a simple phenomenological model. It was concluded that this technique adequately simulates severe degradation environments such as those present in high-temperature gas turbine engines. Product analysis reinforced the theory that the first step in ester oxidation is the formation of low MW unstable species which subsequently polymerize into high MW sludge. UV absorption was found to increase with increasing MW of oxidation products and with the extent of oxidation. In addition, GPC analysis combined with atomic absorption (AA) of samples from

432

4-ball tests indicated that the iron surface participates in the reactions generating high MW material.

Further work was reported by Lockwood, et al. (refs. 32 and 86), with esters using the same apparatus. Here a kinetic model was devised which predicted inhibitor oxidation rates, evaporation rates, and lubricant stable life from 174° to 247° C. Post stable life tests with iron catalysts indicated rapid basestock oxidation with the production of high MW products and organic iron products. A model for ester oxidation is presented in reference 86. It is similar to that proposed by Jensen, et al. (ref. 34), but it indicates that a final condensation polymer containing carbonyl groups conjugated with double bonds could be formed by dehydration of β-hydroxy ketones:

$$\underset{R-\overset{\overset{\displaystyle OH}{|}}{C}H\overset{}{C}H_2\overset{\overset{\displaystyle O}{||}}{C}R}{} \xrightarrow{-H_2O} \underset{RCH=CH\overset{\overset{\displaystyle O}{||}}{C}-R}{} \qquad (26)$$

In addition, a mechanism whereby an intermediate product of ketone condensation could react with an iron surface to produce soluble iron products was presented:

$$FeOH + R-\overset{\overset{\displaystyle OH}{|}}{C}H CH_2\overset{\overset{\displaystyle O}{||}}{C}-R \qquad (27)$$

→ Polymeric product
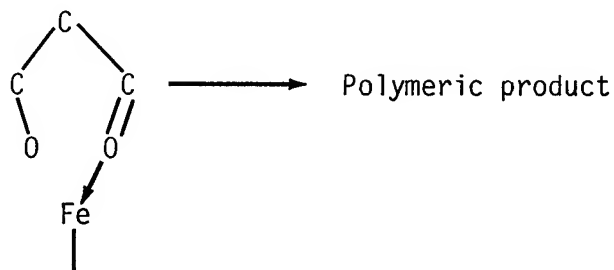
The formation of soluble iron products was almost totally suppressed by the presence of a known metal coater – TCP.

A further description of the microoxidation test appears in reference 69. Here oxidation tests of esters and a superrefined mineral oil are reported. Oxygen diffusion limitations were negligible for small samples (40 μl or less) at 245° C or less. Reaction kinetics indicated that esters and the mineral oil followed a first-order reaction rate from 0 time up to 80 percent conversion. As indicated in previous work, primary oxidation products for the ester were of lower MW than the basestock. For a mineral oil, these products were in the same MW region as the basestock. Secondary and tertiary reactions involve the primary reaction products in a condensation polymerization. The primary products do not accumulate. Therefore, it was concluded that the primary oxidation is the rate determining step and the polymerization reaction is much more rapid.

Catalyst Studies

Catalyst studies indicated that the type of metal affects both the primary rate and the condensation step. For the primary reaction, the order observed was

$$Fe > Al > Pb > Cu$$

The order for the condensation reaction was a little different:

$$Fe > Al > Cu > Pb$$

Qualitative analysis indicated that four characteristic chemical groups were identified in all oxidation products (primary and secondary) from esters and the mineral oil. These were hydroxyl (-OH), carbonyl (C=O), alkenes (C=C), and conjugated dienes (C=C-C=O).

More recent work (ref. 22) with the microreactor indicates that oxygen is definitely required to induce the polymerization reaction with esters. This work also showed that, while low carbon steel and stainless steel catalyze oxidation, lead, zinc, tin, and copper act as inhibitors. AA analysis indicates that the concentration of dissolved metal in a lubricant does not follow the order of catalytic activity. Low concentrations of iron are active promoters while high concentrations of lead are inhibitors.

Polyphenyl Ethers

The polyphenyl ether fluids have been studied (refs. 87 and 88) as possible high-tempeature lubricants for many years. They are thermally stable to approximately 450° C and oxidatively stable to approximately 275° C. Their problems have generally been related to poor low-temperature properties and poor boundary lubricating ability.

Most of the mechanisms of oxidation degradation of these fluids were performed in the early 60's (refs. 55 and 89). At 288° C and above these fluids begin to consume oxygen (after an induction period). These were bulk oxidation tests using a Dornte type apparatus. As oxidation proceeds, the fluid turns black and there is a linear increase in viscosity with increasing oxygen consumption. In addition, EPR spectra indicated the presence of a stable free radical in the oxidized product. In contrast to the previously discussed autoxidation mechanisms of aliphatic hydrocarbons, the initiation step appears to be an attack by molecular oxygen at the phenyl-oxygen-phenyl carbons rather than C-H positions. Symmetrical and unsymmetrical cleavage and dehydrogenation reactions occur to yield phenoxy and substituted phenoxy radicals. Propagation occurs when these radicals attack the parent molecule at the C-O-C carbons producing more phenoxy radicals and with cleavage to form a higher molecular weight product (containing some C-C bridges).

Because of the inherent stability of these fluids, conventional anti-oxidants (such as amines and phenols) are not useful. This is related to the volatility or thermal instability of these additives. However, some additives are effective above 260° C. These include aromatic tin compounds such as tetraphenyl tin (ref. 90), certain other organometallic compounds (ref. 89), and cuprous and cupric oxides (refs. 90 and 91). Continuation of this work (refs. 92 and 93) has shown that soluble alkali or alkaline earth metal phenoxides are also effective inhibitors to 370° C. In addition, oxides, hydroxides, and carbonates of alkali metals and barium are very effective inhibitors to approximately 370° C. A proposed mechanism was the destruction of peroxy radicals by a superoxide formation. In fact, oxidation-corrosion tests (ref. 94) showed that the presence of a variety of metal coupons reduced the oxidation of a polyphenyl ether (measured by viscosity increase). Lead and copper seemed to be the most effective. This is in agreement with the

434

findings of Klaus, et al. (ref. 22), that were discussed previously in the Esters section.

C-Ethers

Another class of fluids, C-ethers or thio-ethers, are structurally similar to the polyphenyl ethers (ref. 95). These fluids have certain advantages over the polyphenyl ethers such as lower pour points and better boundary lubricating performance (ref. 96). However, their inherent thermal stability is somewhat lower (approximately 390° C), and oxidation stability (bulk tests) is about 260° C. However, as with the polyphenyl ethers, these fluids do produce large quantities of a high molecular weight sludge under lubricating conditions (ref. 97).

Macrooxidation-corrosion tests of formulated C-ethers indicated deposit formation was a problem with these fluids (ref. 54). Two C-ether formulations were studied by Jones and Morales (ref. 56) at 353° C using a microreactor. Degradation products were analyzed by gel permeation chromatography. M-50 steel and silver were used as catalysts. In general, both catalyzed C-ether decomposition to about the same extent. This is in contrast to the data reported in reference 54, where silver produced 2 to 5 times the amount of high molecular weight products as M-50 under similar test conditions. In addition, there was little difference between air and nitrogen atmosphere tests based on high MW product formation.

Several discrete peaks of higher MW were seen on many of the chromatograms. Peaks appeared at about 450, 600, 700, and 800 as well as a broad peak centered at 2400. It would appear that coupling reactions resulting in a series of higher MW oligomers basically differing in MW by the addition of another phenyl-sulfur species. A process similar to that described for the polyphenyl eithers could be operating here.

Perfluoroalkylethers

Perfluoroalkylethers are a class of fluids which exhibit excellent thermal and oxidative stability (refs. 98 and 99). Combined with good viscosity characteristics (ref. 46), good elastohydrodynamic film forming capabilities (ref. 100), good boundary lubricating ability (refs. 46 and 49), and non-flammability properties (ref. 51) make these fluids promising candidates for high-temperature lubricant applications.

Basically, there are two types of perfluoroalkylethers, an unbranched and a branched class. The general structures of these classes are as follows:

Hexafluoropropylene oxide (HFPO) based fluids:

$$C_3F_7O(\underset{\underset{CF_3}{|}}{CF}CF_2O)_nR_f$$

Unbranched perfluoroalkylether fluids:

$$R_fO(CF_2CF_2O)_m(CF_2O)_nR_f$$
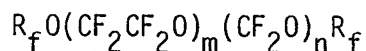
where $R_f = CF_3$ or C_2F_5. The most important representatives of the branched materials are based on the polymerization of hexafluoropropylene oxide (HFPO).

Branched perfluoroalkylethers. - Initial thermal and oxidative stability tests on the branched class were performed on very pure highly characterized materials (ref. 98). These early data indicated that these materials should be thermally stable to 410° C and that oxygen would not accelerate this degradation. However, tests performed on commercial samples never yielded this idealized stability. Thermal stability of about 390° C (ref. 49) and oxidation-corrosion stability to 260° C (ref. 46) in the presence of ferrous and titanium alloys were obtained. This was confirmed by Paciorek, et al. (ref. 47), in bulk oxidation-corrosion experiments.

In the early work by Gumprecht (ref. 101), pure (i.e., completely fluorinated) HFPO fluids theoretically yield mainly $CF_3CF=CF_2$, CF_3COF, and COF_2. Under oxidizing conditions Paciorek, et al. (ref. 47), did not observe any $CF_3CF=CF_2$. This may be due to the oxidation reaction

$$CF_3CF=CF_2 \xrightarrow{\text{O}} CF_3COF + COF_2 \tag{28}$$
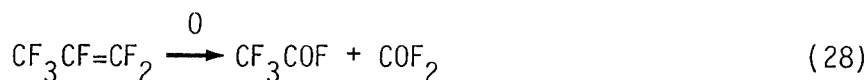
or more likely the unzipping reaction

$$-\!\!\!\bigwedge\!\!\!- \underset{\underset{CF_3}{|}}{CF}-CF_2O \ \underset{\underset{CF_3}{|}}{CF}-CF_2O\cdot \xrightarrow{\text{O}} CF_3COF + COF_2 \tag{29}$$
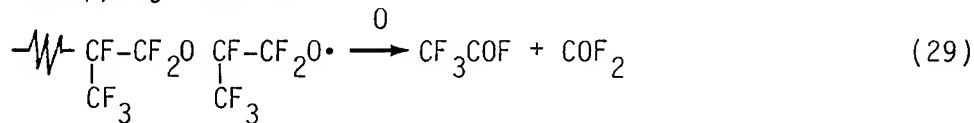
The major products isolated at test conclusion were SiF_4, CO_2, and BF_3. These are obviously due to reaction of the primary products with the glass surface of the oxidation-corrosion apparatus such as

$$2COF_2 + SiO_2 \rightarrow SiF_4 + 2CO_2 \tag{30}$$

Based on the rate of production of these volatile products, it was determined that the commercial HFPO fluids were oxidation stable to about 343° C in the absence of metal. The limited degradation at 343° C was thought to be due to oxidative instability of a weak link or end group. Since at test conclusion the residual fluid was essentially unchanged (i.e., same MW, viscosity, and IR spectra), it was deduced that a certain number of chains had to be hydrogen terminated. Indeed, pretreatment at 343° C with oxygen yielded a more stable fluid, presumably due to burning off the weak hydrogen terminated chains. Proton NMR eventually confirmed this theory. The as-received fluid shows the presence of CF_3CFHO- as a characteristic doublet at 5.9 ppm. After thermal-oxidative exposure at 343° C, these peaks completely disappear.

In the presence of metals and alloys at 316° C, such as Ti(4 Al, 4 Mn), Ti, and Al, degradation rate is increased (fig. 15) and is higher for the non-pretreated fluid. This would indicate that the metals are accelerating the degradation of weak links. However, successive measurements with the Ti(4 Al, 4 Mn) alloy at 288° C show a continual uptake of oxygen with time, indicating that another mechanism is operative. Analysis of the residual fluid indicated a drastic decrease in MW which would indicate that a chain scission process such as the following is likely:

436

$$\underset{\underset{CF_3}{|}}{-\text{W}-\underset{|}{CF}}\underset{\underset{CF_3}{|}}{CFO\underset{|}{CF}CF_2}-\text{W}- + MF_x \longrightarrow -\text{W}-\underset{\underset{CF_3}{|}}{CFCF}\underset{}{^\backprime O}(\underset{\underset{CF_3}{|}}{CFCF_2}O-\text{W}-$$

with

$$\begin{array}{c} F\diagdown\diagup F \\ F\cdots M \diagdown F \end{array}$$

$$\longrightarrow \quad \underset{\underset{CF_3}{|}}{-\text{W}-CFCOF} + C_2F_5CF_2O-\text{W}- + MF_x \qquad (31)$$

A   B
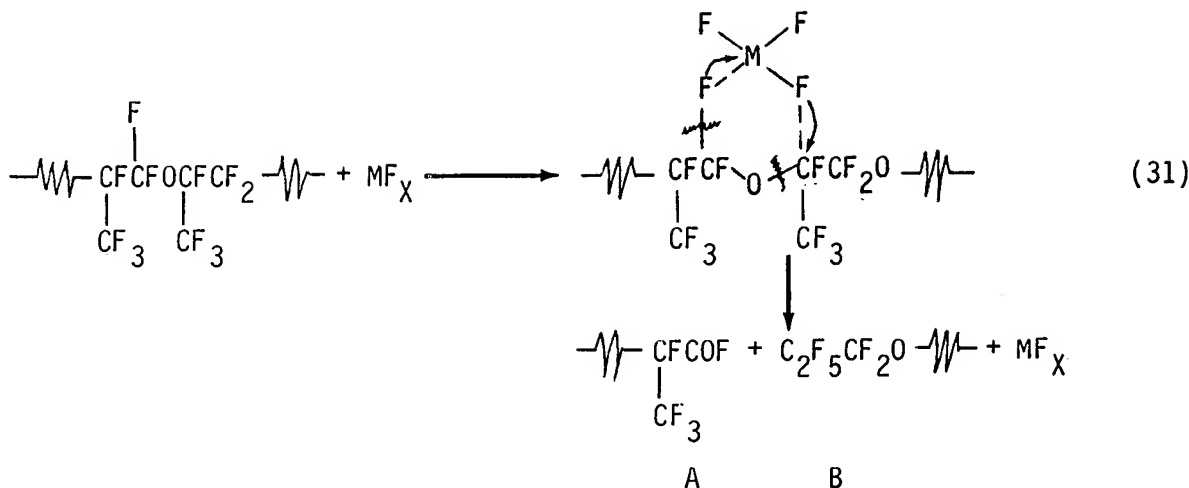
Fragment A can further degrade and B is just a lower MW telomer of the HFPO fluid.

It appears that metals and metal alloys promote degradation in HFPO fluids by a chain scission process. The HFPO fluids that have been thermally pretreated at 343° C in oxygen are stable to oxygen at this temperature. The pretreated fluid is not degraded by M-50 steel or Ti(4 Al, 4 Mn) alloys at 316° C. However, degradation does occur at 343° C with these alloys.

Unbranched perfluoroalkylethers. - A new class of perfluoroalkylethers based on the photooxidation of fluoro-olefins has been developed (ref. 102). This class of materials, whose general chemical structure is $R_fO(CF_2CF_2O)_m(CF_2O)_nR_f$ (where $R_f = CF_3$ or C_2F_2), has an unbranched structure. These fluids have better viscosity-temperature properties than the branched (HFPO) class (ref. 50). However, this unbranched fluid class has exhibited lower thermal-oxidative stability compared to the HFPO fluids (ref. 50). This is surprising since the chemical bonding in both classes is very similar. In fact, it has been shown (ref. 101) that tertiary carbon-fluorine bonds are less stable than those involving primary or secondary carbon atoms. This would lead one to conclude that the HFPO fluids (which contain tertiary carbon atoms) should be less stable than the unbranched fluids.

Recent work (ref. 52) has confirmed that the unbranched fluids are inherently unstable at 316° C in oxidizing atmospheres. This instability is not due to hydrogen chain termination or residual peroxide linkages. In the presence of M-50 steel or Ti(4 Al, 4 Mn) catalysts at 288° and 316° C in oxidizing atmospheres, the unbranched fluids exhibit much greater degradation than in uncatalyzed tests (fig. 16). However, these catalysts do not promote degradation at 316° C in inert (nitrogen) atmospheres.

In addition, catalyzed tests indicated that pure metals (Ti, Al) did not promote as much degradation as alloys (Ti(4 Al, 4 Mn)). Again, as with the HFPO fluids, the metals and alloys promoted degradation by a chain scission process.

GLOSSARY

Free radical	species having an unpaired electron but no charge
Homolysis	breaking of a diamagnetic molecule into two paramagnetic species

Autoxidation	oxidation of an organic compound with molecular oxygen in the absence of a flame
Catalyst	any substance that increases the rate of a chemical reaction
Initiator	substance that starts a free radical chain process
Oxidation	electron removal from a chemical species
Disproportionaton	transfer of an atom from one radical to another forming a saturated and an unsaturaged molecule
Lewis acid	species capable of accepting an electron pair

SYMBOLS

A	preexponential factor
AA	atomic absorption spectroscopy
Aro$\cdot$	phenoxyl radical
CL	chemiluminescence
DES	di-2-ethylhexyl sebacate
E	activation energy
E_{DIS}	bond dissociation energy
ESR	electron spin resonance spectroscopy
$HO_2\cdot$	hydroperoxy radical
In	initiator
IR	infrared spectroscopy
k	rate constant
k_p	rate of chain propagation
k_t	rate of chain termination
MW	molecular weight
NMR	nuclear magentic resonance spectroscopy
PETH	pentaerythrityl tetraheptanoate
PTZ	phenothiazine
R	gas constant
R-H	hydrocarbon
R_i	rate of chain initiation
R$\cdot$	alkyl free radical
RO$\cdot$	alkoxy radical
$RO_2\cdot$	peroxy radical

438

RO_2H	hydroperoxide
RO_4R	tetroxide
SEC	size exclusion chromatography
T	absolute temperature
T_D	thermal decomposition temperature
TCP	tricresyl phosphate
TMPTH	trimethyolpropane triheptanoate
UV	ultraviolet spectroscopy
X	inhibitor

REFERENCES

1. Bisson, E. E.; and Anderson, W. J.: Advanced Bearing Technology. NASA SP-38, 1964.
2. Loomis, W. R.; Townsend, D. P.; and Johnson, R. L.: Lubricants for Inerted Lubrication Systems in Engines for Advanced Aircraft. NASA TN D-5420, Sept. 1969.
3. Parker, R. J.; Bamberger, E. N.; and Zaretsky, E. V.: Bearing Torque and Fatigue Life Studies with Several Lubricants for Use in the Range 500° to 700° F. NASA TN D-3948, May 1967.
4. Zaretsky, E. V.; and Ludwig, L. P.: Advancements in Bearings, Seals, and Lubricants. Aircraft Propulsion, NASA SP-259, 1971, pp. 421-463.
5. Sliney, H. E.: Bearings, Lubricants, and Seals for the Space Shuttle. Space Transportation System Technology Symposium, Vol. III - Structures and Materials, NASA TM X-52876, 1970, pp. 289-296.
6. Bucknell, R. L.: Influence of Fuels and Lubricants on Turbine Engine Design and Performance. Vol. II - Fuel and Lubricant Analyses. PWA-FR-5673, AFAPL-TR-73-52-VOL-2, Pratt and Whitney Aircraft, 1973. (AD-769309.)
7. Lansdown, A. R.: Liquid Lubricants - Functions and Requirements. Interdisciplinary Approach to Liquid Lubricant Technology, P. M. Ku, ed., NASA SP-318, 1973, pp. 1-55.
8. Russell, T. E.; and Mattes, R. E.: A Study of High Temperature Fuels and Lubricants on Supersonic Aircraft/Engine System Performance. SAE Paper 740473, Apr. 1974.
9. Kochi, J. K., ed.: Free Radicals. Vol. I, Wiley, 1973.
10. Back, M. H.: Pyrolysis of Hydrocarbons. The Mechanisms of Pyrolysis, Oxidation, and Burning of Organic Materials, L. A. Wall, ed., NBS SP-357, 1972, pp. 17-31.
11. Layokun, S. K.; and Slater, D. H.: Mechanism and Kinetics of Propane Pyrolysis. Ind. Eng. Chem. Process. Des. Dev., vol. 18, no. 2, 1979, pp. 232-236.
12. Blake, Edward S.; et al.: Thermal Stability as a Function of Chemical Structure. J. Chem. Eng. Data, vol. 6, no. 1, Jan. 1961, pp. 87-98.
13. Vapor Pressure-Temperature Relationship and Initial Decomposition Temperature of Liquids by Isoteniscope. Am. Soc. Test. Mater. Stand. D-2879-75, Part No. 24, 1980.

14. Fowler, L.; and Trump, W. N.: A Recording Tensimeter and Decomposition Temperature Detector. Analysis Instrumentation, Vol. 7. B. Connelly, L. Fowler, and R. Krueger, eds., ISA, 1969, pp. 141-144.

15. Jones, W. R., Jr.; and Hady, W. F.: Boundary Lubrication and Thermal Stability Studies with Five Liquid Lubricants in Nitrogen to 400° C. NASA TN D-6251, Mar. 1971.

16. Beerbower, A.: Environmental Capability of Liquid Lubricants. Interdisciplinary Approach to Liquid Lubricant Technology, P. M. Ku, ed., NASA SP-318, 1973, pp. 365-431.

17. Jones, W. R., Jr.: Friction, Wear, and Thermal Stability Studies of Some Organotin and Organosilicon Compounds. NASA TN D-7175, Mar. 1973.

18. Richardson, G. A.; and Blake, E. S.: Partially Fluorinated Polyaromatic Ethers: Synthesis, Thermal Stability, and Other Physical Properties. USAF Aerospace Fluids and Lubricants Conf., P. M. Ku, ed., Southwest Research Inst., 1963, pp. 130-139.

19. Gunderson, R. C.; and Hart, A. W.: Synthetic Lubricants. Reinhold Publ. Corp., 1962.

20. Klaus, E. E.; and Perez, J. M.: Thermal Stability Characteristics of Some Mineral Oil and Hydrocarbon Hydraulic Fluids and Lubricants. ASLE Trans., vol. 10, 1967, pp. 38-47.

21. Van Krevelen, D. W.: Properties of Polymers, Their Estimation and Correlation with Chemical Structure. Second ed., Elsevier Scientific Publ. Co. (Amsterdam), 1976.

22. Ugwuzor, D. I. K. A.: The Effects of Metals on High Temperature Degradation of Ester-Type Lubricants. M.S. Thesis, The Pennsylvania State University, Nov. 1982.

23. Backstrom, H. L. J.: The Chain-Reaction Theory of Negative Catalysis. J. Am. Chem. Soc., vol. 49, no. 6, June 1927, pp. 1460-1472.

24. Criegee, R.; Pilz, H.; and Flygare, H.: Olefin Peroxides. Chem. Ber., vol. 72B, 1939, pp. 1799-1804.

25. Emanuel, N. M.; Denisov, E. T.; and Maizus, Z. K. (B. J. Hazzard, Transl.): Liquid Phase Oxidation of Hydrocarbons. Plenum, 1967.

26. Dukek, W. G.: Fuels and Lubricants for the Next Generation Aircraft – the Supersonic Transport. J. Inst. Pet. London, vol. 50, no. 491, 1964, pp. 273-296.

27. Booser, E. R.: Liquid-Phase Oxidation of Pure Hydrocarbons. Ph.D. Thesis, The Pennsylvania State University, 1968.

28. Czarnecki, J. R.: High Temperature Degradation of Some Organic Esters. M.S. Thesis, The Pennsylvania State University, Sept. 1971.

29. Ali, A. R.: Characterization of Liquid Phase Oxidation Products. M.S. Thesis, The Pennsylvania State University, 1975.

30. Cvitkovic, E.: Reaction Rate Studies on Ester Oxidation. M.S. Thesis, The Pennsylvania State University, May 1976.

31. Lahijani, J.: Effects of Metals on Oxidation Rates and Products from Esters. M.S. Thesis, The Pennsylvania State University, 1977.

32. Lockwood, F. E.: Ester Oxidation Under Simulated Boundary Lubrication Conditions. Ph.D. Thesis, The Pennsylvania State University, 1978.

33. Korcek, S.; and Jensen, R. K.: Relation Between Base Oil Composition and Oxidation Stability at Increased Temperatures. ASLE Trans., vol. 19, no. 2, 1976, pp. 83-94.

34. Jensen, R. K.; et al.: Liquid-Phase Autoxidation of Organic Compounds at Elevated Temperatures. 1. The Stirred Flow Reactor Technique and Analysis of Primary Products from n-Hexadecane Autoxidation at 120°-180° C. J. Am. Chem. Soc., vol. 101, no. 25, Dec. 1979, pp. 7574-7584.

35. Jensen, R. K., et al.: Liquid-Phase Autoxidation of Ogranic Compounds at Elevated Temperatures. 2. Kinetics and Mechanism of the Formation of Clevage Products in n-Hexadecane Autoxidation. J. Am. Chem. Soc., vol. 103, no. 7, Apr. 1981, pp. 1742-1749.

36. Hamilton, E. J.; et al.: Kinetics and Mechanism of the Autoxidation of Pentaerythrityl Tetraheptanoate at 180°-220° C. Int. J. Chem. Kinet., vol. 12, no. 9, 1980, pp. 577-603.

37. Mahoney, L. R.; et al.: Effects of Structure on the Thermoxidative Stability of Synthetic Ester Lubricants: Theory and Predictive Method Development. Presented at the Div. of Petrol. Chem., Amer. Chem. Soc. (Las Vegas, Nev.), Mar. 28 - Apr. 2, 1982.

38. Boss, B. D.; and Hazlett, R. N.: Oxidation of Hydrocarbons in the Liquid Phase - n-Dodecane in a Borosilicate Glass Chamber at 200° C. Can. J. Chem. vol. 47, 1969, pp. 4175-4182.

39. Mill, T.; et al.: Gas and Liquid-Phase Oxidation of n-Butane. J. Am. Chem. Soc., vol. 94, no. 19, Sept. 1972, pp. 6802-6811.

40. Van Sickle, D. E.; et al.: Intramolecular Propagation in the Oxidation of n-Alkanes, Autoxidation of n-Pentane and n-Octane. J. Org. Chem., vol. 38, no. 26, 1973, p. 4435.

41. Brown, D. M.; and Fish, A.: The Extension to Long-Chain Alkanes and to High Temperatures of the Hydroperoxide Chain Mechanism of Autoxidation. Proc. R. Soc. London Ser. A, vol. 308, no. 1495, Jan. 1969, pp. 547-568.

42. Sniegoski, P. J.: Selectivity of the Oxidative Attack on a Model Ester Lubricant. ASLE Trans., vol. 20, no. 4, 1977, pp. 282-286.

43. Betts, J.: Kinetics of Hydrocarbon Autoxidation in the Liquid Phase. Quart. Rev. Chem. Soc., vol. 25, no. 2, 1971, pp. 265-288.

44. George, P.; Rideal, E. K.; and Robertson, A.: Oxidation of Liquid Hydrocarbons. Proc. R. Soc. London, vol. 185, no. 1002, Mar. 1946, pp. 288-351.

45. Morton, F.; and Bell, R. T. T.: Low-Temperature, Liquid-Phase Oxidation of Hydrocarbons. J. Inst. Pet. London, vol. 44, 1958, pp. 260-272.

46. Snyder, C. E., Jr.; and Dolle, R. E., Jr.: Development of Polyper-fluroalkylethers as High Temperature Lubricants and Hydraulic Fluids. ASLE Trans., vol. 19, 1976, pp. 171-180.

47. Paciorek, K. J. L.; et al.: Thermal Oxidative Studies of Poly (Hexafluoropropene Oxide) Fluids. J. Appl. Polym. Sci., vol. 24, no. 6, 1979, pp. 1397-1411.

48. Snyder, C. E., Jr.; et al.: Synthesis and Development of Improved High-Temperature Additives for Perfluoroalkylether Lubricants and Hydraulic Fluid. Lubr. Eng., vol. 35, no. 8, Aug. 1979, pp. 451-456.

49. Jones, W. R., Jr.; and Snyder, C. E., Jr.: Boundary Lubrication, Thermal and Oxidative Stability of a Fluorinated Polyether and a Perfluoro-polyether Triazine. ASLE Trans., vol. 23, no. 3, July 1980, pp. 253-261.

50. Snyder, C. E., Jr.; Gschwender, L. J.; and Tamborski, C.: Linear Polyperfluoroalkylether-Based Wide-Liquid-Range High-Temperature Fluids and Lubricants. Lubr. Eng., vol. 37, no. 6, June 1981, pp. 344-349.

51. Snyder, C. E., Jr.; Gschwender, L. J.; and Cambell, W. B.: Development and Mechanical Evaluation of Nonflammable Aerospace (-54° C to 135° C) Hydraulic Fluids. Lubr. Eng., vol. 38, no. 1, Jan. 1982, pp. 41-51.

52. Jones, W. R., Jr.; et al.: Thermal Oxidative Degradation Reactions of Linear Perfluoroalkylethers. NASA TM-82834, Apr. 1982.

53. Jones, W. R., Jr.; et al.: Metals and Inhibitors Effects on Thermal Oxidative Degredation Reactions of Perfluoroalkylethers. Presented at the Sixth Winter Symposium on Fluorine Chemistry (Daytona Beach, Fla.), Feb. 6-11, 1983.

441

54. Clark, F. S.; and Miller, D. R.: Formulation and Evaluation of C-Ether Fluids as Lubricants Useful to 260° C. (MRC-SL-1007, Monsanto Research Corp.; NASA Contract NAS3-19746.) NASA CR-159794, Dec. 1980.

55. Wilson, G. R.; Smith, J. O.; and Stemniski, Jr.: Mechanism of Oxidation of Polyphenyl Ethers. ML TDR-64-98, Wright-Patterson AFB, Dec. 1963 (Available as AD-457120).

56. Jones, W. R., Jr.; and Morales, W.: Thermal and Oxidative Degradation Studies of Formulated C-Ethers by Gel-Permeation Chromatography. NASA TP-1994, Mar. 1982.

57. Sheldon, R. A.; and Kochi, J. K.: Metal-Catalyzed Oxidations of Organic Compounds. Academic Press, 1981.

58. Emanuel, N. M.: 80's in the Field of Liquid Phase Oxidation of Organic Compounds. Oxidation Communications, vol. 2, no. 3-4, 1982, pp. 221-238.

59. Korcek, S.; et al.: Absolute Rate Constants For Hydrocarbon Autoxidation XXI. Activation Energies for Propagation and the Correlation of Propagation Rate Constants with Carbon-Hydrogen Bond Strengths. Can. J. Chem., vol. 50, 1972, pp. 2285-2297.

60. Howard, J. A.: Absolute Rate Constants for Reactions of Oxyl Radicals. Advances in Free-Radical Chemistry, G. H. Williams, ed., Academic Press, 1972, pp. 49-165.

61. Bennett, J. E.; Brown, D. M.; and Mile, B.: Electron Spin Resonance of the Reactions of Alkylperoxy Radicals. I. Absolute Rate Constants for the Termination Reactions of Alkylperoxy Radicals. Trans. Faraday Soc., vol. 66, no. 2, 1970, pp. 386-396.

62. Dornte, R. W.: Oxidation of White Oils. Ind. Eng. Chem., vol. 28, Jan. 1936, pp. 26-30.

63. Bolland, J. L.: Kinetic Studies in the Chemistry of Rubber and Related Materials. I. The Thermal Oxidation of Ethyl Linoleate. Proc. R. Soc. London, vol. 186A, no. 1005, July 1946, pp. 218-236.

64. Diamond, H.; Kennedy, H. C.; Larsen, R. G.: Oxidation Characteristics of Lubricating Oils at High Temperature. Ind. Eng. Chem., vol. 44, 1952, pp. 1834-1843.

65. Brook, J. H. T.: A Circulatory (Oil) Oxidation Test. J. Inst. Pet. London, vol. 48, 1962, pp. 7-12.

66. Hepplewhite, H. L.; and Oberright, E. A.: Thin Film Oxidation Test of Lubricants for Gas Turbine Engines. Proc. USAF Aerospace Fluids and Lubricants Conf., P. M. Ku, ed., Southwest Research Inst., 1963, pp. 62-69.

67. Cvitkovic, E.; Klaus, E. E.; and Lockwood, F.: A Thin-Film Test For Measurement of the Oxidation and Evaporation of Ester-Type Lubricants. ASLE Trans., vol. 22, no. 4, 1979, pp. 395-401.

68. Jones, W. R., Jr.; and Morales, W.: Analysis of a MIL-L-27502 Lubricant From a Gas-Turbine Engine Test by Size-Exclusion Chromatography. NASA TP-2063, 1983.

69. Klaus, E. E.; Naidu, S. K.; Berthold, V.; and Duda, J. L.: Stability Studies of Organic Acid Ester Lubricants. NASA CR In Process.

70. Denbigh, K. G.: Velocity and Yield in Continuous-Reaction Systems. Trans. Faraday Soc., vol. 40, 1944, pp. 352-373.

71. Mahoney, L. R.; et al.: Time-Temperature Studies of High Temperature Deterioration Phenomena in Lubricant Systems: Synthetic Ester Lubricants. AFOSR TR-80-0065, Ford Motor Co., 1979. (AD-A080135.)

72. Ravner, H.; and Wohltjen, H.: The Determination of the Oxidative Stability of Several Deuterated Lubricants by an Electronic Gas Sensor. ASLE Preprint 82-AM-5A-4, May 1982.

73. Morales, W.: Use of High Pressure Liquid Chromatography in the Study of Liquid Lubricant Oxidation. NASA TM-83033, Oct. 1982.

74. Silverstein, R. M.; Bassler, G. C.; and Morrill, T. C.: Spectrometric Identification of Organic Compounds. John Wiley and Sons, 1963.

75. Assenheim, H. M.: Introduction to Electron Spin Resonance. Hilger and Watts, LTD (London), 1966.

76. Perry, J. A.: Introduction to Analytical Gas Chromatography. Marcel Dekker, Inc., 1981.

77. Harvey, E. N.: Bioluminescence, Academic Press, 1952.

78. Vassil'ev, R. F.: Chemiluminescence in Liquid-Phase Reactions. Progress in Reaction Kinetics, vol. 4, G. Porter, ed., Pergamon Press, 1967, pp. 305-352.

79. Slawinski, J.: The Use of Chemiluminescence for Investigation of the Kinetics of the Oxidation fo Hydrocarbons in the Liquid Phase. Int. Chem. Engr., vol. 6, no. 1, Jan. 1966, pp. 160-162.

80. Lloyd, R. A.: Low Level Chemiluminescence from Hydrocarbon Autoxidation Reactions. Part I. Apparatus for Studying Thermal Decomposition Reactions and Observations on Benzoyl Peroxide in De-oxygenated Benzene. Trans. Faraday Soc., vol. 61, no. 514, 1965, pp. 2173-2181.

81. Lloyd, R. A.: Thermal Decomposition of Benzoyl Peroxide, Cumene Hydroperoxide, and UV Irradiated Solvents. Part II. Low Level Chemiluminescence From Hydrocarbon Auto-oxidation Reactions. Trans. Faraday Soc., vol. 61, no. 514, 1965, pp. 2182-2193.

82. Hercules, D. M.: Physical Basis of Chemiluminescence. The Current Status of Liquid Scintillation Counting, E. D. Bransome, ed., Grune and Stratton, 1970, pp. 315-336.

83. Clark, D. B.; Weeks, S. J.; and Hsu, S. M.: Chemiluminescence of Fuels and Lubricants - A Critical Review. ASLE Preprint 82-AM-5A-1, May 1982.

84. Larsen, R. G.; Thorpe, R. E.; and Armfield, F. A.: Oxidation Characteristics of Pure Hydrocarbons. Ind. Eng. Chem., vol. 34, no. 2, Feb. 1942, pp. 183-193.

85. Ali, A.; et al.: The Chemical Degradation of Ester Lubricants. ASLE Trans., vol. 22, no. 3, July 1979, pp. 267-276.

86. Lockwood, F.; and Klaus, E. E.: Ester Oxidation - The Effect of an Iron Surface. ASLE Trans., vol. 25, no. 2, 1982, pp. 236-244.

87. Mahoney, C. L.; et al.: Meta-Linked Polyphenyl Ethers as High-Temperature Radiation-Resistant Lubricants. ASLE Trans., vol. 3, no. 1, Apr. 1960, pp. 83-92.

88. Jones, W. R., Jr.; Hady, W. F.; and Swikert, M. A.: Lubrication With Some Polyphenyl Ethers and Superrefined Mineral Oils in a 600° F (316° C) Inerted Vane Pump Loop. NASA TN D-5096, 1969.

89. Archer, W. L.; and Bozer, K. B.: Oxidative Degradation of the Polyphenyl Ethers. Ind. Eng. Chem. Prod. Res. Develop., vol. 5, no. 2, June 1966, pp. 145-149.

90. Smith, J. O.; et al.: Research on High Temperature Additives for Lubricants. WADC-TR-59-191, Part IV, Feb. 1962. (Available as AD 281831.)

91. Ravner, H.; Russ, E. R.; and Timmons, C. O.: Antioxidant Action of Metals and Metal-Organic Salts on Fluoresters and Polyphenyl Ethers. J. Chem. Eng. Data, vol. 8, no. 4, Oct. 1963, pp. 591-596.

92. Ravner, H.; Moniz, W. B.; and Blachly, C. H.: High Temperture Stabilization of Polyphenyl Ethers by Inorganic Salts. ASLE Trans., vol. 15, no. 1, 1972, pp. 45-53.

93. Ravner, H.; and Kaufman, S.: High-Temperature Stabilization of Polyphenyl Ethers by Soluble Metal-Organic Salts. ASLE Trans., vol. 18, no. 1, 1975, pp. 1-4.

94. Stemniski, J. R.; et al.: Antioxidants for High-Temperature Lubricants. ASLE Trans., vol. 7, 1964, pp. 43-54.

95. McHugh, K. L.; and Stark, L. R.: Properties of a New Class of Polyaromatics for Use as High-Temperature Lubricants and Functional Fluids. ASLE Trans., vol. 9, no. 1, Jan. 1966, pp. 13-23.

96. Jones, W. R., Jr.: Boundary Lubrication of Formulated C-Ethers in Air to 300° C. Lubr. Eng., vol. 32, no. 10, 1976, pp. 530-538.

97. Jones, W. R., Jr.: The Effect of Oxygen Concentration on the Boundary-Lubricating Characteristics of a C-Ether and a Polyphenyl Ether to 300° C. Wear, vol. 73, 1981, pp. 123-136.

98. Gumprecht, W. H.: PR-143-A New Class of High Temperature Fluids. ASLE Trans., vol. 9, no. 1, Jan. 1966, pp. 24-30.

99. Sianesi, D.; et al.: Perfluoropolyethers - Their Physical Properties and Behavior at High and Low Temperatures. Wear, vol. 18, 1971, pp. 85-100.

100. Jones, W. R., Jr.; et al.: Pressure-Viscosity Measurements for Several Lubricants to 5.5×10^8 Newtons per Square Meter (8×10^4 psi) and 149° C (300° F). ASLE Trans., vol. 18, no. 4, 1975, pp. 249-262.

101. Gumprecht, W. H.: The Preparation and Thermal Behavior of Hexafluoropropylene Epoxide Polymers. Presented at the Fourth International Symposium on Fluorine Chemistry (Estes Park, Colorado), July 1967.

102. Sianesi, D.; et al.: Perfluoropolyethers by Photo-Oxidation of Fluoroolefins. Chim. Ind. (Milan), vol. 55, no 2, 1973, pp. 208-221.

TABLE I. – THERMAL DECOMPOSITION TEMPERATURES AND

BOND DISSOCIATION ENERGIES FOR VARIOUS COMPOUNDS

Compound	Bonds	E_{DIS}, kJ/mole (ref. 21)	T_D, °C
Octacosane	C–C	337	350
11-Ethyl-11-methyl pentacosane	C –C–C C	314	331
p-Quarterphenyl	$\phi-\phi$	432	454
Polyphenyl ether (5P-4E)	$\phi-O-\phi$	423	443
p-Bis(p-chlorophenoxy) benzene	$\phi-Cl$	419	409
p-Bis(p-bromophenoxy) benzene	$\phi-Br$	335	387
Fluorinated polyether	CF_3-CF_3	406	390
Synthetic paraffin	C–C	337	314
Alkylated benzene	$\phi-C-CH$	335	340

TABLE II. – OXIDIZABILITY OF VARIOUS ORGANIC COMPOUNDS[a]

Substrate	$k_p/(2k_t)^{1/2} \times 10^3 (mol^{-1/2}sec^{-1/2})$
2,3-Dimethyl-2-butene	3.2
Cyclohexene	2.3
1-Octene	.06
Cumene	1.5
Ethylbenzene	.21
Toluene	.01
p-Xylene	.05
Benzaldehyde	290
Benzyl alcohol	.85
2,4,6-Trimethylheptane	.09

[a]Ref. 60.

TABLE III. – X-H BOND ENERGIES[a]

Compound	Energy, (kcal mol^{-1})
CH_3-H	103
n-C_3H_7-H	99
i-C_3H_7-H	94
t-C_4H_9-H	90
CH_2=CH-H	105
C_6H_5-H	103
CH_2=CH-CH_2-H	85
$PhCH_2$-H	85
RCO-H	86
CH_3S-H	88
CH_3PH-H	85
PhO-H	88
PhNH-H	80
ROO-H	90

[a]Ref. 57.

TABLE IV. – RATE CONSTANTS PER LABILE HYDROGEN FOR
REACTION OF SUBSTRATES WITH THEIR OWN PEROXY
RADICALS (k_p) AND WITH tert- BUTYLPEROXY
RADICALS (k_p') at 30° C[a]

Substrate	k_p, ($mol^{-1}sec^{-1}$)	k_p', ($mol^{-1}sec^{-1}$)	k_p/k_p'
1-Octene	0.5	0.084	6.0
Cyclohexene	1.5	.80	1.9
Cyclopentene	1.7	.85	2.0
2,3-Dimethyl-2-butene	1.14	.14	1.0
Toluene	.08	.012	6.7
Ethylbenzene	.65	.10	6.5
Cumene	.18	.22	.9
Tetralin	1.6	.5	3.2
Benzyl ether	7.5	.3	25.0
Benzyl alcohol	2.4	.065	37.0
Benzyl acetate	2.3	.0075	307
Benzyl chloride	1.50	.008	190
Benzyl bromide	.6	.006	100
Benzyl cyanide	1.56	.01	156
Benzaldehyde	33,000	.85	40,000

[a]Ref. 57.

TABLE V. – EFFECTIVENESS OF INHIBITION

BY VARIOUS PHENOLS[a]

|	
Phenol	0.027
2-Methylphenol	.17
4-t-Butylphenol	.05
4-Methylphenol	.095
2-t-Butylphenol	.26
2,6-Dimethylphenol	.314
2,4-Di-t-butylphenol	.465
2,4,6-Tri-t-butylphenol	.47
2-Methyl-4-t-butylphenol	.515
2,6-Di-t-butyl-4-methylphenol	.65
2,4,6-Trimethylphenol	1.00
2,4-Di-t-butyl-6-methylphenol	1.05

[a]Ref. 25.
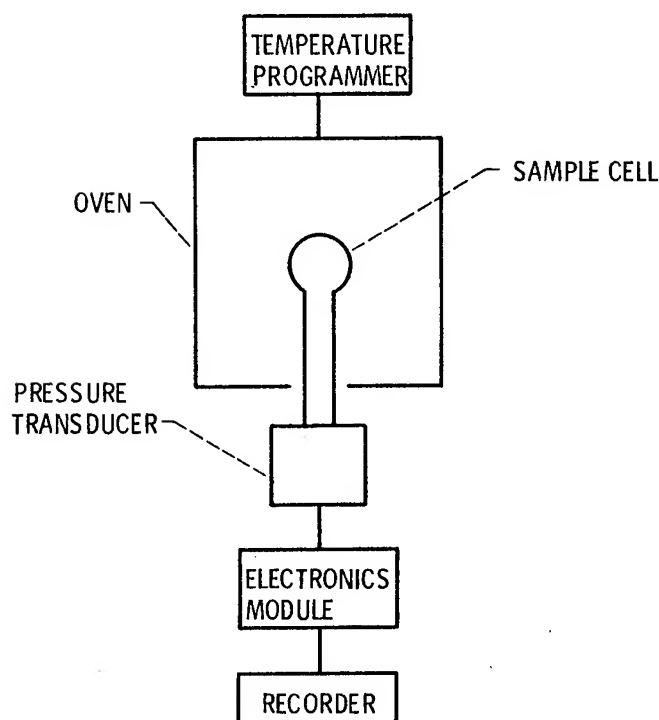
Figure 1. - Recording tensimeter.
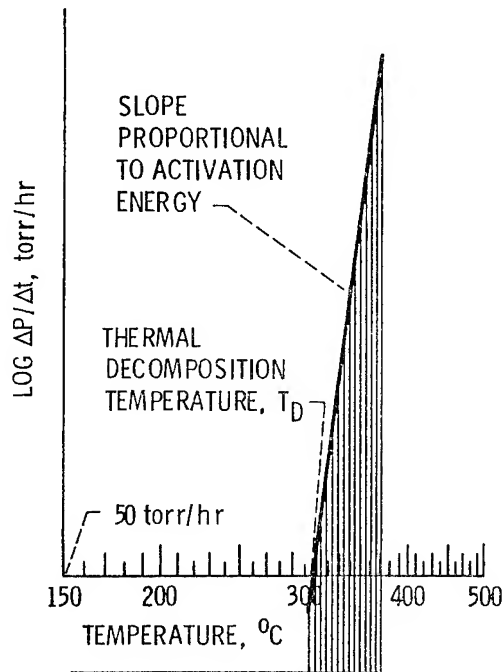
Figure 2. - Thermal decomposition curve
for synthetic hydrocarbon. Heating in-
terval, 5^0 C.
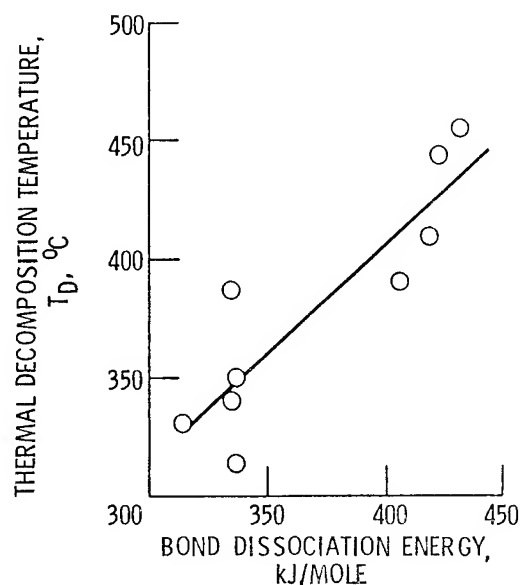
Figure 3. - Thermal decomposition
temperature (T_D) as function of
bond dissociation energy.
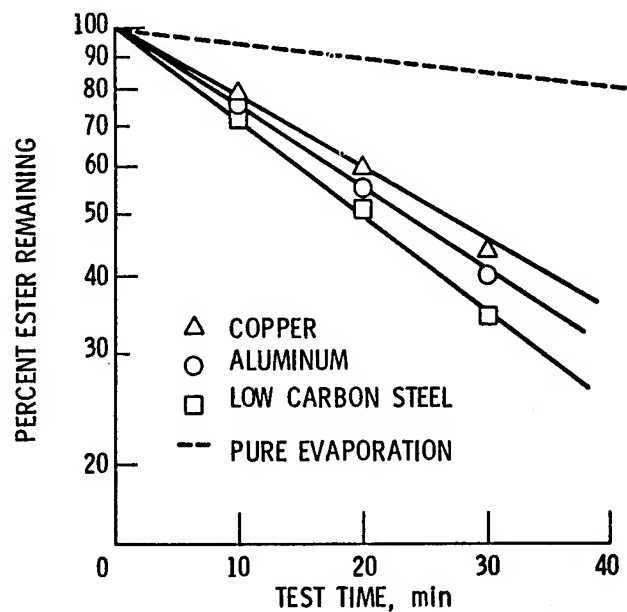
Figure 4. - Time-concentration relationship
of diethylhexyl sebacate in evaporation test
at 270° C in nitrogen atmosphere (ref. 22).
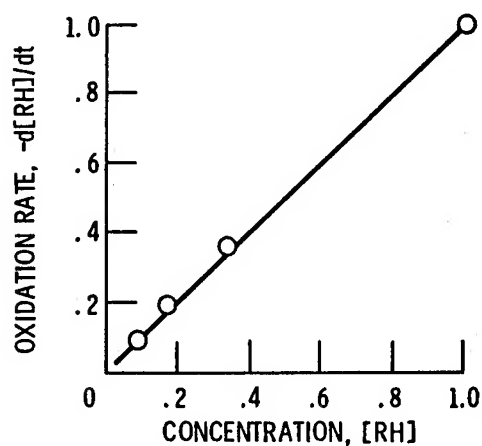
Figure 5. - Oxidation rate as func-
tion of concentration for ethyl
linoleate (ref. 25).

449
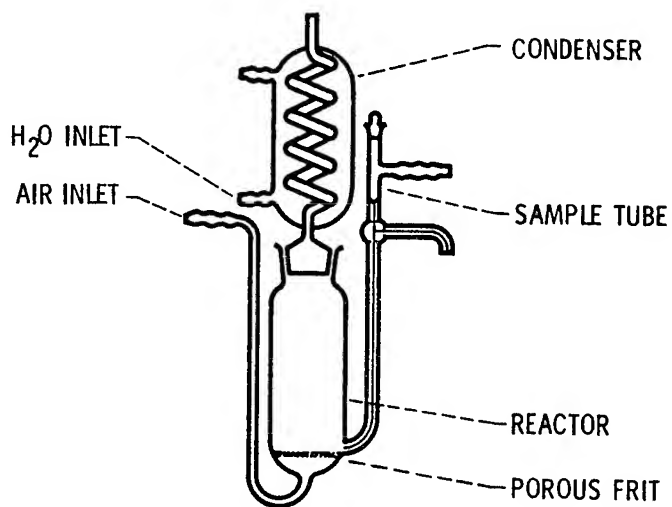
Figure 6. - Typical macrooxidation cell (ref. 25).
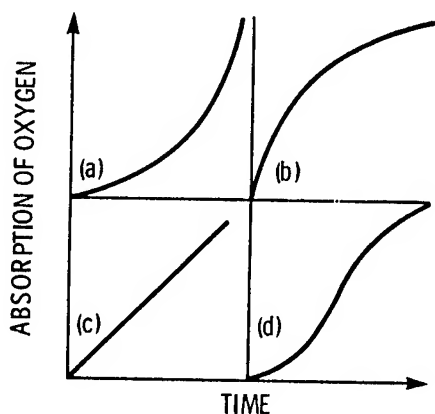
Figure 7. - Types of kinetic curves of the absorption of oxygen (ref. 25).

450
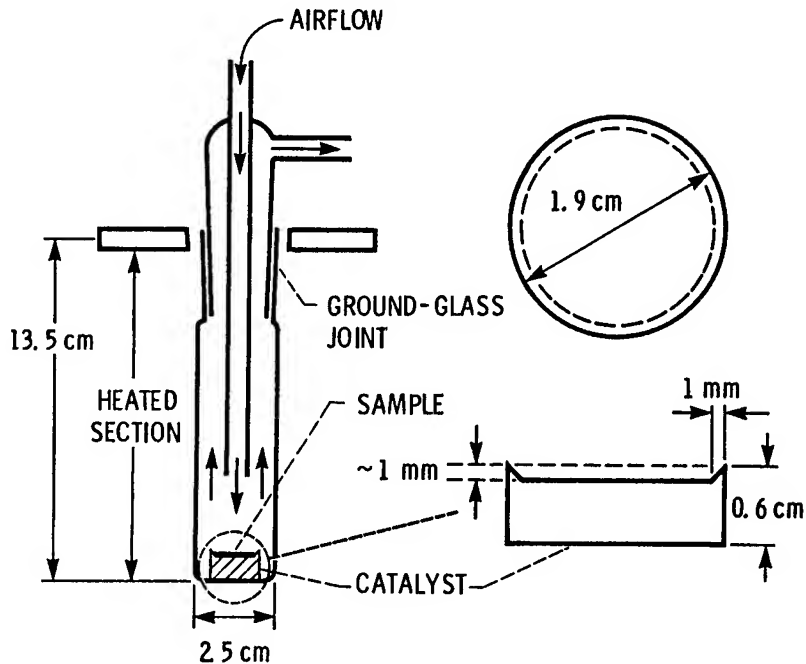
Figure 8. - Microoxidation apparatus (refs. 30 and 66).
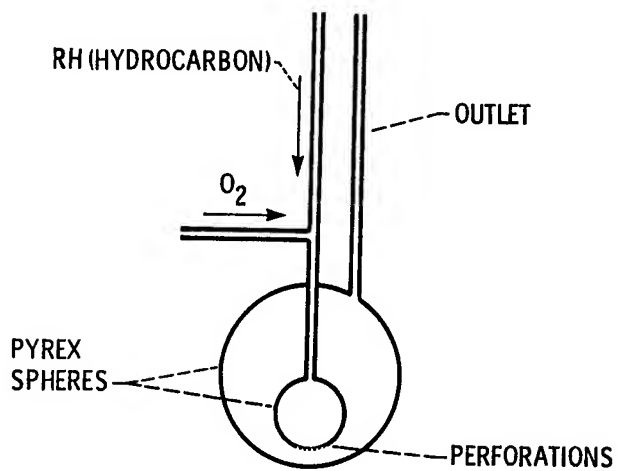
Figure 9. - Stirred flow microreactor (ref. 34).
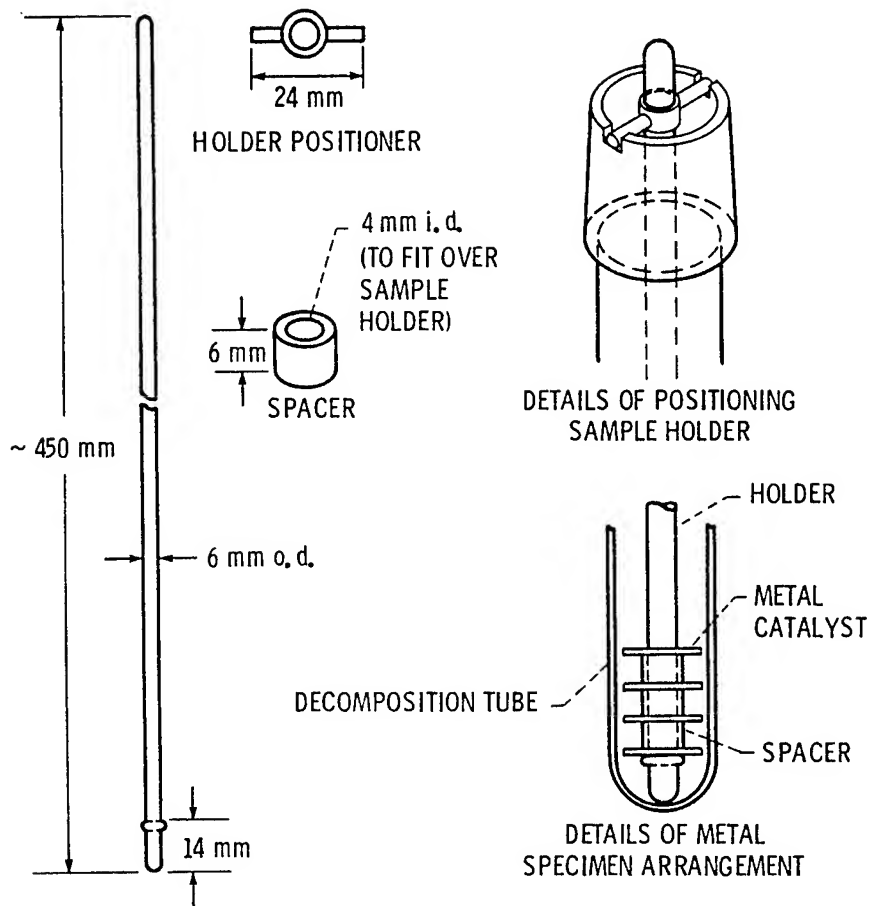
Figure 10. – Thermal oxidative decomposition tube.
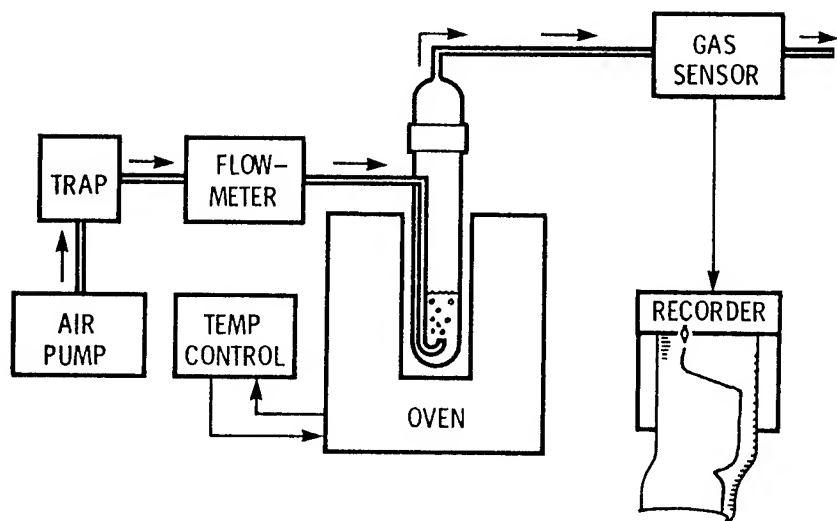
Figure 11. – Oxidative degradation apparatus using electronic gas sensor (ref. 72).
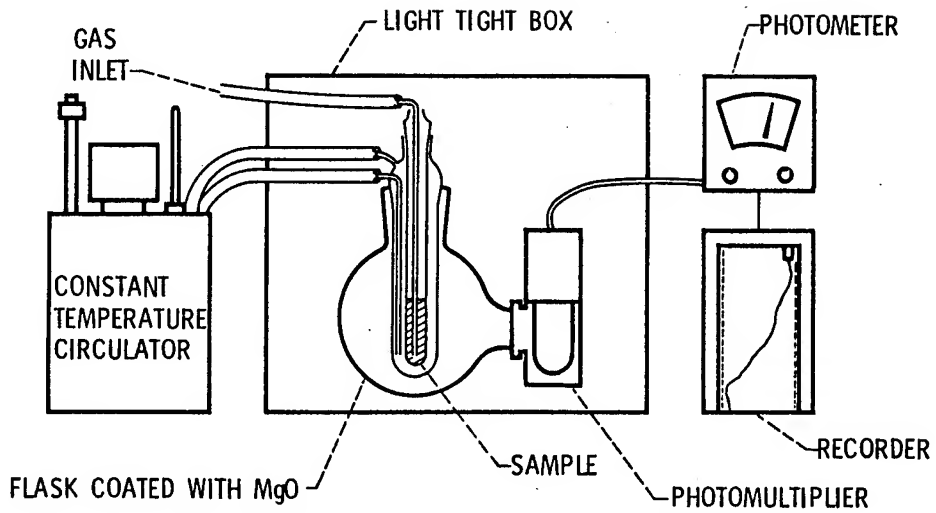
Figure 12. - Apparatus for chemiluminescence studies.
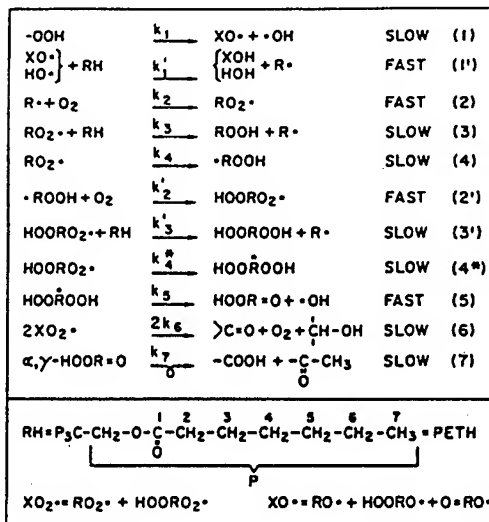
Figure 13. - Reaction scheme for autoxidation of PETH (ref. 36).
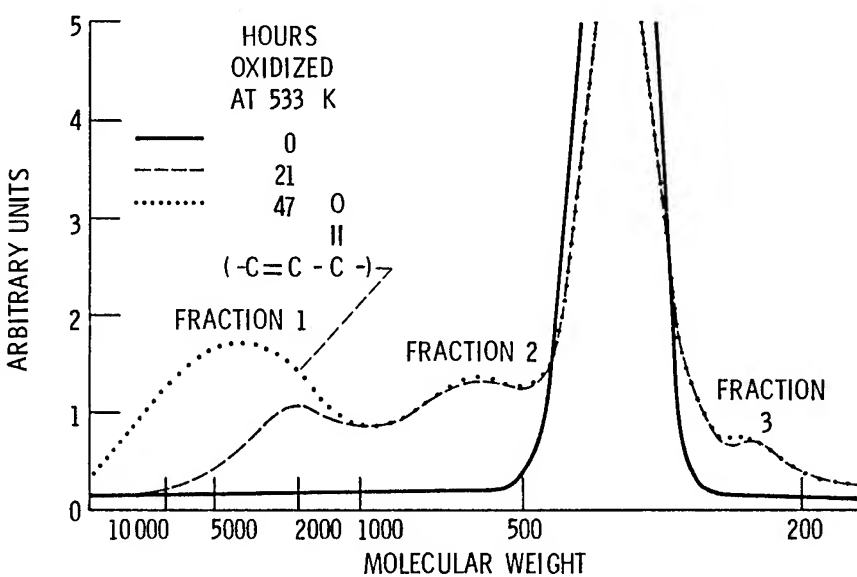
Figure 14. - Gel permeation chromatograms of oxidized di-2-ethyl-hexyl sebacate, no catalyst (ref. 85).
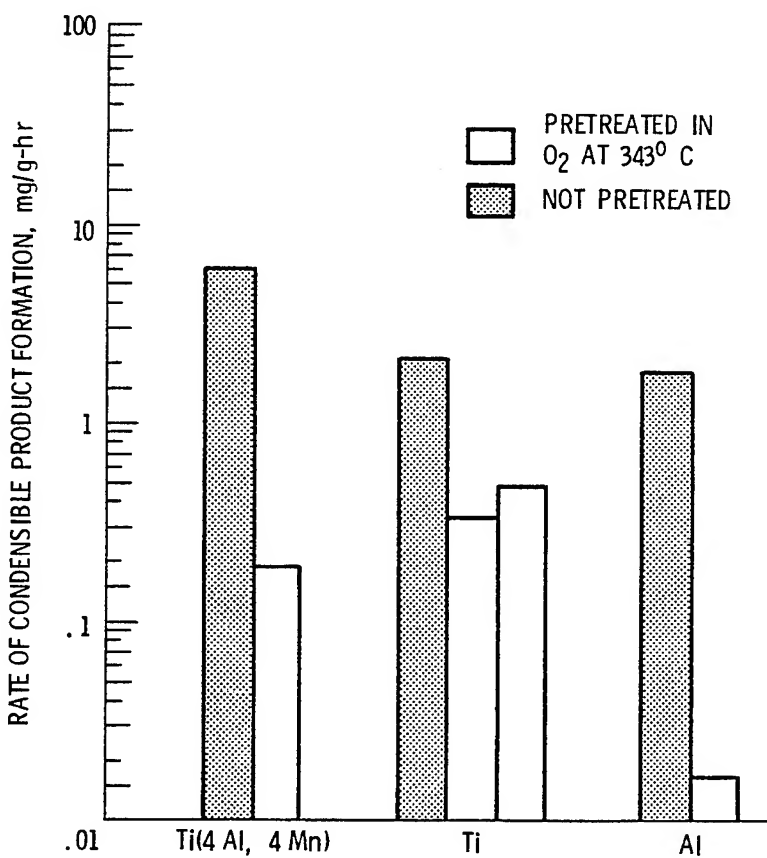
Figure 15. - Effect of metals on degradation of branched per-fluoroalkylether in oxygen at 316° C for 24 hours (ref. 53).
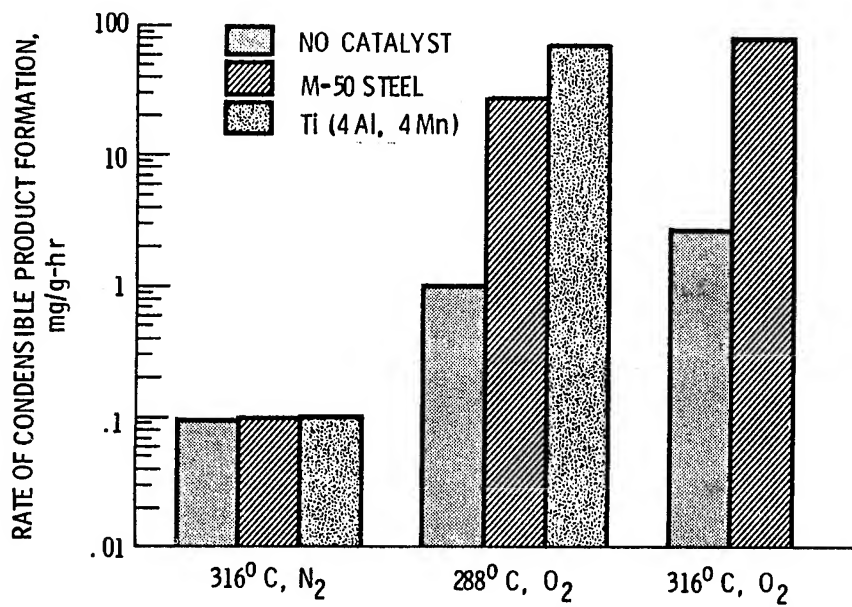
Figure 16. – Rates of condensible product formation for un-branched fluoroalkylether in presence of metal catalysts (ref. 52).

DISCUSSION

Robert N. Bolster
Department of the Navy
Naval Research Laboratory
Washington, D.C.

This paper is a good and comprehensive survey of the technology involved in the use of fluid lubricants at high temperatures. The differences between thermal and oxidative degradation and the mechanisms for both are well described. The effects of catalytic metals and oxidation inhibiting additives are also well covered. The information on oxidation testing and modern analytical techniques should be very helpful to researchers in this field. Petroleum and ester lubricants are covered in detail, and there is also information on some of the high-temperature fluids developed for aerospace applications.

More information on the conditions and problems encountered in service, and how they relate to laboratory results, would have been welcome. However, this was apparently beyond the already-considerable scope of the paper.

The author deserves our thanks for the preparation of this review and its extensive list of references.

DISCUSSION

Stephen M. Hsu
National Bureau of Standards
Washington, D.C.

The author presents a comprehensive survey and summary of the degradation mechanisms on a variety of liquid lubricants. The author describes experimental techniques, catalysis by metal surfaces, useful life prediction under oxidative and thermal conditions. The discussor agreees with the paper and commend the author for an excellent review and assessment.

Two topics need clarification: the distinction between thermal and oxidative stability, and the use of oxidation kinetic expressions to predict lubricant useful life.

In considering the thermal and oxidative stabilities of liquid lubricants, the author emphasizes the decomposition aspect of the degradation. This is true for the initial stage of the reaction sequence. As reaction proceeds, under thermal and oxidative conditions for complex hydrocarbons such as lubricants, an equally significant reaction pathway is to form high molecular weight products through condensation, polymerization, etc. This can be illustrated by a novel thermalgravimetric technique developed at the National Bureau of Standards (NBS). A lubricant is first tested for thermal stability in Argon atmosphere. A typical trace is shown in Figure 1. The same lubricant is then tested under identical conditions in oxygen atmosphere. The two thermograms are then normalized and super-imposed as shown in Figure 1. The weight loss curve in oxygen shows a much higher rate of decomposition due to oxygen. However, as reactions proceed, the oxidation curve crosses over the thermal degradation curve, showing slower rate of weight loss. This can be explained in terms of the formation of the high molecular weight products which have higher boiling points. The formation of the high molecular weight products is important as these products are generally believed to cause viscosity increase, acidity increase, varnish and sludge formations.

The author made a distinction between thermal and oxidative stability. The discussor agrees with the distinction in terms of mechanistic processes. In real systems, the two processes are difficult to distinguish. It is difficult to conceive an absolute oxygen free system. The discussor believes that whether a molecule undergoes oxidation via free radical mechanism or β-carbon scission depends on the microenvironment around the molecule. Reaction will always take place via the lowest energy requirement. From heats of formation data on chemical bonds, oxidation in general is energetically favored. For a particular molecule under oxidative and thermal stresses, if oxygen is readily available, oxidation will occur. If oxygen is not available, but sufficient kinetic energy is available, thermal decomposition will take place. The two processes therefore, usually complement each other in real systems and are difficult to separate one from another. Once sufficient free radicals are generated, either from oxidation or thermal decomposition, chain propagation will proceed to further degradate the lubricants.

The author discussed several methods using oxidation or thermal kinetic rate expressions to predict useful life of lubricants. Care should be taken in applying these methods. Lubricant life is usually defined in terms of wear, viscosity increase, sludge, and varnish. These parameters are related to the bulk lubricant property change as a result of extensive reactions. The kinetic expressions using the oxygen uptake or pressure change indicate the initiate rate of reaction but do not take into account the high molecular weight generation reactions nor the additive decay characteristics. Oils having the same initial reaction rate may have different additive depletion mechanisms, which may result in different useful lives.
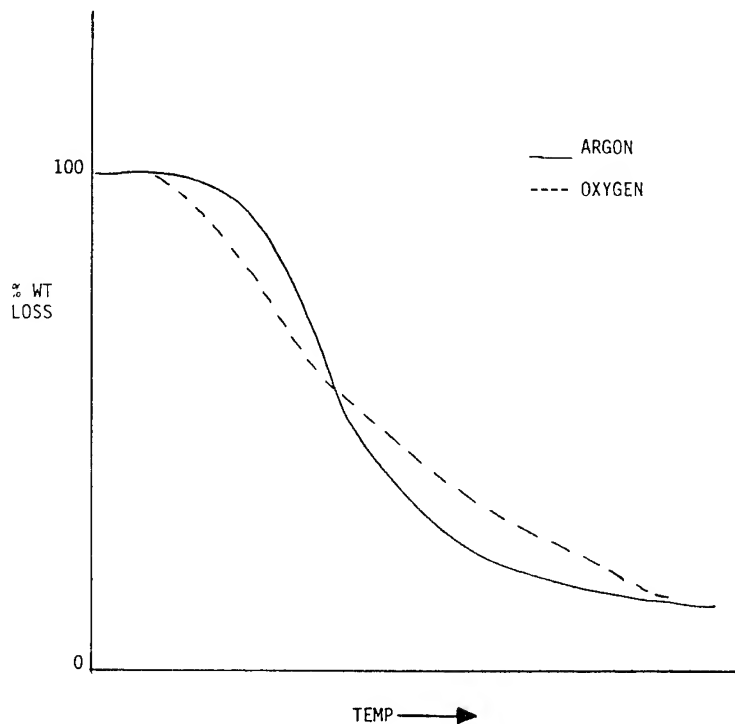
Figure 1. Comparison of Thermal and Oxidative
Stability of Lubricants

458

BEHAVIORS OF POLYMER ADDITIVES UNDER EHL AND INFLUENCES OF

INTERACTIONS BETWEEN ADDITIVES ON FRICTION MODIFICATION

Toshio Sakurai

Tokyo Institute of Technology
Yokohama, Japan

SUMMARY

Polymer additives have become requisite for the formulation of multigrade engine oils. The behavior of polymethacrylate (PMA)-thickened oils as lubricants in concentrated contacts under nominal rolling and pure sliding conditions was investigated by conventional optical interferometry. PMA-thickened oils behaved differently from the base oil in the formation of elastohydrodynamic (EHL) films. The higher the elastohydrodynamic molecular weight of the PMA contained in the lubricant, the thinner was the oil film under EHL conditions. The film thickness of shear-degraded PMA-thickened oils was also investigated. The behavior of graphite particles dispersed in both the base oil and the PMA-thickened oil was studied under pure sliding by taking photomicrographs.

Since, in modern lubricant formulations, many kinds of additives are contained in lubricating oil, it is significant to consider the interactions between additives. This paper is concerned, particularly, with the interactions of zinc-organodithiophosphates (ZDP) with other additives.

INTRODUCTION

The purpose of this paper is to assess the present understanding of the behavior of some additives under lubrication of concentrated contacts. In the modern formulation of lubricating oils, particularly engine oils, many kinds of additives are combined with base oils. Polymer additives have become requisite for the formulation of multigrade engine oils. Winer (refs. 1 and 2) has reported that the addition of high-molecular-weight polymers to the base oil increased traction only slightly and caused molecular degradation of the polymers as a reult of their being sheared in EHL contact. Dyson (ref. 3) has made a pioneering study analyzing the frictional force in EHL contacts by considering lubricants as a viscoelastic liquid. The thicknesses of polyisobutene-thickened oil films have been measured under pure sliding conditions by optical interferometry (ref. 4). With oil-in-water and water-in-oil emulsions, slight or negligible film formation under elastohydrodynamic lubrication (EHL) was observed (refs. 5 and 6).

This paper is concerned with the behavior of PMA molecules in oils under the lubrication of concentrated contacts (unpublished work by Yoshida, Hosonuma, and Sakurai) and also with the interactions between lubricant additives. Although there are synergistic effects in some combinations of additives, antagonistic effects due to the interactions are obviously present as well. In this paper, the antagonistic effects are of primary concern.

FILM THICKNESS DETERMINATION

The apparatus and procedure used under nominally rolling conditions are schematically shown in figure 1. The contact is formed with a steel ball (A1S1 52100) 25.4 mm in diameter on the flat surface of a glass disk. The surface roughness of the glass disk and steel ball were 0.039 μm rms and 0.018 μm rms, respectively. The composite roughness was 0.043 μm. The apparatus represents the point-contact version described in detail elsewere (refs. 5 to 7). For taking photomicrographs of the contact, another apparatus was used under pure sliding conditions in which a highly polished steel ball (AISI 52100) 38 mm in diameter was loaded against a stationary glass plate (ref. 4). The steel ball was rotated at different speeds.

MATERIALS AND PROCEDURES

The physical properties of the mineral oils used in this investigation are shown in table 1. Polymethacrylate (PMA) was used as a polymer additive. The average molecular weights of PMA's are tabulated in table 2.

RESULTS AND DISCUSSION

The relation between the viscosity of the various base oils and the central film thickness in EHL contact is shown in figure 2. The film thickness of the base oils increased with increasing viscosity and entrainment velocity; however, it appeared to be almost independent of applied load.

Behavior of Polymer-Thickened Oils

Polymer-thickened oils are formulated by adding selected polymer thickeners in concentrations up to 20 percent to a light base-stock lubricating oil. Although polymer-thickened oils exhibit distinct advantages in performance characteristics over conventional crankcase lubricants, there may exist serious problems, such as the unanticipated wear of cam-followers (refs. 8 and 9) and the susceptibility of the polymer concentrates to mechanical shear degradation.

The physical properties of PMA-thickened oil A are shown in table 3. The relation between the viscosity of PMA-thickened oil A and the film thickness under rolling conditions is shown in figure 3. The film thickness of PMA-thickened oils increased as the viscosity increased; the rate of increment, however, declined with increasing molecular weight. The film thickness of PMA-5-thickened oil (molecular weight, 900 000) hardly increased and was equivalent to that of the base oil. At the higher load, the same behavior was found in both base oils A and D although the films became thinner than those under the lighter load.

It is interesting that all polymer-thickened oil films were thinner than base oil films. The complex behavior of polymer-thickened oil could be affected by the following factors:

1. The molecular size, molecular structure, and molecular weight distribution of PMA

460

2. The solubility or dispersivity of PMA in the base oil, particularly under higher loads

3. The mechanical shear degradation of PMA at or near the EHL contact

The larger PMA molecules appear to have difficulty passing through the contact. Thus these molecules may accumulate at the inlet and sweep around the EHL contact. However, some of the larger molecules may pass through the contact if the molecules become alined during flow and if the molecules are shear degraded at the inlet. These behaviors should be related to the molecular weight distributions of PMA, which can be narrow or wide.

The polymer concentrates, by means of their solubility in the base oil, exerted a thickening action that increased the viscosity. However, as the molecular weight increased considerably, the solubility became poorer. Thus these molecules are likely to separate from the base oil, particularly under higher loads.

Shear Degradation of PMA-Thickened Oil

The PMA solution was degraded by means of the sonic shear tester, which uses a 10-kHz sonic oscillator. The viscosity of degraded PMA solutions is plotted against irradiation time in figure 4. The average molecular weights of PMA after shear degradation are shown in table 4. The effect of the viscosity of the degraded oils on film thickness under rolling conditions was examined as shown in figure 5(a). The film thickness of the degraded oils gradually increases as the molecular weight of PMA decreases (unpublished work by Yoshida, Hosonuma, and Sakurai). This suggests that the higher molecular weight polymers accumulated at the inlet may be obstructing some of the oil supply to the contact and thus creating a condition of lubricant starvation. The distribution curves for molecular weight become narrower with increasing irradiation time (fig. 5(b)). This may be related to the film thickness in the contact region.

Photomicrographs of EHL Contacts Under Pure Sliding Conditions

Cusano and Sliney (ref. 10) recently presented many interesting photomicrographs of graphite-dispersed oils that show the distribution of the graphite in and around the EHL contact. This paper presents photomicrographs, taken under the pure sliding condition, of contacts lubricated with graphite-dispersed PMA-thickened oils (figs. 6 and 7). The graphite particle size was less than 0.3 µm, and concentrations of graphite oil A and PMA-5-thickened oil A were 1.0 wt%. The results presented in these figures are representative of the many photomicrographs that were taken. The load was 9.8 N (1 kg) and the sliding velocity was 0.01 m/s.

In the base oil alone, graphite did not accumulate in the inlet region as shown in figure 6. On the contrary, in the PMA-thickened oil, the amount of graphite passing through the contact seemed to be very small under the same conditions as shown in figure 7. Under the conditions shown in figure 6, the linear abrasive wear caused by graphite particles was observed on the chromium-evaporated glass surface when the experiment was continued for a longer period.

In pure sliding under boundary conditions the graphite accumulated, to various degrees, at the inlet (ref. 10). Graphite particles passed through

461

the contact when the base oil alone was used as the lubricant. The experiment seems to have been conducted under partial EHL conditions. These pure sliding conditions are quite different from the nominally rolling conditions; however, the same phenomena probably occur under thin film lubrication. The foregoing results suggest that PMA, because of its higher molecular weight, accumulates with graphite particles at the inlet. From these results, it is concluded that PMA molecules are generally difficult to pass through the contact as the molecular size increases, even under rolling conditions. The blocking action of polymers at the inlet cuts off some of the oil supply to the contact and thus is related to a condition of lubricant starvation. Therefore, there may be a critical range of molecular weights for polymers that is dependent on their structure and the distribution of their molecular weights.

## INTERACTIONS BETWEEN SOME ADDITIVES

In the modern formulation of lubricating oils, many kinds of additives are combined with base oils. Synergistic effects may exist in some combinations of additives such as organosulfur compounds and fatty acids (refs. 11 and 12). However, there are also antagonistic effects due to the interactions between zinc-organodithiophosphates (ZDP) and some coadditives.

Gallopoulos and Murphy (ref. 13) observed that ZDP interacts with poly-amino monoalkyl-succinimide to immediately decrease infrared spectrum (IR) absorbance in the intensity of the P-O-C or P-S bonds. Vipper et al. (ref. 14) found that the interactions between ZDP and succinimides provide a marked synergistic effect on the solubilizing ability of the mixture by the use of dye solubilization and 'H-NMR.

Willermet et al. (ref. 15) have recently revealed that ZDP reacts with peroxy radicals, from the evidence of IR results, and that the products of ZDP with peroxy radicals are not effective as antiwear agents. Wear data obtained in fleet tests indicate that the deterioration products of ZDP in a fully formulated engine oil are ineffective for antiwear performance in normal service.

Shiomi et al. (ref. 16) have recently proposed that ZDP easily forms complexes with amines, in the oils, that have smaller steric hindrances in their structures. The various complexes formed in the oils were separated and were analyzed by using 'H-NMR and elementary analysis. It is presumed that the structures of these complexes are coordination compounds, with the complexes in the ratio of 1:1 and 1:2 (fig. 8). These complexes generally have lower antiwear properties than ZDP (ref. 16).

Inoue and Watanabe (ref. 17) have demonstrated by means of modified differential vapor pressure osmometry that succinimides interact with ZDP and metallic detergents. Whereas ZDP interacts strongly with succinimides, it is observed that the chain length of ZDP is not effective for the interaction. Rather, the strength of the interactions depends on the structure of the succinimides. One of the interactions between ZDP and a succinimide may be shown as follows:

$$-CH_2\ -CH_2\ -NH_2 -$$

$$\begin{array}{c} RO \diagdown \quad | \diagup\!\!\!\diagup S \\ P \diagup\!\!\!\diagup \\ RO \diagup \qquad \diagdown S-Zn1/2 \end{array}$$

462
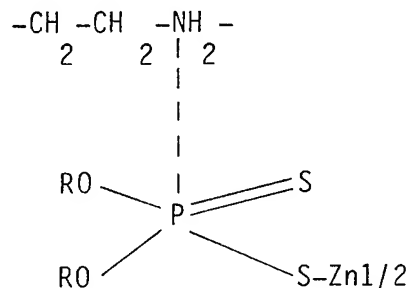
Rounds (ref. 18) has investigated the ZDP-amine interaction as a model of such an interaction. Above a critial concentration, amines can cancel the antiwear performance of ZDP as measured in the four-ball machine (FBM). Two wt% succinimide also interacts with ZDP to reduce the antiwear performance. He postulates that a mechanism for the antiwear action of ZDP depends on the formation of an acid phosphate as a decomposition product.

The ZDP decomposition sequence proposed by Dickert and Rowe (ref. 19) gives one route to an acid phosphate formation. Rounds has proposed another route to provide acid phosphate from pyrophosphate as shown in figure 9. It seems that the mechanism of ZDP antiwear properties has not been fully understood; however, acid phosphate formed from the decomposition of ZDP plays an important role in its antiwear performance.

Amines react easily with acid phosphate to form amine salts. Amine salts have been reported to be effective antiwear agents when coating the rubbing surfaces (ref. 20). Synergistic effects in load-carrying and wear-reducing abilities are revealed in both sulfurized olefin and oleyl amine salts of acid 2-ethylhexylphosphate (ref. 21). This effect appears to be due to the mechanism in which hydrolyzed acid phosphate adsorbs strongly on the sulfidized iron surfaces (ref. 12). Decomposed acid phosphate also appears to be adsorbed on iron sulfide surfaces formed by RSH and H_2S, which are decomposition products of ZDP (ref. 19).

Dacre and Bovington (ref. 22) have demonstrated the adsorption-desorption mechanism of ZDP by using radiolabeling ^{65}Zn and ^{14}C. At temperatures of 60° C or higher, ZDP adsorbed on steel but underwent a chemical reaction. Acid phosphate decomposed from ZDP appeared to be one of the antiwear agents; the antiwear properties of ZDP have not been precisely understood. However, it should be considered that acid phosphate easily interacted with basic compounds in the oil to form compounds that remarkably reduce antiwear performance.

Shoji and Sakurai have compared ZDP with oil-soluble organo-molybdenum-dithiocarbamate (MoDC, (R_2NCS_2MoS) 1/2) in reference 23 and with succinimide in antiwear properties when they coexist with other compounds (in an unpublished work). The effects of adding lauryl amine, cumylperoxide, and succinimide to oils containing ZDP or MoDC on the antiwear performance were examined by using the four-ball machine (FBM). These results are shown in figures 10 and 11. Figure 10 shows 0.1 wt% cumylperoxide added to ZDP (1000 ppm as Zn) oil and to MoDC (600 ppm as Mo) oil. ZDP was more strongly affected by the addition of cumylperoxide (fig. 10(a)) than was MoDC (fig. 10(b)). The wear scar diameter obtained in ZDP was about 1.4 times larger than that in MoDC. Similar results are shown in figure 11 when 1.0 wt% lauryl amine was added to these two oils. The wear scar diameter obtained in ZDP was considerably larger than that in MoDC. From the results of FBM, it is observed that lauryl amine interacts very strongly with ZDP to decrease its antiwear properties. Succinimide also strongly interacts with ZDP. In FBM tests, MoDC with succinimide oil showed negligible wear (0.00 mg/3 balls). On the contrary ZDP oil with 3 wt% succinimide (high basicity, 2 wt% in N concentration) allowed greater wear (0.3 mg/3 balls) under the same conditions.

Finally, the interactions between some additives are summarized in figure 12.

CONCLUSIONS

The behavior of PMA additives under partial or total EHL conditions was studied in nominally rolling and pure sliding apparatuses. The interactions between some additives are reviewed.

463

1. Under rolling conditions, the oil film thickness of PMA-thickened oils gradually increased but the molecular weight remained the same as that of the base oil, reaching a 900 000 average. In PMA-thickened oils, the larger molecules may accumulate at the inlet region. This barrier may disturb some of the oil supply to the contact and be related to oil starvation. There may be a critical range of molecular weight for the film formation at the EHL contact.

2. Under pure sliding, graphite particles dispersed to the base oil and the PMA-thickened oil were studied by taking photomicrographs. It was observed that the large PMA molecules accumulated with graphite particles at the inlet. The same behavior occurred under rolling conditions.

3. With the shear-degraded PMA-thickened oils, the oil film thickness increased as the molecular weight of the PMA decreased under rolling conditions. In practical use of polymer additives, the film formation at the contact becomes effective even if the viscosity of the polymer-thickened oil decreases.

4. The interactions between ZDP and other additives were reviewed. Acid phosphate decomposed from ZDP appeared to be an effective antiwear compound, although the antiwear properties of ZDP have not been clearly understood. However, acid phosphate easily interacted with basic compounds in the oils, and thus the complex or salt formed had considerably lower antiwear properties even considering their decomposition and hydrolysis. MoDC showed better antiwear properties in the presence of coadditives than did ZDP. The interactions between ZDP and other additives were summarized.

5. For effective lubrication it is very important to fully understand additive chemistry. In the modern formulation of lubricants, many kinds of additives are required to impart the desirable properties for lubricants. Some additives interact with each other to deteriorate the function of the lubricant during lubrication. The knowledge of additive chemistry of lubricants should be developed further.

REFERENCES

1. Sanborn, D.M.; and Winer, W.O.: Fluid Rheological Effects in Sliding Elastohydrodynamic Point Contacts with Transient Loading: 2 - Traction. J. Lubr. Technol., vol. 93, no. 3, July 1971, pp. 342-348.

2. Walker, D.L.; Sanborn, D.M.; and Winer, W.O.: Molecular Degradation of Lubricants in Sliding Elastohydrodynamic Contacts. J. Lubr. Technol., vol. 97, no. 3, July 1975, pp. 390-397.

3. Dyson, A.; and Wilson, A.R.: Film Thickness in Elastohydrodynamic Lubrication of Rollers by Greases. Inst. Mech. Eng. (London) Proc. 1969-1970, vol. 184, pt. 3F, 1970, pp. 1-11.

4. Hironaka, S.; Nagai, M.; and Sakurai, T.: Behaviors of Polymer Additives in Elastohydrodynamic Contact. J. Jpn. Pet. Inst., vol. 22, no. 1, 1979, pp. 52-58.

5. Hamaguchi, H.; Spikes, H.A.; and Cameron, A.: Elastohydrodynamic Properties of Water in Oil Emulsions. Wear, vol. 43, 1977, pp. 17-24.

6. Dalmaz, G.: Traction and Film Thickness Measurements of a Water Glycol and a Water in Oil Emulsion in Rolling-Sliding Point Contacts. Proc. 7th Leeds-Lyon Symposium on Tribology, D. Dowson, ed., Westbury House, 1981, pp. 231-240.

7. Wedeven, L.D.; Evans, D.; and Cameron, A.: Optical Analysis of Ball Bearing Starvation. J. Lubr. Technol., vol. 93, no. 3, July 1971, pp. 349-363.

8. Chida, J.: Wear on Engine Parts. Presented at the JSLE 7th Wear Symposium, Mar. 1975.

9. Kawamura, M.; et al.: Lubricity of Various Engine Oils. JSLE Kyushu Meeting, preprint A-16, 1976.

10. Cusano, C.; and Sliney, H.E.: Dynamics of Solid Dispersions in Oil During the Lubrication of Point Contacts, Part 1 - Graphite. ASLE Trans., vol. 25, no. 2, Apr. 1982, pp. 183-189.

11. Davey, W.: Boundary Lubrication of Steel. Blends of Acids, Ester and Soaps in Mineral Oil. Ind. Eng. Chem., vol. 42, no. 9, Sept. 1950, pp. 1837-1840.

12. Kagami, M.; et al.: Wear Behavior and Chemical Modification in Binary-Additive System Under Boundary Lubrication Conditions. ASLE Trans., vol. 24, no. 4, Oct. 1981, pp. 517-525.

13. Gallopoulos, E.; and Murphy, C.K.: Interactions Between a Zinc Dialkyl-phosphorodithioate and Lubricating Oil Dispersants. ASLE Trans., vol. 14, no. 1, Jan. 1971, pp. 1-7.

14. Vipper, A.B.; et al.: Investigations of Interaction Between Succinimides and Antioxidants of Different Structures. Effect of Interaction on Efficiency and Synergism of Additives. Proc. JSLE-ASLE International Lubrication Conference, T. Sakurai, ed., Elsevier (Amsterdam), pp. 738-746.

15. Willermet, P.A.; Mahoney, L.R.; and Bishop, C.M: "Lubricant Degradation and Wear III. Antioxidant Reactions and Wear Behavior of a Zinc Dialkyldithiophosphate in a Fully Formulated Lubricant. ASLE Trans., vol. 23, no. 3, July 1980, pp. 225-231.

16. Shiomi, M.; Tokashiki, M.; and Yamaji, T.: Interactions Between Zinc Organodithiophosphates and Amines. JSLE Tohoku Meeting preprint A-18, 1982, pp. 69-72.

17. Inoue, K.; and Watanabe, H.: Interactions Between Engine Oil Additives. J. Jpn. Pet. Inst., vol. 24, 1981, pp. 101-107.

18. Rounds, F. G.: Some Effects of Amines on Zinc Dialkyldithiophosphate Antiwear Performance as Measured in 4-Ball Wear Tests. ASLE Trans., vol. 24, no. 4, Oct. 1981, pp. 431-440.

19. Dickert, J.J.; and Rowe, C.N.: Thermal Decomposition of Metal O,O-Dialkylphosphorodithioates. J. Org. Chem., vol. 32, no. 3, Mar. 1967, pp. 647-653.

20. Masuko, A.; Hirata, M.; and Watanabe, H.: Electron Probe Microanalysis of Wear Scars of Timken Test Blocks on Sulfur-Phosphorus Type Industrial Gear Oils. ASLE Trans., vol. 20, no. 4, Oct. 1977, pp. 304-308.

21. Forbes, E.S.; and Upsdell, N.T.: Phosphorus Load-Carrying Additives; Adsorption/Reaction Studies of Amine Phosphate and Their Load-Carrying Mechanism. 1st European Tribology Congress, Mechanical Engineering Publications, 1973, pp. 277-286.

22. Dacre, B.; and Bovington, C.H.: The Adsorption and Desorption of Zinc Diisopropyldithiophosphate on Steel. ASLE Trans., vol. 25, no. 4, Oct. 1982, pp. 546-554.

23. Isoyama, H.; and Sakurai, T.: The Lubricating Mechanism of di-μ-thiodithio-bis (diethyldithiocarbamate) dimolybdenum during Extreme Pressure Lubrication. Tribol. Int., vol. 7, no. 4, Aug. 1974, pp. 151-160.

Table 1 The Properties of Hydrocarbon Oils

		Oil A*	Oil B*	Oil C*	Oil D**
Viscosity (cSt)	25℃	153.5	191.6	222.3	155.0
	40℃	67.5	82.0	93.0	65.1
	100℃	8.83	10.0	10.8	7.93
Viscosity Index		104	101	99	84
Refractive Index n_D^{25}		1.4835	1.4828	1.4851	1.4792
Density d_4^{15}		0.8766	0.8795	0.8809	0.8789

*   highly refined Paraffinic oil

**   hydrogenated naphthenic oil

Table 2 Average Molecular Weight of Polymers

Polymethacrylate	Average Molecular Weight(MW)
PMA−1	40,000
PMA−2	100.000
PMA−3	350,000
PMA−4	480,000
PMA−5	900.000

467

Table 3 Physical Properties of PMA-Thickened Oils

Base Oil	PMA	Concentration (wt. %)	Density d_4^{15}	Refractive Index(n^{25})	Viscosity (cst) 25℃	40℃	100℃	V I
A	1	2.0	0.8781	1.4836	164.25	73.47	9.80	113
		4.0	0.8862	1.4836	178.30	80.54	10.82	121
		5.8	0.8818	1.4830	194.82	88.76	11.98	128
		7.5	0.8835	1.4829	214.33	98.07	13.20	133
	2	2.0	0.8780	1.4829	171.47	78.42	10.80	124
		4.0	0.8799	1.4830	195.03	91.36	12.93	139
		5.8	0.8810	1.4821	220.62	105.40	15.26	152
		7.5	0.8819	1.4826	249.27	120.80	17.75	163
	3	1.5	0.8778	1.4815	180.66	83.15	11.51	129
		2.8	0.8781	1.4814	209.78	100.00	14.49	149
		4.1	0.8796	1.4814	243.65	118.80	17.69	165
	4	1.2	0.8776	1.4811	185.30	85.81	11.97	132
		2.3	0.8781	1.4810	220.11	105.80	15.49	155
		3.3	0.8786	1.4811	259.12	127.80	19.34	172
	5	0.9	0.8768	1.4808	171.08	80.89	11.79	139
		1.7	0.8766	1.4809	192.34	97.01	15.71	173
		2.5	0.8778	1.4808	220.37	113.50	18.88	187
D	5	2.5	0.8794	1.4778	210.60	106.80	17.34	178

Table 4 Degradation of PMA-5 Thickened Oil A with Irradiation Time

Irradiation Time (min)	Viscosity at 25℃(cst)	Molecular* weight	MW/MN
0	220.57	900,000	4.38
5	192.41	461,000	2.92
10	184.03	334,000	2.38
15	179.07	276,000	2.16
30	171.51	189,000	1.68

* Weight average molecular weight measured by Gel permiation chromatography which are corrected by molecular weight of polystyrene

468
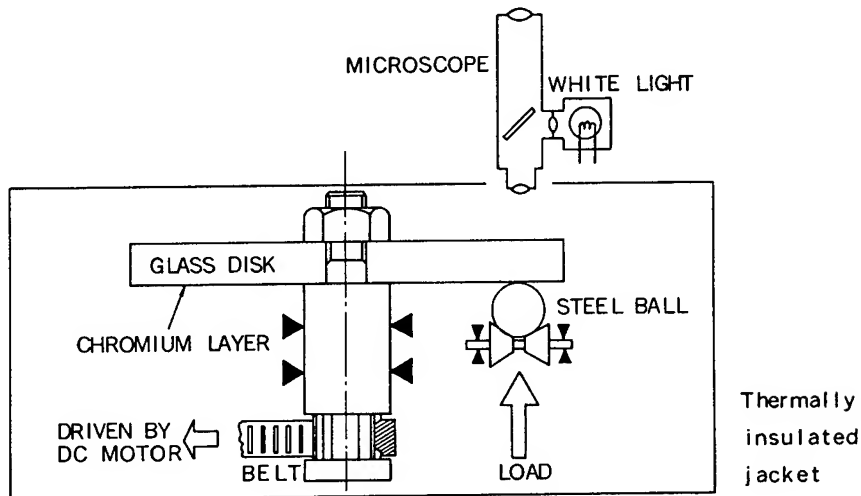
Figure 1. - Schematic diagram of test apparatus.
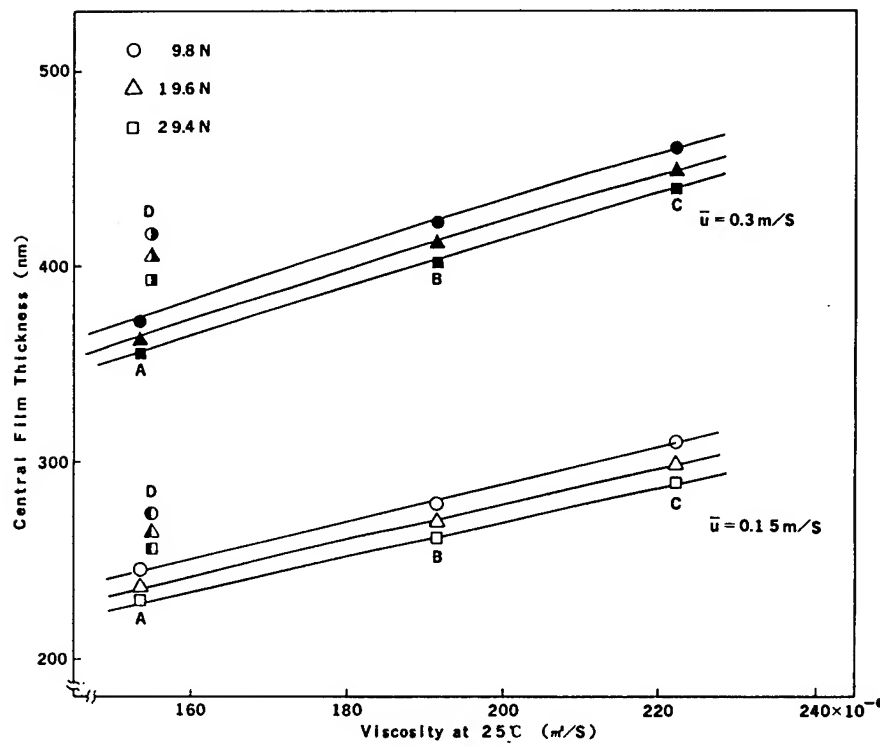
Figure 2. - Central film thickness as a function of viscosity for various base oils at two entrainment velocities u and three loads.
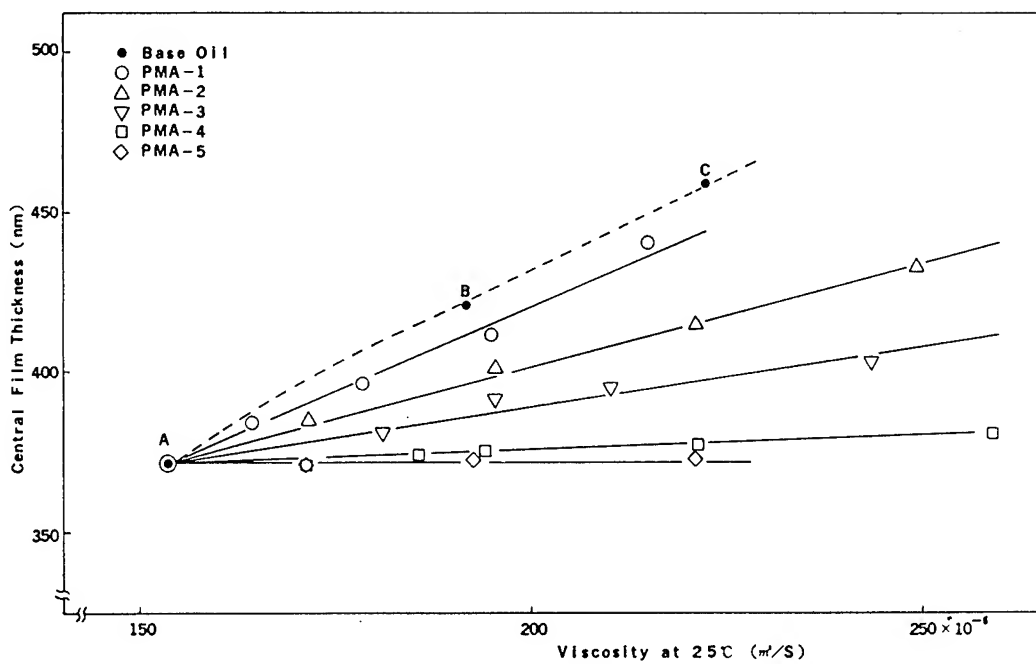
Figure 3. - Central film thickness as a function of viscosity of PMA-thickened oil A. Entrainment velocity, $\bar{u}$, 0.3 m/s; load, P, 9.8 N; maximum Hertz pressure, p_{max}, 0.35 GPa.
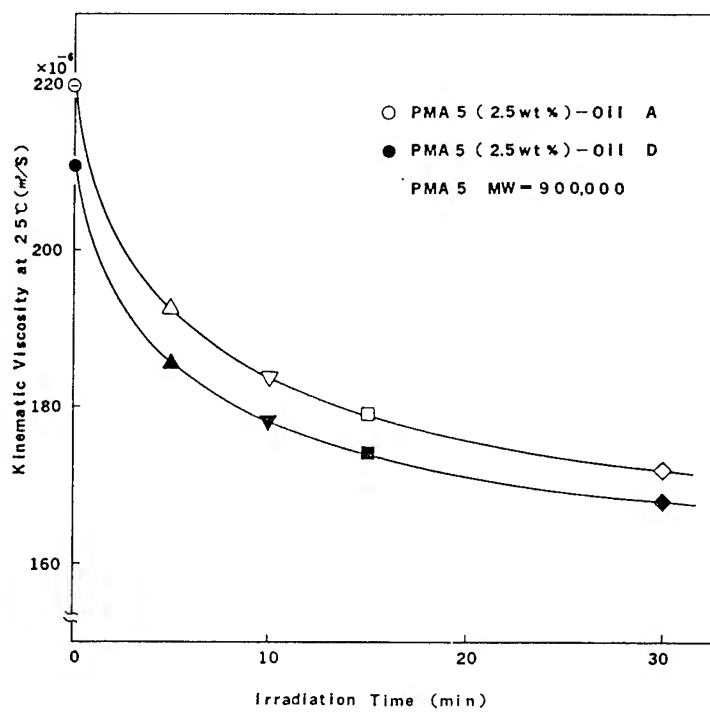
Figure 4. - Kinematic viscosity of PMA-5 degraded oils as a function of irradiation time.
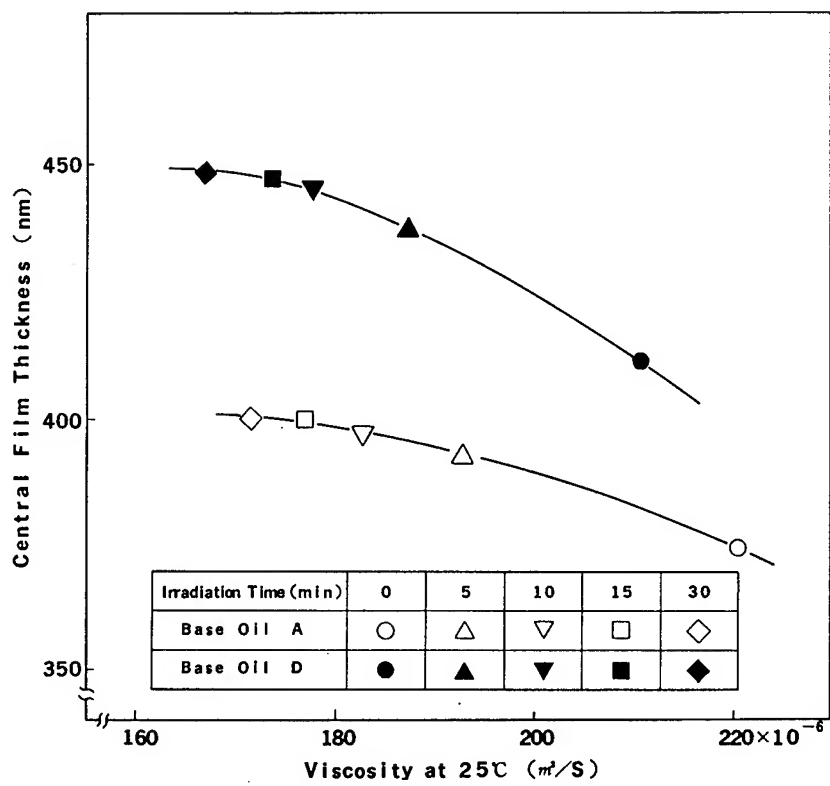
Figure 5(a). - Central film thickness as a function of shear degradation. Entrainment velocity, u, 0.3 m/s; load, P, 9.8 N; maximum Hertz pressure, p_{max}, 0.35 GPa.
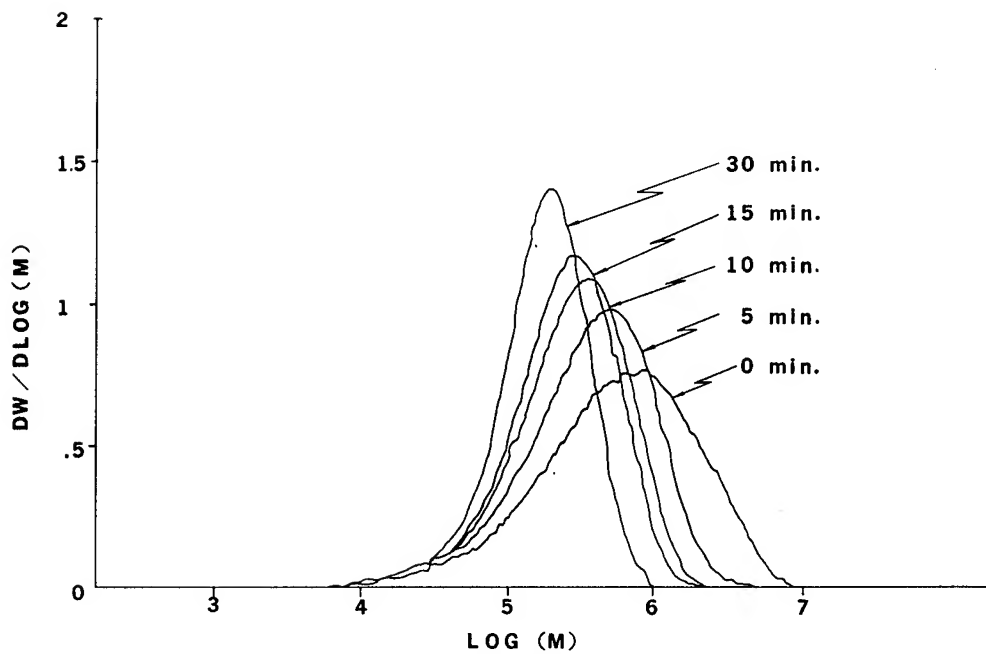
Figure 5(b). - Molecular weight distribution of degraded PMA-thickened oil. Frequency, 10 kHz.

471
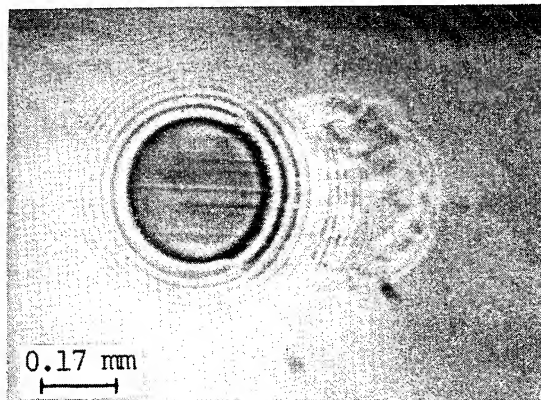
Figure 6. - Graphite-dispersed base oil. Entrainment velocity, u, 1 cm/s; load, P, 9.8 N; maximum Hertz pressure, p_{max}, 0.35 GPa; temperature, 20° C.
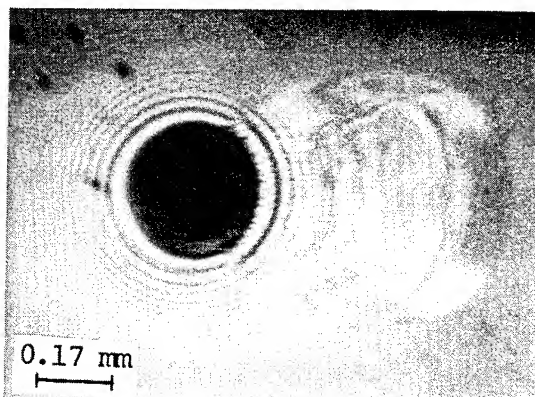
Figure 7. - Graphite-dispersed PMA-5-thickened oil. Entrainment velocity, u, 1 cm/s; load, P, 9.8 N; maximum Hertz pressure, p_{max}, 0.35 GPa; temperature, 20° C.
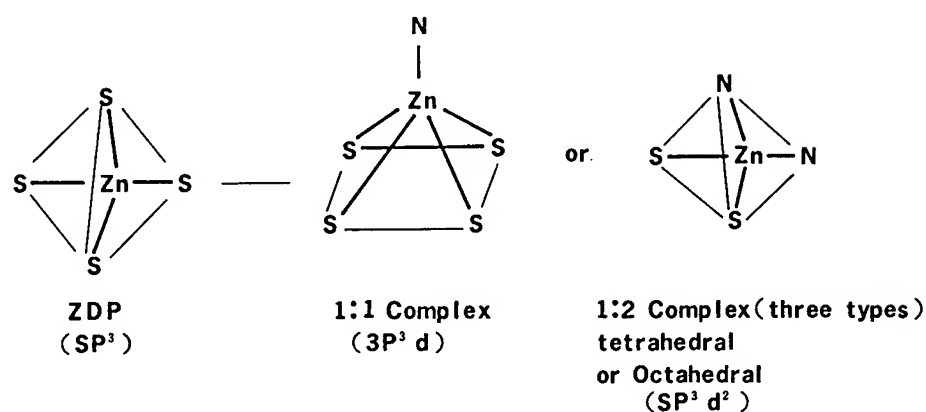
Figure 8. - Complex of ZDP with amines.
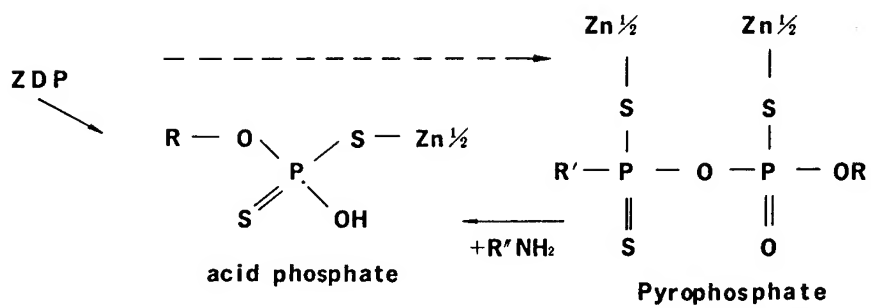
Figure 9. - Mechanism of acid phosphate formation from ZDP.
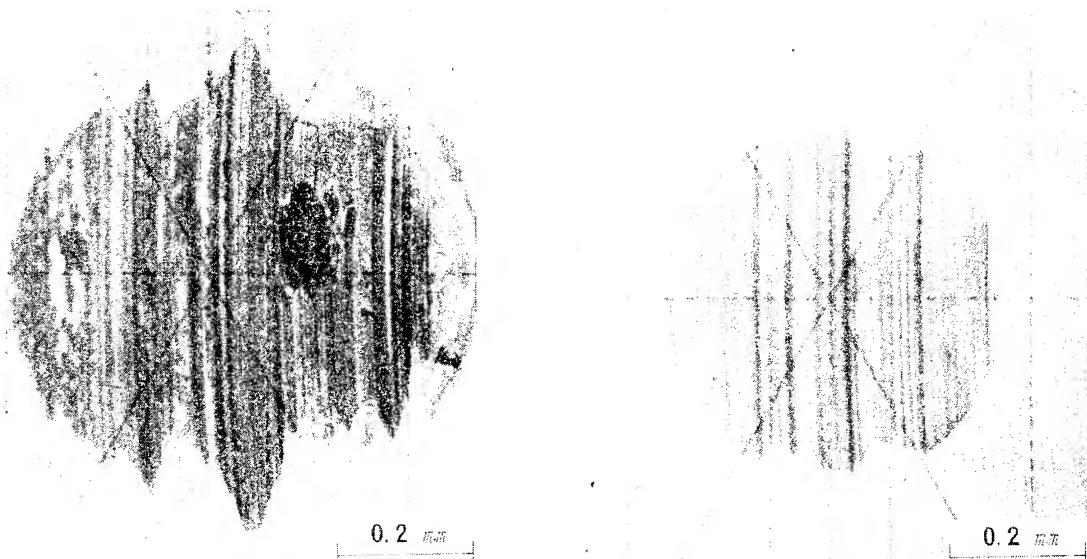
(a) ZDP and cumylperoxide.
(b) MoDC and cumylperoxide.

Figure 10. - Effects of adding cumylperoxide to oils containing ZDP or
MoDC. Entrainment velocity, u, 0.57 m/s; load, P, 314 N; sliding
duration, 30 min; temperature, 80° C.
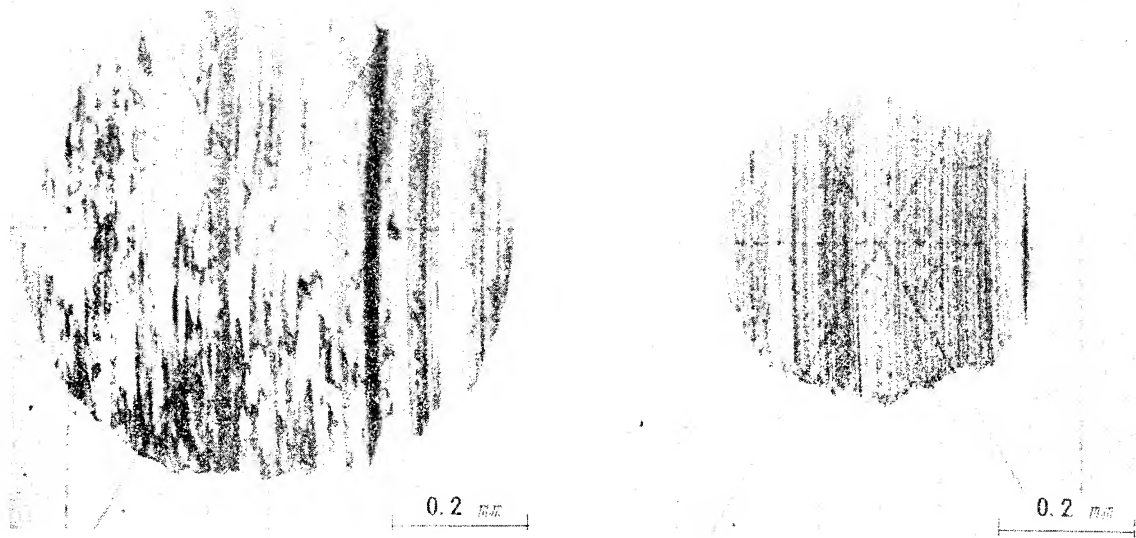
(a) ZPP and lauryl amine.
(b) MoDC and lauryl amine.

Figure 11. - Effects of adding lauryl amine to oils containing ZDP or
MoDC. Entrainment velocity, u, 0.57 m/s; load, P, 392 N; sliding
duration, 30 min; temperature, 80° C.
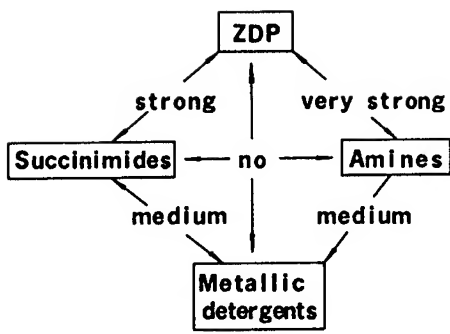
Figure 12. - Interactions between lubricant additions.

WHAT'S SO HOT ABOUT FORMULATED SYNTHETICS?

Alan Beerbower
University of California at San Diego
San Diego, California

The recent appearance on the market of a synthetic automotive engine oil marks the end of a half-century of patient work by many teams. This paper traces the history of synthetic lubricants, and of the additives that are required to make them able to compete in a market developed by and for petroleum oils. Some examples are shown by means of real data, and enlarged using heat transfer properties obtained by chemical engineering thermodynamic methods. The prospects for future successes and ideas on the additives that would most help to bring them about are also presented, as are some thoughts on markets not worth capturing.

INTRODUCTION

The story of synthetic lubricants is long, and mostly painful. Very few people still remember that it began in oil-poor Germany during World War I. Ironically, one of those products still survives, but only because it was a useful additive. It is made by alkylating naphthalene with wax, and was the first pour depressant discovered. There was little progress until World War II, when the need for aircraft turbine lubricants led to adapting available diester plasticizers to that service. Fortunately, the next step did not require a world war, and the use of synthetics for ordinary service has begun without bloodshed.

AIRCRAFT TURBINE LUBRICANTS

The success story of diesters in jet engines is far too well known (1) to need more than cursory mention here. It is still important, though, to remind readers that it was not due to their being "better lubricants" in any general way than petroleum. On the contrary, diesters are quite inferior to mineral oils in some ways that are quite important in most applications, and were only accepted because they were superior in two important respects. A comparison with mineral oil is given in Table 1.

The key factors were the excellent volatility-viscosity relation, and the very good low temperature fluidity. These were each composed of two aspects. The low volatility was inherently related to their higher heat of vaporization, provided by the ester group. However, of equal importance was the fact that they were essentially pure compounds, and so free from any need for fractionation. Even today, commercial petroleum stills are not capable of such control.

Low temperature fluidity was also inherently built into the molecules by their near-linear structure which tends to give the best possible viscosity-temperature slope. The branching gave increased entropy of fusion, which resulted in low freezing

points, and the absence of waxy contamination caused the pour point to equal the freezing point.

The most notorious difficulty with diesters was their poor thermal stability (in the absence of oxygen). This was traced to the tendency of the hydrogen atom in the beta position of the alcohol part to interact with the O in the ester group, and was eventually solved by using polyol esters such as MIL-L-23699. While there were problems with oxidation resistance, they differed from those with petroleum mainly in that different additives were required. Fortunately, the very powerful antioxidant phenothiazine (which is insoluble in hydrocarbons) was discovered quite early. It is still the most widely used despite much research for better additives. Another difficulty was that esters can hydrolyze in storage, giving corrosive acids. Two other problems arose from the use of these oils to lubricate the heavily loaded power take-off gears as well as the turbine bearings. Esters are not as good at preventing gear scuffing as mineral oils, and the extreme pressure additives used for further improvement of petroleum are quite destructive to oxidation stability. That problem was solved with tricresyl phosphate, but the fact that esters are also very much poorer at preventing pitting fatigue (ref. 2) has not been solved yet. In fact, it may never be solved, since recent evidence tends to show that fatigue is proportional to chemical activity (ref. 3). Fortunately, even the worst esters appear to have adequate fatigue protection for most aircraft applications. It is likely that both kinds of gear damage, as well as the hydrolysis noted above, are related to the high solubility of water in esters.

The point of this recital is that the aircraft industry was willing to make sacrifices, and the oil industry to do massive research on minimizing them, to obtain the very real gains attached to using esters. The results appear to be a classic success story, but it must be remembered that the Russians are still using mineral oils in equivalent service. That is surely not due to lack of knowledge, so it must be due to real belief that our sacrifices were not justified.

Future trends are not difficult to predict, as this is the one part of the synthetics business that can be described as mature. There no longer seems to be any prospect of superior base stocks. Polyphenyl ethers have won a limited place in the market, but their poor low temperature properties preclude further expansion.

There is little incentive for better antioxidants. Most of these oils are drained for other reasons long before serious deterioration starts. In fact, there is a small industry based on collecting such drainings and cleaning them up a little for sale as cut-rate plasticizers. The search for better antiscuff agents could be more rewarding. Some oils have been marketed since 1960 containing additives designed to polymerize on the working gear surfaces. While they suffered from side effects, the case is not closed. One interesting example was butyl titanate, which gave a dramatic Ryder gear load, but was too easily hydrolysed. Dimethyl silicone of such low molecular weight as to be soluble in esters also showed a similar effect, but caused excessive foaming. That may sound paradoxical, but the defoaming action of silicone is tied to its insolubility at the usual high chain length. Additive makers are secretive, for obvious reasons, and there may be some new developments behind the scenes, but nothing is visible yet.

AUTOMOTIVE ENGINE LUBRICANTS

Of all the potential markets for synthetic lubricants, that of automotive oils is by far the largest and correspondingly the most attractive. It is also exceptionally challenging because of the many functions of the lubricant in an internal combustion engine. As the result of this combination of high volume and very complex requirement, there have been many frustrated developments. One particularly unhappy example was a polyglycol synthetic that appeared in the late 1940s to have everything needed for success, only to fail because of its incompatibility with petroleum based products.

Many services performed by the oil are so far removed from lubrication that it often seems misnamed "lubricant." These include the following, and perhaps others not yet recognized:

* Heat transfer fluid

* Rust preventive

* Dirt scavenger

* Acid neutralizer

While performing these activities, the oil must not do a number of harmful things:

* Solidify when cold

* Thicken to asphalt

* Ruin the seals

* Oxidize to acid

* Evaporate excessively

* Form gum and varnish

* Form combustion chamber deposits

Finally, having performed these essential housekeeping duties, it is also expected to lubricate under cyclic conditions in the following regimes:

* Hydrodynamic in bearings

* Boundary-EHD in valve train

* Squeeze film in ring zone

All of these requirements are satisfied by petroleum based lubricants containing suitably sophisticated additives. One might well marvel at this happy coincidence were it not for the fact that the modern engines and lubricants grew up together, as classmates in the "school of hard knocks." If Henry Ford had used a modern high

compression engine in his Model T it would not have lasted an hour on the raw distillates then offered as lubricants.

In view of this long success story, it is reasonable to ask "Why use a synthetic base oil?", or, in Ann Landers' phrase, "If it's working, don't fix it." The fact is that the engine makers now, as always in the past, have designs waiting that can hardly even be tested with current premium oils. There is also the fact that "satisfactory" is a very subjective word, and the user who was recently delighted with 16,000 km between changes is now demanding 40,000 km. There are even those among us who dream of "sealed crankcase" engines, replaceable like spent cartridges at 160,000 or so km. While there are probably hydrocarbons in the petroleum that could do these things, refining them free from the inferior molecules would cost more then synthesis.

Chamberlin (ref. 4) has done a good job of answering these questions in terms of presently available oils in current (1977) engines. His data on the physical properties of the base stocks used are shown in Table 2. Since all of them were chosen to be in a narrow range of viscosities at $99^{\circ}C$, it is possible to compare them directly in terms of thickening at lower temperatures. (The first mineral oil "A" required pour depressant before it could be run in the Cold Cranking Simulator at $-18^{\circ}C$, and presumably "B" could not be run there at all). Obviously, building up the VI of Mineral "A" with polymeric additive would still not provide as good low temperature properties as even the poorest synthetics.

Similarly, the volatility relations speak for themselves, and no amount of care in distillation would make mineral oils as good as synthetics. It must be noted, however, that some of the superiority of the polyolefin and the blend is due to very fine fractionation, as shown by the small spreads between 1% and 20% temperatures. If the polyolefin were cut in ordinary refinery equipment, the difference would be less dramatic, while the superior properties of the polyol ester indicate that only unreacted ingredients removable by simple stripping were present.

Since the heat transfer properties of engine lubricants are of interest, estimates of the specific heat and thermal conductivities of the same oils were made, using methods previously published (ref. 5), and compared with older literature data (ref. 1). The results are shown in Table 3. Since the individual values are not easily interpreted, heat transfer engineers group them into the "Prandtl number" or thermal diffusivity. This is defined as the specific heat times viscosity divided by conductivity, and is a dimensionless group. The conclusion is that the synthetics fall in the same range as mineral oils, and neither offer advantages nor create problems in this context.

Chamberlin found that the diester and blend caused more swelling than allowed on automatic transmission fluids. That will be no surprise to the aircraft turbine people, who learned long ago that high nitrile or fluoro rubbers were required. He points out that this does not preclude the use of esters with ordinary seals, and field tests with ester-base oils have not led to any dramatic failures.

His bench oxidation tests are not really relevant as he ran them on base oils without additives. As he should have known, many base stocks, such as super-refined mineral oil, behave very badly under those conditions but are outstanding in response to antioxidants. His laboratory engine tests, on complete lubricants formulated to SAE 5W-40 grade and performance above the SE level, showed the polyol ester/polyolefin blend to be equal or superior to the mineral oil in all respects. Wear and oil consumption were lowered, while engine cleanliness was similar except for the V-C test,

which the synthetic failed to pass on engine varnish. He easily corrected that with a modified additive. The viscosity increase was zero in the IIIC test, which is spectacular. This is attributable to both low volatility and absence of asphalt forming molecules.

These results were confirmed by simulated road service tests for 40,000 km. One additional observation was that the synthetic blend did not suspend as much of the lead halides from the fuel as did the mineral oil formulation, which is not usually a quality criterion. However, the lead deposited on the engine surfaces in a way that has been known to cause problems. Concern over that is limited by the trend to unleaded fuel.

Barton (ref. 6) presented comments on this paper which tend to confirm the above conculsions. Since he worked for Mobil, his data were related to polyolefins rather than esters. He was quick to point out that these are compatible with conventional sealing elastomers. His additive package was optimized to fit these oils, in distinction from Chamberlin's which was modified only to overcome a failure. The two studies are not exactly comparable, but together show that there is a substantial incentive to use these new base stocks in premium engine oils. The five years since they were presented have certainly confirmed that, since the product Barton described is now being widely marketed as "Mobil 1." Ester based products are still in the running, but polyolefin is surely here to stay.

In contrast to the aircraft turbine oil market, that for synthetic automotive oils is too immature to predict any new trends in additives. However, it does seem that the success of a polyolefin shows the validity of Chamberlin's comment that all of the available additives have been fine-tuned to mineral oil. The change to polyolefin is surely much less difficult than that to ester. Probably the biggest problem is that these oils have lower solubility parameters than mineral oils, and additives that tend to drop out in long term storage will be found completely insoluble. The principles for solving that sort of problem are well established (ref. 5,7). On the other hand, esters have higher solubility parameters than hydrocarbons, and so will not cause the same additives to drop out. Some problems have been noted with polybutene, but not the usual highly oxygenated additives. It is more conceivable that some colloidal additives might be rendered less effective because of higher critical micelle concentrations. For example, the lower ability to suspend lead halide noted above may result from this effect. There are those who feel that esters can replace hydrocarbons as we run out of petroleum, but that is illfounded. For one thing, a major part of the esters is also made from petroleum carbons. For another, with modern processes such as hydrocracking, mineral oils and fuels are essentially interchangeable, so any synfuel production can release an equal weight of lubricants. The old mystique of accepting lubes only from "approved crude sources" is already unrealistic.

One can only speculate on what sort of materials could result from as massive a search as has brought forth the present crop of mineral oil additives. Such a project seems unlikely, in view of the current acceptance of polyolefins. One new function has been added to the list given above, energy conservation by reducing friction. The exact nature of the process is still the subject of controversy, because it involves both reducing the viscosity below what was long regarded as the safe minimum, and then using an additive to protect the metal from damage during contacts. There are those who feel that classic hydrodynamics is an adequate explanation, and point to the fact that colloidal graphite or molybdenum disulfide will serve as the additive.

On the other side, others (Exxon in particular) claim that their own highly secret additive goes further than just providing a solid film as a final defense, and actually is more slippery than oil. Regardless of the mechanism, there is not doubt that such oils do reduce fuel consumption. As predicted by HDL, they give greater savings at lower temperatures. An even more controversial matter is adding colloidal polytetrafluoroethene to oils of ordinary viscosity. One article says it works, but du Pont warns against using the PTFE they make in this way (ref. 8).

Other than that, it is probably safe to assume that the list of problems given above will continue into the future. Thus, the new additives will have to be nearly as numerous as they are now. One type that is already undergoing changes is the so-called "detergents," which never had much in common with the far bigger household detergent market. They began as metal salts of organic acids, and seemed to clean off the deposits. Actually, they were preventing them from forming, by two unrelated mechanisms. The metal was neutralizing the acids from combustion, while the rest of the molecule was keeping the sludge dispersed. These functions are now being handled separately, with the metal salt retaining the traditional name. The other additive, quite properly called "dispersant," tends to have a long hydrocarbon (i.e., polybutene) tail and a highly polar organic head. The head is rich in oxygen and nitrogen, as is the soot and other sludge to be dispersed. It is theoretically possible to optimize the dispersant by matching its partial solubility parameters to those of the sludge, while those of the tail match the base stock (ref. 7).

Another change already mentioned is that polyolefin oil does not require a polymeric viscosity improver to meet the needs of viscosity versus temperature. This could be both a blessing and a loss, since Okrent (ref. 9) showed that such additives reduce both friction and wear. It is to be hoped that the fuel-saving additives will more than make up for this loss.

One additive that can be considered indispensible for modern engine oils is zinc dialkyldithiophosphate (ZDDP) in one or more of its many varieties. However, it does seem possible that better varieties might be made if more consideration were given to the possibility that it works by preventing low-cycle fatigue wear, rather than adhesive wear as commonly supposed. It has been shown that some iron sulfides and phosphorus compounds are formed on the cam surface, but it is also well known that a good deal of "friction polymer" is produced there. Presumably it can help lubrication by occupying the valleys among asperities and thus increasing the ratio of EHD film thickness to roughness. Since that reduces the stress concentration on the asperities, it could result in the dramatic decrease in wear rate noted with ZDDP. Better understanding of the mechanism of protection could help to limit the concentration of phosphorus to avoid damage to the catalytic converters used for emission control.

INDUSTRIAL LUBRICANTS

In comparison with the above transportation oriented lubricants, those for ordinary industry resemble an old-fashioned drug store. A partial list of the machinery involved is given in Table 4. At the height of the "hard sell" era, Exxon had over 900 products in that category, including greases. By 1960, these were reduced to 200, thanks to the "multipurpose" trend, but even so it is hard to put a finger on the legitimate target for exploitation of synthetics. In many cases, the demand and the new synthetic to fill it grew up together, as in the classic case of fire resistant phos-

482

phate esters. While these were first thought of as hydraulic fluids, cross-over into
lubricating compressors and high temperature turbines (ref. 10,11) proved to be a
natural next step. However, such cases tend to be self-limiting. A more recent story
concerns the alkyl-aromatics. These were a byproduct from the old alkyl-benzene sul-
fonate detergents, now outlawed because they were non-biodegradable. Someone in
France realized that they might be compatible with R-22, and the synthetic refrigerator
oil industry was born. This seemed very specialized at first, but (as shown in Tables
2 and 3) is now considered a candidate engine oil base stock.

Despite the disappointment in the 1950s on engine oils, the manufacturere of
polygycols have not given up. These have won places as heat transfer and hydraulic
fluids, and offer some good properties as lubricants. They can be made either water
soluble or insoluble depending on whether the chain ends in OH or methyl, and each
has found modest markets. They are seriously weak on thermal stability, but can be
inhibited against oxidation to have excellent lifetimes. The nature of the additives
is proprietary, but they are probably quite unlike those used in mineral oils because
of solubility problems.

The outlook for including even the leading synthetics of Table 2 as industrial
oil base stocks is limited, since these lubricants tend to be selected by very cost-
conscious personnel. Unless there is a proved need for better oil, that will be the
basis for decision. The large scale manufacture of polyolefin base stocks will
naturally lower their cost, so that chances will improve (ref. 12).

There are many more additives used industrially than most customers realize.
From the beginning of the petroleum lubes they have been criticized for lack of
"oiliness," an elusive sort of property that previous users of fatty oils missed. As
a result, the first additives were nothing but a little fat added to bridge the gap,
and that is still fairly common. Better versions such as methyl oleate are also
used. Where those are not enough, stronger chemicals such as tricresyl phosphate
take over. TCP bridges the gap between the "oiliness" agents that work by chemisorp-
tion and the extreme pressure agents that work by irreversible reactions. Of course,
both are used to form films preventing metal-metal contact. For the highest pres-
sures, those used in metal-working, sulfur in very reactive forms is usually used.
Other additives are used to make emulsifiable oils; the oil-in-water for metal cutting
and grinding, the invert for fire resistant lubricants and hydraulic fluids. Other
emulsifiers are used in a whole range of rust preventing products from steam turbine
oils to protective greases and coatings with little or no function in lubrication.
The antioxidant can be chosen to function at temperatures below about $125^{\circ}C$, where
the engine oil types take over. Uses above this temperature are noted by * in Table
4. A very valuable aid to the antioxidant is a "metal deactivator," the purpose of
which is to form a protective coating on any copper in the system.

The prospects for new additives in this field are not very bright because of
the diverse uses and limited markets for individual products. Formulators tend to
depend on the additive makers for research. Since no one of the problem areas in
Table 4 is capable of supporting more than the most modest effort, they are inclined
to aim for wide-spectrum solutions, and also to seek fall-out from their automotive
colleagues. The result is a rather slow-moving activity, occasionally sparked by
some new development or problem. The sudden popularity of mist lubrication a few
years ago was an example of the former, and led to drop-size controlling additives.
However, these were really the descendants of much older high molecular weight poly-
mers used to prevent oils from slinging off shafts in textile and lumber mills.

Toxicity considerations have led to finding substitutes for chlorine and lead compounds previously used for load carrying ability, except where the lubricant can be kept away from human contact.

Some efforts are being made to exploit the automotive energy-saving combination of low viscosity synthetic and additive for use in compressors and gear drives. Success has not been very conspicuous, and if it becomes so will probably not involve any specially developed additives.

CONCLUSIONS

It appears that the "Age of Synthetics" has finally dawned, after years of hopes and disappointments. So far, impact on demand for new additives has not been at all burdensome, and it does not appear likely to become so in the near future.

Of the many additive types looked at, only two seem to be in much need of investigation, and those only in hopes that improved understanding will lead to more efficient ways of doing things that are already being done fairly well. They are:

1. Design dispersants to match partial solubility parameters with specific species of sludge particles and base stocks,

2. Design load carrying agents of the ZDDP type so as to provide the right sort of friction polymer at the right rate to improve EHD lift and reduce surface fatigue.

However, it must be added that synthetics will be more dependent on additives than mineral oils ever were. It is almost axiomatic that the more highly oils are refined, the less oxidation resistance and load carrying ability they have, and in these synthetic base stocks we have the ultimate in refinement. Fortunately, there is another axiom that says the most highly refined oils have the most dramatic response to the right additives.

REFERENCES

1. Gunderson, R. C. and Hart, A. W.: Synthetic Lubricants. Reinhold Publishing Co., New York, 1962.

2. Valori, R.: Evaluation of the Effects of MIL-L-23699 Lubricants on Gear Pitting in Full Scale Helicopter Transmission Tests and Correlation with a Small Scale Tester. NAPTCH-AED-1923, January 1970.

3. Cantley, R. E.: Predicting the Effects of Lubricant Chemistry on Bearing Fatigue Life. ASLE Trans., vol. 26, no. 1, Jan 1983, pp. 80-86

4. Chamberlin, W. B.: Performance of Synthetic Engine Oils. Lubr. Eng., vol. 35, no. 2, Feb. 1979, pp. 80-87.

5. Beerbower, A.: Environmental Capability of Liquid Lubricants. In Interdisciplinary Approach to Liquid Lubricant Technology. NASA SP-318, Supt. of Documents, U.S. Government Printing Office, Washington, D.C. 20402. Ed. P. M. Ku, pp, 365-432, 1973.

6. Barton, D. B.: Discussion. Lubr. Eng., vol. 35, no. 2, Feb. 1979, pp. 87-90.

7. Beerbower, A.: Boundary Lubrication-Scientific and Technical Forecast. Off. Chief of Res. and Dev., Dept. of the Army, 1972, AD 747 336.

8. Reick, F. G.: Energy-Saving Lubricants Containing Colloidal PTFR. Lubr. Eng., vol. 38, no. 10, Oct. 1982, pp. 6350646.

9. Okrent, E. H.: The Effect of Lubricant Viscosity and Composition on Engine Friction and Bearing Wear - II. ASLE Trans., vol. 4, 1961, pp. 257-262.

10. Arbocus, G. R. and Weber, H.J.: Synthetic Compressor Lubricants - State of the Art. Lubr. Eng., vol. 34, no. 7, June 1978, pp. 372-374.

11. Wolfe, G. F. and Whitehead, A.: Experience with Phosphate Ester Fluids as Industrial Steam Turbine-Generator Lubricants. Lubr. Eng., vol. 34, no. 8, Aug. 1978, pp. 413-420.

12. Anonymous: Facts about Synthetic Lubricants. Mobil Oil Corporation, Commercial Marketing, Technical Publications, 3225 Gallows Road, Fairfax, VA 22037 (1981).

TABLE I.–COMPARATIVE PROPERTIES OF MINERAL AND SYNTHETIC OILS

PROPERTY	MINERAL OILS	POLYOL ESTERS	POLY-OLEFINS	POLY-GLYCOLS
Viscosity Index	Good	Excellent	Excellent	Excellent
Pour Point	Fair	Excellent	Excellent	Good
Antioxidant Response	Good	Good	Excellent	Good
Thermal Stability	Good	Good	Good	Poor
Solubility Parameter	Normal	High	Low	Very High
Volatility	Poor	Excellent	Excellent	*

* Not obtainable due to thermal instability.

TABLE II.–PHYSICAL DATA ON BASE STOCKS

Base Stock	Density g/ml 15°C	VI D 2270	Viscosities			Distillation	
			mm^2/s 99°C	mm^2/s 99°C	$Pa \cdot s$ -18°C	*1%	*20%
Mineral A	0.861	98	4.13	21.8	0.61	168	180
Mineral B	0.864	95	5.00	30.8	--	188	200
Polyolefin	0.817	127	3.93	17.9	<0.55	208	214
Alkyl Aromatic	0.864	107	5.12	26.7	0.75	190	219
Diester	0.915	134	5.41	29.2	1.04	220	238
Blend	0.914	134	4.02	18.1	<0.55	217	218

* Boiling point (°C) at 133 Pa by ASTM D 2160

TABLE III.-HEAT TRANSFER PROPERTIES OF BASE STOCKS

Base Stock	Heat Capacity (kJ/kg.K)	Conductivity (W/m.K)	Prandtl Number
Mineral A	2.25	0.115	65.5
Mineral B	2.18	0.115	77.2
Polyolefin	1.92	0.120	48.4
Aklyl Aromatic	2.12	0.110	80.3
Diester	2.18	0.135	75.3
Blend	2.05	0.132	53.8

TABLE IV.—INDUSTRIAL MACHINERY REQUIRING LUBRICATION

*Air Compressors

*Aluminum Smelters

Asphalt Pavers

*Blowers

*Cement Mills

*Clay Products Plants

Conveyers

Cranes

Earth Movers

*Electric Motors

Elevators

*Extruders

Farm Machinery

Gas Compressors

Knitting Machines

Machine Tools

Mining Machines

Nuclear Power Plants

Packaging Machines

*Paper Machines

Pneumatic Tools

*Pumps

Refrigerators

*Rubber Mills

Saw Mills

*Steam Engines

Steam Turbine Bearings

*Steel Mill Bearings

*Steel Mill Gears

Sugar Mills

Textile Machinery

Vacuum Pumps

*Sometimes bearing temperatures exceed 125°C.

DISCUSSION

L. Rozeanu
Israel Institute of Technology
Haifa, Israel

Dr. Beerbower's paper, sober and comprehensive, suggests that the present status of lubricants - while not bad - shows few outstanding prospects. By this is understood that mineral oils, inferior to synthetic oils in certain respects, remain a satisfactory base stock for producing high quality lubricants with the help of additives.

This conclusion may not fit the overall picture showing the great research efforts made by oil producers. It is difficult to consider this as a luxury which rich companies can afford. More likely there are field reports which show that the available lubricants are not as good as the laboratory tests would suggest. It is easy to conceive what can go wrong. For example there are no quantitative answers to the questions:

How long it takes the lubricant to travel through the lubrication system in order to reach remote friction parts?

How long can the lubricant maintain its nominal properties and its expected performance.

How can the lubricant contribute to the energy conservation problem?

Referring to a specific case, there are undisputed data showing that most of the car engine wear occurs during few seconds or minutes after start. Very likely in the same time friction is high. The most probable reason seems to be the slow arrival of the lubricant in the necessary amount at the sites where it is needed. There are indications

489

that tixotrapic structures developed after long periods of rest and high viscosity at low start temperatures are - at least partly - responsible [1]. The efficiency of gear pumps [2] and the phenomena of boundary slippage [3] - higher at low temperatures - may also bring their own contribution. So far little has been done to understand, to evaluate quantitatively and to control these factors.

Regarding the qualitative stability of the lubricant three aspects seem worth considering:

contamination

mechanical degradation

chemical degradation

Contamination refers to dust from air intake, wear debris, solid degradation products and unburned fuel which found its way to the crankcase. It is evident that at a certain level of contamination the lubricant intrinsic quality becomes a secondary consideration. It makes no sense to develop lubricants capable of 100000 Km service if they must be changed after 20000 Km for the more down to earth reasons of excessive contamination.

Mechanical degradation is a specific problem for the high molecular weight long chain molecules used as V.I. improvers. It is unanimously accepted and commonly indicated in articles and textbooks that their molecular weight is drastically reduced in service to as low as 1/10 their original value [4]. They also show a marked decrease of efficiency at high rates of shear [5] normally found in engines thus making questionable the wisdom of their use.

While the   facts cannot be disputed the case against these additives is not convincing. The degradation mechanism suggested so

far implies mechanical interactions difficult to conveive and the description of the lubricants'performance in service has not been made.

This suggests the possible contribution of other destructive mechanisms which - so far - have not been taken into consideration in which case new ways for controlling the break down of long chain polymers should be investigated.

Our own experience is limited to tests conducted in Couette type viscometers at rates of shear of less than $50000 \, s^{-1}$ and at small Reynolds numbers. We did not find any evidence of mechanical degradation. There is a good probability that the conditions were too mild for having a destructive effect but it is also possible that in the same nominal conditions degradation occurs in an engine but not in a Coutte type viscometer.

Chemical degradation of some additives in service is normally expected for at least two reasons:

- Thermal degradation at hot spots or by reaction with wear debris and other contaminants dispersed in the lubricant.

- Desired reaction in the fulfillment of their duties.

To these qualitative changes one should consider the quantitative aspect:decrease of the additive concentration in lubricant by adsorption on the surface of solid particles (wear debris and contaminants mentioned earlier) present in the filter in steadily increasing amounts.

It is evident that knowing the rate of additive depletion readjustment of the additive concentration becomes an objective which cannot be long time neglected.

Energy Conservation. This is the top priority goal of non-chemist

tribologists. Without going into details it can be said that this

problem has no evident solution such as the use of lighter oils which

is reported to lead to higher lubricant consumption, excessive wear and

bearing failure [6].

Confining the discussion to hydrodynamically lubricated systems

it is convenient to refer to the Stribeck curve presented in a slightly

modified from in Fig.1. In addition to the usual terms used in the

original form the modified curve contains the turbulent domain and

stresses the "minimum friction" zone which corresponds to complete

separation of the friction parts by continuous boundary layers of adsorbed

lubricant but not yet a hydrodynamic load carrying film. The use of the

term "boundary" in that region may seem contrary to classical terminology

but it is the closest to the physical reality.

Energy conservation in this case implies passing from curve 1 to

curve 2 in Fig.1. A tentative solution seems to be offered by lubricants

containing a stable V.I. improver [7]. Indeed the long chain additive will

certainly delay the onset of turbulence; at high rates of shear it aligns

in the flow direction loosing its effect of viscosity increase; when the

clearance between friction parts decreases dangerously the entangled

molecules are squeezed away less readily than the fluid lubricant in which

they are disposed. Furthermore, their presence may help in shifting to the

left the "Mixt" branch of the curve. This is, in fact, more than a guess; as

Dr. Beerbower mentions, there is evidence that the overall wear rate is

reduced in the presence of long chain molecules [8]. The benefits of

lubricants (both mineral and sythetic) containing long chain molecules

extend in other directions as well [7].

492

For example:

- Increase of V.I. with rate of Shear

- Reduction of lateral leakage - as a consequence of the
  3-directional viscosity exhibited by the flowing lubricant.

The problem of volatility is not covered by the above discussion but in the chemist's hands it may find an imaginative solution such as developing an additive interacting with the lubricant in the same way way (partial molar effect) as common salt interacts with water.

To conclude, although the present status is that so competently presented by Dr. Beerbower, the prospects for the eighties are not at all bleak.

References

1. Rozeanu, L., "A model for cylinder lubrication", Wear, 40 (1976), 361-369.

2. Papok, C.C., and Semenido, E.E., "Fuels lubricants and special liquids for engines, Ed. Gostoptehizdat (1956) Moscow.

3. Rozeanu, L., and Tipei, N., "Slippage phenomena at the interface between the adsorbed layer and the bulk of the lubricant", Wear, 64 (1980) 245-257.

4. Cameron, A., and Ettles, C.M., "Principles of Lubrication", Longmans, London, 2nd Ed., Longman, London, 1979, 608 pp.

5. Fowle, T.I., "Lubricants for fluid film and Hertzian contact conditions", Proc. I. Mech. E. 1967-68, Vol. 182 pt. 3A, Lubrication and Wear, pp. 568-584.

6. Hamaguchi, H., Maeda, Y., and Maeda, T., "Fuel efficient motor oil for Japanese passenger car", SAE Technical Paper 1981, No. 810316.

7. Mayan, M., Ciobotaru, S., and Rozeanu, L., "P.I.B. and V.I." To be presented at the 1983 conference of Applied Mechanics, Tel-Aviv 12-14 July 1983.

8. Okrent, E.H., "The effect of lubricant viscosity and composition on engine friction and bearing wear II"ASLE Trans. $\underline{4}$ (1961) pp. 257-262.
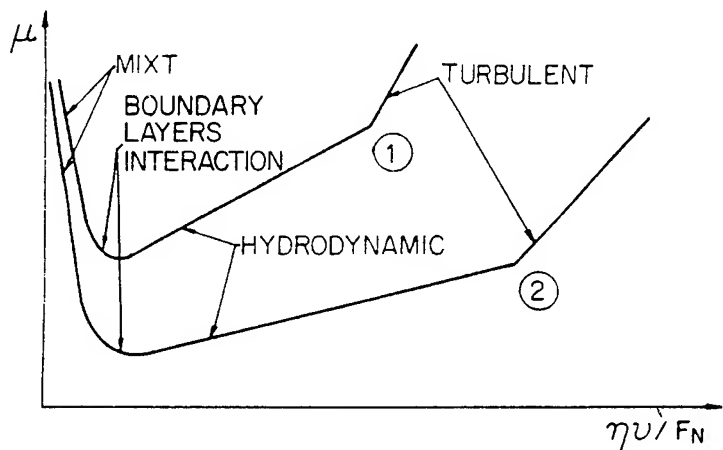
Fig. 1

Stribeck curves modified to include the turbulent regime. Taking MIXT = solid-solid/(solid-liquid+solid-solid). Because $0 < M \leq 1$ the "Boundary" regime at the left of the "Mixt" regime has been eliminated. M=0 has been taken to correspond to the minimum of the curve : interaction between boundary layers of adsorbed lubricant molecules, no load carrying hydrodynamic film.

μ – friction coefficient; η – dynamic viscosity; v – velocity; F_N – normal load.

DISCUSSION

P. A. Willermet
Ford Motor Company
Dearborn, Michigan

Dr. Beerbower has presented a clear and concise summary of the history and the future prospects for formulated synthetic lubricants. It may be, however, of some interest to expand on a few issues he has raised relating to automotive applications.

As the author has pointed out, synthetics differ widely in solubility parameter leading to problems such as additive drop-out and seal swell. These problems can be and are in practice addressed by blending synthetic base stocks. However, these differences may offer new opportunities for improving lubricant performance. The author has alluded to one such potential opportunity, that of reducing oil phosphorus to alleviate poisoning of automotive exhaust catalysts. Another potential opportunity may arise from the observation that hydrocarbons in the combustion chamber can dissolve in the oil layer under pressure and be released during the exhaust stroke contributing to emissions.[1] Recently published results[1] show that the amounts of hydrocarbons dissolved in the oil layer in combustion bomb experiments differ greatly for oils of different structure. In figure 1, Oil A is an SAE 5W20 oil having a poly α-olefin/ester base, oil B is a petroleum based oil, oil C is an alcohol started polypropylene oxide and oil D is a polypropylene-polyethylene oxide copolymer.

Longer oil drain intervals are indeed likely to be an issue of continuing interest. However, it is questionable whether the limiting factor in extending service life will ultimately be oil deterioration or the desirability of performing periodic preventive maintenance. If oil deterioration is the limiting factor, then it appears that additive depletion may be a greater problem than base stock stability. Results obtained in our laboratory for a long drain field test using a synthetic oil[2] indicated that the antioxidant capacity was maintained at an adequate level only by the periodic addition of make-up oil (Figure 2).

Finally, it is worth noting that partial synthetic blends can significantly reduce low temperature viscosity without adversely affecting high temperature viscosity or volatility. Typical data for blends of a synthetic and conventional automatic transmission fluid are given in figure(3). Such applications can potentially extend the scope of synthetics by minimizing the cost penalties for their use.

REFERENCES

1. A. A. Adamczyk and R. A. Kach, "The Effect of Oil Layers on Hydrocarbon Emissions: Low Solubility Oils", Western States Section Meeting of the' Cobustion Institute, Paper No. WSCI 83-39, April 11-12, 1983.

2. S. Korcek, L. R. Mahoney, M. D. Johnson and S. Hoffman, "Antioxidant Decay in Engine Oils During Laboratory Tests and Long Drain Interval Service", Paper No. 780955, SAE International Fuels and Lubricants Meeting, Toronto, November 13-16, 1978.
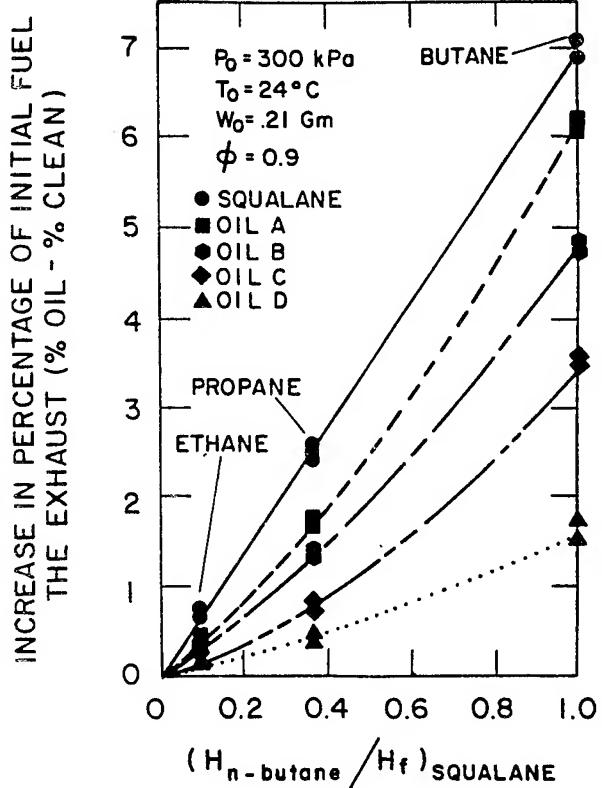
FIG 1 - FUEL HYDROCARBON UPTAKE IN OILS VERSUS THE NORMALIZED
FUEL HYDROCARBON SOLUBILITY PARAMETER
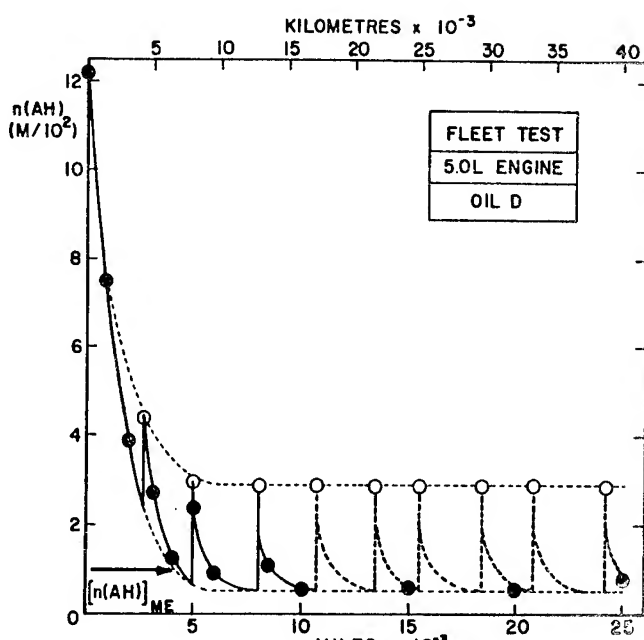
FIG 2 - VALUES OF THE ANTIOXIDANT CAPACITY, n(AH), VERSUS
TEST MILES OBTAINED FROM A LONG DRAIN FLEET TEST.
OPEN CIRCLES INDICATE VALUES CALCULATED FROM THE
AMOUNT AND INITIAL ANTIOXIDANT CAPACITY OF OIL ADDED.
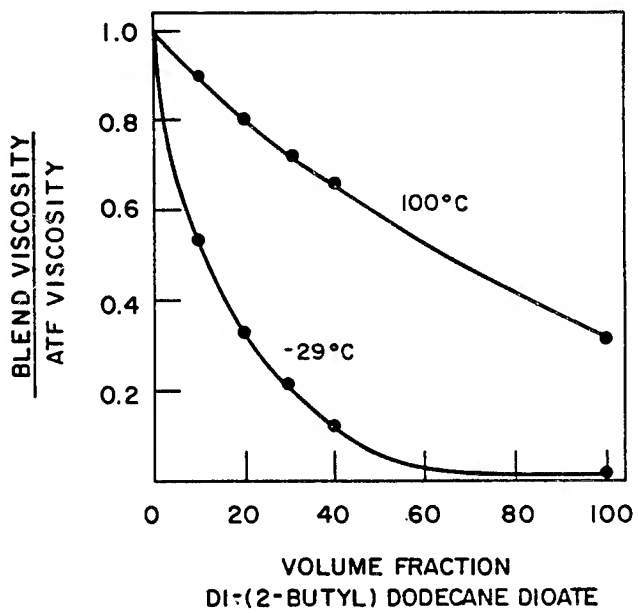
FIG 3 - THE EFFECT OF BLENDING A SYNTHETIC ESTER
WITH A CONVENTIONAL AUTOMATIC TRANSMISSION
FLUID ON VISCOSITY AT TWO TEMPERATURES

496

RESPONSE

Alan Beerbower
University of California at San Diego
San Diego, California

Dr. Willermet's comments are especially interesting, since the author was not aware of the paper by Adamczyk and Kach. It is not possible to estimate the solubility of these gases in all five oils by the published method (B1,B2), but calculations by means of some related unpublished work certainly indicate that the relative positions of the data points are quite in accord with solubility parameter theory.

His point about additive depletion is also well taken. Depletion of the antioxidant is a complex matter, with at least three competing mechanisms. Depletion by performing its function of mutual destruction with a peroxide or free radical is a very necessary evil. Almost as inescapable is the direct oxidation of the additive by atmospheric oxygen. Our best hope lies in trying to limit thermal decomposition, a reaction to which the ZDDP family is especially susceptible. Some progress has been made by using highly deuterated lubricants (B3). Though that paper does not include it, some work was later done with deuterated additives, which also resulted in longer lives. That gives a valuable insight, since deuteration tends to slow most chemical reactions. Peroxide and radical destruction tend to be limited by supply rather than reaction rate, so the increased lubricant lives observed are probably due to slower thermal decomposition. If so, more economical means to this end can be sought.

A fourth mechanism for antioxidant depletion has been proposed, in which the additive adsorbs on sludge, solid surfaces and wear particles. However, it seems most unlikely that this would take place in competition with the powerful surfactants present.

His point on the tendency of blends to give good low temperature viscosities is not a new one, nor is it really surprising if one looks at viscosity with an open mind. Unfortunately, the ASTM D 341 viscosity-temperature chart has been so successful in use on petroleum lubricants that we tend to forget that it is purely empirical in fitting straight lines to data on that specific class. Synthetic hydrocarbons and super-refined oils give lines that are concave downward, while esters plot concave upwards. Blends of the three classes tend to violate even those rules.

Professor Rozeanu's discussion is more complicated, and some of his points cannot be answered at all. For example, while we know the overall oil circulation rate the existence of parallel paths through various thermal zones poses a difficult distribution network problem that it is scarcely worth solving.

The high wear at starting is a regrettable fact of life, and it is alleviated in large steam turbines by starting the oil pumps before turning the shaft. However, the automotive engine cannot afford this sort of luxury, so we depend on bound organic films known variously as "friction polymer" or "third body"

for early protection. These are formed during break-in, often with oils specially formulated for the purpose. A major function of the additives in them and the regular oils is to form and renew the films. Whether they are thixotropic or not is speculative, but it is known that a well run-in engine can be restarted after long storage without catastrophic wear, provided it has been protected from atmospheric corrosion. That implies that the films have such high yield stresses that they are not subject to thixotropy.

The efficiency of gear pumps as a function of viscosity, pressure and rotational speed has been studied (B4) and is quite well understood.

While it is commonly believed that particulate contamination is a major factor in automotive engine wear, some careful studies have failed to verify that idea. Oil and air filters collect most of the road dust before it does much harm, unless neglected to the point of bypassing flow. Even then, it takes surprising doses of particles to do much harm, enough that the failure may be due to plugged oil channels. The opposite is true in systems using rolling element bearings, recently proved to be extremely vulnerable to contamination. Soot is also no problem; the surfactants prevent plugging, and the carbon particles are so fine that carbon black has actually been used as thickener for high temperature industrial greases. Dr. Willermet has touched on the problem of unburned fuel, and the effects of sulfur and nitrogen oxides are notorious, but there may be need for some research on whether free radicals from the combustion chamber are implicated in antioxidant depletion.

Mechanical degradation of polymers is an easily demonstrated reaility, using capillary viscometers rather than the Couette tested at Technion. At that rate of shear it would take a long time to produce measurable results on the usual VI improvers, but those are much improved over what was available 40 years ago. At that time, experiments were conducted in a capillary at about twice their rate of shear. It was found from the molecular weight distributions before and after that the main point of scission was near the middle, indicating failure in tension of molecules caught at an angle to the streamlines. The work was not published, and the data are beyond retrieval.

Oil soluble friction reduction additives were the subject of a very recent review by Papay (B5), whose status in the additive business makes his comments more germane than any response the present author could possibly make to Dr. Rozeanu's question.

REFERENCES

B1. Beerbower, A., "Estimating the Solubility of Gases in Petroleum and Synthetic Lubricants," ASLE Trans., vol. 23, no. 4, Oct. 1980, pp. 335-342.

B2. ASTM Method D 3827, "Estimation of Solubility of Gases in Petroleum and Other Organic Liquids," American Society for Testing and Materials, 1916 Race St., Philadelphia, PA 19103.

B3. Rebuck, N. D., Conte, A. A., Jr., and Stallings, L., "The Effect of Deuterium Exchange on a Synthetic Hydrocarbon Lubricant," ASLE Trans., vol. 20, no. 2, Apr. 1977, pp. 108-114.

B4.   Beerbower, A., "Predicting Performance of Metering Pumps," Control Eng., vol. 8, no. 1, Jan. 1961, pp. 95-97.

B5.   Papay, A. G., "Oil-Soluble Friction Reducers - Theory and Application," Lubr. Eng., vol. 39, no. 7, July 1983, pp. 419-426.

TRIBOLOGY FOR THE 90's AND BEYOND

Duncan Dowson
The University of Leeds
Leeds, England

It is a pleasure to be with you this evening to discuss tribology for the 90's and beyond. I was not allowed to choose the title. Some of you perhaps found it a little difficult preparing your papers for the technical session, but this title really is impossible. I think it was probably put on my plate for one of two reasons - because I have an interest in the history of tribology, or because I am getting old.

I took the invitation seriously, but decided that I would leave the final preparation until I came to the United States. With some friends and colleagues, I attended the Wear Conference in Weston, Virginia, last week and we had 2 or 3 days to travel north from Washington to Cleveland. It was a good opportunity to discover something of the history of this nation.

We went to Gettysburg, in the rain, we crossed the mountains, in the snow, and we stopped in Titusville. How many of the Americans here have been to Titusville? Very good, I'm delighted. We were most impressed by the museum which recognizes the birth of the oil industry. We saw Drake's Well, the McClintock Well, which has been producing oil since 1861, and I was getting involved again in the history of an important aspect of tribology. I thought I was putting together some good background information for this title, Tribology for the 90's and Beyond. And then my colleagues said, "It's 1990 they want to hear about." So all that I had prepared is gone.

I suppose the first thing we should ask is whether or not the subject of tribology will be around in the 1990's and beyond. The long history, that I have mentioned briefly, suggests that it certainly will. The sessions that we have attended already, and even those on subjects like hydrodynamics and old-fashioned elastrohydrodynamics, suggest that there are still a few problems to be solved. So, I think we will be around. Tribology will certainly be a subject for discussion in the 1990's and beyond.

Perhaps we have been a little introspective. David Tabor opened the conference with his penetrating view of the subject and the direction in which it is moving in the 80's. As I listened to him and heard of the outstanding problems I was reminded of the highly humorous, but equally perceptive, view presented by Ernest Rabinowicz at the joint conference last autumn. Although I was not able to be present, I enjoyed reading his article. Perhaps Tabor was a little sober in his view about the changes that have taken place in tribology for the last 20 years and the present status of the subject and the future. He made the point that it is perhaps a low level technology in some ways and this is one of the difficulties we have. We all know the excitement created in the studies of the interacting surface, contact stress problems, and lubrication problems. But to the outside world, we must realize it is a very simple subject.

It must be simple. If you take away friction, lubrication, and wear, what do all these talented people do? We can just say that $\mu = f/w$, that's friction. Wear is a bit more sophisticated: perhaps $(V) = kwx$, or you put in hardness. Lubrication, that's straightforward. Reynolds told us what to

do with that. You just need a gradually tapering wedge, and, indeed, if you just wrap a piece of metal around a rotating shaft, it creates that wedge automatically for you.

Well, then, tribology is a very straightforward and simple subject. In many ways it appears too simple to the outside world. The challenges we face, as scientists and engineers, in this field have to be recognized. The young people of the day, the young scientists, the young engineers, are tempted and led into such terrible things as microelectronics, computing, robotics, etc. Terribly dull things compared with tribology. But we have a job to attract them, to hold their interest, to excite their interest, to emphasize the importance of tribology. This has to be built into our teaching, and certainly into the professional activities of the younger generation.

Having revealed to you that I really was thinking of the 1890's, we should perhaps start with a little historical perspective. We should look at the past to see if it gives us any guidance for the future, see if we can't extrapolate in some way. We are having an exciting time this week hearing about the problems in tribology, the outstanding problems, and many of you are addressing these. But what was happening 100 years ago in 1883? Heinrich Hertz had very recently, in fact the previous year, published his paper on elastic stresses, contact stresses. In that same year Petrov, in Russia, was discovering for the first time the existence of a fluid film in well-acting journal bearings. And, quite independently, Beechum Tow, in the United Kingdom, was finding the same. Within 3 years, Osborne Reynolds, perhaps the most famous tribologist of them all, put lubrication on a firm scientific basis when he applied the laws of slow viscous flow to this problem.

All this was happening in the 1880's. It was a very hectic and exciting time. In this country, Robert Thursten, the first president of the American Society of Mechanical Engineers, one of the greatest engineers of all time, was preaching up and down the country, with an evangelical zeal it appears, not only of the challenge of the technology, but also of the economic significance. His treatise on friction and lost work in machinery and his many writings and talks indicate his dedication and conviction of the importance of the subject that we now call tribology.

Now, 100 years later, as I look around this audience it is a great pleasure to see so many young workers in the field. It is also nice to see older colleagues, many of whom have retired, but who have come back to give us the benefit of their views on this occasion. Some of you might share with me the 50's in age and if you do, just let me ask you for a moment to think that if you just doubled your life span, you're back in the 1880's, it's not that long ago.

If we take the 1880's as the period in which many of the basic principles were established, and also the time in which the economic relevance of tribology was noted, we can look at the subsequent decades and select many equally exciting developments. But on the whole, things did slow down a little. It's not surprising, though, after all those stimulating developments in contact mechanics and lubrication. There were, of course, very notable developments, and I think one of the most important was the development of the tilting pad bearing, or pivoting shoe bearing, the simultaneous development of Michele and Kingsley in the first decade of this century. Also, formation of the bearing companies was happening about this same time. Nothing, however, was quite like the excitement of the 1880's until perhaps the 1920's.

At that time, Hardy drew attention to the phenomenon of boundary lubri-
cation: equally signficant as the 1880's in relation to fluid film lubri-
cation. At the same time, and I hope you will pardon me if I take another
example from the United Kingdom, the Department of Scientific and Industrial
Research established a special committee to look into the subject of lubri-
cation. It concentrated not only on the technological problems and signifi-
cance of lubrication but also on the economic aspect, the cost to the nation
of lubricants, and the effects of poor design relating to bearings.

Now this happened some 40 years after the 1880's and many of you are
talking in this conference about the profile of surfaces, surface topography.
In the same way, I would like to paint for you a little profile of tribology.
You will see that I have an indisputable graph. Like some I've seen already,
it has two points on it, but it is a wave and these are peaks, the first one
1880, the second 1920. So we know the wavelength, it's 40 years.

It is perhaps significant that the 1920 development and the concentra-
tion on economic development aspects of lubrication followed, sadly, by the
First World War. If we look further ahead to the period after the Second
World War, when again some problems were recognized for which there was no
adequate research and development, the subject once again started to blossom.
So we had another peak in the 1960's, the wave comes back after another
40 years.

Also in the 1960's, the Department of Education and Science in the
United Kingdom set up the Working Party under the chairmanship of Peter Jost.
In his address last autumn, Ernest Rabinowicz described the report of that
committee as having both unified our field and elevated our status by coining
the work tribology. The word itself is not particularly significant. What
is important is the unification: the recognition that many of the aspects
of the subject (lubrication, friction, wear, contact mechanics) are inter-
dependent. That they are related brings together the community. I think
that the introduction of the word in the 1960's certainly confirmed the
efforts of Thursten and Goodman and others in the 1880's in preaching the
economic importance of the subject as well as the efforts of a similar group
in the 1920's.

It is interesting that we have to take note of the need, it appears, to
address the politician, to address those who direct scientific and engineer-
ing research. In the United States, I am always impressed by the way in
which your professional engineering societies have representatives in
Washington to speak to Congressmen, to tell them of the priorities in engi-
neering and in science. I don't think we're quite as well organized in the
United Kingdom. I suppose from time to time some of us might try to bend
the ear of a Member of Parliment, or, if we have any sense, a Peer of the
Realm, which is more likely to be successful. But maybe there are other
ways. I've been reminded recently that we have to take account of these
national differences. I think the French would talk to the wives of the
Congressmen. But however we do it, however we wish to influence the politi-
cians, I think it is important that we recognize the need to do so. It's
not a thing that many of us take too kindly. We would rather get on with
our research. We would rather stay in the laboratory or run the computer.
But it is important to keep the subject to the fore, if we genuinely believe
that, among all the problems facing engineering, tribology is indeed a highly
significant one.

The subject of the historical background, and the wavelength that I have
established, suggest that we are now in a trough. The next peak comes along
in approximately 20 years. All I can say to encourage you is that, if this

503

gathering this week represents the trough of tribology, think of all the excitement that's ahead. I suppose that if I steal the words of a well-known sportsman who graces Wimbeldon annually, we are then the pits of tribology.

I think that there are a few qualifications to what I have just said. I have to introduce these qualifications because many of you have achieved great things in the field of tribology, in similar troughs. I think that David Tabor will excuse me if a draw attention to the fact that, with the late Phillip Bowden, much of their stirring work took place in what might be a trough. Perhaps a trough might be a good time to get into this subject and to solve some of these problems, to build for the next recognition in different countries of the importance of the subject.

But, if we are in a trough, then what are we going to be doing in the 1990's. Well, when I recognized that it was the 1990's (not the 1890's) being referred to, I was also reminded that in 1970 I was persuaded to give a talk to the tribology group of the Institution of Mechanical Engineers. I was asked to say what we might be doing in the 1980's. Now, of course, my past has caught up with me. But I had to look at some of these things then and I think that I can get out of this challenge now by simply telling you again what I said in the 1970's.

At that time, I said that it seems quite likely that improvements in tribological materials will be more spectactular than changes in the form of bearings in the next decades. I think I would stick to that again. In particular, the development of improved materials, with operation at high temperature, both in the lubricated state and not, seems quite probable. I drew attention to the fact that, in the previous 10 years, there had been much concern for failure analysis, diagnosis of problems, but that we were moving into an era of prognosis and of monitoring machinery and trying to anticipate events and to avoid failure.

A further development, which I felt was relevant in the 1970's, was the growing interest in the optimum design of tribological components. I expected that ever-increasing demands for power and efficiency would carry that development forward during the next decade. That statement is equally true today, and optimization is developing quite rapidly. At the present time we can see much more interest in the effective design of bearings, gears, and seals: not just the design of something that will work, but the design of something that will work in an optimum and reliable manner. And this, of course, was promoted very much by the consciousness of the energy supply and the need to conserve energy.

In 1970 it seemed safe to assume that we would see a great deal of activity devoted to exposing the mysteries of boundary and mixed film lubrication. That still stands. I think we're still waiting for answers to those questions.

I mentioned also the application of tribology to human joints. I'm not sure how you'll take to this one. I said that I also expect tribologists, 10 years hence (that's now), to have a better understanding of basic wear processes. I think I'll leave that on the list for the 1990's.

In 1970 I felt that courses in tribology, as part of the natural teaching process for engineers and scientists, would be one of the most important developments. I think we have seen this develop in many nations, and it is still developing today in others. Technology transfer (although I do not like the term) wrapped up with education, i.e., the presentation of adequate material and courses, is going to be most important in solving some of the outstanding problems. A genuine, and I mean genuine, recognition and consciousness must be instilled in the minds of all engineers of the importance

of tribology at the outset, at the design stage, or at the conceptual stage. Tribology is not something that you try to put right at the end when things go wrong. We are still battling this one. This same problem was recognized in the 1880's, in the 1920's, and again in the 1960's.

Apart from studies of wear in general and the question of technology transfer, I would put third on my list the question of adequate design of equipment to ensure reliability and appropriate efficiency. There is much concern at present for power losses in equipment, and a lot of good work is leading toward solutions to many of the problems facing the operators of expensive equipment.

I think that the question of materials still stands. We've heard a good deal about composites, polymers, and ceramics (in a sense the glamour material of the present time) attracting a lot of attention. These might very well be the focus of attention in the last decade of this century.

I think I must, if only to defend some of my good colleagues, both present and past (and indeed former students), address one other subject. I will put EHL on the list. There is still a lot to be done in EHL. It is, in fact, presently experiencing something of a revival. I think there are more people working on EHL in the United Kingdom now than I can ever recall. I am conscious in this conference of similar activity in many other countries. I'm not sure that we shall solve all the problems in the next few years, so I think I shall put that on the list for the 1990's and beyond.

I'm now going to rest my arm. I'm not going to list any more speculative topics that you might be addressing in the future. I'm going to try to identify who will be doing it. Some of you know that I have enjoyed writing biographical sketches of a number of famous men who have contributed to our subject. I mentioned 23 such men in my book: five of them were French, five were German, one Russian, three Americans, one Australian, and just to show that I am not at all prejudiced, seven Englishmen, plus the international Leonardo da Vinci. According to my statistics of their birthdates, if we are going to try to identify the people who are going to make the big breakthroughs when the next wave comes in 15 or 20 years, there's a high chance that the individuals were born in October or December. If you were born in November, there's no chance. I looked at the distribution of birthdates, and with an impeccable statistical analysis, found that the average date, from the beginning of the year, of these distinguished gentlemen was 6.45 months, so the leading figure in tribology in the future, who is now perhaps 5 or 10 years old, was born on July 14th, Bastille Day.

Having drawn attention to the economic significance of our subject, as well as the scientific and technological fascination, I would like to say that at the end of the day I hope that we do not lose sight of our major need: to establish and develop the highest standards in our subject, the highest standards of science and of engineering skills. On these points we will be judged, not only within our own community by ourselves, but also by those outside. Thus, the establishment of these standards is extremely important.

Gatherings like this are a real contribution toward the firmness of these standards and their preservation. We will, of course, be able to judge the achievements of the tribologists of the future when we meet again in 5 or 10 years. And we can hope that there will have been many notable achievements by that time. At conferences like this, we hear some tremendous achievements and a lot of challenging questions and this, of course, is the challenge and excitement that we enjoy.

I would, however, just like to end by saying that had Vogelpohl lived a little longer, I understand that his last book would have contained the following words: that new thoughts are not numerous, just tell us the old ones fluently. Thank you very much.